



Università  
di Catania



Department of Biomedical and Biotechnological Sciences

Ph.D. in Biotechnology

Curriculum in Pharmaceutical Biotechnology

XXXIV Cycle

---

ANTONINO NICOLÒ FALLICA

**Targeting the Heme Oxygenase enzymatic system  
as a new approach for anticancer therapy**

*PhD Thesis*

Tutor: *Prof. Valeria Pittalà*

Coordinator: *Prof. Vito De Pinto*

---

ACADEMIC YEARS 2018/2021

**Affiliation**

Department of Drug and Health Sciences, University of Catania, V.le Andrea Doria 6, 95125 Catania, Italy – Prof. Valeria Pittalà.

Interdisciplinary Nanoscience Center (iNANO), Aarhus University, Gustav Wieds Vej 14, 8000, Aarhus C, Denmark – Prof. Kurt Vesterager Gothelf, 14 June 2021–30 January 2022.

## **Table of contents**

Abstract	1
Sommario	2
Abbreviations	3
<b>CHAPTER 1:</b>	
Introduction	5
1.1. Heme degradation pathway	5
1.2. Physiological roles of heme metabolites	8
1.3. Heme oxygenase isoforms	10
1.4. Regulation of heme oxygenase expression	15
1.5. Heme oxygenase 1 and cancer	18
1.6. Heme oxygenase inhibitors	24
1.6.1. Metalloporphyrins	24
1.6.2. Azole-based HO inhibitors	26
<b>CHAPTER 2:</b>	
Aim of the thesis	54
<b>CHAPTER 3:</b>	
Results and discussion	56
<b>Concluding remarks</b>	64
<b>References</b>	65
<i>Identification of a potent heme oxygenase-2 (HO-2) inhibitor by targeting the secondary hydrophobic pocket of the HO-2 western region</i>	83
<i>Discovery of novel acetamide-based heme oxygenase-1 inhibitors with potent in vitro antiproliferative activity</i>	108
<i>Growing the molecular architecture of imidazole-like ligands in HO-1 complexes</i>	162
<i>From far west to east: joining the molecular architecture of imidazole-like ligands in HO-1 complexes</i>	190
<b>Supplementary information</b>	S1
<b>List of papers (2018–2021)</b>	I
<b>List of conference participations (2018–2021)</b>	III

## Abstract

The intrinsic complexity of the molecular mechanisms involved in tumor pathogenesis surely represents one of the main issues that contributes to the failure of common anticancer therapies. Current anticancer approaches are based on the application of different therapeutic protocols aimed at slowing down tumor growth and spread or at killing tumor cells. However, the polypharmacological approach usually applied, even if successful in some conditions, can give rise to cytotoxicity to healthy cells and trigger the appearance of chemoresistance phenomena. The modulation of the activity of biological targets specifically detectable in tumor cells could represent a valid approach for the definition of novel antitumor regimens. In this context, it has been discovered that beyond its physiological role, the inducible isoform of heme oxygenase (HO-1) contributes in the sustenance of a cytoprotective condition that is often exploited by cancer cells to survive and spread to healthy tissues. A wide plethora of studies proved that the specific inhibition of this enzyme is associated to reduced tumor growth and invasiveness, and it also contributes to reversal of chemoresistance. The present PhD thesis focuses on the design, synthesis and *in vitro* evaluation of novel classes of HO inhibitors with potential application in anticancer therapy. The research was carried out by the application of traditional and more innovative drug discovery approaches using as guidelines the information obtained by structure-activity relationship studies concerning HO inhibitors. *In vitro* enzymatic assays and biological studies led to the identification of potent compounds that could be used in the future for the design of selective inhibitors of HO-1 or HO-2, with the latter representing the constitutive enzymatic isoform. Finally, marked antiproliferative properties were discovered for a class of inhibitors characterized by the presence of an acetamide function in the chemical structure of the molecule, with potential application for future *in vivo* studies.



## Sommario

La complessità intrinseca dei meccanismi molecolari coinvolti nell'insorgenza del tumore rappresenta uno dei principali problemi che contribuisce al fallimento delle comuni terapie antineoplastiche. Gli attuali regimi terapeutici si basano sull'applicazione di diversi protocolli volti a rallentare la crescita e la diffusione del tumore o ad uccidere le cellule cancerose. Tuttavia, l'approccio polifarmacologico solitamente utilizzato, sebbene efficace in alcune condizioni, può dar luogo a citotossicità nei confronti di cellule sane e innescare la comparsa di fenomeni di chemioresistenza. La modulazione dell'attività di bersagli biologici specificamente rilevabili nelle cellule tumorali potrebbe rappresentare un valido metodo per la definizione di nuovi regimi antitumorali. In questo contesto, è stato scoperto che, al di là del suo ruolo fisiologico, l'isoforma inducibile dell'eme ossigenasi (HO-1) contribuisce al mantenimento di una condizione citoprotettiva che è spesso sfruttata dalle cellule tumorali per sopravvivere e diffondersi ai tessuti sani. Un'ampia serie di studi ha dimostrato che l'inibizione specifica di questo enzima è associata a una ridotta crescita e invasività del tumore e contribuisce ad invertire i fenomeni di chemioresistenza. La presente tesi di dottorato si concentra sulla progettazione, sintesi e valutazione *in vitro* di nuove classi di inibitori di HO con potenziale applicazione nella terapia antitumorale. La ricerca è stata condotta mediante l'utilizzo di approcci tradizionali e più innovativi di *drug discovery* utilizzando come linee guida le informazioni ottenute da studi di correlazione struttura-attività riguardanti gli inibitori di HO. Saggi enzimatici e studi biologici *in vitro* hanno permesso l'identificazione di potenti derivati che potrebbero essere utilizzati in futuro per la progettazione di inibitori selettivi di HO-1 o HO-2, con quest'ultimo rappresentante l'isoforma enzimatica costitutiva. Infine, sono state riscontrate spiccate proprietà antiproliferative per una classe di inibitori caratterizzati dalla presenza di una funzione acetammidica nella struttura molecolare, potenzialmente utilizzabili per futuri studi *in vivo*.

## **Abbreviations**

3'-UTR, 3'-untranslated region

5-FU, 5-fluorouracil

ARE, antioxidant-response element

Bach1, BTB and CNC homology 1

BK<sub>Ca</sub>, large conductance Ca<sup>2+</sup>-activated K<sup>+</sup> channels

BVR, biliverdin

CBS, cystathionine-β-synthase

cGMP, cyclic guanosine monophosphate

CK2, casein kinase 2

CMA, chaperone-mediated autophagy

Cul3, cullin-3

ER, regulatory elements

ERAD, endoplasmic-reticulum-associated protein degradation

F-2,6-BP, fructose 2,6-bisphosphate

G6PDH, glucose-6-phosphate dehydrogenase

GRE, glucocorticoid responsive element

GSH, glutathione

GSK3β, glycogen synthase kinase 3 beta

HIF-1α, hypoxia inducible factor-1α

HO, heme oxygenase

HRM, heme regulatory motif

Hsp32, heat shock protein 32

IL-10, interleukin 10

IL-2, interleukin 2

IRP, iron regulatory protein

Jak-STAT, Janus kinase-signal transducer and activator of transcription

Keap1, Kelch-like ECH associated protein 1

MAPK, mitogen activated protein kinase

NF- $\kappa$ B, nuclear factor kappa B

NOS, nitric oxide synthase

NPAS2, neuronal PAS domain protein 2

Nrf-2, nuclear factor erythroid 2 p45-related factor 2

PD-L1, programmed death-ligand 1

PFK1, phosphofructokinase 1

PI3K, phosphoinositide 3-kinase

PKC, protein kinase C

ROS, reactive oxygen species

SAR, structure-activity relationships

SDF-1, stromal cell-derived factor 1

sGC, soluble guanyl cyclase

SPP, signal peptide peptidase

TAM, tumor associated macrophages

TLR-4, Toll-like receptor 4

TME, tumor microenvironment

Tregs, regulatory T cells

VEGF, vascular endothelial growth factor

## 1. Introduction

---

### 1.1. Heme degradation pathway

Heme is an electrically neutral tetradentate complex made of an organic part called protoporphyrin IX and ferrous iron ( $\text{Fe}^{2+}$ ), which represents the 95% of the total iron in humans [1]. Heme structure is made of four substituted pyrrole rings linked through methene bridges, with the ferrous iron coordinated by the nitrogen atoms of the pyrrole rings [2]. In eukaryotes heme is synthesized in the mitochondrial matrix and in the cytosol in eight reaction steps, using glycine and succinyl-CoA as starting materials [3]. After its production, heme is transferred in hemoproteins or used for the synthesis of cytochromes; however, the mechanism underlying its trafficking within the different cell compartments has not been perfectly clarified and is currently being studied [4]. In the organism, heme has several physiological functions: it has an active role in sensing the intracellular levels of gasotransmitters, such as nitric oxide (NO) and carbon monoxide (CO), it regulates cells differentiation and protein synthesis through the regulation of the activity of transcription factors, ion channels, kinases and membrane receptors and acts as a prosthetic group in hemoproteins (hemoglobin, myoglobin, cytochrome P450, nitric oxide synthase, peroxidase, cyclooxygenase and catalase) promoting electron transfer, catalysis and oxygen storage [5-8]. These phenomena contribute to preserve cellular homeostasis. The imbalance of the intracellular redox potential mediated by the production of reactive oxygen species (ROS) in certain conditions gives rise to oxidative stress, which damages DNA, proteins and membrane lipids [9]. In its free form, heme possesses powerful pro-oxidant and proinflammatory properties. On the basis of the oxidation state of iron, heme participates in the generation of ROS through the Fenton and Haber-Weiss reaction [10]. Moreover, Wagener and coworkers have also demonstrated that heme proinflammatory properties are

caused by the infiltration of leucocytes into organs in an *in vivo* experimental inflammation [11]. Heme homeostasis can be modulated by its binding with specific proteins, which remove heme and undo its potential cellular toxicity, or by interfering with its biosynthetic route by virtue of feedback mechanisms on the activity of enzymes involved in the rate limiting synthetic steps, such as  $\delta$ -aminolevulinate synthase [12-16]. However, heme degradation represents the most important strategy used by cells to regulate the heme pool and in this context, the key regulator of this process is represented by the heme oxygenase enzymatic family. First discovered in 1968 [17,18], the heme oxygenase family (HO) is a distinctive class of enzymes highly conserved in phylogenetic kingdoms [19]. It is located mostly in the endoplasmic reticulum, but detectable also in mitochondria, caveolae, plasma membrane and cell nucleus [20,21]. The enzyme allows a selective oxidative cleavage of the heme  $\alpha$ -mesocarbon with the consequent release of stoichiometric quantities of three catabolites: carbon monoxide, ferrous iron and biliverdin, a greenish bile pigment later converted in bilirubin by the enzyme biliverdin reductase [22,23]. The reaction requires three  $O_2$  molecules, NADPH and cytochrome P-450 reductase and occurs in three steps (Figure 1) [24,25]. In this metabolic pathway, heme acts both as a prosthetic group and substrate:

- In the first step heme forms a complex with the enzyme. Ferric iron is reduced to a ferrous state by NADPH and cytochrome P-450 reductase allowing oxygen to bind to the complex. The newly formed metastable oxy-form (not shown in Figure 1) is then converted to a ferric hydroxyperoxyheme intermediate thanks to the action of NADPH and the cytochrome P-450 reductase. The distal oxygen attacks the  $\alpha$ -mesocarbon of the porphyrin ring forming the  $\alpha$ -meso-hydroxyheme after loss of a water molecule. The reaction is regiospecific;

- In the second step the HO-bound  $\alpha$ -meso-hydroxyheme is converted in the HO-bound verdoheme using oxygen and one electron. The iron is reduced to a ferrous state. In this step carbon monoxide (CO) is released;
- In the third and last step the HO-verdoheme complex reacts with the third oxygen molecule and electrons, causing the porphyrin ring opening and the oxidation of the iron ion. The resulting ferric iron-biliverdin chelate intermediate (not shown in Figure 1) reacts with an additional electron allowing the release of biliverdin and  $\text{Fe}^{2+}$ , formed after reduction of  $\text{Fe}^{3+}$ ;
- Finally, biliverdin is converted in bilirubin by the cytosolic enzyme biliverdin reductase (BVR). Bilirubin is made water soluble after binding with albumin and then reaches the liver. Herein it is conjugated with glucuronic acid and released in the bile. After bile secretion in the small intestine, bilirubin is converted once again in its free form and is reduced by the intestinal flora to urobilinogen. A small part of urobilinogen is absorbed from the bowel, oxidized to urobilin in the kidney and excreted in urine; the unabsorbed urobilinogen is converted in stercobilinogen in the lower intestine, oxidized to stercobilin and excreted with feces [26].

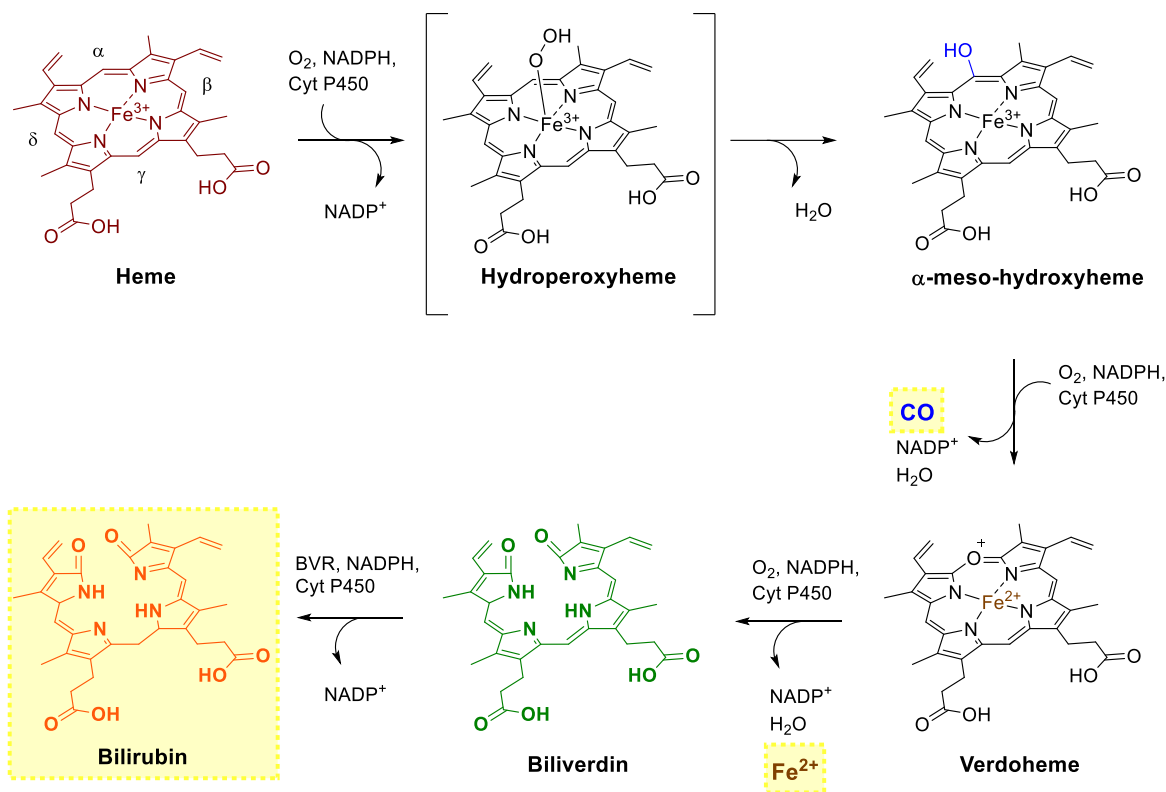


**Figure 1.** The heme degradation pathway promoted by heme oxygenase.

## 1.2. Physiological roles of heme metabolites

Interestingly, CO, bilirubin and Fe<sup>2+</sup> are not useless heme end-products but have beneficial effects that can be summarized into cytoprotective, antiapoptotic and antioxidant properties (Figure 2).

CO is a relatively stable gaseous molecule that traverses cell membranes and acts as a messenger affecting several signaling pathways. With nitric oxide, it upregulates the production of cGMP through modulation of soluble guanyl cyclase (sGC) exerting vasorelaxant, antiplatelet and antiproliferative properties [27]. In particular, it has been shown that in the liver CO increases the activity of nitric oxide synthase (NOS) promoting the production of NO that potentiates HO activity; the result is an additional release of CO with a positive feedback mechanism [28]. The vasodilating property is also due to the

modulation of ion channels such as large conductance  $\text{Ca}^{2+}$ -activated  $\text{K}^+$  channels ( $\text{BK}_{\text{Ca}}$ ) [29]. CO is also able to bind to other hemoproteins. Indeed, it is able to interfere with transcription factors such as Bach1 and NPAS2, contributing to the maintenance of cellular homeostasis and regulating the circadian cycle respectively [29]. Antiapoptotic, antiproliferative and anti-inflammatory functions have been ascribed through the stabilization of hypoxia-inducible factor 1 $\alpha$  (HIF-1 $\alpha$ ) and the modulation of MAPK (mitogen-activated protein kinases) pathways, decreasing leukocyte adhesion and increasing the release of interleukine-10 (IL-10) [30,31]. In addition, CO inhibits NADPH oxidase decreasing the synthesis of superoxide [29]. Finally, CO has the potential to promote angiogenesis [32].

Several studies using animal models of inflammation showed that bilirubin is a powerful antioxidant and possesses also anti-inflammatory properties by scavenging free radicals, decreasing peroxidation of membrane fatty acids and inhibiting the complement cascade [33,34]. At nanomolar concentrations, bilirubin reduces the risk of cardiac ischemia and infarct damage [35]. Moreover, a finely controlled biliverdin/bilirubin oxidation-reduction cycle is involved in neuroprotection [36]. On the other hand, high levels of bilirubin can be harmful, indeed, promoting neonatal jaundice and neurologic damages [37].

Among the three heme catabolites, ferrous iron is the most dangerous because of its intrinsic potential to give rise to oxidative stress. Heme oxygenase strictly affects free iron concentration and its removal by binding with specific proteins. Firstly, freshly released iron is trapped by Fe-ATPase, an iron transporter located on the endoplasmic reticulum lumen, where it is oxidized from  $\text{Fe}^{2+}$  to  $\text{Fe}^{3+}$  [38]. In addition, HO induces the synthesis of ferritin, a globular protein that sequesters iron and renders it ready to be used for the synthesis of new heme molecules [39]. Ferritin synthesis is tuned by post-transcriptional mechanisms:



when high concentration of iron are present, the iron regulatory protein (IRP) binds with iron de-repressing ferritin mRNA so that it can be translated [40].

Considering the properties of each heme metabolite it can be said that heme oxygenase is an antioxidant and cytoprotective enzyme. However, it must be noticed that an excessive activity of the enzyme can reverse its antioxidant activity because of an excessive release of reactive iron that can alter its sequestration and reutilization pathways [41,42].

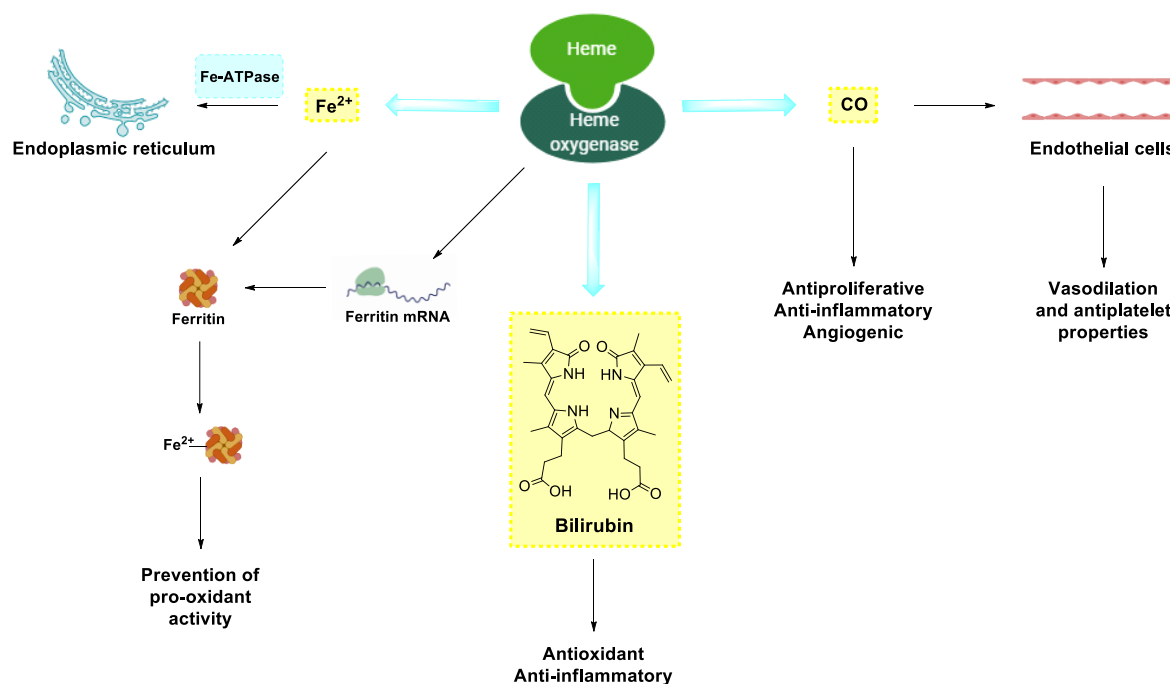


**Figure 2.** Heme metabolites and their physiological roles.

### 1.3. Heme oxygenase isoforms

Until now, two major heme oxygenase isoforms have been discovered and characterized, with an additional isoform (HO-3) which is devoid of any catalytic activity and whose physiologic significance is still poorly understood [43]. The first isoenzyme, named heme oxygenase-1 (HO-1) represents the inducible isoform. HO-1, also called heat shock protein 32 (Hsp32), is a 32 kDa protein made of 288 aminoacidic residues [44] basally

expressed in low levels in spleen, liver and bone marrow [45]. In response to hyperoxia, high heme concentrations, heat shock, toxins, heavy metals, xenobiotics, UV radiations and oxidizing agent, HO-1 is practically over-expressed in every tissue [46], exerting its cytoprotective properties through the production of the three metabolites previously described. The second isoenzyme, heme oxygenase-2 (HO-2), is a 36 kDa protein made of 316 aminoacids [44] constitutively expressed mainly in brain and testis [47], and it is not induced by any HO-1 inducers [48]. It seems that the constitutive expression in these two organs is related to the neuroprotective functions of CO and the modulation of sperm cells maturation respectively [49,50]. The two enzymes are encoded by two different genes, *HMOX1* in chromosome 22 and *HMOX2* in chromosome 16 [51], respectively. In the 5'-flanking region, the *HMOX1* gene is characterized by GT microsatellite polymorphism whose repeats vary between 11 and 40. A low number of GT sequences within the polymorphic sequence (less than 40) causes a higher induction of gene expression in response to oxidative stress [52]. This condition has been associated with major protection against cardiovascular pathologies, as well as in higher risk of cancer onset [53,54]. In humans, the HO-2 gene is transcribed into two transcripts of 1.3 and 1.7 kb that after mRNA encoding give rise to the same molecule. The two transcripts origin from different splicing mechanisms and use of two potential polyadenylation signals located in 3'-UTR region [55]. Despite the existence of two different isozymes, HO-1 and HO-2 catalyze the same reaction. Even so, the two enzymatic isoforms not only differ for their mechanism of induction and tissue localization, but they also present small differences in their structure. HO-1 and HO-2 share a 55% of identity, 76% of similarity and an  $\alpha$ -helical conformation in their secondary structure as shown by crystallographic studies [56]. The best results in terms of crystal resolution have been obtained with truncated and fully active enzymatic forms of both HO-1 and HO-2 (Figure 3) [57,58]. Several portions of the molecule are highly conserved, such

as the catalytic core made of 24 aminoacidic residues. In this area the only difference between the two isoforms regards the substitution of Leu138 in HO-1 with Met157 in HO-2 [59].

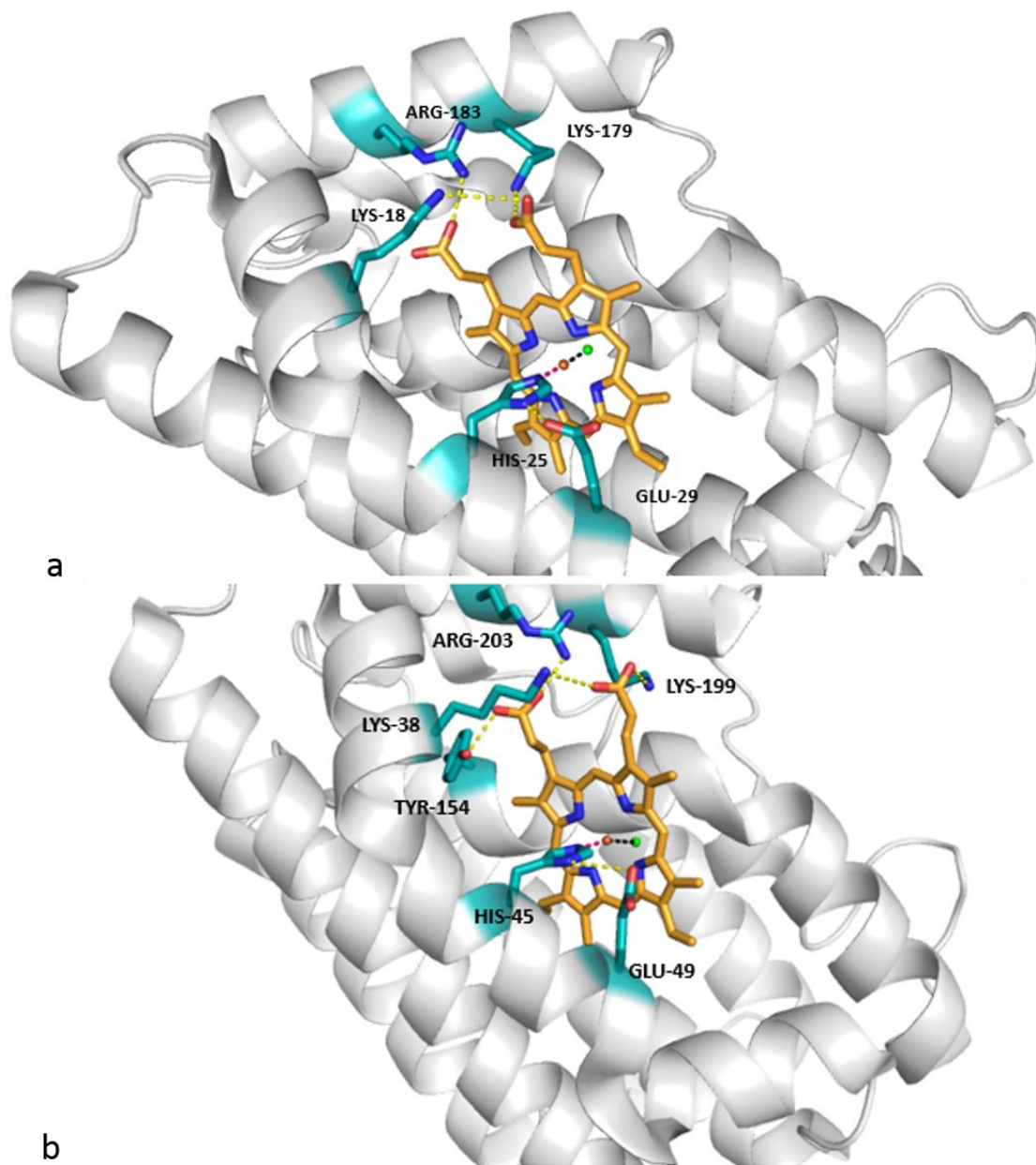


**Figure 3.** Docking of heme with HO-1 (PDB ID #1N45) (a) and HO-2 (PDB ID #2QPP) (b). The water molecule that acts as the heme sixth ligand is represented as a green sphere; iron is shown as an orange sphere. Hydrogen bonds are depicted as yellow dashed lines; the coordination bond between iron and histidine is shown with hot pink dashed lines; the coordination bond between iron and the water molecule with black dashed lines.

In both proteins the catalytic site is comprised inside a space limited by a proximal and a distal helix. The spatial conformation of the two helices are different in the apoenzyme and the holoenzyme. In fact, in the apoenzyme the molecule takes on a more open conformation due to the high flexibility of the distal helix. This inherent flexibility is explained by the presence in this part of the protein of several glycine residues. In HO-1 great importance is given to Gly139 and Gly143 that in the apo-form shift away from the zone that will be occupied by heme whereas in the holoenzyme they take a direct interaction with heme itself [57]. In HO-2 the distal helix flexibility is assured by five aminoacidic residues (Gly159-Asp-Leu-Ser-Gly164) where Gly159 interacts with a water molecule that coordinates the heme iron serving as a sixth ligand [58]. The proximal helix contains a histidine residue (His25 in HO-1, His45 in HO-2) whose nitrogen atom coordinates the heme iron. In addition to this, in the apoenzyme His25 does not have a precise spatial orientation. Contrariwise, in the heme-bound enzyme, His25 position is maintained in the right place thanks to a hydrogen bond with Glu29 (Glu49 in HO-2), which favors a better interaction between iron and histidine [57]. In the holoenzyme the distal helix is less distant from heme, indeed, it is possible to highlight that the enzyme substrate is sandwiched between the two helices. This conformation is typical of the fully active enzyme, whereas the open conformation allows heme to wedge in the catalytic site and biliverdin to be released after heme degradation [57]. The closed conformation is the result of an intricate network of hydrogen bonds in which a fundamental role is played by Asp140 (Asp160 in HO-2), Tyr58, Tyr114, Arg136, Asn210 and water molecules trapped in the catalytic cavity [44,57]. These interactions may serve as a system that promotes a proton shuttle that is necessary to trigger the enzymatic activity. This hypothesis has been confirmed by mutagenesis studies in HO-1 in which Asp140 has been replaced with Ala140 turning the enzymatic function into a peroxidase instead of an oxidoreductase [60]. Heme positioning and selective cleavage at the  $\alpha$ -mesocarbon is also

guaranteed by ionic and hydrogen bonds between the two propionic heme groups with Lys18, Lys22, Lys179 and Arg183. In such manner the  $\alpha$ -mesocarbon is buried in a lipophilic pocket made by Met34, Phe37 and Phe214 residues strengthening the interaction between heme and the enzyme. Obviously, these interactions are not present in the apoenzyme because of electrostatic repulsions between Lys18 and Lys22 basic residues that promote the open conformation [57]. In HO-2 Tyr154 and Arg203 coordinate the carbonyl oxygen of a propionate group buried in a lipophilic area made by Phe53, Val54, Phe57 and Phe234; the other propionate is surrounded by a hydrophilic space and binds with Lys38 and Lys199 in a likewise fashion seen in HO-1 [58]. The major divergences between HO-1 and HO-2 pertain the *N*-terminal region and the *C*-terminal region. In HO-2 the *N*-terminal is 20 aminoacids longer; in both isoforms the *C*-terminal is responsible of HO dimerization, oligomerization and anchoring to the endoplasmic reticulum [44]. In HO-1, but not in HO-2, the region comprised amidst the catalytic core and the membrane anchor possess a protein degradation signal sequence (PEST domain), in which the peptide bond between Ser275 and Phe276 is cleaved by a peptidase [61]. The resulting truncated HO-1 is thus able to translocate to the nucleus modulating gene expression and promoting DNA repair [62]. The resulting cytoprotective effect encouraged by the truncated form is often exploited by many types of cancers to escape apoptosis [63,64]. The HO-2 isoform is characterized by the presence in its structure of three cysteine residues that are part of the so-called heme regulatory motifs (HRMs) [44,65]. Considering that HRMs are not present in HO-1 it was thought that this motifs could have a unique role in HO-2. Three HRMs have been detected: the first one is present in the catalytic core (Cys127-Pro128), the other two are located at the *C*-terminus (Cys265-Pro266 and Cys282-Pro283), where the cysteine thiol residues can form a disulfide bond or can be reduced to a dithiolate state according to the intracellular redox potential [56,66-68]. In order to investigate a hypothetical role of HRMs in HO-2

enzymatic activity, cysteines have been substituted with alanine in a mutagenesis study [50]. Interestingly, menadione, a selective HO-2 inducer, was still able to activate the mutated enzyme, suggesting that HRMs do not have any role in heme degradation [69]. Further studies revealed that HRMs seem to have a role in heme binding regulation or may function as intracellular heme sensors on the basis of a redox-regulated switch that affects the thiol residues of Cys265 and Cys282 [67]. Additional studies investigated the number of heme molecules that can be bound by HO-2. In particular, it was proposed that the reduced thiol residue of Cys265 may coordinate the heme iron serving as the sixth heme ligand displacing the water molecule usually present. In this way the Cys265-Pro266 HRM can bind heme in the catalytic pocket serving as an antenna that senses the changing of the redox potential [56]. Other studies showed that HO-2 can bind at least two heme molecules, the first one in the catalytic core and the second one in the Cys265-Pro266 HRM or with a lower affinity in the Cys282-Pro283 HRM [66]. Recently, it was confirmed that upon heme binding to the HRMs motifs, a conformational change facilitates the docking of the HRM to the core of the HO-2 apoenzyme, allowing heme transfer and degradation. In addition, a transfer from the catalytic core and the HRM can also happen rebalancing the heme pool [70].

#### **1.4. Regulation of heme oxygenase expression**

HO-1 and HO-2 differ for their mechanism of enzymatic activation, gene expression and degradation. In rats, the expression of the constitutive isoform HO-2 is regulated by glucocorticoids through the glucocorticoid responsive element (GRE) [71], whereas its enzymatic activity seems to be boosted by activation of protein kinase C (PKC). In these conditions, PKC phosphorylates casein kinase 2 (CK2), which in turn phosphorylates the Ser79 residue of HO-2, leading to augmented heme catabolism and consequent CO synthesis in hippocampal cultures [72]. Very recently, Liu and co-workers reported that HO-2 is post-

translationally regulated by the presence of heme in the catalytic core. Indeed, heme deficiency and its consequent absence in the catalytic core destabilizes HO-2, favoring HO-2 degradation through a CMA mechanism after recognition of a KFERQ-like motif (absent in HO-1) and/or lysosomal degradation promoted by the presence of a di-leucine motif (<sup>32</sup>DLSELL<sup>37</sup>), also absent in HO-1 [73]. When heme is bound to the catalytic core, the two motifs cannot be recognized by their targets, preventing HO-2 degradation. This discovery was of particular interest, indeed, HO-1 follows an ERAD degradation pathway promoted by poly-ubiquitination and proteasomal degradation, pointing out another difference between the two isozyme. On the other hand, enzymatic activation and gene expression modulation of the inducible isoform HO-1 is far more complex due to the participation of different actors in this regulation. HO-1 gene stimulation is mainly controlled at the transcriptional level. In the promoter 5'-flanking region there are several regulatory elements (ER) whose binding with specific transcriptional factors enhance HO-1 expression in pro-oxidant conditions [74]. The most important key regulator of HO-1 expression in oxidative stress is the cytosolic nuclear factor erythroid 2 p45-related factor 2 (Nrf2). In normoxic conditions (Figure 4, a), Nrf2 is inhibited by the cytosolic Kelch-like ECH associated protein 1 (Keap1), which in turn is a substrate for Cul3 (Cullin-3), a component of Cul3-E3 ubiquitin ligases complex. Indeed, Nrf2 binding with Keap1 determines a constant ubiquitylation and subsequent proteasomal degradation of Nrf2. Meanwhile, in the nucleus, the transcription repressor Bach1 binds to Maf proteins forming a heterodimer that binds to the antioxidant-response element (ARE) on the promoter. During oxidative stress (Figure 4, b), two cysteine residues of Keap1 are oxidized determining a conformational change that frees a phosphorylated Nrf2, allowing its translocation into the nucleus. Herein, Bach1 dissociates from the promoter, Nrf2 forms a heterodimer with Maf proteins and binds to ARE, activating the expression of about 200 antioxidant genes, including HO-1 [9,75].

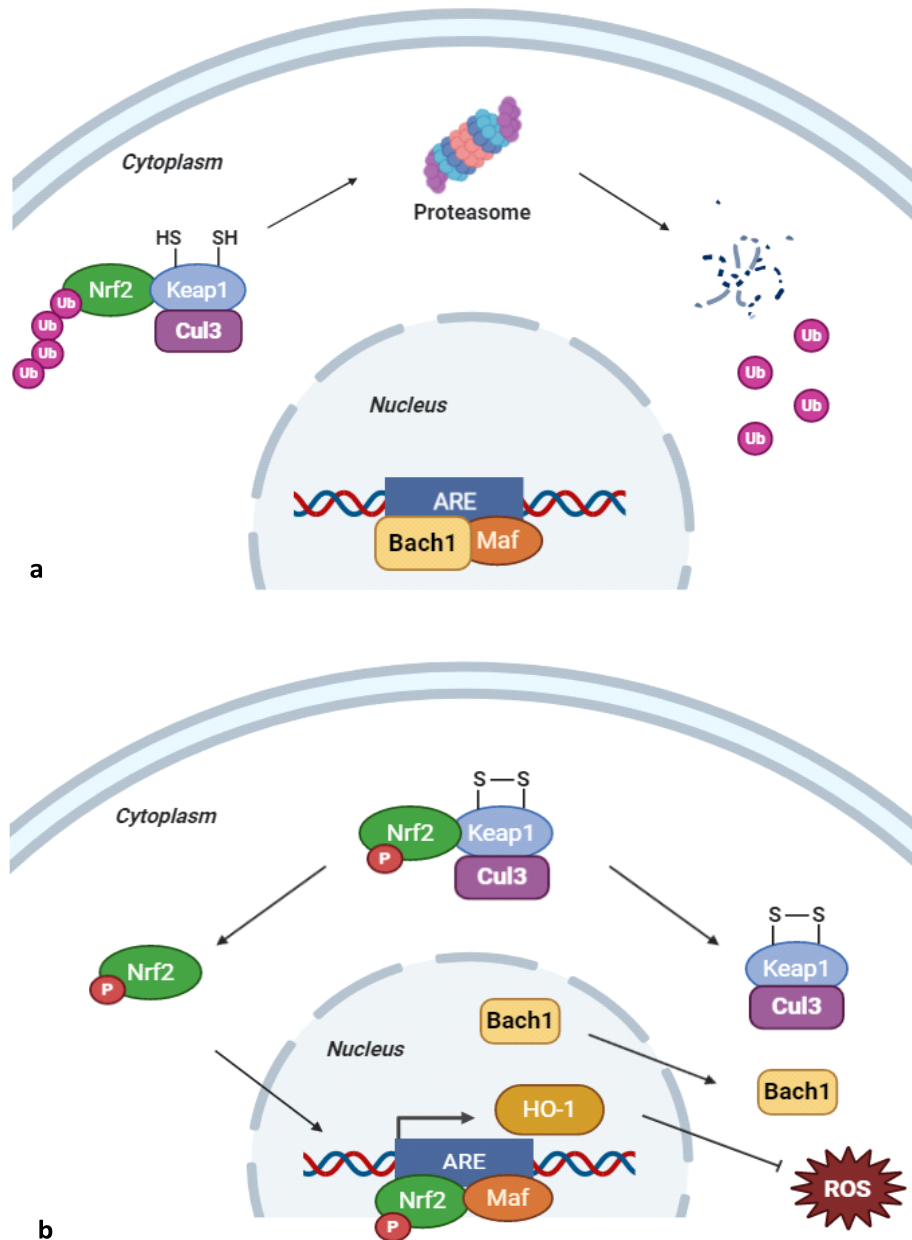


**Figure 4.** The Nrf2/HO-1 axis. a) Normoxic conditions; b) Pro-oxidant conditions.

The splicing mechanisms to which HO-1 is subject can bring to the formation of the well-known 32 kDa protein, but also to a smaller 14 kDa splice isoform after removal of exon 3 [76]. It has been demonstrated that HO-1 expression depends also by other pathways that includes AP-1 (activating protein-1), PKC, NF- $\kappa$ B, PI3K/Akt, IL-10, Jak-STAT, TLR-4 (Toll-like receptor 4) and MAPK [77]. Independently from Keap1, Nrf2 ubiquitylation is also promoted by the activity of glycogen synthase kinase 3 $\beta$  (GSK-3 $\beta$ ) which



phosphorylates specific serine residues in a domain of Nrf2 making it recognizable to the E3 ubiquitin ligase complex ( $\beta$ -TrCP-Skp1-Cul1-Rbx1), indirectly reducing HO-1 gene expression [78,79]. Furthermore, in vascular smooth muscle cells an increase of intracellular  $\text{Ca}^{2+}$  concentration promoted by angiotensin II downregulates HO-1 gene expression [80], whereas in glioblastoma cells suppression of the HO-1 gene is ensured by interferon- $\gamma$  [81]. Loss of function mutations, hypermethylation or interactions of Keap1 with other proteins could enhance HO-1 gene expression due to the failure of Nrf2 inactivation [75]. The consequent expression and activation of HO-1 can support a cytoprotective regimen that can lead to apoptosis evasion. A prolonged activation of the Nrf2/HO-1 axis is considered dangerous in certain pathologies, such as cancer [82]. For these reasons, the evidence of HO-1 overexpression in cancer cells boosted the interest in understanding which mechanisms are entailed for the onset of this pathology in order to define a potential pharmacological approach.

### **1.5. Heme oxygenase 1 and cancer**

From a therapeutic point of view, HO-1 could represent a potential pharmacological target for the treatment of different pathologies. Even though HO-1 induction could represent an optimal approach for the treatment of diseases related to oxidative stress, an heightened enzymatic activity has been found in many types of cancers. The link between HO-1 overexpression and cancer has been and still is deeply investigated; however, results reported so far have been somehow contradictory. Indeed, HO-1 overexpression and cancer progression are cell and tissue-dependent; namely, in some kind of prostate and colon cancers HO-1 overexpression determines antiproliferative activity [83], whereas in lung, pancreatic, gastric, renal and gynecological cancers and in gliomas, glioblastoma, leukemia and multiple myeloma the same overexpression is synonymous of poor prognosis [84-93].

HO-1 can promote tumor growth, higher tumor aggressiveness, angiogenesis, metastasization, failure of apoptosis and resistance to chemotherapy, radiotherapy and photodynamic therapy. The mechanisms by which HO-1 plays its tumorigenic role involve the nature of the HO-1 splice isoform, the localization of HO-1 truncated form in the nucleus, the exploitation of complex cytoprotective biochemical pathways, the metabolic changes in tumor cells and finally the modulation of the immune response (Figure 5).

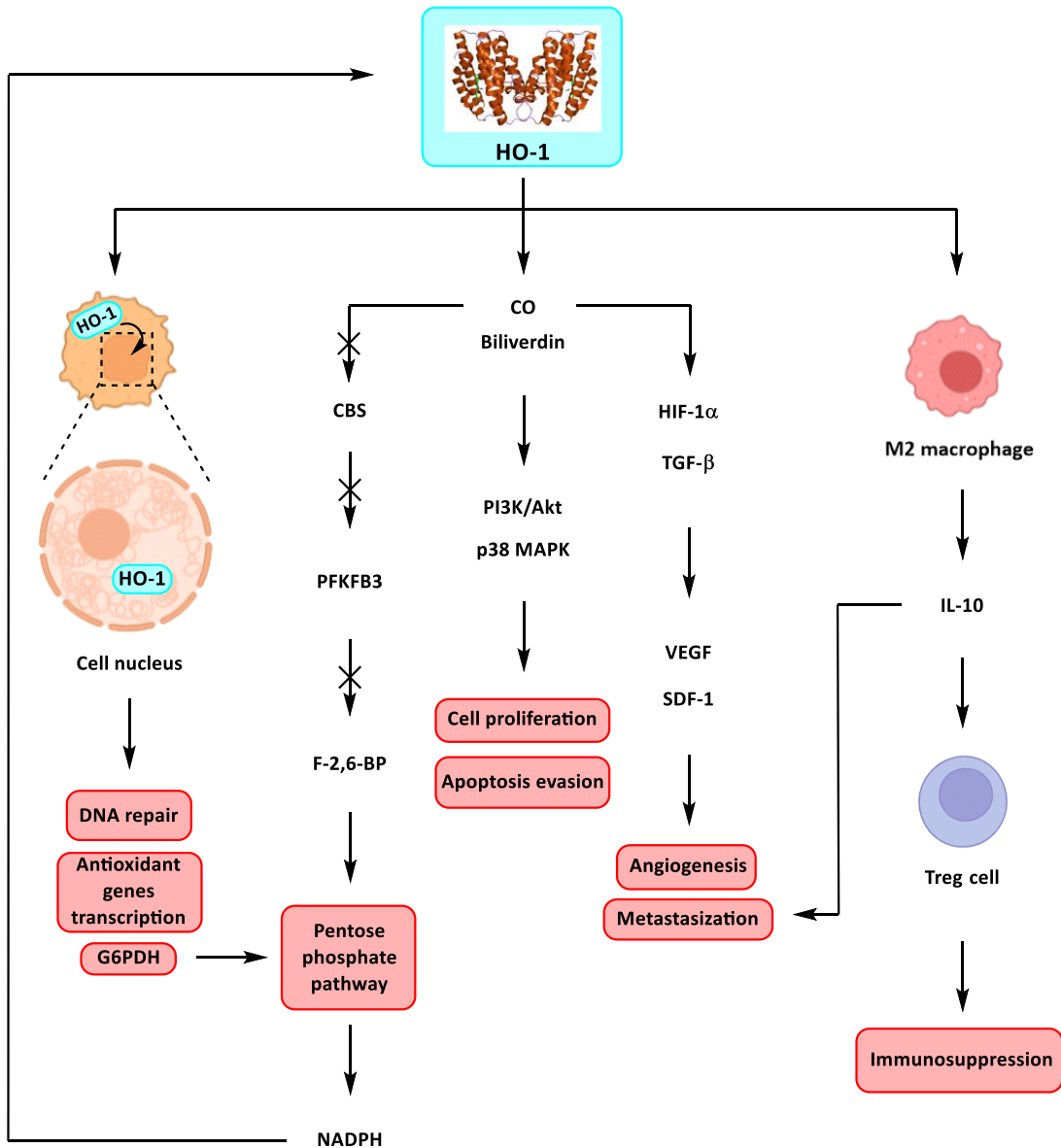


**Figure 5.** Mechanisms of cancer progression promoted by HO-1.

The 14 kDa HO-1 splice isoform has been found in immortalized cells and, differently from the 32 kDa isoform, is not able to translocate into the nucleus. In addition, it has been reported that the shorter isoform increases the telomere length, thus favoring cell proliferation and tumorigenesis [76]. CO produced after heme breakdown is responsible for the activation of HIF-1 $\alpha$  and TGF- $\beta$  which in turn allow the production of VEGF and SDF-1, leading to the endothelial cells proliferation and angiogenesis in melanoma, Kaposi sarcoma, glioma, pancreatic, prostate, bladder, lung and gastric cancer [94-96]. In addition, CO and biliverdin can trigger the activation of PI3K/Akt and p38 MAPK pathways leading to cell proliferation and apoptosis evasion [97-100].

Cytoprotection can be also promoted by translocation of HO-1 into the nucleus. In the cytosol, the signal peptide peptidase (SPP) allows the cleavage of the C-terminal region of the enzyme leading to a HO-1 truncated protein with loss of enzymatic activity [101]. This protein can interact in the nucleus with Nrf2 stabilizing its binding with DNA and favoring the transcription of antioxidant genes, including HO-1 itself, and can participate in DNA repair processes [102-104]. These events, usually enhanced by HO-1 acetylation [105], are coupled with an increased tumor aggressiveness, metastasis formation and chemoresistance as it has been reported in lung, prostate, breast, colon, gliomas and neck and head cancers, as well as in multiple myeloma and chronic myeloid leukemia [103,106,107].

The tumorigenic role of HO-1 is also related to changes in the metabolism of cancer cells. Indeed, it has been reported that HO-1 overexpression, nuclear HO-1 translocation and CO production have a strong impact on cellular metabolism, favoring a metabolic shift from glycolysis to the pentose phosphate pathway [103]. Specifically, nuclear HO-1 is able to induce the expression of the G6PDH mRNA [108], allowing an increased production of G6PDH which represents the rate-limiting enzyme involved in the pentose phosphate pathway. Furthermore, HO-1 overexpression and CO production promote the inhibition of

the cystathionine  $\beta$ -synthase (CBS) [109]. This inhibition decreases the methylation of PFKFB3, an enzyme involved in the synthesis of fructose 2,6-bisphosphate (F-2,6-BP). When methylation of PFKFB3 occurs, the enzymatic activity is enhanced, leading to a higher production of F-2,6-BP which in turns acts as an allosteric activator of phosphofructokinase-1 (PFK1), a rate-limiting enzyme required for glycolysis. On the other hand, PFKFB3 reduced methylation leads to its polyubiquitination and subsequent proteasomal degradation, thus reducing the available amount of F-2,6-BP necessary for glycolysis and determining a shift from the glycolytic to the pentose phosphate pathway [110]. Overall, these events lead to an increased biosynthesis of NADPH and GSH, bringing to a reductive intracellular environment necessary to counteract the oxidative stress promoted by anticancer drugs or by tumor itself, and restoring the NADPH pool required for the full activation of the heme degradation pathway promoted by HO-1.

As far as the activity of HO-1 in immune cells is concerned, several evidence show that overexpression of the enzyme affects the reprogramming of tumor associated macrophages (TAM) population and regulates the crosstalk between cancerous and non-cancerous cells in the tumor microenvironment (TME) through the release of specific cytokines and growth factors [111]. In particular, cell debris released after tumor cell death caused by anticancer therapies are digested by macrophages generating ROS that trigger the expression of HO-1 [112]. In these conditions HO-1 is able to reprogram macrophages from a proinflammatory and antiproliferative M1 phenotype to an anti-inflammatory and pro-tumorigenic M2 phenotype which overexpresses in its cell surface the immune suppressor programmed cell death-ligand 1 (PD-L1) protein and releases IL-10. M2 macrophages are able to infiltrate the tumor surrounding tissues contributing in the establishment of an immunosuppressive environment responsible for the increased risk of metastasis, as shown in pancreatic ductal adenocarcinoma [113]. Furthermore, the higher release of IL-10 from M2 cells stimulates

the activity of T regulatory cells (Tregs) which suppress IL-2 production and CD8<sup>+</sup> T cells activity, thereby enhancing immunosuppression and tumor growth [96,114]. Interestingly, HO-1 inhibition performed by applying genetic engineering approaches or by using specific inhibitors showed beneficial effects either in the reprogramming of TAMs towards the M1 phenotype or restored the sensitivity of cancer cells whose HO-1 overexpression led to chemoresistance to common antineoplastic drugs such as cisplatin, doxorubicin, bortezomib, carfilzomib, cytarabine, 5-fluorouracil, gemcitabine and tyrosine kinase inhibitors [87,90,112,113,115-119]. These data suggest that HO-1 inhibition could be beneficial for the treatment of cancer and HO-1 inhibitors could represent promising pharmacological tools to be used in combination with anticancer drugs or in stand-alone antitumoral therapeutic regimens.

Despite HO-1 overexpression has been predominantly seen as a survival mechanism, an antiproliferative role has been recently reported through the induction of a different form of regulated cell death known as ferroptosis [120]. Distinct both mechanistically and morphologically from other forms of regulated cell deaths, ferroptosis can be triggered by the imbalance of numerous pathways, involving the disruption of the activity of the cystine/glutamate antiporter  $x_c^-$ , glutathione depletion, inactivation of the GPX4 selenocysteine enzyme with consequent accumulation of lipid peroxides, and increase of the intracellular concentration of iron [121]. Iron overload is responsible for the accumulation of ROS species generated through the Fenton reaction, which in turn determines the inactivation of intracellular proteins and oxidation of DNA and polyunsaturated fatty acids [122]. Overall, these events disrupt the fluidity and the integrity of lipids present in the cell membrane, with altered cell permeability and consequent cell death [123]. The interplay between HO-1 and ferroptosis is quite intricate. Indeed, the pro-tumorigenic or antiproliferative effects exerted by HO-1 seem to be dependent on the intracellular ROS

levels. At lower concentrations, ROS trigger a moderate expression of HO-1 in order to protect cells from oxidative insults. On the other hand, a higher accumulation of ROS and overexpression of HO-1 enhance heme metabolism and sequentially dictate the increase of intracellular iron concentration, obtaining as a result the events previously described [123].

Some studies carried out with small molecules acting as positive or negative regulators of ferroptosis highlighted that HO-1 can trigger ferroptosis in a tumor cell-dependent manner. As an example, renal proximal tubule cells treated with erastin, a ferroptotic agent acting as an inhibitor of the  $x_c^-$  system, displayed a different cell death susceptibility on the basis of the presence (HO-1<sup>+/+</sup>) or deficiency (HO-1<sup>-/-</sup>) of HO-1. HO-1<sup>+/+</sup> renal cells treated with erastin showed an overexpression of HO-1 and a less remarkable reduction of cell viability when compared with HO-1<sup>-/-</sup> cells. Treatment with an iron chelator such as deferoxamine, with a ferroptosis inhibitor such as ferrostatin-1, or with a supplier of GSH, such as *N*-acetyl-cysteine, caused an increase of cell viability in both HO-1<sup>+/+</sup> and HO-1<sup>-/-</sup>, demonstrating that HO-1 had an anti-ferroptotic activity in renal proximal tubule cells [124]. On the other hand, HO-1<sup>+/+</sup> HT-1080 fibrosarcoma cells treated with erastin showed an increased expression of HO-1 and a marked reduction of cell viability, an effect that was counterbalanced after treatment with zinc protoporphyrin IX (ZnPP), a HO-1 inhibitor [125]. These results showed that HO-1 upregulation cannot solely be seen as a cytoprotective mechanism and questioned its role in tumor progression or suppression, suggesting that HO-1 overexpression and ferroptosis could represent additional mechanisms of action worthy of attention for the establishment of alternative anticancer therapies.

As regards the role of HO-2 in cancer, very low information have been reported. He and co-workers found that HO-2 silencing in human umbilical vein endothelial cells (HUVEC) and human aortic endothelial cells (HAEC) treated with H<sub>2</sub>O<sub>2</sub> determines mitochondrial membrane depolarization, caspase activation and apoptosis [126]. In addition, Li *et al* used

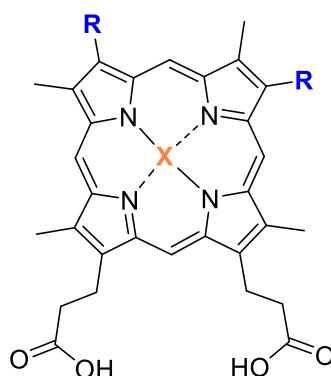
a protein microarray that demonstrated the interplay between HO-2 and PFKFB4, a protein that regulates glycolysis in hepatic cells [127]. Interestingly, liver cancer cells and glioblastoma cells require PFKFB4 for their survival. Interestingly, HO-2 silencing, but not HO-1, reduces PFKFB4 levels, an event that triggers apoptosis in liver cancer cells [128]. These evidences may suggest a role of HO-2 in cell survival, and the biological effects of its inhibition in the context of cancer need to be further elucidated in order to understand if HO-2 could represent a druggable target for the treatment of cancer.

## **1.6. Heme oxygenase inhibitors**

Heme oxygenase inhibitors are classified on the basis of their chemical structure and their mechanism of action. Specifically, two main classes have been distinguished: metalloporphyrins and azole-based compounds derived from the chemical structure of Azalanstat.

### **1.6.1. Metalloporphyrins**

The first reported compounds with HO inhibiting properties were metalloporphyrins. From a structural point of view, they differ from heme by the presence of different substituents on the porphyrin ring and of a metallic cation coordinated by the pyrrole nitrogen atoms that replaces the ferrous ion. Interestingly, some compounds possess inhibitory activities, whereas others are able to strongly enhance the HO enzymatic activity [116]. On the basis of the nature of the substituents in the porphyrin ring it is possible to classify deuteroporphyrins, mesoporphyrins, protoporphyrins and bis-glycolporphyrins [129]. Some inhibitory potencies of metalloporphyrins are reported in Table 1.

**Table 1.** General structure and HO IC<sub>50</sub> values of tin, zinc and chromium metalloporphyrins.

Compd	Class	R	X	IC <sub>50</sub> (μM) HO-1 <sup>a</sup>	IC <sub>50</sub> (μM) HO-2 <sup>a</sup>	SI (HO- 2/HO-1)
<b>SnPP</b>	Protoporphyrin	CH=CH <sub>2</sub>	Sn	0.47	0.10	0.21
<b>SnDP</b>	Deuteroporphyrin	H	Sn	3.15	0.80	0.25
<b>ZnBG</b>	Bis-glycolporphyrin	CHOH-CH <sub>2</sub> OH	Zn	0.12	0.08	0.67
<b>SnMP</b>	Mesoporphyrin	CH <sub>2</sub> CH <sub>3</sub>	Sn	0.08	0.03	0.38
<b>ZnMP</b>	Mesoporphyrin	CH <sub>2</sub> CH <sub>3</sub>	Zn	1.60	0.70	0.44
<b>SnBG</b>	Bis-glycolporphyrin	CHOH-CH <sub>2</sub> OH	Sn	0.80	0.15	0.19
<b>CrPP</b>	Protoporphyrin	CH=CH <sub>2</sub>	Cr	0.30	0.18	0.60
<b>CrMP</b>	Mesoporphyrin	CH <sub>2</sub> CH <sub>3</sub>	Cr	0.05	0.05	1.00
<b>CrBG</b>	Bis-glycolporphyrin	CHOH-CH <sub>2</sub> OH	Cr	2.80	2.10	0.75
<b>ZnDP</b>	Deuteroporphyrin	H	Zn	5.25	2.10	0.40
<b>CrDP</b>	Deuteroporphyrin	H	Cr	0.42	0.25	0.60
<b>ZnPP</b>	Protoporphyrin	CH=CH <sub>2</sub>	Zn	6.00	2.65	0.58

<sup>a</sup>Data taken from [129].

Sn, Cr and Zn porphyrins inhibit HO to a different extent. In general, Cr porphyrins are better HO-1 inhibitors when compared to their Sn or Zn counterparts. On the contrary, Sn porphyrins are better HO-2 inhibitors, with SnPP representing one of the most potent HO inhibitor and possessing the lowest selectivity index (SI). On the other hand, Mg, Ni, Cu and Cd porphyrins do not possess any inhibitory activity towards both enzymes, whereas FeDP and FeMP only slightly inhibit both enzymes (data not reported) [130]. Interestingly, it has been reported that CoPP is a strong inducer of HO-1 expression [131]. This class of

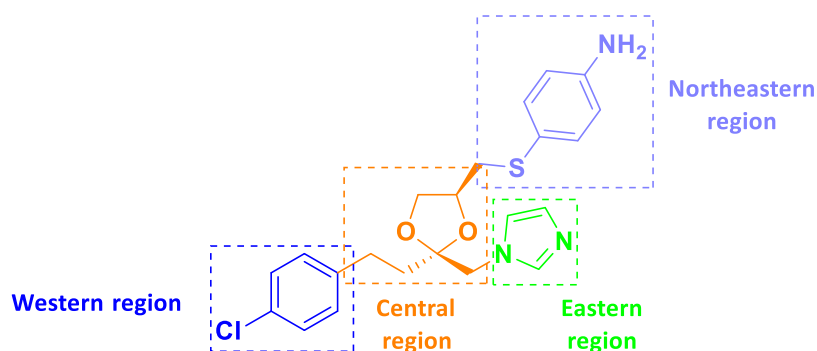


compounds lacks of selectivity between the two isoforms and possesses a competitive mechanism of action which causes a strong interference with other heme proteins such as NOS, cytochrome P450 and sGC [116]. In addition, despite their strong inhibitory activity, metalloporphyrins are able to induce the expression of the HO-1 mRNA, rendering them less useful from a therapeutic point of view. Despite this, these molecules have been proposed as useful tools for the treatment of hyperbilirubinemia and neonatal jaundice [132-134], an harmful pathology caused by the accumulation of bilirubin in children that can determine serious damages to the central nervous system. With the exception of mesoporphyrins, the main side effect of these compounds is also related to their photosensitizing properties that can also restrict their translation in therapeutic regimens [116]. Moreover, Sn and Cr are not biocompatible metals, and this aspect adds another issue for their therapeutic utilization [135]. Finally, an additional issue is represented by their poor solubility or bioavailability that can be partially overcome by pegylation or encapsulation in styrene-maleic anhydride nanoparticles [136-139]. Nevertheless, metalloporphyrins find application as research tools whenever it is desirable to understand the role of HO inhibition in *in vitro* studies.

### **1.6.2. Azole-based HO inhibitors**

The first non-porphyrinic compound discovered as an HO inhibitor was Azalanstat. Firstly investigated in 1993 as an inhibitor of lanosterol 14 $\alpha$ -demethylase [140], an enzyme involved in cholesterol biosynthesis, in 2005 Vlahakis and coworkers chose this molecule as the lead compound for the discovery of novel HO inhibitors whose chemical structure was not related to metalloporphyrins in order to overcome the problems that arise by their utilization [141], as previously discussed. The chemical structure of Azalanstat can be virtually broken down in four regions: northeastern, western, central and eastern region. The northeastern region contains the methylthioaniline moiety, the western region is occupied by

the 4-chlorophenyl ring, the central region contains a four carbon chain and the dioxolane ring, the eastern region presents the imidazole ring (Figure 6).



#### Azalanstat

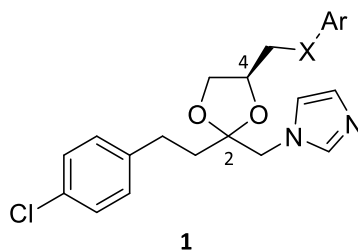
HO-1 IC<sub>50</sub> = 6.0 ± 1 μM

HO-2 IC<sub>50</sub> = 28 ± 18 μM

**Figure 6.** Chemical structure of Azalanstat and HO inhibitory potency values.

The first structural modifications introduced in the Azalanstat molecule aimed at understanding the role of the diastereomeric configuration of the dioxolane ring (2*S*,4*S* in Azalanstat) and the nature of the substituents tolerated in the northeastern region. The general structure of the newly synthesized compound is reported in Table 2.

**Table 2.** General structure of the firstly reported Azalanstat derivatives and their HO IC<sub>50</sub> values.



Compd	Chiral centers	X	Ar	IC <sub>50</sub> (μM) HO-1 <sup>a</sup>	IC <sub>50</sub> (μM) HO-2 <sup>a</sup>	SI (HO-2/HO-1)
<b>1a</b>	2 <i>S</i> ,4 <i>S</i>	S	3-NH <sub>2</sub> Ph	1 ± 0.2	35 ± 6	35

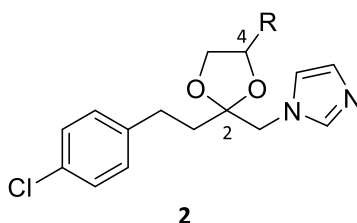
<b>1b</b>	2 <i>S</i> ,4 <i>S</i>	S	2-NH <sub>2</sub> Ph	5 ± 0.1	68 ± 5	13.6
<b>1c</b>	2 <i>R</i> ,4 <i>S</i>	S	4-NH <sub>2</sub> Ph	0.52 ± 0.03	5 ± 3	9.6
<b>1d</b>	2 <i>R</i> ,4 <i>S</i>	S	2-NH <sub>2</sub> Ph	2.5 ± 0.1	63 ± 3	25.2
<b>1e</b>	2 <i>R</i> ,4 <i>S</i>	S	3-NH <sub>2</sub> Ph	1.6 ± 0.7	32 ± 9	20
<b>1f</b>	2 <i>R</i> ,4 <i>S</i>	S	Ph	1.03 ± 0.07	34 ± 12	33
<b>1g</b>	2 <i>R</i> ,4 <i>S</i>	S	Pyridin-4-yl	25 ± 5	69 ± 8	2.8
<b>1h</b>	2 <i>R</i> ,4 <i>S</i>	S	4-OHPh	1.59 ± 0.03	7 ± 2	4
<b>1i</b>	2 <i>R</i> ,4 <i>S</i>	S	4-BrPh	2.1 ± 0.9	2.4 ± 0.1	1.1
<b>1j</b>	2 <i>R</i> ,4 <i>S</i>	S	4-OCH <sub>3</sub> Ph	0.7 ± 0.3	2.5 ± 0.4	4
<b>1k</b>	2 <i>R</i> ,4 <i>S</i>	S	4-ClPh	2.8 ± 0.4	12 ± 5	4.3
<b>1l</b>	2 <i>R</i> ,4 <i>S</i>	S	4-FPh	2.2 ± 0.2	5 ± 4	2
<b>1m</b>	2 <i>R</i> ,4 <i>S</i>	S	4-NO <sub>2</sub> Ph	6 ± 2	19 ± 2	3
<b>1n</b>	2 <i>R</i> ,4 <i>S</i>	S	4-CF <sub>3</sub> -pyridin-2-yl	2.1 ± 0.6	16 ± 8	7.6
<b>1o</b>	2 <i>R</i> ,4 <i>S</i>	S	3-BrPh	5 ± 2	22 ± 9	4
<b>1p</b>	2 <i>R</i> ,4 <i>S</i>	S	2-BrPh	6 ± 1	12.3 ± 0.5	2
<b>1q</b>	2 <i>R</i> ,4 <i>R</i>	O	4-NH <sub>2</sub> Ph	1.4 ± 0.3	13 ± 4	9.3
<b>1r</b>	2 <i>R</i> ,4 <i>R</i>	O	4-OHPh	1.8 ± 0.5	7.1 ± 0.7	3.9
<b>1s</b>	2 <i>R</i> ,4 <i>R</i>	O	Ph	0.59 ± 0.04	1.6 ± 0.3	2.7
<b>1t</b>	2 <i>R</i> ,4 <i>R</i>	O	4-BrPh	3.5 ± 0.2	22 ± 8	6.3
<b>1u</b>	2 <i>R</i> ,4 <i>R</i>	O	4-FPh	0.28 ± 0.01	0.5 ± 0.2	2
<b>1v</b>	2 <i>R</i> ,4 <i>R</i>	O	4-OCH <sub>3</sub> Ph	1.33 ± 0.03	19 ± 7	14
<b>1w</b>	2 <i>R</i> ,4 <i>R</i>	O	4-IPh	9 ± 3	15 ± 4	2
<b>1x</b>	2 <i>R</i> ,4 <i>R</i>	O	4-CNPh	0.67 ± 0.02	1.7 ± 0.2	2.5
<b>Azalanstat</b>	2 <i>S</i> ,4 <i>S</i>	S	4-NH <sub>2</sub> Ph	6 ± 1	28 ± 18	4.7

<sup>a</sup>Data taken from Refs [141,142].

Interestingly, it was found that the preferred configuration of the dioxolan ring is 2*R*,4*S* (**1d** vs **1b**, **1c** vs Azalanstat) [141]. Later on, it was reported that the aryl group in the northeastern region can be linked to the dioxolan moiety also through a oxymethylene group. Moreover, halogens, hydroxy, methoxy, trifluoromethyl, nitro and nitrile substituents in the *para* position of the aryl group are better tolerated when compared to the same substitutions in the *ortho* or *meta* positions. Furthermore, the 4-aminophenylthiomethyl moiety can also be removed in favor of a methyl group, fluorine, chlorine, hydroxy, methoxy, amino, methylthio or azide substituents (Table 3) [142,143]. With the exception of the methyl

substitution, results obtained from this work showed that the new derivatives did not yield any significant improvement in the selective inhibition of one of the two HO isoforms.

**Table 3.** General structure of 4-substituted dioxolane derivatives and their HO IC<sub>50</sub> values.

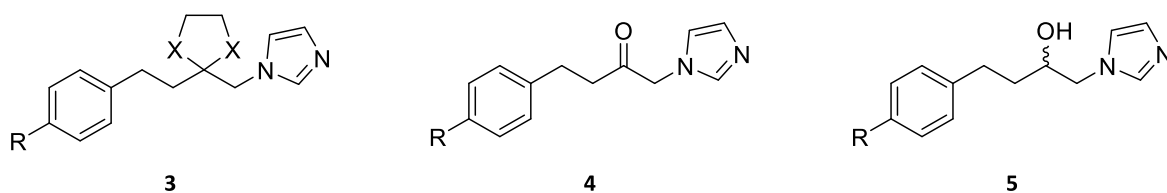


Compd	Chiral centers	R	IC <sub>50</sub> (μM) HO-1 <sup>a</sup>	IC <sub>50</sub> (μM) HO-2 <sup>a</sup>	SI (HO-2/HO-1)
<b>2a</b>	2 <i>R</i> ,4 <i>R</i>	CH <sub>3</sub>	0.8 ± 0.2	305 ± 25	381
<b>2b</b>	2 <i>R</i> ,4 <i>S</i>	CH <sub>3</sub>	2.6 ± 0.4	> 100	> 38
<b>2c</b>	2 <i>S</i> ,4 <i>S</i>	CH <sub>3</sub>	12 ± 4	> 100	> 8
<b>2d</b>	2 <i>S</i> ,4 <i>R</i>	CH <sub>3</sub>	20 ± 4	> 100	> 5
<b>2e</b>	2 <i>R</i> ,4 <i>R</i>	CH <sub>2</sub> OH	12 ± 2	> 100	> 8
<b>2f</b>	2 <i>R</i> ,4 <i>S</i>	CH <sub>2</sub> SCH <sub>3</sub>	9 ± 2	19 ± 7	2
<b>2g</b>	2 <i>R</i> ,4 <i>S</i>	CH <sub>2</sub> F	1.20 ± 0.01	4.4 ± 0.4	3.7
<b>2h</b>	2 <i>R</i> ,4 <i>S</i>	CH <sub>2</sub> Cl	3.5 ± 0.1	122 ± 30	35
<b>2i</b>	2 <i>R</i> ,4 <i>R</i>	CH <sub>2</sub> N <sub>3</sub>	3.6 ± 0.2	38 ± 5	11
<b>2j</b>	2 <i>R</i> ,4 <i>R</i>	CH <sub>2</sub> NH <sub>2</sub>	21 ± 3	> 100	> 5
<b>2k</b>	2 <i>R</i> ,4 <i>R</i>	CH <sub>2</sub> OCH <sub>3</sub>	1.73 ± 0.01	3.3 ± 0.9	1.9

<sup>a</sup>Data taken from Refs [142,143].

Subsequently, the same research group put the attention on substitutions of the chlorine atom in the western region with other halogens and on the modification of the dioxolane ring in the central region [144]. In particular, replacement of the dioxolane ring with a ketone or an alcohol was taken into consideration. Molecules with the general structures **3**, **4**, and **5** were synthesized and their inhibitory potency towards HO-1 and HO-2 was calculated using rat spleen and brain microsomal fractions as sources of the two isozymes, respectively. Results obtained from the biological assays are reported in Table 4.

**Table 4.** General structures of imidazole-dioxolanes, imidazole-ketones and imidazole-alcohols and their HO IC<sub>50</sub> values.



Compd	R	X	IC <sub>50</sub> (μM) HO-1 <sup>a</sup>	IC <sub>50</sub> (μM) HO-2 <sup>a</sup>	SI (HO-2/HO-1)
<b>3a</b>	H	O	0.7 ± 0.4	> 100	> 143
<b>3b</b>	F	O	3.8 ± 1.1	> 100	> 26.3
<b>3c</b>	Cl	O	4.3 ± 2.1	> 100	> 23.2
<b>3d</b>	Br	O	1.9 ± 0.2	> 100	> 52.6
<b>3e</b>	I	O	3.7 ± 0.9	> 100	> 27
<b>3f</b>	Cl	S	4.7 ± 0.6	16 ± 4	3.4
<b>4a</b>	H	–	4.0 ± 1.8	11.3 ± 4.7	2.8
<b>4b</b>	F	–	2.7 ± 0.9	1.9 ± 0.2	1.4
<b>4c</b>	Cl	–	4.7 ± 0.5	43.1 ± 5.4	16.4
<b>4d</b>	Br	–	1.7 ± 0.7	9.5 ± 4.6	9.2
<b>4e</b>	I	–	0.11 ± 0.06	1.8 ± 0.7	5.6
<b>5a</b>	H	–	6.2 ± 0.8	16 ± 8.2	2.6
<b>5b</b>	F	–	1.4 ± 1.1	17.9 ± 11.8	12.8
<b>5c</b>	Cl	–	0.5 ± 0.1	4.0 ± 0.6	8
<b>5d</b>	Br	–	0.14 ± 0.06	2.6 ± 0.5	18.6
<b>5e</b>	I	–	0.06 ± 0.03	1.8 ± 1.5	30

<sup>a</sup>Data taken from Refs [143,144].

This study allowed to define some structure-activity relationships for Azalanstat derivatives. All dioxolane-imidazoles with general structure **3** displayed selectivity towards HO-1. Interestingly, substitution of the dioxolane ring with a dithiolane ring (compound **3f**) slightly reduced the HO-1 inhibitory potency of the compound whereas inhibition of HO-2 is restored. Removal of the dioxolane ring in favor of a ketone or an alcohol functional group was tolerated, and all compounds with general structures **4** and **5** showed remarkable HO-1 IC<sub>50</sub> values, although a lack of selectivity was highlighted. In addition, replacement of the

chlorine atom with bromine and iodine brought to a strong inhibition of HO-1, meaning that a bigger and less electronegative substituent in the *para* position of the phenyl ring in the western region gives better results when compared to fluorine or chlorine. These results paved the way for the potential discovery of novel inhibitors whose chemical structure could be simplified by removal of the chiral centers and substituents in the northeastern region. Moreover, the presence of an oxygen linked to position 2 in the central region seemed to be important for a better inhibition of the inducible isoenzyme and structural modifications in the western region could potentially be acceptable for the discovery of more potent and selective inhibitors.

With the aim to rationally design and define the structural features required for strong inhibition of HO-1, compounds **1n**, **3c**, and **6–8** (Figure 7) were chosen to perform co-crystallization studies [145-151].

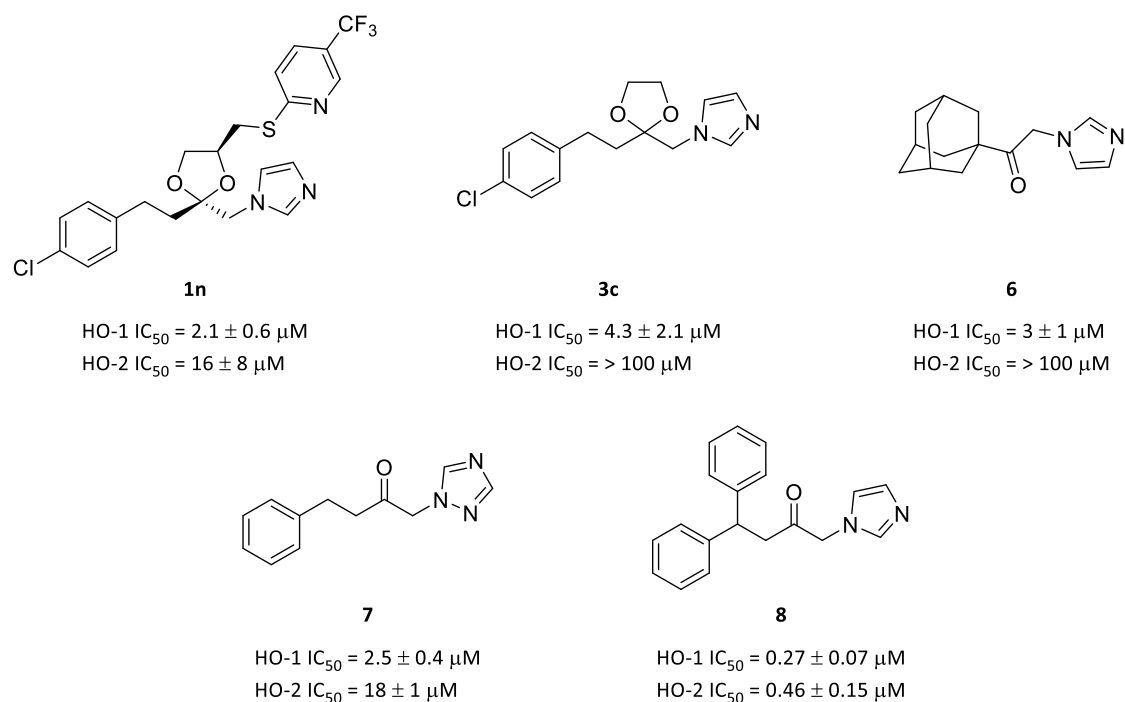


**Figure 7.** Chemical structures of HO inhibitors used for co-crystallization studies and their HO IC<sub>50</sub> values. Data taken from Refs [142,144,149,151,152].

Binding of the compounds to a truncated form of HO-1 spanning residues 1-233 showed that all compounds possess a common binding behavior (Figure 8).

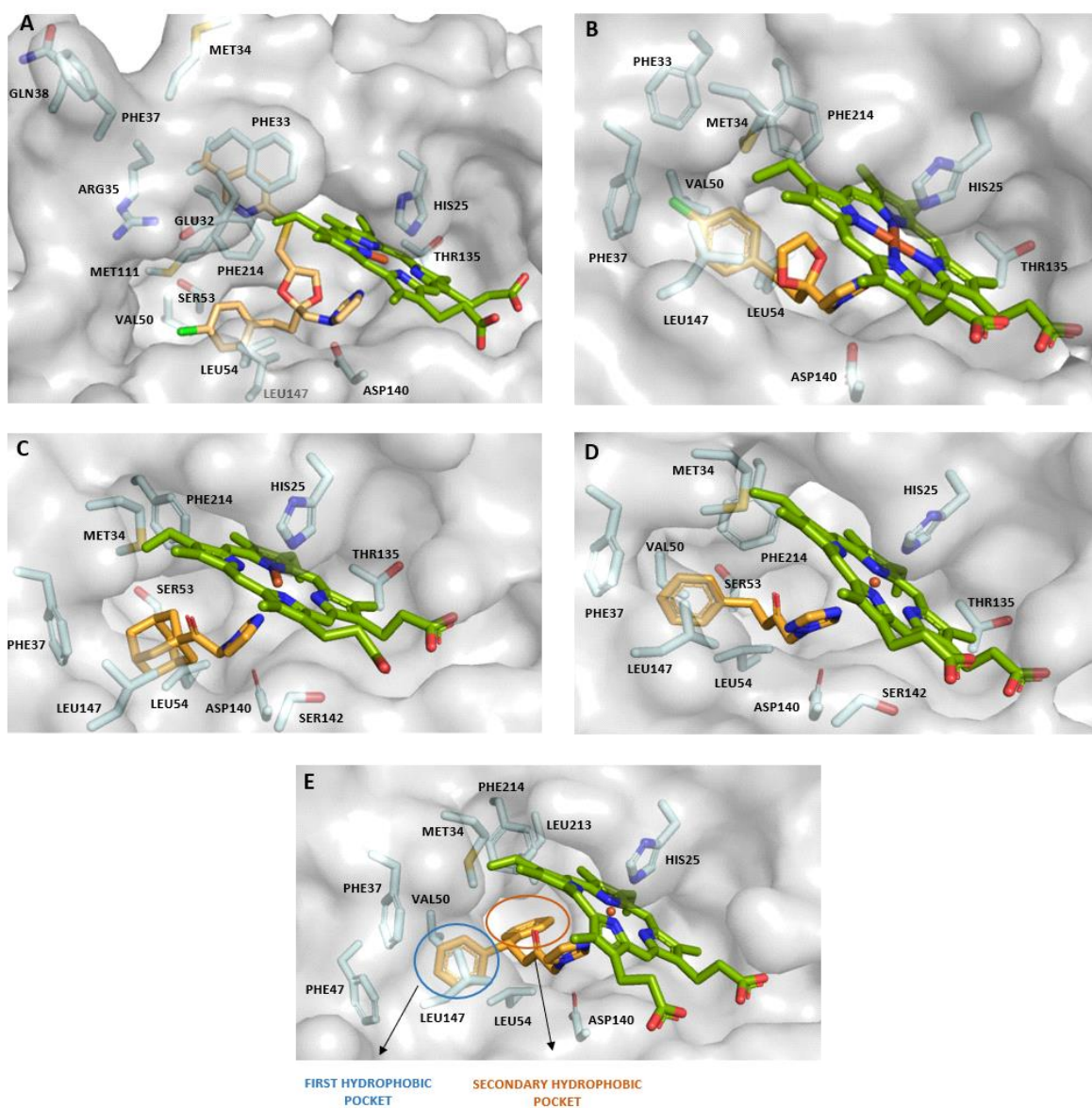


**Figure 8.** Docking of compounds **1n** (A, PDB ID #3HOK), **3c** (B, PDB ID #2DY5), **6** (C, PDB ID #3CZY), **7** (D, PDB ID #3K4F), and **8** (E, PDB ID #3TGM) in HO-1. Ligands are depicted as orange sticks, heme as green sticks, aminoacidic residues in cyan sticks.

Indeed, the *N*3 atom of the imidazole ring in the eastern region coordinates the iron atom in the heme ring replacing water as the sixth heme ligand. This coordination disrupts a well-ordered pattern of hydrogen bonds between water molecules inside the binding pocket and

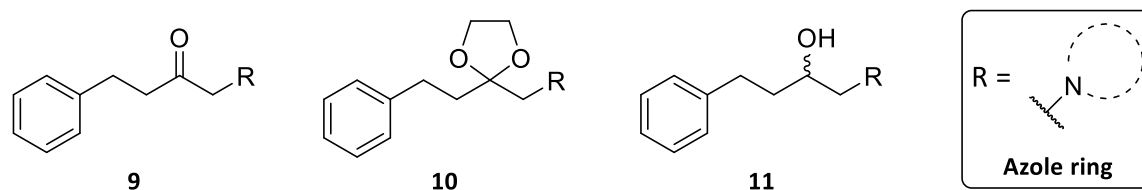
aminoacidic residues, including Asp140 and Thr135, and prevents heme oxidation at the  $\alpha$ -mesocarbon. Differently from metalloporphyrins, all the new compounds do not compete with heme in order to bind to the catalytic pocket. The proposed non-competitive mechanism of action could be particularly interesting in light of a further clinical development of these inhibitors; indeed, interference with other heme-proteins could be significantly reduced. Despite the different chemical structures, all compounds are able to dock inside the binding pocket thanks to the inherent flexibility of the distal helix of the enzyme. The western region of the molecule can be located in a corresponding hydrophobic area in which residues Phe33, Met34, Phe37, Phe47, Val50, Ser53, Leu54, and Leu147 can undertake hydrophobic interactions with lipophilic substituents. In addition, the presence of Met34 could explain the strong inhibitory potency of compounds possessing an halogen substituent in the phenyl ring of the western region. In compound **1n** (Figure 8A) the presence of substituents in the northeastern region of the molecule induces the formation of a proximal hydrophobic pocket able to locate the (4-trifluoropyridin-2-yl)methylthio moiety linked to the 4-position of the dioxolane ring. Residues Glu32, Met34, Arg35, Phe37 and Gln38 can play an important role in the definition of this hydrophobic pocket. Contrariwise, in compound **3c** (Figure 8B) the proximal hydrophobic pocket is not apparent, indeed, Met34 adopts a different conformation when compared to its spatial disposition in Figure 8A, thus prohibiting any interactions in this region of the binding pocket. The presence of bulky lipophilic moieties such as the adamantane group in compound **6** (Figure 8C) is also tolerated because of the wider conformation assumed by the binding pocket when such substituents are present. Looking at the docked poses of the compounds in Figure 8, it is also possible to highlight that in compound **3c** (Figure 8B) the 4-chlorophenyl ring digs deeper in the hydrophobic pocket when compared to adamantane moiety of compound **6** (Figure 8C). This observation could also rationalize the development of compounds in which the central linker could be



elongated in order to establish stronger hydrophobic interactions with this region of the enzyme. In the eastern region the presence of Ser142 and Gly143 could be exploited to establish an additional interaction with the imidazole ring: replacement of C5 of imidazole with a nitrogen atom, *i.e.* 1,2,4-triazole (compound **7**, Figure 8D) can be applied to enact an additional hydrogen bond with this aminoacidic residue with a consequent strengthened enzymatic inhibition. This assumption is further validated from results obtained with compound **7** and its imidazole derivative **4a** (Table 4) whose HO-1 IC<sub>50</sub> values are 2.5 vs 4.0 μM, respectively. The addition of a secondary phenyl ring in the western region helped in the discovery of a small, secondary hydrophobic pocket (Figure 8E) not appreciable in all the crystal structures discussed so far. This additional pocket can take strong hydrophobic interactions with proper molecular scaffolds in the western region, justifying the strong IC<sub>50</sub> values calculated for compound **8**.

Later on the attention was put on the azole ring of the western region [151]. Replacement of imidazole with 1*H*-pyrazole, 1*H*-1,2,3-triazole, 2*H*-1,2,3-triazole, 1*H*-benzo[*d*]imidazole, 1*H*-benzo[*d*][1,2,3]triazole and 2*H*-benzo[*d*][1,2,3]triazole afforded inactive compounds, whereas 1*H*-1,2,4-triazole, 1*H*-tetrazole and 2*H*-tetrazole rings brought to 1-azolyl-4-phenylbutanes with interesting inhibitory potencies. Furthermore, substituents in the azole moiety were not tolerated, with few exceptions represented by a single phenyl ring. The active compounds derived from this study are reported in Table 5.

**Table 5.** General structures and HO IC<sub>50</sub> values of 1-azolyl-4-phenylbutanes.

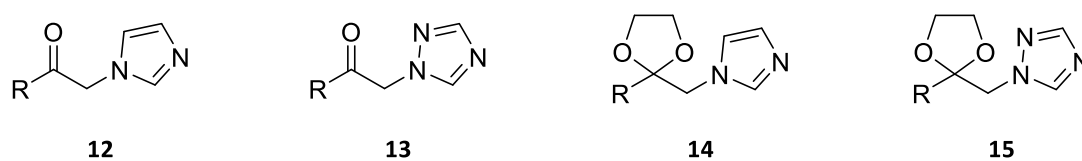


Compd	R	IC <sub>50</sub> (μM) HO-1 <sup>a</sup>	IC <sub>50</sub> (μM) HO-2 <sup>a</sup>	SI (HO-2/HO-1)
<b>9a</b>	1 <i>H</i> -tetrazole	2.6 ± 1	30 ± 4	11.5
<b>9b</b>	2 <i>H</i> -tetrazole	9.6 ± 0.2	> 100	> 10.5
<b>9c</b>	4,5-diphenylimidazole	40 ± 2	> 100	> 2.5
<b>9d</b>	4-phenylimidazole	32 ± 2	> 100	> 3.1
<b>9e</b>	5-bromoimidazole	22 ± 2	> 100	> 4.5
<b>9f</b>	5-methoxycarbonylimidazole	69 ± 19	> 100	> 1.4
<b>9g</b>	3-phenyl-1,2,4-triazole	9 ± 2	90 ± 33	> 10
<b>10a</b>	1,2,4-triazole	13 ± 2	> 100	> 7.6
<b>10b</b>	1 <i>H</i> -tetrazole	39 ± 5	> 100	> 2.6
<b>10c</b>	2 <i>H</i> -tetrazole	72 ± 1	> 100	> 1.4
<b>11a</b>	1,2,4-triazole	10.2 ± 0.2	54 ± 12	5.3
<b>11b</b>	1 <i>H</i> -tetrazole	56 ± 6	> 100	> 1.8
<b>11c</b>	4-phenylimidazole	15 ± 1	> 100	> 6.7

<sup>a</sup>Data taken from Ref [151].

After confirmation of the preference of imidazole or 1,2,4-triazole moieties in the eastern region, structural investigation on the central region led to a series of compounds having a shorter connecting chain [153]. The rationale of this research was based on the observation that also shorter chains, such as in compound **6**, can afford potent inhibitors. The new compounds were characterized by a common 1-aryl-2-(1*H*-azol-1-yl)ethanone chemical structure (**12**, **13**); in addition, some of their dioxolane derivatives (**14**, **15**) were also synthesized. Detailed information about the nature of the substituents and biological results are reported in Table 6.

**Table 6.** General structures and HO IC<sub>50</sub> values of ethanones and dioxolanes **12–15**.



Compd	R	IC <sub>50</sub> (μM) HO-1 <sup>a</sup>	IC <sub>50</sub> (μM) HO-2 <sup>a</sup>	SI (HO-2/HO-1)
<b>12a</b>	Ph	28 ± 3	> 100	> 3.6
<b>12b</b>	4-CH <sub>3</sub> Ph	17 ± 3	69 ± 11	4.1
<b>12c</b>	4-CH <sub>3</sub> OPh	39 ± 7	62 ± 3	1.6
<b>12d</b>	4-FPh	25 ± 4	> 100	> 4
<b>12e</b>	4-ClPh	4 ± 1	20 ± 6	5
<b>12f</b>	3-BrPh	2.06 ± 0.09	35 ± 2	17
<b>12g</b>	4-BrPh	3.2 ± 0.6	14 ± 1	4.4
<b>12h</b>	4-IPh	4.0 ± 0.6	25 ± 11	6.3
<b>12i</b>	4-O <sub>2</sub> NPh	2.5 ± 0.2	> 100	> 40
<b>12j</b>	4-(Ph)Ph	2.1 ± 0.5	3.0 ± 0.5	1.4
<b>12k</b>	4-(4'-BrPh)Ph	1.5 ± 0.3	0.43 ± 0.07	0.29
<b>12l</b>	4-(PhCH <sub>2</sub> )Ph	1.99 ± 0.04	2.3 ± 0.2	1.2
<b>12m</b>	4-(PhCH <sub>2</sub> CH <sub>2</sub> )Ph	4 ± 1	0.9 ± 0.1	0.2
<b>12n</b>	4-(PhCH <sub>2</sub> O)Ph	11 ± 2	> 100	> 9
<b>12o</b>	4-(cyclohexyl)Ph	5 ± 1	6 ± 2	1
<b>12p</b>	Naphtalen-1-yl	2.24 ± 0.07	10 ± 2	4.5
<b>12q</b>	Naphtalen-2-yl	1.9 ± 0.1	12.05 ± 0.04	6.3
<b>12r</b>	3,4-ClPh	1.24 ± 0.05	4.7 ± 0.5	3.8
<b>12s</b>	2,4-ClPh	2.2 ± 0.3	15 ± 1	6.8
<b>12t</b>	2,5-ClPh	6.6 ± 0.1	58 ± 7	8.8
<b>12u</b>	2,3,4-ClPh	2.103 ± 0.002	6 ± 1	3
<b>13a</b>	Ph	11.9 ± 0.7	> 100	> 8
<b>13b</b>	4-ClPh	2.2 ± 0.4	121.56 ± 0.08	55
<b>13c</b>	3-BrPh	1.8 ± 0.5	> 100	> 55
<b>13d</b>	4-BrPh	2.7 ± 0.4	50 ± 17	19
<b>13e</b>	4-O <sub>2</sub> NPh	19.2 ± 0.4	> 100	> 5
<b>13f</b>	4-(Ph)Ph	0.74 ± 0.04	7 ± 3	10
<b>13g</b>	4-(PhCH <sub>2</sub> )Ph	2.7 ± 0.4	7 ± 2	3
<b>13h</b>	Naphtalen-1-yl	0.79 ± 0.02	16 ± 4	20
<b>13i</b>	Naphtalen-2-yl	0.7 ± 0.1	42 ± 7	60
<b>13j</b>	3,4-ClPh	1.3 ± 0.3	> 100	> 77
<b>13k</b>	2,4-ClPh	4.1 ± 0.6	> 100	> 24
<b>13l</b>	2,5-ClPh	18.4 ± 0.3	> 100	> 5
<b>14a</b>	Ph	31 ± 2	> 100	> 3
<b>14b</b>	4-ClPh	19 ± 2	> 100	> 5
<b>14c</b>	3-BrPh	4 ± 0.5	> 100	> 25
<b>14d</b>	4-BrPh	12 ± 1	> 100	> 8
<b>14e</b>	4-(Ph)Ph	16.2 ± 0.3	> 100	> 6

<b>14f</b>	4-(PhCH <sub>2</sub> )Ph	4.98 ± 0.05	> 100	> 20
<b>14g</b>	Naphtalen-2-yl	2.63 ± 0.04	> 100	>38
<b>14h</b>	3,4-ClPh	8 ± 1	> 100	> 13
<b>14i</b>	2,4-ClPh	29 ± 10	> 100	> 3
<b>15a</b>	4-ClPh	68.7 ± 0.4	> 100	> 1.5
<b>15b</b>	4-BrPh	38 ± 5	> 100	> 3
<b>15c</b>	Naphtalen-2-yl	3.58 ± 0.06	> 100	> 28

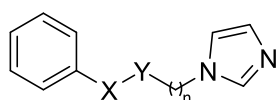
<sup>a</sup>Data taken from Ref [153].

In general, all compounds displayed potent HO-1 inhibition, however, the large majority of them still lacked isozyme selectivity. Among the best substitutions in the western region, halogens are better preferred as hypothesized in previous works. In addition, the aryl moiety can also be substituted by a biphenyl or naphthyl scaffold. Interestingly, ethanones possessed slightly reduced HO-1 inhibiting properties when compared to their respective derivatives with a four-membered central connecting chain (**12a** vs **4a**, **12d** vs **4b**, **12g** vs **4d**, **12h** vs **4e**). Triazole-ethanones with general structure **13** were slightly more potent than their respective imidazole counterparts and showed a better selectivity toward the inducible isoform. Although retaining selectivity, dioxolane-azole derivatives with general structures **14** and **15** were less potent inhibitors when compared to their respective ketone counterparts, showing an opposite trend seen for compounds with general structures **3** and **4** possessing a long chain in the central region. Finally, compound **12k** showed to be a better HO-2 inhibitor.

Further investigation of the structural modifications tolerated in the central region led to the design of  $\alpha$ -(1*H*-imidazol-1-yl)- $\omega$ -phenylalkanes (**16**, Table 7) [154]. In this class of compound different heteroatoms were introduced in central region and the length of the chain was shortened or elongated. Deletion of the central chain brought to inactive compounds. Elongation of the chain from 1 to 5 carbon atoms progressively increased the HO-1 inhibitory potency (compounds **16b–16e**), whereas inhibition of the constitutive isoform was seen only with a five-membered alkyl chain (compound **16e**). Insertion of

oxygen or sulfur in the alkyl chain led to compounds with an ether or thioether functional group. In the ether series, good results were obtained with an oxybutyric chain (compound **16i**), even though the compound did not display any degree of selectivity. Of note, insertion of sulfur gave better results when compared with the oxygen counterparts (**16j–m** vs **16f–i**); moreover inhibition of HO-2 was also observed. Insertion of nitrogen in the alkyl chain was not deeply investigated; only one compound was synthesized but was inactive toward both isozymes.

**Table 7.** General structure and HO IC<sub>50</sub> values of  $\alpha$ -(1*H*-imidazol-1-yl)- $\omega$ -phenylalkanes.



**16**

Compd	X	Y	n	IC <sub>50</sub> (μM) HO-1 <sup>a</sup>	IC <sub>50</sub> (μM) HO-2 <sup>a</sup>	SI (HO-2/HO-1)
<b>16a</b>	CH <sub>2</sub>	–	0	44 ± 6	> 100	> 2.3
<b>16b</b>	CH <sub>2</sub>	CH <sub>2</sub>	0	72 ± 8	> 100	> 1.4
<b>16c</b>	CH <sub>2</sub>	CH <sub>2</sub>	1	14 ± 3	> 100	> 7.1
<b>16d</b>	CH <sub>2</sub>	CH <sub>2</sub>	2	3.5 ± 0.7	> 100	> 28.6
<b>16e</b>	CH <sub>2</sub>	CH <sub>2</sub>	3	2.8 ± 0.3	20 ± 11	7.1
<b>16f</b>	O	CH <sub>2</sub>	1	61 ± 20	> 100	> 2.4
<b>16g</b>	O	CH <sub>2</sub>	2	42 ± 9	> 100	> 10
<b>16h</b>	CH <sub>2</sub>	O	2	32 ± 1	> 100	> 3.1
<b>16i</b>	O	CH <sub>2</sub>	3	4 ± 1	4.6 ± 0.4	1.2
<b>16j</b>	S	CH <sub>2</sub>	1	6.0 ± 0.1	> 100	> 16.7
<b>16k</b>	S	CH <sub>2</sub>	2	2.4 ± 0.1	16 ± 2	6.7
<b>16l</b>	CH <sub>2</sub>	S	2	4.4 ± 0.7	> 100	> 22.7
<b>16m</b>	S	CH <sub>2</sub>	3	1.2 ± 0.1	5 ± 2	4.2

<sup>a</sup>Data taken from Ref [154].

Pushed by these results, our research group set up a research line focused on the discovery of novel HO-1 inhibitors starting from an in store library of NOS inhibitors [155].

These compounds possessed the same structural features required for HO inhibition. The HO-1 inhibiting properties of six compounds (Figure 9) inactive on NOS were evaluated using an enzymatic assay that differed from the one used in the past by other research groups. In fact, the former evaluates HO inhibition through the spectroscopical quantification of the amount of bilirubin produced in presence of the inhibitor, whereas the latter used an assay in which the inhibition was evaluated by the amount of CO generated in presence of the small molecule. The biological studies confirmed the previous SAR previously discussed. Unsurprisingly, the  $IC_{50}$  value obtained for compound **18** (**16f** in Table 7) was different from the value reported by Vlahakis and co-workers. This difference could be ascribable to the different experimental assay used for the determination of HO inhibition.

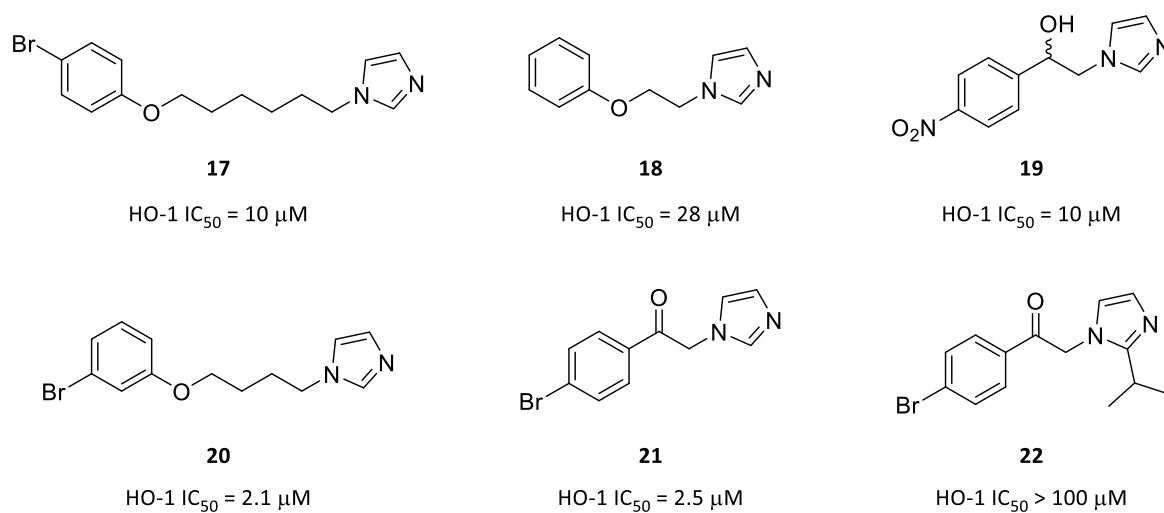
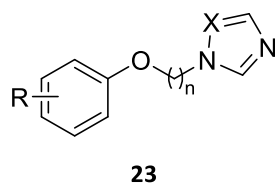


**Figure 9.** Chemical structures and HO-1  $IC_{50}$  values of compounds **17–22** derived from a library of NOS inhibitors.

Further studies were carried out in order to discover more potent HO-1 [156]. Compound **20** was chosen as the lead compound for the design of novel HO inhibitors possessing an aryloxyalkyl-imidazole or aryloxyalkyl-triazole chemical structure (Table 8)

[157,158]. The main structural modifications regarded the length of the alkyloxy chain, the nature of the substituents in the phenyl ring and theazole moiety present in the eastern region. Results showed that an oxybutyl chain is preferred over the oxypropyl chain and imidazole derivatives are better inhibitors than triazole derivatives for HO-1 best inhibition. The most potent compound of the series was compound **23n**, bearing an iodine atom in the *para* position of the phenyl ring. Compounds bearing an oxohexyl chain were devoid of activity towards both HO-1 and HO-2. Surprisingly, compounds with an oxopentyl chain were potent HO-2 inhibitors (**23r**, **23s**, **23u**) with IC<sub>50</sub> values below 1 μM.

**Table 8.** General structure of aryloxyalkyl-azole derivatives and their HO IC<sub>50</sub> values.



Compd	R	X	n	IC <sub>50</sub> (μM) HO-1 <sup>a</sup>	IC <sub>50</sub> (μM) HO-2 <sup>a</sup>
<b>23a</b>	H	CH	3	31 ± 2	> 100
<b>23b</b>	H	N	3	> 100	> 100
<b>23c</b>	H	CH	4	21 ± 1	30 ± 1
<b>23d</b>	H	N	4	92 ± 5	27 ± 2
<b>23e</b>	4-NO <sub>2</sub>	CH	3	> 100	44.7 ± 4.1
<b>23f</b>	4-NO <sub>2</sub>	N	3	> 100	77.6 ± 5.2
<b>23g</b>	4-NO <sub>2</sub>	CH	4	56 ± 2	21 ± 1
<b>23h</b>	4-NO <sub>2</sub>	N	4	> 100	41.7 ± 3.3
<b>23i</b>	3-Br	CH	3	69 ± 3	> 100
<b>23j</b>	3-Br	N	3	> 100	33.9 ± 2.5
<b>23k</b>	3-Br	N	4	> 100	11.2 ± 0.9
<b>23l</b>	4-I	CH	3	> 100	36.3 ± 2.8
<b>23m</b>	4-I	N	3	75 ± 5	90 ± 4
<b>23n</b>	4-I	CH	4	1 ± 0.01	10 ± 0.5
<b>23o</b>	4-I	N	4	38 ± 1	70 ± 3
<b>23p</b>	2-Br	CH	4	53 ± 3	24 ± 3

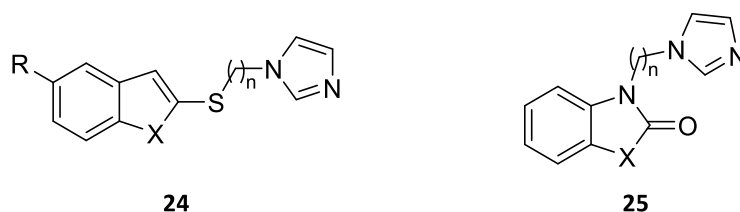
<b>23q</b>	4-Br	CH	4	31 ± 1	75 ± 4
<b>23r</b>	3-Br	CH	5	42.6 ± 1.2	0.9 ± 0.01
<b>23s</b>	3-Br	N	5	20 ± 1	0.8 ± 0.01
<b>23t</b>	3-Br	CH	6	34 ± 3	41 ± 3
<b>23u</b>	4-I	CH	5	44 ± 2	0.9 ± 0.02
<b>23v</b>	4-I	CH	6	42 ± 1	> 100

<sup>a</sup>Data taken from Refs [157,158].

Compounds **20** and **23n** were selected to investigate potential of their *in vitro* antitumor properties in an imatinib resistant human chronic myeloid leukemia (LAMA-84) cell line. The two HO-1 inhibitors were active not only in cell lysates, but also in intact cells. In addition, they both reduced the expression of HO-1 mRNA while they did not interfere with the expression of HO-2 mRNA. Finally, both compounds did not display a significant antitumoral effect when administered alone, whereas in combination with imatinib they were able to revert the resistance of LAMA-84 cells to the tyrosine kinase inhibitor causing an increase of intracellular ROS and triggering apoptosis.

Considering that the western region possesses a high flexibility, it can be assumed that hydrophobic scaffolds different from a phenyl ring can be accommodated in this area of the binding pocket. This hypothesis was examined through the design of heterocyclic bicyclic alkyl-imidazole derivatives with general structures **24** and **25** (Table 9) [158].

**Table 9.** General structures of heterocyclic bicyclic alkyl-imidazole derivatives **24** and **25** and their HO IC<sub>50</sub> values.





Compd	R	X	n	IC <sub>50</sub> (μM) HO-1 <sup>a</sup>	IC <sub>50</sub> (μM) HO-2 <sup>a</sup>
<b>24a</b>	H	O	3	16.9 ± 2.1	49 ± 4
<b>24b</b>	H	O	4	30.9 ± 1.3	74.1 ± 5.1
<b>24c</b>	H	S	3	0.9 ± 0.01	12.5 ± 1.5
<b>24d</b>	H	S	4	1 ± 0.02	0.8 ± 0.01
<b>24e</b>	H	S	5	39.8 ± 3.1	11.2 ± 2.1
<b>24f</b>	Cl	S	3	18.4 ± 1.5	0.9 ± 0.02
<b>24g</b>	Cl	S	4	> 100	0.9 ± 0.01
<b>24h</b>	Cl	S	5	36.3 ± 2.3	0.9 ± 0.02
<b>25a</b>	–	O	4	17.7 ± 1.2	35.5 ± 1.3
<b>25b</b>	–	S	3	16.6 ± 1.1	28.8 ± 3.1

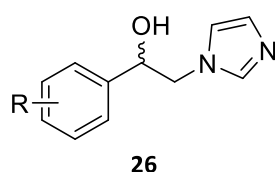
<sup>a</sup>Data taken from Ref [158].

Benzothiazoles **24c–g** gave the most interesting results among the two new series of compounds. Specifically, compound **24c** was slightly more potent in inhibiting HO-1 while elongation of its central region of a methylene unit brought to compound **24d** which did not discriminate in inhibiting both HO-1 and HO-2. Insertion of a chlorine atom in the benzothiazole nucleus lowered or erased any HO-1 inhibition in favor of the constitutive isozyme. Excitingly, compound **24g** was selective over HO-2 and still represents the most potent and selective HO-2 inhibitor discovered so far. Elongation of the chain of compound **24g** (compound **24h**) somehow restored HO-1 inhibition, although the molecule behaved as a better HO-2 inhibitor, confirming that a five-membered chain brings to better HO-2 IC<sub>50</sub> values. Cytotoxicity of compounds **20**, **23n**, **23u**, **24c** and **24d** was evaluated on hormone therapy resistant and sensitive breast (MDA-MB-231, MCF7) and prostate (PC3, DU-145, LnCaP) cancer cell lines. Despite being a potent HO-2 inhibitor, the best results were obtained with compound **23u** in all the investigated cell lines; compound **20** displayed antiproliferative properties on the MDA-MB-231 cell line, compound **23n** was particularly effective in inhibiting LnCap cancer cell proliferation.

In 2017 a free database gathering all the HO inhibitors published or patented till that year was created [159]. At the same time, a 3D-quantitative structure–activity relationship (3D-QSAR) model was also created with the aim of virtually find novel potential inhibitors. An in-depth analysis of the database highlighted that only four compounds are selective HO-1 inhibitors and the strongest HO-1 inhibitors are characterized by the presence of an alcoholic function in the central region. For this reason, an novel series of 1*H*-imidazol-1-yl-phenylethanol derivatives was designed and compounds synthesized (Table 10) [160].

Compounds **26a**, **26b**, **26f**, **26h** and **26j** displayed strong inhibitory potency over HO-1 with IC<sub>50</sub> values below 1 μM, with the 3-bromophenyl derivative **26a** being the most potent of the series. Replacement of the 3-bromo substituent with a bulkier phenyl group in the same position brought to the potent and selective HO-1 inhibitor **26b**. Of note, insertion of a second phenyl ring in the 4-position of the first aromatic ring decreased the activity (compounds **26d**, and **26e**), the same trend was observed when a methylene unit was inserted as a spacer (compound **26g**) between the two rings. Separation of the two aromatic moieties by an ether linkage restored the activity for both enzymatic isoforms (compound **26f**). Elongation of the spacer between the two rings was also tolerated, leading to benzyloxy and 4-bromobenzyloxy compounds **26h** and **26j**, with the latter being also a selective HO-1 inhibitor. Finally, replacement of bromine in compound **26j** with a bulkier iodine (compound **26k**) lowered the activity, demonstrating again that bulky hydrophobic substituents are tolerated in the western region within certain limits.

**Table 10.** General structure of 1*H*-imidazol-1-yl-phenylethanols and their HO IC<sub>50</sub> values.



Compd	R	IC <sub>50</sub> (μM) HO-1 <sup>a</sup>	IC <sub>50</sub> (μM) HO-2 <sup>a</sup>	SI (HO-2/HO-1)
<b>26a</b>	3-Br	0.40 ± 0.01	32 ± 2.2	80
<b>26b</b>	3-Ph	0.90 ± 0.08	> 100	> 111
<b>26c</b>	4-I	14.80 ± 0.8	ND <sup>b</sup>	–
<b>26d</b>	4-Ph	11.70 ± 0.3	ND <sup>b</sup>	–
<b>26e</b>	4-(4'-ClPh)	26.90 ± 0.8	ND <sup>b</sup>	–
<b>26f</b>	4-PhO	0.90 ± 0.1	10.50 ± 0.2	11.6
<b>26g</b>	4-PhCH <sub>2</sub>	26.90 ± 1.1	ND <sup>b</sup>	–
<b>26h</b>	4-PhCH <sub>2</sub> O	0.50 ± 0.01	11.70 ± 0.9	23.4
<b>26i</b>	4-(4-ClPh)CH <sub>2</sub> O	13.10 ± 0.9	ND <sup>b</sup>	–
<b>26j</b>	4-(4-BrPh)CH <sub>2</sub> O	0.95 ± 0.02	> 100	> 105
<b>26k</b>	4-(4-IPh)CH <sub>2</sub> O	24.50 ± 0.4	ND <sup>b</sup>	–

<sup>a</sup>Data taken from Ref [160].

<sup>b</sup>ND = Not determined

All compounds belonging to the ethanolic series just discussed were tested as racemates. Chromatographic resolution of the most selective compounds **26b** and **26j**, *in silico* absolute stereochemistry assignment and subsequent enzymatic assays emphasized a strong preference of the *R*-enantiomers over the *S*-enantiomers for HO-1 inhibition, with IC<sub>50</sub> values of 0.80 ± 0.07 μM for (*R*)-**26b** and 1.10 ± 0.05 μM for (*R*)-**26j** [161]. Molecular modeling studies explained this preferential enantiomeric inhibition through the presence of a consensus water molecule in the HO-1 binding pocket which establishes a hydrogen bond with Thr135. The spatial orientation of the alcoholic function in the *R*-enantiomers allows the molecules to establish an additional hydrogen bond with the consensus water molecule with a consequent better binding in the catalytic pocket.

Compound **26a** was selected for cytotoxicity studies [162]. Among the chosen cancer cell lines (MDA-MB-231, MCF-7, PC3, DU-145, LnCap and B16), moderate cytotoxic activity was detected for MCF-7 and the murine melanoma B16 cell line. Treatment of B16 cells with co-administration of doxorubicin and **26a** produced a synergic cytotoxic effect,

demonstrating that combination of an HO-1 inhibitor and a common anticancer drug can represent an additional weapon in the establishment of novel anticancer therapies.

Compounds **6**, **8**, and **26a** were chosen for further structural modifications aimed at expanding the SARs of HO-1 (Figure 10). In particular, the ketone function of compound **6** was reduced to obtain alcohol **27**, compound **8** was modified in the central region by insertion of an amide function (compound **28**) and compound **26a** was benzylated in order to check if this substitution could give a better enzymatic inhibition from interaction with the secondary hydrophobic pocket of HO-1 (compound **29**) [162].

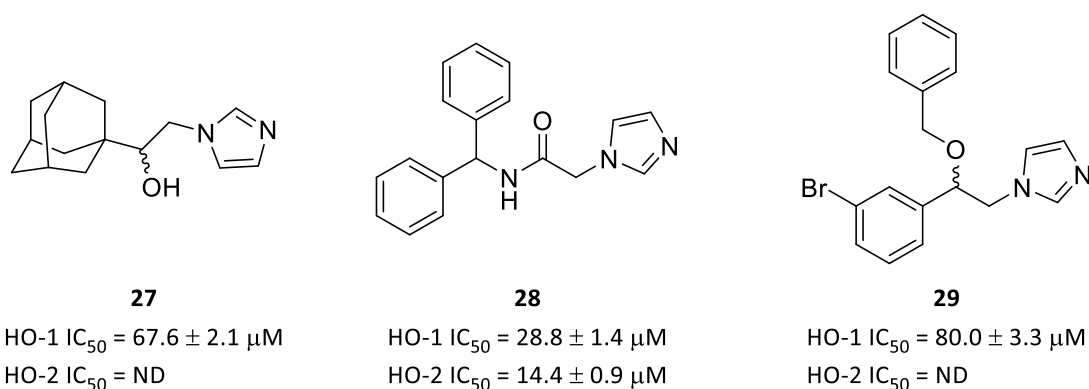


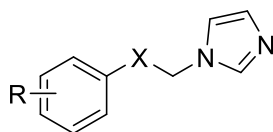
**Figure 10.** Chemical structures and HO IC<sub>50</sub> values of compounds **27–29**.

Results obtained were not promising, indeed, poor IC<sub>50</sub> values were detected for compounds **27** and **29**. Intriguingly compound **28**, the first and only HO inhibitor possessing an amide function in the central connecting chain, was moderately potent towards both HO-1 and HO-2, with a slight preference for the latter.

Overall, results obtained with compounds with general structure **26** seemed to suggest that the ethanolic linker plays a pivotal role in determining strong HO-1 inhibition and HO-1 selectivity. With the aim to further optimize the inhibitory potency of these compounds, a new series of derivatives (general structure **30**, Table 11) was designed and compounds synthesized and subjected to biological studies [163]. Considering that the central region can

also contain a simple non-functionalized alkyl linker or a ketone functional group, some derivatives possessing these chemical features were also tested. In general, results confirmed the importance of the alcoholic function for proper binding to the catalytic pocket of the enzyme, indeed ethylenes **30a–c** and ethanones **30d–f** did not display optimal potency. Subsequently, the attention was focused on the HO-1 selective compound **26j**. The 4-bromobenzyloxy moiety was moved from the *para* to the *ortho* (compound **30h**) and *meta* positions (compounds **30g**, and **30k,l**) in order to evaluate the importance of the spatial disposition of this substituent for optimal binding. In addition, the bromine substituent was also shifted in the *ortho* (compounds **30j** and **30l**) or *meta* (compounds **30i** and **30k**) position of the second phenyl ring for the abovementioned purposes. Results showed that only compounds **30g** and **30j** had inhibitory potency values under 10  $\mu\text{M}$ , with the 3-substituted-4-bromobenzyloxy derivative **30g** being the most potent (HO-1  $\text{IC}_{50} = 0.90 \pm 0.02$ ) and moderately selective. These two derivatives were also tested *in vitro* in MCF-7 and MDA-MB-231 breast cancer cell lines, with compound **30g** displaying a moderate cytotoxic activity in MCF-7 cells.

**Table 11.** HO  $\text{IC}_{50}$  values of compounds with general structure **30**.



**30**

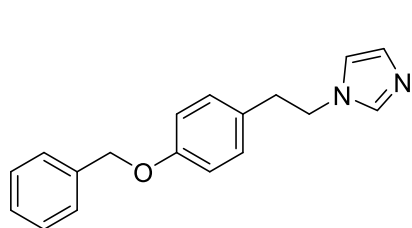
Compd	R	X	$\text{IC}_{50}$ ( $\mu\text{M}$ ) HO-1 <sup>a</sup>	$\text{IC}_{50}$ ( $\mu\text{M}$ ) HO-2 <sup>a</sup>
<b>30a</b>	3-Br	$\text{CH}_2$	$100 \pm 5.60$	ND <sup>b</sup>
<b>30b</b>	4-(4-BrPh) $\text{CH}_2\text{O}$	$\text{CH}_2$	$62.87 \pm 3.20$	ND <sup>b</sup>
<b>30c</b>	3-Ph	$\text{CH}_2$	$46.77 \pm 1.80$	ND <sup>b</sup>
<b>30d</b>	3-Br	CO	$38.17 \pm 1.80$	ND <sup>b</sup>
<b>30e</b>	3-Ph	CO	$19.87 \pm 2.50$	ND <sup>b</sup>

<b>30f</b>	4-(4-BrPh)CH <sub>2</sub> O	CO	55.46 ± 0.05	ND <sup>b</sup>
<b>30g</b>	3-(4-BrPh)CH <sub>2</sub> O	CHOH	0.90 ± 0.02	53.59 ± 1.20
<b>30h</b>	2-(4-BrPh)CH <sub>2</sub> O	CHOH	> 100	ND <sup>b</sup>
<b>30i</b>	4-(3-BrPh)CH <sub>2</sub> O	CHOH	41 ± 1.50	ND <sup>b</sup>
<b>30j</b>	4-(2-BrPh)CH <sub>2</sub> O	CHOH	9.0 ± 2.20	15.85 ± 1.60
<b>30k</b>	3-(3-BrPh)CH <sub>2</sub> O	CHOH	46 ± 1.90	ND <sup>b</sup>
<b>30l</b>	3-(2-BrPh)CH <sub>2</sub> O	CHOH	44 ± 1.80	ND <sup>b</sup>

<sup>a</sup>Data taken from Ref [163].

<sup>b</sup>ND = Not determined

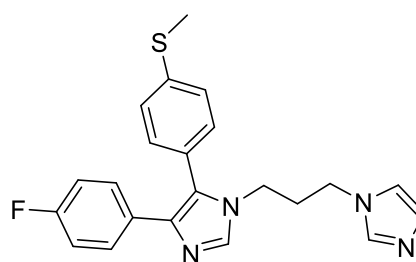
Recently, several computational tools have been exploited to speed up the identification of novel HO-1 inhibitors [164]. Coupling of 3D-QSAR models with a scaffold-hopping analysis approach was successful in the validation of the predictivity of the 3D-QSAR model and led to the identification of a small molecule (compound **31**, Figure 11) whose HO-1 inhibitory potency reached a value of 0.9 μM [165].



**31**

HO-1 IC<sub>50</sub> = 0.9 ± 0.07 μM

HO-2 IC<sub>50</sub> = ND



**32**

HO-1 IC<sub>50</sub> = 2.23 ± 0.35 μM

HO-2 IC<sub>50</sub> = 1.07 μM

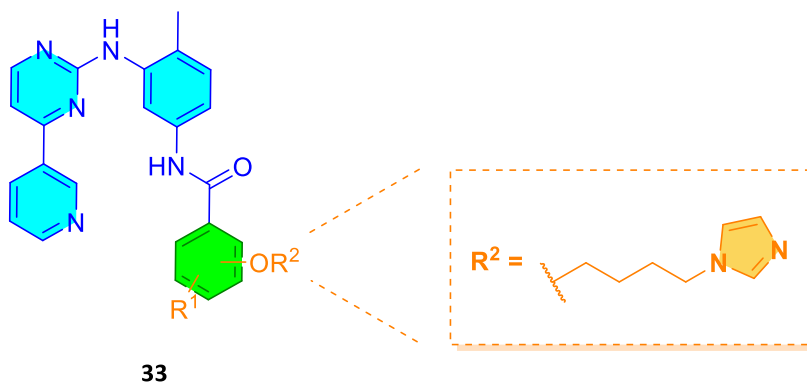
**Figure 11.** Chemical structures and HO IC<sub>50</sub> values of compounds **31** and **32**.

Likewise, a virtual high throughput screening identified a prototype molecule whose chemical optimization led to compound **32** [166]. Interestingly, this molecule possesses in the central region a second imidazole nucleus to which are linked two hydrophobic moieties that take interactions with the western region and the secondary hydrophobic pocket of the enzyme. However, this different chemical structure did not allow to selectively discriminate

between the two isozymes. Of note, compound **32** did not induce HO-1 and HO-2 mRNA overexpression and displayed a good pharmacokinetic profile. Finally, antiproliferative activity was observed in prostate (DU-145) and pancreatic (PANC-1) cancer cell lines, also when administered in combination with doxorubicin and gemcitabine to DU-145 and PANC-1 cancer cell lines, respectively.

The potential utilization of HO-1 inhibitors for restoring the cytotoxicity of anticancer drugs in resistant cancer cell lines has been further investigated through the design of molecular hybrids and prodrugs. As discussed in Paragraph 1.5, HO-1 overexpression is often linked to the raise of chemoresistance. The use of molecular hybrids that contain at the same time the chemical features required for HO-1 inhibition and a molecular portion able to interact with targets of common anticancer drugs could be an useful approach for improving antiproliferative activity and reducing unwanted side effects. Recently, a new series of imatinib/HO-1 inhibitor hybrids were synthesized and tested in sensitive (K562S) and resistant (K562R) CML cancer cell lines. These molecules contain an “imatinib-like” portion which was merged with an aryloxybutylimidazole structure chosen on the basis of the optimal results obtained with compounds **20** and **23n** [167]. The most potent compounds in terms of HO-1 inhibition are reported in Table 11.

**Table 11.** General structure of imatinib/HO-1 hybrids and their HO-1 IC<sub>50</sub> values. The imatinib-like portion is represented in blue color, the HO-1 inhibitor portion in light orange color, the merged portion of the two pharmacophores in green color.



Compd	R <sup>1</sup>	OR <sup>2</sup> position	IC <sub>50</sub> (μM) HO-1 <sup>a</sup>
<b>33a</b>	4-Br	2	0.95 ± 0.01
<b>33b</b>	5-CH <sub>3</sub>	2	0.95 ± 0.02
<b>33c</b>	3-Br	4	0.92 ± 0.01

<sup>a</sup>Data taken from Ref [167].

Among all the synthesized compounds, the best results were obtained when the oxybutylimidazole chain was linked to the 2- or 4-position of the aromatic ring. Molecular modeling studies highlighted the binding mode of the novel derivatives in HO-1 and confirmed the interaction between the nitrogen atom of imidazole and heme iron. The novel hybrids were also able to inhibit the BCR-ABL protein, which represent the target of the tyrosine kinase inhibitor imatinib. *In vitro* biological studies showed that compounds **33a–c** did not induce HO-1 overexpression and reduced cell proliferation than imatinib itself. Therefore, the design of HO-1 inhibitor molecular hybrids represents a valid strategy for novel anticancer therapies.

Very recently, a 5-fluorouracil-HO-1 inhibitor mutual prodrug has been reported [168]. In the novel compound **34** (Figure 13) 5-fluorouracil (5-FU) is linked to the alcoholic function of compound **26a** through a succinic linker. Chemical stability was evaluated *in vitro* at acidic, neutral and alkaline pH. Results showed that the compound is hydrolyzed at alkaline



pH and was stable in an acidic environment. In addition, compound **34** reduced viability of DU-145 prostate cancer cells and A549 lung cancer cells with results comparable to those observed with singular treatment with 5-FU. Finally, compound **34** was non-toxic to the non-tumorigenic BEAS-2B cell line and displayed an optimal drug-like profile evaluated *in silico*.

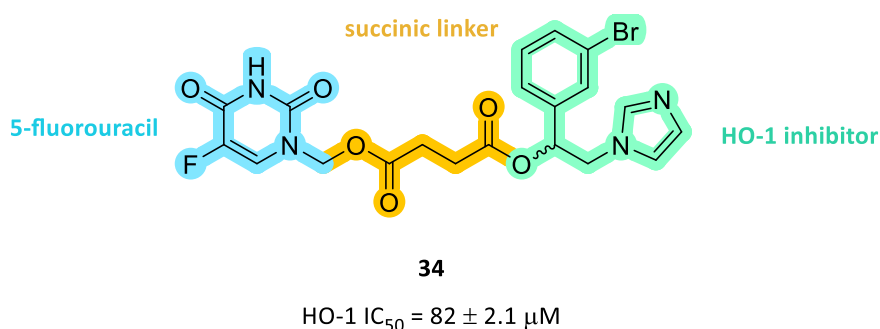
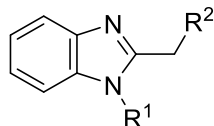


**Figure 13.** Chemical structure and HO-1 inhibitory potency of 5-FU/HO-1 mutual prodrug **34**.

As far as concerns HO-2, only two papers reported a small number of selective inhibitors starting from 2013 [169,170]. Unexpectedly, these compounds did not follow the SARs described so far. Their general structure is based on clemizole, a benzimidazole compound identified as HO-2 selective inhibitor after screening of a library of compounds [169]. The main structural modifications explored regarded the substituent linked at the *N1* atom of the benzimidazole core and the cyclic moiety linked to position 2 through a methylene bridge (Table 12).

**Table 12.** General structure of HO-2 selective clemizole derivatives and their HO IC<sub>50</sub> values.



**35**

Compd	R <sup>1</sup>	R <sup>2</sup>	IC <sub>50</sub> (μM) HO-1 <sup>a</sup>	IC <sub>50</sub> (μM) HO-2 <sup>a</sup>
<b>Clemizole</b>	4-Cl-PhCH <sub>2</sub>	Pyrrolidin-1-yl	> 100	3.4 ± 0.3
<b>35a</b>	4-F-PhCH <sub>2</sub>	Pyrrolidin-1-yl	> 100	2.0 ± 0.2
<b>35b</b>	4-Br-PhCH <sub>2</sub>	Pyrrolidin-1-yl	> 100	2.6 ± 0.4
<b>35c</b>	4-I-PhCH <sub>2</sub>	Pyrrolidin-1-yl	> 100	7.6 ± 0.6
<b>35d</b>	4-Me-PhCH <sub>2</sub>	Pyrrolidin-1-yl	> 100	5 ± 1
<b>35e</b>	3-Cl-PhCH <sub>2</sub>	Pyrrolidin-1-yl	> 100	1.65 ± 0.08
<b>35f</b>	3-Br-PhCH <sub>2</sub>	Pyrrolidin-1-yl	> 100	1.5 ± 0.3
<b>35g</b>	3-Me-PhCH <sub>2</sub>	Pyrrolidin-1-yl	> 100	5 ± 1
<b>35h</b>	3-NO <sub>2</sub> -PhCH <sub>2</sub>	Pyrrolidin-1-yl	> 100	1.3 ± 0.2
<b>35i</b>	2-Cl-PhCH <sub>2</sub>	Pyrrolidin-1-yl	> 100	4.8 ± 0.4
<b>35j</b>	2-CN-PhCH <sub>2</sub>	Pyrrolidin-1-yl	> 100	4 ± 1
<b>35k</b>	2-NO <sub>2</sub> -PhCH <sub>2</sub>	Pyrrolidin-1-yl	> 100	3.5 ± 0.6
<b>35l</b>	2,6-diCl-PhCH <sub>2</sub>	Pyrrolidin-1-yl	> 100	9.2 ± 0.2
<b>35m</b>	3,5-diCl-PhCH <sub>2</sub>	Pyrrolidin-1-yl	> 100	2.1 ± 0.3
<b>35n</b>	PhCH <sub>2</sub>	Pyrrolidin-1-yl	> 100	3.1 ± 0.7
<b>35o</b>	PhCH <sub>2</sub> CH <sub>2</sub>	Pyrrolidin-1-yl	> 100	2.7 ± 0.2
<b>35p</b>	(Ph) <sub>2</sub> CH	Pyrrolidin-1-yl	> 100	4.1 ± 0.1
<b>35q</b>	(Naphthalene-2-yl)-CH <sub>2</sub>	Pyrrolidin-1-yl	> 100	5 ± 2
<b>35r</b>	Cyclohexyl-CH <sub>2</sub>	Pyrrolidin-1-yl	> 100	6 ± 1
<b>35s</b>	PhCH <sub>2</sub>	Norborn-2-yl	> 100	6.3 ± 1.3
<b>35t</b>	4-Cl-PhCH <sub>2</sub>	Norborn-2-yl	> 100	4.3 ± 0.1
<b>35u</b>	4-Br-PhCH <sub>2</sub>	Norborn-2-yl	> 100	5.1 ± 0.2
<b>35v</b>	4-Cl-PhCH <sub>2</sub>	Cyclohexyl	> 100	5.4 ± 0.5
<b>35w</b>	4-Br-PhCH <sub>2</sub>	Cyclohexyl	> 100	5.4 ± 0.7

<sup>a</sup>Data taken from Refs [169,170].

SARs were built for this class of compounds. In general, benzyl, phenethyl, benzhydryl, naphthyl and cyclohexyl rings are tolerated in position 1 of the benzimidazole rings. Benzyl

substituents can be further substituted with halogens, nitro, methyl, and cyano substituents. The methylene group in position 2 of the benzimidazole scaffold can be substituted with norborn-2-yl, cyclohexyl and pyrrolidin-1-yl moieties, with a strong preference for the latter (compounds **35a–r** vs **35s–w**). However, none of these compounds reached an IC<sub>50</sub> value stronger than the one reported for compound **24g** (Table 9). In general, the identification of selective HO-2 inhibitors could pave the way for a better understanding of the physiological role of this isoform and its potential targeting for the treatment of certain pathologies, as reviewed in [171].

To sum up, most of the HO-1 and HO-2 inhibitors discovered so far derives from the chemical structure of Azalanstat, the first HO inhibitor ever reported in literature. An iterative chemical modification of the different regions of its structure led to the design of several classes of compounds that allowed to build up the following SARs (Figure 14):

1. The presence of substituents in the northeastern region is not mandatory for proper inhibition of the enzymatic activity. Structural modifications in this can increase the inhibitory potency of the compounds although no gaining in isoform selectivity is generally observed;
2. An unsubstituted azole ring (imidazole or *1H*-1,2,4-triazole) in the eastern region is mandatory for the activity. Its presence is required for the non-competitive mechanism of action of the inhibitors, indeed, the *N* atom not linked to the central region of the molecule coordinates the ferrous iron in the heme ring blocking its oxidation at the  $\alpha$ -mesocarbon;
3. The central region is required to tether the azole nucleus and the lipophilic substituent in the western region helping in defining additional and fruitful interactions in the binding pocket. Structural modifications in this region can be performed to tune the inhibitory potency of the compounds. In particular, ethanolic spacers allow the

selective inhibition of the inducible HO isoform; a ketone, a dioxolane ring, heteroatoms such oxygen or sulfur or a simple alkyl chain not longer than four atoms are tolerated. Longer connecting chain shift the activity towards the constitutive isoform;

- Due to the higher flexibility of the distal chain of HO, the western region can be highly modified with bulky and lipophilic substituents, such as aryl rings substituted with halogens or benzyloxy moieties. Modifications in this region are responsible for better HO-1 inhibition and isozyme selectivity. Insertion of additional lipophilic substituents can also allow the interaction with a secondary hydrophobic pocket through additional hydrophobic bonds.

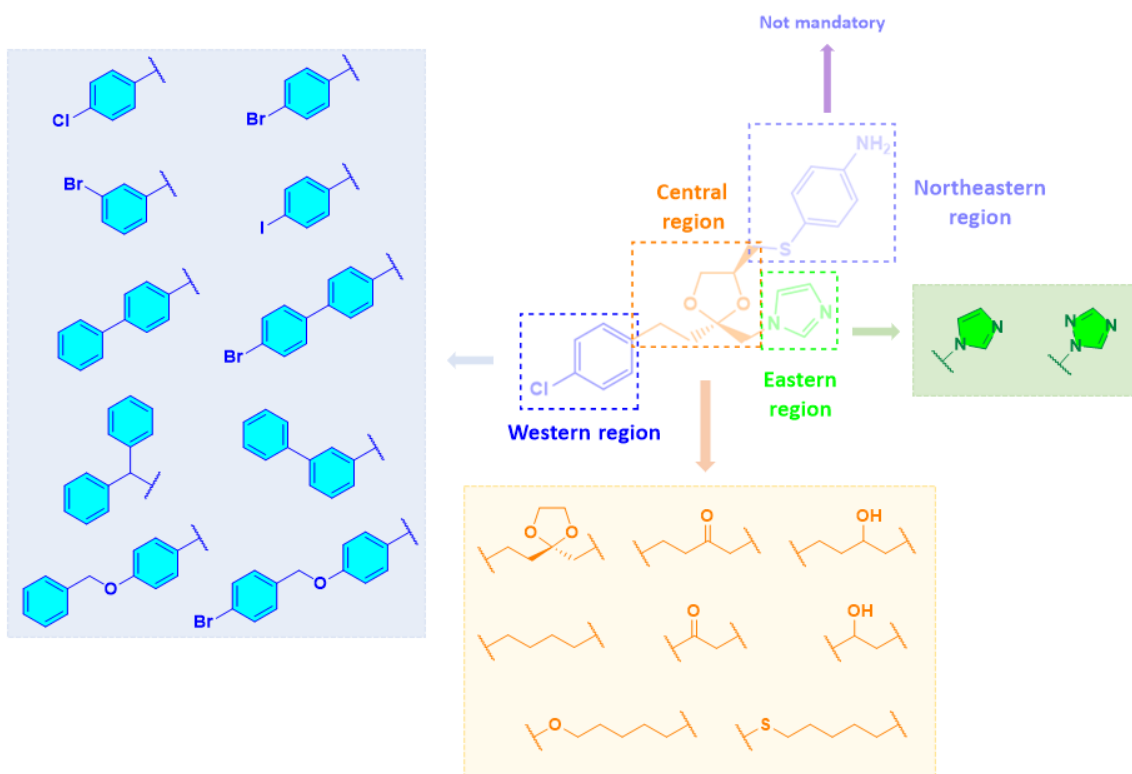


**Figure 14.** Summary of structure-activity relationships of HO-1 inhibitors.

## 2. Aim of the thesis

---

HO-1 overexpression has gained much attention in these last years because of its role in tumor outbreak, proliferation and involvement in the onset of chemoresistance phenomena. Considering its relative specific overexpression in tumor cells, HO-1 could represent an intriguing target exploitable for novel anticancer therapies. The main advantages could be summarized as follows: specific targeting of tumor cells; additive or synergistic effect in co-administration regimens with common anticancer drugs; reversal of chemoresistance phenomena, where present. In addition, the involvement of HO-2 in tumor progression cannot be completely excluded. Indeed, antiproliferative properties observed with compound **23u** (Table 8) in breast and prostate cancer cell lines suggest that the constitutive isoform could also represent a pharmacological target for cancer treatment. However, in order better comprehend the role of HO-2 in tumor biology, it is necessary to find novel potent and selective inhibitors that could be helpful in unraveling its implication in cancer progression. On these grounds, this research project aimed at targeting the HO system with novel and selective inhibitors for both isoforms with potential antitumor properties. In particular, three different strategies were pursued:

I) Define the structural requirements necessary for the selective inhibition of HO-1 or HO-2. In particular, the heme oxygenase database reported in literature highlighted that HO-1 inhibitors possess a smaller Van der Waals volume, whereas HO-2 inhibition is better granted by compounds having a bigger volume. This observation suggested the design of a small series of compounds originated from a non-selective HO inhibitor in which the essential imidazole ring was maintained in the eastern region and the molecular portion in the western region was modified with a bigger substituent to validate the hypothesis;

II) Expand the SAR of HO-1 inhibitors through the design, synthesis and *in vitro* biological evaluation of a novel and synthetically affordable class of compounds possessing

an amide bond in the central region of the molecule. The restricted known information about the tolerance of an amide bond in the central region of HO inhibitors and the moderate HO inhibitory properties of compound **28** (Figure 10) led to its choice as *hit compound* for the design of novel derivatives. Structural modifications were investigated in the central region, in the western region and at the amide function with the aim to understand which types of substitutions could lead to better potency and/or selectivity;

III) Take advantage of computational tools for the identification of novel HO-1 inhibitors. These tools are used to speed up the discovery of potential active compounds possessing novel molecular structures otherwise hardly detectable by common medicinal chemistry procedures. Specifically, growing ligand and joining ligand approaches were used. The former finds its rationale in a multistep growing of a molecular scaffold usually necessary for the interaction with the target into a bigger and more complex molecule. Molecules generated *in-silico* are further validated through a 3D-QSAR model, and the best predicted ones are synthesized and biologically evaluated to validate the approach. The latter works in a similar fashion, but in this case two fragments usually required for a proper interaction with the target are joined through other fragments identified *in-silico*.

### 3. Results and discussion

---

The focus of this PhD thesis was devoted to the design, synthesis, characterization and *in vitro* biological studies of novel HO inhibitors endowed with a potential antitumor activity. The project has been carried out applying classic and novel drug discovery approaches using some well-known HO inhibitors as starting point for the design of newly abovementioned molecules. In general, results herein obtained helped in widening the structure-activity relationships knowledge of HO inhibitors that could be further exploited in the future for the identification of potent and selective inhibitors towards one of the two enzymatic isoforms. The project can be divided in three parts: *i*) development of novel selective HO-2 inhibitors; *ii*) development of novel HO-1 inhibitors with potent antiproliferative properties; *iii*) identification of novel *hit compounds* behaving as HO-1 inhibitors by combination of fragment-based approaches and *in-silico* computational studies.

Every study was performed at the Department of Drug and Health Sciences at the University of Catania in collaboration with the Organic Chemistry and Biochemistry and Advanced Biology research groups. Each project brought to the publication of the following list of papers:

*Paper 1. Identification of a potent heme oxygenase-2 (HO-2) inhibitor by targeting the secondary hydrophobic pocket of the HO-2 western region (Bioorg. Chem. 2020, 104, 104310, second author).*

My contributions to this work were:

1. Design, synthesis and characterization of the novel compounds;
2. Draft original writing and editing.

*Paper 2: Discovery of novel acetamide-based heme oxygenase-1 inhibitors with potent in vitro antiproliferative activity (J. Med. Chem. 2021, 64 (18), 13373-13393, first author).*

My contributions to this work were:

1. Design, synthesis and characterization of the novel compounds;
2. Draft original writing and editing.

*Paper 3: Growing the molecular architecture of imidazole-like ligands in HO-1 complexes (Bioorg. Chem. 2021, 117, 105428, co-first author).*

My contributions to this work were:

1. Design, synthesis and characterization of the novel compounds;
2. Draft original writing and editing.

*Paper 4: From far west to east: joining the molecular architecture of imidazole-like ligands in HO-1 complexes (Pharmaceuticals, 2021, 14 (12), 1289, co-first author).*

My contributions to this work were:

1. Design, synthesis and characterization of the novel compounds;
2. Draft original writing and editing.

Herein are discussed the most important results obtained in each single paper. For full details, the reader is invited to read the published articles that are fully reported at the end of the present thesis.

### **Paper 1: Identification of a potent heme oxygenase-2 (HO-2) inhibitor by targeting the secondary hydrophobic pocket of the HO-2 western region**

The comprehension of the physiological role of HO-2 still represent a challenge for researchers working in the HO field. Despite the knowledge of HO-2 tissue distribution, still poor information has been gained during the years both for the preponderant interest towards the inducible isoform and the lack of selective small molecules that could target the constitutive isoform. However, compounds possessing a better selectivity for HO-2



displayed antiproliferative properties, suggesting that also the constitutive isoform could play a role in tumor biology.

Interestingly, HO-2 inhibitors reported in literature possess a bigger Van der Waals volume when compared to HO-1 inhibitors. This observation pushed us to choose a potent but unselective HO inhibitor possessing a benzyloxyphenyl moiety with the aim to shift its inhibitory potency towards the constitutive isoform simply playing with the volume of substituents located in the western region. Indeed, years of SARs studies highlighted that this region is prone to tolerate a wide range of structural modifications that can tune a selective inhibition over HO-1 or HO-2. Reshaping of the volume of the benzyloxyphenyl ring occupying the western region by the insertion of a nitrile substituent in position 4 and contemporary modification of the central region by the insertion of a ketone, an alcohol or a simple alkyl chain led to the rational design of three novel derivatives. Among them, compound **36** emerged as the best HO-2 inhibitor with a HO-2 IC<sub>50</sub> value of 0.9 μM (Figure 14).

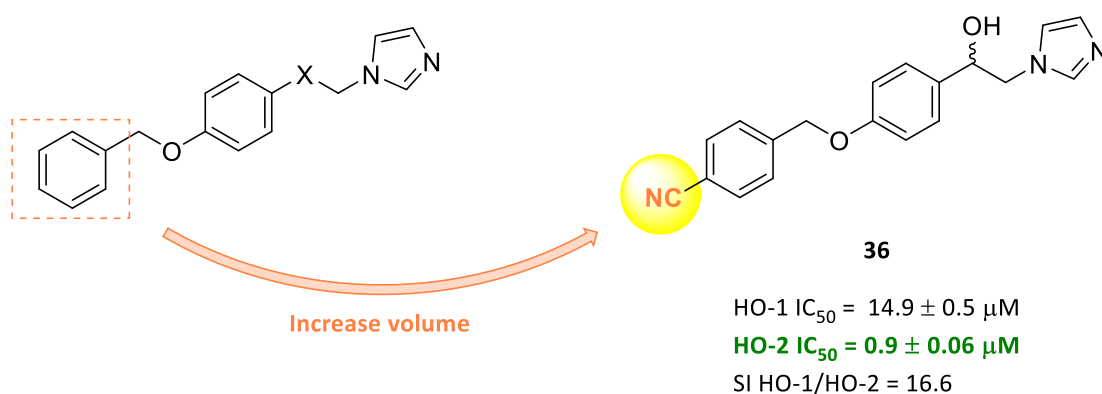


**Figure 14.** Chemical structure and experimental HO-1 and HO-2 IC<sub>50</sub> values of compound **36**.

Molecular modeling studies highlighted that the first aromatic ring of compound **36** is well-located in the western region, whereas the 4-cyanophenyl ring takes interactions with aminoacidic residues in the secondary hydrophobic pocket of the enzyme. Differently from HO-1, HO-2 possesses a Tyr187 residue in the western region that acts as a gate that prevents the interaction of bigger substituents with aminoacidic residues located in this part of the binding pocket, determining a folding of the substituted benzyloxy moiety into the secondary pocket, thus explaining the better inhibition of HO-2. In addition, the alcoholic functional group in the central region takes interactions with the consensus water molecule present in the binding pocket, overall strengthening the inhibition. An *in-silico* ADMET evaluation showed that compound **36** possesses optimal pharmacokinetic properties. This information is particularly useful in light of future *in vitro* studies. In general, this work helped in defining proper structural requirements for HO-2 inhibition and selectivity. These results could be useful not only for helping in the design of novel selective HO-2 inhibitors, but also to understand which structural modifications should be avoided for a selective targeting of HO-1.

## **Paper 2: Discovery of novel acetamide-based heme oxygenase-1 inhibitors with potent *in vitro* antiproliferative activity**

Despite the wide number of series of compounds reported in literature, few information is known about the tolerability of an amide function in the central connecting chain of HO inhibitors. Several marketed drugs are characterized by the presence of this functional group; indeed, its physicochemical properties are often required for optimal pharmacokinetic properties. Moreover, from a chemical point of view, amides are quite easy to synthesize. In light of this and interested in expanding more the SARs of HO-1 inhibitors, in this work were rationally synthesized nineteen compounds possessing an amide function in the central

connecting chain. Compound **28** (Figure 10), the amide derivative of compound **8** (Figure 7) was chosen as *hit compound*. Several structural modifications were analyzed: removal of one phenyl ring; insertion of substituents in one phenyl ring; replacement of one phenyl ring with saturated cycles; insertion of smaller or bulkier substituents at the nitrogen atom of the amide bond; elongation or shortening of the central region. *In vitro* enzymatic assays allowed the identification of six *N*-methylacetamides with potent HO-1 inhibition. Unfortunately, the most potent compounds of this series were generally characterized by poor enzymatic selectivity. An in-depth study of the potential antitumor properties of these compounds brought to the discovery of the 4-chloro-*N*-methyl derivative **37** (Figure 15).

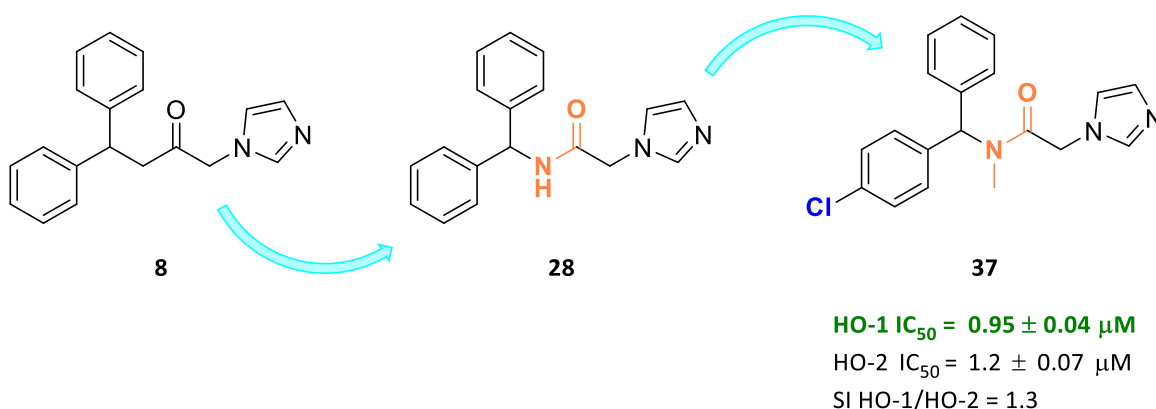


**Figure 15.** Chemical structure and experimental HO-1 and HO-2 IC<sub>50</sub> values of compound **37**.

Molecular modeling studies highlighted again a “double-clamp” binding mode for this compound. Indeed, one phenyl ring is located in the western region, while the second one takes interactions with the smaller secondary hydrophobic pocket of the enzyme. Moreover, the *E/Z* conformation of the molecule and the role of the chiral center were also analyzed. Results showed that a potential enantiomeric resolution would not bring any better inhibition of the enzyme and the equilibrium between the *E* and *Z* conformer is in favor of the latter,

even if this observation does not bring any additive ameliorment of inhibitory potency.

The novel compounds were tested for their antiproliferative properties against glioblastoma, lung and prostate cancer cell lines. Excitingly, compound **37** stood out for its ability to reduce the cell viability of the glioblastoma multiforme U87MG cancer cell line by more than 70 % when administered at a concentration of 1  $\mu$ M. In addition, compound **37** was also able to inhibit HO-1 activity in intact cells and did not induce HO-1 overexpression at the transcriptional level, which represents a common issue observed with other inhibitors, such as metalloporphyrins. Over and above that, U87MG cells treated with 10  $\mu$ M of compound **37** reduced their VEGF release, pointing to a potential antiangiogenic effect exerted by the novel HO-1 inhibitor. Finally, *in-silico* and *in vitro* pharmacokinetic evaluation suggested an exquisite drug-like profile for compound **37**, with blood–brain barrier crossing potential, good oral absorption, good metabolic stability, low cardiotoxicity and reduced cytochrome inhibition which could corroborate a potential *in vivo* utilization.

**Paper 3 (Growing the molecular architecture of imidazole-like ligands in HO-1 complexes) and Paper 4 (From far west to east: joining the molecular architecture of imidazole-like ligands in HO-1 complexes)**

Computational tools represent a powerful weapon that can be used in the drug discovery field to speed up the identification of lead compound that can be successively optimized in potential marketable drugs. In this context, fragment-based approaches make use of libraries of small fragments that can be differently combined in order to find new active molecular entities.

Starting from common fragments required for optimal HO-1 inhibition, two different approaches have been used in order to discover novel HO-1 inhibitors. The first one consisted in a growing-ligand approach, in which a starting molecular fragment can be

grown inside the binding site of the target to find additional interactions that could be useful to raise up the inhibitory potency of the novel compounds. The second approach consisted in joining two common fragments detectable in common HO-1 inhibitors in order to conceive a large library of compounds with potential biological effects. In both cases, the wide number of molecules thus created were evaluated by docking calculations and aligned and scored in the 3D-QSAR model described in the introduction of this thesis. The most interesting predicted molecules were synthesized and their inhibiting properties were evaluated *in vitro*. The most interesting compounds that emerged from this study are reported in Figure 16.

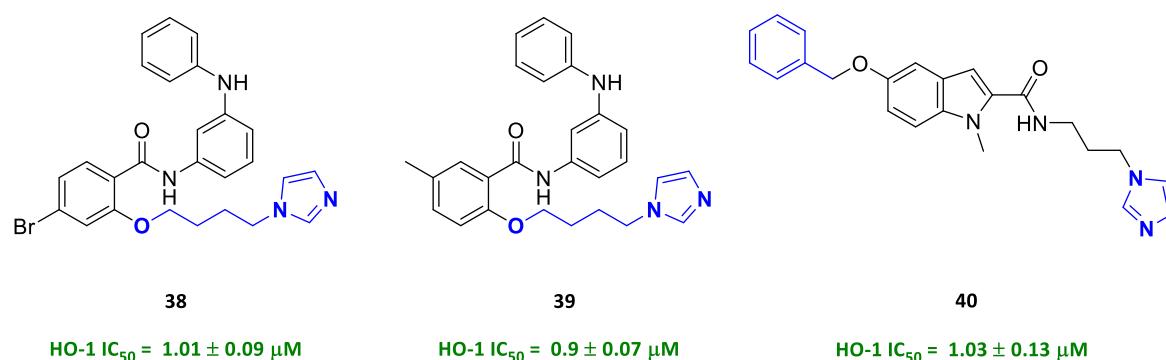


**Figure 16.** Chemical structure and experimental HO-1 and HO-2 IC<sub>50</sub> values of compounds **38–40**. In blue are highlighted the fragments used for the growing ligand or joining ligand experiments.

Compounds **38** and **39** were identified through the growing ligand approach using the oxybutylimidazole fragment as starting point for a two-step ligand growing experiment. Both compounds share some common structural features, such as the oxybutylimidazole substituent linked at position 2 of the aromatic ring and a (phenylamino)phenyl substituent linked to the aromatic ring through an amide bond. A binding mode analysis performed *in-*

*in-silico* showed that the (phenylamino)phenyl substituent identified in the second step of the growing experiment takes interactions with aminoacidic residues located in the northeastern region, thus explaining the strong inhibitory potency of both compounds. The pharmacokinetic properties of compounds **38** and **39** were evaluated *in-silico*. Results showed a potential oral bioavailability and intestinal absorption; however, both compounds are not predicted to cross the blood–brain barrier.

Compound **40** was identified through the joining ligand experiment using as starting fragments the imidazole ring and a benzyl moiety. This approach led to the identification of the indole heterocycle as a suitable moiety for joining the two fragments. Of note, the most potent predicted compounds are substituted at the 5- and/or 5- and 6- positions of the indole ring; moreover better results are predicted when the nitrogen atom of the indole ring is substituted with a methyl group. Interestingly, compounds **38–40** are characterized by the presence of an amide function, demonstrating again the tolerability of this functional group in the central region, as discovered in Paper 2. The good results obtained with these two different *in-silico* strategies, that is  $IC_{50}$  values in the low micromolar range, showed that the predictive power of the two approaches is consistent. Therefore, these models, and in general these computational approaches, will be further investigated for the discovery and optimization of novel *hit compounds*.

## Concluding remarks

---

The compounds herein described allowed to broaden knowledge in the structure-affinity relationships of HO inhibitors. Results showed that the novel *in-silico* identified HO-1 inhibitors and the high selective HO-2 inhibitor could be used as *hit compounds* for the development of more potent and selective compounds. Finally, the potent *in vitro* antitumoral effects exerted by the *N*-methylacetamide derivatives further corroborated HO-1 as a valid druggable target to combat cancer.

In conclusion, the goal of the research carried out during my PhD was achieved and successfully brought to the identification of novel compounds acting as HO inhibitors. This result was possible by strengthening my knowledge in the organic and medicinal chemistry fields and thanks to the fruitful collaborations established with different research groups.

## REFERENCES

- [1] Hooda, J.; Shah, A.; Zhang, L. Heme, an essential nutrient from dietary proteins, critically impacts diverse physiological and pathological processes. *Nutrients* **2014**, *6* (3), 1080-1102.
- [2] Kumar, S.; Bandyopadhyay, U. Free heme toxicity and its detoxification systems in human. *Toxicol. Lett.* **2005**, *157* (3), 175-188.
- [3] Heinemann, I. U.; Jahn, M.; Jahn, D. The biochemistry of heme biosynthesis. *Arch. Biochem. Biophys.* **2008**, *474* (2), 238-251.
- [4] Donegan, R. K.; Moore, C. M.; Hanna, D. A.; Reddi, A. R. Handling heme: The mechanisms underlying the movement of heme within and between cells. *Free Radic. Biol. Med.* **2019**, *133*, 88-100.
- [5] Hanna, D. A.; Martinez-Guzman, O.; Reddi, A. R. Heme Gazing: Illuminating Eukaryotic Heme Trafficking, Dynamics, and Signaling with Fluorescent Heme Sensors. *Biochemistry* **2017**, *56* (13), 1815-1823.
- [6] Immenschuh, S.; Vijayan, V.; Janciauskiene, S.; Gueler, F. Heme as a Target for Therapeutic Interventions. *Front. Pharmacol.* **2017**, *8*, 146.
- [7] Podkalicka, P.; Mucha, O.; Józkwicz, A.; Dulak, J.; Łoboda, A. Heme oxygenase inhibition in cancers: possible tools and targets. *Contemp. Oncol.* **2018**, *22* (1A), 23-32.
- [8] Ponka, P. Cell biology of heme. *Am. J. Med. Sci.* **1999**, *318* (4), 241-256.
- [9] Furfaro, A. L.; Traverso, N.; Domenicotti, C.; Piras, S.; Moretta, L.; Marinari, U. M.; Pronzato, M. A.; Nitti, M. The Nrf2/HO-1 Axis in Cancer Cell Growth and Chemoresistance. *Oxid. Med. Cell Longev.* **2016**, *2016*, 1958174.
- [10] Vincent, S. H. Oxidative effects of heme and porphyrins on proteins and lipids. *Semin. Hematol.* **1989**, *26* (2), 105-113.
- [11] Wagener, F. A.; Abraham, N. G.; van Kooyk, Y.; de Witte, T.; Figdor, C. G. Heme-induced cell adhesion in the pathogenesis of sickle-cell disease and inflammation. *Trends. Pharmacol. Sci.* **2001**, *22* (2), 52-54.
- [12] Iwahara, S.; Satoh, H.; Song, D. X.; Webb, J.; Burlingame, A. L.; Nagae, Y.; Muller-Eberhard, U. Purification, characterization, and cloning of a heme-binding protein (23 kDa) in rat liver cytosol. *Biochemistry* **1995**, *34* (41), 13398-13406.



- [13] Taketani, S.; Adachi, Y.; Kohno, H.; Ikehara, S.; Tokunaga, R.; Ishii, T. Molecular characterization of a newly identified heme-binding protein induced during differentiation of urine erythroleukemia cells. *J. Biol. Chem.* **1998**, *273* (47), 31388-31394.
- [14] Vincent, S. H.; Grady, R. W.; Shaklai, N.; Snider, J. M.; Muller-Eberhard, U. The influence of heme-binding proteins in heme-catalyzed oxidations. *Arch. Biochem. Biophys.* **1988**, *265* (2), 539-550.
- [15] Vincent, S. H.; Muller-Eberhard, U. A protein of the Z class of liver cytosolic proteins in the rat that preferentially binds heme. *J. Biol. Chem.* **1985**, *260* (27), 14521-14528.
- [16] Wijayanti, N.; Katz, N.; Immenschuh, S. Biology of heme in health and disease. *Curr. Med. Chem.* **2004**, *11* (8), 981-986.
- [17] Tenhunen, R.; Marver, H. S.; Schmid, R. The enzymatic conversion of heme to bilirubin by microsomal heme oxygenase. *Proc. Natl. Acad. Sci. U.S.A.* **1968**, *61* (2), 748-755.
- [18] Tenhunen, R.; Marver, H. S.; Schmid, R. Microsomal heme oxygenase. Characterization of the enzyme. *J. Biol. Chem.* **1969**, *244* (23), 6388-6394.
- [19] Li, C.; Stocker, R. Heme oxygenase and iron: from bacteria to humans. *Redox Rep.* **2009**, *14* (3), 95-101.
- [20] Hopper, C. P.; Meinel, L.; Steiger, C.; Otterbein, L. E. Where is the Clinical Breakthrough of Heme Oxygenase-1 / Carbon Monoxide Therapeutics? *Curr. Pharm. Des.* **2018**, *24* (20), 2264-2282.
- [21] Dunn, L. L.; Midwinter, R. G.; Ni, J.; Hamid, H. A.; Parish, C. R.; Stocker, R. New insights into intracellular locations and functions of heme oxygenase-1. *Antioxid. Redox Signal.* **2014**, *20* (11), 1723-1742.
- [22] Abraham, N. G.; Kappas, A. Pharmacological and clinical aspects of heme oxygenase. *Pharmacol. Rev.* **2008**, *60* (1), 79-127.
- [23] Maines, M. D. Overview of heme degradation pathway. *Curr. Protoc. Toxicol.* **2001**, *Chapter 9*, Unit 9.1.
- [24] Yoshida, T.; Migita, C. T. Mechanism of heme degradation by heme oxygenase. *J. Inorg. Biochem.* **2000**, *82* (1-4), 33-41.
- [25] Zhang, X.; Fujii, H.; Matera, K. M.; Migita, C. T.; Sun, D.; Sato, M.; Ikeda-Saito, M.; Yoshida, T. Stereoselectivity of each of the three steps of the heme oxygenase

- reaction: hemin to meso-hydroxyhemin, meso-hydroxyhemin to verdoheme, and verdoheme to biliverdin. *Biochemistry* **2003**, *42* (24), 7418-7426.
- [26] Vitek, L.; Ostrow, J. D. Bilirubin chemistry and metabolism; harmful and protective aspects. *Curr. Pharm. Des.* **2009**, *15* (25), 2869-2883.
- [27] Morita, T.; Kourembanas, S. Endothelial cell expression of vasoconstrictors and growth factors is regulated by smooth muscle cell-derived carbon monoxide. *J. Clin. Invest.* **1995**, *96* (6), 2676-2682.
- [28] Zuckerbraun, B. S.; Billiar, T. R.; Otterbein, S. L.; Kim, P. K.; Liu, F.; Choi, A. M.; Bach, F. H.; Otterbein, L. E. Carbon monoxide protects against liver failure through nitric oxide-induced heme oxygenase 1. *J. Exp. Med.* **2003**, *198* (11), 1707-1716.
- [29] Motterlini, R.; Otterbein, L. E. The therapeutic potential of carbon monoxide. *Nat. Rev. Drug Discov.* **2010**, *9* (9), 728-743.
- [30] Otterbein, L. E.; Bach, F. H.; Alam, J.; Soares, M.; Tao Lu, H.; Wysk, M.; Davis, R. J.; Flavell, R. A.; Choi, A. M. Carbon monoxide has anti-inflammatory effects involving the mitogen-activated protein kinase pathway. *Nat. Med.* **2000**, *6* (4), 422-428.
- [31] Morita, T.; Mitsialis, S. A.; Koike, H.; Liu, Y.; Kourembanas, S. Carbon monoxide controls the proliferation of hypoxic vascular smooth muscle cells. *J. Biol. Chem.* **1997**, *272* (52), 32804-32809.
- [32] Dulak, J.; Jozkowicz, A.; Foresti, R.; Kasza, A.; Frick, M.; Huk, I.; Green, C. J.; Pachinger, O.; Weidinger, F.; Motterlini, R. Heme oxygenase activity modulates vascular endothelial growth factor synthesis in vascular smooth muscle cells. *Antioxid. Redox Signal.* **2002**, *4* (2), 229-240.
- [33] Willis, D.; Moore, A. R.; Frederick, R.; Willoughby, D. A. Heme oxygenase: a novel target for the modulation of the inflammatory response. *Nat. Med.* **1996**, *2* (1), 87-90.
- [34] Kapitulnik, J.; Maines, M. D. Pleiotropic functions of biliverdin reductase: cellular signaling and generation of cytoprotective and cytotoxic bilirubin. *Trends Pharmacol. Sci.* **2009**, *30* (3), 129-137.
- [35] Clark, J. E.; Foresti, R.; Sarathchandra, P.; Kaur, H.; Green, C. J.; Motterlini, R. Heme oxygenase-1-derived bilirubin ameliorates postischemic myocardial dysfunction. *Am. J. Physiol. Heart Circ. Physiol.* **2000**, *278* (2), H643-651.

- [36] Dore, S.; Takahashi, M.; Ferris, C. D.; Zakhary, R.; Hester, L. D.; Guastella, D.; Snyder, S. H. Bilirubin, formed by activation of heme oxygenase-2, protects neurons against oxidative stress injury. *Proc. Natl. Acad. Sci. U.S.A.* **1999**, *96* (5), 2445-2450.
- [37] Hyman, C. B.; Keaster, J.; Hanson, V.; Harris, I.; Sedgwick, R.; Wursten, H.; Wright, A. R. CNS abnormalities after neonatal hemolytic disease or hyperbilirubinemia. A prospective study of 405 patients. *Am. J. Dis. Child.* **1969**, *117* (4), 395-405.
- [38] Baranano, D. E.; Wolosker, H.; Bae, B. I.; Barrow, R. K.; Snyder, S. H.; Ferris, C. D. A mammalian iron ATPase induced by iron. *J. Biol. Chem.* **2000**, *275* (20), 15166-15173.
- [39] Eisenstein, R. S.; Garcia-Mayol, D.; Pettingell, W.; Munro, H. N. Regulation of ferritin and heme oxygenase synthesis in rat fibroblasts by different forms of iron. *Proc. Natl. Acad. Sci. U.S.A.* **1991**, *88* (3), 688-692.
- [40] Eisenstein, R. S.; Munro, H. N. Translational regulation of ferritin synthesis by iron. *Enzyme* **1990**, *44* (1-4), 42-58.
- [41] Ryter, S. W.; Tyrrell, R. M. The heme synthesis and degradation pathways: role in oxidant sensitivity. Heme oxygenase has both pro- and antioxidant properties. *Free Radic. Biol. Med.* **2000**, *28* (2), 289-309.
- [42] Suttner, D. M.; Dennery, P. A. Reversal of HO-1 related cytoprotection with increased expression is due to reactive iron. *FASEB J.* **1999**, *13* (13), 1800-1809.
- [43] Hayashi, S.; Omata, Y.; Sakamoto, H.; Higashimoto, Y.; Hara, T.; Sagara, Y.; Noguchi, M. Characterization of rat heme oxygenase-3 gene. Implication of processed pseudogenes derived from heme oxygenase-2 gene. *Gene* **2004**, *336* (2), 241-250.
- [44] Kochert, B. A.; Fleischhacker, A. S.; Wales, T. E.; Becker, D. F.; Engen, J. R.; Ragsdale, S. W. Dynamic and structural differences between heme oxygenase-1 and -2 are due to differences in their C-terminal regions. *J. Biol. Chem.* **2019**, *294* (20), 8259-8272.
- [45] Keyse, S. M.; Tyrrell, R. M. Heme oxygenase is the major 32-kDa stress protein induced in human skin fibroblasts by UVA radiation, hydrogen peroxide, and sodium arsenite. *Proc. Natl. Acad. Sci. U.S.A.* **1989**, *86* (1), 99-103.
- [46] Ferrandiz, M. L.; Devesa, I. Inducers of heme oxygenase-1. *Curr. Pharm. Des.* **2008**, *14* (5), 473-486.

- [47] Zakhary, R.; Gaine, S. P.; Dinerman, J. L.; Ruat, M.; Flavahan, N. A.; Snyder, S. H. Heme oxygenase 2: endothelial and neuronal localization and role in endothelium-dependent relaxation. *Proc. Natl. Acad. Sci. U.S.A.* **1996**, *93* (2), 795-798.
- [48] Maines, M. D.; Trakshel, G. M.; Kutty, R. K. Characterization of two constitutive forms of rat liver microsomal heme oxygenase. Only one molecular species of the enzyme is inducible. *J. Biol. Chem.* **1986**, *261* (1), 411-419.
- [49] Parfenova, H.; Leffler, C. W. Cerebroprotective functions of HO-2. *Curr. Pharm. Des.* **2008**, *14* (5), 443-453.
- [50] McCoubrey, W. K., Jr.; Huang, T. J.; Maines, M. D. Heme oxygenase-2 is a hemoprotein and binds heme through heme regulatory motifs that are not involved in heme catalysis. *J. Biol. Chem.* **1997**, *272* (19), 12568-12574.
- [51] Kutty, R. K.; Kutty, G.; Rodriguez, I. R.; Chader, G. J.; Wiggert, B. Chromosomal localization of the human heme oxygenase genes: heme oxygenase-1 (HMOX1) maps to chromosome 22q12 and heme oxygenase-2 (HMOX2) maps to chromosome 16p13.3. *Genomics* **1994**, *20* (3), 513-516.
- [52] Exner, M.; Minar, E.; Wagner, O.; Schillinger, M. The role of heme oxygenase-1 promoter polymorphisms in human disease. *Free Radic. Biol. Med.* **2004**, *37* (8), 1097-1104.
- [53] Okamoto, I.; Krogler, J.; Endler, G.; Kaufmann, S.; Mustafa, S.; Exner, M.; Mannhalter, C.; Wagner, O.; Pehamberger, H. A microsatellite polymorphism in the heme oxygenase-1 gene promoter is associated with risk for melanoma. *Int. J. Cancer.* **2006**, *119* (6), 1312-1315.
- [54] Yamada, N.; Yamaya, M.; Okinaga, S.; Nakayama, K.; Sekizawa, K.; Shibahara, S.; Sasaki, H. Microsatellite polymorphism in the heme oxygenase-1 gene promoter is associated with susceptibility to emphysema. *Am. J. Hum. Genet.* **2000**, *66* (1), 187-195.
- [55] McCoubrey, W. K., Jr.; Ewing, J. F.; Maines, M. D. Human heme oxygenase-2: characterization and expression of a full-length cDNA and evidence suggesting that the two HO-2 transcripts may differ by choice of polyadenylation signal. *Arch. Biochem. Biophys.* **1992**, *295* (1), 13-20.
- [56] Yi, L.; Ragsdale, S. W. Evidence that the heme regulatory motifs in heme oxygenase-2 serve as a thiol/disulfide redox switch regulating heme binding. *J. Biol. Chem.* **2007**, *282* (29), 21056-21067.

- [57] Lad, L.; Schuller, D. J.; Shimizu, H.; Friedman, J.; Li, H.; Ortiz de Montellano, P. R.; Poulos, T. L. Comparison of the heme-free and -bound crystal structures of human heme oxygenase-1. *J. Biol. Chem.* **2003**, *278* (10), 7834-7843.
- [58] Bianchetti, C. M.; Yi, L.; Ragsdale, S. W.; Phillips, G. N., Jr. Comparison of apo- and heme-bound crystal structures of a truncated human heme oxygenase-2. *J. Biol. Chem.* **2007**, *282* (52), 37624-37631.
- [59] Rotenberg, M. O.; Maines, M. D. Characterization of a cDNA-encoding rabbit brain heme oxygenase-2 and identification of a conserved domain among mammalian heme oxygenase isozymes: possible heme-binding site? *Arch. Biochem. Biophys.* **1991**, *290* (2), 336-344.
- [60] Lightning, L. K.; Huang, H.; Moenne-Loccoz, P.; Loehr, T. M.; Schuller, D. J.; Poulos, T. L.; de Montellano, P.R. Disruption of an active site hydrogen bond converts human heme oxygenase-1 into a peroxidase. *J. Biol. Chem.* **2001**, *276* (14), 10612-10619.
- [61] Dwyer, B. E.; Nishimura, R. N.; De Vellis, J.; Yoshida, T. Heme oxygenase is a heat shock protein and PEST protein in rat astroglial cells. *Glia* **1992**, *5* (4), 300-305.
- [62] Dennery, P. A. Signaling function of heme oxygenase proteins. *Antioxid. Redox Signal.* **2014**, *20* (11), 1743-1753.
- [63] Hsu, F. F.; Yeh, C. T.; Sun, Y. J.; Chiang, M. T.; Lan, W. M.; Li, F. A.; Lee, W. H.; Chau, L. Y. Signal peptide peptidase-mediated nuclear localization of heme oxygenase-1 promotes cancer cell proliferation and invasion independent of its enzymatic activity. *Oncogene* **2015**, *34* (18), 2410-2411.
- [64] Schaefer, B.; Moriishi, K.; Behrends, S. Insights into the mechanism of isoenzyme-specific signal peptide peptidase-mediated translocation of heme oxygenase. *PLoS one* **2017**, *12* (11), e0188344.
- [65] Fleischhacker, A. S.; Carter, E. L.; Ragsdale, S. W. Redox Regulation of Heme Oxygenase-2 and the Transcription Factor, Rev-Erb, Through Heme Regulatory Motifs. *Antioxid. Redox Signal.* **2018**, *29* (18), 1841-1857.
- [66] Bagai, I.; Sarangi, R.; Fleischhacker, A. S.; Sharma, A.; Hoffman, B. M.; Zuiderweg, E. R.; Ragsdale, S. W. Spectroscopic studies reveal that the heme regulatory motifs of heme oxygenase-2 are dynamically disordered and exhibit redox-dependent interaction with heme. *Biochemistry* **2015**, *54* (17), 2693-2708.

- [67] Fleischhacker, A. S.; Sharma, A.; Choi, M.; Spencer, A. M.; Bagai, I.; Hoffman, B. M.; Ragsdale, S. W. The C-terminal heme regulatory motifs of heme oxygenase-2 are redox-regulated heme binding sites. *Biochemistry* **2015**, *54* (17), 2709-2718.
- [68] Varfaj, F.; Lampe, J. N.; Ortiz de Montellano, P.R. Role of cysteine residues in heme binding to human heme oxygenase-2 elucidated by two-dimensional NMR spectroscopy. *J. Biol. Chem.* **2012**, *287* (42), 35181-35191.
- [69] Vukomanovic, D.; Rahman, M. N.; Maines, M. D.; Ozolins, T. R.; Szarek, W. A.; Jia, Z.; Nakatsu, K. Cysteine-independent activation/inhibition of heme oxygenase-2. *Med. Gas. Res.* **2016**, *6* (1), 10-13.
- [70] Fleischhacker, A. S.; Gunawan, A. L.; Kochert, B. A.; Liu, L.; Wales, T. E.; Borowy, M. C.; Engen, J. R.; Ragsdale, S. W. The heme-regulatory motifs of heme oxygenase-2 contribute to the transfer of heme to the catalytic site for degradation. *J. Biol. Chem.* **2020**, *295* (16), 5177-5191.
- [71] Liu, N.; Wang, X.; McCoubrey, W. K.; Maines, M. D. Developmentally regulated expression of two transcripts for heme oxygenase-2 with a first exon unique to rat testis: control by corticosterone of the oxygenase protein expression. *Gene* **2000**, *241* (1), 175-183.
- [72] Boehning, D.; Moon, C.; Sharma, S.; Hurt, K. J.; Hester, L. D.; Ronnett, G. V.; Shugar, D.; Snyder, S. H. Carbon monoxide neurotransmission activated by CK2 phosphorylation of heme oxygenase-2. *Neuron* **2003**, *40* (1), 129-137.
- [73] Liu, L.; Dumbrepatil, A. B.; Fleischhacker, A. S.; Marsh, E. N. G.; Ragsdale, S. W. Heme oxygenase-2 is post-translationally regulated by heme occupancy in the catalytic site. *J. Biol. Chem.* **2020**, *295* (50), 17227-17240.
- [74] Immenschuh, S.; Ramadori, G. Gene regulation of heme oxygenase-1 as a therapeutic target. *Biochem. Pharmacol.* **2000**, *60* (8), 1121-1128.
- [75] Na, H. K.; Surh, Y. J. Oncogenic potential of Nrf2 and its principal target protein heme oxygenase-1. *Free Radic. Biol. Med.* **2014**, *67*, 353-365.
- [76] Bian, C.; Zhong, M.; Nisar, M. F.; Wu, Y.; Ouyang, M.; Bartsch, J. W.; Zhong, J. L. A novel heme oxygenase-1 splice variant, 14kDa HO-1, promotes cell proliferation and increases relative telomere length. *Biochem. Biophys. Res. Commun.* **2018**, *500* (2), 429-434.

- [77] Paine, A.; Eiz-Vesper, B.; Blasczyk, R.; Immenschuh, S. Signaling to heme oxygenase-1 and its anti-inflammatory therapeutic potential. *Biochem. Pharmacol.* **2010**, *80* (12), 1895-1903.
- [78] Rada, P.; Rojo, A. I.; Chowdhry, S.; McMahon, M.; Hayes, J. D.; Cuadrado, A. SCF/ $\beta$ -TrCP promotes glycogen synthase kinase 3-dependent degradation of the Nrf2 transcription factor in a Keap1-independent manner. *Mol. Cell. Biol.* **2011**, *31* (6), 1121-1133.
- [79] Chowdhry, S.; Zhang, Y.; McMahon, M.; Sutherland, C.; Cuadrado, A.; Hayes, J. D. Nrf2 is controlled by two distinct beta-TrCP recognition motifs in its Neh6 domain, one of which can be modulated by GSK-3 activity. *Oncogene* **2013**, *32* (32), 3765-3781.
- [80] Ishizaka, N.; Griendling, K. K. Heme oxygenase-1 is regulated by angiotensin II in rat vascular smooth muscle cells. *Hypertension* **1997**, *29* (3), 790-795.
- [81] Takahashi, K.; Nakayama, M.; Takeda, K.; Fujia, H.; Shibahara, S. Suppression of heme oxygenase-1 mRNA expression by interferon-gamma in human glioblastoma cells. *J. Neurochem.* **1999**, *72* (6), 2356-2361.
- [82] Nitti, M.; Piras, S.; Marinari, U. M.; Moretta, L.; Pronzato, M. A.; Furfaro, A. L. HO-1 Induction in Cancer Progression: A Matter of Cell Adaptation. *Antioxidants (Basel)* **2017**, *6* (2), 29.
- [83] Gueron, G.; De Siervi, A.; Ferrando, M.; Salierno, M.; De Luca, P.; Elguero, B.; Meiss, R.; Navone, N.; Vazquez, E. S. Critical role of endogenous heme oxygenase 1 as a tuner of the invasive potential of prostate cancer cells. *Mol. Cancer Res.* **2009**, *7* (11), 1745-1755.
- [84] Was, H.; Dulak, J.; Jozkowicz, A. Heme oxygenase-1 in tumor biology and therapy. *Curr. Drug Targets.* **2010**, *11* (12), 1551-1570.
- [85] Castruccio Castracani, C.; Longhitano, L.; Distefano, A.; Di Rosa, M.; Pittalà, V.; Lupo, G.; Caruso, M.; Corona, D.; Tibullo, D.; Li Volti, G. Heme Oxygenase-1 and Carbon Monoxide Regulate Growth and Progression in Glioblastoma Cells. *Mol. Neurobiol.* **2020**, *57* (5), 2436-2446.
- [86] Lu, J. J.; Abudukeyoumu, A.; Zhang, X.; Liu, L. B.; Li, M. Q.; Xie, F. Heme oxygenase 1: a novel oncogene in multiple gynecological cancers. *Int. J. Biol. Sci.* **2021**, *17* (9), 2252-2261.

- [87] Ghosh, D.; Ulasov, I. V.; Chen, L.; Harkins, L. E.; Wallenborg, K.; Hothi, P.; Rostad, S.; Hood, L.; Cobbs, C. S. TGF $\beta$ -Responsive HMOX1 Expression Is Associated with Stemness and Invasion in Glioblastoma Multiforme. *Stem Cells* **2016**, *34* (9), 2276-2289.
- [88] Sferrazzo, G.; Di Rosa, M.; Barone, E.; Li Volti, G.; Musso, N.; Tibullo, D.; Barbagallo, I. Heme Oxygenase-1 in Central Nervous System Malignancies. *J. Clin. Med.* **2020**, *9* (5), 1562.
- [89] Li Volti, G.; Tibullo, D.; Vanella, L.; Giallongo, C.; Di Raimondo, F.; Forte, S.; Di Rosa, M.; Signorelli, S. S.; Barbagallo, I. The Heme Oxygenase System in Hematological Malignancies. *Antioxid. Redox Signal.* **2017**, *27* (6), 363-377.
- [90] Salerno, L.; Romeo, G.; Modica, M. N.; Amata, E.; Sorrenti, V.; Barbagallo, I.; Pittalà, V. Heme oxygenase-1: A new druggable target in the management of chronic and acute myeloid leukemia. *Eur. J. Med. Chem.* **2017**, *142*, 163-178.
- [91] Huang, Y.; Yang, Y.; Xu, Y.; Ma, Q.; Guo, F.; Zhao, Y.; Tao, Y.; Li, M.; Guo, J. Nrf2/HO-1 Axis Regulates the Angiogenesis of Gastric Cancer via Targeting VEGF. *Cancer Manag. Res.* **2021**, *13*, 3155-3169.
- [92] Sorrenti, V.; D'Amico, A. G.; Barbagallo, I.; Consoli, V.; Grosso, S.; Vanella, L. Tin Mesoporphyrin Selectively Reduces Non-Small-Cell Lung Cancer Cell Line A549 Proliferation by Interfering with Heme Oxygenase and Glutathione Systems. *Biomolecules* **2021**, *11* (6), 917.
- [93] Nuhn, P.; Künzli, B. M.; Hennig, R.; Mitkus, T.; Ramanauskas, T.; Nobile, R.; Meuer, S. C.; Friess, H.; Berberat, P. O. Heme oxygenase-1 and its metabolites affect pancreatic tumor growth in vivo. *Mol. Cancer.* **2009**, *8*, 37.
- [94] Chin, B. Y.; Jiang, G.; Wegiel, B.; Wang, H. J.; Macdonald, T.; Zhang, X. C.; Gallo, D.; Cszimadia, E.; Bach, F. H.; Lee, P. J.; Otterbein, L. E. Hypoxia-inducible factor 1 $\alpha$  stabilization by carbon monoxide results in cytoprotective preconditioning. *Proc. Natl. Acad. Sci. U.S.A.* **2007**, *104* (12), 5109-5114.
- [95] Loboda, A.; Jozkowicz, A.; Dulak, J. HO-1/CO system in tumor growth, angiogenesis and metabolism - Targeting HO-1 as an anti-tumor therapy. *Vascul. Pharmacol.* **2015**, *74*, 11-22.
- [96] Nitti, M.; Ivaldo, C.; Traverso, N.; Furfaro, A. L. Clinical Significance of Heme Oxygenase 1 in Tumor Progression. *Antioxidants* **2021**, *10* (5), 789.



- [97] Wegiel, B.; Baty, C. J.; Gallo, D.; Csizmadia, E.; Scott, J. R.; Akhavan, A.; Chin, B. Y.; Kaczmarek, E.; Alam, J.; Bach, F. H.; Zuckerbraun B. S.; Otterbein L. E. Cell surface biliverdin reductase mediates biliverdin-induced anti-inflammatory effects via phosphatidylinositol 3-kinase and Akt. *J. Biol. Chem.* **2009**, *284* (32), 21369-21378.
- [98] Brouard, S.; Otterbein, L. E.; Anrather, J.; Tobiasch, E.; Bach, F. H.; Choi, A. M.; Soares, M. P. Carbon monoxide generated by heme oxygenase 1 suppresses endothelial cell apoptosis. *J. Exp. Med.* **2000**, *192* (7), 1015-1026.
- [99] Zhang, X.; Shan, P.; Alam, J.; Fu, X. Y.; Lee, P. J. Carbon monoxide differentially modulates STAT1 and STAT3 and inhibits apoptosis via a phosphatidylinositol 3-kinase/Akt and p38 kinase-dependent STAT3 pathway during anoxia-reoxygenation injury. *J. Biol. Chem.* **2005**, *280* (10), 8714-8721.
- [100] Al-Owais, M. M.; Scragg, J. L.; Dallas, M. L.; Boycott, H. E.; Warburton, P.; Chakrabarty, A.; Boyle, J. P.; Peers, C. Carbon monoxide mediates the anti-apoptotic effects of heme oxygenase-1 in medulloblastoma DAOY cells via K<sup>+</sup> channel inhibition. *J. Biol. Chem.* **2012**, *287* (29), 24754-24764.
- [101] Hsu, F. F.; Yeh, C. T.; Sun, Y. J.; Chiang, M. T.; Lan, W. M.; Li, F. A.; Lee, W. H.; Chau, L. Y. Signal peptide peptidase-mediated nuclear localization of heme oxygenase-1 promotes cancer cell proliferation and invasion independent of its enzymatic activity. *Oncogene* **2015**, *34* (18), 2360-2370.
- [102] Gandini, N. A.; Fermento, M. E.; Salomón, D. G.; Blasco, J.; Patel, V.; Gutkind, J. S.; Molinolo, A. A.; Facchinetti, M. M.; Curino, A. C. Nuclear localization of heme oxygenase-1 is associated with tumor progression of head and neck squamous cell carcinomas. *Exp. Mol. Pathol.* **2012**, *93* (2), 237-245.
- [103] Mascaró, M.; Alonso, E. N.; Alonso, E. G.; Lacunza, E.; Curino, A. C.; Facchinetti, M. M. Nuclear Localization of Heme Oxygenase-1 in Pathophysiological Conditions: Does It Explain the Dual Role in Cancer? *Antioxidants* **2021**, *10* (1), 87.
- [104] Vanella, L.; Barbagallo, I.; Tibullo, D.; Forte, S.; Zappalà, A.; Li Volti, G. The non-canonical functions of the heme oxygenases. *Oncotarget* **2016**, *7* (42), 69075-69086.
- [105] Hsu, F. F.; Chiang, M. T.; Li, F. A.; Yeh, C. T.; Lee, W. H.; Chau, L. Y. Acetylation is essential for nuclear heme oxygenase-1-enhanced tumor growth and invasiveness. *Oncogene* **2017**, *36* (49), 6805-6814.

- [106] Tibullo, D.; Barbagallo, I.; Giallongo, C.; La Cava, P.; Parrinello, N.; Vanella, L.; Stagno, F.; Palumbo, G. A.; Li Volti, G.; Di Raimondo, F. Nuclear translocation of heme oxygenase-1 confers resistance to imatinib in chronic myeloid leukemia cells. *Curr. Pharm. Des.* **2013**, *19* (15), 2765-2770.
- [107] Tibullo, D.; Barbagallo, I.; Giallongo, C.; Vanella, L.; Conticello, C.; Romano, A.; Saccone, S.; Godos, J.; Di Raimondo, F.; Li Volti, G. Heme oxygenase-1 nuclear translocation regulates bortezomib-induced cytotoxicity and mediates genomic instability in myeloma cells. *Oncotarget* **2016**, *7* (20), 28868-28880.
- [108] Biswas, C.; Shah, N.; Muthu, M.; La, P.; Fernando, A.P.; Sengupta, S.; Yang, G.; Dennery, P. A. Nuclear heme oxygenase-1 (HO-1) modulates subcellular distribution and activation of Nrf2, impacting metabolic and anti-oxidant defenses. *J. Biol. Chem.* **2014**, *289* (39), 26882-26894.
- [109] Consoli, V.; Sorrenti, V.; Grosso, S.; Vanella, L. Heme Oxygenase-1 Signaling and Redox Homeostasis in Physiopathological Conditions. *Biomolecules* **2021**, *11* (4), 589.
- [110] Yamamoto, T.; Takano, N.; Ishiwata, K.; Ohmura, M.; Nagahata, Y.; Matsuura, T.; Kamata, A.; Sakamoto, K.; Nakanishi, T.; Kubo, A.; Hishiki, T.; Suematsu, M. Reduced methylation of PFKFB3 in cancer cells shunts glucose towards the pentose phosphate pathway. *Nat. Commun.* **2014**, *5*, 3480.
- [111] Consonni, F. M.; Bleve, A.; Totaro, M. G.; Storto, M.; Kunderfranco, P.; Termanini, A.; Pasqualini, F.; Ali, C.; Pandolfo, C.; Sgambelluri, F.; Grazia, G.; Santinami, M.; Maurichi, A.; Milione, M.; Erreni, M.; Doni, A.; Fabbri, M.; Gribaldo, L.; Rulli, E.; Soares, M. P.; Torri, V.; Mortarini, R.; Anichini, A.; Sica, A. Heme catabolism by tumor-associated macrophages controls metastasis formation. *Nat. Immunol.* **2021**, *22* (5), 595-606.
- [112] Kim, S. H.; Kim, S. J.; Park, J.; Joe, Y.; Lee, S. E.; Saeidi, S.; Zhong, X.; Kim, S. H.; Park, S. A.; Na, H. K.; Chung, H. T.; Surh, Y. J. Reprogramming of Tumor-Associated Macrophages in Breast Tumor-Bearing Mice under Chemotherapy by Targeting Heme Oxygenase-1. *Antioxidants* **2021**, *10* (3), 470.
- [113] Ahmad, I. M.; Dafferner, A. J.; O'Connell, K. A.; Mehla, K.; Britigan, B. E.; Hollingsworth, M. A.; Abdalla, M. Y. Heme Oxygenase-1 Inhibition Potentiates the Effects of Nab-Paclitaxel-Gemcitabine and Modulates the Tumor Microenvironment in Pancreatic Ductal Adenocarcinoma. *Cancers* **2021**, *13* (9), 2264.

- [114] Luu Hoang, K. N.; Anstee, J. E.; Arnold, J. N. The Diverse Roles of Heme Oxygenase-1 in Tumor Progression. *Front. Immunol.* **2021**, *12*, 658315.
- [115] Chiang, S. K.; Chen, S. E.; Chang, L. C. The Role of HO-1 and Its Crosstalk with Oxidative Stress in Cancer Cell Survival. *Cells* **2021**, *10* (9), 2401.
- [116] Fernández-Fierro, A.; Funes, S. C.; Rios, M.; Covián, C.; González, J.; Kalergis, A. M. Immune Modulation by Inhibitors of the HO System. *Int. J. Mol. Sci.* **2020**, *22* (1), 294.
- [117] Barbagallo, I.; Giallongo, C.; Li Volti, G.; Distefano, A.; Camiolo, G.; Raffaele, M.; Salerno, L.; Pittalà, V.; Sorrenti, V.; Avola, R.; Di Rosa, M.; Vanella, L.; Di Raimondo, F.; Tibullo, D. Heme Oxygenase Inhibition Sensitizes Neuroblastoma Cells to Carfilzomib. *Mol. Neurobiol.* **2019**, *56* (2), 1451-1460.
- [118] Sass, G.; Leukel, P.; Schmitz, V.; Raskopf, E.; Ocker, M.; Neureiter, D.; Meissnitzer, M.; Tasika, E.; Tannapfel, A.; Tiegs, G. Inhibition of heme oxygenase 1 expression by small interfering RNA decreases orthotopic tumor growth in livers of mice. *Int. J. Cancer.* **2008**, *123* (6), 1269-1277.
- [119] Alaoui-Jamali, M. A.; Bismar, T. A.; Gupta, A.; Szarek, W. A.; Su, J.; Song, W.; Xu, Y.; Xu, B.; Liu, G.; Vlahakis, J. Z.; Roman, G.; Jiao, J.; Schipper, H. M. A novel experimental heme oxygenase-1-targeted therapy for hormone-refractory prostate cancer. *Cancer. Res.* **2009**, *69* (20), 8017-8024.
- [120] Yang, W. S.; Stockwell, B. R. Ferroptosis: Death by Lipid Peroxidation. *Trends Cell Biol.* **2016**, *26* (3), 165-176.
- [121] Xie, Y.; Hou, W.; Song, X.; Yu, Y.; Huang, J.; Sun, X.; Kang, R.; Tang, D. Ferroptosis: process and function. *Cell Death Differ.* **2016**, *23* (3), 369-379.
- [122] Thévenod, F. Iron and Its Role in Cancer Defense: A Double-Edged Sword. *Met. Ions Life Sci.* **2018**, *18*.
- [123] Chiang, S. K.; Chen, S. E.; Chang, L. C. A Dual Role of Heme Oxygenase-1 in Cancer Cells. *Int. J. Mol. Sci.* **2018**, *20* (1), 39.
- [124] Adedoyin, O.; Boddu, R.; Traylor, A.; Lever, J. M.; Bolisetty, S.; George, J. F.; Agarwal, A. Heme oxygenase-1 mitigates ferroptosis in renal proximal tubule cells. *Am. J. Physiol. Renal Physiol.* **2018**, *314* (5), 702-714.
- [125] Kwon, M. Y.; Park, E.; Lee, S. J.; Chung, S. W. Heme oxygenase-1 accelerates erastin-induced ferroptotic cell death. *Oncotarget* **2015**, *6* (27), 24393-24403.

- [126] He, J. Z.; Ho, J. J. D.; Gingerich, S.; Courtman, D. W.; Marsden, P. A.; Ward, M. E. Enhanced translation of heme oxygenase-2 preserves human endothelial cell viability during hypoxia. *J. Biol. Chem.* **2010**, 285 (13), 9452-9461.
- [127] Li, B.; Takeda, K.; Ishikawa, K.; Yoshizawa, M.; Sato, M.; Shibahara, S.; Furuyama, K. Coordinated expression of 6-phosphofructo-2-kinase/fructose-2,6-bisphosphatase 4 and heme oxygenase 2: evidence for a regulatory link between glycolysis and heme catabolism. *Tohoku J. Exp. Med.* **2012**, 228 (1), 27-41.
- [128] Satarug, S.; Moore, M. R. Emerging roles of cadmium and heme oxygenase in type-2 diabetes and cancer susceptibility. *Tohoku J. Exp. Med.* **2012**, 228 (4), 267-288.
- [129] Wong, R. J.; Vreman, H. J.; Schulz, S.; Kalish, F. S.; Pierce, N. W.; Stevenson, D. K. In vitro inhibition of heme oxygenase isoenzymes by metalloporphyrins. *J. Perinatol.* **2011**, 31 Suppl 1, S35-41.
- [130] Yoshinaga, T.; Sassa, S.; Kappas, A. Purification and properties of bovine spleen heme oxygenase. Amino acid composition and sites of action of inhibitors of heme oxidation. *J. Biol. Chem.* **1982**, 257 (13), 7778-7785.
- [131] Li, J.; Wu, B.; Teng, D.; Sun, X.; Li, J.; Li, J.; Zhang, G.; Cai, J. Cobalt-protoporphyrin enhances heme oxygenase 1 expression and attenuates liver ischemia/reperfusion injury by inhibiting apoptosis. *Mol. Med. Rep.* **2018**, 17 (3), 4567-4572.
- [132] Bhutani, V. K.; Poland, R.; Meloy, L. D.; Hegyi, T.; Fanaroff, A. A.; Maisels, M. J. Clinical trial of tin mesoporphyrin to prevent neonatal hyperbilirubinemia. *J. Perinatol.* **2016**, 36 (7), 533-539.
- [133] Stevenson, D. K.; Rodgers, P. A.; Vreman, H. J. The use of metalloporphyrins for the chemoprevention of neonatal jaundice. *Am. J. Dis. Child.* **1989**, 143 (3), 353-356.
- [134] Kappas, A.; Drummond, G. S.; Henschke, C.; Valaes, T. Direct comparison of Sn-mesoporphyrin, an inhibitor of bilirubin production, and phototherapy in controlling hyperbilirubinemia in term and near-term newborns. *Pediatrics* **1995**, 95 (4), 468-474.
- [135] Stevenson, D. K.; Wong, R. J. Metalloporphyrins in the management of neonatal hyperbilirubinemia. *Semin. Fetal Neonatal. Med.* **2010**, 15 (3), 164-168.
- [136] Tsukigawa, K.; Nakamura, H.; Fang, J.; Otagiri, M.; Maeda, H. Effect of different chemical bonds in pegylation of zinc protoporphyrin that affects drug release,

- intracellular uptake, and therapeutic effect in the tumor. *Eur. J. Pharm. Biopharm.* **2015**, *89*, 259-270.
- [137] Nakamura, H.; Fang, J.; Gahininath, B.; Tsukigawa, K.; Maeda, H. Intracellular uptake and behavior of two types zinc protoporphyrin (ZnPP) micelles, SMA-ZnPP and PEG-ZnPP as anticancer agents; unique intracellular disintegration of SMA micelles. *J. Control Release* **2011**, *155* (3), 367-375.
- [138] Fang, J.; Greish, K.; Qin, H.; Liao, L.; Nakamura, H.; Takeya, M.; Maeda, H. HSP32 (HO-1) inhibitor, copoly(styrene-maleic acid)-zinc protoporphyrin IX, a water-soluble micelle as anticancer agent: In vitro and in vivo anticancer effect. *Eur. J. Pharm. Biopharm.* **2012**, *81* (3), 540-547.
- [139] Sahoo, S. K.; Sawa, T.; Fang, J.; Tanaka, S.; Miyamoto, Y.; Akaike, T.; Maeda, H. Pegylated zinc protoporphyrin: a water-soluble heme oxygenase inhibitor with tumor-targeting capacity. *Bioconjug. Chem.* **2002**, *13* (5), 1031-1038.
- [140] Walker, K. A.; Kertesz, D. J.; Rotstein, D. M.; Swinney, D. C.; Berry, P. W.; So, O. Y.; Webb, A. S.; Watson, D. M.; Mak, A. Y.; Burton, P. M.; Mills-Dunlap, B.; Chiou, M. Y.; Tokes, L. G.; Kurz, L. J.; Kern, J. R.; Chan, K. W.; Salari, A.; Mendizabal, J. R. Selective inhibition of mammalian lanosterol 14  $\alpha$ -demethylase: a possible strategy for cholesterol lowering. *J. Med. Chem.* **1993**, *36* (15), 2235-2237.
- [141] Vlahakis, J. Z.; Kinobe, R. T.; Bowers, R. J.; Brien, J. F.; Nakatsu, K.; Szarek, W. A. Synthesis and evaluation of azalanstat analogues as heme oxygenase inhibitors. *Bioorg. Med. Chem. Lett.* **2005**, *15* (5), 1457-1461.
- [142] Vlahakis, J. Z.; Hum, M.; Rahman, M. N.; Jia, Z.; Nakatsu, K.; Szarek, W. A. Synthesis and evaluation of imidazole-dioxolane compounds as selective heme oxygenase inhibitors: effect of substituents at the 4-position of the dioxolane ring. *Bioorg. Med. Chem.* **2009**, *17* (6), 2461-2475.
- [143] Vlahakis, J. Z.; Kinobe, R. T.; Bowers, R. J.; Brien, J. F.; Nakatsu, K.; Szarek, W. A. Imidazole-dioxolane compounds as isozyme-selective heme oxygenase inhibitors. *J. Med. Chem.* **2006**, *49* (14), 4437-4441.
- [144] Roman, G.; Riley, J. G.; Vlahakis, J. Z.; Kinobe, R. T.; Brien, J. F.; Nakatsu, K.; Szarek, W. A. Heme oxygenase inhibition by 2-oxy-substituted 1-(1H-imidazol-1-yl)-4-phenylbutanes: effect of halogen substitution in the phenyl ring. *Bioorg. Med. Chem.* **2007**, *15* (9), 3225-3234.

- [145] Rahman, M. N.; Vlahakis, J. Z.; Szarek, W. A.; Nakatsu, K.; Jia, Z. X-ray crystal structure of human heme oxygenase-1 in complex with 1-(adamantan-1-yl)-2-(1H-imidazol-1-yl)ethanone: a common binding mode for imidazole-based heme oxygenase-1 inhibitors. *J. Med. Chem.* **2008**, *51* (19), 5943-5952.
- [146] Sugishima, M.; Higashimoto, Y.; Oishi, T.; Takahashi, H.; Sakamoto, H.; Noguchi, M.; Fukuyama, K. X-ray crystallographic and biochemical characterization of the inhibitory action of an imidazole-dioxolane compound on heme oxygenase. *Biochemistry* **2007**, *46* (7), 1860-1867.
- [147] Rahman, M. N.; Vlahakis, J. Z.; Vukomanovic, D.; Szarek, W. A.; Nakatsu, K.; Jia, Z. X-ray crystal structure of human heme oxygenase-1 with (2R,4S)-2-[2-(4-chlorophenyl)ethyl]-2-[(1H-imidazol-1-yl)methyl]-4[(5-trifluoromethylpyridin-2-yl)thio)methyl]-1,3-dioxolane: a novel, inducible binding mode. *J. Med. Chem.* **2009**, *52* (15), 4946-4950.
- [148] Rahman, M. N.; Vlahakis, J. Z.; Roman, G.; Vukomanovic, D.; Szarek, W. A.; Nakatsu, K.; Jia, Z. Structural characterization of human heme oxygenase-1 in complex with azole-based inhibitors. *J. Inorg. Biochem.* **2010**, *104* (3), 324-330.
- [149] Rahman, M. N.; Vlahakis, J. Z.; Vukomanovic, D.; Lee, W.; Szarek, W. A.; Nakatsu, K.; Jia, Z. A novel, "double-clamp" binding mode for human heme oxygenase-1 inhibition. *PloS one* **2012**, *7* (1), e29514.
- [150] Rahman, M. N.; Vukomanovic, D.; Vlahakis, J. Z.; Szarek, W. A.; Nakatsu, K.; Jia, Z. Structural insights into human heme oxygenase-1 inhibition by potent and selective azole-based compounds. *J. R. Soc. Interface* **2013**, *10* (78), 20120697.
- [151] Roman, G.; Rahman, M. N.; Vukomanovic, D.; Jia, Z.; Nakatsu, K.; Szarek, W. A. Heme oxygenase inhibition by 2-oxy-substituted 1-azolyl-4-phenylbutanes: effect of variation of the azole moiety. X-ray crystal structure of human heme oxygenase-1 in complex with 4-phenyl-1-(1H-1,2,4-triazol-1-yl)-2-butanone. *Chem. Biol. Drug. Des.* **2010**, *75* (1), 68-90.
- [152] Hum, M.; McLaughlin, B. E.; Roman, G.; Vlahakis, J. Z.; Szarek, W. A.; Nakatsu, K. The effects of azole-based heme oxygenase inhibitors on rat cytochromes P450 2E1 and 3A1/2 and human cytochromes P450 3A4 and 2D6. *J. Pharmacol. Exp. Ther.* **2010**, *334* (3), 981-987.

- [153] Roman, G.; Vlahakis, J. Z.; Vukomanovic, D.; Nakatsu, K.; Szarek, W. A. Heme oxygenase inhibition by 1-aryl-2-(1H-imidazol-1-yl/1H-1,2,4-triazol-1-yl)ethanones and their derivatives. *ChemMedChem* **2010**, *5* (9), 1541-1555.
- [154] Vlahakis, J. Z.; Lazar, C.; Roman, G.; Vukomanovic, D.; Nakatsu, K.; Szarek, W. A. Heme oxygenase inhibition by  $\alpha$ -(1H-imidazol-1-yl)- $\omega$ -phenylalkanes: effect of introduction of heteroatoms in the alkyl linker. *ChemMedChem* **2012**, *7* (5), 897-902.
- [155] Sorrenti, V.; Guccione, S.; Di Giacomo, C.; Modica, M. N.; Pittalà, V.; Acquaviva, R.; Basile, L.; Pappalardo, M.; Salerno, L. Evaluation of imidazole-based compounds as heme oxygenase-1 inhibitors. *Chem. Biol. Drug. Des.* **2012**, *80* (6), 876-886.
- [156] Salerno, L.; Floresta, G.; Ciaffaglione, V.; Gentile, D.; Margani, F.; Turnaturi, R.; Rescifina, A.; Pittalà, V. Progress in the development of selective heme oxygenase-1 inhibitors and their potential therapeutic application. *Eur. J. Med. Chem.* **2019**, *167*, 439-453.
- [157] Salerno, L.; Pittalà, V.; Romeo, G.; Modica, M. N.; Siracusa, M. A.; Di Giacomo, C.; Acquaviva, R.; Barbagallo, I.; Tibullo, D.; Sorrenti, V. Evaluation of novel aryloxyalkyl derivatives of imidazole and 1,2,4-triazole as heme oxygenase-1 (HO-1) inhibitors and their antitumor properties. *Bioorg. Med. Chem.* **2013**, *21* (17), 5145-5153.
- [158] Salerno, L.; Pittalà, V.; Romeo, G.; Modica, M. N.; Marrazzo, A.; Siracusa, M. A.; Sorrenti, V.; Di Giacomo, C.; Vanella, L.; Parayath, N. N.; Greish, K. Novel imidazole derivatives as heme oxygenase-1 (HO-1) and heme oxygenase-2 (HO-2) inhibitors and their cytotoxic activity in human-derived cancer cell lines. *Eur. J. Med. Chem.* **2015**, *96*, 162-172.
- [159] Amata, E.; Marrazzo, A.; Dichiara, M.; Modica, M. N.; Salerno, L.; Prezavento, O.; Nastasi, G.; Rescifina, A.; Romeo, G.; Pittalà, V. Heme Oxygenase Database (HemeOxDB) and QSAR Analysis of Isoform 1 Inhibitors. *ChemMedChem* **2017**, *12* (22), 1873-1881.
- [160] Salerno, L.; Amata, E.; Romeo, G.; Marrazzo, A.; Prezavento, O.; Floresta, G.; Sorrenti, V.; Barbagallo, I.; Rescifina, A.; Pittalà, V. Potholing of the hydrophobic heme oxygenase-1 western region for the search of potent and selective imidazole-based inhibitors. *Eur. J. Med. Chem.* **2018**, *148*, 54-62.

- [162] Floresta, G.; Carotti, A.; Ianni, F.; Sorrenti, V.; Intagliata, S.; Rescifina, A.; Salerno, L.; Di Michele, A.; Sardella, R.; Pittalà, V. Chromatographic resolution of phenylethanolic-azole racemic compounds highlighted stereoselective inhibition of heme oxygenase-1 by (R)-enantiomers. *Bioorg. Chem.* **2020**, *99*, 103777.
- [162] Greish, K. F.; Salerno, L.; Al Zahrani, R.; Amata, E.; Modica, M. N.; Romeo, G.; Marrazzo, A.; Prezzavento, O.; Sorrenti, V.; Rescifina, A.; Floresta, G.; Intagliata, S.; Pittalà, V. Novel Structural Insight into Inhibitors of Heme Oxygenase-1 (HO-1) by New Imidazole-Based Compounds: Biochemical and In Vitro Anticancer Activity Evaluation. *Molecules* **2018**, *23* (5), 1209.
- [163] Ciaffaglione, V.; Intagliata, S.; Pittalà, V.; Marrazzo, A.; Sorrenti, V.; Vanella, L.; Rescifina, A.; Floresta, G.; Sultan, A.; Greish, K.; Salerno, L. New Arylethanolimidazole Derivatives as HO-1 Inhibitors with Cytotoxicity against MCF-7 Breast Cancer Cells. *Int. J. Mol. Sci.* **2020**, *21* (6), 1923.
- [164] Floresta, G.; Amata, E.; Dichiara, M.; Marrazzo, A.; Salerno, L.; Romeo, G.; Prezzavento, O.; Pittalà, V.; Rescifina, A. Identification of Potentially Potent Heme Oxygenase 1 Inhibitors through 3D-QSAR Coupled to Scaffold-Hopping Analysis. *ChemMedChem* **2018**, *13* (13), 1336-1342.
- [165] Floresta, G.; Pittalà, V.; Sorrenti, V.; Romeo, G.; Salerno, L.; Rescifina, A. Development of new HO-1 inhibitors by a thorough scaffold-hopping analysis. *Bioorg. Chem.* **2018**, *81*, 334-339.
- [166] Mucha, O.; Podkalicka, P.; Mikulski, M.; Barwacz, S.; Andrysiak, K.; Biela, A.; Mieczkowski, M.; Kachamakova-Trojanowska, N.; Ryszawy, D.; Białas, A.; Szelażek, B.; Grudnik, P.; Majewska, E.; Michalik, K.; Jakubiec, K.; Bień, M.; Witkowska, N.; Gluza, K.; Ekonomiuk, D.; Sitarz, K.; Gałęzowski, M.; Brzózka, K.; Dubin, G.; Józkwicz, A.; Dulak, J.; Łoboda, A. Development and characterization of a new inhibitor of heme oxygenase activity for cancer treatment. *Arch. Biochem. Biophys.* **2019**, *671*, 130-142.
- [167] Sorrenti, V.; Pittalà, V.; Romeo, G.; Amata, E.; Dichiara, M.; Marrazzo, A.; Turnaturi, R.; Prezzavento, O.; Barbagallo, I.; Vanella, L.; Rescifina, A.; Floresta, G.; Tibullo, D.; Di Raimondo, F.; Intagliata, S.; Salerno, L. Targeting heme Oxygenase-1 with hybrid compounds to overcome Imatinib resistance in chronic myeloid leukemia cell lines. *Eur. J. Med. Chem.* **2018**, *158*, 937-950.



- [168] Salerno, L.; Vanella, L.; Sorrenti, V.; Consoli, V.; Ciaffaglione, V.; Fallica, A. N.; Canale, V.; Zajdel, P.; Pignatello, R.; Intagliata, S. Novel mutual prodrug of 5-fluorouracil and heme oxygenase-1 inhibitor (5-FU/HO-1 hybrid): design and preliminary in vitro evaluation. *J. Enzyme Inhib. Med. Chem.* **2021**, *36* (1), 1378-1386.
- [169] Vlahakis, J. Z.; Vukomanovic, D.; Nakatsu, K.; Szarek, W. A. Selective inhibition of heme oxygenase-2 activity by analogs of 1-(4-chlorobenzyl)-2-(pyrrolidin-1-ylmethyl)-1H-benzimidazole (clemizole): Exploration of the effects of substituents at the N-1 position. *Bioorg. Med. Chem.* **2013**, *21* (21), 6788-6795.
- [170] Kong, X.; Vukomanovic, D.; Nakatsu, K.; Szarek, W. A. Structure-Activity Relationships of 1,2-Disubstituted Benzimidazoles: Selective Inhibition of Heme Oxygenase-2 Activity. *ChemMedChem* **2015**, *10* (8), 1435-1441.
- [171] Intagliata, S.; Salerno, L.; Ciaffaglione, V.; Leonardi, C.; Fallica, A. N.; Carota, G.; Amata, E.; Marrazzo, A.; Pittalà, V.; Romeo, G. Heme Oxygenase-2 (HO-2) as a therapeutic target: Activators and inhibitors. *Eur. J. Med. Chem.* **2019**, *183*, 111703.

## Identification of a potent heme oxygenase-2 (HO-2) inhibitor by targeting the secondary hydrophobic pocket of the HO-2 western region

Giuseppe Floresta <sup>a, b</sup>, Antonino N. Fallica <sup>a</sup>, Giuseppe Romeo <sup>a</sup>, Valeria Sorrenti <sup>a</sup>, Loredana Salerno <sup>a</sup>, Antonio Rescifina <sup>a</sup>, Valeria Pittalà <sup>a,\*</sup>

<sup>a</sup> Department of Drug Sciences, University of Catania, V.le A. Doria 6, 95125 – Catania, Italy

<sup>b</sup> Department of Analytics, Environmental & Forensics, King's College London, Stamford Street, London SE1 9NH, UK

*Bioorganic Chemistry*

Received: July 16, 2020; Received in revised form: September 15, 2020; Accepted: September 20, 2020

**ABSTRACT:** The enzymatic family of heme oxygenase (HO) is accountable for heme breakdown. Among the two isoforms characterized to date, HO-2 is poorly investigated due to the lack of potent HO-2 chemical modulators and the greater attentiveness towards HO-1 isoform. In the present paper, we report the rational design and synthesis of HO-2 inhibitors achieved by modulating the volume of known HO-1 inhibitors. The inhibition preference has been moved from HO-1 to HO-2 by merely increasing the volume of the substituent in the western region of the inhibitors. Docking studies demonstrated that new derivatives soak differently in the two binding pockets, probably due to the presence of a Tyr187 residue in HO-2. These findings could be useful for the design of new selective HO-2 compounds.

**KEYWORDS:** Heme oxygenase-2, heme oxygenase-1, imidazole derivatives, structure-activity relationships, western region, azalanstat.

**\*Corresponding author:**

Valeria Pittalà (vpittala@unict.it)

## 1. Introduction

Endogenous enzymes in control of heme breakdown are known as heme oxygenases (HOs). These enzymes exert cytoprotective roles in organs and are responsible for degrading senescent red-blood cells through the removal of the pro-inflammatory heme and the production of protecting by-products such as carbon monoxide (CO) and bilirubin [1]. This group of enzymes includes two well-characterized isoforms, heme oxygenase-1 (HO-1) and heme oxygenase-2 (HO-2), differing for distribution and expression level under different conditions. HO-1 is highly represented only in limited areas such as the liver and spleen, whereas HO-2 is widely distributed among different endogenous areas with a prevalence in the brain, testes, endothelial and smooth muscle cells, myenteric gut plexus, nephrons, and liver [2]. However, while HO-2 distribution remains unchanged regardless of the endogenous oxidative stress status, HO-1 undergoes an overexpression process, controlled by the transcription factor nuclear factor erythroid 2-related factor-2 (Nrf2), with consequent increment in districts where cellular stress must be reduced [1, 3-5]. For such reason, HO-1 received considerable attention in recent years, and the use of HO-1 inducers are advantageous in various oxidative stresses dependent syndromes [6-12].

Nonetheless, an increasing amount of literature recently suggests that HO-1 might play its part in tumor initiation. HO-1 expression is frequently heightened in cancer tissues promoting atypical cellular growth and metastasis onset in different types of cancer and eventually leads to reduced chances of survival [13, 14]. Also, HO-1 levels could be further boosted when those tissues are exposed to different types of tumor treatment, such as radio-, chemo-, or photodynamic [15-18]. It can powerfully improve the growth and spread of cancers suggesting that the role of HO-1 in heme metabolism makes it an essential mediator to protective effects not only towards healthy cells but also towards the cancerous ones. Previous studies demonstrated the involvement of HO-1 in different tumors, including leukemia, glioblastoma, neuroblastoma, prostate, breast, lung, head, and neck cancers [14, 19-21]. Because of this, HO-1 inhibition might reduce aberrant cellular proliferation, tumor invasion, and progression [22-26].

Dissimilar to HO-1 inhibitors/activators, the possible beneficial applications of HO-2 ligands have not been systematically investigated so far [27]. Moreover, the functional role of HO-2 is still elusive, mostly owing to the absence of highly potent HO-2 chemical modulators and the higher interest towards HO-1 isoform. HO-2 physiological roles have been studied mostly in organs such as the liver, testis, and brain, where this isoform is

expressed constitutively and is more abundant [2, 28]. For instance, in testis, HO-2 seems to take part in male reproduction and in the modulation of the ejaculatory activity. The role of HO-2 in the brain is still puzzling, and it is the subject of numerous investigations due to its favorable involvement in neuroprotection and brain injuries [29]. Although increasing knowledge has been gained over the past decade to unravel the physiological role of HO-2, its full potential as a druggable target remains to be elucidated. Therefore, the development of selective and potent HO-2 inhibitors and/or activators is required as pharmacological tools to gain knowledge in the field.

Historically, heme analogs (metalloporphyrins, MPs) lead the research to the development of HO inhibitors; however, their off-target effects limited their translation into the clinic. Therefore, the attention was devoted to azalanstat (Figure 1, compound **1**) that served as a lead compound for the development of selective non-competitive HO-1 and HO-2 inhibitors.

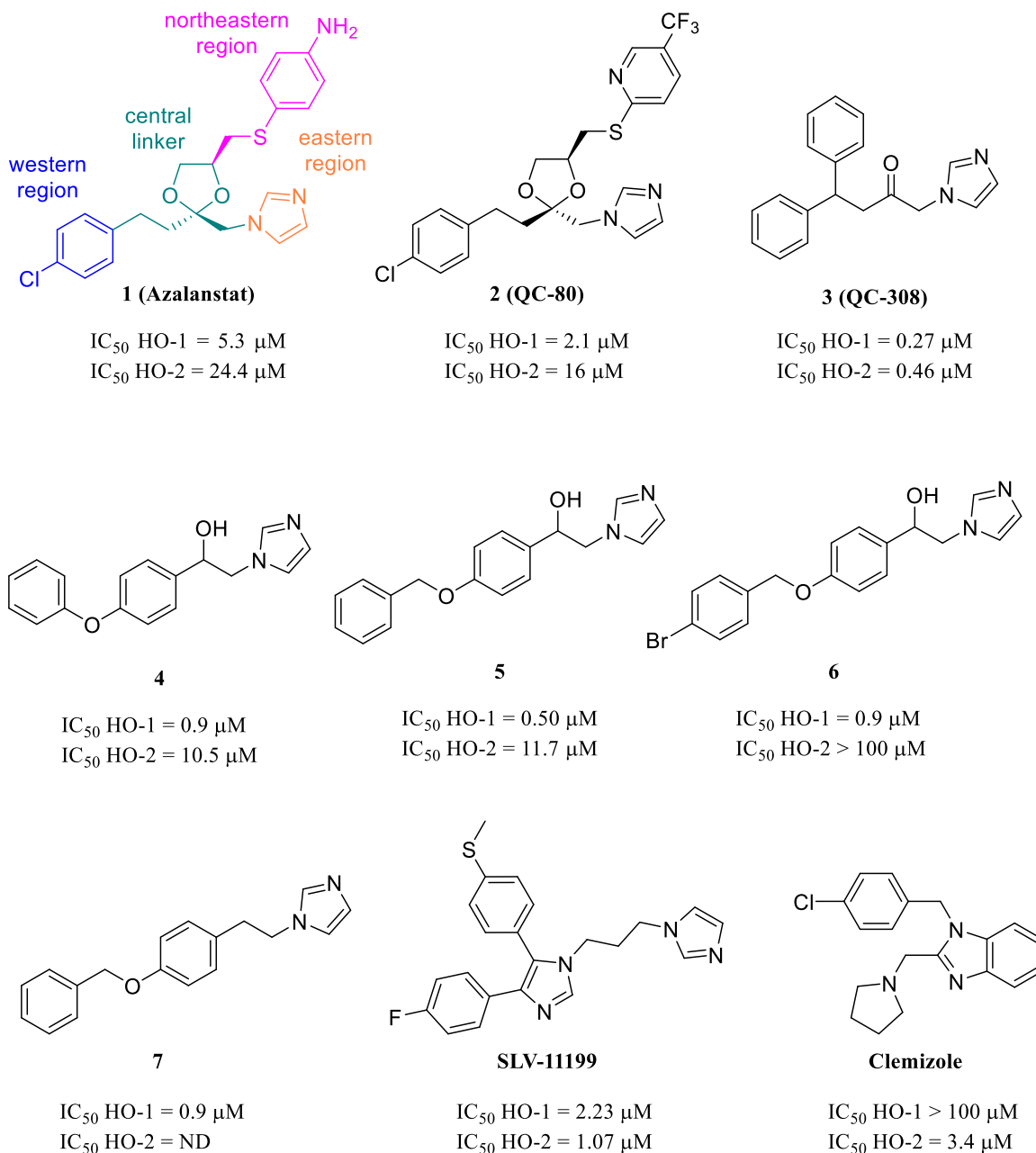


**Figure 1.** Chemical structure of lead compounds, azalanstat, QC-80, QC-308, and other representatives HO selective and non-selective inhibitors.

More than fifteen years of studies on the structure-activity relationships (SARs) on azalanstat focused on the development of selective HO-1 inhibitors allowed the identification of the main key features for HO inhibition, as confirmed by crystallization studies of HO-1 inhibitors complexed with the enzyme [29-31]. Briefly, four main regions (northeastern, eastern, central, and western) can be recognized in the chemical structure of

azalanstat corresponding to four primary areas of interactions inside the HO binding pocket. The northeastern area is not mandatory for HO-1 inhibition, and it is often removed. The eastern region is the most preserved portion of the molecule since it permits the binding to the Fe<sup>2+</sup> of heme. An unsubstituted imidazole provides the best results in term of potency; limited modifications are tolerated in this area, and the majority of them leads to loss of inhibition potency. The central part can be subjected to various modifications regarding the length and the presence of different functional groups/heteroatoms, allowing the optimization of the inhibitory activity. The western region offers a right area for the modulation of activity and selectivity. The type, volume, and nature of the substituents present in this area (large hydrophobic groups seem to be preferred) can additionally stabilize the heme-binding. Substituents in this area interact with the distal hydrophobic pocket of HO. Of interest is the high flexibility of this pocket and the consequent capability to receive moieties of different sizes. Also, crystallization studies on QC-80 and QC-308 (Figure 1, compounds **2** and **3**, respectively) brought to light the presence of a secondary small hydrophobic pocket in the western region [32, 33]. Interactions with this secondary pocket seem to enhance binding potency towards both HO-1 and HO-2 isoforms.

Over the past decade, our research group has been continuously involved in the rational design of selective inhibitors directed towards the two HO isoforms using azole-based scaffolds [23, 25, 34-37]. To this extent, we built a free-internet accessible database bringing together all the HO inhibitors published so far, whose analysis empowered the design of potent selective and non-selective HO-1 inhibitors such as compounds **4-7** (Figure 1) [37-39]. Recently, Mucha and coworkers reported the development and characterization of a novel non-selective HO inhibitor, SLV-11199 (Figure 1), with anticancer effects on human pancreatic (PANC-1) and prostate (DU-145) cancer cell lines [40]. The chemical structure of this novel compound presents the usual imidazole ring in the eastern region; however, an additional 1,4,5-trisubstituted imidazole ring is present in the central region, allowing a more rigid structure and an additional hydrogen bond with the Arg136 sidechain in the catalytic pocket of the enzyme. This additional interaction, together with the binding mode similar to that of QC-308, explains the potent inhibitory activity of SLV-11199 towards both HO isoforms, even if selectivity issues remain. Pushed by these results, the activity of SLV-11199 was evaluated in hereditary leiomyomatosis and renal cell carcinoma (HLRCC), a cancer cell line characterized by deficiency in the fumarate hydratase (FH) gene. Genetic or pharmacological inhibition of HO-1 with SLV-11199 in FH deficient cell lines leads to

synthetic lethality [41]. Fewer studies have been specifically conducted in search of selective HO-2 inhibitors, which lead to the identification of the highly selective clemizole (Figure 1), possessing a benzimidazole scaffold [42]. Structure-activity relationships studies on clemizole have been performed by changing the substituents at N-1 position. The novel derivatives showed to possess similar or slight better potencies against HO-2, and their development represented the first attempt for the search of selective HO-2 inhibitors.

The aim of the present study is the rational design and synthesis of a small series of derivatives oriented towards HO-2 selective inhibition. To this extent, we maintained fixed the imidazole ring and the length of the spacer, rationally modifying the nature of the spacer and the volume of the western region in order to switch both selectivity and potency towards HO-2.

## 2. Results and discussion

### 2.1. Rationale design

As already pointed out in our previous work, the selectivity between the two different isoforms can be triggered by the volume of the molecules and so the design of a novel inhibitor can be tuned exploiting these observations [37]. In fact, even if the binding pockets of the two proteins are relatively flexible, the four most selective, and also potent HO-1 inhibitors, retrieved by the heme-oxygenase database (HemeOxDB2, HemeOxDB16, HemeOxDB18, HemeOxDB20; <http://www.researchdsf.unict.it/hemeoxdb/>) possess a mean Van der Waals volume of 274.34 Å<sup>3</sup> with an interval of 239.00–302.87 Å<sup>3</sup>; differently, potent and selective HO-2 inhibitors (HemeOxDB187, HemeOxDB200, HemeOxDB202, and HemeOxDB286) have a mean volume of 284.10 Å<sup>3</sup> with an interval of 274.37–306.75 Å<sup>3</sup> [37-39]. These observations lead us to think that the volume of the ligands is an essential factor influencing the selectivity, considering as a rule of thumb that the larger the cavity of the isoform, the greater the volume of the ligand to achieve the best binding potency and selectivity. This empirical rule was already successful for the design of novel HO-1 inhibitors [37] (*i.e.*, smaller molecules for selective and potent HO-1 compounds). This work aimed to apply the same rule for the design of novel HO-2 selective compounds (*i.e.*, bigger molecules for selective and potent HO-2 compounds); moreover, the bigger ligand should be easily accommodated in the secondary hydrophobic pocket of the HO-2 western region.

To actively validate this hypothesis, we designed the HO-2 inhibitors starting from two molecules with high HO-1 inhibition activity but not with high selectivity. So, we simply increased the volume of the compounds **5** and **7** adding them a cyano group, as shown in Table 1. In both cases, the selected cyano group added about 20 Å<sup>3</sup> to the final volume of the molecules (Table 1, *i.e.*, increasing the volume size and so theoretically moving the selectivity from HO-1 to HO-2); moreover, the position 4 of the ring system was selected to explore possible interactions with the bottom of the secondary hydrophobic pocket of the HO-2 western region (Figure 2). The cyano group has also been selected because able to be placed deeper in the HO-2 cavity. In fact, despite molecule **9** has a bigger but similar volume than the bromo-derivative **6** (336.32 Å<sup>3</sup> vs. 334.46 Å<sup>3</sup>), the cyano group led the molecule to reach the bottom of the secondary hydrophobic pocket of the HO-2 western region, differently to compound **6** (Figure 1). The measured distances between the nitrogen of molecule **9**, the bromine of **6**, and the respective benzylic CH<sub>2</sub> are 6.88 and 6.10 Å, respectively (Figure 3).

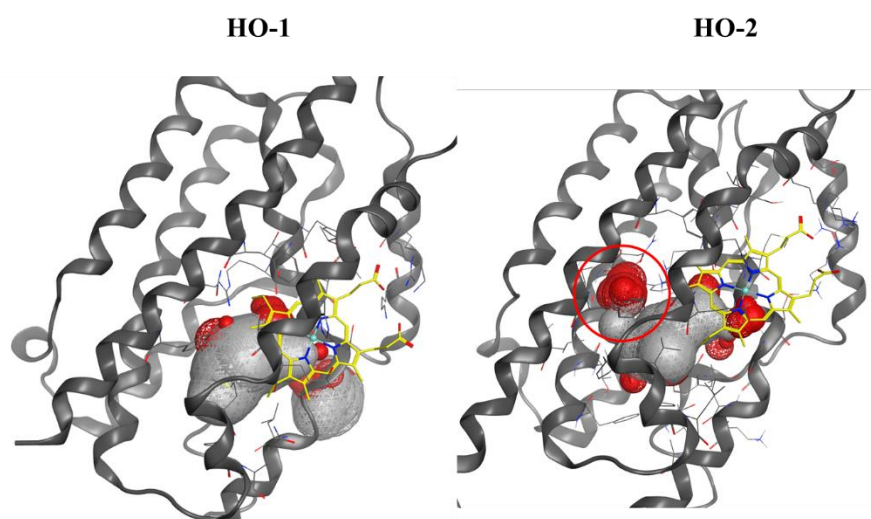


**Figure 2.** Left. HO-1 binding pocket (PDB ID: 2DY5). Right, HO-2 binding pocket (PDB ID: 2QPP), the secondary hydrophobic pocket of the HO-2 western region, is circled in red.



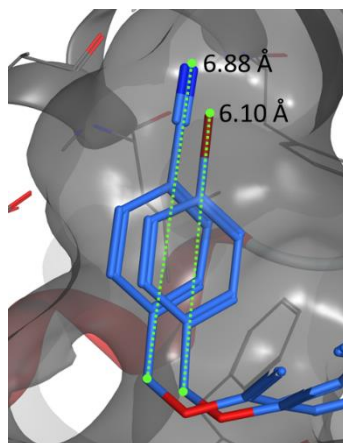
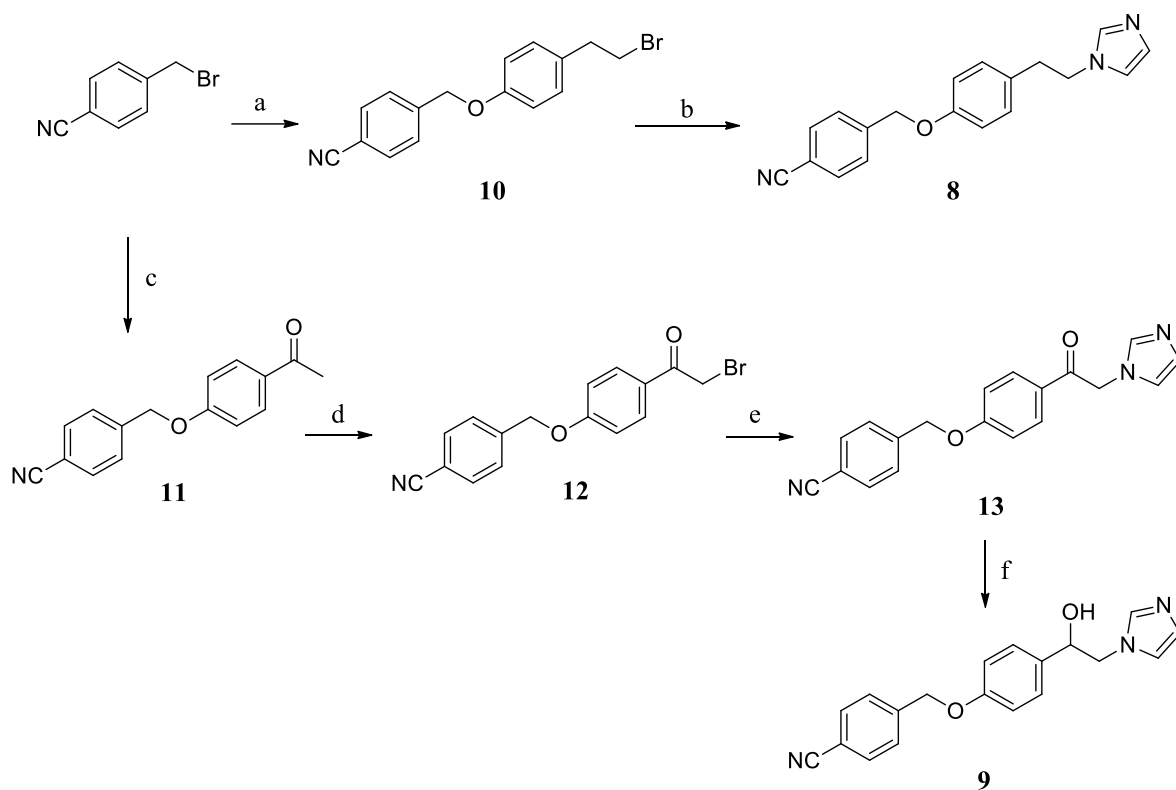


**Figure 3.** Distances between the nitrogen of molecule **9**, the bromine of molecule **6**, and the respectively benzylic CH<sub>2</sub> inside the secondary hydrophobic pocket of the HO-2 western region.

## 2.2. Chemistry

The general synthetic pathway to the new compounds is depicted in Scheme 1. Compound **8** was prepared in two steps as follows: the reaction between 4-(bromomethyl)benzonitrile and 4-(2-bromoethyl)phenol in acetone afforded the bromide derivative **10**. This intermediate was converted to the final compound **8** through a nucleophilic displacement using an excess of imidazole in the presence of TEA and TBAB, using dry CH<sub>3</sub>CN as solvent.

The synthesis of compounds **13** and **9** passes through the formation of the intermediate **11** that was prepared by reaction of 1-(4-hydroxyphenyl)ethanone with 4-(bromomethyl)benzonitrile, as reported in Scheme 1. The 1-substituted bromomethyl ketone **12** was obtained by bromination, in the glacial acetic acid, of the corresponding ketone **11**. The latter has been used without purification to synthesize compound **13**, through a nucleophilic displacement using an excess of imidazole in the presence of K<sub>2</sub>CO<sub>3</sub>. The obtained ketone **13** was then reduced with NaBH<sub>4</sub> to the final compound **9**.

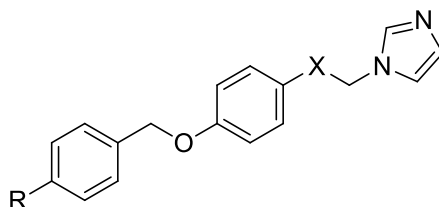


**Scheme 1.** Reagents and conditions: (a) 4-(2-bromoethyl)phenol,  $K_2CO_3$ , acetone, room temperature, 20 h; (b) imidazole, TEA, TBAB,  $CH_3CN$  dry, 90 °C, 45 min; (c) 1-(4-hydroxyphenyl)ethanone,  $K_2CO_3$ , acetone, room temperature, 20 h; (d) glacial acetic acid, HCl,  $Br_2$ , room temperature; (e)  $K_2CO_3$ , imidazole, DMF, room temperature, 2 h; (f)  $NaBH_4$ ,  $CH_3OH$ , room temperature, reflux, 2 h.

### 2.3. HO inhibition and docking studies

The inhibitory activity of the newly synthesized compounds was measured using HO-1 and HO-2 isoforms extracted from rat spleen and rat brain microsomal fractions, respectively. The inhibitory activity is reported as  $IC_{50}$  ( $\mu M$ ), and obtained data are outlined in Table 1, employing azalanstat as the reference compound. All the compounds exhibited good inhibitory potency towards HO-1 and HO-2. Compound 9 showed remarkable HO-2  $IC_{50}$  values  $<1 \mu M$  and interesting selectivity towards HO-1 ( $SI >15$ ). Furthermore, a comparison between the HO-2  $IC_{50}$  values of compound 9 and clemizole highlights that the former is about 5-fold more potent than clemizole ( $0.9 \mu M$  vs  $3.4 \mu M$ , respectively), but less selective in terms of HO-1 inhibition.

**Table 1.** Chemical structures of rationally designed compounds **8** and **9** starting from known HO-1 inhibitors **5** and **7** and experimental IC<sub>50</sub> values and selectivity index (SI) of compounds **8**, **9**, and **13** towards HO-1 and HO-2.



Compound	R	X	HO-1 IC <sub>50</sub> (μM) <sup>a</sup>	HO-2 IC <sub>50</sub> (μM) <sup>a</sup>	SI (HO-1/HO-2)	Volume
<b>5</b>	H	CHOH	0.50 ±0.01 <sup>b</sup>	11.7 ±0.9	0.04	316.81 Å <sup>3</sup>
<b>7</b>	H	CH <sub>2</sub>	0.9 ±0.07 <sup>c</sup>	ND	ND	309.44 Å <sup>3</sup>
<b>8</b>	CN	CH <sub>2</sub>	50.5 ±0.8	56.1 ±1.6	0.90	328.96 Å <sup>3</sup>
<b>9</b>	CN	CHOH	14.9 ±0.5	0.9 ±0.06	16.6	336.32 Å <sup>3</sup>
<b>13</b>	CN	C=O	75.4 ±1.2	72.8 ±2.0	1.04	ND
<b>Azalanstat</b> <sup>c</sup>			5.30 ±0.4	24.40 ±0.8	0.23	ND

<sup>a</sup> Data are reported as IC<sub>50</sub> values in μM ±standard deviation (SD). Values are the mean of triplicate experiments. <sup>b</sup> Data from reference [37], <sup>c</sup> data from reference [34].

A docking study was performed to rationalize the obtained results. Docking was performed as described in the experimental section. The two binding pockets HO-1 and HO-2 were analyzed and aligned, resulted in a mean RMSD of 0.71 and a sequence identity of 77% (Table S1).

The results of the docking calculations are collected in Table 2, and the docking poses are shown in Figures 4 and S1–8. All of the studied compounds are located inside the binding pockets of both proteins with the nitrogen atom of the imidazole rings in the proximity of the ferrous iron of heme, and the calculated binding energies are in the right relationship with the measured ones (Table 2). In this way, the iron is protected from oxidation, and the enzymes are not able to perform their activity. The three different molecules (**8**, **13**, and **9**) have similar interactions within the same binding pocket of HO-1 as well as HO-2. However, it is interesting to notice that the molecules interact differently in the two different binding pockets, as reported in Figure 4. All the molecules inside the HO-1 interact in a similar way of classical HO-1 inhibitors, where the aromatic groups are in the principal western binding pocket (Phe37, Met34, Val50, Leu147, Ala151, Phe166, Phe167, Phe214).

Interestingly, the molecules inside the HO-2 are differently positioned, although the first aromatic ring can occupy the same spot inside the pocket, the terminal aromatic ring of all compounds is not located inside the principal western region but is located in the secondary western region of the HO-2. Interesting to notice that the Phe167 controls the gate access to the western region in HO-1 that is substituted by Tyr187 in HO-2. The presence of the Tyr187 closes the access for the principal western region and drives the terminal ring in the secondary western region of HO-2. The presence of the consensus water molecule inside the binding pockets was also studied. In fact, a similarly located consensus water molecule (that mediates the interaction with Thr135 in HO-1) is present in HO-2 interacting with Thr155. We already reported this consensus water molecule as a key factor in the enantiomer recognition for HO-1 [43]. For molecule **9**, in both the studied proteins, the consensus water can mediate an interaction between Thr135/155 and the hydroxyl group of **9**. In particular, the stronger interaction is the one with the *R*-enantiomer. Analyzing the binding pose of the most potent compound inside the HO-2 (Figure 5), it is possible to see that the compound is optimally placed inside the binding pocket interacting with Thr155 (through the consensus water) and with the Tyr 187, in this way **9** has optimum contact with the binding pocket residues of HO-2 and reach the highest binding energy value. The binding pose of this compound could be exploited for future designed HO-2 selective molecules based on a similar structure and targeting the consensus water and Tyr187 while occupying the secondary western region.

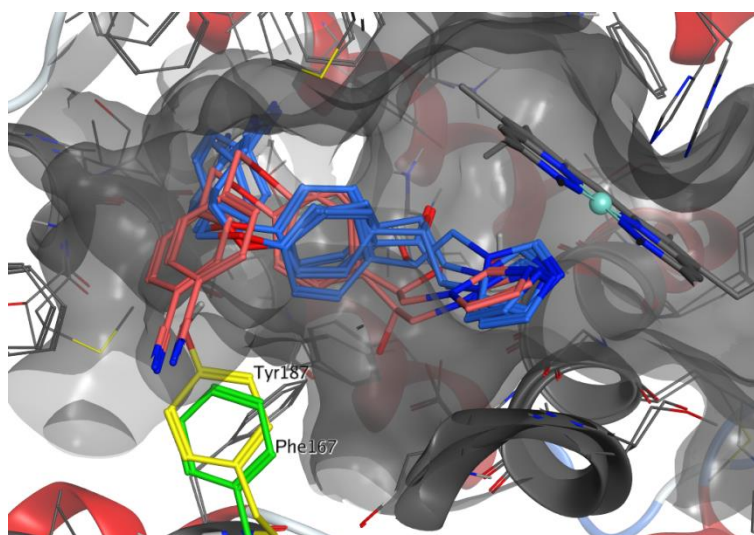


**Figure 4.** Binding poses of **8**, **13**, and **9** (*R* and *S*) in the aligned HO-1 and HO-2 binding pockets. In light red, the molecules inside HO-1, and in light blue the molecules inside HO-2. In yellow, the HO-2 Tyr187 and green the HO-1 Phe167.

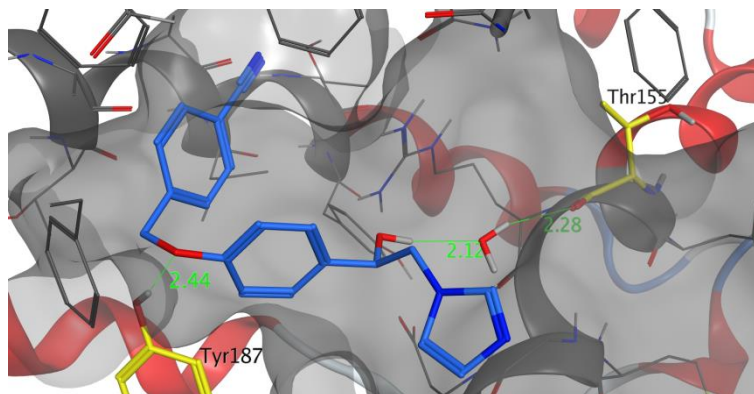


**Figure 5.** Binding poses of (*R*)-**9** in HO-2 binding pockets. Heme is removed for clarity, and Tyr187 and Thr155 are highlighted in yellow. The consensus water molecule is mediating an interaction between Thr155 and the -OH group of **9**.

**Table 2.** Docking results for the studied molecules **8**, **13**, and **9** (*R* and *S*).

Compound	HO-1 $\Delta G_B$ calcd. kcal/mol ( $K_i$ )	HO-2 $\Delta G_B$ calcd. kcal/mol ( $K_i$ )
	calcd. $\mu\text{M}$ )	calcd. $\mu\text{M}$ )
<b>8</b>	-5.82 (54.83)	-5.77 (58.67)
<b>13</b>	-5.40 (109.59)	-5.48 (95.74)
<b>(R)-9</b>	-6.60 (14.44)	-8.16 (1.03)
<b>(S)-9</b>	-6.23 (26.98)	-7.81 (1.87)

#### 2.4. ADMET assessment

To help us for a future selection of lead compounds and to further corroborate the molecular modeling and the in vitro evaluation, we also performed an in-silico absorption, distribution, metabolism, and excretion-toxicity (ADMET) pharmacokinetics evaluation. The *in-silico* assessment has been generated through the evaluation of pharmacokinetic profiles and possible adverse side effects for the molecules **8**, **9** and **13**. ADMET molecular studies were conducted using SwissADME (<http://swissadme.ch>) [44] and pkCSM (<http://biosig.unimelb.edu.au/pkcsm/>) [45], results are reported in the supporting information (Figures S9-S14).

All the three compounds resulted as orally available, with high gastrointestinal absorption and highly soluble in water. None of the compounds resulted as P-glycoprotein substrates; differently, most of the compounds are inhibitors of the CYP family proteins. Interestingly all of the compounds have no violation of the Lipinski rule of 5; they also have no violation of other drug-likeness rules (Ghose, Egan, Veber, and Muegee) [46-49]. The absorption and distribution calculated parameters have been depicted by the Edan–Egg model in Figure 6 (Brain or IntestinaL EstimateD, BOILED-Egg). The Edan-Egg model highlights that all compounds were predicted to passively permeate the blood-brain barrier and are not predicted to be effluated from the CNS by the P-glycoprotein. pkCSM calculated absorption properties showed a higher than 94% intestinal absorption due to the optimal ( $> 0.90$ ) Caco-2 cell permeability. Moreover, most of the compounds can be absorbed by the skin (exploitable for transdermal drug delivery), as showed by the  $\text{Log } K_p < -2.5$ .

The calculated values of the total clearance indicate that most of the compounds have a good renal elimination (1.07–1.11 mL/min kg) and all of them are substrates of the renal organic cation transporter 2. pkCSM calculated toxicity properties did not point out concerns about the AMES test. However, compounds **9** and **13** were predicted as hepatotoxic, and all compounds are predicted as inhibitors of the hERG II. On the other hand, the compounds have not skin sensitisation properties and are not inhibitors of the hERG I.

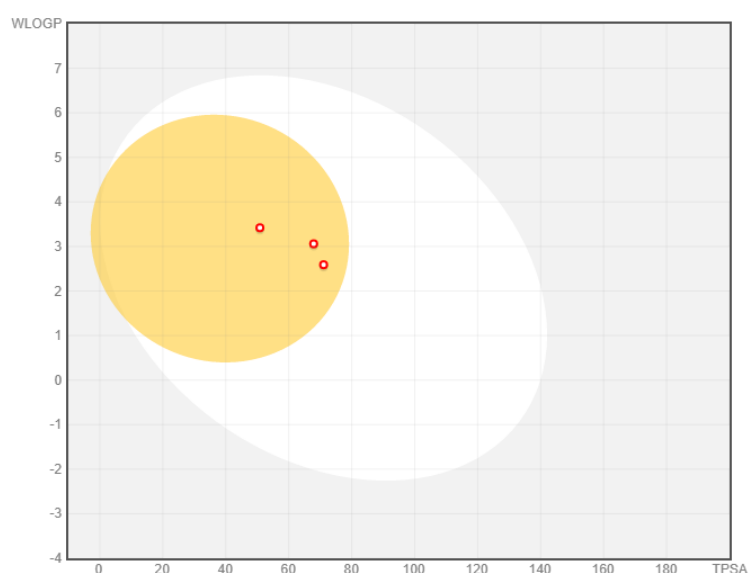


**Figure 6.** BOILED-Egg plot. Points located in the BOILED-Egg's yellow are the compounds predicted to permeate the BBB passively; differently, the ones in the white are

the molecules predicted to be only passively absorbed by the gastrointestinal tract. Blue dots indicate molecules expected to be refluxed from the central nervous system (CNS) by the P-glycoprotein, whereas the red ones are not transported by the P-glycoprotein.

### 3. Conclusions

The present study was aimed at unraveling the chemical requirements to obtain new selective HO-2 inhibitors. To this extent, we rationally designed a small, focused series of derivatives by playing with the volume of the molecules. Starting from HO-1 inhibitors previously reported in the literature and by merely increasing the volume of the western region, we switched the inhibition preference from HO-1 to HO-2. Molecular modeling studies helped in understanding the binding mode of these compounds, highlighting that the molecules correctly interact with the HO-1 and HO-2 binding site. The molecular modeling showed that the molecules differently interact with the two binding sites and that the presence of the HO-2 Tyr187 should represent the main reason for such a differentiation. Moreover, the consensus water molecule present in both binding sites can mediate an interaction with a Thr155 for the *R* enantiomer mainly. This set of described interactions can be useful for the design of new selective HO-2 compounds.

### 4. Experimental section

#### 4.1. Chemistry

Reactions were followed by TLC carried out on Sigma Aldrich silica plates (60 F254), using UV light (254 nm and 366 nm) for visualization and developed using I<sub>2</sub> chamber. Flash chromatographic purification on glasses columns was achieved employing Merck silica gel 60, 0.040–0.063 mm (230–400 mesh). Chemical syntheses requiring microwave irradiation were performed with a CEM Discover instrument using closed Pyrex glass tubes (ca. 10 mL) with Teflon-coated septa. Melting points were assigned by using an IA9200 Electrothermal apparatus furnished with a digital thermometer in capillary glass tubes and are uncorrected. Infrared spectra were recorded on a spectrometer in KBr disks or NaCl crystal windows. <sup>1</sup>H NMR spectra were recorded on a 200 or 500 MHz spectrometer in DMSO-*d*<sub>6</sub> solution. Chemical shifts are given in  $\delta$  values (ppm), using tetramethylsilane (TMS) as the internal standard; coupling constants (*J*) are given in Hz. Signal multiplicities are characterized as s (singlet), d (doublet), t (triplet), q (quartet), m (multiplet), br (broad). Elemental analyses for

C, H, N, and O were within  $\pm 0.4\%$  of theoretical values and were accomplished through a Carlo Erba Elemental Analyzer Mod. 1108 apparatus. Reagents, solvents, and starting materials were acquired from commercial suppliers.

#### 4.1.1. 4-[[4-(2-Bromoethyl)phenoxy]methyl]benzonitrile (**10**)

A mixture of 4-(bromomethyl)benzonitrile (3.5 mmol), 4-(2-bromoethyl)phenol (6.9 mmol), and  $\text{K}_2\text{CO}_3$  (6.9 mmol) in acetone (20 mL) was left stirring for 20 h, at room temperature. Then it was evaporated to dryness, added with deionized water (40 mL). The obtained suspension was left stirring for 15 min, filtered under vacuum, and washed twice with cold water. The white solid was left in the stove at 50 °C and crystallized using  $\text{C}_2\text{H}_5\text{OH}$  as solvent. The title compound was obtained as a pure white solid (59%): mp 90–92 °C;  $^1\text{H}$  NMR (200 MHz,  $\text{DMSO}-d_6$ ):  $\delta$  7.87 (d,  $J = 8.2$  Hz, 2H aromatic), 7.63 (d,  $J = 8.0$  Hz, 2H aromatic), 7.20 (d,  $J = 8.2$  Hz, 2H, aromatic), 6.95 (d,  $J = 8.4$  Hz, 2H, aromatic), 5.20 (s, 2H,  $\text{CH}_2\text{O}$ ), 3.67 (t,  $J = 7.2$  Hz, 2H,  $\text{CH}_2\text{CH}_2$ ), 3.05 (t,  $J = 7.2$  Hz, 2H,  $\text{CH}_2\text{CH}_2$ ). Anal. Calcd. for ( $\text{C}_{16}\text{H}_{14}\text{BrNO}$ ): C, 60.78; H, 4.46; N, 4.43. Found: C, 60.69; H, 4.48; N, 4.19.

#### 4.1.2. 4-[[4-[2-(1H-Imidazol-1-yl)ethyl]phenoxy]methyl]benzonitrile (**8**)

Compound **10** (0.95 mmol) was dissolved in anhydrous  $\text{CH}_3\text{CN}$  (5 mL). Then, imidazole (1.4 mmol), TEA (0.95 mmol) and TBAB (0.95 mmol) were added and the reaction mixture was left refluxing for 45 min in microwave (90 °C, 200 W, 150 Psi). The mixture was concentrated and the residue was dissolved in EtOAc (100 mL), washed with NaOH 0.1 N (3 $\times$ 50 mL) and brine (1 $\times$ 50 mL). The organic layer was dried over anhydrous  $\text{Na}_2\text{SO}_4$ , filtered and concentrated under vacuum. The obtained yellow oil was purified by flash chromatography (9.5 EtOAc/0.5  $\text{CH}_3\text{OH}$ ) affording a pure white solid (32%): mp 110–112 °C;  $^1\text{H}$  NMR (500 MHz,  $\text{DMSO}-d_6$ ):  $\delta$  7.86 (d,  $J = 8.4$  Hz, 2H, aromatic), 7.63 (d,  $J = 8.4$  Hz, 2H, aromatic), 7.47 (s, 1H, imidazole), 7.12 (s, 1H, imidazole), 7.09 (d,  $J = 8.6$  Hz, 2H, aromatic), 6.92 (d,  $J = 8.6$  Hz, 2H, aromatic), 6.84 (s, 1H, imidazole), 5.18 (s, 2H,  $\text{CH}_2\text{O}$ ), 4.15 (t,  $J = 7.3$  Hz, 2H,  $\text{CH}_2\text{CH}_2$ ), 2.95 (t,  $J = 7.3$  Hz, 2H,  $\text{CH}_2\text{CH}_2$ );  $^{13}\text{C}$  NMR (125 MHz,  $\text{DMSO}-d_6$ ):  $\delta$  156.52, 142.98, 132.33, 130.63, 129.67, 128.16, 127.98, 119.09, 118.69, 114.64, 110.36, 68.14, 47.29, 35.82. Anal. Calcd. for ( $\text{C}_{19}\text{H}_{17}\text{N}_3\text{O}$ ): C, 75.23; H, 5.65; N, 13.85. Found: C, 74.92; H, 5.66; N, 13.91.

#### 4.1.3. 4-[(4-Acetylphenoxy)methyl]benzonitrile (**11**)

A mixture of the appropriate commercially available 1-(4-hydroxyphenyl)ethanone (10 mmol) and 4-(bromomethyl)benzonitrile (10 mmol), in acetone (40 mL) and in the presence



of  $\text{K}_2\text{CO}_3$  (20 mmol) and a catalytic amount of KI was refluxed for 3 h. The reaction was checked for completion by TLC (7 Cy/3 EtOAc), and then, the solvent was evaporated. Distilled water was added, and the suspension was left stirring for 15 min, filtered and washed with water to obtain an off-white solid that was recrystallized from  $\text{C}_2\text{H}_5\text{OH}$ . Analytical characterization is in agreement with previously reported data [50].

#### 4.1.4. 4-[[4-(Bromoacetyl)phenoxy]methyl]benzonitrile (**12**)

4-[(4-Acetylphenoxy)methyl]benzonitrile **11** (5 mmol) was dissolved in glacial acetic acid (20 mL) and 0.5 mL of conc. HCl, then bromine (5 mmol) was added dropwise. The mixture was left stirring at room temperature until colorless. The obtained solution was dropped in saturated  $\text{NaHCO}_3$ , and the pH was adjusted to 9. The suspension obtained was filtered in vacuum to obtain a white solid. The residue was dissolved in DCM and washed with brine. The organic layer was dried over  $\text{Na}_2\text{SO}_4$ , filtered, and concentrated. The obtained crude **12** was used as such in the following step.

#### 4.1.5. 4-[[4-(1*H*-Imidazol-1-yl)acetyl]phenoxy]methyl]benzonitrile (**13**)

4-[[4-(Bromoacetyl)phenoxy]methyl]benzonitrile **12** (5 mmol), was dissolved in anhydrous DMF (15 mL) and added dropwise to a previously prepared suspension of imidazole (15 mmol) and  $\text{K}_2\text{CO}_3$  (15 mmol) in anhydrous DMF (20 mL). The obtained reaction mixture was left stirring for 2 h; then, water was added and the resulting suspension was filtered in vacuum. The obtained crude material was purified by column chromatography using 9.5 EtOAc/0.5  $\text{CH}_3\text{OH}$  as eluent. The residue was recrystallized from EtOAc to obtain a pure yellow solid (74%): mp 178–180 °C;  $^1\text{H}$  NMR (500 MHz,  $\text{DMSO}-d_6$ ):  $\delta$  8.01 (d,  $J = 8.9$  Hz, 2H, aromatic), 7.87 (d,  $J = 8.3$  Hz, 2H, aromatic), 7.66 (d,  $J = 8.3$  Hz, 2H, aromatic), 7.57 (s, 1H, imidazole), 7.19 (d,  $J = 8.9$  Hz, 2H, aromatic), 7.09 (s, 1H, imidazole), 6.91 (s, 1H, imidazole), 5.66 (s, 2H,  $\text{CH}_2\text{N}$ ), 5.35 (s, 2H,  $\text{CH}_2\text{O}$ );  $^{13}\text{C}$  NMR (125 MHz,  $\text{DMSO}-d_6$ ):  $\delta$  191.95, 162.33, 142.25, 138.40, 132.54, 130.44, 128.23, 127.82, 127.80, 121.01, 118.77, 115.05, 110.73, 68.63, 52.28. Anal. Calcd. for ( $\text{C}_{19}\text{H}_{15}\text{N}_3\text{O}_2$ ): C, 71.91; H, 4.76; N, 13.24. Found: C, 72.21; H, 4.79; N, 13.19.

#### 4.1.6. 4-[[4-[1-hydroxy-2-(1*H*-imidazol-1-yl)ethyl]phenoxy]methyl]benzonitrile (**9**)

A mixture of the imidazole-ketone **13** (0.63 mmol) and  $\text{NaBH}_4$  (1.26 mmol) in anhydrous  $\text{CH}_3\text{OH}$  (10 mL) was refluxed for 2 h; then it was evaporated to dryness, added with deionized water (40 mL), acidified with HCl 1 N and heated to 110 °C for 0.5 h. After cooling to room temperature, the reaction mixture was treated with a 1 N NaOH solution up

to a pH of 8.5 and the obtained suspension was filtered, washed repeatedly with water to neutrality, dried and crystallized from C<sub>2</sub>H<sub>5</sub>OH. The title compound was obtained as pure off-white solid (89%): mp 165–166 °C; <sup>1</sup>H NMR (500 MHz, DMSO-*d*<sub>6</sub>): δ 7.86 (d, *J* = 8.2 Hz, 2H, aromatic), 7.62 (d, *J* = 8.2 Hz, 2H, aromatic), 7.48 (s, 1H, imidazole), 7.25 (d, *J* = 8.6 Hz, 2H, aromatic), 7.09 (s, 1H, imidazole), 6.96 (d, *J* = 8.6 Hz, 2H, aromatic), 6.81 (s, 1H, imidazole), 5.63 (d, *J* = 3.9 Hz, 1H, OH), 5.20 (s, 2H, CH<sub>2</sub>O), 4.78–4.71 (m, 1H, CHOH), 4.08 (dd, *J* = 13.9, *J* = 4 Hz, 1H, CH<sub>A</sub>CH<sub>B</sub>), 4.00 (dd, *J* = 13.9, *J* = 8 Hz, 1H, CH<sub>A</sub>CH<sub>B</sub>); <sup>13</sup>C NMR (125 MHz, DMSO-*d*<sub>6</sub>): δ 157.23, 143.05, 135.25, 132.46, 129.37, 128.07, 127.69, 127.33, 120.08, 118.83, 114.43, 110.44, 71.65, 68.20, 53.59. Anal. Calcd. for (C<sub>19</sub>H<sub>17</sub>N<sub>3</sub>O<sub>2</sub>): C, 71.46; H, 5.37; N, 13.16. Found: C, 71.13; H, 5.33; N, 13.26.

## 4.2. Biology

### 4.2.1. Preparation of spleen and brain microsomal fractions

Rat spleen and brain microsomal fractions were prepared by differential centrifugation to obtain HO-1 and HO-2, respectively; the dominance of HO-1 protein in the rat spleen and of HO-2 in the rat brain has been widely documented [51]. Rat spleen and brain microsomal fractions were selected in order to use the most native (*i.e.*, closest to *in vivo*) forms of HO-1 and HO-2. Spleen and brain (Sprague-Dawley rats) microsomal fractions were prepared according to the procedure outlined by Ryter et al. [52]. The experiments reported in the present paper complied with current Italian law and met the guidelines of the Institutional Animal Care and Use Committee of MINISTRY OF HEALTH (Directorate General for Animal Health and Veterinary Medicines) (Italy). The experiments were performed in male Sprague-Dawley albino rats (150 g body weight and age 45 d). Animals had free access to water and were maintained in a temperature- and light-controlled facility. Each rat was sacrificed and their spleen and brain were excised, weighed and pooled to obtain homogenates. Spleen and brain homogenates (15%, w/v) pooled from four rats was prepared in ice-cold HO-homogenizing buffer (50 mM Tris buffer, pH 7.4, containing 0.25 M sucrose) using a Potter-Elvehjem homogenizing system with a Teflon pestle. Centrifugation at 10,000g for 20 min at 4 °C, followed by centrifugation of the supernatant at 100,000g for 60 min at 4 °C was used to obtain microsomal fraction of rat spleen and brain homogenates. The 100,000g pellet (microsomes) was resuspended in 100 mM potassium phosphate buffer, pH 7.8, containing 2 mM MgCl<sub>2</sub> with a Potter-Elvehjem homogenizing system. Equal

aliquots of the rat spleen and brain microsomal fractions were and stored at  $-80\text{ }^{\circ}\text{C}$  for up to 2 months. Protein concentration was measured using TAKE 3 nanodrop.

#### 4.2.2. Preparation of biliverdin reductase

Biliverdin reductase (BVR) was obtained from the liver cytosol. Rat liver was perfused through the hepatic portal vein with cold 0.9% NaCl; then, it was cut and perfused with  $2\times 20$  mL of ice-cold PBS to remove all of the blood. Liver homogenates were obtained with 3 volumes of a solution containing 1.15% KCl w/v and Tris buffer 20 mM, pH 7.8 on ice. Homogenates were centrifuged at 10,000g for 20 minutes at  $4\text{ }^{\circ}\text{C}$  and then the supernatant was centrifuged at 100,000g for 1 h at  $4\text{ }^{\circ}\text{C}$  to sediment the microsomes. Small amounts of the 100,000g supernatant were stored at  $-80\text{ }^{\circ}\text{C}$  after its protein concentration was measured.

#### 4.2.3. Measurement of HO-1 and HO-2 enzymatic activities in the microsomal fraction of rat spleen and brain

The HO-1 and HO-2 activities were measured following the bilirubin formation, as described by Ryter et al. [52]. Reaction mixtures (500  $\mu\text{L}$ ) contained: 20 mM Tris-HCl, pH 7.4, (1 mg/mL) microsomal extract, 0.5–2.0 mg/mL biliverdin reductase, 1 mM NADPH, 2 mM glucose 6-phosphate (G6P), 1 U G6P dehydrogenase, 25  $\mu\text{M}$  hemin, 10  $\mu\text{L}$  of DMSO (or the same volume of DMSO solution of test compounds to a final concentration of 100, 10, and 1  $\mu\text{M}$ ). 60 min incubations at  $37\text{ }^{\circ}\text{C}$  were carried out in a circulating water bath in the dark. 1 volume of chloroform was added to stop reactions. After recovering the chloroform phase, the amount of bilirubin formed was measured with a double-beam spectrophotometer as OD<sub>464-530 nm</sub> (extinction coefficient,  $40\text{ mM}/\text{cm}^{-1}$  for bilirubin). One unit of the enzyme was defined as the amount of enzyme catalyzing the formation of 1 nmol of bilirubin/mg protein/h.

#### 4.3. Computational methods

The three-dimensional structures of all the studied molecules were generated using Marvin Sketch (18.24, ChemAxon Ltd., Budapest, Hungary) [53]. The input 2D structures were minimized using the Merck molecular force field (MMFF94) present in Marvin Sketch at neutral pH. Then, the obtained geometries were further optimized using the PM3 Hamiltonian in MOPAC (MOPAC2016 v. 18.151, Stewart Computational Chemistry, Colorado Springs, CO, USA) [54]. The docking model was validated as we already published in a different paper using the classical inhibitors of HO-1 (Azalanstat, QC-15, QC-

80, QC-82, QC-86, and QC-308) [37]. The protein and the ligands were prepared using YASARA (v. 19.5.5, YASARA Biosciences GmbH, Vienna, Austria). The protein structures were downloaded from the protein data bank (<https://www.rcsb.org/>, ID: 2DY5 for HO-1 and 2QPP for HO-2). Chain A and the heme group were maintained for HO-1, while chain B was used for HO-2. All the water molecules were removed apart from the described consensus water [43]. In the docking experiments, the amino acid residues of the proteins were kept rigid; differently, the single bonds of the ligands were kept free to rotate. Docking was performed by applying the Lamarckian genetic algorithm (LGA) implemented in AutoDock using YASARA GUI. The ligand-centered maps were generated by the AutoGrid with a spacing of 0.375Å and dimensions that surround all atoms extending 5Å from the surface of the ligand in a cuboid box. All of the parameters were at their default settings.

### Supplementary data

Supplementary data related to this article can be found at <https://doi.org/10.1016/j.bioorg.2020.104310>.

### Acknowledgements

This work was supported by 1) Research Funding for University (Piano per la Ricerca 2016–2018, project code 57722172107 and Programma Ricerca di Ateneo UNICT 2020-22 linea 2); 2) Project authorized by the Ministry of Health (Directorate General for Animal Health and Veterinary Medicines) “Dosing of enzymatic activities in rat microsomes” (2018–2022) (project code 02769.N.VLY); 3) PON R&I funds 2014-2020 (CUP: E66C18001320007, AIM1872330, activity 1).

### REFERENCES

- [1] Abraham, N. G.; Kappas, A., Pharmacological and clinical aspects of heme oxygenase. *Pharmacol Rev.* **2008**, *60* (1), 79-127.
- [2] Ewing, J. F.; Maines, M. D., Histochemical localization of heme oxygenase-2 protein and mRNA expression in rat brain. *Brain Res Brain Res Protoc.* **1997**, *1* (2), 165-74.
- [3] Battino, M.; Giampieri, F.; Pistollato, F.; Sureda, A.; de Oliveira, M. R.; Pittala, V.; Fallarino, F.; Nabavi, S. F.; Atanasov, A. G.; Nabavi, S. M., Nrf2 as regulator of

- innate immunity: A molecular Swiss army knife! *Biotechnol Adv.* **2018**, *36* (2), 358-370.
- [4] Amata, E.; Pittala, V.; Marrazzo, A.; Parenti, C.; Prezzavento, O.; Arena, E.; Nabavi, S. M.; Salerno, L., Role of the Nrf2/HO-1 axis in bronchopulmonary dysplasia and hyperoxic lung injuries. *Clin Sci (Lond)*. **2017**, *131* (14), 1701-1712.
- [5] Bauer, M.; Bauer, I., Heme oxygenase-1: redox regulation and role in the hepatic response to oxidative stress. *Antioxid. Redox Signal.* **2002**, *4* (5), 749-58.
- [6] Carota, G.; Raffaele, M.; Sorrenti, V.; Salerno, L.; Pittala, V.; Intagliata, S., Ginseng and heme oxygenase-1: The link between an old herb and a new protective system. *Fitoterapia* **2019**, *139*, 104370.
- [7] Pittala, V.; Salerno, L.; Romeo, G.; Acquaviva, R.; Di Giacomo, C.; Sorrenti, V., Therapeutic Potential of Caffeic Acid Phenethyl Ester (CAPE) in Diabetes. *Curr. Med. Chem.* **2018**, *25* (37), 4827-4836.
- [8] Pittala, V.; Salerno, L.; Romeo, G.; Siracusa, M. A.; Modica, M. N.; Romano, G. L.; Salomone, S.; Drago, F.; Bucolo, C., Effects of novel hybrids of caffeic acid phenethyl ester and NSAIDs on experimental ocular inflammation. *Eur. J. Pharmacol.* **2015**, *752*, 78-83.
- [9] Pittala, V.; Vanella, L.; Salerno, L.; Di Giacomo, C.; Acquaviva, R.; Raffaele, M.; Romeo, G.; Modica, M. N.; Prezzavento, O.; Sorrenti, V., Novel Caffeic Acid Phenethyl Ester (Cape) Analogues as Inducers of Heme Oxygenase-1. *Curr. Pharm. Des.* **2017**, *23* (18), 2657-2664.
- [10] Pittala, V.; Vanella, L.; Salerno, L.; Romeo, G.; Marrazzo, A.; Di Giacomo, C.; Sorrenti, V., Effects of Polyphenolic Derivatives on Heme Oxygenase-System in Metabolic Dysfunctions. *Curr. Med. Chem.* **2018**, *25* (13), 1577-1595.
- [11] Pittala, V.; Vanella, L.; Maria Platania, C. B.; Salerno, L.; Raffaele, M.; Amata, E.; Marrazzo, A.; Floresta, G.; Romeo, G.; Greish, K.; Intagliata, S.; Bucolo, C.; Sorrenti, V., Synthesis, in vitro and in silico studies of HO-1 inducers and lung antifibrotic agents. *Future Med. Chem.* **2019**, *11* (13), 1523-1536.
- [12] Ferrandiz, M. L.; Devesa, I., Inducers of heme oxygenase-1. *Curr. Pharm. Des.* **2008**, *14* (5), 473-86.
- [13] Chau, L. Y., Heme oxygenase-1: emerging target of cancer therapy. *J. Biomed. Sci.* **2015**, *22*, 22.

- [14] Podkalicka, P.; Mucha, O.; Jozkowicz, A.; Dulak, J.; Loboda, A., Heme oxygenase inhibition in cancers: possible tools and targets. *Contemp Oncol (Pozn)*. **2018**, *22* (1A), 23-32.
- [15] Dichiara, M.; Prezzavento, O.; Marrazzo, A.; Pittala, V.; Salerno, L.; Rescifina, A.; Amata, E., Recent advances in drug discovery of phototherapeutic non-porphyrinic anticancer agents. *Eur. J. Med. Chem.* **2017**, *142*, 459-485.
- [16] Salerno, L.; Pittala, V.; Romeo, G.; Modica, M. N.; Siracusa, M. A.; Di Giacomo, C.; Acquaviva, R.; Barbagallo, I.; Tibullo, D.; Sorrenti, V., Evaluation of novel aryloxyalkyl derivatives of imidazole and 1,2,4-triazole as heme oxygenase-1 (HO-1) inhibitors and their antitumor properties. *Bioorg. Med. Chem.* **2013**, *21* (17), 5145-53.
- [17] Salerno, L.; Romeo, G.; Modica, M. N.; Amata, E.; Sorrenti, V.; Barbagallo, I.; Pittala, V., Heme oxygenase-1: A new druggable target in the management of chronic and acute myeloid leukemia. *Eur. J. Med. Chem.* **2017**, *142*, 163-178.
- [18] Berberat, P. O.; Dambrauskas, Z.; Gulbinas, A.; Giese, T.; Giese, N.; Kunzli, B.; Autschbach, F.; Meuer, S.; Buchler, M. W.; Friess, H., Inhibition of heme oxygenase-1 increases responsiveness of pancreatic cancer cells to anticancer treatment. *Clin. Cancer Res.* **2005**, *11* (10), 3790-8.
- [19] Salerno, L.; Pittala, V.; Romeo, G.; Modica, M. N.; Marrazzo, A.; Siracusa, M. A.; Sorrenti, V.; Di Giacomo, C.; Vanella, L.; Parayath, N. N.; Greish, K., Novel imidazole derivatives as heme oxygenase-1 (HO-1) and heme oxygenase-2 (HO-2) inhibitors and their cytotoxic activity in human-derived cancer cell lines. *Eur. J. Med. Chem.* **2015**, *96*, 162-72.
- [20] Barbagallo, I.; Giallongo, C.; Li Volti, G.; Distefano, A.; Camiolo, G.; Raffaele, M.; Salerno, L.; Pittala, V.; Sorrenti, V.; Avola, R.; Di Rosa, M.; Vanella, L.; Di Raimondo, F.; Tibullo, D., Heme Oxygenase Inhibition Sensitizes Neuroblastoma Cells to Carfilzomib. *Mol. Neurobiol.* **2019**, *56* (2), 1451-1460.
- [21] Castruccio Castracani, C.; Longhitano, L.; Distefano, A.; Di Rosa, M.; Pittala, V.; Lupo, G.; Caruso, M.; Corona, D.; Tibullo, D.; Li Volti, G., Heme Oxygenase-1 and Carbon Monoxide Regulate Growth and Progression in Glioblastoma Cells. *Mol. Neurobiol.* **2020**, *57* (5), 2436-2446.
- [22] Ciaffaglione, V.; Intagliata, S.; Pittala, V.; Marrazzo, A.; Sorrenti, V.; Vanella, L.; Rescifina, A.; Floresta, G.; Sultan, A.; Greish, K.; Salerno, L., New

- Arylethanolimidazole Derivatives as HO-1 Inhibitors with Cytotoxicity against MCF-7 Breast Cancer Cells. *Int. J. Mol. Sci.* **2020**, *21* (6), 1923.
- [23] Greish, K. F.; Salerno, L.; Al Zahrani, R.; Amata, E.; Modica, M. N.; Romeo, G.; Marrazzo, A.; Prezzavento, O.; Sorrenti, V.; Rescifina, A.; Floresta, G.; Intagliata, S.; Pittala, V., Novel Structural Insight into Inhibitors of Heme Oxygenase-1 (HO-1) by New Imidazole-Based Compounds: Biochemical and In Vitro Anticancer Activity Evaluation. *Molecules* **2018**, *23* (5), 1209.
- [24] Raffaele, M.; Pittala, V.; Zingales, V.; Barbagallo, I.; Salerno, L.; Li Volti, G.; Romeo, G.; Carota, G.; Sorrenti, V.; Vanella, L., Heme Oxygenase-1 Inhibition Sensitizes Human Prostate Cancer Cells towards Glucose Deprivation and Metformin-Mediated Cell Death. *Int. J. Mol. Sci.* **2019**, *20* (10), 2593.
- [25] Sorrenti, V.; Pittala, V.; Romeo, G.; Amata, E.; Dichiaro, M.; Marrazzo, A.; Turnaturi, R.; Prezzavento, O.; Barbagallo, I.; Vanella, L.; Rescifina, A.; Floresta, G.; Tibullo, D.; Di Raimondo, F.; Intagliata, S.; Salerno, L., Targeting heme Oxygenase-1 with hybrid compounds to overcome Imatinib resistance in chronic myeloid leukemia cell lines. *Eur. J. Med. Chem.* **2018**, *158*, 937-950.
- [26] Spampinato, M.; Sferrazzo, G.; Pittala, V.; Di Rosa, M.; Vanella, L.; Salerno, L.; Sorrenti, V.; Carota, G.; Parrinello, N.; Raffaele, M.; Tibullo, D.; Li Volti, G.; Barbagallo, I., Non-competitive heme oxygenase-1 activity inhibitor reduces non-small cell lung cancer glutathione content and regulates cell proliferation. *Mol. Biol. Rep.* **2020**, *47* (3), 1949-1964.
- [27] Intagliata, S.; Salerno, L.; Ciaffaglione, V.; Leonardi, C.; Fallica, A. N.; Carota, G.; Amata, E.; Marrazzo, A.; Pittala, V.; Romeo, G., Heme Oxygenase-2 (HO-2) as a therapeutic target: Activators and inhibitors. *Eur. J. Med. Chem.* **2019**, *183*, 111703.
- [28] Trakshel, G. M.; Kutty, R. K.; Maines, M. D., Purification and characterization of the major constitutive form of testicular heme oxygenase. The noninducible isoform. *J. Biol. Chem.* **1986**, *261* (24), 11131-7.
- [29] Salerno, L.; Floresta, G.; Ciaffaglione, V.; Gentile, D.; Margani, F.; Turnaturi, R.; Rescifina, A.; Pittala, V., Progress in the development of selective heme oxygenase-1 inhibitors and their potential therapeutic application. *Eur. J. Med. Chem.* **2019**, *167*, 439-453.

- [30] Rahman, M. N.; Vukomanovic, D.; Vlahakis, J. Z.; Szarek, W. A.; Nakatsu, K.; Jia, Z. C., Structural insights into human heme oxygenase-1 inhibition by potent and selective azole-based compounds. *J. R. Soc. Interface* **2013**, *10* (78), 20120697.
- [31] Pittala, V.; Salerno, L.; Romeo, G.; Modica, M. N.; Siracusa, M. A., A focus on heme oxygenase-1 (HO-1) inhibitors. *Curr. Med. Chem.* **2013**, *20* (30), 3711-32.
- [32] Rahman, M. N.; Vlahakis, J. Z.; Vukomanovic, D.; Lee, W.; Szarek, W. A.; Nakatsu, K.; Jia, Z. C., A Novel, "Double-Clamp" Binding Mode for Human Heme Oxygenase-1 Inhibition. *Plos One* **2012**, *7* (1), e29514.
- [33] Rahman, M. N.; Vlahakis, J. Z.; Vukomanovic, D.; Szarek, W. A.; Nakatsu, K.; Jia, Z. C., X-ray Crystal Structure of Human Heme Oxygenase-1 with (2R,4S)-2-[2-(4-Chlorophenyl)ethyl]-2-[(1H-imidazol-1-yl)methyl]-4[[(5-trifluoromethyl)pyridin-2-yl)thio)methyl]-1,3-dioxolane: A Novel, Inducible Binding Mode. *J. Med. Chem.* **2009**, *52* (15), 4946-4950.
- [34] Floresta, G.; Pittala, V.; Sorrenti, V.; Romeo, G.; Salerno, L.; Rescifina, A., Development of new HO-1 inhibitors by a thorough scaffold-hopping analysis. *Bioorg Chem.* **2018**, *81*, 334-339.
- [35] Floresta, G.; Amata, E.; Gentile, D.; Romeo, G.; Marrazzo, A.; Pittala, V.; Salerno, L.; Rescifina, A., Fourfold Filtered Statistical/Computational Approach for the Identification of Imidazole Compounds as HO-1 Inhibitors from Natural Products. *Mar. Drugs* **2019**, *17* (2), 113.
- [36] Floresta, G.; Amata, E.; Dichiara, M.; Marrazzo, A.; Salerno, L.; Romeo, G.; Prezzavento, O.; Pittala, V.; Rescifina, A., Identification of Potentially Potent Heme Oxygenase 1 Inhibitors through 3D-QSAR Coupled to Scaffold-Hopping Analysis. *ChemMedChem* **2018**, *13* (13), 1336-1342.
- [37] Salerno, L.; Amata, E.; Romeo, G.; Marrazzo, A.; Prezzavento, O.; Floresta, G.; Sorrenti, V.; Barbagallo, I.; Rescifina, A.; Pittala, V., Potholing of the hydrophobic heme oxygenase-1 western region for the search of potent and selective imidazole-based inhibitors. *Eur. J. Med. Chem.* **2018**, *148*, 54-62.
- [38] Amata, E.; Marrazzo, A.; Dichiara, M.; Modica, M. N.; Salerno, L.; Prezzavento, O.; Nastasi, G.; Rescifina, A.; Romeo, G.; Pittala, V., Comprehensive data on a 2D-QSAR model for Heme Oxygenase isoform 1 inhibitors. *Data Brief.* **2017**, *15*, 281-299.



- [39] Amata, E.; Marrazzo, A.; Dichiara, M.; Modica, M. N.; Salerno, L.; Prezzavento, O.; Nastasi, G.; Rescifina, A.; Romeo, G.; Pittala, V., Heme Oxygenase Database (HemeOxDB) and QSAR Analysis of Isoform 1 Inhibitors. *ChemMedChem* **2017**, *12* (22), 1873-1881.
- [40] Mucha, O.; Podkalicka, P.; Mikulski, M.; Barwacz, S.; Andrysiak, K.; Biela, A.; Mieczkowski, M.; Kachamakova-Trojanowska, N.; Ryszawy, D.; Bialas, A.; Szelazek, B.; Grudnik, P.; Majewska, E.; Michalik, K.; Jakubiec, K.; Bien, M.; Witkowska, N.; Gluza, K.; Ekonomiuk, D.; Sitarz, K.; Galezowski, M.; Brzozka, K.; Dubin, G.; Jozkowicz, A.; Dulak, J.; Loboda, A., Development and characterization of a new inhibitor of heme oxygenase activity for cancer treatment. *Arch Biochem Biophys* **2019**, *671*, 130-142.
- [41] Podkalicka, P.; Mucha, O.; Kruczek, S.; Biela, A.; Andrysiak, K.; Stepniewski, J.; Mikulski, M.; Galezowski, M.; Sitarz, K.; Brzozka, K.; Jozkowicz, A.; Dulak, J.; Loboda, A., Synthetically Lethal Interactions of Heme Oxygenase-1 and Fumarate Hydratase Genes. *Biomolecules* **2020**, *10* (1), 143.
- [42] Vlahakis, J. Z.; Vukomanovic, D.; Nakatsu, K.; Szarek, W. A., Selective inhibition of heme oxygenase-2 activity by analogs of 1-(4-chlorobenzyl)-2-(pyrrolidin-1-ylmethyl)-1H-benzimidazole (clemizole): Exploration of the effects of substituents at the N-1 position. *Bioorg. Med. Chem.* **2013**, *21* (21), 6788-6795.
- [43] Floresta, G.; Carotti, A.; Ianni, F.; Sorrenti, V.; Intagliata, S.; Rescifina, A.; Salerno, L.; Di Michele, A.; Sardella, R.; Pittala, V., Chromatographic resolution of phenylethanoic-azole racemic compounds highlighted stereoselective inhibition of heme oxygenase-1 by (R)-enantiomers. *Bioorg Chem.* **2020**, *99*, 103777.
- [44] Daina, A.; Michielin, O.; Zoete, V., SwissADME: a free web tool to evaluate pharmacokinetics, drug-likeness and medicinal chemistry friendliness of small molecules. *Sci. Rep.* **2017**, *7*, 42717.
- [45] Pires, D. E.; Blundell, T. L.; Ascher, D. B., pkCSM: Predicting Small-Molecule Pharmacokinetic and Toxicity Properties Using Graph-Based Signatures. *J. Med. Chem.* **2015**, *58* (9), 4066-72.
- [46] Lipinski, C. A.; Lombardo, F.; Dominy, B. W.; Feeney, P. J., Experimental and computational approaches to estimate solubility and permeability in drug discovery and development settings. *Adv Drug Deliv Rev* **2001**, *46* (1-3), 3-26.

- [47] Ghose, A. K.; Viswanadhan, V. N.; Wendoloski, J. J., A knowledge-based approach in designing combinatorial or medicinal chemistry libraries for drug discovery. 1. A qualitative and quantitative characterization of known drug databases. *J. Comb. Chem.* **1999**, *1* (1), 55-68.
- [48] Egan, W. J.; Merz, K. M., Jr.; Baldwin, J. J., Prediction of drug absorption using multivariate statistics. *J. Med. Chem.* **2000**, *43* (21), 3867-77.
- [49] Veber, D. F.; Johnson, S. R.; Cheng, H. Y.; Smith, B. R.; Ward, K. W.; Kopple, K. D., Molecular properties that influence the oral bioavailability of drug candidates. *J. Med. Chem.* **2002**, *45* (12), 2615-23.
- [50] Ma, Y. T.; Fan, H. F.; Gao, Y. Q.; Li, H.; Zhang, A. L.; Gao, J. M., Natural Products as Sources of New Fungicides (I): Synthesis and Antifungal Activity of Acetophenone Derivatives Against Phytopathogenic Fungi. *Chem. Biol. Drug Des.* **2013**, *81* (4), 545-552.
- [51] Maines, M. D., Heme Oxygenase - Function, Multiplicity, Regulatory Mechanisms, and Clinical-Applications. *Faseb J.* **1988**, *2* (10), 2557-2568.
- [52] Ryter, S. W.; Alam, J.; Choi, A. M. K., Heme oxygenase-1/carbon monoxide: From basic science to therapeutic applications. *Physiol. Rev.* **2006**, *86* (2), 583-650.
- [53] Csizmadia, F., JChem: Java applets and modules supporting chemical database handling from web browsers. *J. Chem. Inf. Comput. Sci.* **2000**, *40* (2), 323-4.
- [54] Stewart, J. J., MOPAC: a semiempirical molecular orbital program. *J. Comput.-Aided Mol. Des.* **1990**, *4* (1), 1-105.

“This article was published in *Bioorganic Chemistry*, 104, Floresta G.; Fallica AN; Romeo G; Sorrenti V; Salerno L; Rescifina A; Pittalà V, Identification of a potent heme oxygenase-2 (HO-2) inhibitor by targeting the secondary hydrophobic pocket of the HO-2 western region, 104310, Copyright Elsevier (2020).”

## Discovery of novel acetamide-based heme oxygenase-1 inhibitors with potent in vitro antiproliferative activity

Antonino N. Fallica,<sup>a ‡</sup> Valeria Sorrenti,<sup>a ‡</sup> Agata G. D'Amico,<sup>a</sup> Loredana Salerno,<sup>a</sup> Giuseppe Romeo,<sup>a</sup> Sebastiano Intagliata,<sup>a</sup> Valeria Consoli,<sup>a</sup> Giuseppe Floresta,<sup>b</sup> Antonio Rescifina,<sup>a</sup> Velia D'Agata,<sup>c</sup> Luca Vanella,<sup>a</sup> Valeria Pittalà<sup>a\*</sup>

<sup>a</sup> Department of Drug and Health Sciences, University of Catania, 95125 – Catania, Italy.

<sup>b</sup> Department of Analytics, Environmental & Forensics, King's College London, Stamford Street, London SE1 9NH, UK

<sup>c</sup> Sections of Human Anatomy and Histology, Department of Biomedical and Biotechnological Sciences, University of Catania, 95123 – Catania, Italy

*Journal of Medicinal Chemistry*

Received: April 6, 2021; Published: September 2, 2021

**ABSTRACT:** Heme oxygenase-1 (HO-1) promotes heme catabolism exercising cytoprotective roles in normal and cancer cells. Herein, we report the design, synthesis, molecular modeling, and biological evaluation of novel HO-1 inhibitors. Specifically, an amide linker in the central spacer and an imidazole were fixed, and the hydrophobic moiety required by pharmacophore was largely modified. In many tumors, overexpression of HO-1 correlates with poor prognosis and chemoresistance, suggesting inhibition of HO-1 as a possible antitumor strategy. Accordingly, compounds **7i** and **7l-p**, emerged for their potency against HO-1, and were investigated for their anticancer activity against prostate (DU-145), lung (A549), and glioblastoma (U87MG, A172) cancer cells. The selected compounds showed the best activity towards U87MG cells. Compound **7l** was further investigated for its in-cells enzymatic HO-1 activity, expression levels, and effects on cell invasion and VEGF extracellular release. Obtained data suggest that **7l** can reduce cell invasivity acting through modulation of HO-1 expression.

**KEYWORDS:** Heme oxygenase-1, heme oxygenase-2, structure-activity relationships, inhibitors, glioblastoma, U87MG.

### Author contributions

<sup>‡</sup> These authors contributed equally

### \*Corresponding Author:

Valeria Pittalà: vpittala@unict.it

## 1. Introduction

Heme metabolism is under the tight control of a family of phase II detoxifying enzymes known as heme oxygenase (HO) [1]. HOs include heme oxygenase-1 (HO-1) and heme oxygenase-2 (HO-2) isoforms. HO-2 is a constitutive isoform and has been characterized generally in testis and the brain, where this isoform is more abundant. While HO-2 distribution remains unchanged regardless of the endogenous oxidative stress status, HO-1, whose expression is mainly under the control of the transcription factor nuclear factor erythroid 2-related factor 2 (Nrf2), is an inducible isoform implicated in counteracting inflammation and oxidative stress responses [1, 2]. Metabolites produced upon heme breakdown, biliverdin, bilirubin, carbon monoxide, and  $\text{Fe}^{2+}$ , further support HO-1 cytoprotective roles. As a result, HO-1 gained interest over the years, and its induction is valuable in several oxidative stress-dependent diseases [3-5]. At the same time, literature reports indicate a key role of HO-1 in promoting cell survival in cancerous cells and resistance to the current anticancer therapies. Patients presenting HO-1 aberrant overexpression appear to have lesser survival chances and more unsatisfactory clinical outcomes. In fact, the detrimental role of HO-1 has been demonstrated in leukemia, glioblastoma (GBM), prostate, lung, and colon cancers [6-12]. Also, whereas HO-1 is generally found in the cytoplasm, a different subcellular localization was detected in cancerous tissues. In fact, higher levels of nuclear HO-1 have been detected in malignant tissues than those in normal ones, which has been speculated to be strictly linked with cancer progression [13, 14]. These aspects pushed for the search of selective HO-1 inhibitors. Though growing information has been gained in the recent past to unravel the involvement of HO-1 in tumors, its pharmacological tractability as a new target remains to be elucidated. Therefore, the identification of new potent HO-1 inhibitors is desirable to gather knowledge faster. Structure-activity relationship (SAR) studies to identify new HO-1 inhibitors has been initially focused on metalloporphyrins (MPs), soon abandoned due to different side-effects and subsequently on the non-porphyrin lead compound azalanstat (Figure 1) [15].

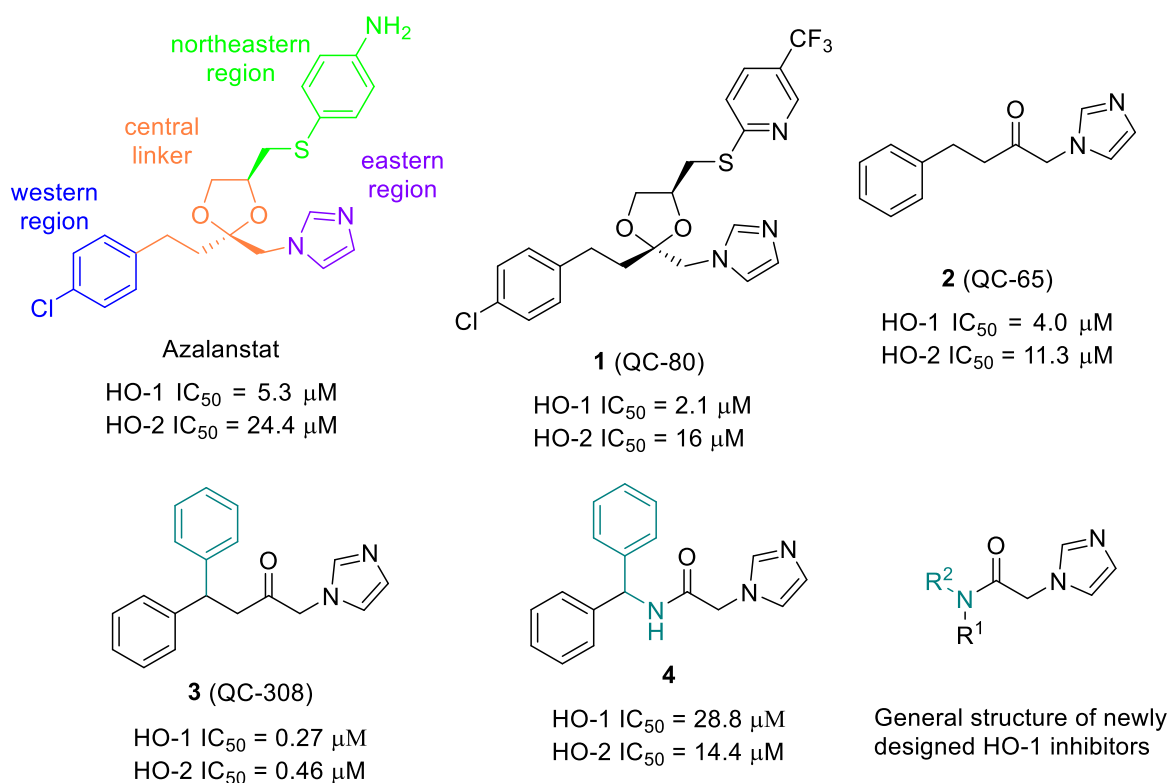


**Figure 1.** Chemical structures of azalanstat, **1** (QC-80), **2** (QC-65), **3** (QC-308), and hit compound **4**.

Main modification able to increase potency and selectivity occurred mainly through structural modifications on the central connecting chain or in the western region, while the northeastern region demonstrated to be not mandatory and the eastern region not prone to modifications [16-19].

Over the years, co-crystallization studies of HO-1 with selected inhibitors (including azalanstat and **1–3**, Figure 1) contributed to understanding the binding mode and the critical requirements for binding (Figure 2) [20-22]. Our research group has long been focused on the design of inhibitors oriented towards HO-1 and HO-2 usingazole-based scaffolds, including the identification of the new hit compound **4** (Figure 1) [23].

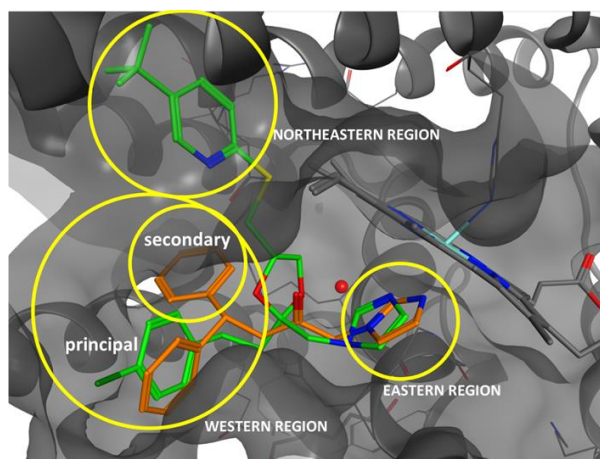


**Figure 2.** Compound **1** (green) and **3** (orange) inside the HO-1 binding pocket.

Based on such premises, we designed a new series of HO-1 inhibitors with an amide function in the central connecting chain. Obtained compounds (Table 1) behaving as potent HO-1 inhibitors have been screened for their antiproliferative activity and HO-1 expression levels against a small panel of cancer cell lines, showing the best activity towards GBM cell line U87MG. This exploration also identified compound **71** as suitable for further investigating its in-cells enzymatic HO-1 activity and its effects on cell invasion. Encouraging results obtained on compound **71** will pave the way to study more in depth its pharmacological profile.

## 2. Results and discussion

### 2.1. Rational design

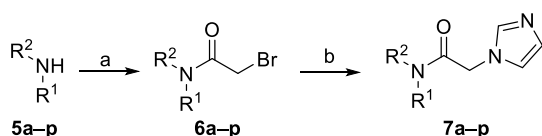
The classical pharmacophore for HO-1 inhibition consists of (i) an iron(II)-binding group that coordinates  $\text{Fe}^{2+}$  in the HO-1 active site; (ii) a hydrophobic portion; (iii) a central spacer connecting the two groups. This pharmacophore pattern has been investigated in the past years to derive novel series of HO-1 inhibitors and will be herein further exploited [16-18]. Moreover, co-crystallization studies performed with compound **3** highlighted the presence of an additional smaller secondary hydrophobic pocket in HO-1 and HO-2 [21]. This information allowed to explain the 15-fold higher inhibitory potency towards HO-1 of **3** with respect to its monophenyl analog, **2** ( $0.27 \mu\text{M}$  vs  $4.0 \mu\text{M}$ , respectively, Figure 1). This “double-clamp” binding mode has been poorly exploited in the search for more powerful HO-1 inhibitors. Substituents in the aromatic rings can help fine-tune both the potency and the selectivity of the resulted compounds over HO-1 or HO-2.

SAR studies performed on HO-1 inhibitors revealed that the central connecting chain could contain heteroatoms such as sulfur, oxygen, hydroxyl groups, and carbonyl functions [16]. However, insufficient information has been reported on the tolerability of an amide function in the central connecting chain. The ability to establish critical hydrogen bonding interactions and the consequent increase in polarity can affect the pharmacological profile of compounds possessing this functional group. Thereby, amide functional groups represent one of the most easily found structural motifs in marketed drugs and drug candidates [24]. Recently, our research group reported the synthesis of compound **4** (Figure 1) and its IC<sub>50</sub> values towards both enzymatic isoforms [23]. Insertion of the amide function in the central connecting chain increased the HO-1 IC<sub>50</sub> value from 0.27 μM for **3** to 28.8 μM for compound **4**; besides, a slight preference for the constitutive isoform was detected (HO-2 IC<sub>50</sub> = 14.4 μM). Nevertheless, the amide function's chemical versatility in medicinal chemistry and the easy-to-synthesize compounds with this functional group are appealing. To expand the SAR studies of HO-1 inhibitors, we chose compound **4** as the hit compound to design novel amide-imidazole-based HO-1 inhibitors (Table 1). Five main strategies have been pursued: (i) structural simplification by removal of the secondary phenyl ring; (ii) shortening or elongation of the central connecting chain; (iii) substitution of the nitrogen atom on the amide function to obtain tertiary amides; (iv) inversion of the amide bond; (v) insertion of substituents on one phenyl ring or its removal in favor of saturated cycles to explore the steric and electronic requirements of the smaller secondary hydrophobic pocket.

## 2.2. Chemistry

Final compounds **7a–p** have been synthesized as depicted in Scheme 1. The first step involves the reaction of the appropriate primary or secondary amines **5a–p** with bromoacetyl bromide and TEA in dry acetonitrile at room temperature for three hours, affording the *N*-mono or *N,N*-disubstituted  $\alpha$ -bromo-acetamide intermediates **6a–p**. The last step is an aliphatic nucleophilic substitution of compounds **6a–p** with imidazole. For compounds **7a**, **7c–d**, **7f–g**, **7i**, and **7o**, the reaction was conducted in dry DMF and K<sub>2</sub>CO<sub>3</sub> at room temperature for 2 hours. However, low reaction yields have been obtained with this synthetic strategy. In order to scale up the reaction yield and obtain larger quantities of compounds intended for biological tests, a more efficient base able to fully deprotonate the nitrogen atom of imidazole has been chosen for the nucleophilic substitution. Therefore, compounds **7b**, **7e**, **7h**, **7j–n**, and **7p** have been synthesized using an excess of NaH 80% in oil dispersion as

base and dry THF as reaction solvent at room temperature for 16 hours.

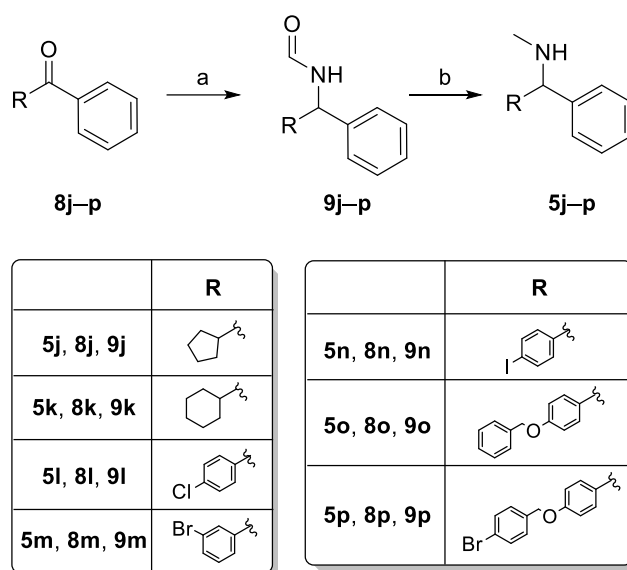


	R <sup>1</sup>	R <sup>2</sup>		R <sup>1</sup>	R <sup>2</sup>
<b>5a, 6a, 7a</b>		H	<b>5i, 6i, 7i</b>		CH <sub>3</sub>
<b>5b, 6b, 7b</b>		CH <sub>3</sub>	<b>5j, 6j, 7j</b>		CH <sub>3</sub>
<b>5c, 6c, 7c</b>		H	<b>5k, 6k, 7k</b>		CH <sub>3</sub>
<b>5d, 6d, 7d</b>		H	<b>5l, 6l, 7l</b>		CH <sub>3</sub>
<b>5e, 6e, 7e</b>		CH <sub>3</sub>	<b>5m, 6m, 7m</b>		CH <sub>3</sub>
<b>5f, 6f, 7f</b>		H	<b>5n, 6n, 7n</b>		CH <sub>3</sub>
<b>5g, 6g, 7g</b>		CH <sub>3</sub>	<b>5o, 6o, 7o</b>		CH <sub>3</sub>
<b>5h, 6h, 7h</b>			<b>5p, 6p, 7p</b>		CH <sub>3</sub>

**Scheme 1.** Reagents and conditions: a)  $\alpha$ -bromo-acetyl bromide, TEA, dry CH<sub>3</sub>CN, room temperature, 3 h; b) imidazole, K<sub>2</sub>CO<sub>3</sub>, dry DMF, room temperature, 2 h or 80% NaH in oil dispersion, dry THF, room temperature, 16 h.

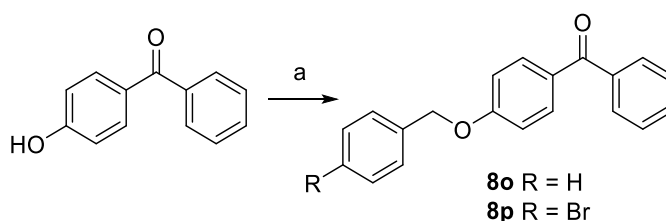
Amines **5j–p** have been synthesized employing the Leuckart reaction, a synthetic procedure in which an appropriate starting ketone **8j–p** is converted into the corresponding *N*-methyl amine derivative by reductive amination of the carbonyl function (Scheme 2). The reaction classically requires two steps: in the first one, ketones **8j–p** were treated with formamide and formic acid at 170 °C for 18 hours. To reduce the reaction time, a microwave-assisted procedure has been developed, and the best results have been obtained at 170 °C for 90 min. The formamide function of derivatives **9j–p** has been subsequently reduced to a methylamino group using LiAlH<sub>4</sub> in THF 1M (for the synthesis of compounds **5j–k** and **5o–p**) or DIBAL-H in 1M *n*-hexane (for the synthesis of compounds **5l–n**).





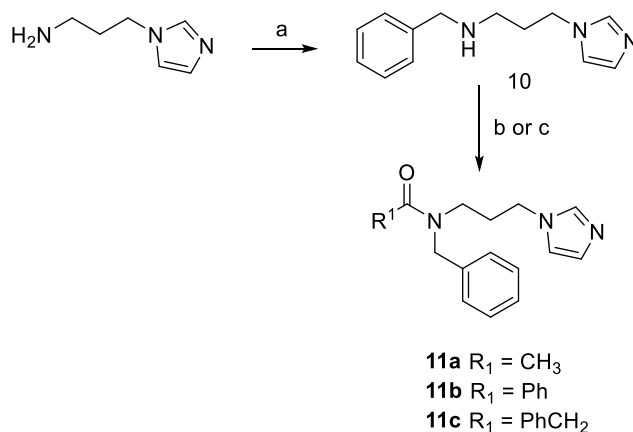
**Scheme 2.** Reagents and conditions: a)  $\text{H}_2\text{NCHO}$ ,  $\text{HCOOH}$ , MW, 150 W, 150 psi, 170 °C, 1.5 h; b)  $\text{LiAlH}_4$  in THF 1M, dry THF, reflux, 2 h or DIBAL-H in 1M *n*-hexane, THF, reflux, 3.5 h, then room temperature, 16 h.

4-Benzyloxyketones **8o–p** were synthesized as depicted in Scheme 3. The reaction involves the etherification of 4-hydroxybenzophenone with the appropriate benzyl bromide in refluxing acetone with  $\text{K}_2\text{CO}_3$  and KI as catalyst for 3 hours.



**Scheme 3.** Reagents and conditions: a) appropriate benzyl bromide,  $\text{K}_2\text{CO}_3$ , KI, acetone, reflux, 3 h.

In Scheme 4 is reported the synthesis of final compounds **11a–c**. The synthesis of these compounds required two steps: a reductive alkylation of 3-(1*H*-imidazol-1-yl)propan-1-amine with benzaldehyde and  $\text{NaBH}_4$  in dry methanol afforded intermediate **10**, that was condensed with acetic anhydride or an appropriate acyl chloride in dry dichloromethane, affording compounds **11a** and **11b,c**, respectively.



**Scheme 4.** Reagents and conditions: a) benzaldehyde, CH<sub>3</sub>CO<sub>2</sub>Na, activated 3Å molecular sieves, dry CH<sub>3</sub>OH, room temperature, 12 h, then NaBH<sub>4</sub>, room temperature, 3 h; b) acetic anhydride, TEA, DMAP, dry CH<sub>2</sub>Cl<sub>2</sub>, 0 °C, 10 min, then room temperature, 12 h; c) appropriate acyl chloride, TEA, dry CH<sub>2</sub>Cl<sub>2</sub>, room temperature, 12 h.

All compounds have been characterized by IR, <sup>1</sup>H-NMR, melting point, and elemental analysis; final compounds also by <sup>13</sup>C-NMR. Intermediates and final compounds possessing a tertiary amide functional group exist as an *E/Z* mixture, as evidenced by NMR spectra. The steric hindrance around the amide bond and the partial nature of the C–N double bond does not grant the free rotation of the different parts of the molecule around a single bond, giving rise to “*E/Z*” isomers. From NMR spectra, it has been possible to highlight this phenomenon by doubling specific identifying peaks, such as the methyl group linked to the nitrogen atom, CH<sub>2</sub>, or imidazole CH groups.

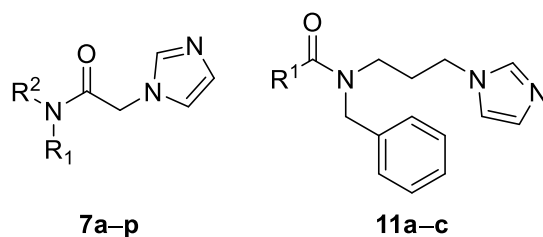
### 2.3. HO inhibition and SAR analysis

Compounds **7a–p** and **11a–c** were tested to evaluate their inhibitory properties toward HO-1, obtained from rat spleen microsomal fractions. Data are expressed as IC<sub>50</sub> (μM) and are summarized in Table 1. Compounds with an HO-1 IC<sub>50</sub> ≤ 8 μM have also been screened to inhibit the constitutive HO-2, which was obtained from rat brain microsomal fractions. IC<sub>50</sub> values of **1** and **4** are also reported. Based on the results obtained by the enzymatic assays, SARs can be built. Shortening of the central connecting chain of compound **4** from four to three atoms afforded anilide compounds **7a–e**. This specific structural modification does not allow the presence of the secondary phenyl ring. Except for **7d**, which displayed an HO-1 IC<sub>50</sub> value of 8.34 μM, all anilides exhibited poor inhibitory activity, and all of them are less potent than hit compound **4**. Furthermore, *N*-methylation of anilides **7a** and **7d** afforded **7b** and the **7e**, respectively, showing a strong drop in activity. To verify if the

“double clamp” binding mode also plays a role in this class of amide derivatives, we removed the second phenyl ring of compound **4** affording **7f**, which showed a 2-fold decrease in potency with respect to **4** (57.60  $\mu\text{M}$  vs 28.8  $\mu\text{M}$ , respectively). *N*-methylation of **7f** (compound **7g**) did not produce a significant improvement of the inhibitory potency. A bulkier substituent such as a benzyl moiety linked to the nitrogen atom of the amide function (compound **7h**) showed comparable activity to its *N*-methyl analog **7g** (64.80  $\mu\text{M}$  vs 50.63  $\mu\text{M}$ , respectively). From these results, we can assume that shortening of the central connecting chain or deletion of the secondary phenyl ring reduces the affinity. In light of the previous considerations, we then decided to add a small substituent at the nitrogen atom of compound **4**. The corresponding *N*-methyl derivative **7i** displayed an  $\text{IC}_{50}$  value of 0.9  $\mu\text{M}$  and is about 32-fold more potent than the parent compound **4**. Therefore, compound **7i** has been considered the lead compound for the design and synthesis of derivatives **7j–p**. Interestingly, all *N*-methylated **7i** derivatives improved potency, showing an opposite trend than anilide derivatives **7b**, **7e**. Considering that the two hydrophobic pockets of the HO-1 enzyme seem smaller than the HO-2 ones, we can speculate that both enzymes will accommodate bulky hydrophobic moieties differently and with different affinity [25]. Consequently, we removed one phenyl ring in favor of a saturated cyclopentyl or cyclohexyl one (compounds **7j** and **7k**, respectively). However, both compounds showed slightly reduced inhibitory activity against HO-1; specifically, **7j** displayed a value of 11.43  $\mu\text{M}$ , whereas **7k** exhibited a value of 26.84  $\mu\text{M}$  being 13- and 30-fold less potent than compound **7i**, respectively. Insertion of electron-withdrawing or electron-donating groups in one phenyl ring led to compounds **7l–p**. Halogen-substituted compounds **7l–n** showed inhibitory potencies perfectly comparable with that of the unsubstituted compound **7i**. A benzyloxy or 4-bromobenzyloxy moiety at the 4-position of one phenyl ring of **7i** afforded compounds **7o** and **7p**, respectively. Both compounds can inhibit the HO-1 enzyme, although at different levels. Indeed, **7o** has an inhibitory potency similar to **7i** (1.2  $\mu\text{M}$  vs 0.9  $\mu\text{M}$ ), whereas **7p** is about 6.5- and 9-fold less potent than **7o** and **7i**, respectively (8.0  $\mu\text{M}$  vs 1.2  $\mu\text{M}$  and 0.9  $\mu\text{M}$ ). HO-1 inhibition data for compounds **7i–p** overall reconfirm the importance of the secondary hydrophobic pocket and the so-called “double clamp” binding mode as already highlighted by compound **3**. Elongation of the central connecting chain to five atoms and concomitant inversion of the amide bond led to the design of compounds **11a–c** maintaining a benzyl substituent at the nitrogen atom of the amide bond. The lipophilic portion of the molecule has been changed from an acetyl group to a more lipophilic phenyl or

phenylmethyl substituents. The *N*-acetyl derivative **11a** resulted almost inactive, whereas compounds **11b** and **11c** showed IC<sub>50</sub> values comparable to the hit compound **4** (Table 1). Interestingly, these results confirmed that the HO-1 enzyme less tolerates substituents linked to the *N*-atom bulkier than a methyl group. The most potent HO-1 inhibitors of this series, possessing an IC<sub>50</sub> ≤ 8 μM, have also been tested to evaluate their selectivity towards the HO-2 isozyme. Compounds **7i**, **7l** and **7m** showed superimposable HO-1 and HO-2 IC<sub>50</sub> values, compounds **7o** and **7p** are 9- and 3-fold more selective for the inducible isoform (1.20 μM vs 11.19 μM for **7o**, 8.0 μM vs 24.71 μM for **7p**, respectively). The most selective compound of this series, 4-iodo-monosubstituted derivative **7n**, is about 48-fold more selective for HO-1 (0.95 μM vs. 45.89 μM).

**Table 1.** Experimental IC<sub>50</sub> values (μM) of compounds **7a–p** and **11a–c** towards HO-1 and HO-2.



Compd	R <sup>1</sup>	R <sup>2</sup>	IC <sub>50</sub> (μM)		SI (HO-2/HO-1)
			HO-1	HO-2	
<b>7a</b>	Ph	H	110.0 ± 3.1	ND	–
<b>7b</b>	Ph	CH <sub>3</sub>	2.50 (mM)	ND	–
<b>7c</b>	3-BrPh	H	35.71 ± 1.20	ND	–
<b>7d</b>	4-IPh	H	8.34 ± 0.21	ND	–
<b>7e</b>	4-IPh	CH <sub>3</sub>	96.14 ± 1.44	ND	–
<b>7f</b>	PhCH <sub>2</sub>	H	57.60 ± 2.38	ND	–
<b>7g</b>	PhCH <sub>2</sub>	CH <sub>3</sub>	50.63 ± 1.84	ND	–
<b>7h</b>	PhCH <sub>2</sub>	PhCH <sub>2</sub>	64.80 ± 1.56	ND	–
<b>7i</b>	Ph(Ph)CH	CH <sub>3</sub>	0.90 ± 0.07	0.90 ± 0.05	1
<b>7j</b>	C <sub>5</sub> H <sub>9</sub> (Ph)CH	CH <sub>3</sub>	11.43 ± 0.97	ND	–
<b>7k</b>	C <sub>6</sub> H <sub>11</sub> (Ph)CH	CH <sub>3</sub>	26.84 ± 1.61	ND	–
<b>7l</b>	4-ClPh(Ph)CH	CH <sub>3</sub>	0.95 ± 0.04	1.2 ± 0.07	1.3
<b>7m</b>	3-BrPh(Ph)CH	CH <sub>3</sub>	0.90 ± 0.03	1.1 ± 0.04	1.2
<b>7n</b>	4-IPh(Ph)CH	CH <sub>3</sub>	0.95 ± 0.09	45.89 ± 1.67	48.3
<b>7o</b>	PhCH <sub>2</sub> OPh(Ph)CH	CH <sub>3</sub>	1.20 ± 0.11	11.19 ± 0.18	9.3
<b>7p</b>	4-BrPhCH <sub>2</sub> OPh(Ph)CH	CH <sub>3</sub>	8.0 ± 0.39	24.71 ± 0.14	3.1
<b>11a</b>	CH <sub>3</sub>	–	224.0 ± 8.10	ND	–
<b>11b</b>	Ph	–	31.0 ± 1.74	ND	–

<b>11c</b>	PhCH <sub>2</sub>	–	31.99 ± 1.48	ND	–
<b>4<sup>b</sup></b>	Ph(Ph)CH	H	28.8 ± 1.41	14.4 ± 0.9	0.5
<b>Azalanstat<sup>b</sup></b>	–	–	5.30 ± 0.4	24.40 ± 0.8	4.6

<sup>a</sup>Data are reported as IC<sub>50</sub> values in μM ± standard deviation (SD). Values are the mean of triplicate experiments. <sup>b</sup>Data from reference [23].

#### 2.4. Molecular modeling studies

A molecular docking study was performed as described in the experimental section to study the interactions of the reported compounds with HO-1 and HO-2. Initially, we focused our attention on the most potent and selective compound **7n** to explain the selectivity and understand the possible different potencies of the *R/S* and *E/Z* isomers. The poses of the four different isomers inside the binding pocket of HO-1 are shown in Figure 3. The four different isomers all have a similar pose inside the pocket where the iron(II) of the heme substrate in HO-1 is correctly coordinated by the nitrogen atom of the imidazole ring of the analyzed molecules in the eastern pocket. Through this coordination binding, iron(II) is protected from oxidation by disrupting an ordered solvent structure involving the critical Asp140 hydrogen-bond network (Tyr58, Tyr114, Arg136, and Asn210) and consequent displacement of water residues needed for catalysis. In all the docked structures, the unsubstituted phenyl moiety is always located in the principal western region of the binding pocket, whereas the 4-I substituted phenyl ring is always perfectly allocated inside the secondary western region. As shown in Figure 3, the consensus water was retained during the calculation inside the pocket; in fact, it was already showed that this molecule could have a fundamental importance in the enantiomers' recognitions for ethanolic linkers [26]. However, differently to the ethanolic linker compounds, our new series of reported molecule cannot interact with the water molecule, nor the *R* or the *S* stereoisomer. Actually, compounds **7n** all interact with a pose similar to **3**, where the lone pairs of the carbonyl oxygen in the linker are located in a different plane far away from acting as an H-bond acceptor with the conserved water molecule. Notably, the carbonyl oxygen of compounds *Z,R*, and *Z,S* are placed in an upward-like fashion as in **3**; differently, the carbonyl oxygen of compounds *E,R*, and *E,S* are placed in a downward style. In none of the four different isomers, the oxygen is engaging relevant interactions with the protein.

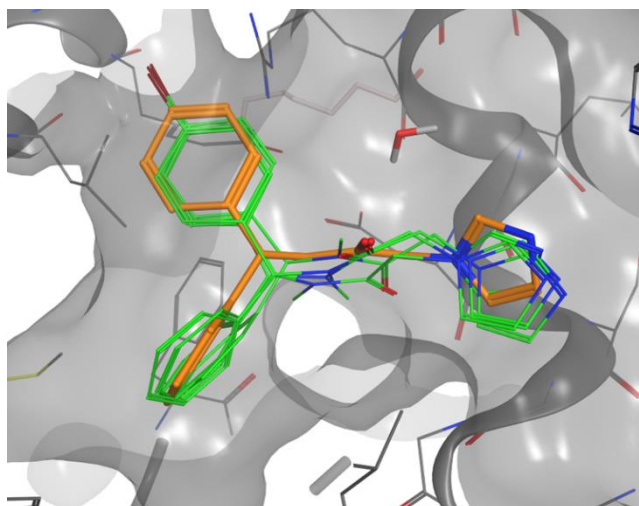


**Figure 3.** Binding interactions of the four different isomers of **7n** (green) compared with the binding pose of **3** in HO-1.

The calculated binding energies for the four isomers of **7n** are reported in Table 2. As expected from the binding poses, the calculated energies are very similar for all the compounds with slightly higher energies for the isomers where the carbonyl linker's oxygen is located in an upward specimen similar to **3**. These findings could lead to the conclusion that an enantiomeric resolution could not be an avenue worth pursuing. On the other hand, the *E/Z* interconversion, which occurs at room temperature, would move the *E* to *Z* equilibrium toward the most active isomer consumed during the reaction with HO-1.

**Table 2.** Docking results for **7n** isomers.

Compd	$\Delta G_B$ calcd. (kcal/mol)	$K_i$ calcd. ( $\mu\text{M}$ )
<i>R,E</i>	-6.51	16.81
<i>R,Z</i>	-6.63	13.73
<i>S,E</i>	-6.55	15.71
<i>S,Z</i>	-6.60	14.44

Once the most active compound's binding pose was studied, our attention was focused on the selectivity of the same compound **7n** toward HO-2. The sequence alignment of the HO-2 holoenzyme with that of the HO-1 confirmed that the catalytic cores of these two enzymes are structurally conserved with an RMSD of 0.874 Å over the 202 aminoacids alignment length [21]. Indeed, among the binding pocket residues, only four differences were seen between the two HO-1 and HO-2: Phe167Tyr187, Val50Ala70, Met34Val54, and Leu213Ile233. The modeling calculation started with the docking of **3** inside HO-2;

interestingly, the molecule interacts with the enzyme in a similar but different pose to the one it has in the HO-1 isoform. Remarkably, the predicted most active pose has the two phenyl rings pointing higher in the hydrophobic pocket, with a ring in the secondary western region, as in HO-1, and the second ring pointing in a different area of the pocket, probably due to the presence of Tyr 167 in HO-2 (Figure 4), that partially occupies the binding area [25].

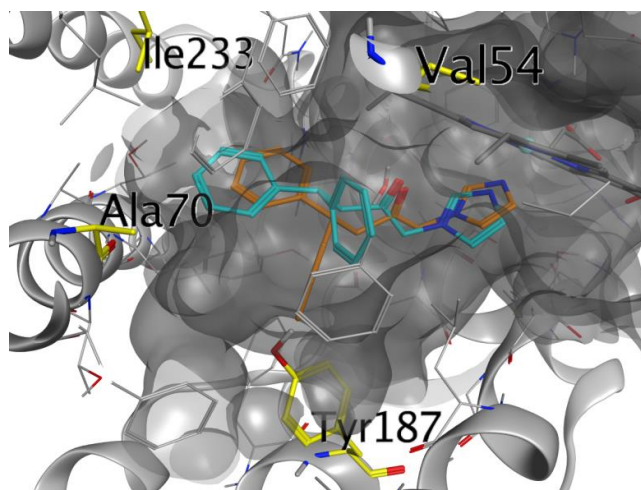


**Figure 4.** Comparison of compound **3** poses in HO-1 (orange) and HO-2 (light blue). The different residues between HO-2 and HO-1 binding pocket are highlighted in yellow. The highlighted residues belong to HO-2.

Closer inspection of the residues involved in compound's **3** interaction in HO-1 and HO-2 showed that the already reported gate closure by 167 Tyr in HO-2 is most likely the reason for this different pose inside the HO-2 isoform [25]. Molecules **7i** and **7l–n** were then docked in both isoforms to study the binding interactions and the selectivity, only the *R*, *Z* isomers were studied considering the already reported considerations for compound **7n**. The docked poses of **7i** and **7l–n** inside HO-1 and HO-2 are reported in Figures 5 and 6. All the molecules have similar poses of **3** inside both the HO-1 and HO-2 isoforms. The calculated binding potencies are in good agreement with the experimental values in the HO-1 and HO-2 inhibition assay (Table 3). These findings suggest that the proposed “double clamp” binding interaction of **3** can be fine-tuned by the presence of a substituent in a phenyl ring, increasing both the potency and the selectivity of the resulted compounds. The presence of no substituent, as in molecule **7i**, resulted in a similar no-selectivity as in **3** for HO-2. Small halogen atoms in molecules **7l** and **7m** are easily accommodated inside the HO-2 pocket as in HO-1, resulting in an overall no selectivity over the two isoforms. Unlike the 4-I in the

phenyl ring of **7n**, it is too sterically hindered for the pocket and pushes the imidazole ring away from the optimal distance for an effective interaction with the iron, resulting in less potency of the molecule in HO-2.

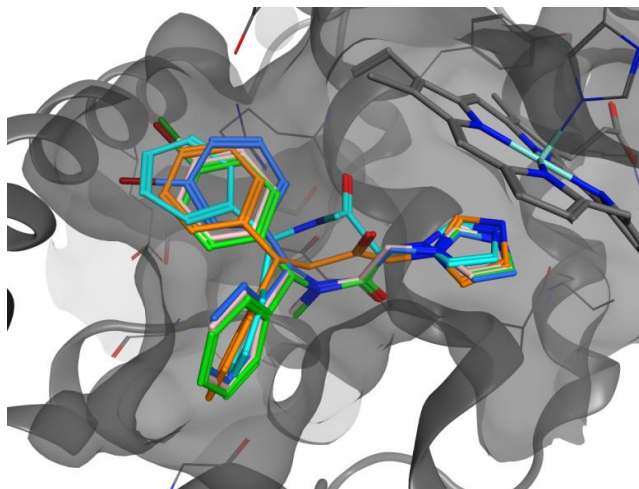


**Figure 5.** Comparison of **3** binding pose (orange) and **7i** (light blue), **7l** (light pink), **7m** (blue) and **7n** (green) in HO-1.

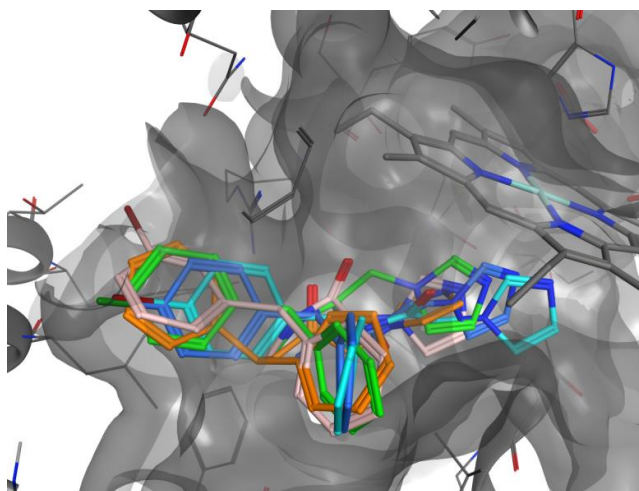


**Figure 6.** Comparison of **3** binding pose (orange) and **7i** (light blue), **7l** (light pink), **7m** (blue) and **7n** (green) in HO-2.

**Table 3.** Docking results for **7i**, **7l–n** in HO-1 and HO-2.

Cmpd	HO-1 $\Delta G_B$ calcd. (kcal/mol)	HO-1 $K_i$ calcd. ( $\mu\text{M}$ )	HO-2 $\Delta G_B$ calcd. (kcal/mol)	HO-2 $K_i$ calcd. ( $\mu\text{M}$ )
<b>7i</b>	-6.76	11.02	-6.61	14.20
<b>7l</b>	-6.52	16.53	-6.46	18.29
<b>7m</b>	-6.71	11.99	-6.54	15.98
<b>7n</b>	-6.63	13.73	-5.64	73.07



Finally, the lower selectivity and potency of the most potent compound with the more sterically hindered group, molecule **7o**, could be explained if the compound does not allocate the hindered group in the secondary binding pocket of the western region of HO-1; but in the northeastern pocket (Asn210, Ala31, Ile211, Ala28, and Glu32) in a similar pose of the aromatic region (trifluoromethylpyridine) analog in compound **1**. Unfortunately, it was concluded that modification in this region would result in neither potency nor selectivity increases and may not be an efficient avenue in developing highly selective HO-1 inhibitors [23]. Our docking calculation confirmed this; in fact, when the molecule is docked inside the HO-1, it prefers to allocate the hindered group in the northeastern pocket as in compound **1** (Figure 7), with calculated binding energy of  $-6.63$  kcal/mol for HO-1 and  $-5.78$  kcal/mol for HO-2 in agreement with the experimental ones.

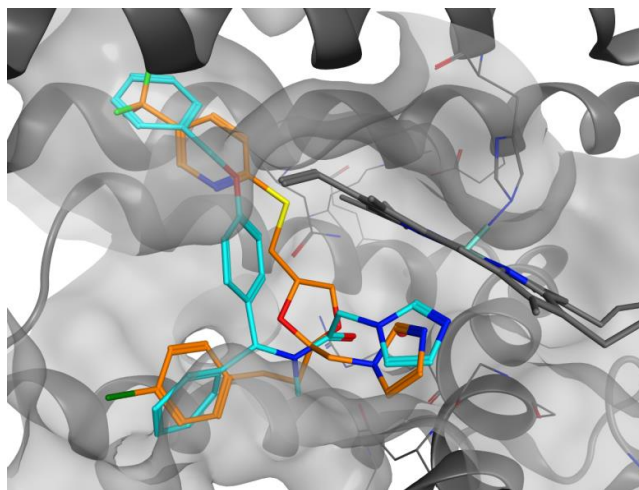


**Figure 7.** Comparison of compound **1** binding pose (orange) and **7o** (light blue) in HO-1.

### 2.5. **7l** *in silico* ADMET assessment

A suitable drug-like profile is an essential element for increasing the chance to advance a preclinical candidate through the drug discovery stages successfully. Therefore, we performed an *in-silico* absorption, distribution, metabolism, and excretion-toxicity (ADMET) pharmacokinetics evaluation. The *in-silico* assessment has been generated through the evaluation of pharmacokinetic profiles and possible adverse side effects for the molecule **7l**. ADMET molecular studies were conducted using SwissADME (<http://swissadme.ch>) [27] and pkCSM (<http://biosig.unimelb.edu.au/pkcsm/>) [28], results are reported in Tables S2 and S3. Compound **7l** resulted predicted as orally available, with high gastrointestinal absorption and soluble in water. The compound does not result as P-glycoprotein and CYP2D6 and CYP2C9 substrate, but differently can be a substrate for

CYP3A4 (Table S3). Moreover, most of the classical enzyme of the CYP family may be inhibited by our compound, i.e. CYP1A2, CYP2C19, CYP2C9, CYP2D6 and CYP3A4 (Table S2). Interestingly compound **71** has no violation to the Lipinski rule of 5, it also has no violation to other drug-likeness rules (Ghose, Egan, Veber, and Muegge) [29-33]. The absorption and distribution calculated parameters have been depicted by the Edan–Egg model in Figure S35 (Brain or IntestinaL Estimated, BOILED-Egg). The Edan–Egg model highlights that compound **71** was predicted to passively permeate the blood-brain barrier. pkCSM calculated absorption properties showed a higher than 94% intestinal absorption, due to the optimal (> 0.90) Caco-2 cell permeability. The calculated value of steady state volume of distribution is relatively high for the compounds (Log VD<sub>ss</sub> > 0.45), differently, the compound's unbound fraction in the plasma is relatively low resulting in a calculated unbound fraction in human of 0.019. The calculated values of the total clearance indicate that the compound has a good renal elimination (0.662 log ml/min/kg) and it is a substrate of the renal organic cation transporter 2. Finally, no toxicity issues were pointed out by pkCSM, also the compound resulted as non-toxic in the AMES test, not hepatotoxic, it does not have skin sensitization properties and should be generally well tolerated.

## 2.6. **71** preliminary *in vitro* ADMET assessment

To further corroborate the *in-silico* evaluation, preliminary experimental *in vitro* ADME (i.e., aqueous solubility, bidirectional permeability, metabolic stability, CYP450 inhibition) and toxicology testing (i.e., binding towards hERG potassium channel) were performed on compound **71** (Table 4).

**Table 4.** *In vitro* ADMET profile of **71**.

Test type	<b>71</b>	Reference cmpd.
Aqueous solubility <sup>a</sup>	195.8 μM	-
Bidirectional permeability (Caco-2, pH 6.5/7.4) <sup>b</sup>	P <sub>app A-B</sub> = 44.1 × 10 <sup>-6</sup> cm/s P <sub>app B-A</sub> = 19.4 × 10 <sup>-6</sup> cm/s	P <sub>app A-B</sub> = 26.9 × 10 <sup>-6</sup> cm/s P <sub>app B-A</sub> = 39.7 × 10 <sup>-6</sup> cm/s (propranolol)
Microsomal stability <sup>c</sup> (half-life/intrinsic clearance)	t <sub>1/2</sub> = 118.9 min Cl <sub>int</sub> = 58.3 μL/min/mg protein	t <sub>1/2</sub> = 88.5 min Cl <sub>int</sub> = 7.8 μL/min/mg protein (imipramine)
CYP2D6 inhibition <sup>d</sup>	2.5 μM	0.018 μM (quinidine)
CYP3A4 inhibition <sup>d</sup>	0.18 μM	0.046 μM (ketoconazole)

Potassium Channel hERG  
binding

5.7<sup>e</sup>

78<sup>f</sup>  
(terfenadine)

<sup>a</sup>Measured in simulated gastric fluid; <sup>b</sup>tested concentration 10  $\mu$ M; <sup>c</sup>assessed at a protein concentration of 0.1 mg/mL in human liver microsomes assay; <sup>d</sup>CYP isoforms inhibition is expressed as an IC<sub>50</sub> value; <sup>e</sup> % inhibition at 1  $\mu$ M; <sup>f</sup>  $K_i$  value in nM.

Since poor solubility and permeability are important factors that might affect both the ADME and the pharmacokinetic properties of a molecule, we initially investigated whether or not compound **71** was soluble in mimicking gastric fluid media and able to move across the intestinal epithelial barrier. As predicted by the *in-silico* calculations compound **71** showed good aqueous solubility at the selected pH, supporting its possible absorption from the stomach (Table 4). In addition, **71** displayed a suitable apparent permeability coefficient ( $P_{app}$ ) in either the A-B (apical to basolateral) or B-A (basolateral to apical) direction, with an efflux ratio <2 ( $P_{app\ BA}/P_{app\ AB} = 0.44$ ). Taken together, these data on solubility and permeability of **71** are likely indicative of a proper oral bioavailability.

Afterward, *in vitro* metabolic stability of **71** in human liver microsomes was tested, revealing suitable stability over the period of incubation (up to 1 h) better than imipramine used as a relatively stable reference compound.

As pointed in the *in silico* ADMET profiling, **71** as well as manyazole-based compounds are often able to inhibit heme-containing enzymes, including human cytochromes P450 (CYPs), thus potentially interfering and affecting oxidative metabolism of other drugs [34-35]. With this in mind, compound **71** was tested for its effects on human CYP2D6 and CYP3A4, the two CYP isoforms most involved in drug metabolism. The reference compounds quinidine and ketoconazole showed 139-fold and 4-fold higher inhibition of the two CYP isoforms than **71**.

Finally, to preliminary investigate potential undesirable cardiovascular side effects of **71**, binding toward the off-target hERG potassium channel was assessed (**71** was predicted as a non-inhibitor of hERG I, but a hERG II inhibitor, Table S3). Notably, **71** did not display any significant affinity for the selected target (% inhibition at 1  $\mu$ M = 5.7%), thus suggesting a low risk of cardiovascular liabilities.

### 2.7. **71** isosteric replacement and SAR analysis

In order to enlarge the chemical landscape evaluation and the SAR evaluation of **71**, a bioisosteric and fragment replacement software tool (Spark v10.4.0, Cresset, New Cambridge House, Hertfordshire, United Kingdom) was adopted to produce a scaffold-hopping analysis and to generate a virtual library of HO-1 ligands. The molecule **71** was

divided in two parts and a scaffold hopping analysis was performed for each part (Figure S36). In series 1 the two aromatic rings located in the western region were substituted and in series 2 the amide linker was substituted. The imidazole nucleus was not replaced due to the important interaction with heme. 200 molecules were generated for each substitution and the best 10 molecules of each series are reported in Tables S4 and S5. All the molecules were evaluated by the 3D superposition on an already published HO-1 3D-QSAR model, as reported in the experimental section, allowing a fast screening of the dataset. As demonstrated by the result of the series 1, a different aromatic ring can be used instead of the two phenyls (western region), particularly the substitution achieved optimal results with an imidazole, tetrazole and a pyridine ring. Moreover, an aromatic ring of molecule **71** can also be substituted by non-aromatic substituents (entries 7, 8 and 10, Table S4). The pivot carbon between the two phenyl rings of the western region can also be substituted by a nitrogen without losing activity (entries 4, 5, 6 and 9, Table S4). The length of the connecting unit between the imidazole (eastern region) and the aromatic rings of the western region was studied in the series 2. As showed by the results in Table S5, the connecting unit can easily contain small alkyl substituents (entries 1, 2, 4 and 4, Table S5), a different length can also be used without losing HO-1 inhibitory activity (entries 3 and 10, Table S5). Overall, thanks to the scaffold hopping analysis the SAR of molecule **71** was further explored and the results indicate that the scaffold replacement generated new structures with the appropriate chemical features for the binding to the HO-1. Some of the selected compounds resulted more potent than their precursor (3D-QSAR calculated  $pIC_{50}$  of **71** = 6.0), showing again the potential of the models to identify new hits among library of compounds and would deserve further research investigation to better understand the potential HO-1 inhibitory activity.

### *2.8. Biological evaluation – HO-1 levels in different tumoral cell lines*

As suggested by data reported in the literature, HO-1 is differentially expressed in cellular specific manner [36]. To select cancer cell lines more appropriate for studying the effects of our newly identified HO-1 inhibitors, we measured by western blot analysis the basal HO-1 protein expression in four different cancer cell lines, namely GBM (U87MG and A172), prostate carcinoma (DU-145) and lung adenocarcinoma (A549) (Figure 8A). We choose these cell lines since the associated cancers overexpress HO-1 protein, and their treatment still represents an unmet clinical need [6, 8, 10]. As clearly shown in Figure 8 panels A and B, HO-1 levels are significantly higher in U87MG when compared to the

others. These data were confirmed by immunofluorescence analysis assessing HO-1 immunoreactivity (green fluorescence) in all cell lines under basal condition (Figure 8C). Microphotographs show HO-1 high signal intensity in U87MG; whereas, HO-1 is weakly expressed in A172 mirroring western blot data. From the immunolocalization panel, we can also highlight that U87MG showed small spots in the perinuclear compartment, allowing us to suppose that in this cell line, HO-1 shows both cytoplasmic and nuclear localization.

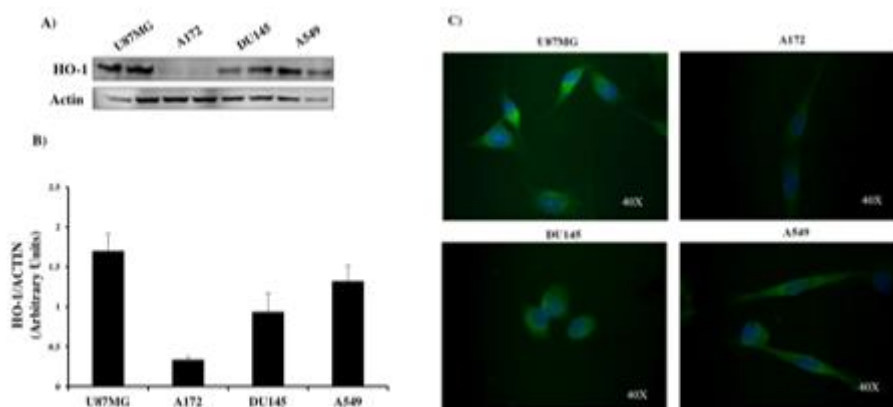


**Figure 8.** Expression levels of HO-1 in different cancer cell lines. A) Representative immunoblot of basal HO-1 protein expression detected on cell homogenate of U87MG, A172, DU145, and A549 cell lines; B) The bar graphs are representative of results from three independent experiments. Each protein level was expressed as arbitrary units obtained after normalization to Actin; C) Immunolocalization of HO-1 (green fluorescence) in tumor cell lines under basal condition. Nuclei were stained (blue) with DAPI. Photomicrographs are representative results of fields taken randomly from slides and scanned by a Zeiss fluorescent microscope.

### 2.9. Effect of compounds on cancer cell viability and HO-1 protein expression

Following the results obtained from the evaluation of the microsomal enzymatic activity in the presence of the tested compounds, compounds possessing an  $IC_{50}$  value  $\leq 8 \mu M$  (**7i** and **7l-p**) were selected for investigation on cell viability in cancer cell lines. To this extent, we performed an MTT assay at different concentrations (1, 10, and 50  $\mu M$ ) after 48 h of exposure to the selected compounds. Panels A and B of Figure 9 showed that the best results were obtained in both GBM cell lines with reduced cell viability at all concentrations tested. In the U87MG cell line (Figure 9A), all compounds, at 50  $\mu M$ , showed potent cell viability

reduction, except **7i**. Compounds **7m,n** determined more than 30% reduction at both concentrations 1 and 10  $\mu\text{M}$ ; whereas, **7o,p** around 20%. By analyzing the cell viability rate induced by the compounds at various concentrations, we can observe that **7l** is the most efficacious inhibitor in the U87MG cell line inducing more than 60% cell viability reduction at all the tested concentrations. In A172 cell lines (Figure 9B), compounds **7i-l** and **7o** showed a remarkable reduction of cell viability at all the tested concentrations, whereas compounds **7n** and **7p** only at 50  $\mu\text{M}$ , and milder activity at 10  $\mu\text{M}$ . Compound **7m** showed weak activity at all the tested concentrations. Conversely, in the lung adenocarcinoma cell line (A549, Figure 9, panel C) no substances demonstrated efficacy at 1  $\mu\text{M}$  concentration, whereas **7o** and **7p** showed weak effect at 10  $\mu\text{M}$ . Only compounds **7n-p** at 50  $\mu\text{M}$  concentration showed a significant reduction of cell viability. In prostate carcinoma cell line (DU-145, Figure 9, panel D), exclusively **7o**, and **7p** had efficacy at 1  $\mu\text{M}$  and 10  $\mu\text{M}$ , whereas **7n-p** showed a significant cell viability reduction at 50  $\mu\text{M}$ .

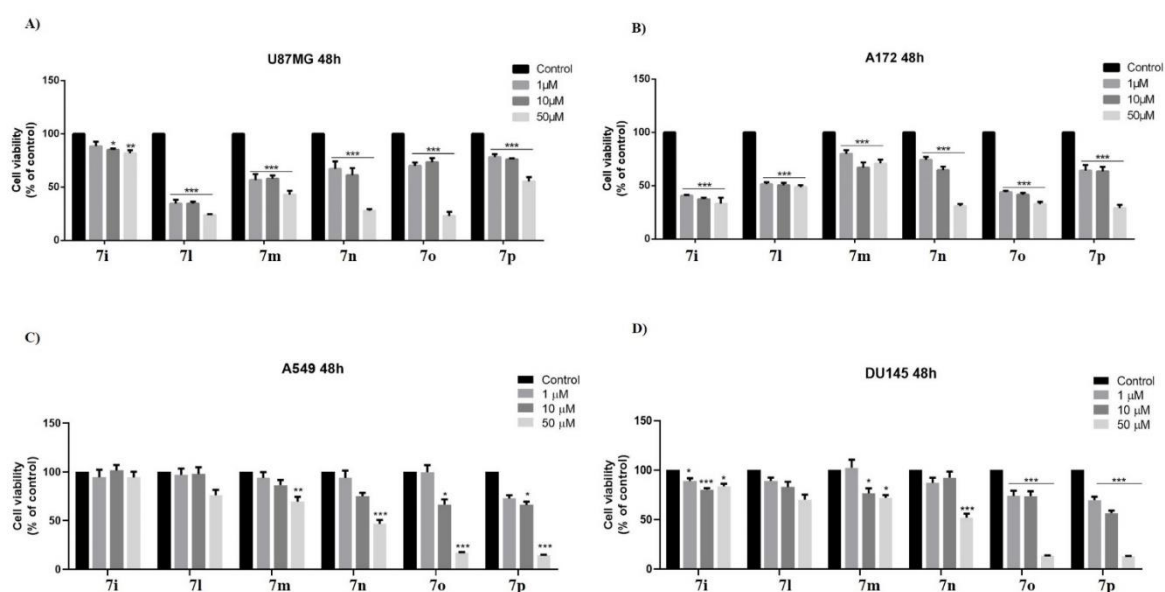


**Figure 9.** Effect of **7i** and **7l-p** treatments on cell viability of A) U87MG; B) A172; C) A549 and D) DU145 cell lines, assessed by MTT assay. Results are representative of at least three independent experiments, and the values are expressed as percentage of control (% of control). Data represent means  $\pm$  SEM. \* $p < 0.05$ ; \*\* $p < 0.01$  or \*\*\* $p < 0.001$  vs. control.

To investigate the link between cell viability reduction and HO-1 expression, we measured HO-1 levels in cancer cells after 48 h treatments with 10  $\mu\text{M}$  of each compound, **7i** and **7l-p**. Representative immunoblots of the signal detected in U87MG, A172, A549, and DU-145 are reported in Figure 10 (panels A–D, respectively). As shown in Figures 10A' and

B', **7l** reduced HO-1 expression only in U87MG. Quite unexpectedly, **7n** enhanced its levels in both U87MG and A172 cell lines, whereas **7i** and **7m** only in A172. In A549 (panel C'), **7l–n** weakly downregulated HO-1 levels; conversely, **7o** upregulated its expression. Finally, in DU-145, treatment with **7i** and **7n** reduced HO-1 protein expression. By careful analysis of data, compound **7l** was selected further to investigate its molecular mechanism in the U87MG cell line since it was able to significantly reduce cell viability and concomitantly HO-1 expression (Figures 9A and 10A).

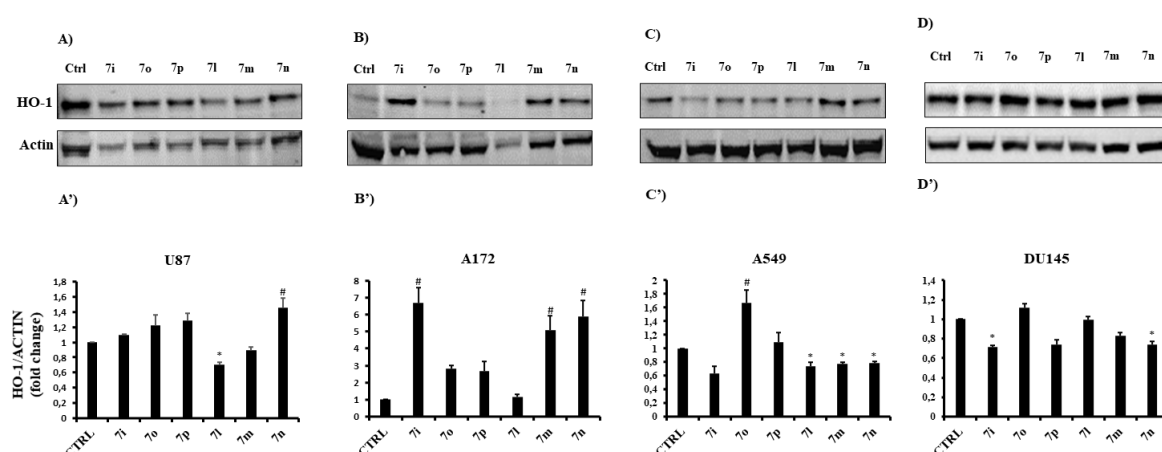


**Figure 10.** HO-1 expression after **7i** and **7l–p** treatments for 48h. A–D) Representative immunoblot of HO-1 protein expression detected on cell homogenate of U87MG, A172, A549, and DU145 cell lines treated with the selected compounds (10  $\mu$ M); A'–D') The bar graphs are representative of results from three independent experiments. Relative band density was quantified by using LI-COR software. Each protein level was expressed as a fold of change after normalization to actin used as a housekeeping protein. Data represent means  $\pm$  SEM. \* $p < 0.05$  vs. control # $p < 0.05$  vs. control

## 2.10. Effect of compound **7l** on HO-1 levels and enzymatic activity in U87MG cells

To evaluate whether HO activity inhibition was maintained in the intact cells, we measured HO enzymatic activity in U87MG cell line untreated and treated with 10  $\mu$ M of compound **7l**. The results, described in Figure 11 (Panel A), showed that **7l** reduced HO activity in cell lysates behaving as a HO inhibitor. Therefore, compound **7l** is effective in microsome preparation and in intact cells, suggesting that it can cross the cellular membrane and might have potential *in vivo* application. However, it is known that Mps, which are HO-1 inhibitors structurally related to heme and which consequently act as competitive HO-1 inhibitors, may induce upstream HO-1 expression *in vivo*, giving rise to opposite effects to

the expected results [37]. Consequently, HO-1 induction, together with other side-effects of Mps, limit their clinical use. Therefore, we measured HO-1 expression in intact U87MG cells treated and untreated with compound **71**.

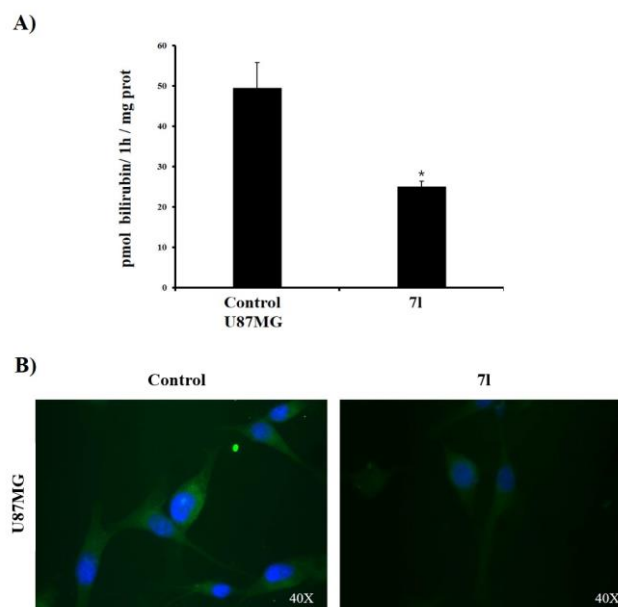


**Figure 11.** A) HO enzymatic activity in U87MG cell line untreated and treated with 10  $\mu$ M compound **71**; the results are representative of at least three independent experiments, and values are expressed as pmol of bilirubin/1h/mg protein. Data represent means  $\pm$  SEM. \* $p < 0.01$ ; vs. control. B) Immunolocalization of HO-1 (green fluorescence) in U87MG cell line under basal condition or after 48 h treatment with **71** at 10  $\mu$ M. Nuclei were stained (blue) with DAPI. Photomicrographs are representative results of fields taken randomly from slides and scanned by Zeiss fluorescent microscope.

Using immunofluorescence analysis, a technique that allows the detection of antigen in tissue or cells and localizes its distribution in cytoplasmic or perinuclear layers, we showed immunolocalization of HO-1 in the U87MG cell line under basal condition or after 48 h treatment with **71** at 10  $\mu$ M. We demonstrated that the treatment with **71** reduced the immunoreactivity of HO-1 in U87MG compared to control cells (Figure 11, panel B). These data are in agreement with immunoblot analysis (Figure 10A'). Thus, compound **71**, contrarily to other HO-1 inhibitors such as Mps, does not behave as an HO-1 inducer but can down-regulate HO-1 expression and inhibit HO-1 activity.



### 2.11. Effect of **7I** treatment on GBM rate of cell invasion and angiogenesis process

It is largely demonstrated that HO-1 is directly linked to neoangiogenesis occurring in tumoral mass with consequent increase of cell invasion rate [13, 38]. In fact, HO-1 can upregulate vascular endothelial growth factor (VEGF) that represents the main trophic factor involved in cancer progression [6]. Noteworthy, HO-1 gene is considered a potential marker of human glioma neovascularization; therefore, we evaluated the effect of **7I** on cell invasion and neoangiogenesis process [39, 40]. As shown in Figure 12 (panels A and B), we evaluated the effects of **7I** on U87MG cell motility through wound healing assay. As reported in Figure 12B, cell motility was drastically reduced following 48 h of **7I** treatment compared to control at 24 h and 48 h.

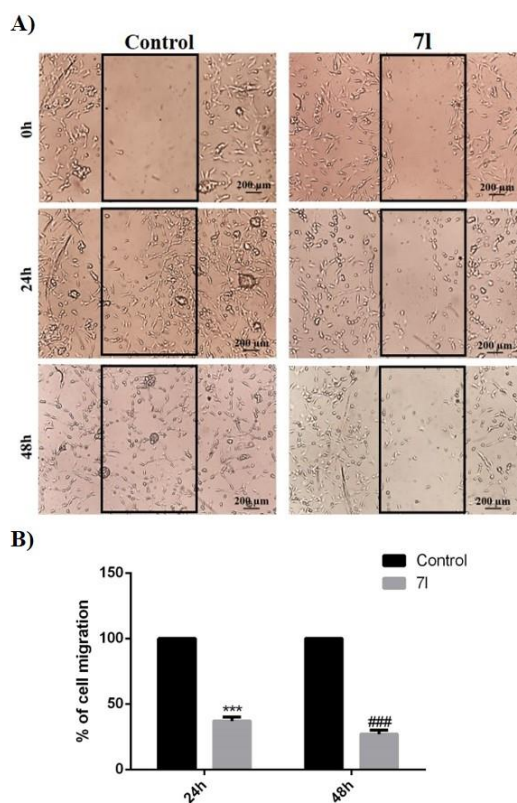


**Figure 12.** Effect of **7I** on GBM cells migration A) Cell monolayer was scraped by a pipette tip and incubated with **7I** compound or vehicle for 48 h. The wounded areas were visualized under a microscope for quantification. Migration was calculated as the average number of cells observed in three random wounded fields/per well in duplicate wells. Scale bar (200 μm). B) The bar graph shows data expressed as percentage of control (% of cell migration). Data represent means ± SEM. \*\*\* p<0.0001 vs. control 24 h; ### p<0.0001 vs. control 48 h.

Furthermore, as reported in Figure 13 (panels A, B, and C), **71** treatment caused a significant reduction of VEGF intracellular expression and its release in culture medium of U87MG cells, as demonstrated by western blot and ELISA assay, respectively. Since VEGF secretion in tumor microenvironment leads to neoangiogenesis, we have further investigated the effect of **71** in this process. To this end, we have tested the effect of the compound by using endothelial H5V cells that are able to form a network of tube-like structures, mimicking neo-vessels formation. These cells were cultured with 200  $\mu$ l of conditioned medium (CM) derived from U87MG cells treated with vehicle (CM1) or **71** (CM2) for 48 h. As shown in Figure 13 (panels D and E), incubation of H5V cells with CM2, medium derived from U87MG cells cultured with 10  $\mu$ M of compound **71**, significantly decreased the number of tube-like structures with respect to control cells.

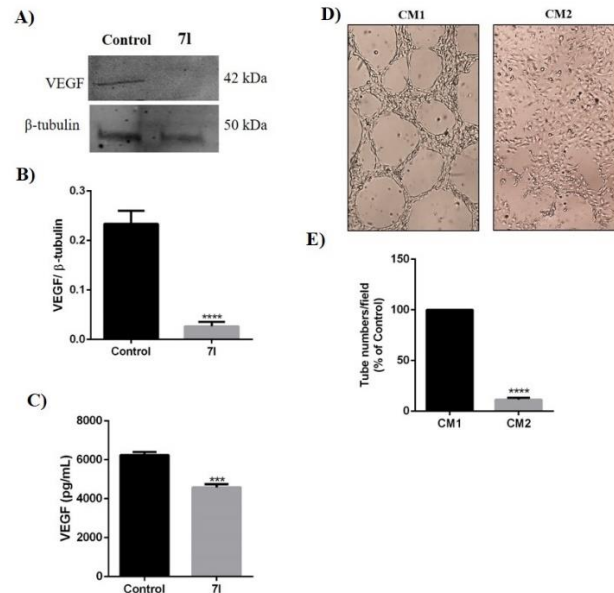


**Figure 13.** Effect of **71** on VEGF expression/release in U87MG human GBM cells, and new vessels formation. The expression and release of VEGF was evaluated in U87MG cells treated with vehicle or 10  $\mu$ M of **71** for 48 h by using western blot analysis (A and B) and ELISA assay (C). New vessel formation was evaluated by using tube formation assay (D and E). H5V cells were cultured with conditioned medium (CM) derived from U87MG cells treated with vehicle (CM1) or **71** (CM2) for 48 h. In the bar graph values are expressed as percentage of control (\*\*\*\* $p$ <0.0001 vs. Control).

These data allow us to suggest that **71** can reduce cell invasivity acting through modulation of HO-1 expression and would encourage further investigation to better understand the modulation of the angiogenesis process by compound **71**.

### 3. Conclusions

In the present paper, we report knowledge and structure-based design of new HO-1 inhibitors. Synthetic pathways described above enabled the exploration of the hydrophobic portion and the central linker of the HO-1 pharmacophore employing five different strategies. This exploration clarified the importance of the secondary hydrophobic pocket and the so-called “double clamp” binding mode. This binding interaction can be fine-tuned by the presence of a substituent in one out of the two phenyl rings, increasing both the potency and the selectivity of resulted compounds. Molecular modeling experiments showed how the newly designed compounds interact with the HO-1 and the molecular properties that lead to potent and selective compounds at the molecular level. Most potent compounds **7i** and **7l-p**, tested in a small panel of cancer cell lines, showed interesting antiproliferative profiles, especially in the GBM U87MG cell line. Potent antiproliferative activity and HO-1 expression levels in the U87MG cell line allowed the identification of **7l** as a promising lead compound for further characterization. Compound **7l** was able to potently inhibit enzymatic activity in intact U87MG cells in agreement with immunofluorescence analysis. Also, compound **7l** showed to significantly reduce VEGF release and new tube formation suggesting an important role in reducing cell invasivity. Considering that GBM remains still incurable due to its resistance to conventional therapies, this newly reported HO-1 inhibitor **7l** could be considered an interesting starting point to be further explored and optimized as a lead molecule in the management of GBM.

### 4. Experimental

#### 4.1. General

Melting points were determined in an IA9200 Electrothermal apparatus equipped with a digital thermometer in capillary glass tubes and are uncorrected. Infrared spectra were recorded on a Perkin Elmer 281 FTIR spectrometer using KBr disks or NaCl plates. Purity of all compounds was  $\geq 95\%$  as determined by elemental analyses (C, H, N) which was performed on a Carlo Erba Elemental Analyzer Mod. 1108; results were within  $\pm 0.4\%$  of the theoretical values.  $^1\text{H}$ - and  $^{13}\text{C}$ -NMR spectra were recorded on Varian Unity Inova 200 and 500 MHz spectrometers in  $\text{DMSO-}d_6$  or  $\text{CDCl}_3$  solution. Chemical shifts are given in ppm values, using tetramethylsilane (TMS) as the internal standard; coupling constants ( $J$ ) are given in Hz. Signal multiplicities are characterized as s (singlet), d (doublet), t (triplet),

q (quartet), m (multiplet), br (broad). All reactions were monitored on TLC (aluminum sheet coated with silica gel 60 F254, Merck, Kenilworth, NJ, USA) and visualized by UV ( $\lambda = 254$  and 366 nm) and iodine chamber. Purification of synthesized compounds by flash column chromatography was performed using silica gel 60 (Merck, Kenilworth, NJ, USA) or a Biotage FlashMaster Personal Plus system with prepacked silica gel columns of 25, 50, and 100 g (Biotage® SNAP cartridge KP-Sil, Uppsala, Sweden). Microwaves assisted reactions were accomplished with a CEM Discover instrument using closed Pyrex glass tubes with Teflon-coated septa. Where indicated, Celite® was used as a filter aid. All chemicals and solvents were reagent grade and were purchased from commercial vendors (Sigma Aldrich, Fluorochem, TCI chemicals). Compounds **5l–m**, **6a–d**, **6f–h**, **7a**, **7f**, **8o**, **9l**, and **10** have been reported in the literature, and characterization data match those reported [41-50].

#### 4.2. General procedure for the synthesis of 2-bromo-N-substituted-acetamides (**6a–p**)

In a round bottom flask, the appropriate starting amine **5a–p** (1 eq) was dissolved in dry CH<sub>3</sub>CN (10 mL). TEA (1.1 eq) was added, then  $\alpha$ -bromo-acetyl bromide (1.1 eq) was slowly dropped in the solution. The resulting mixture was left stirring at room temperature for 3 h. After this period of time, EtOAc (50 mL) was added, and the organic phase was washed with NaHCO<sub>3</sub> (2×50 mL) and brine (50 mL). The organic phase was dried over anhydrous Na<sub>2</sub>SO<sub>4</sub>, filtered, and evaporated. The resulting crude was purified by flash chromatography eluting with a mixture of Cy/EtOAc (7:3). Using this procedure, the following intermediates have been obtained.

##### 4.2.1. 2-Bromo-N-(4-iodophenyl)-N-methylacetamide (**6e**)

Yellow oil (17%): IR (neat) cm<sup>-1</sup> 3580 (broad), 2983, 1665 (C=O stretch), 1595, 1482, 1431, 1377, 1298, 1221, 1110, 1008, 832; <sup>1</sup>H NMR (200 MHz, CDCl<sub>3</sub>): Mixture of two *E/Z* conformers (approximately 50:50)  $\delta$  7.79 (d, *J* = 8.6 Hz, 1H, aromatic), 7.50–7.40 (m, 1H, aromatic), 7.30 (m, 1H, aromatic), 7.06 (d, *J* = 8.8 Hz, 1H, aromatic), 3.69 (s, 2H, COCH<sub>2</sub>, conformer *E* (or *Z*)), 3.66 (s, 2H, COCH<sub>2</sub>, conformer *Z* (or *E*)), 3.32 (s, 3H, NCH<sub>3</sub>, conformer *E* (or *Z*)), 3.29 (s, 3H, NCH<sub>3</sub>, conformer *Z* (or *E*)). Anal. Calcd. for: C<sub>9</sub>H<sub>9</sub>BrINO: C, 30.54; H, 2.56; N, 3.96. Found: C, 30.44; H, 2.55; N, 3.97.

##### 4.2.2. N-Benzhydryl-2-bromo-N-methylacetamide (**6i**)

Colorless oil (90%): IR (neat) cm<sup>-1</sup> 3060, 3028, 2932, 1652 (C=O stretch.), 1495, 1447, 1396, 1328, 1081, 1031, 977, 751, 731, 699, 600; <sup>1</sup>H NMR (200 MHz, DMSO-*d*<sub>6</sub>): Mixture

of two *E/Z* conformers (approximately 84:16)  $\delta$  7.43–7.29 (m, 6H, aromatic), 7.22–7.13 (m, 4H, aromatic), 6.86 (s, 1H, CHN, conformer *E* (or *Z*)), 6.49 (s, 1H, CHN, conformer *Z* (or *E*)), 4.28 (br s, 2H, COCH<sub>2</sub>), 2.82 (s, 3H, NCH<sub>3</sub>, conformer *E* (or *Z*)), 2.63 (s, 3H, NCH<sub>3</sub>, conformer *Z* (or *E*)). Anal. Calcd. for: C<sub>16</sub>H<sub>16</sub>BrNO: C, 60.39; H, 5.07; N, 4.40. Found: C, 60.21; H, 5.05; N, 4.41.

#### 4.2.3. 2-Bromo-*N*-(cyclopentyl(phenyl)methyl)-*N*-methylacetamide (**6j**)

White semisolid (63%): mp 70–72 °C; IR (neat) cm<sup>-1</sup> 3447, 2941, 2864, 1634 (C=O stretch.), 1498, 1448, 1402, 1328, 1215, 1134, 1091, 969, 744, 700, 610, 560, 520; <sup>1</sup>H NMR (200 MHz, DMSO-*d*<sub>6</sub>): Mixture of two *E/Z* conformers (approximately 88:12)  $\delta$  7.52–7.27 (m, 5H, aromatic), 5.36 (d, *J* = 12.0 Hz, 1H, CHN, conformer *E* (or *Z*)), 4.69 (d, *J* = 12.0 Hz, 1H, CHN, conformer *Z* (or *E*)), 4.18, 4.04 (ABq, *J*<sub>AB</sub> = 28.0 Hz, 2H, CH<sub>2</sub>Br), 2.75 (s, 3H, NCH<sub>3</sub>, conformer *E* (or *Z*)), 2.64 (s, 3H, NCH<sub>3</sub>, conformer *Z* (or *E*)), 1.78–1.48 (m, 7H, cyclopentyl), 1.31–0.95 (m, 2H, cyclopentyl). Anal. Calcd. for: C<sub>15</sub>H<sub>20</sub>BrNO: C, 58.07; H, 6.50; N, 4.51. Found: C, 58.24; H, 6.52; N, 4.49.

#### 4.2.4. 2-Bromo-*N*-(cyclohexyl(phenyl)methyl)-*N*-methylacetamide (**6k**)

Whitish solid (54%): mp 90–93 °C; IR (KBr) cm<sup>-1</sup> 3448 (broad), 2936, 2851, 1633 (C=O stretch.), 1449, 1402, 1326, 1088, 982, 955, 924, 892, 744, 703, 616, 559; <sup>1</sup>H NMR (200 MHz, DMSO-*d*<sub>6</sub>): Mixture of two *E/Z* conformers (approximately 83:17)  $\delta$  7.52–7.23 (m, 5H, aromatic), 5.30 (d, *J* = 10.0 Hz, 1H, CHN, conformer *E* (or *Z*)), 4.65–4.34 (m, 2H + 1H, CH<sub>2</sub>Br + CHN, conformer *Z* (or *E*)), 4.16, 4.04 (ABq, *J*<sub>AB</sub> = 24.0 Hz, 2H, CH<sub>2</sub>Br, conformer *E* (or *Z*)), 2.76 (s, 3H, NCH<sub>3</sub>, conformer *E* (or *Z*)), 2.63 (s, 3H, NCH<sub>3</sub>, conformer *Z* (or *E*)), 2.18 (m, 1H, cyclohexyl), 1.75–0.71 (m, 10H, cyclohexyl). Anal. Calcd. for: C<sub>16</sub>H<sub>22</sub>BrNO: C, 59.27; H, 6.84; N, 4.32. Found: C, 59.12; H, 6.82; N, 4.33.

#### 4.2.5. 2-Bromo-*N*-((4-chlorophenyl)(phenyl)methyl)-*N*-methylacetamide (**6l**)

Yellow oil (34%): IR (neat) cm<sup>-1</sup> 3030, 2886, 1659 (C=O stretch.), 1644, 1493, 1452, 1394, 1331, 1091, 1015, 978, 848, 742, 703; <sup>1</sup>H NMR (200 MHz, CDCl<sub>3</sub>): Mixture of two *E/Z* conformers (approximately 71:29)  $\delta$  7.40–7.32 (m, 5H, aromatic), 7.20–7.13 (m, 4H, aromatic), 7.04 (s, 1H, CHN, conformer *E* (or *Z*)), 6.38 (s, 1H, CHN, conformer *Z* (or *E*)), 3.95 (s, 2H, CH<sub>2</sub>Br, conformer *E* (or *Z*)), 3.85 (s, 2H, CH<sub>2</sub>Br, conformer *Z* (or *E*)), 2.89 (s, 3H, NCH<sub>3</sub>, conformer *E* (or *Z*)), 2.75 (s, 3H, NCH<sub>3</sub>, conformer *Z* (or *E*)). Anal. Calcd. for: C<sub>16</sub>H<sub>15</sub>BrClNO: C, 54.49; H, 4.29; N, 3.97. Found: C, 54.35; H, 4.27; N, 3.98.

#### 4.2.6. 2-Bromo-*N*-((3-bromophenyl)(phenyl)methyl)-*N*-methylacetamide (**6m**)

Yellow oil (50%): IR (neat)  $\text{cm}^{-1}$  3060, 2932, 1660 (C=O stretch.), 1644, 1568, 1471, 1393, 1325, 1250, 1232, 1174, 1079, 979, 882, 777, 740, 701;  $^1\text{H}$  NMR (200 MHz,  $\text{CDCl}_3$ ): Mixture of two *E/Z* conformers (approximately 70:30)  $\delta$  7.47–7.28 (m, 5H, aromatic), 7.19 (m, 4H, aromatic), 7.04 (s, 1H, CHN, conformer *E* (or *Z*)), 6.37 (s, 1H, CHN, conformer *Z* (or *E*)), 3.96 (s, 2H,  $\text{CH}_2\text{Br}$ , conformer *E* (or *Z*)), 3.84 (s, 2H,  $\text{CH}_2\text{Br}$ , conformer *Z* (or *E*)), 2.90 (s, 3H,  $\text{NCH}_3$ , conformer *E* (or *Z*)), 2.76 (s, 3H,  $\text{NCH}_3$ , conformer *Z* (or *E*)). Anal. Calcd. for:  $\text{C}_{16}\text{H}_{15}\text{Br}_2\text{NO}$ : C, 48.39; H, 3.81; N, 3.53. Found: C, 48.51; H, 3.82; N, 3.52.

#### 4.2.7. 2-Bromo-*N*-((4-iodophenyl)(phenyl)methyl)-*N*-methylacetamide (**6n**)

Pale yellow oil (78%): IR (neat)  $\text{cm}^{-1}$  3452 (broad), 2954, 2361, 1654 (C=O stretch.), 1482, 1399, 1081, 1006, 790;  $^1\text{H}$  NMR (200 MHz,  $\text{DMSO-}d_6$ ): Mixture of two *E/Z* conformers (approximately 85:15)  $\delta$  7.75 (d,  $J = 8.2$  Hz, 2H, aromatic), 7.40–7.33 (m, 3H, aromatic), 7.15–7.12 (m, 2H, aromatic), 6.96 (d,  $J = 8.4$  Hz, 2H, aromatic), 6.80 (s, 1H, CHN), 4.28 (s, 2H,  $\text{CH}_2\text{Br}$ ), 2.81 (s, 3H,  $\text{NCH}_3$ , conformer *E* (or *Z*)), 2.61 (s, 3H,  $\text{NCH}_3$ , conformer *Z* (or *E*)). Anal. Calcd. for:  $\text{C}_{16}\text{H}_{15}\text{BrINO}$ : C, 43.27; H, 3.40; N, 3.15. Found: C, 43.38; H, 3.41; N, 3.14.

#### 4.2.8. *N*-((4-(Benzyloxy)phenyl)(phenyl)methyl)-2-bromo-*N*-methylacetamide (**6o**)

White solid (91%): mp 170 °C (dec); IR (neat)  $\text{cm}^{-1}$  3292, 3031, 2931, 1734, 1652 (C=O stretch.), 1610, 1509, 1454, 1396, 1244, 1176, 1080, 1025, 845, 736, 698;  $^1\text{H}$  NMR (200 MHz,  $\text{DMSO-}d_6$ ): Mixture of two *E/Z* conformers (approximately 81:19)  $\delta$  7.48–7.28 (m, 8H, aromatic), 7.15–6.99 (m, 6H, aromatic), 6.80 (s, 1H, CHN), 5.10 (s, 2H,  $\text{CH}_2\text{O}$ ), 4.27 (s, 2H,  $\text{CH}_2\text{Br}$ ), 2.81 (s, 3H,  $\text{NCH}_3$ , conformer *E* (or *Z*)), 2.62 (s, 3H,  $\text{NCH}_3$ , conformer *Z* (or *E*)). Anal. Calcd. for:  $\text{C}_{23}\text{H}_{22}\text{BrNO}_2$ : C, 65.10; H, 5.23; N, 3.30. Found: C, 64.99; H, 5.21; N, 3.31.

#### 4.2.9. 2-Bromo-*N*-((4-((4-bromobenzyl)oxy)phenyl)(phenyl)methyl)-*N*-methylacetamide (**6p**)

Colorless oil (78%): IR (neat)  $\text{cm}^{-1}$  3032, 2365, 1654 (C=O stretch.), 1609, 1508, 1457, 1396, 1244, 1175, 1080, 1025, 736, 698, 666;  $^1\text{H}$  NMR (200 MHz,  $\text{DMSO-}d_6$ ): Mixture of two *E/Z* conformers (approximately 83:17)  $\delta$  7.48–7.32 (m, 7H, aromatic), 7.20–7.00 (m, 6H, aromatic), 6.80 (s, 1H, CHN), 5.10 (s, 2H,  $\text{CH}_2\text{O}$ ), 4.56 (s, 2H,  $\text{CH}_2\text{Br}$ , conformer *Z* (or

*E*)), 4.27 (s, 2H, CH<sub>2</sub>Br, conformer *E* (or *Z*)), 2.81 (s, 3H, NCH<sub>3</sub>, conformer *E* (or *Z*)), 2.62 (s, 3H, NCH<sub>3</sub>, conformer *Z* (or *E*)). Anal. Calcd. for: C<sub>23</sub>H<sub>21</sub>Br<sub>2</sub>NO<sub>2</sub>: C, 54.90; H, 4.21; N, 2.78. Found: C, 54.77; H, 4.20; N, 2.79.

#### 4.3. General procedure for the synthesis of final compounds **7c–d**, **7g–i**, and **7o** (Method A)

In a round bottom flask, K<sub>2</sub>CO<sub>3</sub> (3 eq) was suspended in dry DMF (6 mL). Imidazole (3 eq) was added to the suspension under stirring. The appropriate  $\alpha$ -bromo-acetamide intermediate **6** (1 eq) was dissolved in dry DMF (6 mL) and dropped to the suspension, which was left stirring at room temperature for 2 h. The resulting mixture was concentrated under vacuum, then EtOAc (100 mL) was added. The organic phase was washed with NaOH 1N (2×100 mL) and brine (1×100 mL). The organic phase was dried over anhydrous Na<sub>2</sub>SO<sub>4</sub>, filtered, and evaporated. The resulting crude was purified by crystallization in EtOAc or flash chromatography, using a mixture of CH<sub>2</sub>Cl<sub>2</sub>/MeOH (9.5:0.5) as eluent. Using this procedure, the following final compounds have been synthesized.

##### 4.3.1. *N*-(3-Bromophenyl)-2-(1*H*-imidazol-1-yl)acetamide (**7c**)

Purified by flash chromatography (9.5 CH<sub>2</sub>Cl<sub>2</sub>/0.5 MeOH). Brownish solid (16%): mp 158–162 °C; IR (KBr) cm<sup>-1</sup> 3245, 2915, 2849, 2783, 1698 (C=O stretch.), 1623, 1594, 1543, 1509, 1472, 1420, 1307, 1269, 1198, 1108, 1080, 1033, 870, 830, 783, 741, 684, 656; <sup>1</sup>H NMR (500 MHz, DMSO-*d*<sub>6</sub>):  $\delta$  10.50 (s, 1H, NH), 7.91 (s, 1H, imidazole), 7.70 (s, 1H, imidazole), 7.48 (d, *J* = 5.0 Hz, 1H, aromatic), 7.31–7.25 (m, 2H, aromatic), 7.18 (s, 1H, aromatic), 6.93 (s, 1H, imidazole), 4.92 (s, 2H, COCH<sub>2</sub>); <sup>13</sup>C NMR (125 MHz, DMSO-*d*<sub>6</sub>):  $\delta$  166.17, 140.20, 131.02, 127.58, 126.38, 121.72, 121.67, 121.00, 118.08, 49.32. Anal. Calcd for: C<sub>11</sub>H<sub>10</sub>BrN<sub>3</sub>O: C, 47.16; H, 3.60; N, 15.00. Found: C, 47.23; H, 3.60; N, 14.97.

##### 4.3.2. 2-(1*H*-Imidazol-1-yl)-*N*-(4-iodophenyl)acetamide (**7d**)

Purified by flash chromatography (9.5 CH<sub>2</sub>Cl<sub>2</sub>/0.5 MeOH). Beige crystals (66%): mp 222–225 °C; IR (KBr) cm<sup>-1</sup> 3258, 3181, 2954 (broad), 1706 (C=O stretch.), 1617, 1585, 1549, 1508, 1484, 1391, 1302, 1250, 1198, 1108, 1101, 1081, 916, 825; <sup>1</sup>H NMR (500 MHz, DMSO-*d*<sub>6</sub>):  $\delta$  10.45 (s, 1H, NH), 7.66 (d, *J* = 10.0 Hz, 2H, aromatic), 7.64 (s, 1H, imidazole), 7.43 (d, *J* = 10.0 Hz, 2H, aromatic), 7.16 (s, 1H, imidazole), 6.90 (s, 1H, imidazole), 4.90 (s, 2H, CH<sub>2</sub>CO); <sup>13</sup>C NMR (125 MHz, DMSO-*d*<sub>6</sub>):  $\delta$  165.95, 138.47, 138.32, 137.51, 127.89, 121.28, 120.74, 87.12, 49.17. Anal. Calcd for: C<sub>11</sub>H<sub>10</sub>IN<sub>3</sub>O: C, 40.39; H, 3.08; N, 12.85. Found: C, 40.43; H, 3.09; N, 12.82.

#### 4.3.3. *N*-Benzyl-2-(1*H*-imidazol-1-yl)-*N*-methylacetamide (**7g**)

Purified by flash chromatography (9.5 CH<sub>2</sub>Cl<sub>2</sub>/0.5 MeOH). Whitish solid (27%): mp 106–111 °C; IR (KBr) cm<sup>-1</sup> 3313, 3132, 3113, 3025, 2982, 2916, 1674 (C=O stretch.), 1603, 1485, 1453, 1406, 1357, 1341, 1307, 1291, 1235, 1204, 1121, 1071, 1038, 1004, 966, 948, 908, 824, 757, 735, 697, 665, 640, 593; <sup>1</sup>H NMR (500 MHz, DMSO-*d*<sub>6</sub>): Mixture of two *E/Z* conformers (approximately 70:30) δ 7.55 (s, 1H, imidazole), 7.42–7.25 (m, 5H, aromatic), 7.08 (s, 1H, imidazole, conformer *E* (or *Z*)), 7.06 (s, 1H, imidazole, conformer *Z* (or *E*)), 6.87 (s, 1H, imidazole, conformer *E* (or *Z*)), 6.86 (s, 1H, imidazole, conformer *Z* (or *E*)), 5.09 (s, 2H, ArCH<sub>2</sub>N, conformer *E* (or *Z*)), 5.06 (s, 2H, ArCH<sub>2</sub>N, conformer *Z* (or *E*)), 4.63 (s, 2H, COCH<sub>2</sub>, conformer *E* (or *Z*)), 4.53 (s, 2H, COCH<sub>2</sub>, conformer *Z* (or *E*)), 2.97 (s, 3H, NCH<sub>3</sub>, conformer *E* (or *Z*)), 2.80 (s, 3H, NCH<sub>3</sub>, conformer *Z* (or *E*)); <sup>13</sup>C NMR (125 MHz, DMSO-*d*<sub>6</sub>): δ 167.29, 167.06, 138.33, 137.29, 136.77, 128.80, 128.49, 127.60, 127.52, 127.16, 127.09, 120.96, 120.91, 51.69, 50.41, 47.30, 47.16, 33.83, 33.50. Anal. Calcd for: C<sub>13</sub>H<sub>15</sub>N<sub>3</sub>O: C, 68.10; H, 6.59; N, 18.33. Found: C, 68.24; H, 6.60; N, 18.27.

#### 4.3.4. *N,N*-Dibenzyl-2-(1*H*-imidazol-1-yl)acetamide (**7h**)

Purified by flash chromatography (9.5 CH<sub>2</sub>Cl<sub>2</sub>/0.5 MeOH). White solid (42%): mp 99–102 °C; IR (KBr) cm<sup>-1</sup> 3026, 2943, 1641 (C=O stretch.), 1513, 1495, 1451, 1438, 1422, 1346, 1315, 1291, 1261, 1218, 1199, 1105, 1078, 1038, 909, 819, 775, 753, 693, 666, 625, 579, 506; <sup>1</sup>H NMR (500 MHz, DMSO-*d*<sub>6</sub>): δ 7.57 (s, 1H, imidazole), 7.40 (t, *J* = 7.0 Hz, 2H, aromatic), 7.32 (t, *J* = 7.5 Hz, 3H, aromatic), 7.26 (t, *J* = 7.0 Hz, 3H, aromatic), 7.21 (d, *J* = 7.5 Hz, 2H, aromatic), 7.07 (s, 1H, imidazole), 6.87 (s, 1H, imidazole), 5.10 (s, 2H, COCH<sub>2</sub>), 4.58 (s, 2H, ArCH<sub>2</sub>N), 4.48 (s, 2H, ArCH<sub>2</sub>N); <sup>13</sup>C NMR (125 MHz, DMSO-*d*<sub>6</sub>): δ 167.74, 138.57, 137.10, 136.56, 129.01, 128.64, 127.88, 127.76, 127.38, 127.20, 121.12, 49.60, 48.56, 47.39. Anal. Calcd for: C<sub>19</sub>H<sub>19</sub>N<sub>3</sub>O: C, 74.73; H, 6.27; N, 13.76. Found: C, 74.98; H, 6.29; N, 13.75.

#### 4.3.5. *N*-Benzhydryl-2-(1*H*-imidazol-1-yl)-*N*-methylacetamide (**7i**)

Crystallized from EtOAc. White crystals (11%): mp 121–126 °C; IR (KBr) cm<sup>-1</sup> 3445 (broad), 3030, 2937, 1659 (C=O stretch.), 1643, 1508, 1498, 1477, 1451, 1400, 1233, 1109, 1073, 1031, 969, 901, 818, 751, 725, 699; <sup>1</sup>H NMR (500 MHz, DMSO-*d*<sub>6</sub>): Mixture of two *E/Z* conformers (approximately 85:15) δ 7.56 (s, 1H, imidazole), 7.41–7.32 (m, 6H, aromatic), 7.24–7.17 (m, 4H, aromatic), 7.09 (s, 1H, imidazole), 6.89 (s, 1H, imidazole), 6.87 (s, 1H, CHN, conformer *E* (or *Z*)), 6.53 (s, 1H, CHN, conformer *Z* (or *E*)), 5.17 (s, 2H,



COCH<sub>2</sub>, conformer *E* (or *Z*)), 5.13 (s, 2H, COCH<sub>2</sub>, conformer *Z* (or *E*)), 2.83 (s, 3H, NCH<sub>3</sub>, conformer *E* (or *Z*)), 2.64 (s, 3H, NCH<sub>3</sub>, conformer *Z* (or *E*)); <sup>13</sup>C NMR (125 MHz, DMSO-*d*<sub>6</sub>): δ 167.77, 138.87, 138.34, 128.53, 128.50, 127.79, 127.61, 127.46, 120.98, 60.34, 47.53, 30.97. Anal. Calcd for: C<sub>19</sub>H<sub>19</sub>N<sub>3</sub>O: C, 74.73; H, 6.27; N, 13.76. Found: C, 74.81; H, 6.28; N, 13.73.

4.3.6. *N*-((4-(Benzyloxy)phenyl)(phenyl)methyl)-2-(1*H*-imidazol-1-yl)-*N*-methylacetamide (**7o**).

Purified by flash chromatography (9.5 CH<sub>2</sub>Cl<sub>2</sub>/0.5 MeOH). White solid (14%): mp 119–121 °C; IR (KBr) cm<sup>-1</sup> 3447 (broad), 3111, 3034, 2977, 1654 (C=O stretch.), 1638, 1513, 1476, 1456, 1401, 1301, 1254, 1235, 1178, 1113, 1074, 1042, 1028, 844, 732, 705; <sup>1</sup>H NMR (500 MHz, DMSO-*d*<sub>6</sub>): Mixture of two *E/Z* conformers (approximately 80:20) δ 7.58 (s, 1H, imidazole), 7.46 (d, *J* = 5.0 Hz, 2H, aromatic), 7.40 (q, *J* = 7.0 Hz, 3H, aromatic), 7.34 (q, *J* = 7.0 Hz, 2H, aromatic), 7.24–7.23 (m, 1H, aromatic), 7.17 (d, *J* = 10.0 Hz, 2H, aromatic), 7.09 (d, *J* = 5.0 Hz, 2H, aromatic), 7.03 (d, *J* = 10.0 Hz, 2H, aromatic), 6.88 (s, 1H, imidazole), 6.82 (s, 1H, imidazole), 5.19–5.11 (m, 2H + 1H, COCH<sub>2</sub> + CHN), 3.62 (s, 2H, CH<sub>2</sub>O) 2.82 (s, 3H, NCH<sub>3</sub>, conformer *E* (or *Z*)), 2.63 (s, 3H, NCH<sub>3</sub>, conformer *Z* (or *E*)); <sup>13</sup>C NMR (125 MHz, DMSO-*d*<sub>6</sub>): δ 167.87, 157.86, 139.32, 138.58, 137.19, 131.10, 130.19, 128.93, 128.72, 128.37, 128.15, 127.96, 127.69, 127.58, 121.31, 114.97, 69.46, 60.07, 47.79, 31.03. Anal. Calcd for: C<sub>26</sub>H<sub>25</sub>N<sub>3</sub>O<sub>2</sub>: C, 75.89; H, 6.12; N, 10.21. Found: C, 76.12; H, 6.12; N, 10.18.

4.4. General procedure for the synthesis of final compounds **7b**, **7e**, **7j–n**, and **7p** (Method B)

In a two-necked round bottom flask, imidazole (3 eq) was dissolved in dry THF (10 mL) under an N<sub>2</sub> flow. Subsequently, NaH (oil dispersion 80%) (5 eq) was added, and the resulting suspension was left stirring for 15 minutes. The appropriate α-bromo-acetamide derivative **6** (1 eq) was dissolved in anhydrous THF (10 mL) in an inert atmosphere and subsequently dropped on the suspension of NaH and imidazole via syringe. The suspension was left under stirring at room temperature for 16 hours. Then, deionized water was added, and the resulting mixture was extracted three times with EtOAc (3×100 mL). The combined organic phases were washed with 150 mL of an aqueous solution of NaOH 1M, dried on Na<sub>2</sub>SO<sub>4</sub>, filtered, and concentrated under vacuum. The resulting oil was purified by flash chromatography using a mixture of CH<sub>2</sub>Cl<sub>2</sub>/MeOH (9.5:0.5) as eluent. The pure oils were

then triturated with cold Et<sub>2</sub>O affording final compounds as white solids, except for compounds **7e** and **7j-l**.

#### 4.4.1. 2-(1*H*-Imidazol-1-yl)-*N*-methyl-*N*-phenylacetamide (**7b**)

White solid (31%): mp 117–119 °C; IR (KBr) cm<sup>-1</sup> 3446 (broad), 3112, 2938, 1670 (C=O stretch.), 1595, 1513, 1495, 1418, 1393, 1329, 1295, 1236, 1125, 1080, 907, 826, 799, 774, 752, 697, 664, 562; <sup>1</sup>H NMR (500 MHz, DMSO-*d*<sub>6</sub>): δ 7.50–7.45 (m, 6H, aromatic + imidazole), 7.01 (s, 1H, imidazole), 6.81 (s, 1H, imidazole), 4.58 (s, 2H, COCH<sub>2</sub>), 3.18 (s, 3H, NCH<sub>3</sub>); <sup>13</sup>C NMR (125 MHz, DMSO-*d*<sub>6</sub>): δ 166.36, 142.17, 138.32, 129.96, 128.25, 127.59, 120.83, 47.86, 37.31. Anal. Calcd for: C<sub>12</sub>H<sub>13</sub>N<sub>3</sub>O: C, 66.96; H, 6.09; N, 19.52. Found: C, 67.03; H, 6.10; N, 19.48.

#### 4.4.2. 2-(1*H*-Imidazol-1-yl)-*N*-(4-iodophenyl)-*N*-methylacetamide (**7e**)

Light yellowish oil (47%): IR (neat) cm<sup>-1</sup> 3375 (broad), 3113, 2919, 1671 (C=O stretch.), 1595, 1508, 1497, 1419, 1394, 1327, 1292, 1235, 1124, 1079, 914, 800, 774, 739, 702, 663; <sup>1</sup>H NMR (500 MHz, DMSO-*d*<sub>6</sub>): Mixture of two *E/Z* conformers (approximately 73:27) δ 7.86–7.84 (m, 1H, aromatic), 7.53–7.42 (m, 2H + 1H, aromatic + imidazole), 7.28–7.26 (m, 1H, aromatic), 7.01 (s, 1H, imidazole), 6.82 (s, 1H, imidazole), 4.63 (s, 2H, COCH<sub>2</sub>, conformer *E* (or *Z*)), 4.59 (s, 2H, COCH<sub>2</sub>, conformer *Z* (or *E*)), 3.20 (s, 3H, NCH<sub>3</sub>, conformer *E* (or *Z*)), 3.18 (s, 3H, NCH<sub>3</sub>, conformer *Z* (or *E*)); <sup>13</sup>C NMR (125 MHz, DMSO-*d*<sub>6</sub>): δ 166.27, 142.15, 138.64, 138.21, 129.85, 128.11, 127.54, 120.72, 109.81, 47.77, 37.21, 37.02. Anal. Calcd for: C<sub>12</sub>H<sub>12</sub>IN<sub>3</sub>O: C, 42.25; H, 3.55; N, 12.32. Found: C, 42.39; H, 3.56; N, 12.28.

#### 4.4.3. *N*-(Cyclopentyl(phenyl)methyl)-2-(1*H*-imidazol-1-yl)-*N*-methylacetamide (**7j**)

White solid (84%): mp 134–136 °C; IR (KBr) cm<sup>-1</sup> 3447 (broad), 2952, 2865, 1654 (C=O stretch.), 1638, 1508, 1456, 1403, 1313, 1234, 1109, 1073, 908, 817, 760, 742, 702, 665, 567; <sup>1</sup>H NMR (500 MHz, DMSO-*d*<sub>6</sub>): Mixture of two *E/Z* conformers (approximately 87:13) δ 7.60 (s, 1H, imidazole, conformer *E* (or *Z*)), 7.52 (s, 1H, imidazole, conformer *Z* (or *E*)), 7.48–7.25 (m, 5H, aromatic), 7.08 (s, 1H, imidazole, conformer *E* (or *Z*)), 7.03 (s, 1H, imidazole, conformer *Z* (or *E*)), 6.85 (s, 1H, imidazole), 5.33–5.16 (m, 2H + 1H, COCH<sub>2</sub> + CHN, conformer *E* (or *Z*)), 5.00, 4.92 (ABq, *J*<sub>AB</sub> = 15.0 Hz, 2H, COCH<sub>2</sub>, conformer *Z* (or *E*)), 4.64 (d, *J* = 11.0 Hz, 1H, CHN, conformer *Z* (or *E*)), 2.75 (s, 3H, NCH<sub>3</sub>, conformer *E* (or *Z*)), 2.63 (s, 3H, NCH<sub>3</sub>, conformer *Z* (or *E*)), 1.75–1.69 (m, 1H, cyclopentyl), 1.63–1.49

(m, 5H, cyclopentyl), 1.25–1.18 (m, 1H, cyclopentyl), 1.00–0.93 (m, 1H, cyclopentyl); <sup>13</sup>C NMR (125 MHz, DMSO-*d*<sub>6</sub>): δ 167.36, 166.72, 139.67, 139.34, 138.50, 128.75, 128.62, 128.45, 127.94, 127.70, 127.63, 121.19, 64.14, 60.85, 47.80, 47.67, 38.24, 30.59, 30.43, 29.96, 29.73, 28.61, 28.01, 25.59, 25.42, 25.29, 25.23. Anal. Calcd for: C<sub>18</sub>H<sub>23</sub>N<sub>3</sub>O: C, 72.70; H, 7.80; N, 14.13. Found: C, 72.88; H, 7.82; N, 14.11.

#### 4.4.4. *N*-(Cyclohexyl(phenyl)methyl)-2-(1*H*-imidazol-1-yl)-*N*-methylacetamide (**7k**)

White solid (70%): mp 130–133 °C; IR (KBr) cm<sup>-1</sup> 3447 (broad), 2923, 2852, 1655 (C=O stretch.), 1645, 1508, 1448, 1405, 1317, 1294, 1234, 1138, 1107, 1077, 812, 742, 702, 662; <sup>1</sup>H NMR (500 MHz, DMSO-*d*<sub>6</sub>): Mixture of two *E/Z* conformers (approximately 83:17) δ 7.60 (s, 1H, imidazole, conformer *E* (or *Z*)), 7.50 (s, 1H, imidazole, conformer *Z* (or *E*)), 7.46–7.25 (m, 5H, aromatic), 7.07 (s, 1H, imidazole, conformer *E* (or *Z*)), 7.03 (s, 1H, imidazole, conformer *Z* (or *E*)), 6.86 (s, 1H, imidazole, conformer *E* (or *Z*)), 6.84 ((s, 1H, imidazole, conformer *Z* (or *E*)), 5.28–5.15 (m, 2H + 1H, COCH<sub>2</sub> + CHN, conformer *E* (or *Z*)), 5.01, 4.88 (ABq, *J*<sub>AB</sub> = 15.0 Hz, 2H, COCH<sub>2</sub>, conformer *Z* (or *E*)), 4.52 (d, *J* = 10.0 Hz, 1H, CHN, conformer *Z* (or *E*)), 2.75 (s, 3H, NCH<sub>3</sub>, conformer *E* (or *Z*)), 2.61 (s, 3H, NCH<sub>3</sub>, conformer *Z* (or *E*)), 2.20–2.10 (m, 1H, cyclohexyl), 1.78–1.55 (m, 4H, cyclohexyl), 1.39–1.06 (m, 4H, cyclohexyl), 0.93–0.86 (m, 1H, cyclohexyl), 0.78–0.70 (m, 1H, cyclohexyl); <sup>13</sup>C NMR (125 MHz, DMSO-*d*<sub>6</sub>): δ 167.54, 167.19, 138.63, 138.13, 128.99, 128.89, 128.16, 127.86, 127.68, 121.38, 64.87, 61.49, 48.01, 47.80, 36.85, 35.44, 30.61, 30.32, 29.41, 29.28, 28.70, 27.94, 26.23, 26.11, 25.84, 25.71, 25.57, 25.49. Anal. Calcd for: C<sub>19</sub>H<sub>25</sub>N<sub>3</sub>O: C, 73.28; H, 8.09; N, 13.49. Found: C, 73.41; H, 8.10; N, 13.45.

#### 4.4.5. *N*-((4-chlorophenyl)(phenyl)methyl)-2-(1*H*-imidazol-1-yl)-*N*-methylacetamide (**7l**)

Colorless solid (84%): mp 60–61 °C: IR (neat) cm<sup>-1</sup> 3384 (broad), 2932, 1660 (C=O stretch.), 1510, 1491, 1404, 1299, 1108, 1078, 1014, 828, 740, 704; <sup>1</sup>H NMR (500 MHz, DMSO-*d*<sub>6</sub>): Mixture of two *E/Z* conformers (approximately 87:13) δ 7.56 (s, 1H, imidazole), 7.48–7.32 (m, 5H, aromatic), 7.25–7.15 (m, 4H, aromatic), 7.08 (s, 1H, imidazole), 6.86 (s, 1H, imidazole), 6.83 (s, 1H, CHN, conformer *E* (or *Z*)), 6.50 (s, 1H, CHN, conformer *Z* (or *E*)), 5.13 (s, 2H, COCH<sub>2</sub>, conformer *E* (or *Z*)), 5.10 (s, 2H, COCH<sub>2</sub>, conformer *Z* (or *E*)), 2.81 (s, 3H, NCH<sub>3</sub>, conformer *E* (or *Z*)), 2.61 (s, 3H, NCH<sub>3</sub>, conformer *Z* (or *E*)); <sup>13</sup>C NMR (125 MHz, DMSO-*d*<sub>6</sub>): δ 168.04, 138.55, 138.11, 132.32, 130.52, 128.87, 128.71, 127.88, 127.69, 121.27, 60.17, 47.78, 31.18. Anal. Calcd for: C<sub>19</sub>H<sub>18</sub>ClN<sub>3</sub>O: C, 67.15; H, 5.34; N, 12.37. Found: C, 67.33; H, 5.34; N, 12.35.

#### 4.4.6. *N-((3-Bromophenyl)(phenyl)methyl)-2-(1H-imidazol-1-yl)-N-methylacetamide (7m)*

Colorless solid (50%): mp 82–83 °C; IR (neat)  $\text{cm}^{-1}$  3375 (broad), 2968, 2361, 1660 (C=O stretch.), 1593, 1568, 1514, 1472, 1402, 1301, 1236, 1108, 1078, 826, 739, 703, 665;  $^1\text{H}$  NMR (500 MHz, DMSO- $d_6$ ): Mixture of two *E/Z* conformers (approximately 84:16)  $\delta$  7.56 (s, 1H, imidazole), 7.53 (d,  $J = 8.0$  Hz, 1H, aromatic), 7.41–7.33 (m, 4H, aromatic), 7.31 (s, 1H, aromatic), 7.22–7.16 (m, 3H, aromatic), 7.08 (s, 1H, imidazole), 6.86 (s, 1H, imidazole), 6.84 (s, 1H, CHN, conformer *E* (or *Z*)), 6.52 (s, 1H, CHN, conformer *Z* (or *E*)), 5.18, 5.13 (ABq,  $J_{\text{AB}} = 20.0$  Hz, 2H, COCH<sub>2</sub>), 2.83 (s, 3H, NCH<sub>3</sub>, conformer *E* (or *Z*)), 2.63 (s, 3H, NCH<sub>3</sub>, conformer *Z* (or *E*));  $^{13}\text{C}$  NMR (125 MHz, DMSO- $d_6$ ):  $\delta$  168.11, 141.99, 138.55, 138.37, 131.10, 130.92, 130.63, 128.87, 128.76, 127.94, 127.64, 122.09, 121.24, 60.31, 47.76, 31.32. Anal. Calcd for: C<sub>19</sub>H<sub>18</sub>BrN<sub>3</sub>O: C, 59.39; H, 4.72; N, 10.94. Found: C, 59.52; H, 4.73; N, 10.94.

#### 4.4.7. *2-(1H-Imidazol-1-yl)-N-((4-iodophenyl)(phenyl)methyl)-N-methylacetamide (7n)*

White solid (74%): mp 69–71 °C; IR (neat)  $\text{cm}^{-1}$  3447 (broad), 2361, 1654 (C=O stretch.), 1508, 1483, 1400, 1300, 1236, 1108, 1078, 1006, 829, 739, 702;  $^1\text{H}$  NMR (500 MHz, DMSO- $d_6$ ): Mixture of two *E/Z* conformers (approximately 84:16)  $\delta$  7.75 (d,  $J = 8.0$  Hz, 2H, aromatic), 7.55 (s, 1H, imidazole), 7.44–7.33 (m, 3H, aromatic), 7.17 (d,  $J = 7.0$  Hz, 2H, aromatic), 7.08 (s, 1H, imidazole), 6.99 (d,  $J = 8.0$  Hz, 2H, aromatic), 6.86 (s, 1H, imidazole), 6.83 (s, 1H, CHN, conformer *E* (or *Z*)), 6.49 (s, 1H, CHN, conformer *Z* (or *E*)), 5.15 (s, 2H, COCH<sub>2</sub>, conformer *E* (or *Z*)), 5.12 (s, 2H, COCH<sub>2</sub>, conformer *Z* (or *E*)), 2.82 (s, 3H, NCH<sub>3</sub>, conformer *E* (or *Z*)), 2.62 (s, 3H, NCH<sub>3</sub>, conformer *Z* (or *E*));  $^{13}\text{C}$  NMR (125 MHz, DMSO- $d_6$ ):  $\delta$  167.82, 138.80, 138.33, 137.26, 130.78, 128.60, 128.52, 127.60, 120.96, 93.58, 60.05, 47.52, 30.96. Anal. Calcd for: C<sub>19</sub>H<sub>18</sub>IN<sub>3</sub>O: C, 52.91; H, 4.21; N, 9.74. Found: C, 53.01; H, 4.22; N, 9.72.

#### 4.4.8. *N-((4-((4-Bromobenzyl)oxy)phenyl)(phenyl)methyl)-2-(1H-imidazol-1-yl)-N-methylacetamide (7p)*

White solid (40%): mp 120–121 °C; IR (KBr)  $\text{cm}^{-1}$  3447 (broad), 3031, 2934, 1655 (C=O stretch.), 1609, 1509, 1456, 1400, 1304, 1245, 1177, 1111, 1076, 1104, 849, 750, 699, 662, 622;  $^1\text{H}$  NMR (500 MHz, DMSO- $d_6$ ): Mixture of two *E/Z* conformers (approximately 82:18)  $\delta$  7.54 (s, 1H, imidazole), 7.45–7.31 (m, 7H, aromatic), 7.20–7.14 (m, 2H, aromatic), 7.08–7.00 (m, 4H, aromatic), 6.85 (s, 1H, imidazole), 6.80 (s, 1H, imidazole), 5.16–5.09 (m, 3H, CHN + COCH<sub>2</sub>), 3.41 (s, 2H, CH<sub>2</sub>O), 2.80 (s, 3H, NCH<sub>3</sub>, conformer *E* (or *Z*)), 2.61 (s,

3H, NCH<sub>3</sub>, conformer *Z* (or *E*)); <sup>13</sup>C NMR (125 MHz, DMSO-*d*<sub>6</sub>): δ 167.70, 157.74, 139.21, 138.41, 137.08, 130.98, 130.02, 128.55, 128.23, 127.96, 127.79, 127.61, 127.39, 121.08, 114.84, 69.35, 59.91, 47.62, 30.89. Anal. Calcd for: C<sub>26</sub>H<sub>24</sub>BrN<sub>3</sub>O<sub>2</sub>: C, 63.68; H, 4.93; N, 8.57. Found: C, 63.70; H, 4.94; N, 8.55.

#### 4.5. Synthesis of 4-benzyloxy-substituted benzophenones **8o-p**

4-Hydroxyacetophenone (5 mmol) and K<sub>2</sub>CO<sub>3</sub> (10 mmol) were suspended in acetone (20 mL), then the appropriate benzyl bromide (10 mmol) and a catalytic amount of KI were added. The mixture was refluxed for 3 hours. The reaction solvent was removed under vacuum, and the resulting solid was crystallized from ethanol.

##### 4.5.1. (4-((4-Bromobenzyl)oxy)phenyl)(phenyl)methanone (**8p**)

Whitish crystals (85%): mp 101–103 °C; IR (KBr) cm<sup>-1</sup> 3448 (broad), 2920, 2861, 1639 (C=O stretch), 1602, 1503, 1489, 1446, 1404, 1378, 1290, 1247, 1224, 1174, 1149, 1074, 1021, 1010, 939, 925, 845, 802, 740, 695, 609, 508; <sup>1</sup>H NMR (200 MHz, DMSO-*d*<sub>6</sub>): δ 7.78–7.43 (m, 11H, aromatic), 7.17 (d, *J* = 8.0 Hz, 2H, aromatic), 5.22 (s, 1H, CH<sub>2</sub>O). Anal. Calcd. for: C<sub>20</sub>H<sub>15</sub>BrO<sub>2</sub>: C, 65.41; H, 4.12. Found: C, 65.27; H, 4.11.

#### 4.6. General procedure for the synthesis of formamides **9j-p**

In a sealed vial equipped with a stirring bar were added ketones **8j-p** (1 eq), formic acid (1.25 eq), and formamide (3 mL). The suspension was stirred under microwave irradiation for 90 minutes (150 W, 150 psi, 170 °C). The resulting hot solution was diluted with EtOAc (100 mL) and washed three times with brine (3×50 mL). The organic phase was dried with Na<sub>2</sub>SO<sub>4</sub>, filtered, and evaporated. The crude was crystallized with a mixture of CHCl<sub>3</sub>/*n*-hexane or purified by flash chromatography using a mixture of Cy/EtOAc (7:3). Using this procedure, the following compounds have been synthesized.

##### 4.6.1. *N*-(Cyclopentyl(phenyl)methyl)formamide (**9j**)

Crystallized from CHCl<sub>3</sub>/*n*-hexane. Whitish solid (57%): mp 65–68 °C; IR (KBr) cm<sup>-1</sup> 3331, 2957, 2859, 1657 (C=O stretch), 1510, 1385, 1223, 755, 701, 525; <sup>1</sup>H NMR (200 MHz, DMSO-*d*<sub>6</sub>): δ 8.62 (d, *J* = 10.0 Hz, 1H, CONH), 8.02 (s, 1H, CHO), 7.34–7.19 (m, 5H, aromatic), 4.69–4.59 (m, 1H, CHN), 2.29–2.13 (m, 1H, cyclopentyl), 1.77–0.99 (m, 8H, cyclopentyl). Anal. Calcd for: C<sub>13</sub>H<sub>17</sub>NO: C, 76.81; H, 8.43; N, 6.89. Found: C, 76.70; H, 8.41; N, 6.91.

#### 4.6.2. *N*-(Cyclohexyl(phenyl)methyl)formamide (**9k**)

Crystallized from CHCl<sub>3</sub>/*n*-hexane. Whitish solid (77%): mp 128–130 °C; IR (KBr) cm<sup>-1</sup> 3334, 3061, 3029, 2923, 2847, 1660 (C=O stretch), 1513, 1444, 1385, 1286, 1232, 1199, 1183, 1138, 1074, 1012, 966, 913, 893, 834, 768, 754, 703, 678, 632, 573, 526; <sup>1</sup>H NMR (200 MHz, DMSO-*d*<sub>6</sub>): δ 8.56 (d, *J* = 8.0 Hz, 1H, CONH), 8.06 (s, 1H, CHO), 7.36–7.22 (m, 5H, aromatic), 4.69–4.60 (m, 1H, CHN), 1.78–1.50 (m, 5H, cyclohexyl), 1.33–0.83 (m, 6H, cyclohexyl). Anal. Calcd for: C<sub>14</sub>H<sub>19</sub>NO: C, 77.38; H, 8.81; N, 6.45. Found: C, 77.57; H, 8.83; N, 6.43.

#### 4.6.3. *N*-((3-Bromophenyl)(phenyl)methyl)formamide (**9m**)

Crystallized from CHCl<sub>3</sub>/*n*-hexane. Pale beige solid (57%): mp 97–100 °C; IR (KBr) cm<sup>-1</sup> 3118, 3023, 2885, 2366, 1676 (C=O stretch), 1652, 1541, 1388, 1244, 1193, 1075, 1027, 788, 761, 745, 705, 610; <sup>1</sup>H NMR (200 MHz, DMSO-*d*<sub>6</sub>): δ 9.18 (d, *J* = 8.0 Hz, 1H, CONH), 8.17 (s, 1H, CHO), 7.51–7.27 (m, 9H, aromatic), 6.20 (d, *J* = 8.0 Hz, 1H, CHN). Anal. Calcd for: C<sub>14</sub>H<sub>12</sub>BrNO: C, 57.95; H, 4.17; N, 4.83. Found: C, 57.81; H, 4.16; N, 4.84.

#### 4.6.4. *N*-((4-Iodophenyl)(phenyl)methyl)formamide (**9n**)

Crystallized from CHCl<sub>3</sub>/*n*-hexane. Beige solid (50%): mp 142–144 °C; IR (KBr) cm<sup>-1</sup> 3327, 3227, 3007, 2904, 2344, 1654 (C=O stretch.), 1522, 1493, 1450, 1397, 1379, 1222, 1062, 1007, 850, 814, 762, 741, 700, 604, 537; <sup>1</sup>H NMR (200 MHz, DMSO-*d*<sub>6</sub>): δ 9.13 (d, *J* = 8.0 Hz, 1H, CONH), 8.16 (s, 1H, CHO), 7.71 (d, *J* = 8.2 Hz, 2H, aromatic), 7.39–7.22 (m, 5H, aromatic), 7.10 (d, *J* = 8.2 Hz, 2H, aromatic), 6.14 (d, *J* = 8.0 Hz, 1H, CHN). Anal. Calcd for: C<sub>14</sub>H<sub>12</sub>INO: C, 49.87; H, 3.59; N, 4.15. Found: C, 49.76; H, 3.60; N, 4.14.

#### 4.6.5. *N*-((4-(Benzyloxy)phenyl)(phenyl)methyl)formamide (**9o**)

Crystallized from CHCl<sub>3</sub>/*n*-hexane. Whitish solid (73%): mp 127–130 °C; IR (KBr) cm<sup>-1</sup> 3331, 3030, 2865, 1658 (C=O stretch.), 1610, 1511, 1452, 1385, 1236, 1181, 1011, 916, 873, 826, 819, 760, 698, 614, 542; <sup>1</sup>H NMR (200 MHz, DMSO-*d*<sub>6</sub>): δ 9.07 (d, *J* = 8.0 Hz, 1H, CONH), 8.14 (s, 1H, CHO), 7.45–7.17 (m, 12H, aromatic), 6.97 (d, *J* = 8.0 Hz, 2H, aromatic), 6.12 (d, *J* = 8.0 Hz, 1H, CHN), 5.07 (s, 2H, CH<sub>2</sub>O). Anal. Calcd for: C<sub>21</sub>H<sub>19</sub>NO<sub>2</sub>: C, 79.47; H, 6.03; N, 4.41. Found: C, 79.65; H, 6.01; N, 4.40.

#### 4.6.6. *N*-((4-((4-Bromobenzyl)oxy)phenyl)(phenyl)methyl)formamide (**9p**)

Purified by flash chromatography (7 Cy/3 EtOAc). Whitish solid (35%): mp 146–149

°C; IR (KBr)  $\text{cm}^{-1}$  3303, 3030, 2919, 2867, 1657 (C=O stretch.), 1610, 1596, 1511, 1490, 1450, 1390, 1236, 1180, 1070, 1012, 876, 826, 816, 801, 761, 734, 702, 582, 542, 510;  $^1\text{H}$  NMR (200 MHz,  $\text{DMSO-}d_6$ ):  $\delta$  9.04 (d,  $J = 8.0$  Hz, 1H, CONH), 8.14 (s, 1H, CHO), 7.58 (d,  $J = 8.0$  Hz, 2H, aromatic), 7.41–7.17 (m, 9H, aromatic), 6.96 (d,  $J = 8.0$  Hz, 2H, aromatic), 6.12 (d,  $J = 8.0$  Hz, 1H, CHN), 5.06 (s, 2H,  $\text{CH}_2\text{O}$ ). Anal. Calcd for:  $\text{C}_{21}\text{H}_{18}\text{BrNO}_2$ : C, 63.65; H, 4.58; N, 3.53. Found: C, 63.46; H, 4.59; N, 3.54.

#### 4.7. General procedure for the synthesis of *N*-methylamines **5j–k**, **5o–p**

A two-necked round bottom flask equipped with a stirring bar was filled with  $\text{N}_2$ . A suspension of  $\text{LiAlH}_4$  in THF 1M (6 eq) was added into the flask. The proper formamide **6** (1 eq) was dissolved in dry THF (10 mL) in an inert atmosphere and slowly dropped via syringe to the suspension. The reaction was refluxed for 2 hours. Then, the reaction mixture was cooled at 0 °C with an ice bath, and an aqueous solution of NaOH 2M (20 eq) was carefully added. The mixture was left under stirring for 30 minutes. The reaction mixture was diluted with EtOAc (50 mL) and extracted with water ( $3 \times 75$  mL) and brine (1x100 mL). The organic phases were dried on  $\text{Na}_2\text{SO}_4$ , filtered, and evaporated under vacuum. The crude product was purified by flash chromatography or column chromatography using a Biotage® chromatographic system with Biotage® SNAP KP-Sil flash chromatography cartridges using gradient mixtures of  $\text{CH}_2\text{Cl}_2/\text{MeOH}$ . Using this procedure, the following compounds have been synthesized.

##### 4.7.1. 1-Cyclopentyl-*N*-methyl-1-phenylmethanamine (**5j**)

Pale yellow oil (52%): IR (neat)  $\text{cm}^{-1}$  3337 (broad) (N-H stretch), 2951, 2868, 2785, 1490, 1474, 1452, 1136, 836, 761, 701;  $^1\text{H}$  NMR (200 MHz,  $\text{DMSO-}d_6$ ):  $\delta$  7.34–7.15 (m, 5H, aromatic), 3.12 (d,  $J = 8.0$  Hz, 1H, CHN), 2.03 (s, 3H,  $\text{NCH}_3$ ), 1.99–1.76 (m, 2H, cyclopentyl), 1.61–1.28 (m, 5H, cyclopentyl), 1.23–0.97 (m, 2H, cyclopentyl). Anal. Calcd for:  $\text{C}_{13}\text{H}_{19}\text{N}$ : C, 82.48; H, 10.12; N, 7.40. Found: C, 82.23; H, 10.11; N, 7.42.

##### 4.7.2. 1-Cyclohexyl-*N*-methyl-1-phenylmethanamine (**5k**)

Pale yellow oil (35%): IR (neat)  $\text{cm}^{-1}$  3343 (broad) (N-H stretch), 2925, 2851, 2787, 1734, 1636, 1602, 1492, 1450, 1133, 1062, 1029, 891, 826, 760, 703, 666;  $^1\text{H}$  NMR (200 MHz,  $\text{DMSO-}d_6$ ):  $\delta$  7.34–7.15 (m, 5H, aromatic), 3.12 (d,  $J = 8.0$  Hz, 1H, CHN), 2.03–1.76 (m, 6H,  $\text{NCH}_3$  + cyclohexyl), 1.61–0.97 (m, 8H, cyclohexyl). Anal. Calcd for:  $\text{C}_{14}\text{H}_{21}\text{N}$ : C, 82.70; H, 10.41; N, 6.89. Found: C, 82.98; H, 10.40; N, 6.91.

#### 4.7.3. 1-(4-(Benzyloxy)phenyl)-N-methyl-1-phenylmethanamine (**5o**)

Whitish solid (76%): mp 67–69 °C; IR (neat)  $\text{cm}^{-1}$  3030 (N-H stretch), 2946, 2784, 1699, 1608, 1583, 1509, 1493, 1469, 1454, 1386, 1341, 1300, 1242, 1172, 1115, 1014, 912, 827, 808, 748, 697, 643, 630, 607, 548;  $^1\text{H}$  NMR (200 MHz,  $\text{DMSO-}d_6$ ):  $\delta$  7.45–7.15 (m, 12H, aromatic), 6.92 (d,  $J = 10.0$  Hz, 2H, aromatic), 5.04 (s, 2H,  $\text{CH}_2\text{O}$ ), 4.58 (s, 1H, CHN), 2.19 (s, 3H,  $\text{NCH}_3$ ). Anal. Calcd for:  $\text{C}_{21}\text{H}_{21}\text{NO}$ : C, 83.13; H, 6.98; N, 4.62. Found: C, 83.33; H, 6.97; N, 4.61.

#### 4.7.4. 1-(4-((4-Bromobenzyl)oxy)phenyl)-N-methyl-1-phenylmethanamine (**5p**)

White solid (63%): mp 80–82 °C; IR (KBr)  $\text{cm}^{-1}$  3448 (broad) (N-H stretch), 3323, 3032, 2931, 2838, 2786, 1607, 1584, 1508, 1470, 1455, 1379, 1298, 1234, 1170, 1125, 1106, 1016, 814, 732, 700, 620, 550;  $^1\text{H}$  NMR (200 MHz,  $\text{DMSO-}d_6$ ):  $\delta$  7.44–7.12 (m, 11H, aromatic), 6.92 (d,  $J = 10.0$  Hz, 2H, aromatic), 5.04 (s, 2H,  $\text{CH}_2\text{O}$ ), 4.58 (s, 1H, CHN), 2.20 (s, 3H,  $\text{NCH}_3$ ). Anal. Calcd for:  $\text{C}_{21}\text{H}_{20}\text{BrNO}$ : C, 65.98; H, 5.27; N, 3.66. Found: C, 65.89; H, 5.26; N, 3.67.

#### 4.8. Synthesis of 1-(4-Iodophenyl)-N-methyl-1-phenylmethanamine (**5n**)

Formamide **9n** (0.7 mmol, 1 eq) was added in a hot flamed three-necked round bottom flask filled with argon and equipped with a magnetic stirring bar and solubilized in dry THF (7 mL). To the clear solution, DIBAL-H in 1M *n*-hexane (2.1 mL, 3 eq) was carefully added through a dropping funnel at room temperature. The reaction mixture was refluxed for 3.5 hours and then was left under stirring at room temperature for 16 hours. Then, the reaction mixture was cooled at 0 °C with an ice bath, and a solution of NaOH 2M (12 eq) was added dropwise. After 30 minutes of stirring at room temperature, the aqueous phase was separated from the organic phase, and the former was extracted three times with EtOAc (3×75 mL). The combined organic phases were dried on  $\text{Na}_2\text{SO}_4$ , filtered, and concentrated under vacuum. The crude was purified by flash chromatography using gradient mixtures of Cy/EtOAc as eluent. The desired product was obtained as pale yellow oil (51%): IR (neat)  $\text{cm}^{-1}$  3336 (N-H stretch.), 3059, 3025, 2948, 2850, 2788, 2360, 1647, 1558, 1541, 1479, 1456, 1397, 1126, 1103, 1006, 801, 749, 698;  $^1\text{H}$  NMR (200 MHz,  $\text{DMSO-}d_6$ ):  $\delta$  7.67–7.61 (m, 2H, aromatic), 7.40–7.18 (m, 7H, aromatic), 4.61 (s, 1H, CHN), 2.20 (s, 3H,  $\text{NCH}_3$ ). Anal. Calcd for:  $\text{C}_{14}\text{H}_{14}\text{IN}$ : C, 52.03; H, 4.37; N, 4.33. Found: C, 51.91; H, 4.38; N, 4.32.



#### 4.9. Synthesis of *N*-benzyl-3-(1*H*-imidazol-1-yl)propan-1-amine (**10**)

In a two-necked round bottom flask, a mixture of benzaldehyde (480  $\mu\text{L}$ , 1 eq), 3-(1*H*-imidazol-1-yl)propan-1-amine (591  $\mu\text{L}$ , 1.05 eq), sodium acetate (386 mg, 1 eq), and 3 Å molecular sieves (860 mg) in anhydrous MeOH (12 mL) was stirred under  $\text{N}_2$  at room temperature overnight. Then, the temperature was lowered to 0 °C, and  $\text{NaBH}_4$  (182 mg, 1.02 eq) was added portion-wise over one hour. The reaction mixture was left under stirring at room temperature for 3 additional hours. The mixture was filtered through a Celite® pad and washed with MeOH. The filtrate was concentrated in vacuo and the residue was diluted with  $\text{CH}_2\text{Cl}_2$  and washed with an aqueous solution of NaOH 10% and with brine. The organic phase was dried with  $\text{Na}_2\text{SO}_4$ , filtered, and concentrated. The pale-yellow oil thus obtained was used in the next step without any further purification.

#### 4.10. Synthesis of *N*-(3-(1*H*-imidazol-1-yl)propyl)-*N*-benzylacetamide (**11a**)

A stirred mixture of *N*-benzyl-3-(1*H*-imidazol-1-yl)propan-1-amine (**10**) (150 mg, 1 eq), TEA (194.3  $\mu\text{L}$ , 2 eq) and a catalytic amount of DMAP (0.1 eq) in anhydrous  $\text{CH}_2\text{Cl}_2$  (3 mL) was cooled to 0 °C. Acetic anhydride (65.3  $\mu\text{L}$ , 1 eq) was added dropwise and the mixture was stirred for 10 minutes at 0 °C and then at room temperature for 12 hours. The mixture was diluted with  $\text{CH}_2\text{Cl}_2$ , washed with a saturated solution of  $\text{NaHCO}_3$  (50 mL), deionized water (50 mL) and brine (50 mL), dried with  $\text{Na}_2\text{SO}_4$ , filtered and concentrated under vacuum. The residue was purified by flash chromatography eluting with a mixture of  $\text{CH}_2\text{Cl}_2/\text{MeOH}$ . Pale yellow oil (69%): IR (neat)  $\text{cm}^{-1}$  3437 (broad), 2937, 1628 (C=O stretch), 1509, 1450, 1362, 1232, 1110, 1081, 1029, 983, 917, 822, 735, 699, 666;  $^1\text{H}$  NMR (500 MHz,  $\text{DMSO}-d_6$ ): Mixture of two *E/Z* conformers (approximately 50:50):  $\delta$  7.59 (s, 1H, imidazole), 7.36 (t,  $J = 7.5$  Hz, 1H, aromatic), 7.31–7.21 (m, 2H, aromatic), 7.18–7.13 (m, 3H, aromatic + imidazole), 6.87 (d,  $J = 10.0$  Hz, 1H, imidazole), 4.52 (s, 2H,  $\text{CH}_2\text{Ar}$ , conformer *E* (or *Z*)), 4.46 (s, 2H,  $\text{CH}_2\text{Ar}$ , conformer *Z* (or *E*)), 3.95–3.89 (m, 2H,  $\text{CH}_2$ -imidazole, conformer *E* (or *Z*) + conformer *Z* (or *E*)), 3.22 (t,  $J = 7.5$  Hz, 2H,  $\text{NCH}_2$ , conformer *E* (or *Z*)), 3.14 (t,  $J = 7.5$  Hz, 2H,  $\text{NCH}_2$ , conformer *Z* (or *E*)), 2.01 (s, 2H,  $\text{COCH}_3$ , conformer *E* (or *Z*)), 1.99 (s, 2H,  $\text{COCH}_3$ , conformer *Z* (or *E*)), 1.98–1.92 (m, 2H,  $\text{CH}_2\text{CH}_2\text{CH}_2$ , conformer *E* (or *Z*)), 1.90–1.84 (m, 2H,  $\text{CH}_2\text{CH}_2\text{CH}_2$ , conformer *Z* (or *E*));  $^{13}\text{C}$  NMR (125 MHz,  $\text{DMSO}-d_6$ ):  $\delta$  170.58, 170.05, 138.23, 137.72, 137.37, 137.30, 128.91, 128.55, 128.34, 127.63, 127.43, 127.13, 126.63, 119.36, 51.29, 47.46, 45.05, 44.07, 43.67, 42.83, 29.45, 28.84, 21.67, 21.13. Anal. Calcd for:  $\text{C}_{15}\text{H}_{19}\text{N}_3\text{O}$ : C, 70.01; H, 7.44; N, 16.33.

Found: C, 70.14; H, 7.46; N, 16.27.

#### 4.11. General procedure for the synthesis of *N*-(3-(1*H*-imidazol-1-yl)propyl)-*N*-benzylamides **11b-c**.

*N*-benzyl-3-(1*H*-imidazol-1-yl)propan-1-amine (**10**) (1.1 eq) and TEA (1.5 eq) were dissolved in a round bottom flask with dry CH<sub>2</sub>Cl<sub>2</sub> (6 mL); then the appropriate acyl chloride (1 eq) was added dropwise at room temperature. The reaction mixture was stirred at room temperature for 12 hours. The mixture was diluted with 20 mL of CH<sub>2</sub>Cl<sub>2</sub> and 10 mL of deionized water; the organic phase was washed twice with a saturated solution of NaHCO<sub>3</sub> and once with brine, dried with Na<sub>2</sub>SO<sub>4</sub>, filtered, and concentrated under vacuum. The crude was purified by flash chromatography using a mixture of EtOAc/MeOH (9.5:0.5). Using this procedure, the following compounds have been synthesized.

##### 4.11.1. *N*-(3-(1*H*-Imidazol-1-yl)propyl)-*N*-benzylbenzamide (**11b**)

Yellow oil (48%): IR (neat) cm<sup>-1</sup> 3434 (broad), 3111, 2940, 1627 (C=O stretch), 1577, 1509, 1496, 1446, 1426, 1360, 1320, 1282, 1231, 1144, 1109, 1080, 1028, 978, 917, 821, 789, 736, 702; <sup>1</sup>H NMR (500 MHz, DMSO-*d*<sub>6</sub>): Mixture of two *E/Z* conformers (approximately 55:45) δ 7.63 (s, 1H, imidazole), 7.41–7.26 (m, 10H, aromatic), 7.17–7.14 (m, 1H, imidazole), 6.93–6.77 (m, 1H, imidazole), 4.68 (br s, 2H, ArCH<sub>2</sub>, conformer *E* (or *Z*)), 4.45 (br s, 2H, ArCH<sub>2</sub>, conformer *Z* (or *E*)), 4.00 (br s, 2H, CH<sub>2</sub>-imidazole, conformer *E* (or *Z*)), 3.76 (br s, 2H, CH<sub>2</sub>-imidazole, conformer *Z* (or *E*)), 3.32 (br s, 2H, NCH<sub>2</sub>, conformer *E* (or *Z*)), 3.07 (br s, 2H, NCH<sub>2</sub>, conformer *Z* (or *E*)), 2.00–1.95 (m, 2H, CH<sub>2</sub>CH<sub>2</sub>CH<sub>2</sub>); <sup>13</sup>C NMR (125 MHz, DMSO-*d*<sub>6</sub>): δ 171.04, 137.69, 137.12, 136.45, 129.32, 128.67, 128.48, 128.35, 127.42, 127.24, 126.83, 126.40, 126.21, 119.22, 118.94, 51.85, 46.99, 45.70, 43.88, 43.36, 41.72, 29.16, 28.33. Anal. Calcd for: C<sub>20</sub>H<sub>21</sub>N<sub>3</sub>O: C, 75.21; H, 6.63; N, 13.16. Found: C, 75.43; H, 6.64; N, 13.12.

##### 4.11.2. *N*-(3-(1*H*-Imidazol-1-yl)propyl)-*N*-benzyl-2-phenylacetamide (**11c**)

Pale yellow oil (49%): IR (neat) cm<sup>-1</sup> 3418 (broad), 3110, 2938, 1640 (C=O stretch), 1496, 1453, 1426, 1360, 1282, 1230, 1155, 1109, 1080, 1030, 916, 821, 733, 698, 665; <sup>1</sup>H NMR (500 MHz, DMSO-*d*<sub>6</sub>): Mixture of two *E/Z* conformers (approximately 50:50) δ 7.57 (s, 1H, imidazole, conformer *E* (or *Z*)), 7.56 (s, 1H, imidazole, conformer *Z* (or *E*)), 7.37–7.11 (m, 10H + 1H, aromatic + imidazole), 6.91 (s, 1H, imidazole, conformer *E* (or *Z*)) 6.85 (s, 1H, imidazole, conformer *Z* (or *E*)), 4.60 (s, 2H, CH<sub>2</sub>Ar, conformer *E* (or *Z*)), 4.50 (s, 2H,

CH<sub>2</sub>Ar, conformer *Z* (or *E*)), 3.93–3.87 (m, 2H, CH<sub>2</sub>-imidazole, conformer *E* (or *Z*) + conformer *Z* (or *E*)), 3.70 (s, 2H, ArCH<sub>2</sub>CO, conformer *E* (or *Z*)), 3.66 (s, 2H, ArCH<sub>2</sub>CO, conformer *Z* (or *E*)), 3.23 (t, *J* = 5.0 Hz, 2H, NCH<sub>2</sub>, conformer *E* (or *Z*)), 3.18 (t, *J* = 5.0 Hz, 2H, NCH<sub>2</sub>, conformer *Z* (or *E*)), 1.95–1.84 (m, 2H, CH<sub>2</sub>CH<sub>2</sub>CH<sub>2</sub>, conformer *E* (or *Z*) + conformer *Z* (or *E*)); <sup>13</sup>C NMR (125 MHz, DMSO-*d*<sub>6</sub>): δ 170.71, 170.26, 138.09, 137.49, 137.24, 137.13, 135.80, 135.77, 129.07, 129.01, 128.71, 128.55, 128.37, 128.30, 127.47, 127.31, 126.99, 126.64, 126.43, 119.16, 50.57, 47.40, 44.32, 43.80, 43.40, 42.83, 29.42, 28.60. Anal. Calcd for: C<sub>21</sub>H<sub>23</sub>N<sub>3</sub>O: C, 75.65; H, 6.95; N, 12.60. Found: C, 75.83; H, 6.97; N, 12.56.

#### 4.12. Molecular modeling

The X-ray crystal structures of the co-crystal HO-1/QC-80 (PDB code 3HOK), co-crystal HO-1/QC-308 (PDB code 3TGM), and HO-2 (PDB code 2QPP) were used as protein structures. To validate the docking model, we used the procedure of our already published HO-1 inhibitors paper [51]. The three-dimensional structures of all the studied molecules were generated using Marvin Sketch (18.24, ChemAxon Ltd., Budapest, Hungary) and all geometries were fully optimized, in the same software, with the semi-empirical PM6 Hamiltonian implemented in MOPAC2016 (17.130 W) [52-54]. Proteins and ligands were prepared within YASARA; the point charges were initially assigned according to the AMBER14 force field and then damped to mimic the less polar Gasteiger charges used to optimize the AutoDock scoring function [55]. Fine docking was performed by applying the Lamarckian genetic algorithm (LGA) implemented in AutoDock. The ligand-centered maps were generated by the program AutoGrid with a spacing of 0.375 Å and dimensions that encompass all atoms extending 5 Å from the surface of the ligand. All of the parameters were inserted at their default settings. In the docking tab, the macromolecule and ligand are selected, and GA parameters are set as *ga\_runs* = 100, *ga\_pop\_size* = 150, *ga\_num\_evals* = 20,000,000, *ga\_num\_generations* = 27,000, *ga\_elitism* = 1, *ga\_mutation\_rate* = 0.02, *ga\_crossover\_rate* = 0.8, *ga\_crossover\_mode* = two points, *ga\_cauchy\_alpha* = 0.0, *ga\_cauchy\_beta* = 1.0, number of generations for picking worst individual = 10. All protein amino acidic residues were kept rigid, whereas all single bonds of the ligands were treated as fully flexible.

#### 4.13. In vitro ADMET testing

*In vitro* ADMET testing has been performed at Eurofins Scientific. Aqueous solubility

in simulated gastric fluid (catalogue product number 2061), intrinsic clearance in liver microsomes-human (catalogue product number 607), CYP2D6 and CYP3A4 inhibition (catalogue product number 1338 and 391, respectively), and hERG human potassium ion channel binding (catalogue product number 4094), were conducted at Eurofins following their experimental protocols (<https://www.eurofins.com/>).

#### 4.14. *Isosteric replacement and compounds alignment for the 3D-QSAR evaluation*

The isosteric replacement was performed using Spark as a software (10.4.0, Cresset, Litlington, Cambridgeshire, UK, <http://www.cresset-group.com/forge>). The replacement was performed through the same 178,558 fragments for each part, which derive from ChEMBL and Zinc databases, as already reported [56, 57]. Two hundred compounds were generated for each substitution. Then, the newly designed molecules were imported into the software Forge (v10.4.2), for the alignment/evaluation of the dataset in the 3D-QSAR model already published [58]. The filed points of each compound (negative, positive, shape and hydrophobic) were calculated and generated using the XED (extended electron distribution) force field in Forge, then the molecules were aligned with the training set of the QSAR model by a maximum common substructure algorithm using a customized and validated set-up [59, 60]. The maximum number of conformations generated for each molecule was set to 500. The root-mean-square deviation of atomic positions cutoff, which is the similarity threshold below which two conformers are assumed identical, was set to 0.5 Å. The gradient cutoff for conformer minimization was set to 0.1 kcal/mol. The energy window was set to 2.5 kcal/mol and all the conformers with calculated energy outside the selected energy window were discarded.

#### 4.15. *Preparation of spleen and brain microsomal fractions*

HO-1 and HO-2 were obtained, respectively, from rat spleen and brain as the microsomal fraction prepared by differential centrifugation; the dominance of HO-1 protein in the rat spleen and HO-2 in the rat brain has been well documented [24]. These particular microsomal preparations were selected to use the most native (*i.e.*, closest to *in vivo*) forms of HO-1 and HO-2. Spleen and brain (Sprague–Dawley rats) microsomal fractions were prepared according to the procedure outlined by Ryter *et al* [2]. The experiments reported in the present paper complied with current Italian law and met the guidelines of the Institutional Animal Care and Use Committee of Ministry of Health (Directorate General for Animal Health and Veterinary Medicines, Italy) “Dosing of enzymatic activities in rat microsomes”

(2018–2022), project code 02769.N.VLY. The experiments were performed in male Sprague–Dawley albino rats (150 g body weight and age 45 d). They had free access to water and were kept at room temperature with a natural photo-period (12 h light-12 h dark cycle). For measuring HO-1 and HO-2 activities, each rat was sacrificed and their spleen and brain were excised and weighed. A homogenate (15%, w/v) of spleens and brains pooled from four rats was prepared in ice-cold HO-homogenizing buffer (50 mM Tris buffer, pH 7.4, containing 0.25 M sucrose) using a Potter–Elvehjem homogenizing system with a Teflon pestle. The microsomal fraction of rat spleen and brain homogenate was obtained by centrifugation at 10,000g for 20 min at 4 °C, followed by centrifugation of the supernatant at 100,000g for 60 min at 4 °C. The 100,000g pellet (microsomes) was resuspended in 100 mM potassium phosphate buffer, pH 7.8, containing 2 mM MgCl<sub>2</sub> with a Potter–Elvehjem homogenizing system. The rat spleen and brain microsomal fractions were divided into equal aliquots, placed into microcentrifuge tubes, and stored at -80 °C for up to 2 months.

#### *4.16. Preparation of biliverdin reductase*

Liver cytosol has been used as a source of biliverdin reductase. Rat liver was perfused through the hepatic portal vein with cold 0.9% NaCl; then, it was cut and flushed with 2×20 mL of ice-cold PBS to remove all of the blood. Liver tissue was homogenized in 3 volumes of a solution containing 1.15% KCl w/v and Tris buffer 20 mM, pH 7.8 on ice. Homogenates were centrifuged at 10,000g for 20 min at 4 °C. The supernatant was decanted and centrifuged at 100,000g for 1 h at 4 °C to sediment the microsomes. The 100,000g supernatant was saved and then stored in small amounts at -80 °C after its protein concentration was measured.

#### *4.17. Measurement of HO-1 and HO-2 enzymatic activities in microsomal fraction of rat spleen and brain*

The HO-1 and HO-2 activities were determined by measuring the bilirubin formation using the difference in absorbance at 464–530 nm as described by Ryter *et al* [2]. Reaction mixtures (500 µL) consisted of 20 mM Tris–HCl, pH 7.4, (1 mg/mL) microsomal extract, 0.5–2 mg/mL biliverdin reductase, 1 mM NADPH, 2 mM glucose 6-phosphate (G6P), 1 U G6P dehydrogenase, 25 µM hemin, and 10 µL of DMSO (or the same volume of DMSO solution of test compounds to a final concentration of 100, 10, and 1 µM). Incubations were carried out for 60 min at 37 °C in a circulating water bath in the dark. Reactions were stopped by adding the same volume of chloroform. After recovering the chloroform phase, the

amount of bilirubin formed was measured with a double-beam spectrophotometer as OD<sub>464–530</sub> nm (extinction coefficient, 40 mM/cm<sup>-1</sup> for bilirubin). One unit of the enzyme was defined as the amount of enzyme catalyzing the formation of 1 nmol of bilirubin/mg protein/h.

#### 4.18. Cell culture and treatments

Experiments were performed on human GBM cell line U87MG (ATCCC number #HTB-14), and A172 (ATCCC #CRL-1620); on DU 145 (ATCC HTB-81) and human lung adenocarcinoma A549 (ATCC CCL-185-LUC2). All cell lines were obtained from the American Type Culture Collection (ATCC, Rockville, Md., USA). Cells were grown in Dulbecco's modified Eagle's medium (DMEM) supplemented with 10% of heat-inactivated fetal bovine serum (FBS), 100 U/ml penicillin, and 100- $\mu$ g/ml streptomycin (Sigma-Aldrich, Steinheim, Germany). Cells were incubated at 37 °C in a humidified atmosphere with 5% CO<sub>2</sub>.

#### 4.19. Cell viability assay

The effect of selected compounds **7i** and **7l–p** on cell viability was assessed by performing an MTT assay. Cells were seeded into 96-well plates at a density of  $7 \times 10^3$  cells/well in 100  $\mu$ l of culture medium. After 24 h, cells were treated with selected compounds at three different concentrations (1  $\mu$ M, 10  $\mu$ M, and 50  $\mu$ M) for 48 h. Following treatments, 0.5 mg/ml of 3-[4,5-dimethylthiazol-2-yl]-2,5-diphenyltetrazolium bromide (MTT) (Sigma Aldrich) was added to each well and incubated for 4 h at 37 °C. Finally, dimethylsulfoxide (DMSO) was used to dissolve formazan salts, and absorbance was measured at 570 nm in a microplate reader (Biotek Synergy-HT). Eight replicate wells were used for each group.

#### 4.20. Western Blot Analysis

Proteins were extracted from total cell lysate, as previously described [61]. Briefly, cell lines were added to a buffer containing 20 mM Tris (pH 7.4), 2 mM EDTA, 0.5 mM EGTA; 50 mM mercaptoethanol, 0.32 mM sucrose supplemented with phosphatase and protease inhibitor cocktails (Roche Diagnostics, Monza, Italy). Subsequently, protein samples were sonicated twice for 20' by using an ultrasonic probe, followed by centrifugation at 10,000 x g for 10 min at 4 °C. Sample proteins (30  $\mu$ g) were diluted in 4X NuPage LDS sample buffer (Invitrogen, NP0007), heated at 80 °C for 5 min and then separated on a Biorad Criterion

XT 4-15% Bis-tris gel (BIO-RAD) by electrophoresis and then transferred to a PVDF membrane (BIO-RAD). Blots were blocked using the Odyssey Blocking Buffer (LI-COR Biosciences) and probed with appropriate antibodies: HO-1 antibody (GeneTex GTX101147), goat polyclonal anti-VEGF (cat. no. sc-1836, Santa Cruz Biotechnology), and rabbit polyclonal anti- $\beta$ -tubulin (cat n.sc-9104, Santa Cruz Biotechnology) and  $\beta$ -Actin antibody (GeneTex GTX109639). The secondary antibodies goat anti-rabbit (Odyssey, #926-32211; Odyssey #926-68021) and donkey anti-goat IRDye 800CW (cat #926-32214; Li-Cor Biosciences) were used at 1:7000. Blots were scanned, and Densitometric analysis was performed with Odyssey Infrared Imaging System. Values were normalized to  $\beta$ -actin and to  $\beta$ -tubulin.

#### *4.21. Immunolocalization*

To determine the cellular distribution of heme oxygenase 1 in tumor cells, immunofluorescence analysis was performed as previously described [62]. Tumor cell lines were cultured on glass cover slips were fixed in 4% paraformaldehyde in PBS (15' at room temperature), permeabilized with 0.2% Triton X100, blocked with 0.1% BSA in PBS, and then probed with rabbit HO-1 antibody. Signal was revealed with Alexa Fluor 488 goat anti-rabbit for 1 h, at room temperature and maintained shielded from light. DNA was counterstained stained with DAPI (#940110, Vector Laboratories). After a series of PBS and double-distilled water washes, the fixed cells were cover-slipped with Vectashield mounting medium (Vector Laboratories, Inc., Burlingame, CA, USA). Localization of antibody was performed by Zeiss fluorescent microscopy.

#### *4.22. Measurement of HO enzymatic activity in U87MG cell line*

U87MG cells were incubated for 24 h in the presence or absence of 10  $\mu$ M compound 7I. Total HO activity in the cell lysate was determined by measuring the bilirubin formation using the difference in absorbance at 464 to 530 nm [2]. Reaction mixtures (500  $\mu$ L) consisted of 20 mM Tris-HCl, pH 7.4, (1 mg/mL) cell lysate, 0.5–2 mg/mL biliverdin reductase, 1 mM NADPH, 2 mM glucose 6-phosphate (G6P), 1 U G6P dehydrogenase, 25  $\mu$ M hemin, 10  $\mu$ L of DMSO. Incubations were carried out for 60 min at 37  $^{\circ}$ C in a circulating water bath in the dark. Reactions were stopped by adding 1 volume of chloroform. After recovering the chloroform phase, the amount of bilirubin formed was measured with a double-beam spectrophotometer as OD 464–530 nm (extinction coefficient, 40 mM/cm<sup>-1</sup> for bilirubin). One unit of the enzyme was defined as the amount of enzyme catalyzing the

formation of 1 nmol of bilirubin/mg protein/h.

#### 4.23. Wound-healing assay

U87MG cells grown to confluence in six-well dishes ( $5 \times 10^4$  cells/well) were scratched with a 200  $\mu$ l pipette tip. Cells were cultured in 1% serum medium with or without 10  $\mu$ M of **71**. Quantitative assessment of the wound area was performed under an inverted microscope, as previously described [63]. The distance that the advancing cells had moved into the wound area was measured after 24 h and 48 h. The migration was calculated as the average number of cells observed in three random of high-power wounded fields/per well in duplicate wells and expressed in percentage of control (% of control).

#### 4.24. ELISA

VEGF-A release in conditioned media was measured using the ELISA sandwich enzymatic method with specific anti-VEGF-A (cat. No. ELH-VEGF) antibodies coated on a 96-well plate, according to the manufacturer's guidelines. Briefly, confluent U87MG cells grown in media supplemented with 1% FBS were treated for 48 h with 10  $\mu$ M of **71**. Standards and supernatants from samples were pipetted into the wells containing the immobilized VEGF antibody. The wells were then washed before adding a biotinylated anti-human VEGF antibody. Following incubation, the unbound biotinylated antibody was washed off, and HRP-conjugated streptavidin was pipetted in each well. After an additional wash step, a TMB substrate solution was added to each well, resulting in blue coloration proportional to the amount of bound VEGF. Finally, the stop solution was added, and the colorimetric intensity of the blue substrate now turned yellow was measured at 450 nm.

#### 4.25. Conditioned medium and tube formation assay

Subconfluent U87MG cell cultures were placed in media supplemented with 1% FBS (representing the conditioned medium 1- CM1 or control) or containing 10 $\mu$ M of **71** molecule (representing the conditioned medium 2- CM2) and incubated at 37 °C for 48 h. Subsequently the CMs were collected, centrifuged at 2000 rpm for 5 min, and the supernatants frozen at -80 °C until use. Geltrex™ reduced growth factor basement membrane matrix (Invitrogen) was thawed at 4 °C overnight before use. Geltrex™ matrix was added to a 24-well plate (95  $\mu$ l/well) and then incubated at 37 °C for 30 min to allow polymerization. Murine microvascular endothelial cells (H5V) were starved overnight in the growth medium, then the cells were seeded onto the layer of Geltrex™ matrix and cultured



with 200  $\mu$ l of CM1 and CM2 at 37 °C for 48 h. Three random selected fields of view were captured with a digital camera (Canon) connected to an inverted microscope (Axio Observer A1; Carl Zeiss, Göttingen, Germany). Tube numbers per field was calculated as percentage of control.

#### 4.26. Statistical analyses

Data are represented as mean  $\pm$  standard error (SEM). One-way analysis of variance (ANOVA) was used to compare differences among groups, and statistical significance was assessed by the Tukey–Kramer post hoc test. The level of significance for all statistical tests was set at  $p \leq 0.05$ .

### ASSOCIATED CONTENT

The Supporting Information is available free of charge at <https://pubs.acs.org/doi/10.1021/acs.jmedchem.1c00633>.

### Author Contributions

All authors contributed to the present paper and have given approval to the final version of the manuscript.

### Funding Sources

This work was founded by (1) University of Catania, Programma Ricerca di Ateneo Pia.Ce.Ri 2020-2022 linea 2, project number 57722172126; (2) Project authorized by the Ministry of Health (Directorate General for Animal Health and Veterinary Medicines) “Dosing of enzymatic activities in rat microsomes” (2018–2022) (project code 02769.N.VLY); (3) PON R&I funds 2014-2020 (CUP: E66C18001320007, AIM1872330, activity 1).

### ABBREVIATIONS

BSA, Bovine Serum Albumin; CH<sub>3</sub>CN, acetonitrile; DAPI, 4',6-diamidino-2-phenylindole; DIBAL-H, diisobutylaluminium hydride; DMAP, 4-dimethylaminopyridine; DMF, *N,N*-dimethylformamide; DMSO, dimethyl sulfoxide; HCOOH, formic acid; H<sub>2</sub>NCHO, formamide; HO-1, heme oxygenase-1; HO-2, heme oxygenase-2; G6P, glucose 6-phosphate; GBM, glioblastoma; IC<sub>50</sub>, inhibitory concentration<sub>50</sub>; MPs, metalloporphyrins; MTT, 3-(4,5-dimethylthiazol-2-yl)-2,5-diphenyl-2*H*-tetrazolium bromide; NaH, sodium hydride; NADPH, nicotinamide adenine dinucleotide phosphate; NMR, nuclear magnetic resonance; PBS, phosphate-buffered saline; RMSD, root-mean-square deviation; SAR,

structure-activity relationship; SD, standard deviation; TEA, triethylamine; THF, tetrahydrofuran; TLC, thin layer chromatography; VEGF, vascular endothelial growth factor.

## REFERENCES

- [1] Abraham, N. G.; Kappas, A., Pharmacological and clinical aspects of heme oxygenase. *Pharmacol. Rev.* **2008**, *60* (1), 79-127.
- [2] Ryter, S. W.; Alam, J.; Choi, A. M., Heme oxygenase-1/carbon monoxide: from basic science to therapeutic applications. *Physiol. Rev.* **2006**, *86* (2), 583-650.
- [3] Chen, S.; Wang, X.; Nisar, M. F.; Lin, M.; Zhong, J. L., Heme oxygenases: cellular multifunctional and protective molecules against UV-induced oxidative stress. *Oxid. Med. Cell. Longev.* **2019**, 5416728.
- [4] Sorrenti, V.; Raffaele, M.; Vanella, L.; Acquaviva, R.; Salerno, L.; Pittala, V.; Intagliata, S.; Di Giacomo, C., Protective effects of caffeic acid phenethyl ester (CAPE) and novel cape analogue as inducers of heme oxygenase-1 in streptozotocin-induced type 1 diabetic rats. *Int. J. Mol. Sci.* **2019**, *20* (10), 2441.
- [5] Pittalà, V.; Vanella, L.; Platania, C. B. M.; Salerno, L.; Raffaele, M.; Amata, E.; Marrazzo, A.; Floresta, G.; Romeo, G.; Greish, K.; Intagliata, S.; Bucolo, C.; Sorrenti, V., Synthesis, in vitro and in silico studies of HO-1 inducers and lung antifibrotic agents. *Future Med. Chem.* **2019**, *11* (13), 1523-1536.
- [6] Podkalicka, P.; Mucha, O.; Jozkowicz, A.; Dulak, J.; Loboda, A., Heme oxygenase inhibition in cancers: possible tools and targets. *Contemp. Oncol. (Pozn)*. **2018**, *22* (1A), 23-32.
- [7] Sorrenti, V.; Pittala, V.; Romeo, G.; Amata, E.; Dichiara, M.; Marrazzo, A.; Turnaturi, R.; Prezzavento, O.; Barbagallo, I.; Vanella, L.; Rescifina, A.; Floresta, G.; Tibullo, D.; Di Raimondo, F.; Intagliata, S.; Salerno, L., Targeting heme Oxygenase-1 with hybrid compounds to overcome Imatinib resistance in chronic myeloid leukemia cell lines. *Eur. J. Med. Chem.* **2018**, *158*, 937-950.
- [8] Castruccio Castracani, C.; Longhitano, L.; Distefano, A.; Di Rosa, M.; Pittala, V.; Lupo, G.; Caruso, M.; Corona, D.; Tibullo, D.; Li Volti, G., Heme oxygenase-1 and carbon monoxide regulate growth and progression in glioblastoma cells. *Mol. Neurobiol.* **2020**, *57* (5), 2436-2446.

- [9] Raffaele, M.; Pittala, V.; Zingales, V.; Barbagallo, I.; Salerno, L.; Li Volti, G.; Romeo, G.; Carota, G.; Sorrenti, V.; Vanella, L., Heme oxygenase-1 inhibition sensitizes human prostate cancer cells towards glucose deprivation and Metformin-mediated cell death. *Int. J. Mol. Sci.* **2019**, *20* (10), 2593.
- [10] Tsai, J. R.; Wang, H. M.; Liu, P. L.; Chen, Y. H.; Yang, M. C.; Chou, S. H.; Cheng, Y. J.; Yin, W. H.; Hwang, J. J.; Chong, I. W., High expression of heme oxygenase-1 is associated with tumor invasiveness and poor clinical outcome in non-small cell lung cancer patients. *Cell. Oncol. (Dordr)* **2012**, *35* (6), 461-471.
- [11] Yin, H.; Fang, J.; Liao, L.; Maeda, H.; Su, Q., Upregulation of heme oxygenase-1 in colorectal cancer patients with increased circulation carbon monoxide levels, potentially affects chemotherapeutic sensitivity. *BMC Cancer* **2014**, *14*, 436.
- [12] Zhu, X.; Fan, W. G.; Li, D. P.; Lin, M. C.; Kung, H., Heme oxygenase-1 system and gastrointestinal tumors. *World J. Gastroenterol.* **2010**, *16* (21), 2633-2637.
- [13] Chau, L. Y., Heme oxygenase-1: emerging target of cancer therapy. *J. Biomed. Sci.* **2015**, *22*, 22.
- [14] Gandini, N. A.; Fermento, M. E.; Salomón, D. G.; Blasco, J.; Patel, V.; Gutkind, J. S.; Molinolo, A. A.; Facchinetti, M. M.; Curino, A. C., Nuclear localization of heme oxygenase-1 is associated with tumor progression of head and neck squamous cell carcinomas. *Exp. Mol. Pathol.* **2012**, *93* (2), 237-245.
- [15] Rahman, M. N.; Vukomanovic, D.; Vlahakis, J. Z.; Szarek, W. A.; Nakatsu, K.; Jia, Z. C., Structural insights into human heme oxygenase-1 inhibition by potent and selective azole-based compounds. *J. R. Soc. Interface* **2013**, *10* (78), 1-14.
- [16] Salerno, L.; Floresta, G.; Ciaffaglione, V.; Gentile, D.; Margani, F.; Turnaturi, R.; Rescifina, A.; Pittala, V., Progress in the development of selective heme oxygenase-1 inhibitors and their potential therapeutic application. *Eur. J. Med. Chem.* **2019**, *167*, 439-453.
- [17] Intagliata, S.; Salerno, L.; Ciaffaglione, V.; Leonardi, C.; Fallica, A. N.; Carota, G.; Amata, E.; Marrazzo, A.; Pittala, V.; Romeo, G., Heme Oxygenase-2 (HO-2) as a therapeutic target: activators and inhibitors. *Eur. J. Med. Chem.* **2019**, *183*, 111703.
- [18] Kinobe, R. T.; Dercho, R. A.; Nakatsu, K., Inhibitors of the heme oxygenase – carbon monoxide system: on the doorstep of the clinic? *Can. J. Physiol. Pharmacol.* **2008**, *86* (9), 577-599.

- [19] Ciaffaglione, V.; Intagliata, S.; Pittala, V.; Marrazzo, A.; Sorrenti, V.; Vanella, L.; Rescifina, A.; Floresta, G.; Sultan, A.; Greish, K.; Salerno, L., New aryloethanolimidazole derivatives as HO-1 inhibitors with cytotoxicity against MCF-7 breast cancer cells. *Int. J. Mol. Sci.* **2020**, *21* (6), 1923.
- [20] Roman, G.; Rahman, M. N.; Vukomanovic, D.; Jia, Z.; Nakatsu, K.; Szarek, W. A., Heme oxygenase inhibition by 2-oxy-substituted 1-azolyl-4-phenylbutanes: effect of variation of the azole moiety. X-Ray crystal structure of human heme oxygenase-1 in complex with 4-phenyl-1-(1H-1,2,4-triazol-1-yl)-2-butanone. *Chem. Biol. Drug Des.* **2010**, *75* (1), 68-90.
- [21] Rahman, M. N.; Vlahakis, J. Z.; Vukomanovic, D.; Lee, W.; Szarek, W. A.; Nakatsu, K.; Jia, Z. C., A novel, "double-clamp" binding mode for human heme oxygenase-1 inhibition. *Plos One* **2012**, *7* (1), e29514.
- [22] Rahman, M. N.; Vlahakis, J. Z.; Vukomanovic, D.; Szarek, W. A.; Nakatsu, K.; Jia, Z. C., X-ray crystal structure of human heme oxygenase-1 with (2R,4S)-2-[2-(4-chlorophenyl)ethyl]-2-[(1H-imidazol-1-yl)methyl]-4-[(5-trifluoromethylpyridin-2-yl)thio)methyl]-1,3-dioxolane: a novel, inducible binding mode. *J. Med. Chem.* **2009**, *52* (15), 4946-4950.
- [23] Greish, K. F.; Salerno, L.; Al Zahrani, R.; Amata, E.; Modica, M. N.; Romeo, G.; Marrazzo, A.; Prezzavento, O.; Sorrenti, V.; Rescifina, A.; Floresta, G.; Intagliata, S.; Pittala, V., Novel structural insight into inhibitors of heme oxygenase-1 (HO-1) by new imidazole-based compounds: biochemical and in vitro anticancer activity evaluation. *Molecules* **2018**, *23* (5), 1209.
- [24] Kumari, S.; Carmona, A. V.; Tiwari, A. K.; Trippier, P. C. Amide bond bioisosteres: strategies, synthesis, and successes. *J. Med. Chem.* **2020**, *63* (21), 12290-12358.
- [25] Floresta, G.; Fallica, A. N.; Romeo, G.; Sorrenti, V.; Salerno, L.; Rescifina, A.; Pittala, V., Identification of a potent heme oxygenase-2 (HO-2) inhibitor by targeting the secondary hydrophobic pocket of the HO-2 western region. *Bioorg. Chem.* **2020**, *104*, 104310.
- [26] Floresta, G.; Carotti, A.; Ianni, F.; Sorrenti, V.; Intagliata, S.; Rescifina, A.; Salerno, L.; Di Michele, A.; Sardella, R.; Pittala, V., Chromatographic resolution of phenylethanol-imidazole racemic compounds highlighted stereoselective inhibition of heme oxygenase-1 by (R)-enantiomers. *Bioorg. Chem.* **2020**, *99*, 103777.

- [27] Daina, A.; Michielin, O.; Zoete, V., SwissADME: a free web tool to evaluate pharmacokinetics, drug-likeness and medicinal chemistry friendliness of small molecules. *Sci. Rep.* **2017**, *7*, 42717.
- [28] Pires, D. E. V.; Blundell, T. L.; Ascher, D. B., pkCSM: predicting small-molecule pharmacokinetic and toxicity properties using graph-based signatures. *J. Med. Chem.* **2015**, *58*, 4066–4072.
- [29] Lipinski, C. A.; Lombardo, F.; Dominy, B. W.; Feeney, P. J., Experimental and computational approaches to estimate solubility and permeability in drug discovery and development settings. *Adv. Drug Deliv. Rev.* **1997**, *23*, 3–25.
- [30] Ghose, A. K.; Viswanadhan, V. N.; Wendoloski, J. J., A knowledge-based approach in designing combinatorial or medicinal chemistry libraries for drug discovery. 1. A qualitative and quantitative characterization of known drug databases. *J. Comb. Chem.* **1999**, *1*, 55–68.
- [31] Egan, W. J.; Merz, K. M.; Baldwin, J. J., Prediction of drug absorption using multivariate statistics. *J. Med. Chem.* **2000**, *43*, 3867–3877.
- [32] Veber, D. F.; Johnson, S. R.; Cheng, H. Y.; Smith, B. R.; Ward, K. M.; Kopple, K. D., Molecular properties that influence the oral bioavailability of drug candidates. *J. Med. Chem.* **2002**, *45*, 2615–2623.
- [33] Muegge, I.; Heald, S. L.; Brittelli, D., Simple selection criteria for drug-like chemical matter. *J. Med. Chem.* **2001**, *4*, 1841–1846.
- [34] Venkatakrisnan, K.; von Moltke, L. L.; Greenblatt, D. J. Effects of the antifungal agents on oxidative drug metabolism: clinical relevance. *Clin. Pharmacokinet.* **2000**, *38*, 111-180.
- [35] Lynch, T.; Price, A. The effect of cytochrome P450 metabolism on drug response, interactions, and adverse effects, *Am. Fam. Phys.* **2007**, *76*, 391-396.
- [36] Bahmani, P.; Hassanshahi, G.; Halabian, R.; Roushandeh, A. M.; Jahanian-Najafabadi, A.; Roudkenar, M. H., The expression of heme oxygenase-1 in human-derived cancer cell lines. *Iran. J. Med. Sci.* **2011**, *36* (4), 260-265.
- [37] Shan, Y.; Pepe, J.; Lu, T. H.; Elbirt, K. K.; Lambrecht, R. W.; Bonkovsky, H. L., Induction of the heme oxygenase-1 gene by metalloporphyrins. *Arch. Biochem. Biophys.* **2000**, *380* (2), 219-227.
- [38] Loboda, A.; Jazwa, A.; Wegiel, B.; Jozkowicz, A.; Dulak, J., Heme oxygenase-1-dependent and -independent regulation of angiogenic genes expression: effect of cobalt

protoporphyrin and cobalt chloride on VEGF and IL-8 synthesis in human microvascular endothelial cells. *Cell. Mol. Biol. (Noisy-le-grand)* **2005**, *51* (4), 347-355.

[39] Nishie, A.; Ono, M.; Shono, T.; Fukushi, J.; Otsubo, M.; Onoue, H.; Ito, Y.; Inamura, T.; Ikezaki, K.; Fukui, M.; Iwaki, T.; Kuwano, M., Macrophage infiltration and heme oxygenase-1 expression correlate with angiogenesis in human gliomas. *Clin. Cancer Res.* **1999**, *5* (5), 1107-1113.

[40] Sferrazzo, G.; Di Rosa, M.; Barone, E.; Li Volti, G.; Musso, N.; Tibullo, D.; Barbagallo, I., Heme oxygenase-1 in central nervous system malignancies. *J. Clin. Med.* **2020**, *9* (5), 1562.

[41] McAllister, L. A.; Turner, K. L.; Brand, S.; Stefaniak, M.; Procter, D. J., Solid phase approaches to N-heterocycles using a sulfur linker cleaved by SmI<sub>2</sub>. *J. Org. Chem.* **2006**, *71* (17), 6497-6507.

[42] Hung, J. M.; Arabshahi, H. J.; Leung, E.; Reynisson, J.; Barker, D., Synthesis and cytotoxicity of thieno[2,3-b]pyridine and furo[2,3-b]pyridine derivatives. *Eur. J. Med. Chem.* **2014**, *86*, 420-437.

[43] Tabrizi, M. A.; Baraldi, P. G.; Preti, D.; Romagnoli, R.; Saponaro, G.; Baraldi, S.; Moorman, A. R.; Zaid, A. N.; Varani, K.; Borea, P. A., 1,3-Dipropyl-8-(1-phenylacetamide-1H-pyrazol-3-yl)-xanthine derivatives as highly potent and selective human A<sub>2B</sub> adenosine receptor antagonists. *Bioorg. Med. Chem.* **2008**, *16* (5), 2419-2430.

[44] Fetzer, C.; Korotkov, V. S.; Sieber, S. A., Hydantoin analogs inhibit the fully assembled ClpXP protease without affecting the individual peptidase and chaperone domains. *Org. Biomol. Chem.* **2019**, *17* (30), 7124-7127.

[45] Miller, K. J.; Saherwala, A. A.; Webber, B. C.; Wu, Y.; Sherry, A. D.; Woods, M., The population of SAP and TSAP isomers in cyclen-based lanthanide(III) chelates is substantially affected by solvent. *Inorg. Chem.* **2010**, *49* (19), 8662-8664.

[46] Iman, M.; Davood, A.; Dehqani, G.; Lotfinia, M.; Sardari, S.; Azerang, P.; Amini, M., Design, synthesis and evaluation of antitubercular activity of novel dihydropyridine containing imidazolyl substituent. *Iran. J. Pharm. Res.* **2015**, *14* (4), 1067-1075.

[47] Ohmura, T.; Awano, T.; Suginome, M., Stereospecific Suzuki-Miyaura coupling of chiral alpha-(acylamino)benzylboronic esters with inversion of configuration. *J. Am. Chem. Soc.* **2010**, *132* (38), 13191-13193.

[48] Bartsch, R. A.; Cho, B. R., Reactions of N-halo-N-methylbenzylamines with sodium methoxide-methanol and potassium tert-butoxide-tert-butyl alcohol. Effects of .beta.-carbon

substituent and base-solvent system upon the imine-forming transition state. *J. Am. Chem. Soc.* **1989**, *111* (6), 2252-2257.

[49] Unger, Y.; Strassner, T., Platinum(II) complexes with amide-functionalized NHC ligands. *J. Organomet. Chem.* **2012**, *713*, 203-208.

[50] Dey, T. K.; Basu, P.; Riyajuddin, S.; Ghosh, A.; Ghosh, K.; Manirul Islam, S., Polymer-incarcerated palladium-catalyzed facile in situ carbonylation for the synthesis of aryl aldehydes and diaryl ketones using CO surrogates under ambient conditions. *New J. Chem.* **2019**, *43* (25), 9802-9814.

[51] Salerno, L.; Amata, E.; Romeo, G.; Marrazzo, A.; Prezzavento, O.; Floresta, G.; Sorrenti, V.; Barbagallo, I.; Rescifina, A.; Pittala, V., Potholing of the hydrophobic heme oxygenase-1 western region for the search of potent and selective imidazole-based inhibitors. *Eur. J. Med. Chem.* **2018**, *148*, 54-62.

[52] Csizmadia, F., JChem: Java applets and modules supporting chemical database handling from web browsers. *J. Chem. Inf. Comput. Sci.* **2000**, *40* (2), 323-324.

[53] Stewart, J. J., MOPAC: a semiempirical molecular orbital program. *J. Comput. Aided. Mol. Des.* **1990**, *4* (1), 1-105.

[54] Krieger, E.; Vriend, G., YASARA View - molecular graphics for all devices - from smartphones to workstations. *Bioinformatics* **2014**, *30* (20), 2981-2982.

[55] Duan, Y.; Wu, C.; Chowdhury, S.; Lee, M. C.; Xiong, G.; Zhang, W.; Yang, R.; Cieplak, P.; Luo, R.; Lee, T.; Caldwell, J.; Wang, J.; Kollman, P., A point-charge force field for molecular mechanics simulations of proteins based on condensed-phase quantum mechanical calculations. *J. Comput. Chem.* **2003**, *24* (16), 1999-2012.

[56] Floresta, G.; Cilibrizzi, A.; Abbate, V.; Spampinato, A.; Zagni, C.; Rescifina, A., 3D-QSAR assisted identification of FABP4 inhibitors: An effective scaffold hopping analysis/QSAR evaluation. *Bioorg. Chem.* **2019**, *84*, 276-284.

[57] Floresta, G.; Cilibrizzi, A.; Abbate, V.; Spampinato, A.; Zagni, C.; Rescifina, A., FABP4 inhibitors 3D-QSAR model and isosteric replacement of BMS309403 datasets. *Data Brief.* **2018**, *22*, 471-483.

[58] Floresta, G.; Amata, E.; Dichiarà, M.; Marrazzo, A.; Salerno, L.; Romeo, G.; Prezzavento, O.; Pittalà, V.; Rescifina, A., Identification of potentially potent heme oxygenase 1 inhibitors through 3D-QSAR coupled to scaffold-hopping analysis. *ChemMedChem.* **2018**, *13*, 1336-1342.

- [59] Floresta, G.; Pittalà, V.; Sorrenti, V.; Romeo, G.; Salerno, L.; Rescifina, A., Development of new HO-1 inhibitors by a thorough scaffold-hopping analysis. *Bioorg. Chem.* **2018**, *81*, 334-339.
- [60] Floresta, G.; Apirakkan, O.; Rescifina, A.; Abbate, V., Discovery of high-affinity cannabinoid receptors ligands through a 3D-QSAR ushered by scaffold-hopping analysis. *Molecules.* **2018**, *23*, 2183.
- [61] D'Amico, A. G.; Maugeri, G.; Saccone, S.; Federico, C.; Cavallaro, S.; Reglodi, D.; D'Agata, V., PACAP modulates the autophagy process in an in vitro model of amyotrophic lateral sclerosis. *Int. J. Mol. Sci.* **2020**, *21* (8), 2943.
- [62] D'Amico, A. G.; Maugeri, G.; Bucolo, C.; Saccone, S.; Federico, C.; Cavallaro, S.; D'Agata, V., Nap interferes with hypoxia-inducible factors and VEGF expression in retina of diabetic rats. *J. Mol. Neurosci.* **2017**, *61* (2), 256-266.
- [63] Maugeri, G.; Longo, A.; D'Amico, A. G.; Rasa, D. M.; Reibaldi, M.; Russo, A.; Bonfiglio, V.; Avitabile, T.; D'Agata, V., Trophic effect of PACAP on human corneal endothelium. *Peptides* **2018**, *99*, 20-26.

*“Adapted with permission from Journal of Medicinal Chemistry, Fallica AN, Sorrenti V, D'Amico AG, Salerno L, Romeo G, Intagliata S, Consoli V, Floresta G, Rescifina A, D'Agata V, Vanella L, Pittalà V. Discovery of Novel Acetamide-Based Heme Oxygenase-1 Inhibitors with Potent In Vitro Antiproliferative Activity, 2021, 64, 18, 13373–13393, Copyright © (2021) The Authors. Published by American Chemical Society”.*



# Growing the molecular architecture of imidazole-like ligands in HO-1 complexes

Giuseppe Floresta <sup>a,1,\*</sup>, Antonino N. Fallica <sup>b,1</sup>, Loredana Salerno <sup>b</sup>, Valeria Sorrenti <sup>b</sup>, Valeria Pittalà <sup>b,\*</sup>, Antonio Rescifina <sup>b</sup>

<sup>a</sup> Department of Analytical, Environmental and Forensic Sciences, King's College London, London, UK

<sup>b</sup> Department of Drug and Health Sciences, University of Catania, Catania – Italy

## *Bioorganic Chemistry*

Received: May 12, 2021; Received in revised form: August 27, 2021; Accepted: October 11, 2021

**ABSTRACT:** Up-regulation of HO-1 had been frequently reported in different cases and types of human malignancies. Since poor clinical outcomes are reported in these cases, but this enzyme's inhibition is considered a valuable and proven anticancer approach. To identify novel HO-1 inhibitors suitable for drug development, we report a structure-guided fragment-based approach to identify new lead compounds. Different parts of the selected molecules were analyzed, and the different series of novel compounds were virtually evaluated. The growing experiments of the classical HO-1 inhibitors structure led us to different hit-compounds. A synthetic pathway for six selected molecules was designed, and the compounds were synthesized. The biological activity revealed that molecules **10** and **12** inhibit the HO-1 activity with an IC<sub>50</sub> of 1.01 and 0.90 μM, respectively. This study suggested that our growing approach was successful, and these results are ongoing for further development.

**KEYWORDS:** Fragment-based ligand design; Fragment growing; Structure-based drug design; Heme Oxygenase; HO-1 inhibitors; Imidazole.

### **Authors contribution**

<sup>1</sup>These authors contributed equally

### **\*Corresponding authors:**

Giuseppe Floresta: giuseppe.floresta@kcl.ac.uk

Valeria Pittalà: vpittala@unict.it

## 1. Introduction

In mammalian cells, heme catabolism is closely controlled by the heme oxygenase (HO) enzymatic family [1]. This class of oxidoreductases breaks the heme molecule into three catabolites: carbon monoxide, ferrous iron, and biliverdin, a bile pigment rapidly converted to bilirubin by the biliverdin reductase enzyme [2]. Heme catabolites are involved in the modulation of vasodilation, voltage channel activation, neuroprotection, and exert potent antioxidant effects [3-5]. Currently, two main isoforms have been described, HO-1 and HO-2. Although they catalyze the same reaction, the two isozymes differ in their genetic origin, tissue distribution, and aminoacidic sequence [6]. HO-1, also described as heat-shock protein 32 (Hsp32), is basally expressed in spleen and liver tissues [7, 8], although its intracellular levels can be highly raised up under stressful conditions and after exposure to ROS, xenobiotics, heavy metals, toxins, UV radiations and high heme concentrations [9]. HO-1 upregulation is under the tight control of the nuclear factor erythroid 2-related factor 2 (Nrf2). In the case of an imbalanced oxidative intracellular status, Nrf2 dissociates from the Kelch-like ECH-associated protein 1 (Keap1) and translocates to the nucleus, where it binds to specific binding domains localized on the DNA, boosting the transcription of several antioxidant proteins, including HO-1 [10]. On the contrary, the HO-2 enzyme represents the constitutive isoform principally detectable in the brain and testis, where it exerts neuroprotective properties through carbon monoxide production and seems to be involved in male reproduction [11, 12]. The cytoprotective effects exerted by high levels of HO-1 make this isozyme a double-edged sword. Indeed, if HO-1 overexpression could be advantageous for the treatment of several pathologies directly related to an imbalanced intracellular oxidative stress status [13-21], the same overexpression has been noticed in several cancers and should be avoided. A large group of papers reported that HO-1 overexpression in tumor cells promotes cell survival, cell proliferation, neovascularization, and failure of apoptosis [22-25]. Moreover, aberrant HO-1 upregulation and overexpression are closely associated with resistance to radiotherapy, chemotherapy, and photodynamic therapy with a consequent fateful prognosis and very low chances of survival. The inducible nature of HO-1 and its overexpression in tumor cells render this enzyme an intriguing target for novel anticancer therapies in which HO-1 inhibitors could be used in stand-alone therapeutic regimens or could be associated with commonly used anticancer drugs in order to reduce toxicity, resistance phenomena, and unwanted side effects. In light of this, we gained extensive knowledge on the design of novel potent HO inhibitors [26, 27], and we

built a database (HemeOxDB, <http://www.researchdsf.unict.it/hemeoxdb>) in which can be found all published HO inhibitors [28]. In addition, we developed a successful 3D-QSAR model to discover novel HO-1 inhibitors [29-31]. Pushed by the successful results previously obtained with our *in-silico* approaches, we decided to exploit these computational techniques further to identify novel lead compounds helpful in designing novel HO-1 inhibitors.

One of the foremost common ways for medicinal chemists to optimize a new chemical entity is to gain further interactions with the targeted receptor by growing a compound. Using this approach, a hit can easily and quickly grow into a lead by gaining novel interactions with the targeted receptor. It has been reported that the evolution of a hit to a clinical candidate increases the structural complexity of the original molecule and gains an average molecular weight of 85 Da [32]. The growth strategy is particularly relevant in the fragment-based drug design, where the starting studied molecules usually are compounds with low MW and marginal potency on the receptor. Molecular modeling is a mainstream technology with applications in all the drug discovery process steps, from early discovery tasks to receptor prioritization, binding site detection, druggability analysis, virtual screening, and lead optimization. Structure-based *in-silico* ligand growing exploration is not an exception [33].

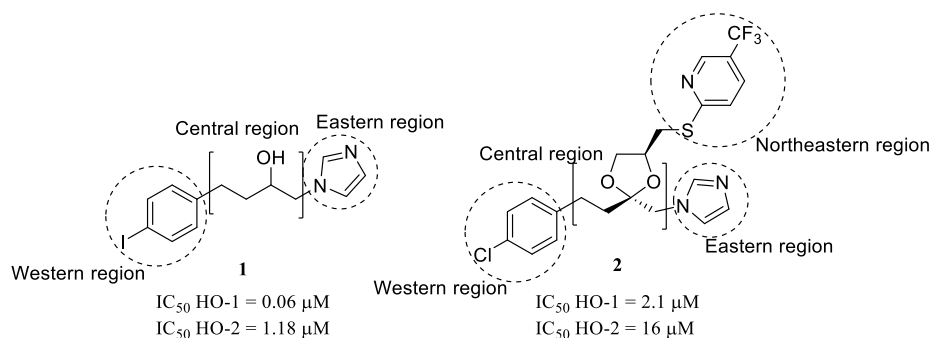
Moreover, our research group has already successfully applied different *in-silico* techniques to develop HO-1 and HO-2 inhibitors [28, 29, 34-39]. This work describes the development of HO-1 inhibitors employing structure-guided optimization of a fragment hit. The molecules were generated and classified *in silico* and then synthesized and tested for their activity in HO-1.

## **2. Results and discussion**

### *2.1. Ligand Growing*

Fragment-based ligand design is now well established as an efficient starting point and optimization method in structure-based drug discovery and can also be assisted by molecular modeling. In a ligand growing experiment, once the candidate fragments are identified from a library, they are merged or linked together, adding functionalities to increase binding and selectivity; then, the energy of binding is evaluated or calculated before synthesizing the designed compounds. In this paper, the ligand growing approach was used to identify new hit compounds as HO-1 inhibitors. The experiments firstly started by selecting a common

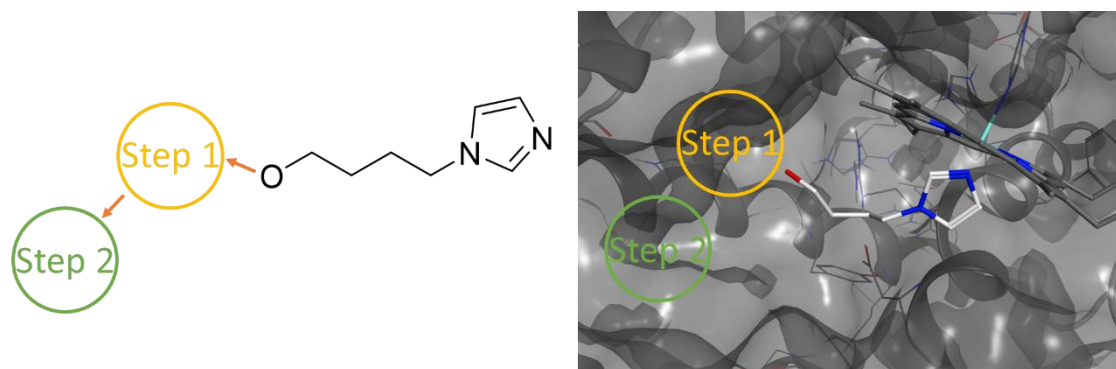
starting moiety in the “classical” HO-1 inhibitors structure. The structure of HO-1 inhibitors can be divided into four different regions, as showed in Figure 1. The northeastern region is not essential for HO-1 inhibition and can increase the activity but not HO-1 versus HO-2 selectivity. Co-crystallization studies performed with compound 2 and hHO-1 highlighted that its binding mode with the enzyme is similar to the binding mode of otherazole-based compounds that lack a substituent in the northeastern region, but with slight differences. The presence of additional moieties in this region induces a conformational change that allows the instauration of fruitful hydrophobic interactions associated with changes in the primary binding pocket (*i.e.*, western region), resulting in a slight reduction of potency and lack of selectivity for HO-1. The eastern region is crucial for the first interaction with HO-1; in fact, the imidazole’s nitrogen can coordinate the iron(II) of the heme substrate in HO-1. Through this coordination binding, iron(II) is protected from oxidation by disrupting an ordered solvent structure involving the critical Asp140 hydrogen-bond network (Tyr58, Tyr114, Arg136, and Asn210) and consequent displacement of water residues needed for catalysis. The central region is the connecting alkyl chain. Different nature and lengths are well-tolerated, but four or five atom chains are preferred. Finally, the western region is the main area responsible for HO-1 potency and selectivity towards HO-2, and it is crucial for the interaction with the distal hydrophobic pocket of the enzyme [40, 41].



**Figure 1.** Chemical structures and IC<sub>50</sub> values of representative HO-1 and HO-2 inhibitors.

Considering the typical structure of the classical HO-1 inhibitors, our ligand growing experiments started from a simple imidazole and a 4-carbon atoms alkyl chain to exploit, in two steps, the filling of the western region cavity of the HO-1 (Figure 2). Indeed, it was already proved in different molecules that a simple alkyl/aryl chain could be conveniently used as a linker between the two fundamental moieties of the “classical” HO-1 inhibitor without affecting the potency [30]. That is, the main contribution of the linker is to properly space the eastern (imidazole) from the western region allowing optimal contacts with heme-

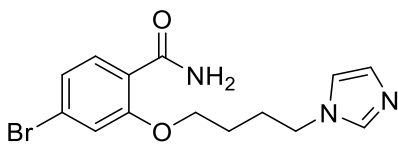
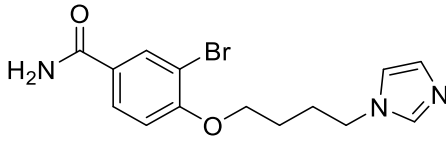
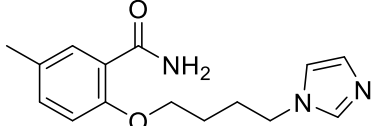
Fe<sup>2+</sup> and the distal hydrophobic pocket, respectively [28].

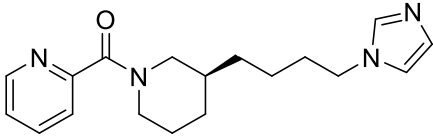
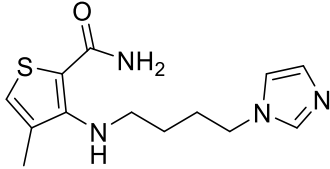


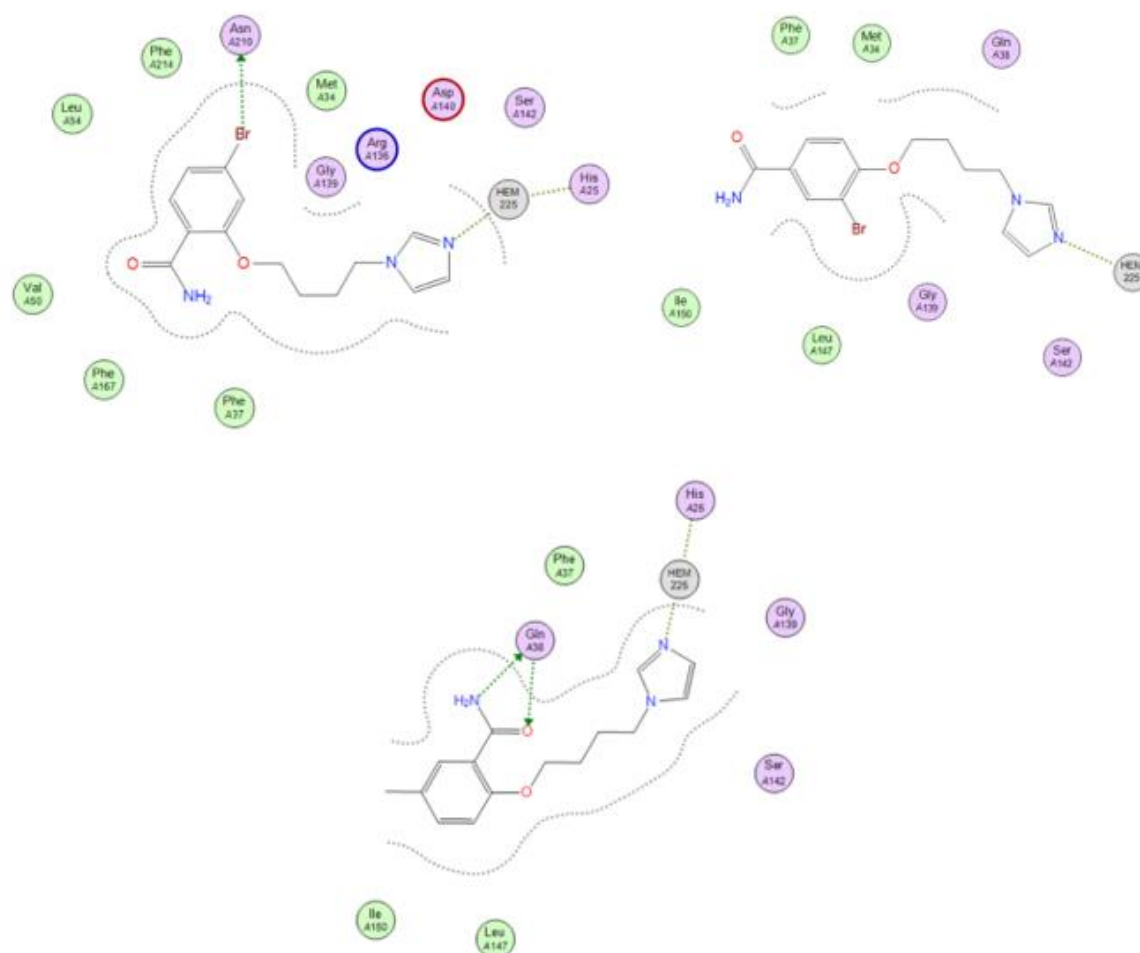
**Figure 2.** Representation of the two steps ligand growing experiments.

In the first step, the oxygen of the 4-(1*H*-imidazol-1-yl)butan-1-ol was substituted, and the 500 best compounds were selected among all the analyzed fragments (Table S1). The potency of the 500 compounds was then calculated by docking calculation and aligning and scoring in our previously published 3D-QSAR model [29]. The mean value between the calculated  $K_i$  (docking calculation) and the calculated  $IC_{50}$  (3D-QSAR model) was used to rank the compounds; we have already validated this strategy [42]. According to HO-1 predicted  $pIC_{50}$  from the 3D-QSAR model and the docking calculations, the five top-scored compounds from step one are reported in Table 1, while the complete set of compounds is reported in the supporting information. Figure 3 shows the docking pose of the three molecules; all of them are correctly placed inside the binding pocket of HO-1, molecule 3 is more inside in the pocket, whereas molecules 4 and 5 are pointing more on the surface, still making optimum interactions with the protein.

**Table 1.** Best-ranked molecules from step 1 of the ligand growing experiment.

Comp.	Structure	3D-QSAR $IC_{50}$ $\mu$ M	Docking $K_i$ $\mu$ M	Average
3		17.01	29.94	23.47
4		20.31	30.84	25.58
5		20.31	32.91	26.61

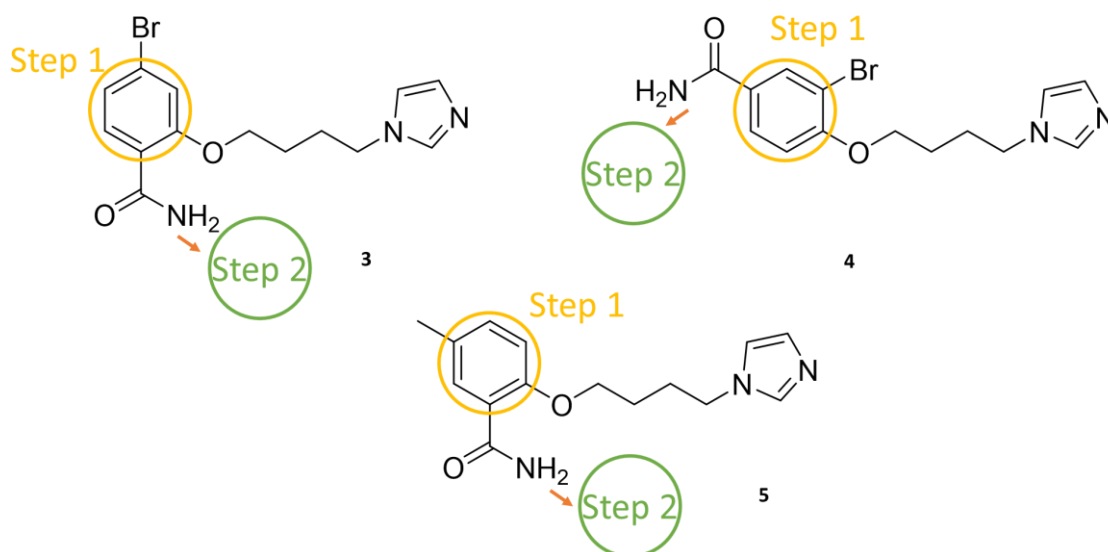
6		34.55	20.54	27.55
7		34.55	26.32	30.44



**Figure 3.** Best three compounds from step 1 of the ligand growing experiment inside HO-1. Top-left molecule **3**, top-right molecule **4**, and bottom molecule **5**.

For the second step, the three top-scored compounds from step 1 were selected and further led to growing inside the binding pocket of the HO-1 (Figure 4). The aromatic portion placed in the western region was selected for further expansion of the molecules. Five hundred compounds were generated for each molecule 3–5 for a total of 1500 new

compounds, which were then aligned and scored in our previously published 3D-QSAR model and by docking calculation (Tables S2–S4).

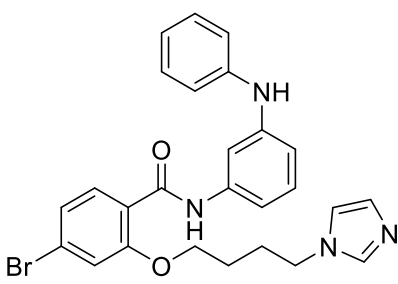
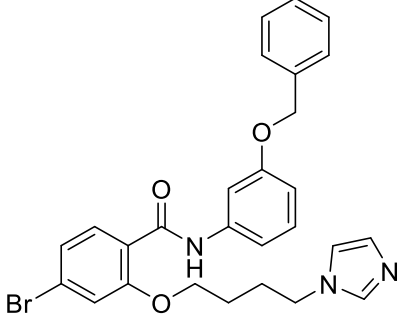
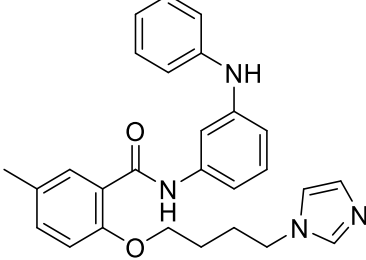
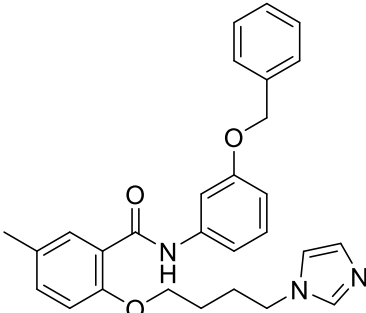


**Figure 4.** Representation of the second step of the ligand growing experiments for molecules 3–5.

The results of the second step of the growing calculations led to predicted potency in the low micromolar range, as an average of the predicted activity from the QSAR model and the docking calculations. To find common scaffolds to facilitate the synthesis of the final compounds, we examined the results of the best-ranked 25 compounds in the three different series. Interestingly, two common scaffolds (3-(phenylamino)phenyl and 3-(benzyloxy)phenyl) were identified in the three series. The structures of the selected compounds are reported in Table 2.

**Table 2.** Selected molecules from step 2 of the ligand growing experiment from molecules 3–5.

Compd	Structure	Rank in the series	Average $\mu\text{M}$ activity
8		2	1.26
9		22	2.86

10		1	0.69
11		14	2.02
12		6	0.86
13		25	1.65

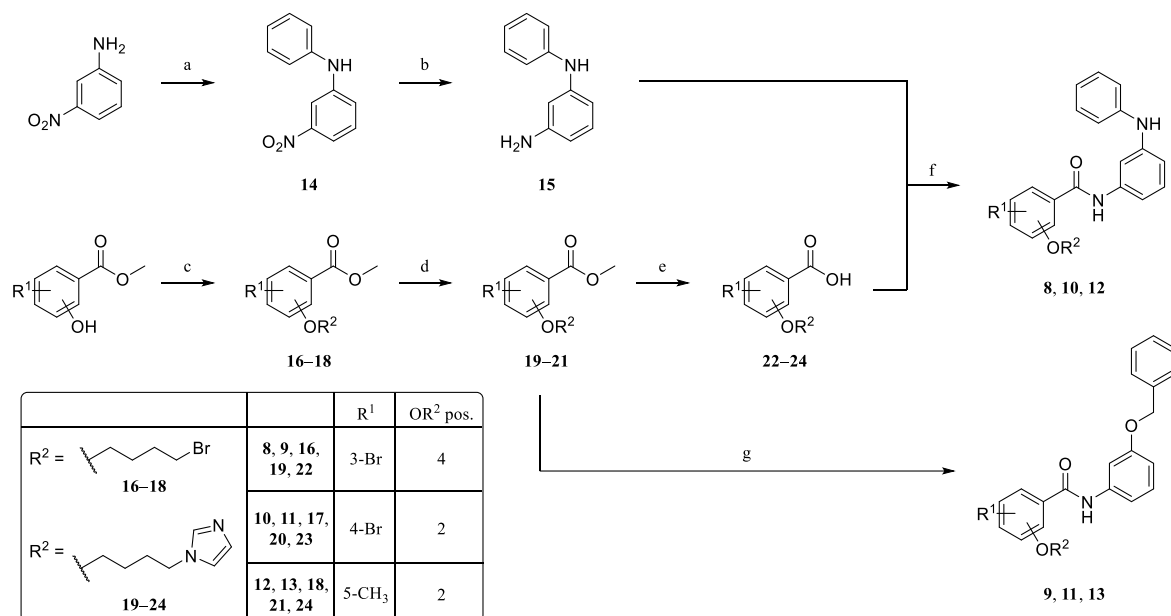
Overall results indicated that the computer-aided growing experiment gave compounds with the appropriate chemical structure for the inhibition of HO-1 with predicted potencies that reach the low micromolar range (as the average of the predicted  $K_i$  and  $IC_{50}$ ). To verify our procedure's predictive capabilities, the molecules selected from the second step, containing a common scaffold (**8–13**), were synthesized and tested for their actual inhibition of HO-1.

## 2.2. Synthesis

The synthesis of final compounds **8–13** was accomplished as depicted in Scheme 1. *N*-1-phenylbenzene-1,3-diamine (compound 15) was obtained by reaction of phenylboronic acid,



3-nitroaniline, and copper (II) acetate ( $\text{Cu}(\text{OAc})_2$ ) as coupling agent affording intermediate 14, which was subsequently reduced using iron powder and  $\text{NH}_4\text{Cl}$  in an ethanol/water mixture at reflux for 1 h. Bromobutoxy benzoates **16–18** were obtained following two different synthetic procedures as previously reported [35]: the first one consisted in the etherification of a substituted hydroxybenzoate methyl ester with 1,4-dibromobutane,  $\text{K}_2\text{CO}_3$  as base and acetone as reaction solvent under microwave irradiation; the second procedure involved the use of  $\text{NaOH}$  as base and DMSO. Imidazolylbutoxy benzoates **19–21** were obtained from intermediates **16–18** by aliphatic nucleophilic substitution with imidazole in acetonitrile as the reaction solvent, triethylamine (TEA) as base, and tetrabutylammonium bromide (TBAB) as catalyst under microwave irradiation. Basic hydrolysis of intermediates **19–21** under microwave irradiation with  $\text{LiOH}$  in a mixture of THF/ $\text{H}_2\text{O}$ / $\text{CH}_3\text{OH}$  led to benzoic acids **22–24**. Final compounds **8, 10, and 12** were obtained by condensation of **15** and **22–24** using 1-ethyl-3-(3-dimethylaminopropyl)carbodiimide hydrochloride ( $\text{EDC}\cdot\text{HCl}$ ) and hydroxybenzotriazole (HOBt) as carboxyl activating agents in dry DMF at room temperature for 24 h. Final compounds **9, 11, and 13** were obtained by condensation of intermediates **19–21** with 3-benzyloxyaniline exploiting a greener synthetic approach that involved the use of potassium tert-butoxide in dry THF at room temperature for 2 h under a nitrogen atmosphere.



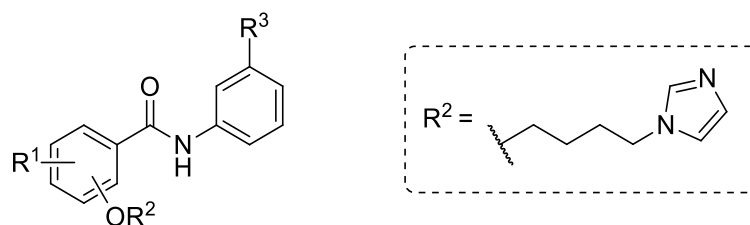
**Scheme 1.** Reagents and conditions: a) phenylboronic acid,  $\text{Cu}(\text{OAc})_2$ , TEA, dry  $\text{CH}_2\text{Cl}_2$ , room temperature, 48 h, under argon; b) Fe powder,  $\text{NH}_4\text{Cl}$ , EtOH/ $\text{H}_2\text{O}$ , 55 °C, then reflux, 1 h; c) method A, 1,4-dibromobutane,  $\text{K}_2\text{CO}_3$ , acetone, MW, 90 °C, 150 psi, 150 W, 45 min;

method B, 1,4-dibromobutane, KOH, DMSO, room temperature, 2 h; d) imidazole, acetonitrile, TEA, TBAB, MW, 95 °C, 150 psi, 150 W, 45 min, e) LiOH, THF/H<sub>2</sub>O/CH<sub>3</sub>OH, MW, 100 °C, 150 psi, 150 W, 45 min; f) EDC hydrochloride, HOBt, dry DMF, 0 °C, then room temperature, 24 h, under Ar; g) 3-benzyloxyaniline, *t*BuOK, dry THF, room temperature, 2 h, under N<sub>2</sub>.

### 2.3. HO-1 inhibition

The inhibitory activity of novel compounds was evaluated with an enzymatic assay. At basal conditions, HO-1 levels are highly detectable in rat spleen tissues, with the result that rat spleen homogenates have been chosen as the source of HO-1 for the measurement of the enzymatic activity. Heme catabolism brings to the formation biliverdin, which is quickly converted in bilirubin by the biliverdin reductase enzyme. Among the three heme catabolites, bilirubin formation can be easily monitored spectrophotometrically [43]. In this way, a higher inhibitory activity of a potential HO-1 inhibitor is mirrored in a lower bilirubin detection. IC<sub>50</sub> values for the new synthesized compounds are reported in Table 3, using azalanstat as the reference compound.

**Table 3.** Structures and experimental IC<sub>50</sub> values for molecules **8–13** and Azalanstat.



Compound	R <sup>1</sup>	OR <sup>2</sup> position	R <sup>3</sup>	IC <sub>50</sub> (μM) HO-1 <sup>a</sup>
<b>8</b>	3-Br	4	PhNH	18.63 ±0.93
<b>9</b>	3-Br	4	PhCH <sub>2</sub> O	84.38 ±1.01
<b>10</b>	4-Br	2	PhNH	1.01 ±0.09
<b>11</b>	4-Br	2	PhCH <sub>2</sub> O	56.38 ±1.09
<b>12</b>	5-CH <sub>3</sub>	2	PhNH	0.90 ±0.07
<b>13</b>	5-CH <sub>3</sub>	2	PhCH <sub>2</sub> O	40.84 ±0.82
Azalanstat <sup>b</sup>	—	—	—	5.3 ±0.4

<sup>a</sup>Data are shown as IC<sub>50</sub> values in μM ± standard deviation (SD) and are the mean of triplicate experiments.

<sup>b</sup>Data taken from Ref. [40].

Overall, compounds possessing a 3-(phenylamino)phenyl moiety (molecules **8**, **10**, and **12**) displayed better IC<sub>50</sub> values than their 3-(benzyloxy)phenyl counterparts (molecules **9**, **11**, and **13**). These results are in agreement with values predicted with the ligand-growing

experiment. In addition, compounds **10** and **12** exhibited IC<sub>50</sub> values in the low micromolar range (1.01 and 0.90 μM, respectively) and were entirely in agreement with the predicted ones (average μM activity of **10** and **12** in HO-1 0.69 and 0.86 μM, respectively. Table 2). Looking at the molecules poses inside the HO-1 derived from the docking calculation (Figures S16-S25), is it possible to classify the poses of the compounds in two different clusters. Molecules **8** and **9** are part of the first, and molecules **10–13** are part of the second (Figure S22). In the first cluster, the molecules are pointing outside of the binding pocket, and beside the imidazole that is interacting correctly with the iron of the prosthetic group, the aromatic rings are not optimally placed inside the western region making the molecules not very strong HO-1 binders. In the second cluster, molecules **10–13** allocate their aromatic rings deep inside the HO-1 western- and part of the northeastern regions. Looking at the pose of the most potent compounds **10** and **12**, both achieved a similar pose inside the binding pocket and, differently to the less potent compounds **11** and **13**, are able to interact with Met34 (Figures S19,21). Compound **10** is also interacting through an H-pi interaction with Phe37 (Figure S18). These two interactions could be the main reason for the compounds' more potency than others in the same cluster (**11** and **13**).

#### 2.4. ADMET assessment

An *in-silico* absorption, distribution, metabolism, and excretion-toxicity (ADMET) pharmacokinetics evaluation was performed for molecules **8–13** to further expand the molecular modelling and the *in vitro* evaluations. The *in-silico* ADMET assessment has been generated using SwissADME (<http://swissadme.ch>) [44], and pkCSM (<http://biosig.unimelb.edu.au/pkcsm/>) [45], and the results are reported in Tables S6,7. Despite the low to moderate predicted solubility for molecules **8–13**, all compounds resulted orally available with good intestinal absorption. All molecules resulted as P-glycoprotein substrates, and they are also classified as P-glycoprotein I and II inhibitors. Differently, none of the studied compounds resulted as CYP2D6 substrate, but all the studied molecules can be metabolized by CYP3A4. Moreover, most of the classical enzymes of the CYP family may be inhibited by the molecules **8–13**, *i.e.*, CYP1A2, CYP2C19, CYP2C9, CYP2D6, and CYP3A4. Interestingly compounds **12** and **13** have no violation of the Lipinski rule of 5, compound **12** also has no violation of Egan rules, and compound **13** has no violations also to Egan and Muegee drug-likeness [46-48]. The absorption and distribution calculated parameters have been depicted by the Egan-Egg model in Figure S26 (Brain or Intestinal

EstimateD, BOILED-Egg). The Edan–Egg model highlights that all compounds were predicted to not passively permeate the blood-brain barrier but to be easily absorbed by the gastrointestinal tract. pkCSM calculated absorption properties showed a high (from 89.9 to 91.9 %) intestinal absorption due to the good Caco-2 cell permeability. The calculated value of the steady-state volume of distribution is relatively high for the compounds (Log VD<sub>ss</sub> > 0.28); differently, the compound's unbound fraction in the plasma is relatively low, resulting in a calculated unbound fraction in human proximal to zero in most cases. The calculated values of the total clearance indicate that the compounds have a good renal elimination (0.98 to 1.09 log mL/min/kg); compounds **8–11** also are substrates of the renal organic cation transporter 2. Finally, some toxicity issues were pointed out by pkCSM, despite the fact the none of the compounds result to have skin sensitization problems, most of them could be hERG I and II inhibitors and resulted predicted as toxic in the AMES test.

### 3. Conclusion

In this paper, we reported a two-step computer-aided fragment-based ligand growing experiments inside the binding pocket of the HO-1 starting from a simple alkyl-linker chain and the classic imidazole of the eastern region of common HO-1 inhibitors. Starting from 4-(1*H*-imidazol-1-yl)butan-1-ol, the oxygen was substituted, and 500 new compounds were generated and evaluated. The evaluation was conducted by docking calculation and by aligning and scoring in our previously published 3D QSAR model. The three best-scored compounds were selected and used as a starting point in the second step of the growing experiments. In this second step, the selected molecules were further gowned inside the binding pocket of HO-1, and 500 compounds were generated for each molecule. Molecules **8–13** were selected among the most potent compounds from step 2 of the growing experiments and synthesized.

The measured IC<sub>50</sub> against HO-1 confirmed the molecules' activity; mainly, molecules with the 3-(phenylamino)phenyl substituent were more potent than compounds with the 3-(benzyloxy)phenyl substituent as predicted by our calculations. Moreover, the predicted most potent molecules **10** and **12** were also the most active in the biological assay, showing an IC<sub>50</sub> of 1.01 and 0.90 μM, respectively. Considering the successful prediction of our ligand growing experiments, we will prompt extend this work to synthesize the other of the most potent predicted derivatives trying to create new scaffolds as potent HO-1 inhibitors. We will also use other fragment-based computer-aided experiments to individuate other hit

compounds. The ADMET *in-silico* evaluation of the molecules will also lead us to select the best candidate for further *in-vitro* and *in-vivo* evaluation.

## 4. Experimental

### 4.1. Molecular modeling

The structures of all the molecules were built using Marvin Sketch [49]. The 2D structures were first subjected to a molecular mechanics energy minimization by the Merck molecular force field (MMFF94) present in Marvin Sketch [49]. The protonation states of the molecules were calculated assuming a neutral pH. Before the ligand growing experiments, the alignment for the 3D-QSAR filter and the docking calculation, and the geometries of the obtained molecular mechanics 3D structures were further optimized at the semiempirical level employing the parameterized model number 3 (PM3) Hamiltonian as implemented in the MOPAC2016 package (Keywords used in MOPAC2016: PM3, EF, PRECISE, GNORM=0.01, DDMIN=0) [50-52]. Ligand growing experiments were performed on Spark (v. 10.6.0, <https://www.cresset-group.com/products/spark/>). Spark is a bioisostere replacement tool for rapidly generating reasonable yet novel scaffold and groups replacements using Cresset's molecular field points. Cresset's field technology condenses the molecular fields down to a set of points around the molecule, termed "field points". Field points are the local extrema of the electrostatic, van der Waals, and the molecule's hydrophobic potentials [53]. The ligand growing experiments were performed using databases of 1589469 fragments (Figure S1). 500 new ligands were generated for each growing step and then evaluated in a 3D-QSAR model and docking calculations. For the QSAR evaluation, all the 3D structures of the selected molecules were imported into the software Forge (v. 10.4.2) for the alignment/evaluation of the dataset in the 3D-QSAR model already published [29]. The field points of each compound (negative, positive, shape, and hydrophobic) were calculated and generated using the XED (extended electron distribution) force field in Forge; then, the molecules were aligned with the training set of the QSAR model by a maximum common substructure algorithm using a customized and validated set-up [29, 54, 55]. All the software parameters used for the conformation hunt and alignment presented in the supplementary material (Figures S2 and S3). The maximum number of conformations generated for each molecule was set to 500. The root-mean-square deviation of atomic positions cutoff, which is the similarity threshold below which two conformers are

assumed identical, was set to 0.5 Å. The gradient cutoff for conformer minimization was set to 0.1 kcal/mol. The energy window was set to 2.5 kcal/mol, and all the conformers with calculated energy outside the selected energy window were discarded. Docking experiments were performed employing AutoDock 4.2.6 software implemented in YASARA (v. 20.12.24) [56, 57] using 3HOK (X-ray Crystal Structure of Human Heme Oxygenase-1 with (2R, 4S)-2-[2-(4-Chlorophenyl)ethyl]-2-[(1*H*-imidazol-1-yl)methyl]-4[[[(5-trifluoromethylpyridin-2-yl)thio)methyl]-1,3-dioxolane) PDB code of the HO-1. The maps were generated by the AutoGrid (4.2.6) program with a spacing of 0.375 Å and dimensions that encompass all atoms extending 5 Å from the surface of the PM3 minimized structure of the crystallized ligand. All the parameters were inserted at their default settings. In the docking tab, the macromolecule and ligand are selected, and GA parameters are set as *ga\_runs* = 100, *ga\_pop\_size* = 150, *ga\_num\_evals* = 20000000, *ga\_num\_generations* = 27000, *ga\_elitism* = 1, *ga\_mutation\_rate* = 0.02, *ga\_crossover\_rate* = 0.8, *ga\_crossover\_mode* = two points, *ga\_cauchy\_alpha* = 0.0, *ga\_cauchy\_beta* = 1.0, number of generations for picking worst individual = 10.

#### 4.2. Chemistry

Microwaves assisted reactions were carried out with a CEM Discover instrument using closed Pyrex glass tubes (ca. 10 mL) with Teflon-coated septa. Reactions were monitored on TLC aluminum sheets coated with silica gel (60 F254, Merck, Kenilworth, NJ, USA) and visualized by UV ( $\lambda = 254$  and 366 nm) and iodine chamber. When needed, Celite<sup>®</sup> was used as a filter aid. Compounds were purified by flash chromatography performed on glass columns employing Merck silica gel (60, 0.040–0.063 mm, 230–400 mesh) as stationary phase. Melting points were determined in an IA9200 Electrothermal apparatus equipped with a digital thermometer in capillary glass tubes and are uncorrected. Infrared spectra were recorded on a Perkin Elmer 281 FTIR spectrometer using KBr disks or NaCl plates. <sup>1</sup>H- and <sup>13</sup>C-NMR spectra were determined with Varian Unity Inova 200 and 500 MHz instruments in CDCl<sub>3</sub> or DMSO-*d*<sub>6</sub> solution. Chemical shifts are given in ppm values, using tetramethylsilane (TMS) as the internal standard; coupling constants (*J*) are given in Hz. Signal multiplicities are characterized as s (singlet), d (doublet), t (triplet), q (quartet), m (multiplet), br (broad). High-resolution mass spectra were acquired with a Q Exactive Orbitrap mass spectrometer equipped with an ESI ion source operating in positive mode. Elemental analyses (C, H, N) were executed on a Carlo Erba Elemental Analyzer Mod. 1108;

results were within  $\pm 0.4\%$  of the theoretical values. All chemicals and solvents were reagent grade and were purchased from commercial sources. Characterization data of compounds **16–21** matched with those previously reported.

#### 4.2.1. Synthesis of 3-nitro-*N*-phenylaniline (**14**)

In an oven-dried two-necked round bottom flask equipped with a magnetic stirring bar and under an argon atmosphere, phenylboronic acid (1.45 mmol, 1 eq) and 3-nitroaniline (1.45 mmol, 1 eq) were dissolved in 5 mL of anhydrous  $\text{CH}_2\text{Cl}_2$ .  $\text{Cu}(\text{OAc})_2$  (1.45 mmol, 1 eq) and TEA (7.25 mmol, 2 eq) were added, and the suspension was left stirring at room temperature for 48 hours. The dark suspension was filtered through a Celite<sup>®</sup> pad, and the filtrate was evaporated under vacuum. The crude was purified by flash chromatography eluting with gradient mixtures of cyclohexane/EtOAc. The title compound was obtained as an orange solid (43%): mp 110–111 °C; IR (KBr)  $\text{cm}^{-1}$  3379, 1619, 1600, 1538, 1492, 1336, 1094, 994, 867, 789, 755; <sup>1</sup>H NMR (200 MHz, DMSO-*d*<sub>6</sub>):  $\delta$  8.77 (s, 1H, NH); 7.81–7.78 (m, 1H, aromatic), 7.63–7.30 (m, 5H, aromatic); 7.20–7.14 (m, 2H, aromatic); 7.04–6.95 (m, 1H, aromatic). Anal. Calcd. for ( $\text{C}_{12}\text{H}_{10}\text{N}_2\text{O}_2$ ): C, 67.28; H, 4.71; N, 13.08. Found: C, 67.24; H, 4.70; N, 13.12.

#### 4.2.2. Synthesis of *N*<sup>1</sup>-phenylbenzene-1,3-diamine (**15**)

In a round bottom flask, 3-nitro-*N*-phenylaniline **14** (0.59 mmol, 1 eq) was dissolved in 5 mL of EtOH and heated to 55 °C with an oil bath. Iron powder (2.95 mmol, 5 eq) and a solution of  $\text{NH}_4\text{Cl}$  (2.95 mmol, 5 eq) in 5 mL of deionized  $\text{H}_2\text{O}$  were added in sequence, and the orange solution was refluxed for 1 hour. The progress of the reaction was monitored on TLC (8 Cy/2 EtOAc). Then, the colorless hot solution was filtered through a Celite<sup>®</sup> pad, and the filtrate was dried under vacuum. The crude was basified with a saturated solution of  $\text{NaHCO}_3$  and the aqueous solution extracted with EtOAc (3×50 mL). The combined organic phases were dried with  $\text{Na}_2\text{SO}_4$ , filtered, and evaporated under vacuum affording a brown oil that was directly used in the next step with no further purification nor characterization.

#### 4.2.3. General procedure for the synthesis of substituted 4-(1*H*-imidazol-1-yl)butoxybenzoic acids (**22–24**)

In a sealed Pyrex glass tube equipped with a stirring bar, the proper methyl benzoate **19–21** (1 eq) was dissolved in a mixture of THF/ $\text{H}_2\text{O}$ / $\text{CH}_3\text{OH}$  (3:1.5:1 ratio). LiOH (2 eq) was added, and the mixture was stirred under microwave irradiation for 45 minutes (150 psi,

150 W, 100 °C). Reaction solvents were removed under reduced pressure, and the residue was acidified till the isoelectric point by dropwise addition of a solution of HCl 1N. The aqueous phase was extracted with EtOAc (3×20 mL); the organic phases were dried with Na<sub>2</sub>SO<sub>4</sub>, filtered, and evaporated under reduced pressure. According to this procedure, the following products were obtained.

#### 4.2.3.1. 4-(4-(1H-imidazol-1-yl)butoxy)-3-bromobenzoic acid (**22**)

The title compound was obtained using 0.52 mmol of **19** and 1.04 mmol of LiOH in 1.09 mL of THF, 544 μL of H<sub>2</sub>O and 363 μL of CH<sub>3</sub>OH. White solid (55%): mp 194–195 °C; IR (KBr) cm<sup>-1</sup> 3438, 2959, 2370, 1684, 1596, 1500, 1468, 1399, 1279, 1086, 1047, 1002, 742; <sup>1</sup>H NMR (200 MHz, DMSO-*d*<sub>6</sub>): δ 8.06 (d, *J* = 1.6 Hz, 1H, aromatic), 7.91 (dd, *J* = 8.6, 1.6 Hz, 1H, aromatic), 7.67 (s, 1H, imidazole), 7.21 (s, 1H, aromatic), 7.16 (s, 1H, imidazole), 6.91 (s, 1H, imidazole), 4.15 (t, *J* = 6.0 Hz, 2H, CH<sub>2</sub>-imidazole), 4.07 (t, *J* = 6.0 Hz, 2H, OCH<sub>2</sub>), 1.98–1.83 (m, 2H, CH<sub>2</sub>CH<sub>2</sub>-imidazole), 1.76–1.63 (m, 2H, OCH<sub>2</sub>CH<sub>2</sub>). Anal. Calcd. for C<sub>14</sub>H<sub>15</sub>BrN<sub>2</sub>O<sub>3</sub>: C, 49.57; H, 4.46; N, 8.26. Found: C, 49.43; H, 4.45; N, 8.29.

#### 4.2.3.2. 2-(4-(1H-Imidazol-1-yl)butoxy)-4-bromobenzoic acid (**23**)

The title compound was obtained using 0.624 mmol of **20** and 1.25 mmol of LiOH in 1.09 mL of THF, 544 μL of H<sub>2</sub>O and 363 μL of CH<sub>3</sub>OH. White solid (56%): mp 125 °C; IR (KBr) cm<sup>-1</sup> 3424 (br), 3134, 2917, 1687, 1587, 1485, 1466, 1389, 1242, 1100, 1018, 876; <sup>1</sup>H NMR (200 MHz, DMSO-*d*<sub>6</sub>): δ 7.69 (s, 1H, imidazole), 7.21 (s, 1H, imidazole), 7.12 (d, *J* = 8.0 Hz, 1H, aromatic), 7.01–6.94 (m, 2H, aromatic), 6.86 (s, 1H, imidazole), 4.06 (t, *J* = 6.0 Hz, 2H, CH<sub>2</sub>-imidazole), 3.94 (t, *J* = 6.0 Hz, 2H, OCH<sub>2</sub>), 1.94–1.79 (m, 2H, CH<sub>2</sub>CH<sub>2</sub>-imidazole), 1.63–1.50 (m, 2H, OCH<sub>2</sub>CH<sub>2</sub>). Anal. Calcd. for C<sub>14</sub>H<sub>15</sub>BrN<sub>2</sub>O<sub>3</sub>: C, 49.57; H, 4.46; N, 8.26. Found: C, 49.49; H, 4.44; N, 8.31.

#### 4.2.3.3. 2-(4-(1H-Imidazol-1-yl)butoxy)-5-methylbenzoic acid (**24**)

The title compound was obtained using 1.08 mmol of **21** and 2.16 mmol of LiOH in 1.87 mL of THF, 942 μL of H<sub>2</sub>O and 628 μL of CH<sub>3</sub>OH. White solid (47%): mp 244–246 °C; IR (KBr) cm<sup>-1</sup> 3362 (br), 1558, 1485, 1434, 1236, 1103, 1059, 866, 667; <sup>1</sup>H NMR (200 MHz, DMSO-*d*<sub>6</sub>): δ 7.68 (s, 1H, imidazole), 7.21 (s, 1H, imidazole), 6.99 (s, 1H, imidazole), 6.89–6.84 (m, 2H, aromatic), 6.70 (d, *J* = 8.0 Hz, 1H, aromatic), 4.05 (t, *J* = 6.0 Hz, 2H, CH<sub>2</sub>-imidazole), 3.89 (t, *J* = 6.0 Hz, 2H, OCH<sub>2</sub>), 2.18 (s, 3H, CH<sub>3</sub>), 1.92–1.78 (m, 2H,



CH<sub>2</sub>CH<sub>2</sub>-imidazole), 1.62–1.49 (m, 2H, OCH<sub>2</sub>CH<sub>2</sub>). Anal. Calcd. for C<sub>15</sub>H<sub>18</sub>N<sub>2</sub>O<sub>3</sub>: C, 65.68; H, 6.61; N, 10.21. Found: C, 65.48; H, 6.59; N, 10.24.

#### 4.2.4. General procedure for the synthesis of substituted (4-(1H-imidazol-1-yl)butoxy)-N-(3-(phenylamino)phenyl)benzamides (**8**, **10**, **12**)

In a round bottom flask, the proper substituted 4-(1H-imidazol-1-yl)butoxybenzoic acid **22–24** (1 eq) was dissolved in 3 mL of anhydrous DMF under an argon atmosphere. The solution was cooled to 0 °C with an ice bath. To the cooled stirred solution, EDC hydrochloride (1.5 eq), HOBt (1.5 eq) and a solution of compound **15** (2 eq) in 2 mL of anhydrous DMF were subsequently added within 30 minutes, and the dark resulting solution was left under stirring at room temperature for 24 hours under an argon atmosphere. The reaction solvent was concentrated under reduced pressure, the residue was diluted with a saturated solution of 80 mL of NaHCO<sub>3</sub>, and the aqueous phase was extracted three times with EtOAc (3×40 mL). The organic phase was dried with Na<sub>2</sub>SO<sub>4</sub>, filtered, and evaporated under vacuum. The crude was purified by flash chromatography eluting with gradient mixtures of CH<sub>2</sub>Cl<sub>2</sub>/CH<sub>3</sub>OH. According to this procedure, the following products were obtained.

##### 4.2.4.1. 4-(4-(1H-Imidazol-1-yl)butoxy)-3-bromo-N-(3-(phenylamino)phenyl)benzamide (**8**)

The title compound was obtained using 0.318 mmol of **22**, 0.477 mmol of EDC hydrochloride, 0.477 mmol of HOBt and 0.636 mmol of **15**. Grey solid (32%): mp 76 °C; IR (KBr) cm<sup>-1</sup> 3314 (br), 1654, 1595, 1544, 1496, 1449, 1308, 1266, 1048, 748; <sup>1</sup>H NMR (500 MHz, CDCl<sub>3</sub>): δ 8.55 (s, 1H, CONH), 8.07 (d, *J* = 2.0 Hz, 1H, aromatic), 7.78 (dd, *J* = 8.5, 2.0 Hz, 1H, aromatic), 7.52 (s, 1H, imidazole), 7.48 (s, 1H, aromatic), 7.26–7.23 (m, 2H, aromatic), 7.18 (t, *J* = 8.0 Hz, 1H, aromatic), 7.12–7.04 (m, 4H, aromatic + imidazole), 6.94–6.90 (m, 2H, aromatic and imidazole), 6.84 (dd, *J* = 8.0, 1.5 Hz, 1H, aromatic), 6.79 (d, *J* = 8.5 Hz, 1H, aromatic), 4.05 (t, *J* = 7.0 Hz, 2H, CH<sub>2</sub>-imidazole), 4.01 (t, *J* = 6.0 Hz, 2H, OCH<sub>2</sub>), 2.04–1.99 (m, 2H, CH<sub>2</sub>CH<sub>2</sub>-imidazole), 1.82–1.77 (m, 2H, OCH<sub>2</sub>CH<sub>2</sub>); <sup>13</sup>C NMR (125 MHz, CDCl<sub>3</sub>): δ 164.38, 157.70, 144.20, 142.78, 139.33, 132.63, 129.83, 129.45, 128.81, 121.41, 118.48, 113.31, 112.78, 112.28, 112.07, 109.49, 68.68, 46.91, 28.02, 25.95. Anal. Calcd. for C<sub>26</sub>H<sub>25</sub>BrN<sub>4</sub>O<sub>2</sub>: C, 61.79; H, 4.99; N, 11.09. Found: C, 61.98; H, 5.00; N, 11.07. HRMS (ESI<sup>+</sup>) *m/z*: calcd. for C<sub>26</sub>H<sub>26</sub>BrN<sub>4</sub>O<sub>2</sub>: 505.1239 [M+H]<sup>+</sup>; found 505.1211.

4.2.4.2. 2-(4-(1*H*-Imidazol-1-yl)butoxy)-4-bromo-*N*-(3-(phenylamino)phenyl)benzamide (**10**)

The title compound was obtained using 0.27 mmol of **23**, 0.405 mmol of EDC hydrochloride, 0.405 mmol of HOBT and 0.54 mmol of **15**. Whitish solid (61%): mp 147–149 °C; IR (KBr)  $\text{cm}^{-1}$  3345, 1664, 1592, 1553, 1493, 1447, 1316, 1230, 1168, 1076, 1009, 891, 837, 745;  $^1\text{H}$  NMR (500 MHz, DMSO- $d_6$ ):  $\delta$  10.0 (s, 1H, CONH), 8.25 (s, 1H, NH), 7.59 (s, 2H, aromatic), 7.55 (d,  $J = 8.0$  Hz, 1H, aromatic), 7.35 (d,  $J = 1.5$  Hz, 1H, aromatic), 7.26–7.22 (m, 3H, aromatic + imidazole), 7.17 (t,  $J = 8.0$  Hz, 1H, aromatic), 7.10 (d,  $J = 8.0$  Hz, 2H, aromatic), 7.06 (d,  $J = 8.0$  Hz, 1H, aromatic), 7.03 (s, 1H, imidazole), 6.85–6.78 (m, 3H, aromatic and imidazole), 4.12 (t,  $J = 6.0$  Hz, 2H,  $\text{CH}_2$ -imidazole), 3.95 (t,  $J = 7.0$  Hz, 2H,  $\text{OCH}_2$ ), 1.86–1.81 (m, 2H,  $\text{CH}_2\text{CH}_2$ -imidazole), 1.70–1.65 (m, 2H,  $\text{OCH}_2\text{CH}_2$ );  $^{13}\text{C}$  NMR (125 MHz, DMSO- $d_6$ ):  $\delta$  163.59, 156.53, 143.94, 143.23, 139.67, 131.24, 129.42, 129.12, 128.03, 124.66, 124.62, 123.47, 119.82, 119.18, 117.07, 115.97, 112.18, 110.90, 107.38, 68.23, 45.50, 27.09, 25.42. Anal. Calcd. for  $\text{C}_{26}\text{H}_{25}\text{BrN}_4\text{O}_2$ : C, 61.79; H, 4.99; N, 11.09. Found: C, 61.68; H, 4.97; N, 11.11. HRMS (ESI $^+$ )  $m/z$ : calcd. for  $\text{C}_{26}\text{H}_{26}\text{BrN}_4\text{O}_2$ : 505.1239 [M+H] $^+$ ; found 505.1215.

4.2.4.3. 2-(4-(1*H*-Imidazol-1-yl)butoxy)-5-methyl-*N*-(3-(phenylamino)phenyl)benzamide (**12**)

The title compound was obtained using 0.445 mmol of **24**, 0.67 mmol of EDC hydrochloride, 0.67 mmol of HOBT and 0.89 mmol of **15**. Brown solid (11%): mp 146 °C; IR (KBr)  $\text{cm}^{-1}$  3333, 2925, 1661, 1594, 1547, 1496, 1311, 1232, 1079, 747;  $^1\text{H}$  NMR (500 MHz,  $\text{CDCl}_3$ ):  $\delta$  9.66 (s, 1H, CONH), 8.01 (d,  $J = 2.0$  Hz, 1H, aromatic), 7.74 (s, 1H, imidazole), 7.29–7.17 (m, 8H, aromatic), 7.08 (s, 1H, imidazole), 6.94–6.90 (m, 2H, aromatic), 6.86 (s, 1H, imidazole), 6.83 (d,  $J = 8.5$  Hz, 1H, aromatic), 4.11 (t,  $J = 6.5$  Hz, 2H,  $\text{CH}_2$ -imidazole), 3.99 (t,  $J = 6.5$  Hz, 2H,  $\text{OCH}_2$ ), 2.33 (s, 3H,  $\text{CH}_3$ ), 2.00–1.94 (m, 2H,  $\text{CH}_2\text{CH}_2$ -imidazole), 1.86–1.81 (m, 2H,  $\text{OCH}_2\text{CH}_2$ );  $^{13}\text{C}$  NMR (125 MHz,  $\text{CDCl}_3$ ):  $\delta$  163.50, 154.35, 144.43, 143.22, 139.64, 133.74, 132.77, 131.52, 130.10, 129.46, 121.92, 121.14, 118.33, 113.05, 112.71, 112.28, 108.78, 68.79, 47.03, 27.79, 26.71, 20.54. Anal. Calcd. for  $\text{C}_{27}\text{H}_{28}\text{N}_4\text{O}_2$ : C, 73.61; H, 6.41; N, 12.72. Found: C, 73.49; H, 6.39; N, 12.76. HRMS (ESI $^+$ )  $m/z$ : calcd. for  $\text{C}_{27}\text{H}_{29}\text{N}_4\text{O}_2$ : 441.2291 [M+H] $^+$ ; found 441.2268.

4.2.5. General procedure for the synthesis of substituted (4-(1*H*-imidazol-1-yl)butoxy)-*N*-(3-(benzyloxy)phenyl)benzamides (**9**, **11**, **13**)

In a two-necked round bottom flask, the proper methyl benzoate **19–21** (1 eq) and 3-benzyloxyaniline (1 eq) were dissolved in 6 mL of anhydrous THF under nitrogen atmosphere. After 5 minutes of stirring, *t*BuOK (6 eq) was added, and the resulting brown suspension was left to stir at room temperature for 2 hours. The reaction was quenched with brine (6 mL), and the mixture was extracted with EtOAc (3×30 mL). The combined organic phases were washed with water, dried with Na<sub>2</sub>SO<sub>4</sub>, filtered, and removed under reduced pressure. The crude was purified by flash chromatography eluting with a mixture of 9.8 CH<sub>2</sub>Cl<sub>2</sub>/0.2 CH<sub>3</sub>OH. According to this procedure, the following products were obtained.

#### 4.2.5.1. 4-(4-(1*H*-Imidazol-1-yl)butoxy)-*N*-(3-(benzyloxy)phenyl)-3-bromobenzamide (**9**)

The title compound was obtained using 0.283 mmol of **19**, 0.283 mmol of 3-benzyloxyaniline and 1.70 mmol of *t*BuOK. Light brown solid (19%): mp 130–132 °C, IR (KBr) cm<sup>-1</sup> 3448, 2942, 1664, 1608, 1552, 1493, 1428, 1380, 1318, 1259, 1181, 1162, 1146, 1033, 915, 746; <sup>1</sup>H NMR (500 MHz, DMSO-*d*<sub>6</sub>): δ 10.15 (s, 1H, CONH), 8.18 (d, *J* = 2.0 Hz, 1H, aromatic), 7.95 (dd, *J* = 8.5, 2.0 Hz, 1H, aromatic), 7.80 (s, 1H, imidazole), 7.50 (t, *J* = 2.0 Hz, 1H, aromatic), 7.45 (d, *J* = 7.0 Hz, 2H, aromatic), 7.38 (t, *J* = 7.5 Hz, 2H, aromatic), 7.33–7.31 (m, 2H, aromatic and imidazole), 7.24 (t, *J* = 8.0 Hz, 2H, aromatic), 7.19 (d, *J* = 8.5 Hz, 1H, aromatic), 6.97 (s, 1H, imidazole), 6.75 (dd, *J* = 8.5, 2.0 Hz, 1H, aromatic), 5.08 (s, 2H, ArCH<sub>2</sub>), 4.14 (t, *J* = 6.0 Hz, 2H, CH<sub>2</sub>-imidazole), 4.08 (t, *J* = 7.0 Hz, 2H, OCH<sub>2</sub>), 1.94–1.88 (m, 2H, CH<sub>2</sub>CH<sub>2</sub>-imidazole), 1.72–1.67 (m, 2H, OCH<sub>2</sub>CH<sub>2</sub>); <sup>13</sup>C NMR (125 MHz, DMSO-*d*<sub>6</sub>): δ 163.98, 158.71, 157.49, 140.38, 137.23, 132.45, 129.71, 129.32, 128.71, 128.22, 128.10, 127.86, 113.21, 110.95, 110.31, 107.39, 69.42, 68.71, 46.16, 27.36, 25.63. Anal. Calcd. for C<sub>27</sub>H<sub>26</sub>BrN<sub>3</sub>O<sub>3</sub>: C, 62.31; H, 5.04; N, 8.07. Found: C, 62.47; H, 5.05; N, 8.05. HRMS (ESI<sup>+</sup>) *m/z*: calcd. for C<sub>27</sub>H<sub>27</sub>BrN<sub>3</sub>O<sub>3</sub>: 520.1236 [M+H]<sup>+</sup>; found 520.1221.

#### 4.2.5.2. 2-(4-(1*H*-Imidazol-1-yl)butoxy)-*N*-(3-(benzyloxy)phenyl)-4-bromobenzamide (**11**)

The title compound was obtained using 0.34 mmol of **20**, 0.34 mmol of 3-benzyloxyaniline and 2.04 mmol of *t*BuOK. Pale yellow oil (20%): IR (neat) cm<sup>-1</sup> 3357 (br), 1670, 1587, 1543, 1490, 1290, 1229, 1159, 1026, 742; <sup>1</sup>H NMR (500 MHz, CDCl<sub>3</sub>): δ 9.56 (s, 1H, CONH), 8.07 (d, *J* = 8.0 Hz, 1H, aromatic), 7.67 (s, 1H, imidazole), 7.57 (t, *J* = 1.5 Hz, 1H, aromatic), 7.44 (d, *J* = 7.0 Hz, 2H, aromatic), 7.38 (t, *J* = 7.5 Hz, 2H, aromatic), 7.32 (t, *J* = 7.5 Hz, 1H, aromatic), 7.27–7.24 (m, 2H, aromatic), 7.10 (d, *J* = 1.5 Hz, 1H, aromatic), 7.04 (s, 1H, imidazole), 6.96 (d, *J* = 8.0 Hz, 1H, aromatic), 6.86 (s, 1H, imidazole),

6.77 (dd,  $J = 8.0, 2.0$  Hz, 1H, aromatic), 5.09 (s, 2H, ArCH<sub>2</sub>), 4.15 (t,  $J = 6.0$  Hz, 2H, CH<sub>2</sub>-imidazole), 4.04 (t,  $J = 6.5$  Hz, 2H, OCH<sub>2</sub>), 2.04–1.98 (m, 2H, CH<sub>2</sub>CH<sub>2</sub>-imidazole), 1.95–1.90 (m, 2H, OCH<sub>2</sub>CH<sub>2</sub>); <sup>13</sup>C NMR (125 MHz, CDCl<sub>3</sub>):  $\delta$  162.53, 159.63, 156.61, 139.51, 136.95, 133.73, 130.02, 128.70, 128.14, 127.71, 127.24, 125.34, 121.30, 116.16, 112.38, 110.93, 107.10, 70.20, 69.16, 46.82, 27.90, 26.51. Anal. Calcd. for C<sub>27</sub>H<sub>26</sub>BrN<sub>3</sub>O<sub>3</sub>: C, 62.31; H, 5.04; N, 8.07. Found: C, 62.22; H, 5.02; N, 8.09. HRMS (ESI<sup>+</sup>)  $m/z$ : calcd. for C<sub>27</sub>H<sub>27</sub>BrN<sub>3</sub>O<sub>3</sub>: 520.1236 [M+H]<sup>+</sup>; found 520.1217.

#### 4.2.5.3. 2-(4-(1*H*-Imidazol-1-yl)butoxy)-*N*-(3-(benzyloxy)phenyl)-5-methylbenzamide (**13**)

The title compound was obtained using 0.45 mmol of **21**, 0.45 mmol of 3-benzyloxyaniline and 2.70 mmol of *t*BuOK. Brown solid (12%): mp 141–142 °C; IR (KBr) cm<sup>-1</sup> 3347, 1666, 1595, 1542, 1498, 1446, 1384, 1288, 1248, 1236, 1206, 1148, 1049, 1021, 763; <sup>1</sup>H NMR (500 MHz, DMSO-*d*<sub>6</sub>):  $\delta$  10.06 (s, 1H, CONH), 7.54 (d,  $J = 5.5$  Hz, 2H, aromatic), 7.46–7.16 (m, 9H, aromatic and imidazole), 7.04–7.02 (m, 2H, aromatic and imidazole), 6.82 (s, 1H, imidazole), 6.75 (d,  $J = 7.5$  Hz, 1H, aromatic), 5.07 (s, 2H, ArCH<sub>2</sub>), 4.07 (t,  $J = 6.0$  Hz, 2H, CH<sub>2</sub>-imidazole), 3.96 (t,  $J = 6.5$  Hz, 2H, OCH<sub>2</sub>), 2.28 (s, 3H, CH<sub>3</sub>), 1.86–1.81 (m, 2H, CH<sub>2</sub>CH<sub>2</sub>-imidazole), 1.70–1.66 (m, 2H, OCH<sub>2</sub>CH<sub>2</sub>); <sup>13</sup>C NMR (125 MHz, DMSO-*d*<sub>6</sub>):  $\delta$  164.58, 158.68, 153.76, 140.21, 137.06, 132.38, 130.00, 129.64, 129.48, 128.45, 128.33, 127.85, 127.69, 124.68, 113.02, 112.00, 109.62, 106.26, 69.19, 67.90, 45.59, 27.31, 25.67, 19.95. Anal. Calcd. for C<sub>28</sub>H<sub>29</sub>N<sub>3</sub>O<sub>3</sub>: C, 73.82; H, 6.42; N, 9.22. Found: C, 73.71; H, 6.39; N, 9.25. HRMS (ESI<sup>+</sup>)  $m/z$ : calcd. for C<sub>28</sub>H<sub>30</sub>N<sub>3</sub>O<sub>3</sub>: 456.2287 [M+H]<sup>+</sup>; found 456.2262.

### 4.3. Biology

#### 4.3.1. Preparation of rat spleen microsomal fractions

It is well documented that HO-1 protein is abundant in the rat spleen (PMID: 22431362). Therefore, rat spleen microsomal fraction prepared by differential centrifugation was used as the source of the HO-1 protein. We selected this particular microsomal preparation to use the most native (*i.e.*, closest to *in vivo*) form of HO-1. Spleen microsomal fractions were obtained according to Ryter et al. [8]. The experiments reported in the present paper complied with current Italian law and met the guidelines of the Institutional Animal Care and Use Committee of the Ministry of Health (Directorate General for Animal Health and Veterinary Medicines, Italy) “Dosing of enzymatic activities in rat microsomes” (2018–2022), project code 02769.N.VLY. Male Sprague–Dawley albino rats (150 g body weight

and age 45 d) with free access to water and kept at room temperature with a natural photoperiod (12 h light-12 h dark cycle) were used to obtain spleen microsomal fraction. For measuring HO-1 activity, each rat was sacrificed, and their spleens were excised and weighed. A homogenate (15%, w/v) of spleens pooled from five rats was prepared in 50 mM Tris buffer, pH 7.4, containing 0.25 M sucrose, using a Potter-Elvehjem homogenizing system with a Teflon pestle. The microsomal fraction of rat spleen homogenate was obtained by differential centrifugation; in particular, the first centrifugation at 10,000g for 20 min at 4 °C was followed by the second centrifugation of the supernatant at 100,000g for 60 min at 4 °C. The 100,000g pellet (microsomes) was resuspended in 100 mM potassium phosphate buffer, pH 7.8, containing 2 mM MgCl<sub>2</sub>. The rat spleen fraction was divided into equal aliquots, placed into microcentrifuge tubes, and stored at -80 °C for up to 2 months.

#### 4.3.2. Preparation of biliverdin reductase

Biliverdin reductase was obtained by using rat liver cytosol. We used three volumes of a 1.15% KCl w/v solution and Tris buffer 20 mM, pH 7.8, to homogenize on ice liver tissue. Homogenates were centrifuged at 10,000g for 20 min at 4 °C, and the obtained supernatant was then centrifuged at 100,000g for 1 h at 4 °C to sediment the microsomes. The 100,000g supernatant was stored in small amounts at -80 °C after its protein concentration was measured.

#### 4.3.3. Measurement of HO-1 enzymatic activities in the microsomal fraction of rat spleen

The HO-1 activity was determined by measuring the bilirubin formation using the difference in absorbance at 464–530 nm as described by Ryter et al. [8]. Incubation mixtures (500 µL) contained 20 mM Tris-HCl, pH 7.4, (1 mg/mL) microsomal extract, 0.5–2 mg/mL biliverdin reductase, 1 mM NADPH, 2 mM glucose 6-phosphate (G6P), 1 U G6P dehydrogenase, 25 µM hemin, and 10 µL of DMSO (or the same volume of DMSO solution of test compounds to a final concentration of 100, 10, and 1 µM). Enzymatic reactions were carried out for 60 min at 37 °C in a circulating water bath in the dark. The addition of 500 µL of chloroform stopped the reactions. After recovering the chloroform phase, the amount of bilirubin formed was measured with a double-beam spectrophotometer as OD 464–530 nm (extinction coefficient, 40 mM/cm<sup>-1</sup> for bilirubin). The enzymatic activity was defined as Units (one Unit is the amount of enzyme catalyzing the formation of 1 nmol of bilirubin/mg protein/h).

## Declaration of Competing Interest

The authors declare that they have no known competing financial interests or personal relationships that could have influenced the work reported in this paper.

## Acknowledgments

This work was founded by (1) University of Catania, Programma Ricerca di Ateneo Pia.Ce.Ri 2020-2022 linea 2, project number 57722172126; (2) Project authorized by the Ministry of Health (Directorate General for Animal Health and Veterinary Medicines) “Dosing of enzymatic activities in rat microsomes” (2018–2022) (project code 02769.N.VLY).

## Appendix A. Supplementary material

Supplementary data to this article can be found online at <https://doi.org/10.1016/j.bioorg.2021.105428>.

## REFERENCES

- [1] Abraham, N. G.; Kappas, A., Pharmacological and clinical aspects of heme oxygenase. *Pharmacol. Rev.* **2008**, *60* (1), 79-127.
- [2] Tenhunen, R.; Marver, H. S.; Schmid, R., The enzymatic conversion of heme to bilirubin by microsomal heme oxygenase. *Proc Natl Acad Sci U S A* **1968**, *61* (2), 748-755.
- [3] Motterlini, R.; Otterbein, L. E., The therapeutic potential of carbon monoxide. *Nat. Rev. Drug Discov.* **2010**, *9* (9), 728-743.
- [4] Morita, T.; Kourembanas, S., Endothelial cell expression of vasoconstrictors and growth factors is regulated by smooth muscle cell-derived carbon monoxide. *J. Clin. Investig.* **1995**, *96* (6), 2676-82.
- [5] Gozzelino, R.; Jeney, V.; Soares, M. P., Mechanisms of cell protection by heme oxygenase-1. *Annu. Rev. Pharmacol.* **2010**, *50*, 323-54.
- [6] Kutty, R. K.; Kutty, G.; Rodriguez, I. R.; Chader, G. J.; Wiggert, B., Chromosomal localization of the human heme oxygenase genes: heme oxygenase-1 (HMOX1) maps to chromosome 22q12 and heme oxygenase-2 (HMOX2) maps to chromosome 16p13.3. *Genomics* **1994**, *20* (3), 513-6.

- [7] Choi, A. M.; Alam, J., Heme oxygenase-1: function, regulation, and implication of a novel stress-inducible protein in oxidant-induced lung injury. *Am. J. Respir. Cell Mol. Biol.* **1996**, *15* (1), 9-19.
- [8] Ryter, S. W.; Alam, J.; Choi, A. M.; Heme oxygenase-1/carbon monoxide: from basic science to therapeutic applications. *Physiol. Rev.* **2006**, *86* (2), 583-650.
- [9] Muñoz-Sánchez, J.; Chánez-Cárdenas, M. E.; A Review on Hemeoxygenase-2: Focus on Cellular Protection and Oxygen Response. *Oxid. Med. Cell. Longev.* **2014**, *2014*, 604981.
- [10] Saha, S.; Buttari, B.; Panieri, E.; Profumo, E.; Saso, L.; An Overview of Nrf2 Signaling Pathway and Its Role in Inflammation. *Molecules* **2020**, *25* (22), 5474.
- [11] Zakhary, R.; Gaine, S. P.; Dinerman, J. L.; Ruat, M.; Flavahan, N. A.; Snyder, S. H.; Heme oxygenase 2: endothelial and neuronal localization and role in endothelium-dependent relaxation. *Proc Natl Acad Sci U S A* **1996**, *93* (2), 795-798.
- [12] McCoubrey, W. K. Jr.; Huang, T. J.; Maines, M. D.; Heme oxygenase-2 is a hemoprotein and binds heme through heme regulatory motifs that are not involved in heme catalysis. *J. Biol. Chem.* **1997**, *272* (19), 12568-74.
- [13] Li, C.; Hossieny, P.; Wu, B. J.; Qawasmeh, A.; Beck, K.; Stocker, R., Pharmacologic induction of heme oxygenase-1. *Antioxid. Redox Signal.* **2007**, *9* (12), 2227-39.
- [14] Calay, D.; Mason, J. C., The multifunctional role and therapeutic potential of HO-1 in the vascular endothelium. *Antioxid. Redox Signal.* **2014**, *20* (11), 1789-809.
- [15] Sorrenti, V.; Vanella, L.; Platania, C. B. M.; Greish, K.; Bucolo, C.; Pittalà, V.; Salerno, L., Novel Heme Oxygenase-1 (HO-1) Inducers Based on Dimethyl Fumarate Structure. *Int. J. Mol. Sci.* **2020**, *21* (24), 9541.
- [16] Carota, G.; Raffaele, M.; Sorrenti, V.; Salerno, L.; Pittalà, V.; Intagliata, S., Ginseng and heme oxygenase-1: The link between an old herb and a new protective system. *Fitoterapia* **2019**, *139*, 104370.
- [17] Pittalà, V.; Vanella, L.; Platania, C. B. M.; Salerno, L.; Raffaele, M.; Amata, E.; Marrazzo, A.; Floresta, G.; Romeo, G.; Greish, K.; Intagliata, S.; Bucolo, C.; Sorrenti, V., Synthesis, in vitro and in silico studies of HO-1 inducers and lung antifibrotic agents. *Future Med. Chem.* **2019**, *11* (13), 1523-1536.
- [18] Pittalà, V.; Salerno, L.; Romeo, G.; Acquaviva, R.; Di Giacomo, C.; Sorrenti, V., Therapeutic Potential of Caffeic Acid Phenethyl Ester (CAPE) in Diabetes. *Curr. Med. Chem.* **2018**, *25* (37), 4827-4836.

- [19] Pittalà, V.; Salerno, L.; Romeo, G.; Siracusa, M. A.; Modica, M. N.; Romano, G. L.; Salomone, S.; Drago, F.; Bucolo, C., Effects of novel hybrids of caffeic acid phenethyl ester and NSAIDs on experimental ocular inflammation. *Eur. J. Pharmacol.* **2015**, *752*, 78-83.
- [20] Pittala, V.; Vanella, L.; Salerno, L.; Di Giacomo, C.; Acquaviva, R.; Raffaele, M.; Romeo, G.; Modica, M. N.; Prezzavento, O.; Sorrenti, V., Novel Caffeic Acid Phenethyl Ester (Cape) Analogues as Inducers of Heme Oxygenase-1. *Curr. Pharm. Des.* **2017**, *23* (18), 2657-2664.
- [21] Pittala, V.; Vanella, L.; Salerno, L.; Romeo, G.; Marrazzo, A.; Di Giacomo, C.; Sorrenti, V., Effects of Polyphenolic Derivatives on Heme Oxygenase-System in Metabolic Dysfunctions. *Curr. Med. Chem.* **2018**, *25* (13), 1577-1595.
- [22] Nitti, M.; Piras, S.; Marinari, U. M.; Moretta, L.; Pronzato, M. A.; Furfaro, A. L.; HO-1 Induction in Cancer Progression: A Matter of Cell Adaptation. *Antioxidants* **2017**, *6* (2), 29.
- [23] Furfaro, A. L.; Traverso, N.; Domenicotti, C.; Piras, S.; Moretta, L.; Marinari, U. M.; Pronzato, M. A.; Nitti, M., The Nrf2/HO-1 Axis in Cancer Cell Growth and Chemoresistance. *Oxid Med Cell Longev* **2016**, *2016*, 1958174.
- [24] Chau, L. Y., Heme oxygenase-1: emerging target of cancer therapy. *J. Biomed. Sci.* **2015**, *22* (1), 22.
- [25] Castruccio Castracani, C.; Longhitano, L.; Distefano, A.; Di Rosa, M.; Pittalà, V.; Lupo, G.; Caruso, M.; Corona, D.; Tibullo, D.; Li Volti, G., Heme Oxygenase-1 and Carbon Monoxide Regulate Growth and Progression in Glioblastoma Cells. *Mol. Neurobiol.* **2020**, *57* (5), 2436-2446.
- [26] Salerno, L.; Floresta, G.; Ciaffaglione, V.; Gentile, D.; Margani, F.; Turnaturi, R.; Rescifina, A.; Pittalà, V., Progress in the development of selective heme oxygenase-1 inhibitors and their potential therapeutic application. *Eur. J. Med. Chem.* **2019**, *167*, 439-453.
- [27] Intagliata, S.; Salerno, L.; Ciaffaglione, V.; Leonardi, C.; Fallica, A. N.; Carota, G.; Amata, E.; Marrazzo, A.; Pittalà, V.; Romeo, G., Heme Oxygenase-2 (HO-2) as a therapeutic target: Activators and inhibitors. *Eur. J. Med. Chem.* **2019**, *183*, 111703.
- [28] Floresta, G.; Pittala, V.; Sorrenti, V.; Romeo, G.; Salerno, L.; Rescifina, A., Development of new HO-1 inhibitors by a thorough scaffold-hopping analysis. *Bioorg. Chem.* **2018**, *81*, 334-339.



- [29] Floresta, G.; Amata, E.; Dichiarà, M.; Marrazzo, A.; Salerno, L.; Romeo, G.; Prezzavento, O.; Pittalà, V.; Rescifina, A., Identification of Potentially Potent Heme Oxygenase 1 Inhibitors through 3D-QSAR Coupled to Scaffold-Hopping Analysis. *ChemMedChem* **2018**, *13* (13), 1336-1342.
- [30] Amata, E.; Marrazzo, A.; Dichiarà, M.; Modica, M. N.; Salerno, L.; Prezzavento, O.; Nastasi, G.; Rescifina, A.; Romeo, G.; Pittalà, V., Heme Oxygenase Database (HemeOxDB) and QSAR Analysis of Isoform 1 Inhibitors. *ChemMedChem* **2017**, *12* (22), 1873-1881.
- [31] Amata, E.; Marrazzo, A.; Dichiarà, M.; Modica, M. N.; Salerno, L.; Prezzavento, O.; Nastasi, G.; Rescifina, A.; Romeo, G.; Pittalà, V., Comprehensive data on a 2D-QSAR model for Heme Oxygenase isoform 1 inhibitors. *Data Brief* **2017**, *15*, 281-299.
- [32] Brown, D. G.; Boström, J., Where Do Recent Small Molecule Clinical Development Candidates Come From? *J. Med. Chem.* **2018**, *61* (21), 9442-9468.
- [33] Bienstock, R. J., Computational methods for fragment-based ligand design: growing and linking. *Methods Mol. Biol.* **2015**, *1289*, 119-35.
- [34] Greish, K. F.; Salerno, L.; Al Zahrani, R.; Amata, E.; Modica, M. N.; Romeo, G.; Marrazzo, A.; Prezzavento, O.; Sorrenti, V.; Rescifina, A.; Floresta, G.; Intagliata, S.; Pittalà, V., Novel Structural Insight into Inhibitors of Heme Oxygenase-1 (HO-1) by New Imidazole-Based Compounds: Biochemical and In Vitro Anticancer Activity Evaluation. *Molecules* **2018**, *23* (5), 1209.
- [35] Sorrenti, V.; Pittalà, V.; Romeo, G.; Amata, E.; Dichiarà, M.; Marrazzo, A.; Turnaturi, R.; Prezzavento, O.; Barbagallo, I.; Vanella, L.; Rescifina, A.; Floresta, G.; Tibullo, D.; Di Raimondo, F.; Intagliata, S.; Salerno, L., Targeting heme Oxygenase-1 with hybrid compounds to overcome Imatinib resistance in chronic myeloid leukemia cell lines. *Eur. J. Med. Chem.* **2018**, *158*, 937-950.
- [36] Floresta, G.; Amata, E.; Gentile, D.; Romeo, G.; Marrazzo, A.; Pittalà, V.; Salerno, L.; Rescifina, A., Fourfold Filtered Statistical/Computational Approach for the Identification of Imidazole Compounds as HO-1 Inhibitors from Natural Products. *Mar. Drugs* **2019**, *17* (2), 113.
- [37] Sorrenti, V.; Raffaele, M.; Vanella, L.; Acquaviva, R.; Salerno, L.; Pittalà, V.; Intagliata, S.; Di Giacomo, C., Protective Effects of Caffeic Acid Phenethyl Ester

- (CAPE) and Novel Cape Analogue as Inducers of Heme Oxygenase-1 in Streptozotocin-Induced Type 1 Diabetic Rats. *Int. J. Mol. Sci.* **2019**, *20* (10), 2441.
- [38] Ciaffaglione, V.; Intagliata, S.; Pittala, V.; Marrazzo, A.; Sorrenti, V.; Vanella, L.; Rescifina, A.; Floresta, G.; Sultan, A.; Greish, K.; Salerno, L., New Arylethanolimidazole Derivatives as HO-1 Inhibitors with Cytotoxicity against MCF-7 Breast Cancer Cells. *Int. J. Mol. Sci.* **2020**, *21* (6), 1923.
- [39] Floresta, G.; Fallica, A. N.; Romeo, G.; Sorrenti, V.; Salerno, L.; Rescifina, A.; Pittala, V., Identification of a potent heme oxygenase-2 (HO-2) inhibitor by targeting the secondary hydrophobic pocket of the HO-2 western region. *Bioorg. Chem.* **2020**, *104*, 104310.
- [40] Salerno, L.; Amata, E.; Romeo, G.; Marrazzo, A.; Prezzavento, O.; Floresta, G.; Sorrenti, V.; Barbagallo, I.; Rescifina, A.; Pittala, V., Potholing of the hydrophobic heme oxygenase-1 western region for the search of potent and selective imidazole-based inhibitors. *Eur. J. Med. Chem.* **2018**, *148*, 54-62.
- [41] Salerno, L.; Floresta, G.; Ciaffaglione, V.; Gentile, D.; Margani, F.; Turnaturi, R.; Rescifina, A.; Pittala, V., Progress in the development of selective heme oxygenase-1 inhibitors and their potential therapeutic application. *Eur. J. Med Chem.* **2019**, *167*, 439-453.
- [42] Gentile, D.; Floresta, G.; Patamia, V.; Chiaramonte, R.; Mauro, G. L.; Rescifina, A.; Vecchio, M., An Integrated Pharmacophore/Docking/3D-QSAR Approach to Screening a Large Library of Products in Search of Future Botulinum Neurotoxin A Inhibitors. *Int. J. Mol. Sci.* **2020**, *21* (24), 9470.
- [43] Sorrenti, V.; Guccione, S.; Di Giacomo, C.; Modica, M. N.; Pittalà, V.; Acquaviva, R.; Basile, L.; Pappalardo, M.; Salerno, L., Evaluation of imidazole-based compounds as heme oxygenase-1 inhibitors. *Chem. Biol. Drug. Des.* **2012**, *80* (6), 876-86.
- [44] Daina, A.; Michielin, O.; Zoete, V., SwissADME: a free web tool to evaluate pharmacokinetics, drug-likeness and medicinal chemistry friendliness of small molecules. *Sci. Rep.* **2017**, *7* (1), 42717.
- [45] Pires, D. E. V.; Blundell, T. L.; Ascher, D. B., pkCSM: Predicting Small-Molecule Pharmacokinetic and Toxicity Properties Using Graph-Based Signatures. *J. Med. Chem.* **2015**, *58* (9), 4066-4072.

- [46] Lipinski, C. A.; Lombardo, F.; Dominy, B. W.; Feeney, P. J., Experimental and computational approaches to estimate solubility and permeability in drug discovery and development settings. *Adv. Drug Deliv. Rev.* **1997**, *23* (1), 3-25.
- [47] Egan, W. J.; Merz, K. M.; Baldwin, J. J., Prediction of Drug Absorption Using Multivariate Statistics. *J. Med. Chem.* **2000**, *43* (21), 3867-3877.
- [48] Muegge, I.; Heald, S. L.; Brittelli, D., Simple Selection Criteria for Drug-like Chemical Matter. *J. Med. Chem.* **2001**, *44* (12), 1841-1846.
- [49] Barf, T.; Lehmann, F.; Hammer, K.; Haile, S.; Axen, E.; Medina, C.; Uppenberg, J.; Svensson, S.; Rondahl, L.; Lundback, T., N-Benzyl-indolo carboxylic acids: Design and synthesis of potent and selective adipocyte fatty-acid binding protein (A-FABP) inhibitors. *Bioorg. Med. Chem. Lett.* **2009**, *19* (6), 1745-8.
- [50] Stewart, J. J., Optimization of parameters for semiempirical methods IV: extension of MNDO, AM1, and PM3 to more main group elements. *J. Mol. Model.* **2004**, *10* (2), 155-64.
- [51] Alemán, C.; Luque, F. J.; Orozco, M., Suitability of the PM3-derived molecular electrostatic potentials. *J. Comput. Chem.* **1993**, *14* (7), 799-808.
- [52] Qiao, F.; Luo, L.; Peng, H.; Luo, S.; Huang, W.; Cui, J.; Li, X.; Kong, L.; Jiang, D.; Chitwood, D. J.; Peng, D., Characterization of Three Novel Fatty Acid- and Retinoid-Binding Protein Genes (Ha-far-1, Ha-far-2 and Hf-far-1) from the Cereal Cyst Nematodes *Heterodera avenae* and *H. filipjevi*. *PLoS One* **2016**, *11* (8), e0160003.
- [53] Cheeseright, T.; Mackey, M.; Rose, S.; Vinter, A., Molecular field extrema as descriptors of biological activity: definition and validation. *J. Chem. Inf. Model.* **2006**, *46* (2), 665-76.
- [54] Floresta, G.; Rescifina, A.; Marrazzo, A.; Dichiaro, M.; Pistara, V.; Pittala, V.; Prezzavento, O.; Amata, E., Hyphenated 3D-QSAR statistical model-scaffold hopping analysis for the identification of potentially potent and selective sigma-2 receptor ligands. *Eur. J. Med. Chem.* **2017**, *139*, 884-891.
- [55] Floresta, G.; Apirakkan, O.; Rescifina, A.; Abbate, V., Discovery of High-Affinity Cannabinoid Receptors Ligands through a 3D-QSAR Ushered by Scaffold-Hopping Analysis. *Molecules* **2018**, *23* (9), 2183.
- [56] Krieger, E.; Vriend, G., YASARA View - molecular graphics for all devices - from smartphones to workstations. *Bioinformatics* **2014**, *30* (20), 2981-2.

- [57] Krieger, E.; Koraimann, G.; Vriend, G., Increasing the precision of comparative models with YASARA NOVA-a self-parameterizing force field. *Proteins* **2002**, *47* (3), 393-402.

*“This article was published in Bioorganic Chemistry, 117, Floresta G.; Fallica AN; Salerno L; Sorrenti V; Pittalà V; Rescifina A, Growing the molecular architecture of imidazole-like ligands in HO-1 complexes, 105428, Copyright Elsevier (2020).”*

## From far west to east: joining the molecular architecture of imidazole-like ligands in HO-1 complexes

Giuseppe Floresta <sup>1,2,†</sup>, Antonino Nicolò Fallica <sup>1,†</sup>, Vincenzo Patamia <sup>1</sup>, Valeria Sorrenti <sup>1</sup>, Khaled Greish <sup>3</sup>, Antonio Rescifina <sup>1,\*</sup>, Valeria Pittalà <sup>1,\*</sup>

<sup>1</sup> Department of Drug and Health Sciences, University of Catania, V.le Andrea Doria 6, 95125 Catania, Italy;

<sup>2</sup> Department of Analytics, Environmental & Forensics, King's College London, London SE1 9NH, UK;

<sup>3</sup> Department of Molecular Medicine and Nanomedicine Unit, Princess Al-Jawhara Center for Molecular Medicine, College of Medicine and Medical Sciences, Arabian Gulf University, Manama 329, Bahrain.

### *Pharmaceuticals*

Received: November 16, 2021 Accepted: December 6, 2021

**ABSTRACT:** HO-1 overexpression has been reported in several cases/types of human malignancies. Unfortunately, poor clinical outcomes are reported in most of these cases, and the inhibition of HO-1 is considered a valuable and proven anticancer approach. To identify novel hit compounds suitable as HO-1 inhibitors, we report here a fragment-based approach where ligand joining experiments were used. The two most important parts of the classical structure of the HO-1 inhibitors were used as a starting point, and 1000 novel compounds were generated and then virtually evaluated by structure and ligand-based approaches. The joining experiments led us to a novel series of indole-based compounds. A synthetic pathway for eight selected molecules was designed, and the compounds were synthesized. The biological activity revealed that some molecules reach the micromolar activity whereas molecule **4d** inhibits the HO-1 with an IC<sub>50</sub> of 1.03 μM. This study suggested that our joining approach was successful, and a novel hit compound was generated. These results are ongoing for further development.

**KEYWORDS:** fragment-based ligand design; fragment growing; ligand joining, structure-based drug design; heme oxygenase; HO-1 inhibitors; imidazole

### **Author contributions**

† These authors contributed equally

### **\*Corresponding authors:**

Antonio Rescifina: arescifina@unict.it

Valeria Pittalà: vpittala@unict.it

## 1. Introduction

Despite the several efforts accomplished by the scientific community, cancer still represents one of the most important causes of death worldwide. This medical condition represents a challenge from both a clinical and an economic point of view, and its treatment is far from being resolute [1]. Modulating the activity of novel biological targets implicated in tumor onset and progression is regarded as a valuable strategy to define novel and better antitumor therapies [2]. In this context, it has been widely reported that heme oxygenase (HO) plays a key role in tumor growth and aggressiveness [3-6]. Heme oxygenase's physiological role consists in the oxidative heme breakdown at the cytoplasmatic level with the consequent stoichiometric production of three catabolites: carbon monoxide, ferrous ion, and biliverdin [7]. After its production, biliverdin is later converted into bilirubin by the biliverdin reductase enzyme. Heme end-products are involved in the control of several physiological activities, ranging from antioxidant to neuroprotective functions [8-12]. Nowadays, two main HO isoforms have been described. Both isoforms possess a similar aminoacidic sequence and catalyze the same reaction but differ in their genetic origin, tissue distribution, and mechanism of induction [13]. HO-1, also referred to as heat-shock protein 32, is basally expressed in high concentrations in the spleen and the liver. In other tissues, its expression is triggered by stressful stimuli such as xenobiotics, toxins, heavy metals, UV radiations, and oxidative stress.

On the other hand, HO-2 represents the constitutive isoform generally expressed in the brain and testis, where it seems to play a role in vasodilation through carbon monoxide production, neuroprotection and male reproduction [14, 15]. Consistently with its overall cytoprotective properties, HO-1 is highly induced in cancerous cells [16-19]. Indeed, its overexpression has been linked to increased tumor aggressiveness, neovascularization, metastasization, failure of apoptosis and poor chances of survival [20, 21]. Moreover, tumor cells overexpressing HO-1 are hardly treatable with common anticancer therapies, such as radiotherapy, chemotherapy, and photodynamic therapy. Finally, HO-1 induction is also related to the acquisition of resistance to common anticancer drugs, such as the antimetabolite fluorouracil [22-24]. In this general perspective, HO-1 inhibition could account for a valid strategy to be pursued in addition to the wide range of the current anticancer therapies [25]. Over the past years, we gained expertise on the design of potent HO inhibitors [15, 26-34], we published a database (HemeOxDB, <http://www.researchdsf.unict.it/hemeoxdb>) containing all published HO inhibitors [35] and

developed a descriptive 3D-QSAR model for HO-1 inhibitors [36, 37]. Motivated by the successful achievements of our *in-silico* approaches, we again decided to exploit these computational techniques to identify novel lead compounds for HO-1 inhibition.

It is common and widely used to gain further interactions with the targeted receptor growing a compound to optimize a new chemical entity. In fact, it has been proved that during the optimization process of a hit to lead compound, the original molecule gains an average molecular weight of 85 Da [38]. This growth strategy is particularly useful in the fragment-based drug design; moreover, with recent molecular modeling technologies, it is also possible to achieve ligand growing exploration from virtual growing experiments [39], and our research group has already successfully applied *in-silico* techniques to develop several HO-1/2 inhibitors [28-30, 32, 36, 37, 40]. This work describes the development of new scaffolds as HO-1 inhibitors exploiting virtual structure-guided ligand joining experiments. The molecules were generated and classified *in-silico* and then synthesized and tested for their activity in HO-1.

## 2. Results and discussion

### 2.1. Molecular modeling

Fragment-based and virtual fragment-based drug designs are now established as productive and cost-effective starting point/optimization methods in structure-based drug discovery. In these experiments, the candidate fragments are identified and then merged or linked together to increase binding and selectivity. We recently reported a successful virtual fragment-based drug design used to develop HO-1 inhibitors where a growing approach was exploited in the growing experiments [41]. Enthusiastic about the results, in this paper, a different virtual fragment-based approach is reported. Differently from the aforementioned growing experiments, the design was achieved using a ligand joining protocol, where two different ligands inside the HO-1 binding pocket were virtually joined to connect the two fragments. The drug design experiments started by selecting common starting moieties in the typical HO-1 inhibitors structure. HO-1 inhibitors can be divided into four different regions, as shown in Figure 1. The northeastern region is not a requisite for HO-1 inhibition and can only increase the activity but not the HO-1/HO-2 selectivity. The eastern region, where usually an imidazole or imidazole-like moiety coordinates the iron(II) of the heme substrate in HO-1, denotes the most critical region for inhibiting heme oxygenase enzymes.

In fact, thanks to this interaction, the iron(II) is protected from oxidation by disrupting an ordered solvent structure involving the critical Asp140 hydrogen-bond network (Tyr58, Tyr114, Arg136, and Asn210) and consequent displacement of water residues needed for catalysis. A central region is a connecting unit. Different types and lengths are well-tolerated, but four or five atom chains are preferred. Finally, the western region is the foremost area in controlling HO-1 potency and selectivity towards HO-2. It is crucial for the interaction with the distal hydrophobic pocket of the enzyme [15, 33].

Taking the typical structure of the HO-1 inhibitors as a starting point, our ligand joining experiments started from a simple imidazole and a benzyl group located in the western region, as already proved by us to be part of the western portion of some of the most powerful compounds against HO-1 (Figure 2) [33].

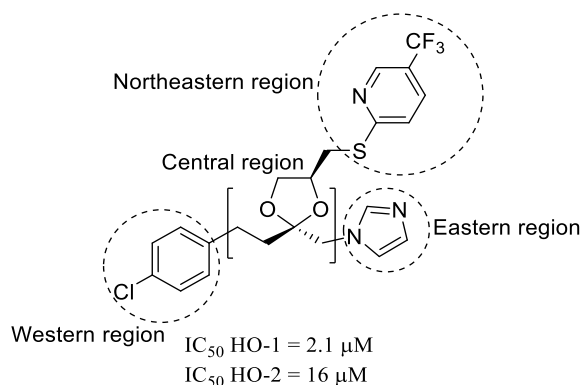


**Figure 1.** Chemical structure and IC<sub>50</sub> values of representative HO-1 and HO-2 inhibitor (QC-80).

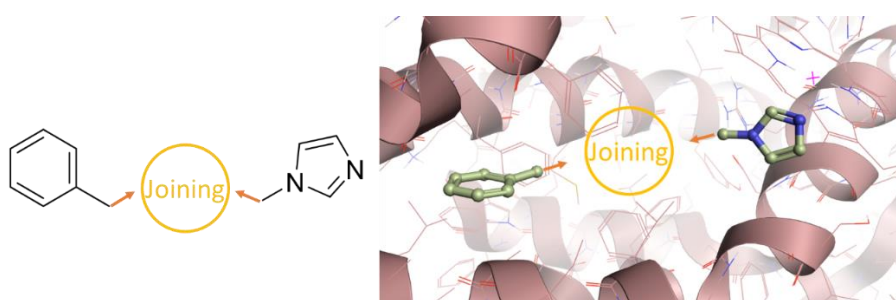


**Figure 2.** Representation of the ligand joining experiments inside HO-1.

In the fragment-based joining experiments, the benzyl group located in the far west area was joined to the imidazole inside the binding pocket of HO-1. One thousand compounds were generated and selected for further analysis (Table S1). The potency of the compounds was then evaluated and ranked by docking calculation and aligned in our previously published 3D-QSAR model [37]. Then, as already proven to be effective [42], the mean



value between the two calculated potencies ( $K_i$  from docking calculation and  $IC_{50}$  from the 3D-QSAR evaluation) was used to rank all the generated molecules. To find common scaffolds to facilitate the synthesis of the final compounds, we examined the results of the best-ranked 50 compounds. To assess the molecular diversity and find out common structural clusters within the compounds, the pairwise similarity was calculated by using ECFP4/FCFP4 circular fingerprints. ECFP4/FCFP4 circular fingerprints showed that the new set of compounds covers a wide range of molecular features; interestingly, two common clusters of compounds containing the indole within the connecting unit and the western region were identified by both fingerprints (Figure 3, Tables S2,3). In the two different sets of compounds, the indole is substituted with starting benzyl group either at its nitrogen atom or the 5-ring position, whereas a common connecting linker is always located in position 2. These newly identified indole-based ligands indicated that the computer-aided joining experiment gave structures with the appropriate chemical features for HO-1 inhibition with predicted potencies that reach the low micromolar range (as the average of the predicted  $K_i$  and  $IC_{50}$ ). To verify our procedure's predictive capabilities, five molecules (**1**, **4d**, and **8a–c**) were selected, synthesized, and tested for their actual inhibition of HO-1. Moreover, other three molecules (**4a–c**) were also synthesized to evaluate the presence of smaller substituents in the newly identified indole central ring.

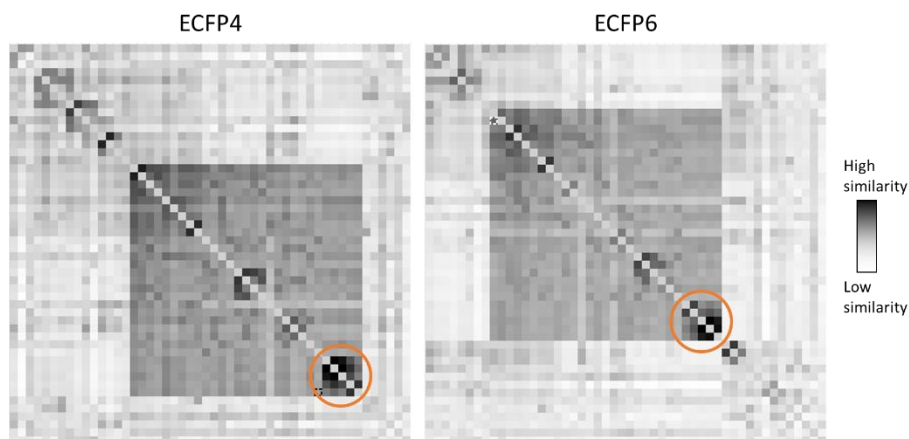
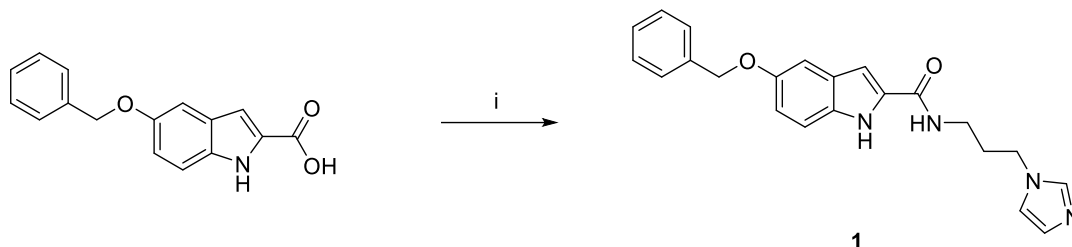


**Figure 3.** ECFP4 and FCFP4 fingerprint similarity matrix. Circled in orange is the highest similarity among the compounds (molecules **1**, **4d**, and **8a–c**).

## 2.2. Chemistry

The synthesis of final compound **1** is shown in Scheme 1. Compound **1** was synthesized in a one-step synthetic procedure by reaction of 5-(benzyloxy)-1*H*-indole-2-carboxylic acid,

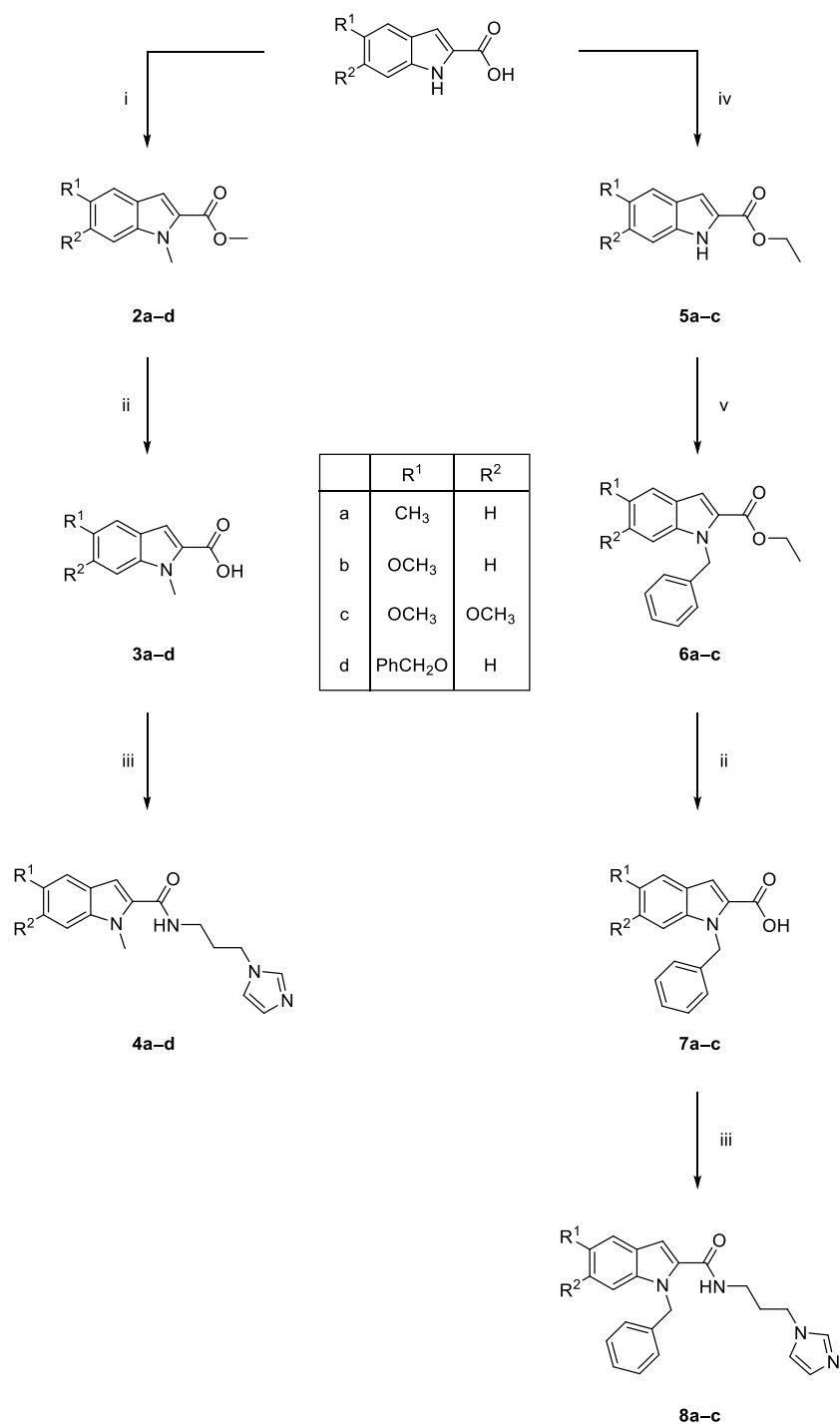
3-(1*H*-imidazol-1-yl)propan-1-amine and 1,1'-carbonyldiimidazole (CDI), as carboxylic acid activator, in anhydrous THF and at room temperature for 24 hours and then at refluxing conditions for 90 minutes.



**Scheme 1.** Synthesis of compound 1. Reagents and conditions: i) CDI, anhydrous THF, 2 h, room temperature; then 3-(1*H*-imidazol-1-yl)propan-1-amine, 22 h, room temperature; reflux, 90 min.

In Scheme 2 is reported the synthesis of final compounds **4a–d** and **8a–c**. Compounds **4a–d** were synthesized in three steps. The first step involved the contemporary esterification of the carboxylic acid function and methylation of the indole nitrogen using a large excess of CH<sub>3</sub>I and K<sub>2</sub>CO<sub>3</sub> in dry DMF at room temperature for 48 hours (intermediates **2a–d**). Hydrolysis of intermediates **2a–d** was performed using LiOH monohydrate in a THF/H<sub>2</sub>O/CH<sub>3</sub>OH mixture under microwave conditions for 90 minutes, affording the substituted methyl-1*H*-indole-2-carboxylic acid **3a–d**. The last step for the synthesis of compounds **4a–d** involved the condensation at 0 °C of intermediates **3a–d** with 3-(1*H*-imidazol-1-yl)propan-1-amine using 1-ethyl-3-(3-dimethylaminopropyl)carbodiimide hydrochloride (EDC·HCl) and hydroxybenzotriazole (HOBt) as coupling agents and anhydrous DMF as the reaction solvent.

Compounds **8a–c** were obtained in four steps. In order to protect the carboxylic function in the subsequent synthetic steps, a Fischer esterification of the appropriate substituted 1*H*-indole-2-carboxylic acid with refluxing ethanol and *p*-toluenesulfonic acid for 16 hours brought intermediates **5a–c**. In the second step, benzylation of compounds **5a–c** was performed using benzyl bromide and NaH (oil dispersion 80%) as base and anhydrous DMF as reaction solvent for 3 hours at room temperature and under an N<sub>2</sub> atmosphere, obtaining intermediates **6a–c**. The final two steps involved the basic hydrolysis of ethyl esters **6a–c** (compounds **7a–c**) and the condensation of carboxylic acids **7a–c** with 3-(1*H*-imidazol-1-yl)propan-1-amine following the same synthetic procedure described above for the synthesis of compounds **3a–d** and **4a–d**, respectively.



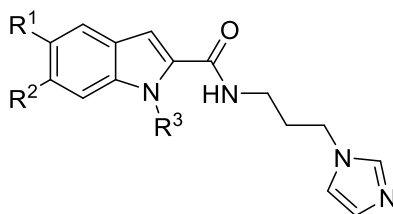
**Scheme 2.** Synthetic procedure adopted for the synthesis of compounds **4a-d** and **8a-c**. Reagents and conditions: i) CH<sub>3</sub>I, K<sub>2</sub>CO<sub>3</sub>, anhydrous DMF, room temperature, 48 h; ii) LiOH, THF/H<sub>2</sub>O/CH<sub>3</sub>OH, MW, 150 psi, 150 W, 100 °C, 90 min; iii) EDC hydrochloride, HOBt, 3-(1H-imidazol-1-yl)propan-1-amine, anhydrous DMF, 0 °C, then room temperature,

24 h, under Ar; iv) EtOH, *p*-TsOH, reflux, 16 hours; v) NaH oil dispersion 80%, 0 °C, 1 h, then benzyl bromide, room temperature, 3 h, under N<sub>2</sub>.

### 2.3. *In vitro* HO-1 inhibition and structure-activity relationships studies

The inhibitory potency of the novel compounds was evaluated reproducing *in vitro* the HO-1 catalytic cycle. Rat spleen microsomal fractions were chosen to isolate HO-1 in its most native form; indeed, it is well known that in basal conditions HO-1 is highly expressed in spleen tissues. In the presence of a strong HO-1 inhibitor, the amount of heme catabolites will be drastically reduced. Among the three catabolites, bilirubin concentrations can easily be monitored spectrophotometrically; the lowest is the absorbance detected with the assay, and the highest is the potency of the putative inhibitor. Results obtained from the *in vitro* enzymatic assay are reported in Table 1, using Azalanstat as the reference compound.

**Table 1.** General structure and experimental IC<sub>50</sub> values of compounds **1**, **4a–d**, **8a–c**, and Azalanstat.



Compd	R <sup>1</sup>	R <sup>2</sup>	R <sup>3</sup>	HO-1 <i>in-silico</i> (μM) <sup>a</sup>	HO-1 IC <sub>50</sub> (μM) <sup>b</sup>
<b>1</b>	PhCH <sub>2</sub> O	H	H	1.19	89.60 ± 6.10
<b>4a</b>	CH <sub>3</sub>	H	CH <sub>3</sub>	—	367.31 ± 34.50
<b>4b</b>	OCH <sub>3</sub>	H	CH <sub>3</sub>	—	113.33 ± 18.50
<b>4c</b>	OCH <sub>3</sub>	OCH <sub>3</sub>	CH <sub>3</sub>	—	55.48 ± 3.82
<b>4d</b>	PhCH <sub>2</sub> O	H	CH <sub>3</sub>	1.03	1.03 ± 0.13
<b>8a</b>	CH <sub>3</sub>	H	PhCH <sub>2</sub>	1.49	2063 ± 412
<b>8b</b>	OCH <sub>3</sub>	H	PhCH <sub>2</sub>	1.29	349.24 ± 37.00
<b>8c</b>	OCH <sub>3</sub>	OCH <sub>3</sub>	PhCH <sub>2</sub>	1.30	81.03 ± 4.65
<b>Azalanstat</b>	—	—	—	—	5.30 ± 0.40

<sup>a</sup>*In-silico* average calculated activity for the virtually evaluated compounds (*K<sub>i</sub>* from docking and IC<sub>50</sub> from QSAR). <sup>b</sup>Data are shown as IC<sub>50</sub> values in μM ± standard deviation (SD) and are the mean of triplicate experiments. <sup>c</sup>Data taken from ref. [33].

Looking at the poses inside the HO-1 from the docking calculation (Figures S17–19), is it possible to classify the poses of the compounds in three different clusters accordingly with their structures. Molecules **1** and **4d** are part of the first, molecules **4a–c** are part of the second, and molecules **8a–c** are part of the third. The *N*-unsubstituted compound **1** showed

a low IC<sub>50</sub> value of 89.6 μM. The insertion of a substituent to the nitrogen atom of the indole ring brought to compounds **4a–d** and **8a–c**. As a general trend, the *N*-methyl-1*H*-indole-2-carboxamides **4a–d** displayed better IC<sub>50</sub> values when compared to their *N*-benzyl derivatives **8a–c**. All the molecules of the second cluster can be correctly allocated inside the binding pocket. However, any of them is able to reach strong stabilizing interaction resulting in binders weaker than molecule **4d**. In the third cluster, the presence of the benzyl group in the nitrogen of the central core produces a series of bulkier compounds where the benzyl is not reaching any relevant interaction inside the pocket. From the obtained results, it is possible to speculate that the nature of the substituent on the indole ring plays an important role in the inhibitory potency of the novel compounds. Indeed, a small electron-donating substituent as the methyl group in the 5 position brought the worst results for both the *N*-methyl and the *N*-benzyl substituted compounds (367.31 μM for compound **4a** and 2063 μM for compound **8a**). The introduction of a methoxy group in the 5 position on the indole ring slightly ameliorated the IC<sub>50</sub> values when compared to the 5-methyl derivatives from 3- to 6-fold (compare **4b** vs. **4a** and **8b** vs. **8a**, respectively), even if the IC<sub>50</sub> values were higher than 100 μM. An additional methoxy group in position 6 on the indole ring afforded compounds **4c** and **8c**, which were 2- and 4-fold more potent than **4b** and **4c**, respectively. Methylation of the nitrogen atom of the indole ring of compound **1** led to the most potent compound of the series (compound **4d**), which displayed an IC<sub>50</sub> value of 1.03 μM and was 87-fold more potent than its parent compound **1**. Molecules of the first docking cluster allocate their benzyl substituent in the far western pocket, whereas the indole at the central core could be flipped in two different ways that apparently are responsible for the difference in potency of the two compounds. When no substituent is present on the nitrogen of the indole, the hydrogen is pointing out the binding pocket; differently, when a methyl group is present, this is allocated in a different way inside the pocket, increasing the hydrophobic interaction and stabilizing the molecule, resulting in a better inhibitor activity of molecule **4d**.

### 3. Conclusions

In this paper, we reported a computer-aided fragment-based ligand joining experiment inside the binding pocket of the HO-1 starting from the imidazole of the eastern region and a benzyl group located far in the western region of the HO-1 pocket. The two structures were then virtually joined, and 1000 new compounds were generated and evaluated by docking

calculation and scoring after alignment in our previously published 3D QSAR model. Five compounds were selected among the 50 best-scored compounds by fingerprint similarity analysis and synthesized along with the other three compounds. The measured IC<sub>50</sub> against HO-1 confirmed the molecules' activity, and molecules with the methyl substituent at the nitrogen atom of the indole were generally more potent than benzyl substituted compounds. Moreover, molecule **4d** showed an IC<sub>50</sub> in the low micromolar range as predicted by the calculation. Considering the success of this approach, we will extend this work by synthesizing other of the most potent derivatives found out by the virtual joining experiments. We will also use other fragment-based computer-aided experiments to individuate other hit compounds.

## 4. Experimental

### 4.1. Chemistry

Materials and chemicals were purchased from Fisher scientific (Waltham, Massachusetts, USA), Merck (Kenilworth, NJ, USA), CEM corporation (Charlotte, NC, USA), as reagent grade or better, and were used with no further manipulation. Solvents and NMR solvents were purchased from Fisher Scientific, Merck, and VWR (Radnor, Pennsylvania, USA). Microwave-assisted reactions were performed using a CEM Discover instrument in closed Pyrex glass tubes (ca. 10 mL) with Teflon-coated septa. Reactions were monitored on TLC aluminum sheets coated with silica gel (60 F254, Merck, Kenilworth, NJ, USA) and visualized by UV ( $\lambda = 254$  and  $366$  nm) and iodine vapors. Compounds were purified by flash chromatography employing Merck silica gel (60, 0.040–0.063 mm, 230–400 mesh) as stationary phase and using glass columns. Infrared spectra were recorded on a Perkin Elmer 281 FTIR spectrometer using KBr disks or NaCl plates. <sup>1</sup>H- and <sup>13</sup>C-NMR spectra were determined with Varian Unity Inova 200 and 500 MHz instruments in CDCl<sub>3</sub> or DMSO-*d*<sub>6</sub> solution. Chemical shifts are given in ppm values, using tetramethylsilane (TMS) as the internal standard; coupling constants (*J*) are given in Hz. Signal multiplicities are characterized as s (singlet), d (doublet), t (triplet), q (quartet), p (pentet), m (multiplet), br (broad). Melting points were determined in an IA9200 Electrothermal apparatus equipped with a digital thermometer in capillary glass tubes and are uncorrected. Elemental analyses (C, H, N) were executed on a Carlo Erba Elemental Analyzer Mod. 1108; purity of compounds was  $\geq 95\%$ , and results were within  $\pm 0.4\%$  of the theoretical values.

#### 4.1.1. Synthesis of *N*-(3-(1*H*-imidazol-1-yl)propyl)-5-(benzyloxy)-1*H*-indole-2-carboxamide (**1**)

In a round bottom flask, 5-(benzyloxy)-1*H*-indole-2-carboxylic acid (0,374 mmol, 1 eq.) and 1,1'-carbonyldiimidazole (0,374 mmol, 1 eq.) were dissolved in anhydrous THF (2 mL) and stirred at room temperature for 2 hours. Then, 3-(1*H*-imidazol-1-yl)propan-1-amine (0,374 mmol, 1 eq.) was added and the obtained suspension was stirred at room temperature for 22 hours and refluxed for 90 minutes. After this time, 200  $\mu$ L of deionized H<sub>2</sub>O were added to the suspension, which turned in a bright yellow solution. The mixture was refluxed for 1 hour and then cooled to room temperature. The reaction solvent was removed under reduced pressure and to the residue were added CH<sub>2</sub>Cl<sub>2</sub> and NaOH 1M. The two phases were separated; the organic phase was washed three times with deionized H<sub>2</sub>O and then dried with anhydrous Na<sub>2</sub>SO<sub>4</sub>, filtered and concentrated. The obtained yellow solid was triturated with diethylether and filtered under vacuum, giving the pure desired product as a pale yellow solid (12%): mp 204–206 °C; IR (KBr) cm<sup>-1</sup> 3446 (br), 3281, 3104, 2946, 1622, 1557, 1508, 1445, 1430, 1388, 1330, 1231, 1180, 1116, 1079, 1013, 916, 846, 820, 745, 696, 660; <sup>1</sup>H NMR (500 MHz, DMSO-*d*<sub>6</sub>):  $\delta$  11.34 (s, 1H, NH), 8.48 (t, *J* = 5,5 Hz, 1H, CONH), 7.74 (s, 1H, imidazole), 7.44 (d, *J* = 7.5 Hz, 2H, aromatic), 7.39–7.29 (m, 4H, aromatic), 7.23 (s, 1H, imidazole), 7.15 (s, 1H, aromatic), 6.99 (s, 1H, aromatic), 6.93–6.90 (m, 2H, aromatic + imidazole), 5.07 (s, 2H, PhCH<sub>2</sub>O), 4.03 (t, *J* = 7.0 Hz, 2H, CH<sub>2</sub>-imidazole), 3.24 (dt, *J* = 5.4, 6.5 Hz, 2H, CH<sub>2</sub>NH), 1.96 (p, *J* = 7.0 Hz, 2H, CH<sub>2</sub>CH<sub>2</sub>CH<sub>2</sub>); <sup>13</sup>C NMR (125 MHz, DMSO-*d*<sub>6</sub>):  $\delta$  161.67, 153.01, 137.83, 132.27, 132.12, 128.72, 128.10, 128.02, 127.94, 127.65, 119.93, 115.36, 113.51, 103.99, 102.64, 69.99, 44.27, 36.38, 31.04. Anal. calcd for: C<sub>22</sub>H<sub>22</sub>N<sub>4</sub>O<sub>2</sub>: C, 70.57; H, 5.92; N, 14.96. Found: C, 70.48; H, 5.91; N, 14.99.

#### 4.1.2. General procedure for the synthesis of substituted 1-methyl-1*H*-indole methyl esters (**2a–d**)

In a round bottom flask, the proper commercial indole (1 mmol, 1 eq.) and K<sub>2</sub>CO<sub>3</sub> (6 mmol, 6 eq.) were suspended in 5 mL of anhydrous DMF. CH<sub>3</sub>I (6 mmol, 6 eq.) was dropped to the suspension, and the mixture was stirred at room temperature for 48 hours. The mixture was diluted with 50 mL of deionized H<sub>2</sub>O and extracted with EtOAc (3×25 mL). The organic phase was dried with anhydrous Na<sub>2</sub>SO<sub>4</sub>, filtered and concentrated under reduced pressure. The residue was purified by flash chromatography eluting with a gradient mixture of cyclohexane/EtOAc. According to this procedure, the following products were obtained.

#### 4.1.2.1. Methyl 1,5-dimethyl-1H-indole-2-carboxylate (**2a**)

White solid (92%): mp 72.5–73.5 °C; IR (KBr)  $\text{cm}^{-1}$  1715, 1523, 1471, 1450, 1399, 1224, 1137, 1089, 798, 764, 740;  $^1\text{H}$  NMR (500 MHz, DMSO- $d_6$ ):  $\delta$  7.48–7.45 (m, 2H, aromatic), 7.19–7.16 (m, 2H, aromatic), 3.99 (s, 3H, NCH<sub>3</sub>), 3.84 (s, 3H, COOCH<sub>3</sub>), 2.38 (s, 3H, CH<sub>3</sub>). Anal. calcd for: C<sub>12</sub>H<sub>13</sub>NO<sub>2</sub>: C, 70.92; H, 6.45; N, 6.89. Found: C, 70.86; H, 6.43; N, 6.90.

#### 4.1.2.2. Methyl 5-methoxy-1-methyl-1H-indole-2-carboxylate (**2b**)

White solid (77%): mp 123–125 °C; IR (KBr)  $\text{cm}^{-1}$  3399 (br), 2955, 1706, 1519, 1474, 1430, 1220, 1141, 1089, 1025, 843, 799, 762, 736;  $^1\text{H}$  NMR (500 MHz, DMSO- $d_6$ ):  $\delta$  7.50 (d,  $J = 9.0$  Hz, 1H, aromatic), 7.17–7.13 (m, 2H, aromatic), 7.00 (dd,  $J = 9.0, 2.5$  Hz, 1H, aromatic), 3.99 (s, 3H, NCH<sub>3</sub>), 3.84 (s, 3H, OCH<sub>3</sub>), 3.77 (s, 3H, COOCH<sub>3</sub>). Anal. calcd for: C<sub>12</sub>H<sub>13</sub>NO<sub>3</sub>: C, 65.74; H, 5.98; N, 6.39. Found: C, 65.87; H, 5.99; N, 6.37.

#### 4.1.2.3. Methyl 5,6-dimethoxy-1-methyl-1H-indole-2-carboxylate (**2c**)

Pale yellow solid (95%): mp 118–120 °C; IR (KBr)  $\text{cm}^{-1}$  2996, 2958, 1703, 1628, 1516, 1474, 1448, 1350, 1223, 1141, 1089, 1007, 846, 799, 760;  $^1\text{H}$  NMR (500 MHz, DMSO- $d_6$ ):  $\delta$  7.13 (s, 1H, aromatic), 7.11 (s, 1H, aromatic), 7.08 (s, 1H, aromatic), 3.99 (s, 3H, NCH<sub>3</sub>), 3.86 (s, 3H, 5-OCH<sub>3</sub>), 3.81 (s, 3H, 6-OCH<sub>3</sub>), 3.77 (s, 3H, COOCH<sub>3</sub>). Anal. calcd for: C<sub>13</sub>H<sub>15</sub>NO<sub>4</sub>: C, 62.64; H, 6.07; N, 5.62. Found: C, 62.73; H, 6.06; N, 5.63.

#### 4.1.2.4. Methyl 5-(benzyloxy)-1-methyl-1H-indole-2-carboxylate (**2d**)

White solid (89%): mp 134–135 °C; IR (KBr)  $\text{cm}^{-1}$  3397 (br), 2956, 2907, 1716, 1516, 1466, 1436, 1386, 1296, 1256, 1226, 1200, 1148, 1090, 1012, 852, 803;  $^1\text{H}$  NMR (200 MHz, DMSO- $d_6$ ):  $\delta$  7.55–7.32 (m, 6H, aromatic), 7.24 (d,  $J = 2.2$  Hz, 1H, aromatic), 7.16 (s, 1H, aromatic), 7.08 (dd,  $J = 9.0, 2.4$  Hz, 1H, aromatic), 5.11 (s, 2H, OCH<sub>2</sub>), 4.00 (s, 3H, NCH<sub>3</sub>), 3.84 (s, 3H, COOCH<sub>3</sub>). Anal. calcd for: C<sub>18</sub>H<sub>17</sub>NO<sub>3</sub>: C, 73.20; H, 5.80; N, 4.74. Found: C, 73.07; H, 5.81; N, 4.73.

#### 4.1.3. General procedure for the synthesis of *N*-substituted 1H-indole-2-carboxylic acids (**3a–d**, **7a–c**)

In a sealed-Pyrex tube equipped with a magnetic stirrer, the proper carboxylic acid (**2a–d**, **6a–c**) (1 eq.) and LiOH monohydrate (2 eq.) were suspended in a mixture of THF/H<sub>2</sub>O/CH<sub>3</sub>OH (3:1.5:1 ratio). The reaction was stirred under microwave irradiation (150 psi, 150 W, 100 °C) for 90 min. The reaction solvents were removed under reduced pressure, and to the residue was added HCl 1M. The suspension was stirred at room temperature for



30 min. The solid was filtered under reduced pressure and repeatedly washed with deionized H<sub>2</sub>O, affording the pure products that needed no further purification. According to this procedure, the following products were obtained.

#### 4.1.3.1. 1,5-dimethyl-1H-indole-2-carboxylic acid (**3a**)

The title compound was obtained using 0.81 mmol of compound **2a** and 1,62 mmol of LiOH monohydrate in a mixture of THF (1.8 mL), H<sub>2</sub>O (904  $\mu$ L) and CH<sub>3</sub>OH (602  $\mu$ L). White solid (85%): mp 219 °C; IR (KBr) cm<sup>-1</sup> 2918, 1679, 1528, 1474, 1414, 1273, 1235, 1134, 910, 882, 785; <sup>1</sup>H NMR (500 MHz, DMSO-*d*<sub>6</sub>):  $\delta$  7.45–7.42 (m, 2H, aromatic), 7.16–7.14 (m, 1H, aromatic), 7.09 (br s, 1H, aromatic), 3.99 (s, 3H, NCH<sub>3</sub>), 2.38 (s, 3H, CH<sub>3</sub>). Anal. calcd for: C<sub>11</sub>H<sub>11</sub>NO<sub>2</sub>: C, 69.83; H, 5.86; N, 7.40. Found: C, 69.98; H, 5.85; N, 7.41.

#### 4.1.3.2. 5-methoxy-1-methyl-1H-indole-2-carboxylic acid (**3b**)

The title compound was obtained using 0.72 mmol of compound **2b** and 1,44 mmol of LiOH monohydrate in a mixture of THF (1.6 mL), H<sub>2</sub>O (818  $\mu$ L) and CH<sub>3</sub>OH (602  $\mu$ L). White solid (88%): mp 217 °C; IR (KBr) cm<sup>-1</sup> 3448, 2959, 1687, 1519, 1472, 1266, 1231, 1217, 1142, 1027, 846, 800; <sup>1</sup>H NMR (500 MHz, DMSO-*d*<sub>6</sub>):  $\delta$  7.47 (d, *J* = 9.0 Hz, 1H, aromatic), 7.14–7.12 (m, 2H, aromatic), 6.98 (dd, *J* = 9.0, 2.0 Hz, 1H, aromatic), 3.99 (s, 3H, NCH<sub>3</sub>), 3.77 (s, 3H, OCH<sub>3</sub>). Anal. calcd for: C<sub>11</sub>H<sub>11</sub>NO<sub>3</sub>: C, 64.38; H, 5.40; N, 6.83. Found: C, 64.44; H, 5.39; N, 6.85.

#### 4.1.3.3. 5,6-dimethoxy-1-methyl-1H-indole-2-carboxylic acid (**3c**)

The title compound was obtained using 0.80 mmol of compound **2c** and 1,6 mmol of LiOH monohydrate in a mixture of THF (1.6 mL), H<sub>2</sub>O (904  $\mu$ L) and CH<sub>3</sub>OH (545  $\mu$ L). White solid (quantitative): mp 210 °C; IR (KBr) cm<sup>-1</sup> 3538, 3489, 2947, 1683, 1636, 1519, 1476, 1231, 1143, 1095, 1003, 858, 803, 768; <sup>1</sup>H NMR (500 MHz, DMSO-*d*<sub>6</sub>):  $\delta$  7.10–7.06 (m, 3H, aromatic), 3.98 (s, 3H, NCH<sub>3</sub>), 3.86 (s, 3H, 5-OCH<sub>3</sub>), 3.77 (s, 3H, 6-OCH<sub>3</sub>). Anal. calcd for: C<sub>12</sub>H<sub>13</sub>NO<sub>4</sub>: C, 61.27; H, 5.57; N, 5.95. Found: C, 61.38; H, 5.55; N, 5.94.

#### 4.1.3.4. 5-(benzyloxy)-1-methyl-1H-indole-2-carboxylic acid (**3d**)

The title compound was obtained using 0.64 mmol of compound **2d** and 1,28 mmol of LiOH monohydrate in a mixture of THF (1.36 mL), H<sub>2</sub>O (682  $\mu$ L) and CH<sub>3</sub>OH (454  $\mu$ L). White solid (96%): mp > 300 °C (dec.); IR (KBr) cm<sup>-1</sup> 3500, 2952, 1700, 1524, 1478, 1428, 1380, 1296, 1207, 1132, 1083, 806; <sup>1</sup>H NMR (200 MHz, DMSO-*d*<sub>6</sub>):  $\delta$  7.50–7.28 (m, 6H, aromatic), 7.11 (d, *J* = 2.0 Hz, 1H, aromatic), 6.87 (dd, *J* = 9.0, 2.0 Hz, 1H, aromatic), 6.71

(s, 1H, aromatic), 5.08 (s, 2H, PhCH<sub>2</sub>O), 4.01 (s, 3H, NCH<sub>3</sub>). Anal. calcd for: C<sub>17</sub>H<sub>15</sub>NO<sub>3</sub>: C, 72.58; H, 5.37; N, 4.98. Found: C, 72.41; H, 5.36; N, 4.99.

#### 4.1.3.5. 1-benzyl-5-methyl-1H-indole-2-carboxylic acid (**7a**)

The title compound was obtained using 0.655 mmol of compound **6a** and 1.31 mmol of LiOH monohydrate in a mixture of THF (1.6 mL), H<sub>2</sub>O (818 μL) and CH<sub>3</sub>OH (545 μL). White solid (81%): mp 198–199 °C; IR (KBr) cm<sup>-1</sup> 3447, 1670, 1531, 1465, 1453, 1426, 1277, 1216, 1127, 903, 791, 736; <sup>1</sup>H NMR (200 MHz, DMSO-*d*<sub>6</sub>): δ 7.47–6.98 (m, 9H, aromatic), 5.85 (s, 2H, PhCH<sub>2</sub>), 2.36 (s, 3H, CH<sub>3</sub>). Anal. calcd for: C<sub>17</sub>H<sub>15</sub>NO<sub>2</sub>: C, 76.96; H, 5.70; N, 5.28. Found: C, 77.12; H, 5.69; N, 5.29.

#### 4.1.3.6. 1-benzyl-5-methoxy-1H-indole-2-carboxylic acid (**7b**)

The title compound was obtained using 0.64 mmol of compound **6b** and 1.28 mmol of LiOH monohydrate in a mixture of THF (1.36 mL), H<sub>2</sub>O (682 μL) and CH<sub>3</sub>OH (454 μL). White solid (80%): mp 174–175 °C; IR (KBr) cm<sup>-1</sup> 3506 (br), 1664, 1519, 1458, 1421, 1266, 1219, 1172, 1032, 708; <sup>1</sup>H NMR (500 MHz, CDCl<sub>3</sub>): δ 7.43 (s, 1H, aromatic), 7.27–7.20 (m, 4H, aromatic), 7.10 (d, *J* = 2.5 Hz, 1H, aromatic), 7.04 (d, *J* = 9.0 Hz, 2H, aromatic), 7.00 (dd, *J* = 9.0, 2.5 Hz, 1H, aromatic), 5.81 (s, 2H, PhCH<sub>2</sub>O), 3.85 (s, 3H, OCH<sub>3</sub>). Anal. calcd for: C<sub>17</sub>H<sub>15</sub>NO<sub>3</sub>: C, 72.58; H, 5.37; N, 4.98. Found: C, 72.70; H, 5.39; N, 4.97.

#### 4.1.3.7. 1-benzyl-5,6-dimethoxy-1H-indole-2-carboxylic acid (**7c**)

The title compound was obtained using 0.133 mmol of compound **6c** and 0.266 mmol of LiOH monohydrate in a mixture of THF (0.327 μL), H<sub>2</sub>O (167 μL) and CH<sub>3</sub>OH (111 μL). White solid (79%): mp 188 °C; IR (KBr) cm<sup>-1</sup> 3457, 1652, 1520, 1493, 1455, 1250, 1216, 1158, 1011; <sup>1</sup>H NMR (200 MHz, CDCl<sub>3</sub>): δ 7.42 (s, 1H, aromatic), 7.28–7.24 (m, 3H, aromatic), 7.07–7.03 (m, 3H, aromatic), 6.69 (s, 1H, aromatic), 5.81 (s, 2H, PhCH<sub>2</sub>O), 3.93 (s, 3H, 5-OCH<sub>3</sub>), 3.86 (s, 3H, 6-OCH<sub>3</sub>). Anal. calcd for: C<sub>18</sub>H<sub>17</sub>NO<sub>4</sub>: C, 69.44; H, 5.50; N, 4.50. Found: C, 69.32; H, 5.51; N, 4.51.

#### 4.1.4. General procedure for the synthesis of *N*-substituted 1H-indole-2-carboxamides (**4a–d**, **8a–c**)

In a flame dried two-necked round bottom flask, the appropriate carboxylic acid (**3a–d**, **7a–c**, 1 eq.) was dissolved in anhydrous DMF in an argon atmosphere. The obtained solution was cooled to 0 °C with an ice bath. EDC hydrochloride (1.5 eq.) was added and the reaction was stirred for 15 minutes. After this time, HOBt (1.5 eq.) was added and the mixture was stirred for further 15 minutes. Finally, 3-(1H-imidazol-1-yl)propan-1-amine (2 eq.) was

added to the solution, and the reaction was slowly warmed at room temperature and left to react for 24 hours under an argon atmosphere. The mixture was concentrated, diluted with an aqueous solution of NaHCO<sub>3</sub> 5%, and extracted three times with EtOAc. The organic phases were dried with anhydrous Na<sub>2</sub>SO<sub>4</sub>, filtered, and concentrated. The crude was purified by flash chromatography eluting with a gradient mixture of CH<sub>2</sub>Cl<sub>2</sub>/CH<sub>3</sub>OH. According to this procedure, the following products were obtained.

#### 4.1.4.1. *N*-(3-(1*H*-imidazol-1-yl)propyl)-1,5-dimethyl-1*H*-indole-2-carboxamide (**4a**)

The title compound was obtained using 0.57 mmol of compound **3a**, 0.78 mmol of EDC hydrochloride, 0.78 mmol of HOBt, and 1.04 mmol of 3-(1*H*-imidazol-1-yl)propan-1-amine in 5 mL of anhydrous DMF. Whitish solid (75%): mp 102–103 °C; IR (KBr) cm<sup>-1</sup> 3447 (br), 3218, 2934, 1645, 1552, 1515, 1466, 1394, 1305, 1270, 1230, 1086; 812, 745; <sup>1</sup>H NMR (500 MHz, DMSO-*d*<sub>6</sub>): δ 8.50 (t, *J* = 5.6 Hz, 1H, CONH), 7.67 (s, 1H, imidazole), 7.44–7.35 (m, 2H, aromatic), 7.21 (s, 1H, aromatic), 7.09 (dd, *J* = 8.6, 1H, aromatic), 6.96 (s, 1H, imidazole), 6.89 (s, 1H, imidazole), 4.03 (t, *J* = 6.9 Hz, 2H, CH<sub>2</sub>-imidazole), 3.92 (s, 3H, NCH<sub>3</sub>), 3.22 (dt, *J* = 5.7, 6.5 Hz, 2H, CONHCH<sub>2</sub>), 2.37 (s, 3H, CH<sub>3</sub>), 1.96 (p, *J* = 6.9 Hz, 2H, CH<sub>2</sub>CH<sub>2</sub>CH<sub>2</sub>); <sup>13</sup>C NMR (125 MHz, DMSO-*d*<sub>6</sub>): δ 162.34, 137.52, 137.11, 132.28, 128.99, 128.44, 125.97, 125.52, 120.95, 119.63, 110.35, 103.88, 44.01, 36.26, 31.50, 30.89, 21.21. Anal. calcd for: C<sub>17</sub>H<sub>20</sub>N<sub>4</sub>O: C, 68.90; H, 6.80; N, 18.90. Found: C, 68.73; H, 6.81; N, 18.86.

#### 4.1.4.2. *N*-(3-(1*H*-imidazol-1-yl)propyl)-5-methoxy-1-methyl-1*H*-indole-2-carboxamide (**4b**)

The title compound was obtained using 0.652 mmol of compound **3b**, 0.978 mmol of EDC hydrochloride, 0.978 mmol of HOBt, and 1.304 mmol of 3-(1*H*-imidazol-1-yl)propan-1-amine in 5 mL of anhydrous DMF. Pale yellow solid (54%): mp 121–122 °C; IR (KBr) cm<sup>-1</sup> 3286, 2938, 1633, 1545, 1509, 1470, 1457, 1397, 1274, 1219, 1024, 840, 804; <sup>1</sup>H NMR (500 MHz, DMSO-*d*<sub>6</sub>): δ 8.49 (t, *J* = 5.5 Hz, 1H, CONH), 7.67 (s, 1H, imidazole), 7.42 (d, *J* = 9.0 Hz, 1H, aromatic), 7.22 (s, 1H, aromatic), 7.10 (d, *J* = 2.0 Hz, 1H, aromatic), 6.98 (s, 1H, imidazole), 6.93–6.90 (m, 2H, aromatic + imidazole), 4.04 (t, *J* = 7.0 Hz, 2H, CH<sub>2</sub>-imidazole), 3.94 (s, 3H, NCH<sub>3</sub>), 3.77 (s, 3H, OCH<sub>3</sub>), 3.23 (dt, *J* = 5.6, 6.5 Hz, 2H, CONHCH<sub>2</sub>), 1.97 (p, *J* = 7.0 Hz, 2H, CH<sub>2</sub>CH<sub>2</sub>CH<sub>2</sub>); <sup>13</sup>C NMR (125 MHz, DMSO-*d*<sub>6</sub>): δ 162.20, 154.16, 137.47, 133.94, 132.52, 128.40, 126.00, 119.57, 114.48, 111.47, 103.93,

102.32, 55.49, 43.96, 36.22, 31.54, 30.86. Anal. calcd for: C<sub>17</sub>H<sub>20</sub>N<sub>4</sub>O<sub>2</sub>: C, 65.37; H, 6.45; N, 17.94. Found: C, 65.29; H, 6.46; N, 17.99.

4.1.4.3. *N*-(3-(1*H*-imidazol-1-yl)propyl)-5,6-dimethoxy-1-methyl-1*H*-indole-2-carboxamide (**4c**)

The title compound was obtained using 0.703 mmol of compound **3c**, 1.055 mmol of EDC hydrochloride, 1.055 mmol of HOBt, and 1.406 mmol of 3-(1*H*-imidazol-1-yl)propan-1-amine in 5 mL of anhydrous DMF. Pale yellow solid (71%): mp 146–147 °C; IR (KBr) cm<sup>-1</sup> 3228, 2942, 1649, 1624, 1540, 1508, 1473, 1395, 1246, 1215, 1094, 1001, 840, 813; <sup>1</sup>H NMR (500 MHz, DMSO-*d*<sub>6</sub>): δ 8.35 (t, *J* = 5.5 Hz, 1H, CONH), 7.68 (s, 1H, imidazole), 7.22 (s, 1H, imidazole), 7.09 (s, 1H, aromatic), 7.04 (s, 1H, aromatic), 6.97 (s, 1H, aromatic), 6.91 (s, 1H, imidazole), 4.03 (t, *J* = 7.0 Hz, 2H, CH<sub>2</sub>-imidazole), 3.95 (s, 3H, NCH<sub>3</sub>), 3.84 (s, 3H, 5-OCH<sub>3</sub>), 3.77 (s, 3H, 6-OCH<sub>3</sub>), 3.22 (dt, *J* = 5.6, 6.5 Hz, 2H, CONHCH<sub>2</sub>), 1.96 (p, *J* = 7.0 Hz, 2H, CH<sub>2</sub>CH<sub>2</sub>CH<sub>2</sub>); <sup>13</sup>C NMR (125 MHz, DMSO-*d*<sub>6</sub>): δ 162.35, 148.70, 145.62, 137.53, 133.78, 130.38, 128.41, 119.66, 118.30, 104.58, 102.82, 93.54, 55.98, 55.90, 44.05, 36.20, 31.73, 30.99. Anal. calcd for: C<sub>18</sub>H<sub>22</sub>N<sub>4</sub>O<sub>3</sub>: C, 63.14; H, 6.48; N, 16.36. Found: C, 63.23; H, 6.49; N, 16.31.

4.1.4.4. *N*-(3-(1*H*-imidazol-1-yl)propyl)-5-(benzyloxy)-1-methyl-1*H*-indole-2-carboxamide (**4d**)

The title compound was obtained using 0.355 mmol of compound **3d**, 0.533 mmol of EDC hydrochloride, 0.533 mmol of HOBt, and 0.71 mmol of 3-(1*H*-imidazol-1-yl)propan-1-amine in 5 mL of anhydrous DMF. White solid (87%): mp 174–175 °C; IR (KBr) cm<sup>-1</sup> 3194, 1635, 1551, 1506, 1452, 1388, 1269, 1235, 1200, 1161, 1101, 1072, 1013, 845, 751, 707; <sup>1</sup>H NMR (500 MHz, DMSO-*d*<sub>6</sub>): δ 8.48 (t, *J* = 5.7 Hz, 1H, CONH), 7.66 (s, 1H, imidazole), 7.48–7.36 (m, 5H, aromatic), 7.34–7.29 (m, 1H, aromatic), 7.22–7.20 (m, 1H, aromatic), 7.19 (d, *J* = 2.4 Hz, 1H, imidazole), 7.01–6.98 (m, 1H, aromatic), 6.97–6.96 (m, 1H, aromatic), 6.90–6.89 (m, 1H, imidazole), 5.11 (s, 2H, PhCH<sub>2</sub>O), 4.03 (t, *J* = 6.9 Hz, 2H, CH<sub>2</sub>-imidazole), 3.93 (s, 3H, NCH<sub>3</sub>), 3.22 (dt, *J* = 5.7, 6.5 Hz, 2H, CONHCH<sub>2</sub>), 1.96 (p, *J* = 6.9 Hz, 2H, CH<sub>2</sub>CH<sub>2</sub>CH<sub>2</sub>); <sup>13</sup>C NMR (125 MHz, DMSO-*d*<sub>6</sub>): δ 162.03, 153.02, 137.57, 133.97, 132.54, 128.42, 128.39, 127.72, 127.70, 125.85, 119.43, 114.92, 111.41, 103.91, 103.85, 69.77, 43.83, 36.12, 31.45, 30.80. Anal. calcd for: C<sub>23</sub>H<sub>24</sub>N<sub>4</sub>O<sub>2</sub>: C, 71.11; H, 6.23; N, 14.42. Found: C, 70.98; H, 6.22; N, 14.45.

4.1.4.5. *N*-(3-(1*H*-imidazol-1-yl)propyl)-1-benzyl-5-methyl-1*H*-indole-2-carboxamide (**8a**)

The title compound was obtained using 0.291 mmol of compound **7a**, 0.437 mmol of EDC hydrochloride, 0.437 mmol of HOBt, and 0.582 mmol of 3-(1*H*-imidazol-1-yl)propan-1-amine in 2.5 mL of anhydrous DMF. White solid (72%): mp 178–179 °C; IR (KBr)  $\text{cm}^{-1}$  3448 (br), 3198, 2923, 1654, 1560, 1506, 1456, 1352, 1302, 1278, 1223, 1082, 917, 789;  $^1\text{H}$  NMR (500 MHz,  $\text{DMSO-}d_6$ ):  $\delta$  8.57 (t,  $J = 5.7$  Hz, 1H, CONH), 7.63 (s, 1H, imidazole), 7.41 (s, 1H, aromatic), 7.36 (d,  $J = 8.5$  Hz, 1H, aromatic), 7.24–7.13 (m, 4H), 7.04 (s, 1H, aromatic), 7.03–6.99 (m, 3H, aromatic + imidazole), 6.89 (s, 1H, imidazole), 5.79 (s, 2H,  $\text{PhCH}_2$ ), 3.94 (t,  $J = 6.9$  Hz, 2H,  $\text{CH}_2$ -imidazole), 3.19 (dt,  $J = 5.8, 6.5$  Hz, 2H,  $\text{CONHCH}_2$ ), 2.35 (s, 3H,  $\text{CH}_3$ ), 1.91 (p, 2H,  $J = 6.9$  Hz  $\text{CH}_2\text{CH}_2\text{CH}_2$ );  $^{13}\text{C}$  NMR (125 MHz,  $\text{DMSO-}d_6$ ):  $\delta$  162.42, 139.10, 136.71, 132.04, 129.40, 128.54, 128.35, 127.16, 126.66, 126.30, 125.79, 121.18, 119.67, 110.92, 104.87, 46.99, 43.95, 36.23, 30.87, 21.20. Anal. calcd for:  $\text{C}_{23}\text{H}_{24}\text{N}_4\text{O}$ : C, 74.17; H, 6.49; N, 15.04. Found: C, 73.99; H, 6.47; N, 15.08.

4.1.4.6. *N*-(3-(1*H*-imidazol-1-yl)propyl)-1-benzyl-5-methoxy-1*H*-indole-2-carboxamide (**8b**)

The title compound was obtained using 0.495 mmol of compound **7b**, 0.743 mmol of EDC hydrochloride, 0.743 mmol of HOBt, and 0.99 mmol of 3-(1*H*-imidazol-1-yl)propan-1-amine in 5 mL of anhydrous DMF. White solid (75%): mp 151–152 °C; IR (KBr)  $\text{cm}^{-1}$  3245, 2928, 1643, 1543, 1450, 1349, 1271, 1230, 1078, 1030, 795;  $^1\text{H}$  NMR (500 MHz,  $\text{DMSO-}d_6$ ):  $\delta$  8.57 (t,  $J = 5.7$  Hz, 1H, CONH), 7.61 (s, 1H, imidazole), 7.39 (d,  $J = 9.0$  Hz, 1H, aromatic), 7.24–7.19 (m, 2H, aromatic), 7.18–7.13 (m, 2H, aromatic + imidazole), 7.12 (d,  $J = 2.4$  Hz, 1H aromatic), 7.05 (s, 1H, aromatic), 7.04–7.01 (m, 2H, aromatic), 6.90–6.84 (m, 2H, aromatic + imidazole), 5.80 (s, 2H,  $\text{PhCH}_2$ ), 3.95 (t,  $J = 6.9$  Hz, 2H,  $\text{CH}_2$ -imidazole), 3.75 (s, 3H,  $\text{OCH}_3$ ), 3.20 (dt,  $J = 5.8, 6.5$  Hz, 2H,  $\text{CONHCH}_2$ ), 1.92 (p,  $J = 6.8$  Hz, 2H,  $\text{CH}_2\text{CH}_2\text{CH}_2$ );  $^{13}\text{C}$  NMR (125 MHz,  $\text{DMSO-}d_6$ ):  $\delta$  162.16, 154.26, 139.00, 137.37, 133.38, 132.23, 128.40, 127.01, 126.54, 126.31, 119.45, 114.58, 111.94, 104.81, 102.50, 55.44, 46.93, 43.76, 36.11, 30.80. Anal. calcd for:  $\text{C}_{23}\text{H}_{24}\text{N}_4\text{O}_2$ : C, 71.11; H, 6.23; N, 14.42. Found: C, 71.00; H, 6.22; N, 14.45.

4.1.4.7. *N*-(3-(1*H*-imidazol-1-yl)propyl)-1-benzyl-5,6-dimethoxy-1*H*-indole-2-carboxamide (**8c**)

The title compound was obtained using 0.104 mmol of compound **7c**, 0.156 mmol of EDC hydrochloride, 0.156 mmol of HOBt, and 0.208 mmol of 3-(1*H*-imidazol-1-yl)propan-1-amine in 1.5 mL of anhydrous DMF. White solid (46%): mp 110–111 °C; IR (KBr)  $\text{cm}^{-1}$

3422 (br), 3309, 1628, 1542, 1443, 1266, 1224, 1163, 1111, 844, 705;  $^1\text{H}$  NMR (500 MHz, DMSO- $d_6$ ):  $\delta$  8.41 (t,  $J = 6.0$  Hz, 1H, CONH), 7.61 (s, 1H, imidazole), 7.23–7.20 (m, 2H, aromatic), 7.17–7.14 (m, 2H, aromatic), 7.10 (s, 1H, imidazole), 7.05–7.02 (m, 4H, aromatic), 6.88 (s, 1H, imidazole), 5.81 (s, 2H, PhCH<sub>2</sub>), 3.93 (t,  $J = 6.5$  Hz, 2H, CH<sub>2</sub>-imidazole), 3.75 (s, 3H, 5-OCH<sub>3</sub>), 3.74 (s, 3H, 6-OCH<sub>3</sub>), 3.17 (dt,  $J = 6.1, 6.9$  Hz, 2H, CONHCH<sub>2</sub>), 1.90 (p,  $J = 6.5$  Hz, 2H, CH<sub>2</sub>CH<sub>2</sub>CH<sub>2</sub>);  $^{13}\text{C}$  NMR (125 MHz, DMSO- $d_6$ ):  $\delta$  162.29, 148.70, 145.74, 139.18, 137.44, 133.33, 130.11, 128.44, 128.40, 127.03, 126.69, 119.55, 118.61, 105.53, 102.94, 94.04, 55.95, 55.89, 46.92, 43.83, 36.06, 30.95. Anal. calcd for: C<sub>24</sub>H<sub>26</sub>N<sub>4</sub>O<sub>3</sub>: C, 68.88; H, 6.26; N, 13.39. Found: C, 69.01; H, 6.27; N, 13.35.

#### 4.1.5. General procedure for the synthesis of substituted 1H-indole ethyl esters (**5a–c**)

The proper commercial indole (1 mmol, 1 eq) was dissolved in 20 mL of EtOH. *p*-toluensulfonic acid (5 mmol, 5 eq) was added to the mixture and the solution was refluxed for 16 hours. After cooling to room temperature, the reaction solvent was removed under reduced pressure, a saturated solution of Na<sub>2</sub>CO<sub>3</sub> was added and the mixture extracted three times with CH<sub>2</sub>Cl<sub>2</sub>. The reunited organic phases were dried with Na<sub>2</sub>SO<sub>4</sub>, filtered and the solvent removed under vacuo. With the exception of compound **5c**, the obtained product did not require any purification. According to this procedure, the following products were obtained.

##### 4.1.5.1. Ethyl 5-methyl-1H-indole-2-carboxylate (**5a**)

Beige solid (53%): mp 158–159 °C; IR (KBr) cm<sup>-1</sup> 3327, 2940, 1686, 1533, 1380, 1331, 1255, 1211, 1023, 800, 773, 743, 669;  $^1\text{H}$  NMR (500 MHz, CDCl<sub>3</sub>):  $\delta$  8.81 (s, 1H, NH), 7.46 (s, 1H, aromatic), 7.31 (d,  $J = 8.5$  Hz, 1H, aromatic), 7.16 (d,  $J = 1.5$  Hz, 1H, aromatic), 7.14 (d,  $J = 1.5$  Hz, 1H, aromatic), 4.40 (q,  $J = 7.0$  Hz, 2H, CH<sub>2</sub>CH<sub>3</sub>), 2.44 (s, 3H, CH<sub>3</sub>), 1.41 (t,  $J = 7.0$  Hz, 3H, CH<sub>2</sub>CH<sub>3</sub>). Anal. calcd for: C<sub>12</sub>H<sub>13</sub>NO<sub>2</sub>: C, 70.92; H, 6.45; N, 6.89. Found: C, 70.79; H, 6.46; N, 6.87.

##### 4.1.5.2. Ethyl 5-methoxy-1H-indole-2-carboxylate (**5b**)

Light brownish solid (89%): mp 154–155 °C; IR (KBr) cm<sup>-1</sup> 3328, 1683, 1528, 1457, 1340, 1251, 1219, 1158, 1027, 858, 774;  $^1\text{H}$  NMR (500 MHz, DMSO- $d_6$ ):  $\delta$  11.72 (s, 1H, NH), 7.37–7.34 (m, 1H, aromatic), 7.10–7.05 (m, 2H, aromatic), 6.94–6.91 (m, 1H, aromatic), 4.34 (q,  $J = 7.0$  Hz, 2H, CH<sub>2</sub>CH<sub>3</sub>), 3.76 (s, 3H, OCH<sub>3</sub>), 1.34 (t,  $J = 7.0$  Hz, 3H, CH<sub>2</sub>CH<sub>3</sub>). Anal. calcd for: C<sub>12</sub>H<sub>13</sub>NO<sub>3</sub>: C, 65.74; H, 5.98; N, 6.39. Found: C, 65.61; H, 5.96; N, 6.41.

#### 4.1.5.3. Ethyl 5,6-dimethoxy-1H-indole-2-carboxylate (**5c**)

Purified by flash chromatography eluting with a mixture of cyclohexane/EtOAc (7:3). White solid (41%): mp 171–172 °C; IR (KBr)  $\text{cm}^{-1}$  3314, 2986, 1682, 1523, 1501, 1458, 1348, 1285, 1250, 1213, 1193, 1145, 1028, 1006, 843, 770;  $^1\text{H}$  NMR (500 MHz,  $\text{CDCl}_3$ ):  $\delta$  8.84 (s, 1H, NH), 7.12 (d,  $J = 2.0$  Hz, 1H, aromatic), 7.04 (s, 1H, aromatic), 6.85 (s, 1H, aromatic), 4.39 (q,  $J = 7.0$  Hz, 2H,  $\text{CH}_2\text{CH}_3$ ), 3.93 (s, 3H, 5-OCH<sub>3</sub>), 3.92 (s, 3H, 6-OCH<sub>3</sub>), 1.40 (t,  $J = 7.0$  Hz, 3H,  $\text{CH}_2\text{CH}_3$ ). Anal. calcd for:  $\text{C}_{13}\text{H}_{15}\text{NO}_4$ : C, 62.64; H, 6.07; N, 5.62. Found: C, 62.72; H, 6.06; N, 5.60.

#### 4.1.6. General procedure for the synthesis of substituted 1-benzyl-1H-indole ethyl esters (**6a–c**)

In a two-necked round bottom flask, NaH (oil dispersion 80%, 2 eq.) was added to 3 mL of anhydrous DMF under  $\text{N}_2$  and the suspension was cooled to 0 °C with an ice bath. The proper 1H-indole ethyl ester (1 eq.) was dissolved in 2 mL of anhydrous DMF and added dropwise via syringe to the stirring suspension and the reaction was warmed to room temperature. After 1 hour, benzyl bromide (2 eq.) was added dropwise and the mixture was stirred at room temperature for 3 hours. Then, the mixture was poured in crushed ice and extracted with EtOAc (3×35 mL). The reunited organic phases were washed with deionized  $\text{H}_2\text{O}$  (1×45 mL) and brine (1×45 mL). After drying with  $\text{Na}_2\text{SO}_4$ , filtering and removing the solvent under reduced pressure, the crude was purified by flash chromatography eluting with a gradient mixture of cyclohexane/EtOAc. According to this procedure, the following products were obtained.

##### 4.1.6.1. Ethyl 1-benzyl-5-methyl-1H-indole-2-carboxylate (**6a**)

The title compound was obtained using 0.59 mmol of compound **5a**, 1.18 mmol of NaH and 1.18 mmol of benzyl bromide. Pale yellow waxy solid (77%): mp 61–63 °C; IR (KBr)  $\text{cm}^{-1}$  2926, 1706, 1523, 1454, 1250, 1200, 1149, 1094, 1029, 867, 703;  $^1\text{H}$  NMR (200 MHz,  $\text{DMSO-}d_6$ ):  $\delta$  7.49–6.97 (m, 9H, aromatic), 5.83 (s, 2H,  $\text{PhCH}_2$ ), 4.27 (q,  $J = 7.0$  Hz, 2H,  $\text{CH}_2\text{CH}_3$ ), 2.37 (s, 3H,  $\text{CH}_3$ ), 1.28 (t,  $J = 7.0$  Hz, 3H,  $\text{CH}_2\text{CH}_3$ ). Anal. calcd for:  $\text{C}_{19}\text{H}_{19}\text{NO}_2$ : C, 77.79; H, 6.53; N, 4.77. Found: C, 77.92; H, 6.54; N, 4.76.

##### 4.1.6.2. Ethyl 1-benzyl-5-methoxy-1H-indole-2-carboxylate (**6b**)

The title compound was obtained using 0.655 mmol of compound **5b**, 1.31 mmol of NaH and 1.31 mmol of benzyl bromide. Pale yellow oil (95%): IR (NaCl)  $\text{cm}^{-1}$  3401 (br), 2982, 2933, 1704, 1624, 1520, 1454, 1419, 1251, 1213, 1094, 1030, 844, 801, 762, 736;  $^1\text{H}$

NMR (500 MHz, CDCl<sub>3</sub>):  $\delta$  7.29 (s, 1H, aromatic), 7.25–7.17 (m, 4H, aromatic), 7.09 (d,  $J$  = 2.5 Hz, 1H, aromatic), 7.04–7.01 (m, 2H, aromatic), 6.97 (dd,  $J$  = 9.0, 2.5 Hz, 1H, aromatic), 5.81 (s, 2H, PhCH<sub>2</sub>), 4.31 (q,  $J$  = 7.0 Hz, 2H, CH<sub>2</sub>CH<sub>3</sub>), 3.84 (s, 3H, OCH<sub>3</sub>), 1.34 (t,  $J$  = 7.0 Hz, 3H, CH<sub>2</sub>CH<sub>3</sub>). Anal. calcd for: C<sub>19</sub>H<sub>19</sub>NO<sub>3</sub>: C, 73.77; H, 6.19; N, 4.53. Found: C, 73.58; H, 6.20; N, 4.54.

#### 4.1.6.3. Ethyl 1-benzyl-5,6-dimethoxy-1H-indole-2-carboxylate (**6c**)

The title compound was obtained using 0.324 mmol of compound **5c**, 0.648 mmol of NaH and 0.648 mmol of benzyl bromide. Colorless oil (41%): IR (NaCl) cm<sup>-1</sup> 3534 (br), 2935, 1694, 1630, 1520, 1494, 1454, 1414, 1251, 1216, 1154, 1089, 1029, 846, 737, 703; <sup>1</sup>H NMR (200 MHz, CDCl<sub>3</sub>):  $\delta$  7.36–7.19 (m, 5H, aromatic), 7.06–7.01 (m, 3H, aromatic), 6.71 (s, 1H, aromatic), 5.80 (s, 2H, PhCH<sub>2</sub>), 4.29 (q,  $J$  = 7.0 Hz, 2H, CH<sub>2</sub>CH<sub>3</sub>), 3.92 (s, 3H, 5-OCH<sub>3</sub>), 3.85 (s, 3H, 6-OCH<sub>3</sub>), 1.33 (t,  $J$  = 7.0 Hz, 3H, CH<sub>2</sub>CH<sub>3</sub>). Anal. calcd for: C<sub>20</sub>H<sub>21</sub>NO<sub>4</sub>: C, 70.78; H, 6.24; N, 4.13. Found: C, 70.59; H, 6.23; N, 4.14.

## 4.2. Molecular modeling

Molecules' structures were built using Marvin Sketch with a protonation state calculated at neutral pH. The 2D molecules were initially subjected to a molecular mechanics energy minimization by the Merck molecular force field (MMFF94), then optimized at the semiempirical level employing the parameterized model number 3 (PM3) Hamiltonian as implemented in the MOPAC2016 package (Keywords used in MOPAC2016: PM3, MMOK, XYZ, BONDS, DDMIN=0, PRECISE, GNORM=0.01, CHECK) [43, 44]. The pairwise similarity was calculated using ECFP4/FCFP4 circular fingerprints using Forge 10.6.0 Revision: 36004 (Cresset Biomolecular Discovery Ltd.). Spark (v. 10.6.0, <https://www.cresset-group.com/products/spark/>) was used for the ligand growing experiments using Cresset's molecular field points (local extrema of the electrostatic, van der Waals, and the molecule's hydrophobic potentials) [45]. The 1000 molecules derived from the ligand growing experiments were generated using a database of 1589469 fragments (Fig. S20). Docking experiments were performed using AutoDock 4.2.6 in YASARA (GUI, v. 20.12.24) [46] using 3HOK (X-ray Crystal Structure of Human Heme Oxygenase-1 with (2*R*, 4*S*)-2-[2-(4-chlorophenyl)ethyl]-2-[(1*H*-imidazol-1-yl)methyl]-4[[[(5-trifluoromethylpyridin-2-yl)thio)methyl]-1,3-dioxolane) PDB code of the HO-1. AutoGrid (4.2.6) was used to generate the grid maps with a spacing of 0.375 Å and dimensions encompassing all atoms extending 5 Å from the surface of the PM3 minimized structure of



the crystallized ligand. All the parameters were inserted at their default settings. In the docking tab, the macromolecule and ligand are selected, and GA parameters are set as  $ga\_runs = 100$ ,  $ga\_pop\_size = 150$ ,  $ga\_num\_evals = 20000000$ ,  $ga\_num\_generations = 27000$ ,  $ga\_elitism = 1$ ,  $ga\_mutation\_rate = 0.02$ ,  $ga\_crossover\_rate = 0.8$ ,  $ga\_crossover\_mode = two\ points$ ,  $ga\_cauchy\_alpha = 0.0$ ,  $ga\_cauchy\_beta = 1.0$ , number of generations for picking worst individual = 10. The QSAR evaluation was achieved using Forge (v. 10.4.2) after alignment with the dataset in the 3D-QSAR model already published [37]. The field points of all the molecules evaluated in the QSAR model (negative, positive, shape, and hydrophobic) were calculated and generated using the XED (extended electron distribution) force field in Forge; then, the molecules were aligned with the training set of the QSAR model by a maximum common substructure algorithm using a customized and validated set-up [37, 47, 48]. All the specifications used for the conformation hunt and alignment are detailed in the supplementary material (Figures S21,22). The maximal number of conformations created for each molecule was set to 500. The root-mean-square deviation of atomic positions cutoff, which is the similarity threshold below which two conformers are assumed identical, was set to 0.5 Å. The gradient cutoff for conformer minimization was set to 0.1 kcal/mol. The energy window was set to 2.5 kcal/mol, and all the conformers with calculated energy outside the selected energy window were rejected.

### 4.3. Biology

#### 4.3.1. Preparation of Spleen Microsomal Fractions

Rat spleen microsomal fraction obtained by differential centrifugation, according to Ryter et al. [49], was used as source of the HO-1 protein. As reported in the literature [50], HO-1 is abundant in the rat spleen. We chose this source because it represents the most native (i.e., closest to *in vivo*) form of HO-1. The experiments reported in the present paper complied with current Italian law and met the guidelines of the Institutional Animal Care and Use Committee of the Ministry of Health (Directorate-General for Animal Health and Veterinary Medicines, Italy) “Dosing of enzymatic activities in rat microsomes” (2018–2022), project code 02769.N.VLY. We used male albino rats of strain Sprague-Dawley (150 g body weight and age 45 d) to obtain spleen microsomal fraction. Rats had free access to water and were kept at room temperature with a natural photoperiod (12 h light-12 h dark cycle). Each rat was sacrificed, and their spleens were pooled and then homogenized in 50 mM Tris buffer, pH 7.4, containing 0.25 M sucrose, using a Potter-Elvehjem homogenizing system with a Teflon pestle. Rat spleen homogenate was centrifuged at 10,000g for 20 min

at 4 °C, and the supernatant was centrifuged at 100,000g for 60 min at 4 °C. The 100,000g pellet (microsomes) was resuspended in 100 mM potassium phosphate buffer, pH 7.8, containing MgCl<sub>2</sub> 2 mM. After measuring its protein concentration, the microsomal fraction was aliquoted and stored at –80 °C for up to 2 months.

#### 4.3.2. Preparation of biliverdin reductase

Liver tissue was used to obtain biliverdin reductase. Liver tissue was homogenized on ice in 3 volumes of a solution 1.15% KCl w/v and Tris buffer 20 mM, pH 7.8. Rat liver homogenate was centrifuged at 10,000g for 20 min at 4 °C, and the supernatant was centrifuged at 100,000g for 1 h at 4 °C. The 100,000g supernatant was aliquoted and stored at –80 °C after its protein concentration was measured.

#### 4.3.3. Measurement of HO-1 enzymatic activity in the microsomal fraction of rat spleen

Determination of HO-1 activity has been performed by measuring the bilirubin formation using the difference in absorbance at 464–530 nm as described by Ryter et al. [49]. The incubation mixture contained in a final volume of 500 µL: 20 mM Tris–HCl, pH 7.4, (1 mg/mL) microsomal extract, 0.5–2 mg/mL biliverdin reductase, 1 mM NADPH, 2 mM glucose 6-phosphate (G6P), 1 U G6P dehydrogenase, 25 µM hemin, and 10 µL of DMSO (or the same volume of DMSO solution of test compounds to a final concentration of 100, 10, and 1 µM). Enzymatic reactions were carried out in the dark for 1 h at 37 °C in a circulating water bath. 500 µL of chloroform was used to stop the reaction. The amount of bilirubin formed was measured in the chloroform phase, with a double-beam spectrophotometer as OD<sub>464–530 nm</sub> (extinction coefficient, 40 mM/cm for bilirubin). The enzymatic activity was defined as Units (one Unit is the amount of enzyme catalyzing the formation of 1 nmol of bilirubin/mg protein/h).

### **Funding**

This research was founded by the University of Catania, Programma Ricerca di Ateneo Pia.Ce.Ri 2020–2022 linea 2, project number 57722172126.

**Institutional Review Board Statement:** The study was conducted according to the guidelines of the Declaration of Helsinki, and approved by project authorized by the Ministry of Health (Directorate General for Animal Health and Veterinary Medicines) “Dosing of enzymatic activities in rat microsomes” (2018–2022) (project code 02769.N.VLY).

**Conflicts of Interest:** The authors declare no conflict of interest.

## REFERENCES

- [1] Mattiuzzi, C.; Lippi, G., Current Cancer Epidemiology. *J. Epidemiol. Glob. Health* **2019**, *9* (4), 217–222.
- [2] Bedard, P. L.; Hyman, D. M.; Davids, M. S.; Siu, L. L., Small molecules, big impact: 20 years of targeted therapy in oncology. *Lancet* **2020**, *395* (10229), 1078–1088.
- [3] Chau, L. Y., Heme oxygenase-1: Emerging target of cancer therapy. *J. Biomed. Sci.* **2015**, *22* (1), 22.
- [4] Na, H. K.; Surh, Y. J., Oncogenic potential of Nrf2 and its principal target protein heme oxygenase-1. *Free Radic. Biol. Med.* **2014**, *67*, 353–365.
- [5] Furfaro, A. L.; Traverso, N.; Domenicotti, C.; Piras, S.; Moretta, L.; Marinari, U. M.; Pronzato, M. A.; Nitti, M., The Nrf2/HO-1 Axis in Cancer Cell Growth and Chemoresistance. *Oxid. Med. Cell. Longev.* **2016**, *2016*, 1958174.
- [6] Was, H.; Dulak, J.; Jozkowicz, A., Heme oxygenase-1 in tumor biology and therapy. *Curr. Drug Targets* **2010**, *11* (12), 1551–1570.
- [7] Abraham, N. G.; Kappas, A., Pharmacological and clinical aspects of heme oxygenase. *Pharmacol. Rev.* **2008**, *60* (1), 79–127.
- [8] Aztatzi-Santillán, E.; Nares-López, F. E.; Márquez-Valadez, B.; Aguilera, P.; Cháñez-Cárdenas, M. E., The protective role of heme oxygenase-1 in cerebral ischemia. *Cent. Nerv. Syst. Agents Med. Chem.* **2010**, *10* (4), 310–316.
- [9] Gozzelino, R.; Jeney, V.; Soares, M. P., Mechanisms of cell protection by heme oxygenase-1. *Annu. Rev. Pharmacol. Toxicol.* **2010**, *50*, 323–354.
- [10] Parfenova, H.; Leffler, C. W.; Basuroy, S.; Liu, J.; Fedinec, A. L., Antioxidant roles of heme oxygenase, carbon monoxide, and bilirubin in cerebral circulation during seizures. *J. Cereb. Blood Flow Metab.* **2012**, *32* (6), 1024–1034.
- [11] Ryter, S. W., Heme oxygenase-1/carbon monoxide as modulators of autophagy and inflammation. *Arch. Biochem. Biophys.* **2019**, *678*, 108186.
- [12] Motterlini, R.; Otterbein, L. E., The therapeutic potential of carbon monoxide. *Nat. Rev. Drug Discov.* **2010**, *9* (9), 728–743.
- [13] Kutty, R. K.; Kutty, G.; Rodriguez, I. R.; Chader, G. J.; Wiggert, B., Chromosomal localization of the human heme oxygenase genes: Heme oxygenase-1 (HMOX1) maps to chromosome 22q12 and heme oxygenase-2 (HMOX2) maps to chromosome 16p13.3. *Genomics* **1994**, *20* (3), 513–516.

- [14] Intagliata, S.; Salerno, L.; Ciaffaglione, V.; Leonardi, C.; Fallica, A. N.; Carota, G.; Amata, E.; Marrazzo, A.; Pittalà, V.; Romeo, G., Heme Oxygenase-2 (HO-2) as a therapeutic target: Activators and inhibitors. *Eur. J. Med. Chem.* **2019**, *183*, 111703.
- [15] Salerno, L.; Floresta, G.; Ciaffaglione, V.; Gentile, D.; Margani, F.; Turnaturi, R.; Rescifina, A.; Pittalà, V., Progress in the development of selective heme oxygenase-1 inhibitors and their potential therapeutic application. *Eur. J. Med. Chem.* **2019**, *167*, 439–453.
- [16] Hemmati, M.; Yousefi, B.; Bahar, A.; Eslami, M., Importance of Heme Oxygenase-1 in Gastrointestinal Cancers: Functions, Inductions, Regulations, and Signaling. *J. Gastrointest. Cancer* **2021**, *52* (2), 454–461.
- [17] Li Volti, G.; Tibullo, D.; Vanella, L.; Giallongo, C.; Di Raimondo, F.; Forte, S.; Di Rosa, M.; Signorelli, S. S.; Barbagallo, I., The Heme Oxygenase System in Hematological Malignancies. *Antioxid. Redox Signal.* **2017**, *27* (6), 363–377.
- [18] Raval, C. M.; Lee, P. J., Heme oxygenase-1 in lung disease. *Curr. Drug Targets* **2010**, *11* (12), 1532–1540.
- [19] Salerno, L.; Romeo, G.; Modica, M. N.; Amata, E.; Sorrenti, V.; Barbagallo, I.; Pittalà, V., Heme oxygenase-1: A new druggable target in the management of chronic and acute myeloid leukemia. *Eur. J. Med. Chem.* **2017**, *142*, 163–178.
- [20] Nitti, M.; Piras, S.; Marinari, U. M.; Moretta, L.; Pronzato, M. A.; Furfaro, A. L., HO-1 Induction in Cancer Progression: A Matter of Cell Adaptation. *Antioxidants* **2017**, *6* (2), 29.
- [21] Seo, G. S.; Jiang, W. Y.; Chi, J. H.; Jin, H.; Park, W. C.; Sohn, D. H.; Park, P. H.; Lee, S. H., Heme oxygenase-1 promotes tumor progression and metastasis of colorectal carcinoma cells by inhibiting antitumor immunity. *Oncotarget* **2015**, *6* (23), 19792–19806.
- [22] Salerno, L.; Vanella, L.; Sorrenti, V.; Consoli, V.; Ciaffaglione, V.; Fallica, A. N.; Canale, V.; Zajdel, P.; Pignatello, R.; Intagliata, S., Novel mutual prodrug of 5-fluorouracil and heme oxygenase-1 inhibitor (5-FU/HO-1 hybrid): Design and preliminary in vitro evaluation. *J. Enzyme Inhib. Med. Chem.* **2021**, *36* (1), 1378–1386.
- [23] Ciaffaglione, V.; Modica, M. N.; Pittalà, V.; Romeo, G.; Salerno, L.; Intagliata, S., Mutual Prodrugs of 5-Fluorouracil: From a Classic Chemotherapeutic Agent to Novel Potential Anticancer Drugs. *ChemMedChem* **2021**, *16* (23), 3496–3512.

- [24] Kang, K. A.; Piao, M. J.; Kim, K. C.; Kang, H. K.; Chang, W. Y.; Park, I. C.; Keum, Y. S.; Surh, Y. J.; Hyun, J. W., Epigenetic modification of Nrf2 in 5-fluorouracil-resistant colon cancer cells: Involvement of TET-dependent DNA demethylation. *Cell Death Dis.* **2014**, *5* (4), e1183.
- [25] Podkalicka, P.; Mucha, O.; Józkwicz, A.; Dulak, J.; Łoboda, A., Heme oxygenase inhibition in cancers: Possible tools and targets. *Contemp. Oncol. (Pozn)* **2018**, *22* (1A), 23–32.
- [26] Salerno, L.; Pittalà, V.; Romeo, G.; Modica, M. N.; Siracusa, M. A.; Di Giacomo, C.; Acquaviva, R.; Barbagallo, I.; Tibullo, D.; Sorrenti, V., Evaluation of novel aryloxyalkyl derivatives of imidazole and 1,2,4-triazole as heme oxygenase-1 (HO-1) inhibitors and their antitumor properties. *Bioorg. Med. Chem.* **2013**, *21* (17), 5145–5153.
- [27] Salerno, L.; Pittalà, V.; Romeo, G.; Modica, M. N.; Marrazzo, A.; Siracusa, M. A.; Sorrenti, V.; Di Giacomo, C.; Vanella, L.; Parayath, N. N.; Greish, K., Novel imidazole derivatives as heme oxygenase-1 (HO-1) and heme oxygenase-2 (HO-2) inhibitors and their cytotoxic activity in human-derived cancer cell lines. *Eur. J. Med. Chem.* **2015**, *96*, 162–172.
- [28] Sorrenti, V.; Pittalà, V.; Romeo, G.; Amata, E.; Dichiarà, M.; Marrazzo, A.; Turnaturi, R.; Prezzavento, O.; Barbagallo, I.; Vanella, L.; Rescifina, A.; Floresta, G.; Tibullo, D.; Di Raimondo, F.; Intagliata, S.; Salerno, L., Targeting heme Oxygenase-1 with hybrid compounds to overcome Imatinib resistance in chronic myeloid leukemia cell lines. *Eur. J. Med. Chem.* **2018**, *158*, 937–950.
- [29] Greish, K. F.; Salerno, L.; Al Zahrani, R.; Amata, E.; Modica, M. N.; Romeo, G.; Marrazzo, A.; Prezzavento, O.; Sorrenti, V.; Rescifina, A.; Floresta, G.; Intagliata, S.; Pittalà, V., Novel Structural Insight into Inhibitors of Heme Oxygenase-1 (HO-1) by New Imidazole-Based Compounds: Biochemical and In Vitro Anticancer Activity Evaluation. *Molecules* **2018**, *23* (5), 1209.
- [30] Ciaffaglione, V.; Intagliata, S.; Pittalà, V.; Marrazzo, A.; Sorrenti, V.; Vanella, L.; Rescifina, A.; Floresta, G.; Sultan, A.; Greish, K.; Salerno, L., New Arylethanolimidazole Derivatives as HO-1 Inhibitors with Cytotoxicity against MCF-7 Breast Cancer Cells. *Int. J. Mol. Sci.* **2020**, *21* (6), 1923.
- [31] Floresta, G.; Carotti, A.; Ianni, F.; Sorrenti, V.; Intagliata, S.; Rescifina, A.; Salerno, L.; Di Michele, A.; Sardella, R.; Pittalà, V., Chromatographic resolution of

- phenylethanolic-azole racemic compounds highlighted stereoselective inhibition of heme oxygenase-1 by (R)-enantiomers. *Bioorg. Chem.* **2020**, *99*, 103777.
- [32] Floresta, G.; Fallica, A. N.; Romeo, G.; Sorrenti, V.; Salerno, L.; Rescifina, A.; Pittalà, V., Identification of a potent heme oxygenase-2 (HO-2) inhibitor by targeting the secondary hydrophobic pocket of the HO-2 western region. *Bioorg. Chem.* **2020**, *104*, 104310.
- [33] Salerno, L.; Amata, E.; Romeo, G.; Marrazzo, A.; Prezzavento, O.; Floresta, G.; Sorrenti, V.; Barbagallo, I.; Rescifina, A.; Pittalà, V., Potholing of the hydrophobic heme oxygenase-1 western region for the search of potent and selective imidazole-based inhibitors. *Eur. J. Med. Chem.* **2018**, *148*, 54–62.
- [34] Fallica, A. N.; Sorrenti, V.; D'Amico, A.G.; Salerno, L.; Romeo, G.; Intagliata, S.; Consoli, V.; Floresta, G.; Rescifina, A.; D'Agata, V.; Vanella, L.; Pittalà, V., Discovery of Novel Acetamide-Based Heme Oxygenase-1 Inhibitors with Potent In Vitro Antiproliferative Activity. *J. Med. Chem.* **2021**, *64* (18), 13373–13393.
- [35] Amata, E.; Marrazzo, A.; Dichiarà, M.; Modica, M. N.; Salerno, L.; Prezzavento, O.; Nastasi, G.; Rescifina, A.; Romeo, G.; Pittalà, V., Heme Oxygenase Database (HemeOxDB) and QSAR Analysis of Isoform 1 Inhibitors. *ChemMedChem* **2017**, *12* (22), 1873–1881.
- [36] Floresta, G.; Pittalà, V.; Sorrenti, V.; Romeo, G.; Salerno, L.; Rescifina, A., Development of new HO-1 inhibitors by a thorough scaffold-hopping analysis. *Bioorg. Chem.* **2018**, *81*, 334–339.
- [37] Floresta, G.; Amata, E.; Dichiarà, M.; Marrazzo, A.; Salerno, L.; Romeo, G.; Prezzavento, O.; Pittalà, V.; Rescifina, A., Identification of Potentially Potent Heme Oxygenase 1 Inhibitors through 3D-QSAR Coupled to Scaffold-Hopping Analysis. *ChemMedChem* **2018**, *13* (13), 1336–1342.
- [38] Brown, D. G.; Boström, J., Where Do Recent Small Molecule Clinical Development Candidates Come from? *J. Med. Chem.* **2018**, *61* (21), 9442–9468.
- [39] Bienstock, R. J., Computational methods for fragment-based ligand design: Growing and linking. *Methods Mol. Biol.* **2015**, *1289*, 119–135.
- [40] Floresta, G.; Amata, E.; Gentile, D.; Romeo, G.; Marrazzo, A.; Pittalà, V.; Salerno, L.; Rescifina, A., Fourfold Filtered Statistical/Computational Approach for the Identification of Imidazole Compounds as HO-1 Inhibitors from Natural Products. *Mar. Drugs* **2019**, *17* (2), 113.

- [41] Floresta, G.; Fallica, A. N.; Salerno, L.; Sorrenti, V.; Pittalà, V.; Rescifina, A., Growing the molecular architecture of imidazole-like ligands in HO-1 complexes. *Bioorg. Chem.* **2021**, *117*, 105428.
- [42] Gentile, D.; Floresta, G.; Patamia, V.; Chiaramonte, R.; Mauro, G. L.; Rescifina, A.; Vecchio, M., An Integrated Pharmacophore/Docking/3D-QSAR Approach to Screening a Large Library of Products in Search of Future Botulinum Neurotoxin A Inhibitors. *Int. J. Mol. Sci.* **2020**, *21* (24), 9470.
- [43] Stewart, J. J., Optimization of parameters for semiempirical methods IV: Extension of MNDO, AM1, and PM3 to more main group elements. *J. Mol. Model.* **2004**, *10* (2), 155–164.
- [44] Alemán, C.; Luque, F. J.; Orozco, M., Suitability of the PM3-derived molecular electrostatic potentials. *J. Comput. Chem.* **1993**, *14*, 799–808.
- [45] Cheeseright, T.; Mackey, M.; Rose, S.; Vinter, A., Molecular field extrema as descriptors of biological activity: Definition and validation. *J. Chem. Inf. Model.* **2006**, *46* (2), 665–676.
- [46] Krieger, E.; Vriend, G., YASARA View—Molecular graphics for all devices—From smartphones to workstations. *Bioinformatics* **2014**, *30* (20), 2981–2982.
- [47] Floresta, G.; Rescifina, A.; Marrazzo, A.; Dichiarà, M.; Pistarà, V.; Pittalà, V.; Prezzavento, O.; Amata, E., Hyphenated 3D-QSAR statistical model-scaffold hopping analysis for the identification of potentially potent and selective sigma-2 receptor ligands. *Eur. J. Med. Chem.* **2017**, *139*, 884–891.
- [48] Floresta, G.; Apirakkan, O.; Rescifina, A.; Abbate, V., Discovery of High-Affinity Cannabinoid Receptors Ligands through a 3D-QSAR Ushered by Scaffold-Hopping Analysis. *Molecules* **2018**, *23* (9), 2183.
- [49] Ryter, S. W.; Alam, J.; Choi, A. M., Heme oxygenase-1/carbon monoxide: From basic science to therapeutic applications. *Physiol. Rev.* **2006**, *86* (2), 583–650.
- [50] Vlahakis, J. Z.; Lazar, C.; Roman, G.; Vukomanovic, D.; Nakatsu, K.; Szarek, W. A., Heme oxygenase inhibition by alpha-(1H-imidazol-1-yl)-omega-phenylalkanes: Effect of introduction of heteroatoms in the alkyl linker. *ChemMedChem* **2012**, *7* (5), 897–902.

## Supplementary information

### Identification of a potent heme oxygenase-2 (HO-2) inhibitor by targeting the secondary hydrophobic pocket of the HO-2 western region

Giuseppe Floresta <sup>a, b</sup>, Antonino N. Fallica <sup>a</sup>, Giuseppe Romeo <sup>a</sup>, Valeria Sorrenti <sup>a</sup>, Loredana Salerno <sup>a</sup>, Antonio Rescifina <sup>a</sup>, Valeria Pittalà <sup>a,\*</sup>

<sup>a</sup> Department of Drug Sciences, University of Catania, V.le A. Doria 6, 95125 – Catania, Italy

<sup>b</sup> Department of Analytics, Environmental & Forensics, King's College London, Stamford Street, London SE1 9NH, UK

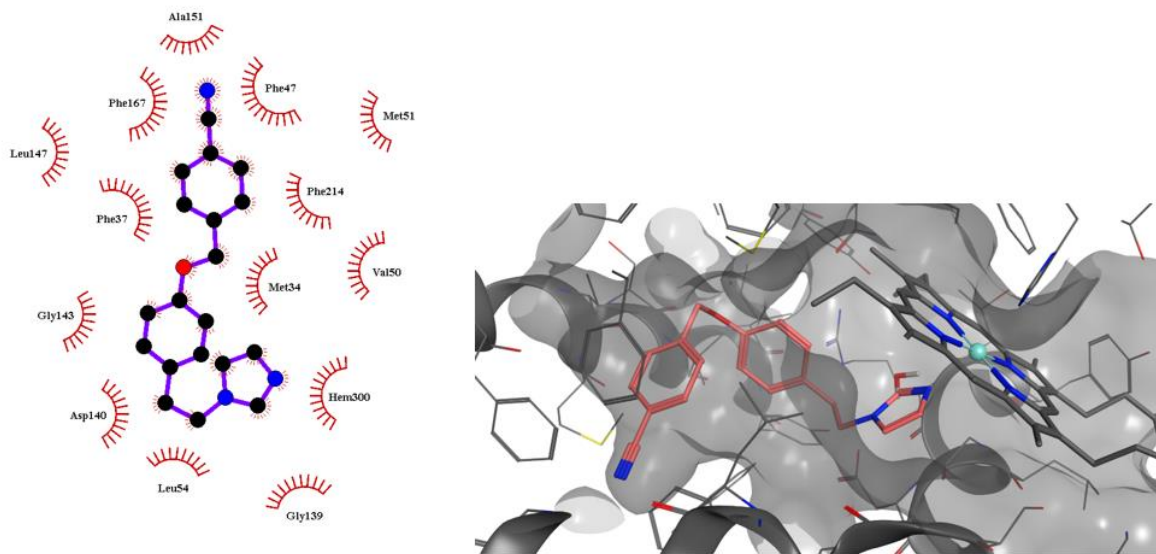
#### \*Corresponding author:

Valeria Pittalà (vpittala@unict.it)

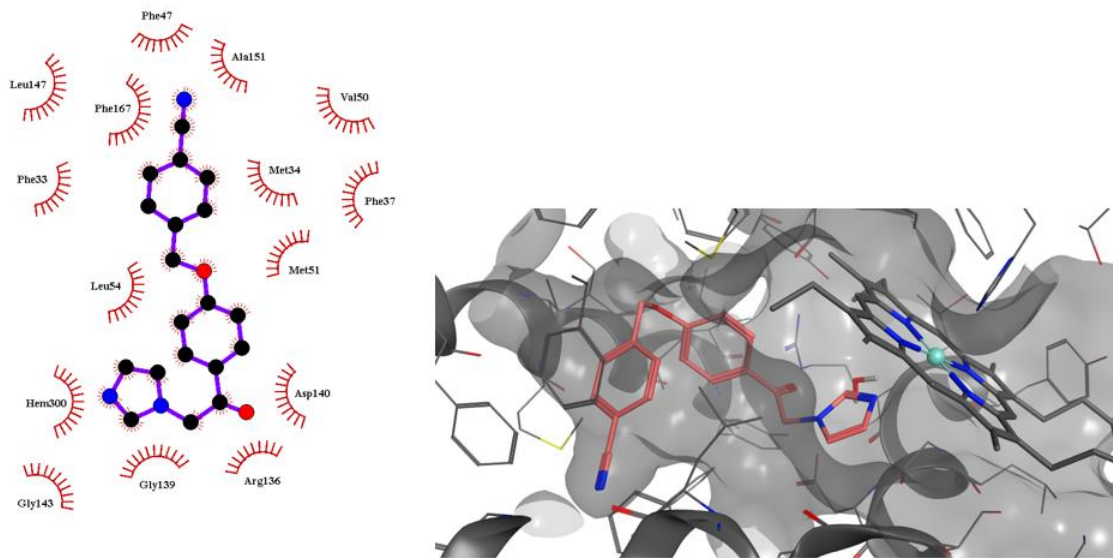
#### Table of contents

Fig. S1. 2D ligand/protein interaction diagram for the molecule 8/HO-1	S2
Fig. S2. 2D ligand/protein interaction diagram for the molecule 13/HO-1	S2
Fig. S3. 2D ligand/protein interaction diagram for the molecule (R)-9/HO-1	S3
Fig. S4. 2D ligand/protein interaction diagram for the molecule (S)-9/HO-1	S3
Fig. S5. 2D ligand/protein interaction diagram for the molecule 8/HO-2	S4
Fig. S6. 2D ligand/protein interaction diagram for the molecule 13/HO-2	S4
Fig. S7. 2D ligand/protein interaction diagram for the molecule (R)-9/HO-2	S5
Fig. S8. 2D ligand/protein interaction diagram for the molecule (S)-9/HO-2	S5
Table S1. Aligned residues of the HO-1 and HO-2 binding sites. The differences are highlighted in yellow	S6
Fig. S9. SwissADME result for molecule 8	S7
Fig. S10. SwissADME result for molecule 9	S8
Fig. S11. SwissADME result for molecule 13	S9
Fig. S12. pkCSM result for molecule 8	S10
Fig. S13. pkCSM result for molecule 9	S11
Fig. S14. pkCSM result for molecule 13	S12
Fig. S15–S20 NMR spectra	S13





**Figure S1.** 2D ligand/protein interaction diagram for the molecule **8**/HO-1.



**Figure S2.** 2D ligand/protein interaction diagram for the molecule **13**/HO-1.

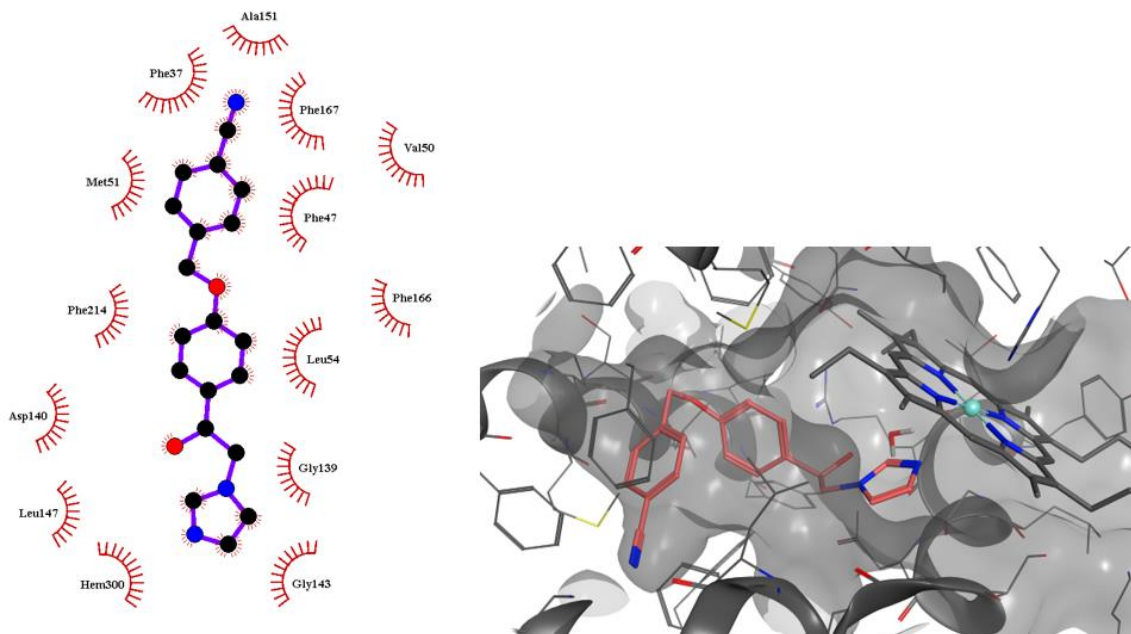


**Figure S3.** 2D ligand/protein interaction diagram for the molecule (*R*)-**9**/HO-1.

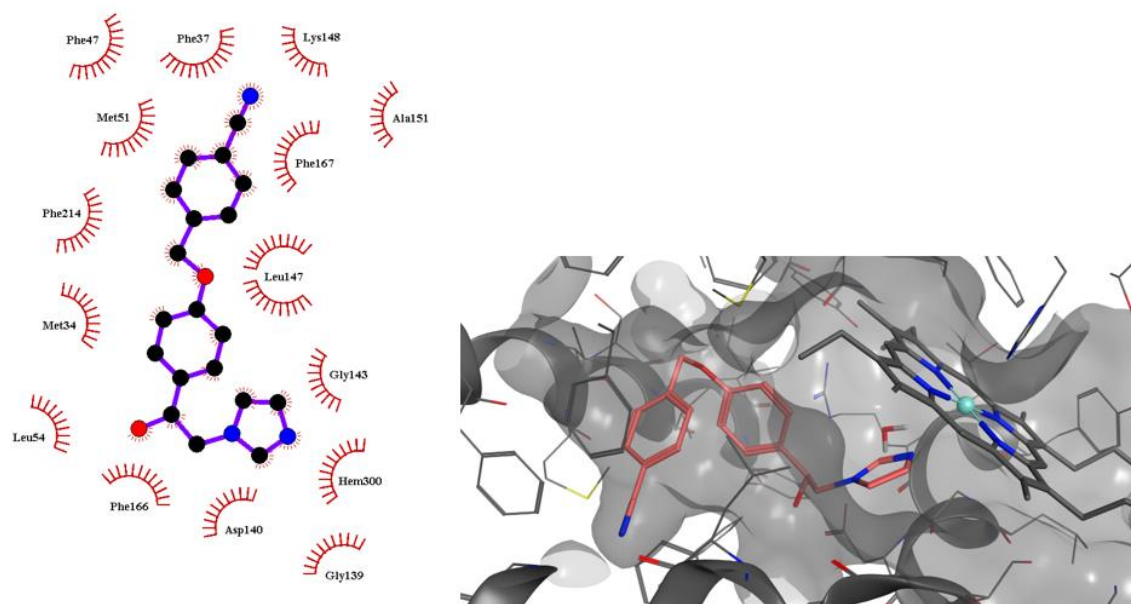


**Figure S4.** 2D ligand/protein interaction diagram for the molecule (*S*)-**9**/HO-1.

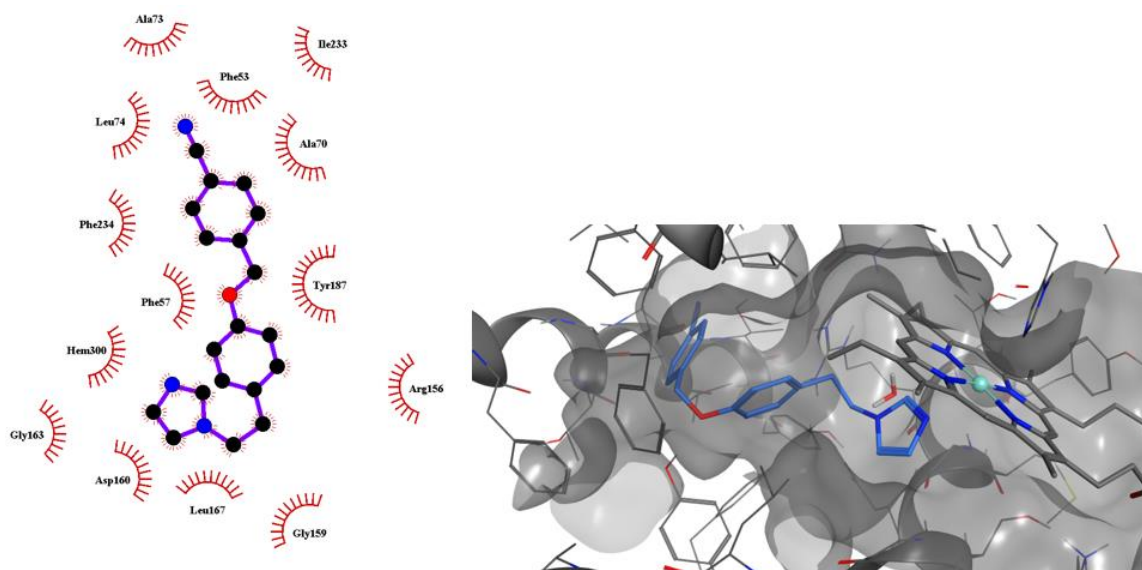


**Figure S5.** 2D ligand/protein interaction diagram for the molecule **9**/HO-2.

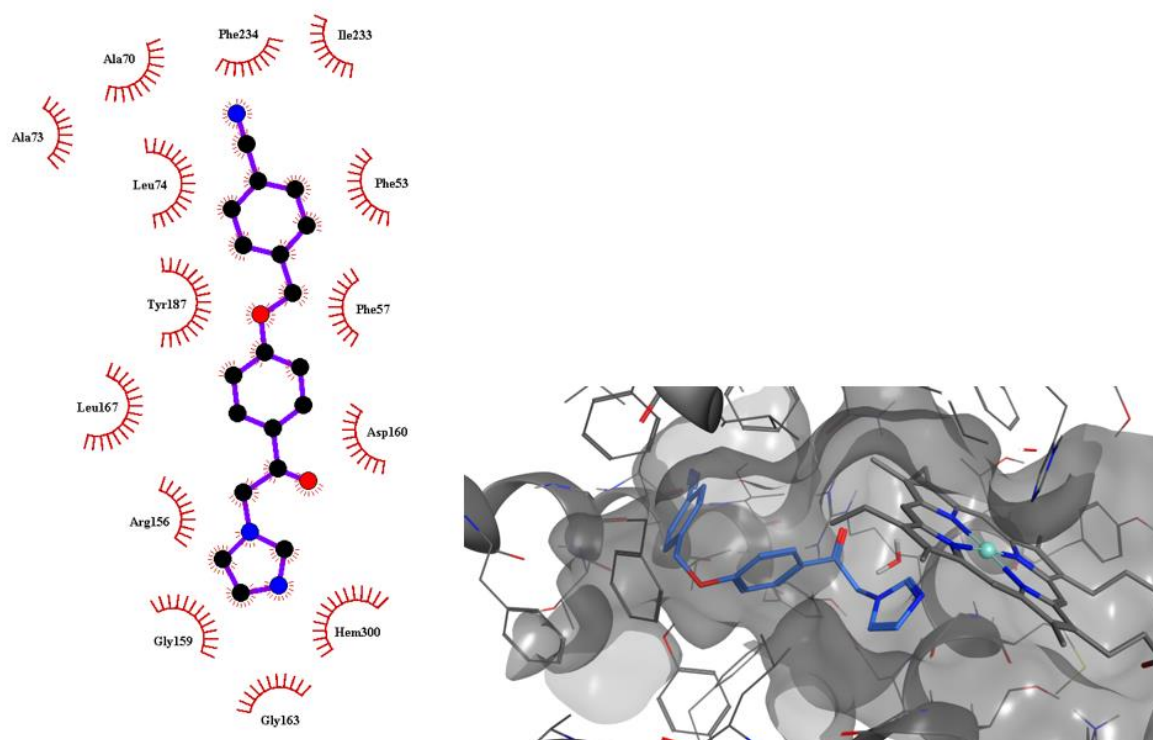


**Figure S6.** 2D ligand/protein interaction diagram for the molecule **12**/HO-2.

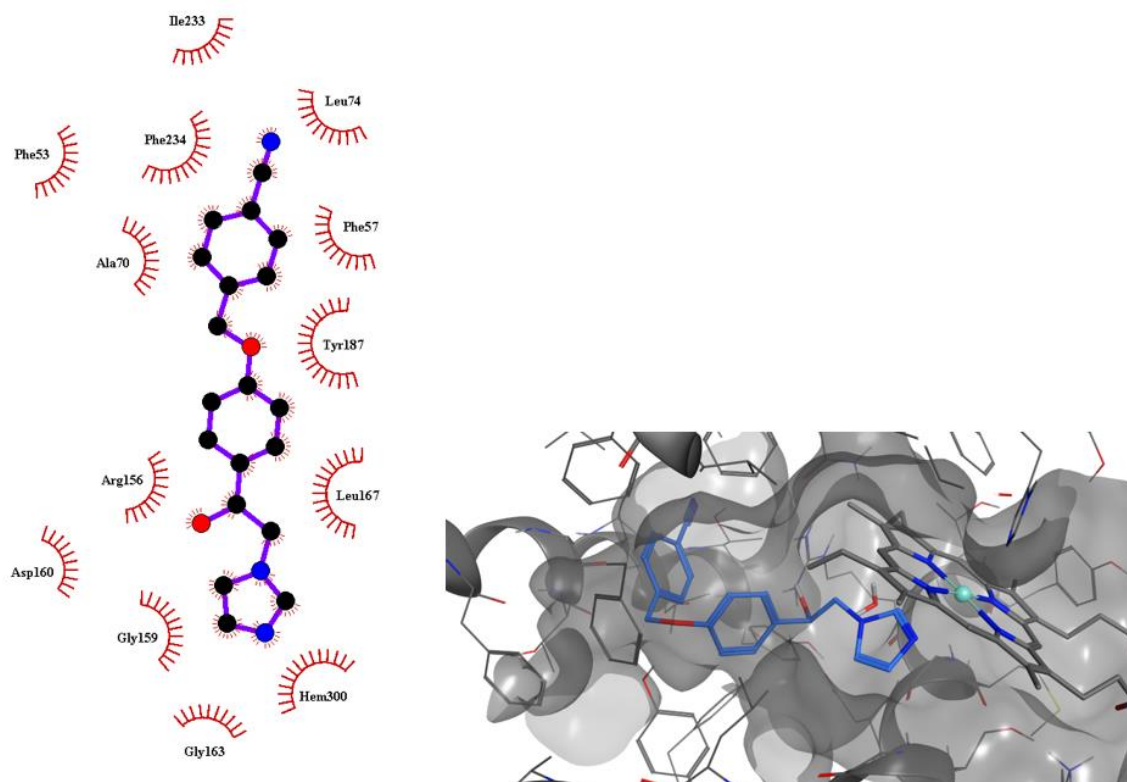


**Figure S7.** 2D ligand/protein interaction diagram for the molecule (*R*)-**13**/HO-2.

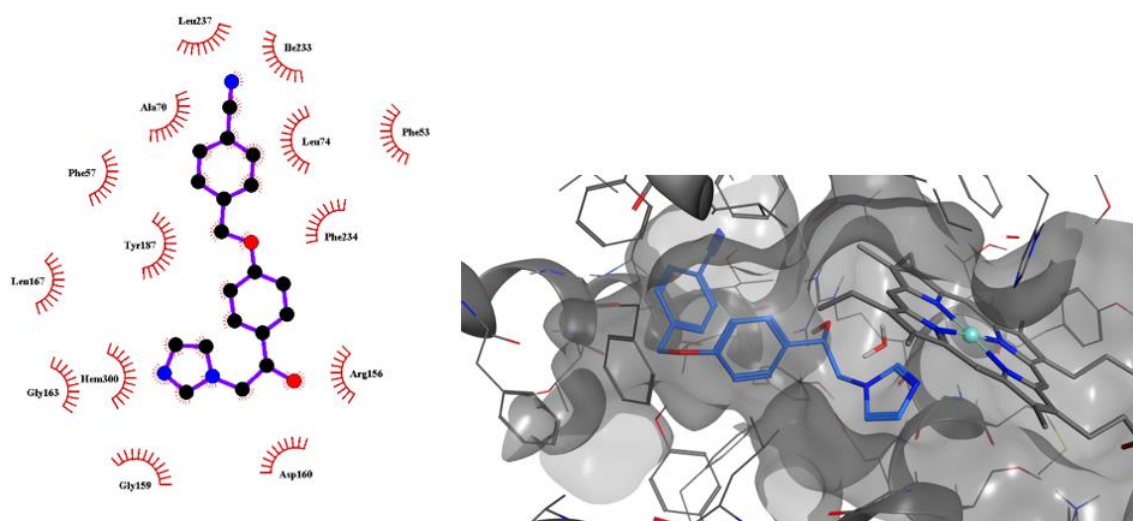


**Figure S8.** 2D ligand/protein interaction diagram for the molecule (*S*)-**13**/HO-2.

**Table S1.** Aligned residues of the HO-1 and HO-2 binding sites. The differences are highlighted in yellow.

HO-1	HO-2	Single aminoacid RMSD
SER 14	SER 34	0.676
LYS 18	LYS 38	0.483
THR 21	THR 41	0.995
HIS 25	HIS 45	0.761
ALA 28	ALA 48	0.417
GLU 29	GLU 49	1.018
PHE 33	PHE 53	0.372
MET 34	VAL 54	0.379
PHE 37	PHE 57	0.552
GLN 38	LEU 58	1.085
PHE 47	PHE 67	0.614
VAL 50	ALA 70	0.371
MET 51	THR 71	0.344
SER 53	ALA 73	0.659
LEU 54	LEU 74	0.429
TYR 134	TYR 154	0.294
THR 135	THR 155	0.382
ARG 136	ARG 156	0.373
LEU 138	MET 158	0.700
GLY 139	GLY 159	0.737
ASP 140	ASP 160	0.553
SER 142	SER 162	0.529
GLY 143	GLY 163	0.562
GLY 144	GLY 164	0.894
GLN 145	GLN 165	1.101
VAL 146	VAL 166	1.046
LEU 147	LEU 167	1.156
LYS 148	LYS 168	1.208
ALA 151	ALA 171	0.528
LEU 164	THR 184	1.011
PHE 166	PHE 186	0.590
PHE 167	TYR 187	0.863
LYS 179	LYS 199	0.765
ARG 183	ARG 203	0.498
PHE 207	PHE 227	0.513
ASN 210	ASN 230	0.328
LEU 213	ILE 233	0.670
PHE 214	PHE 234	0.339
LEU 217	LEU 237	0.846



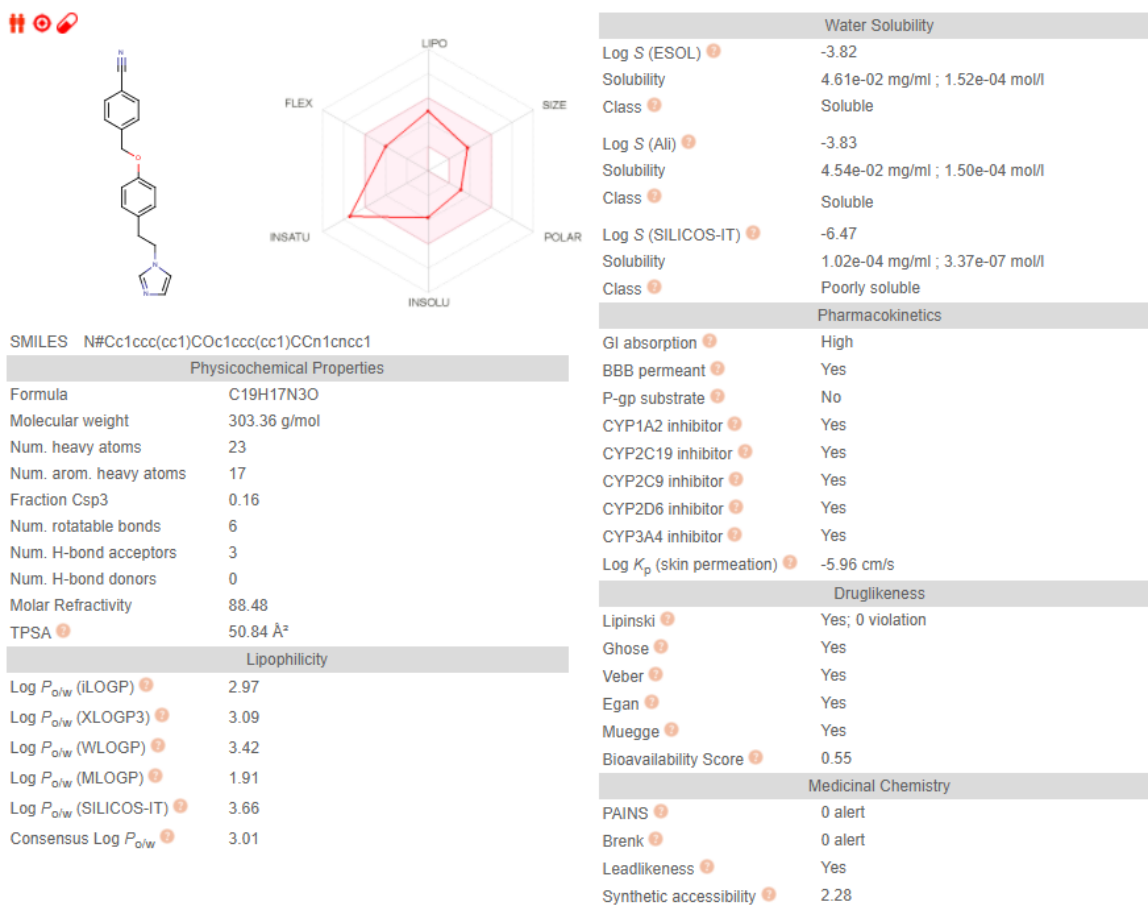
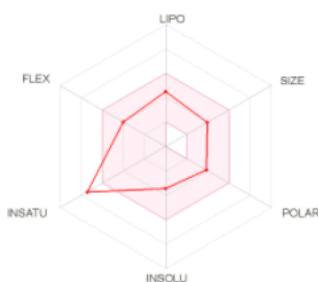
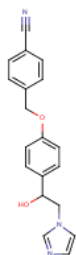


**Figure S9.** SwissADME result for molecule 8.



SMILES N#Cc1ccc(cc1)COc1ccc(cc1)C(Cn1cncc1)O

#### Physicochemical Properties

Formula	C19H17N3O2
Molecular weight	319.36 g/mol
Num. heavy atoms	24
Num. arom. heavy atoms	17
Fraction Csp3	0.16
Num. rotatable bonds	6
Num. H-bond acceptors	4
Num. H-bond donors	1
Molar Refractivity	89.64
TPSA	71.07 Å²

#### Lipophilicity

Log $P_{o/w}$ (iLOGP)	2.73
Log $P_{o/w}$ (XLOGP3)	2.37
Log $P_{o/w}$ (WLOGP)	2.59
Log $P_{o/w}$ (MLOGP)	1.08
Log $P_{o/w}$ (SILICOS-IT)	2.88
Consensus Log $P_{o/w}$	2.33

#### Water Solubility

Log S (ESOL)	-3.44
Solubility	1.16e-01 mg/ml ; 3.62e-04 mol/l
Class	Soluble
Log S (Ali)	-3.50
Solubility	1.00e-01 mg/ml ; 3.14e-04 mol/l
Class	Soluble
Log S (SILICOS-IT)	-5.53
Solubility	9.36e-04 mg/ml ; 2.93e-06 mol/l
Class	Moderately soluble

#### Pharmacokinetics

GI absorption	High
BBB permeant	Yes
P-gp substrate	No
CYP1A2 inhibitor	No
CYP2C19 inhibitor	Yes
CYP2C9 inhibitor	Yes
CYP2D6 inhibitor	Yes
CYP3A4 inhibitor	Yes
Log $K_p$ (skin permeation)	-6.57 cm/s

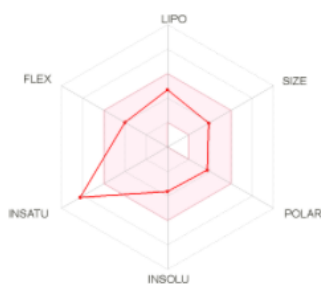
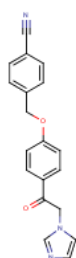
#### Druglikeness

Lipinski	Yes; 0 violation
Ghose	Yes
Weber	Yes
Egan	Yes
Muegge	Yes
Bioavailability Score	0.55

#### Medicinal Chemistry

PAINS	0 alert
Brenk	0 alert
Leadlikeness	Yes
Synthetic accessibility	2.89

Figure S10. SwissADME result for molecule 9.



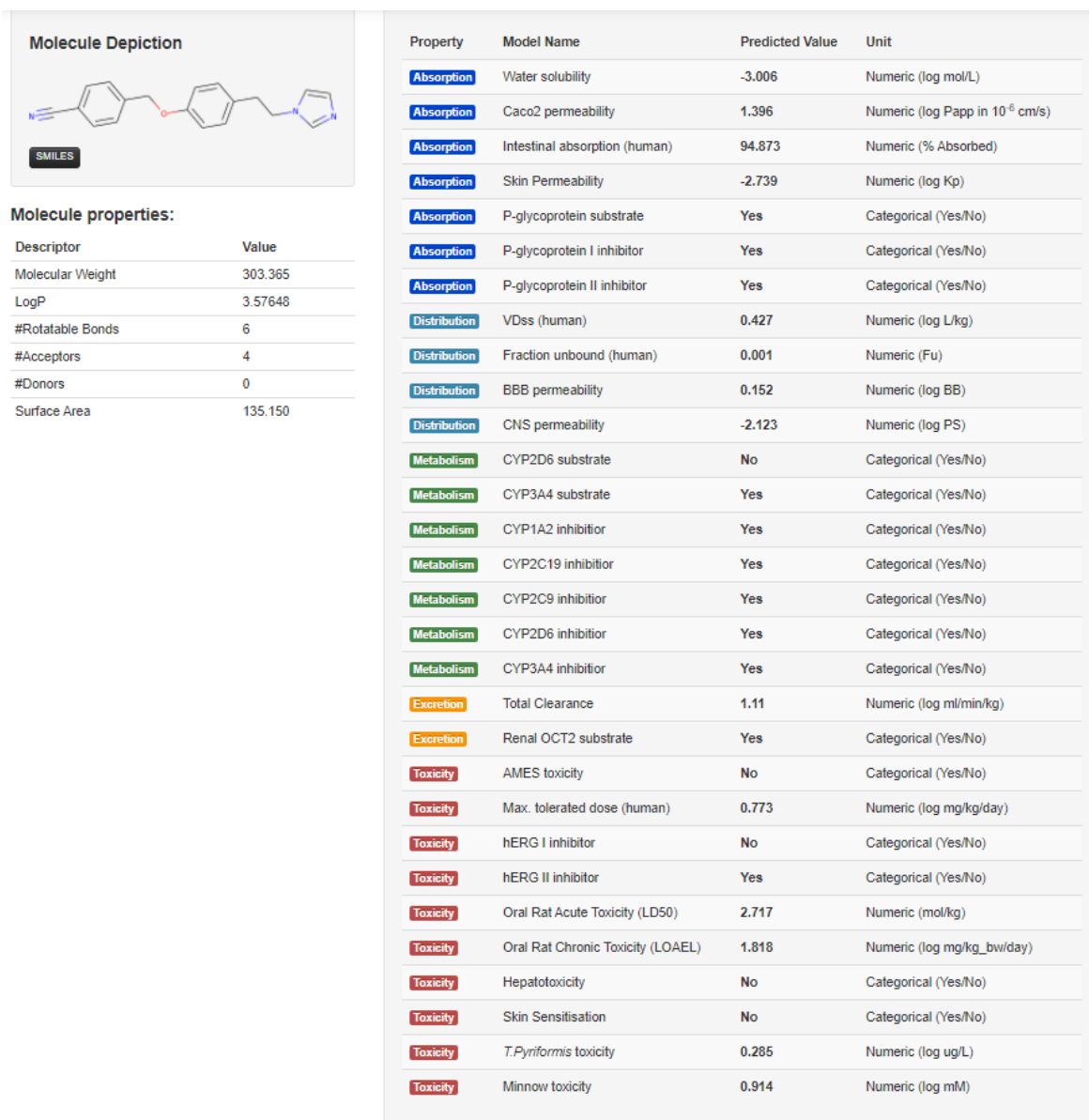
SMILES N#Cc1ccc(cc1)COc1ccc(cc1)C(=O)Cn1cnc1

Physicochemical Properties	
Formula	C19H15N3O2
Molecular weight	317.34 g/mol
Num. heavy atoms	24
Num. arom. heavy atoms	17
Fraction Csp3	0.11
Num. rotatable bonds	6
Num. H-bond acceptors	4
Num. H-bond donors	0
Molar Refractivity	88.90
TPSA	67.91 Å <sup>2</sup>
Lipophilicity	
Log P <sub>o/w</sub> (iLOGP)	2.33
Log P <sub>o/w</sub> (XLOGP3)	2.71
Log P <sub>o/w</sub> (WLOGP)	3.06
Log P <sub>o/w</sub> (MLOGP)	1.01
Log P <sub>o/w</sub> (SILICOS-IT)	3.20
Consensus Log P <sub>o/w</sub>	2.46

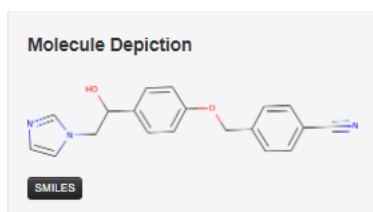
Water Solubility	
Log S (ESOL)	-3.64
Solubility	7.22e-02 mg/ml ; 2.28e-04 mol/l
Class	Soluble
Log S (Ali)	-3.79
Solubility	5.15e-02 mg/ml ; 1.62e-04 mol/l
Class	Soluble
Log S (SILICOS-IT)	-6.01
Solubility	3.11e-04 mg/ml ; 9.79e-07 mol/l
Class	Poorly soluble
Pharmacokinetics	
GI absorption	High
BBB permeant	Yes
P-gp substrate	No
CYP1A2 inhibitor	Yes
CYP2C19 inhibitor	Yes
CYP2C9 inhibitor	Yes
CYP2D6 inhibitor	Yes
CYP3A4 inhibitor	Yes
Log K <sub>p</sub> (skin permeation)	-6.31 cm/s
Druglikeness	
Lipinski	Yes; 0 violation
Ghose	Yes
Veber	Yes
Egan	Yes
Muegge	Yes
Bioavailability Score	0.55
Medicinal Chemistry	
PAINS	0 alert
Brenk	0 alert
Leadlikeness	Yes
Synthetic accessibility	2.30

Figure S11. SwissADME result for molecule 13.





**Figure S12.** pkCSM result for molecule 8.

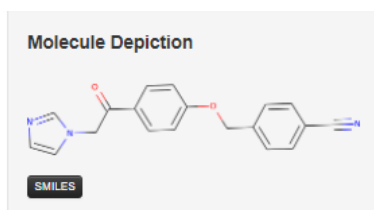


**Molecule properties:**

Descriptor	Value
Molecular Weight	319.364
LogP	3.06738
#Rotatable Bonds	6
#Acceptors	5
#Donors	1
Surface Area	139.944

Property	Model Name	Predicted Value	Unit
<b>Absorption</b>	Water solubility	-3.033	Numeric (log mol/L)
<b>Absorption</b>	Caco2 permeability	0.913	Numeric (log Papp in 10 <sup>-6</sup> cm/s)
<b>Absorption</b>	Intestinal absorption (human)	96.473	Numeric (% Absorbed)
<b>Absorption</b>	Skin Permeability	-2.745	Numeric (log Kp)
<b>Absorption</b>	P-glycoprotein substrate	Yes	Categorical (Yes/No)
<b>Absorption</b>	P-glycoprotein I inhibitor	No	Categorical (Yes/No)
<b>Absorption</b>	P-glycoprotein II inhibitor	Yes	Categorical (Yes/No)
<b>Distribution</b>	VDss (human)	0.368	Numeric (log L/kg)
<b>Distribution</b>	Fraction unbound (human)	0.084	Numeric (Fu)
<b>Distribution</b>	BBB permeability	-0.723	Numeric (log BB)
<b>Distribution</b>	CNS permeability	-2.363	Numeric (log PS)
<b>Metabolism</b>	CYP2D6 substrate	No	Categorical (Yes/No)
<b>Metabolism</b>	CYP3A4 substrate	No	Categorical (Yes/No)
<b>Metabolism</b>	CYP1A2 inhibitor	Yes	Categorical (Yes/No)
<b>Metabolism</b>	CYP2C19 inhibitor	Yes	Categorical (Yes/No)
<b>Metabolism</b>	CYP2C9 inhibitor	Yes	Categorical (Yes/No)
<b>Metabolism</b>	CYP2D6 inhibitor	No	Categorical (Yes/No)
<b>Metabolism</b>	CYP3A4 inhibitor	Yes	Categorical (Yes/No)
<b>Excretion</b>	Total Clearance	1.05	Numeric (log ml/min/kg)
<b>Excretion</b>	Renal OCT2 substrate	Yes	Categorical (Yes/No)
<b>Toxicity</b>	AMES toxicity	No	Categorical (Yes/No)
<b>Toxicity</b>	Max. tolerated dose (human)	1.094	Numeric (log mg/kg/day)
<b>Toxicity</b>	hERG I inhibitor	No	Categorical (Yes/No)
<b>Toxicity</b>	hERG II inhibitor	Yes	Categorical (Yes/No)
<b>Toxicity</b>	Oral Rat Acute Toxicity (LD50)	2.162	Numeric (mol/kg)
<b>Toxicity</b>	Oral Rat Chronic Toxicity (LOAEL)	1.399	Numeric (log mg/kg_bw/day)
<b>Toxicity</b>	Hepatotoxicity	Yes	Categorical (Yes/No)
<b>Toxicity</b>	Skin Sensitisation	No	Categorical (Yes/No)
<b>Toxicity</b>	<i>T. Pyriformis</i> toxicity	0.285	Numeric (log ug/L)
<b>Toxicity</b>	Minnow toxicity	0.12	Numeric (log mM)

**Figure S13.** pkCSM result for molecule 9.



**Molecule properties:**

Descriptor	Value
Molecular Weight	317.348
LogP	3.21668
#Rotatable Bonds	6
#Acceptors	5
#Donors	0
Surface Area	139.312

Property	Model Name	Predicted Value	Unit
<b>Absorption</b>	Water solubility	-3.073	Numeric (log mol/L)
<b>Absorption</b>	Caco2 permeability	0.916	Numeric (log Papp in 10 <sup>-6</sup> cm/s)
<b>Absorption</b>	Intestinal absorption (human)	99.132	Numeric (% Absorbed)
<b>Absorption</b>	Skin Permeability	-2.745	Numeric (log Kp)
<b>Absorption</b>	P-glycoprotein substrate	Yes	Categorical (Yes/No)
<b>Absorption</b>	P-glycoprotein I inhibitor	No	Categorical (Yes/No)
<b>Absorption</b>	P-glycoprotein II inhibitor	Yes	Categorical (Yes/No)
<b>Distribution</b>	VDss (human)	0.34	Numeric (log L/kg)
<b>Distribution</b>	Fraction unbound (human)	0.077	Numeric (Fu)
<b>Distribution</b>	BBB permeability	-0.72	Numeric (log BB)
<b>Distribution</b>	CNS permeability	-2.287	Numeric (log PS)
<b>Metabolism</b>	CYP2D6 substrate	No	Categorical (Yes/No)
<b>Metabolism</b>	CYP3A4 substrate	No	Categorical (Yes/No)
<b>Metabolism</b>	CYP1A2 inhibitor	Yes	Categorical (Yes/No)
<b>Metabolism</b>	CYP2C19 inhibitor	Yes	Categorical (Yes/No)
<b>Metabolism</b>	CYP2C9 inhibitor	Yes	Categorical (Yes/No)
<b>Metabolism</b>	CYP2D6 inhibitor	No	Categorical (Yes/No)
<b>Metabolism</b>	CYP3A4 inhibitor	Yes	Categorical (Yes/No)
<b>Excretion</b>	Total Clearance	1.069	Numeric (log ml/min/kg)
<b>Excretion</b>	Renal OCT2 substrate	Yes	Categorical (Yes/No)
<b>Toxicity</b>	AMES toxicity	No	Categorical (Yes/No)
<b>Toxicity</b>	Max. tolerated dose (human)	1.093	Numeric (log mg/kg/day)
<b>Toxicity</b>	hERG I inhibitor	No	Categorical (Yes/No)
<b>Toxicity</b>	hERG II inhibitor	Yes	Categorical (Yes/No)
<b>Toxicity</b>	Oral Rat Acute Toxicity (LD50)	2.174	Numeric (mol/kg)
<b>Toxicity</b>	Oral Rat Chronic Toxicity (LOAEL)	1.375	Numeric (log mg/kg_bw/day)
<b>Toxicity</b>	Hepatotoxicity	Yes	Categorical (Yes/No)
<b>Toxicity</b>	Skin Sensitisation	No	Categorical (Yes/No)
<b>Toxicity</b>	<i>T.Pyriformis</i> toxicity	0.285	Numeric (log ug/L)
<b>Toxicity</b>	Minnow toxicity	-0.134	Numeric (log mM)

**Figure S14.** pkCSM result for molecule 13.

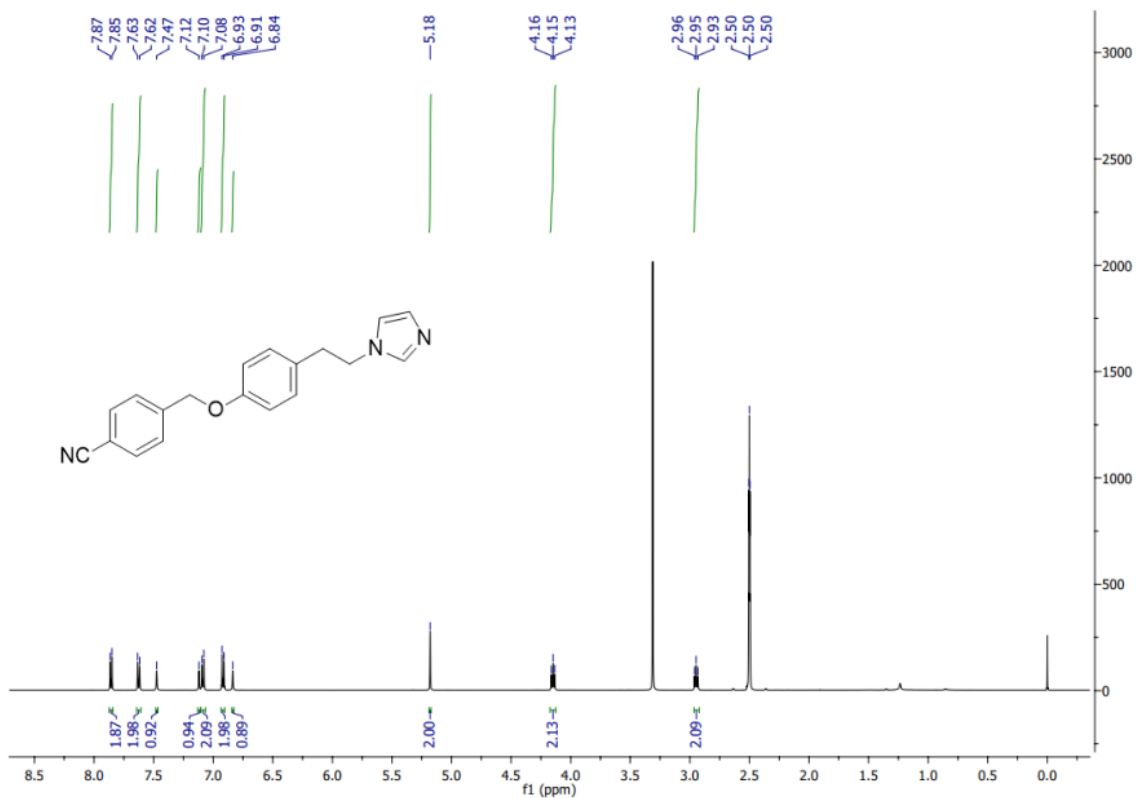


**Figure S15.** <sup>1</sup>H NMR (500 MHz, DMSO-*d*<sub>6</sub>) of compound **8**.

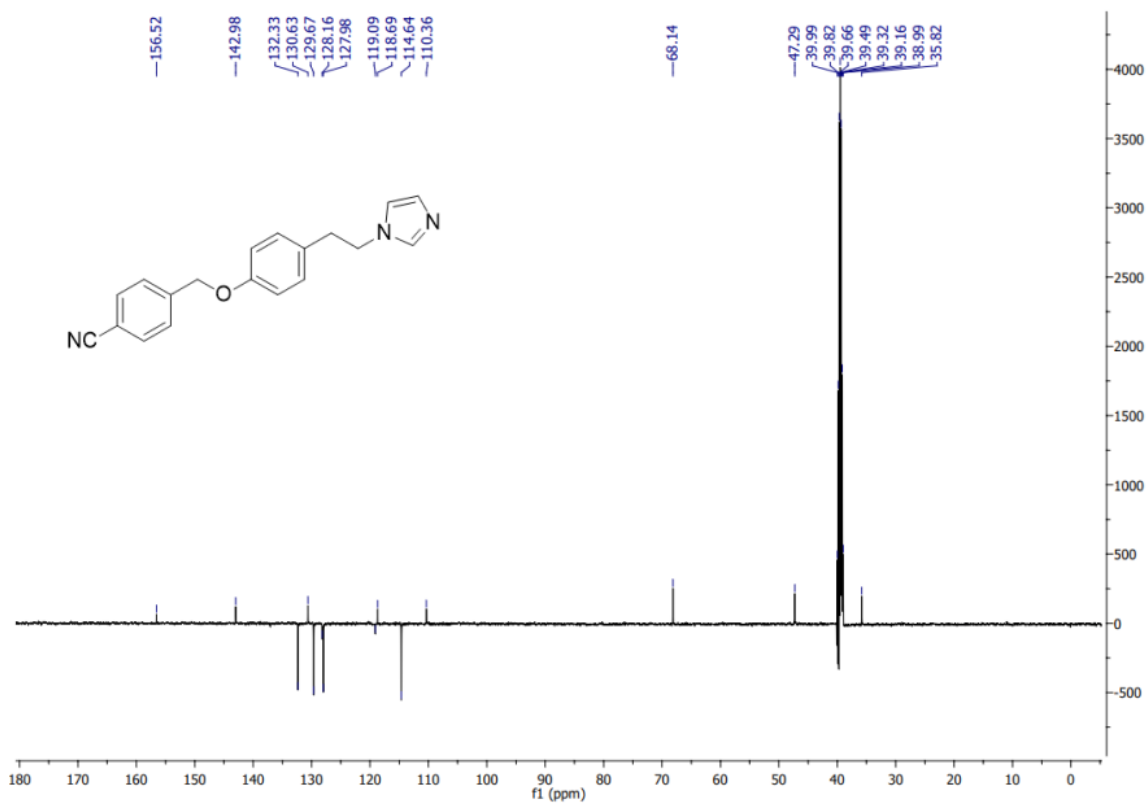


**Figure S16.** <sup>13</sup>C NMR (125 MHz, DMSO-*d*<sub>6</sub>) of compound **8**.

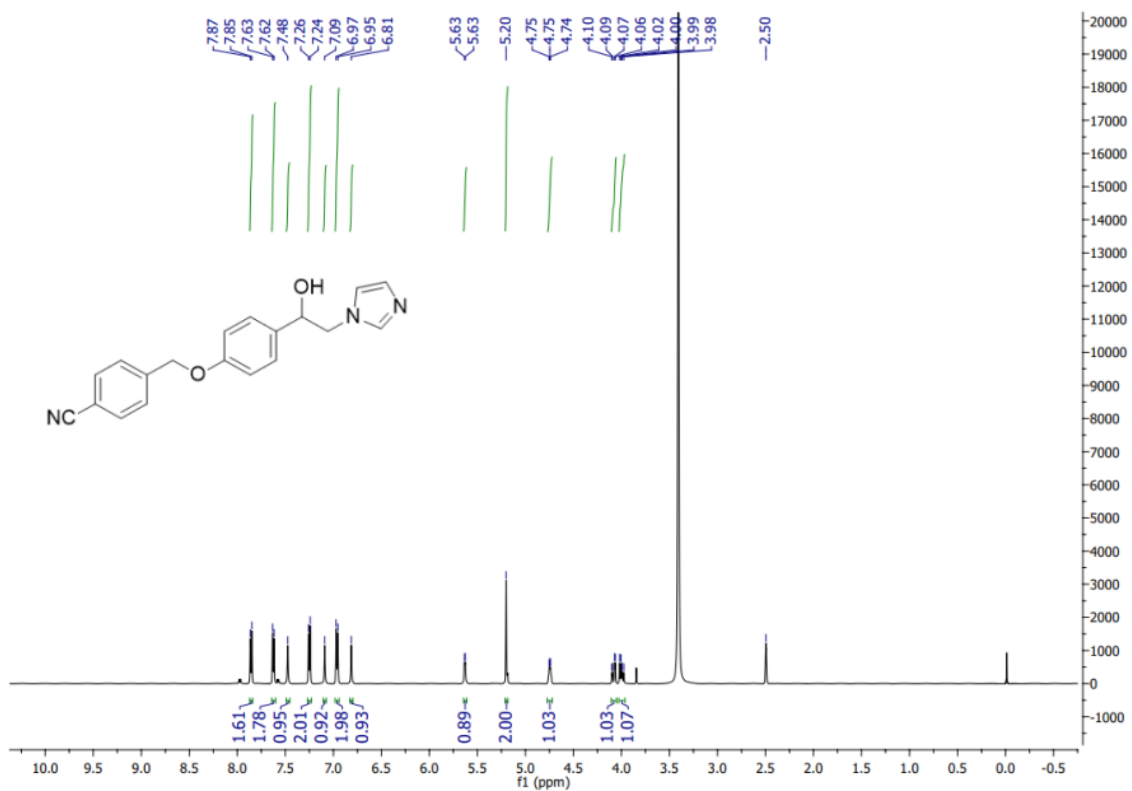


**Figure S17.**  $^1\text{H}$  NMR (500 MHz,  $\text{DMSO}-d_6$ ) of compound **9**.

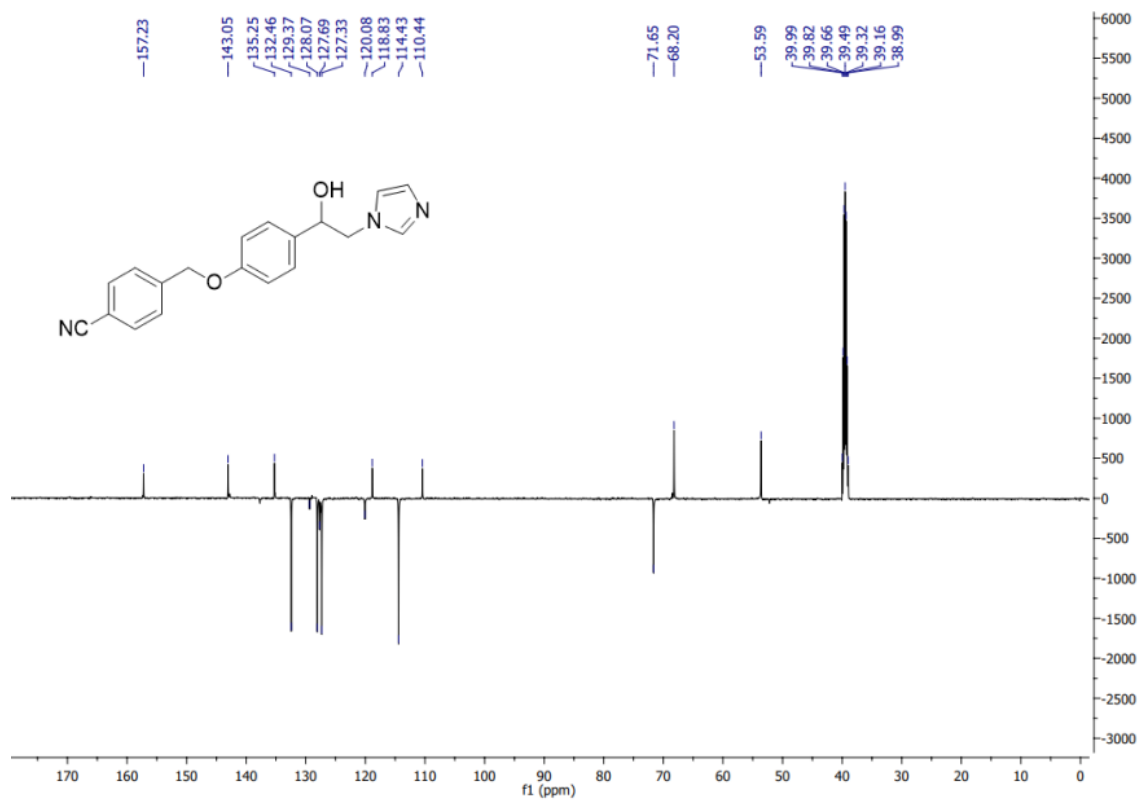


**Figure S18.**  $^{13}\text{C}$  NMR (125 MHz,  $\text{DMSO}-d_6$ ) of compound **9**.

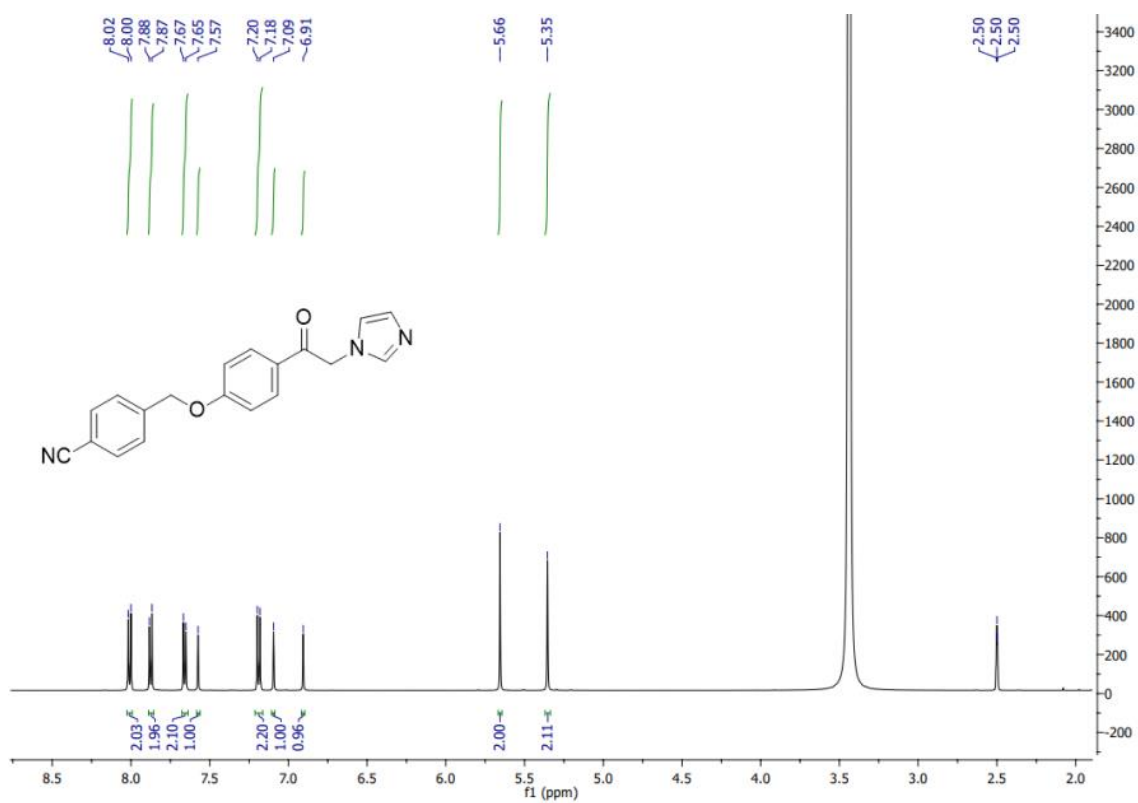


**Figure S19.**  $^1\text{H}$  NMR (500 MHz,  $\text{DMSO}-d_6$ ) of compound **13**.

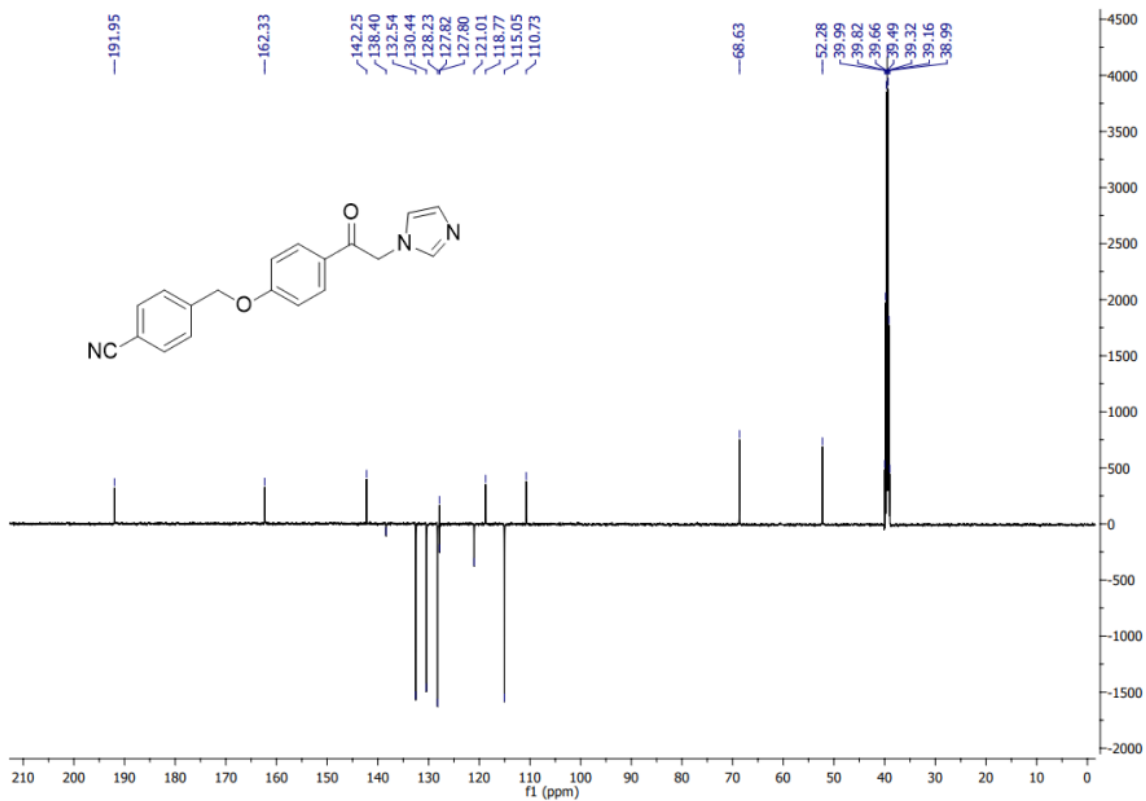


**Figure S20.**  $^{13}\text{C}$  NMR (125 MHz,  $\text{DMSO}-d_6$ ) of compound **13**.

## Discovery of novel acetamide-based heme oxygenase-1 inhibitors with potent in vitro antiproliferative activity

Antonino N. Fallica, <sup>a ‡</sup> Valeria Sorrenti, <sup>a ‡</sup> Agata G. D'Amico, <sup>a</sup> Loredana Salerno, <sup>a</sup> Giuseppe Romeo, <sup>a</sup> Sebastiano Intagliata, <sup>a</sup> Valeria Consoli, <sup>a</sup> Giuseppe Floresta, <sup>b</sup> Antonio Rescifina, <sup>a</sup> Velia D'Agata, <sup>c</sup> Luca Vanella, <sup>a</sup> Valeria Pittalà <sup>a\*</sup>

<sup>a</sup> Department of Drug and Health Sciences, University of Catania, 95125 – Catania, Italy.

<sup>b</sup> Department of Analytics, Environmental & Forensics, King's College London, Stamford Street, London SE1 9NH, UK

<sup>c</sup> Sections of Human Anatomy and Histology, Department of Biomedical and Biotechnological Sciences, University of Catania, 95123 – Catania, Italy

**KEYWORDS:** Heme oxygenase-1, heme oxygenase-2, structure-activity relationships, inhibitors, glioblastoma, U87MG.

### Author contributions

<sup>‡</sup> These authors contributed equally

### \*Corresponding Author:

Valeria Pittalà: vpittala@unict.it

### Table of contents

NMR spectra of compounds	S17-S33
Figure S35. BOILED-Egg plot	S34
Table S2. Results of SwissADME calculations	S34-S36
Table S3. Results of pkCSM calculations	S36-S37
Figure S36. Series 1 and 2 of the scaffold-hopping analysis in <b>71</b> .	S37
Table S4. Series 1 derived from isosteric replacement	S37-S39
Table S5. Series 2 derived from isosteric replacement	S39-S40

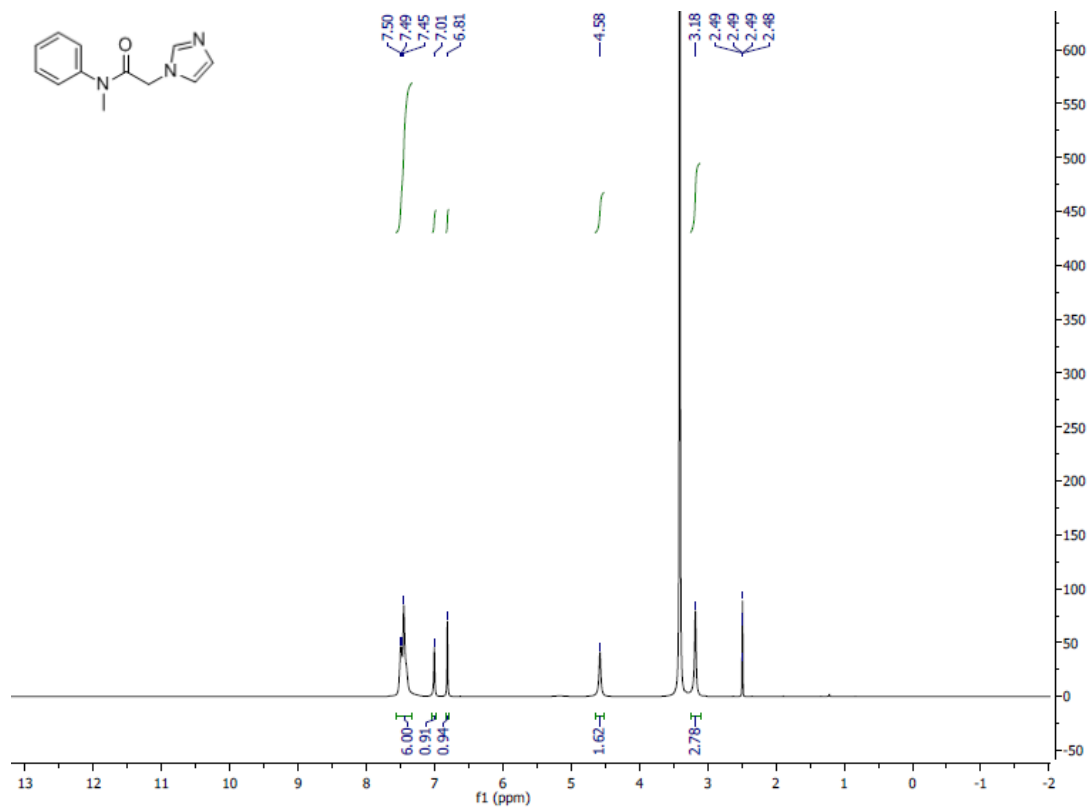


**Figure S1.**  $^1\text{H}$  NMR (500 MHz,  $\text{DMSO-}d_6$ ) of compound **7b**.

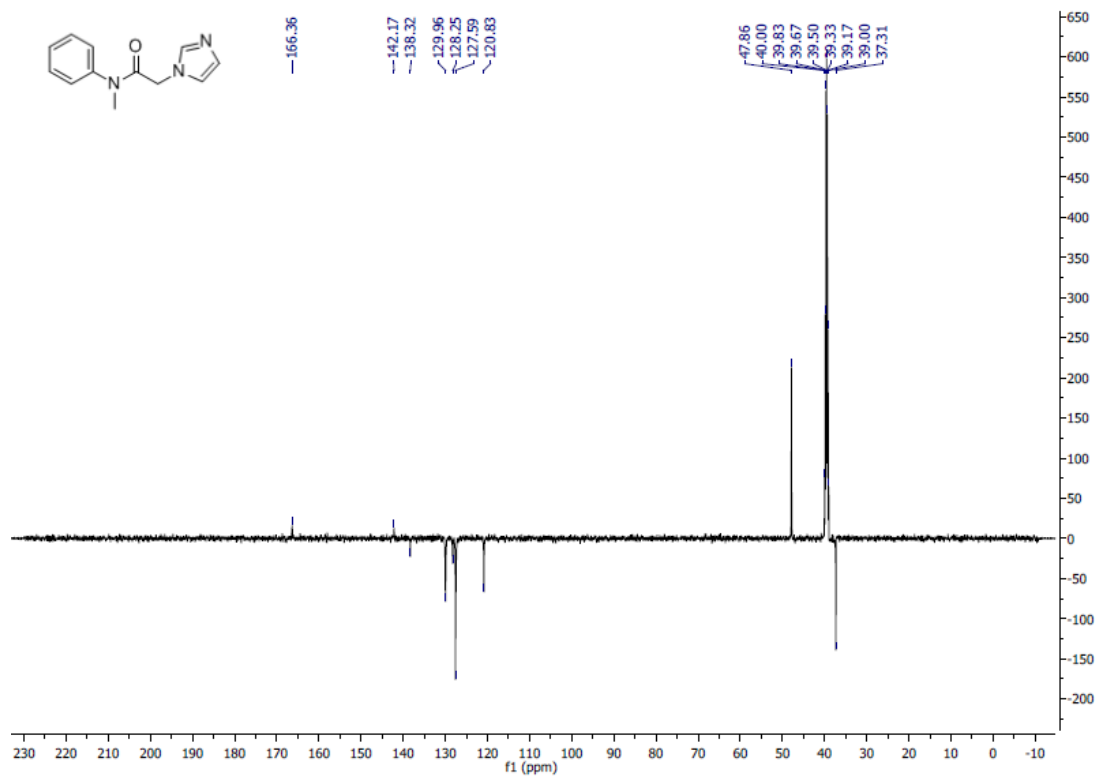


**Figure S2.**  $^{13}\text{C}$  NMR (125 MHz,  $\text{DMSO-}d_6$ ) of compound **7b**.



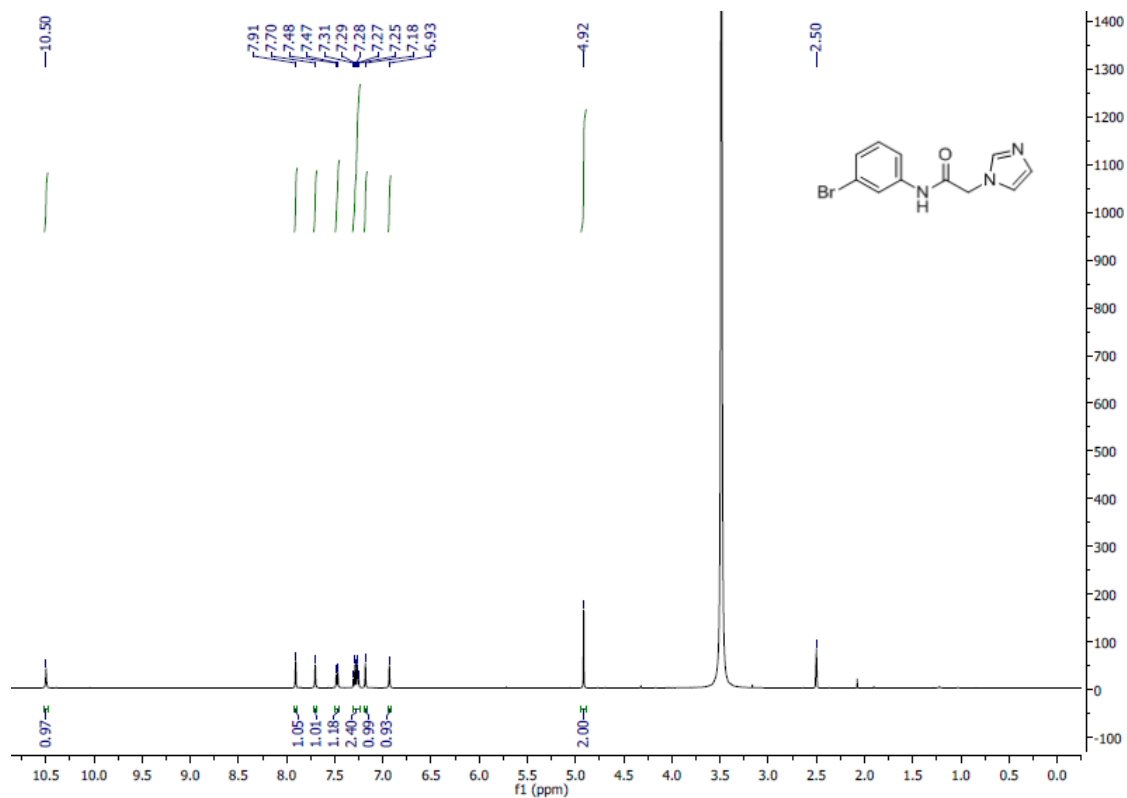


Figure S3.  $^1\text{H}$  NMR (500 MHz,  $\text{DMSO-}d_6$ ) of compound 7c.

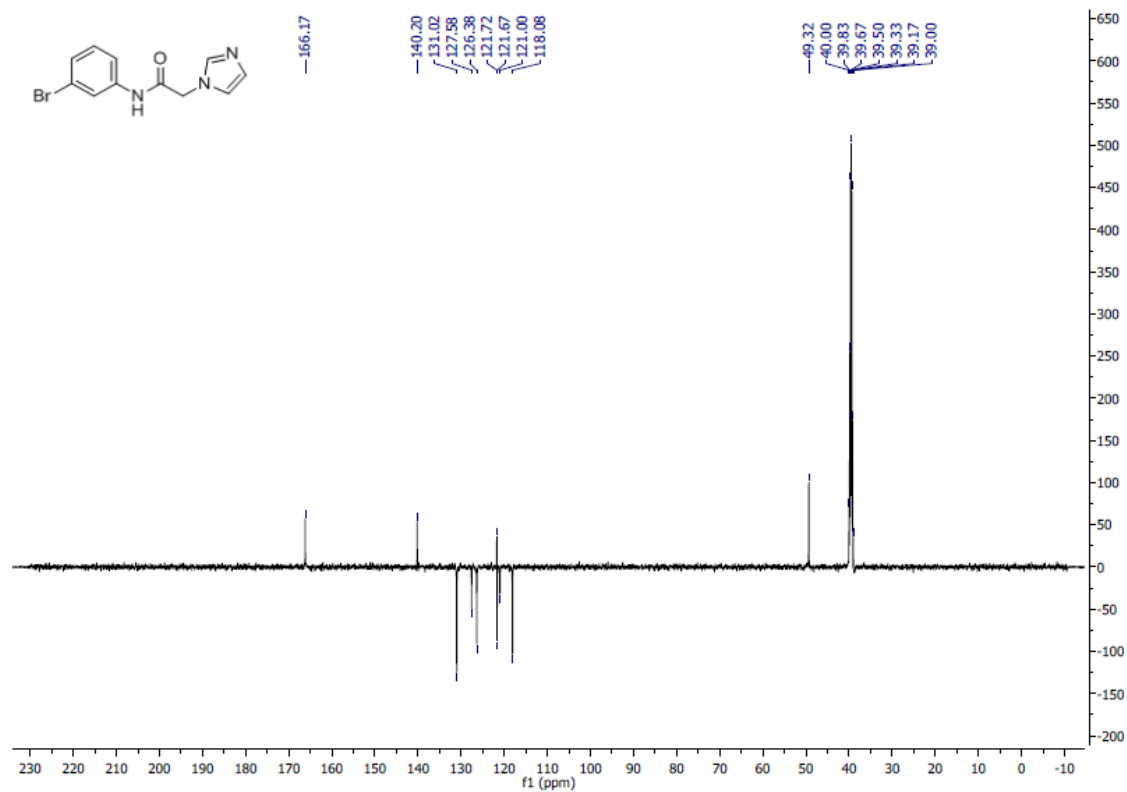
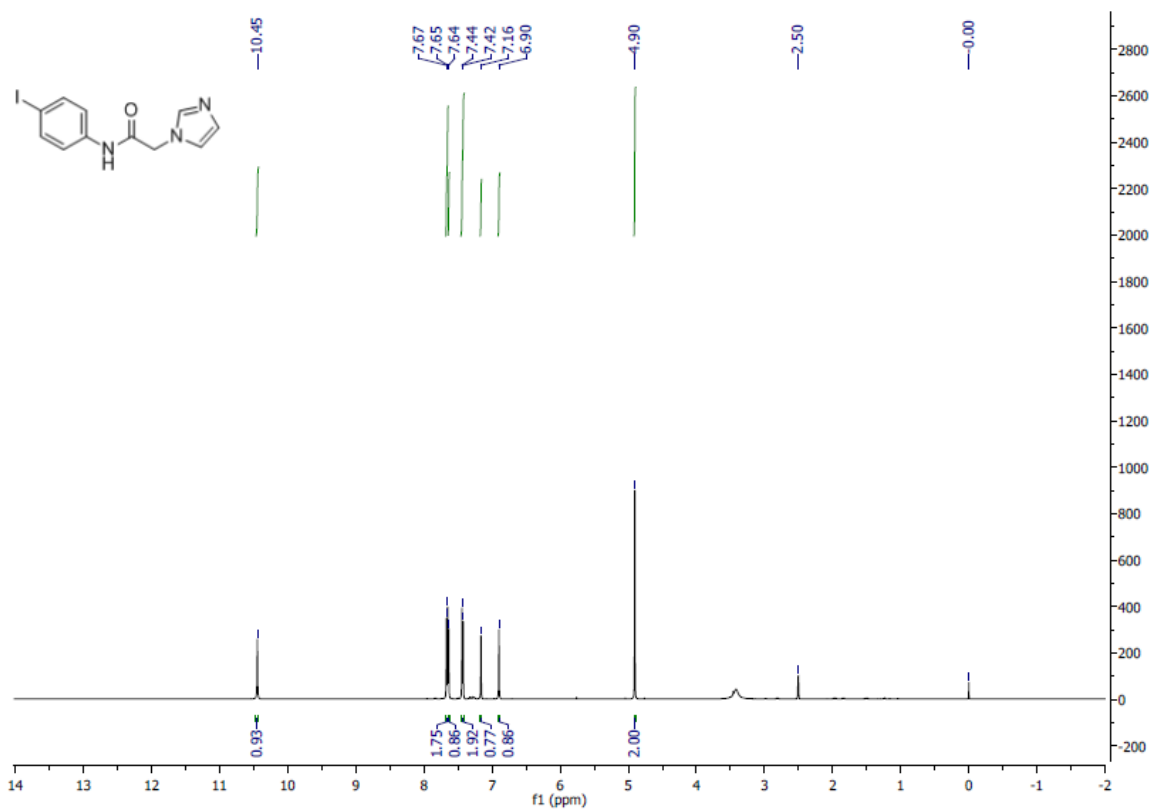
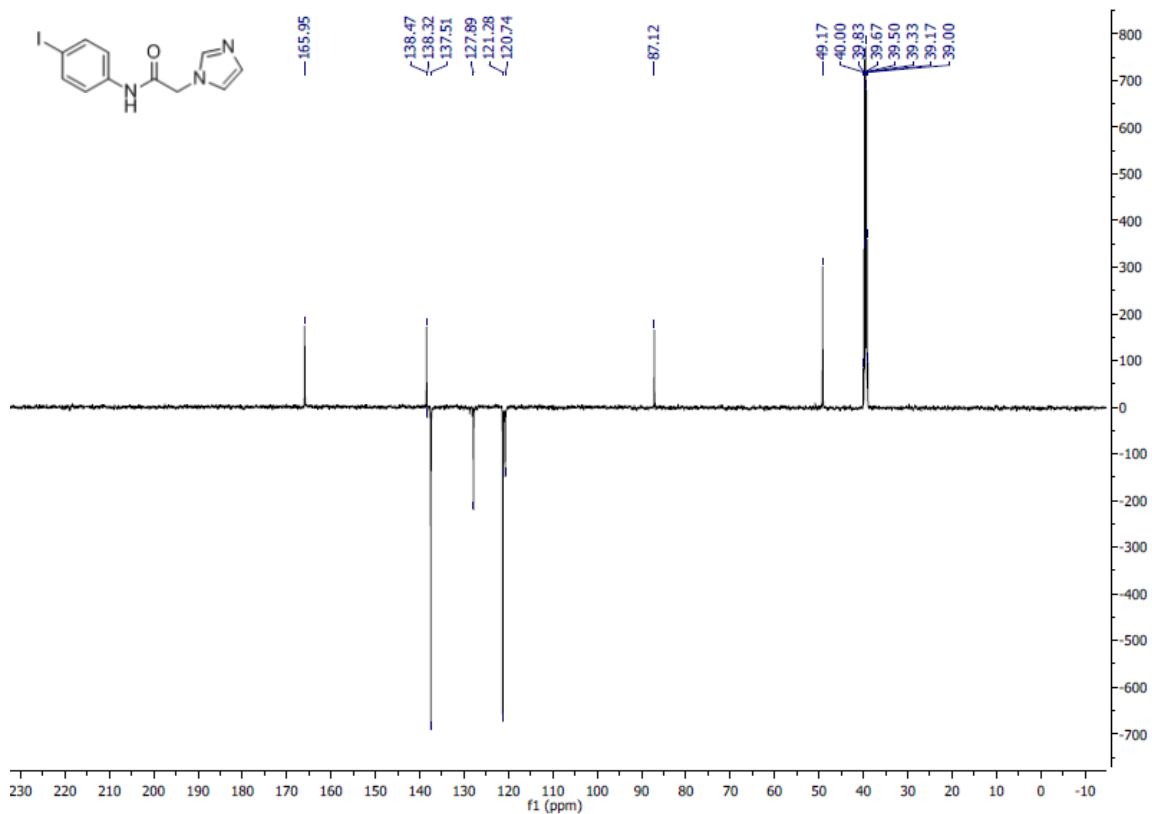


Figure S4.  $^{13}\text{C}$  NMR (125 MHz,  $\text{DMSO-}d_6$ ) of compound 7c.



**Figure S5.**  $^1\text{H}$  NMR (500 MHz,  $\text{DMSO-}d_6$ ) of compound **7d**.



**Figure S6.**  $^{13}\text{C}$  NMR (125 MHz,  $\text{DMSO-}d_6$ ) of compound **7d**.

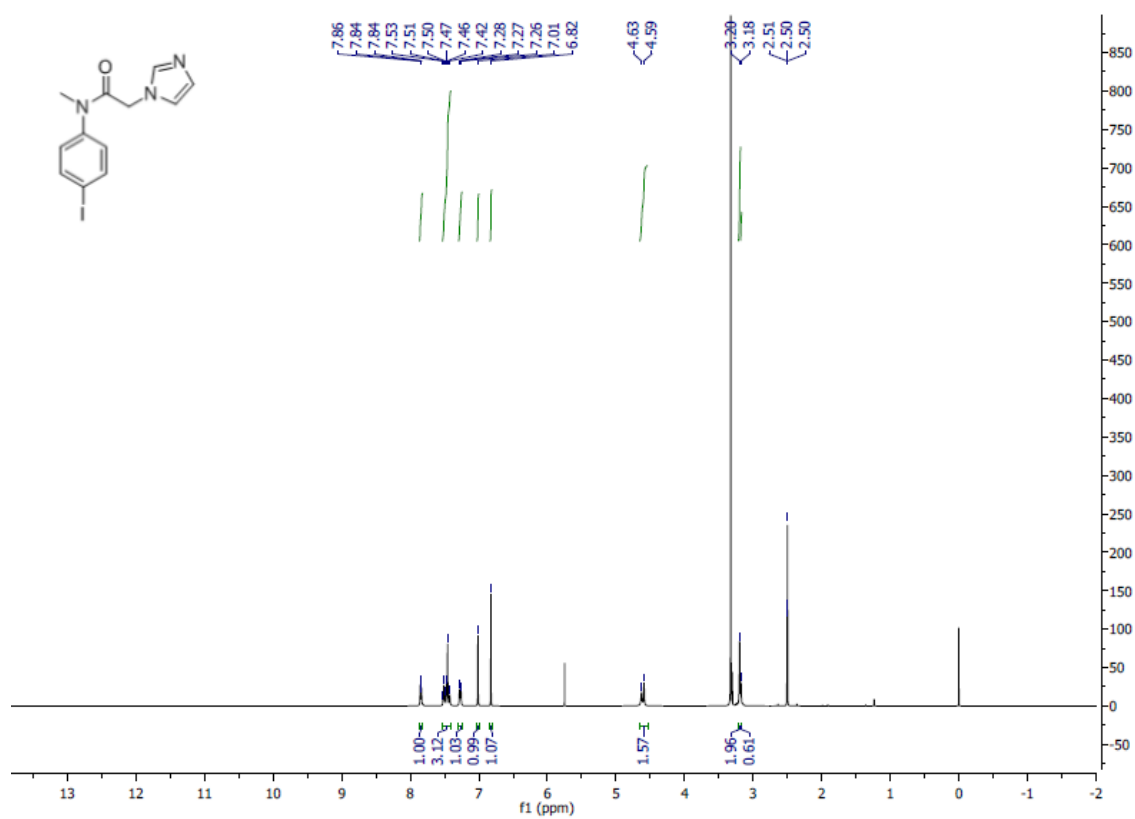


Figure S7.  $^1\text{H}$  NMR (500 MHz,  $\text{DMSO-}d_6$ ) of compound 7e.

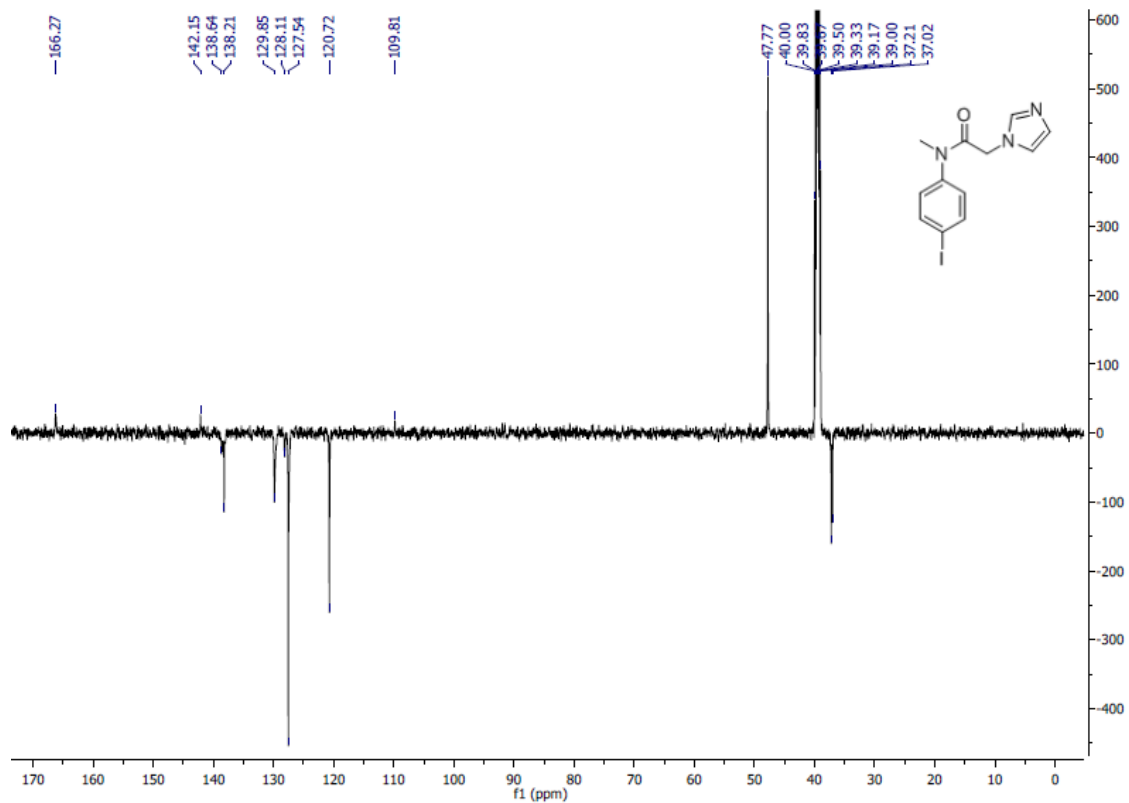


Figure S8.  $^{13}\text{C}$  NMR (125 MHz,  $\text{DMSO-}d_6$ ) of compound 7e.

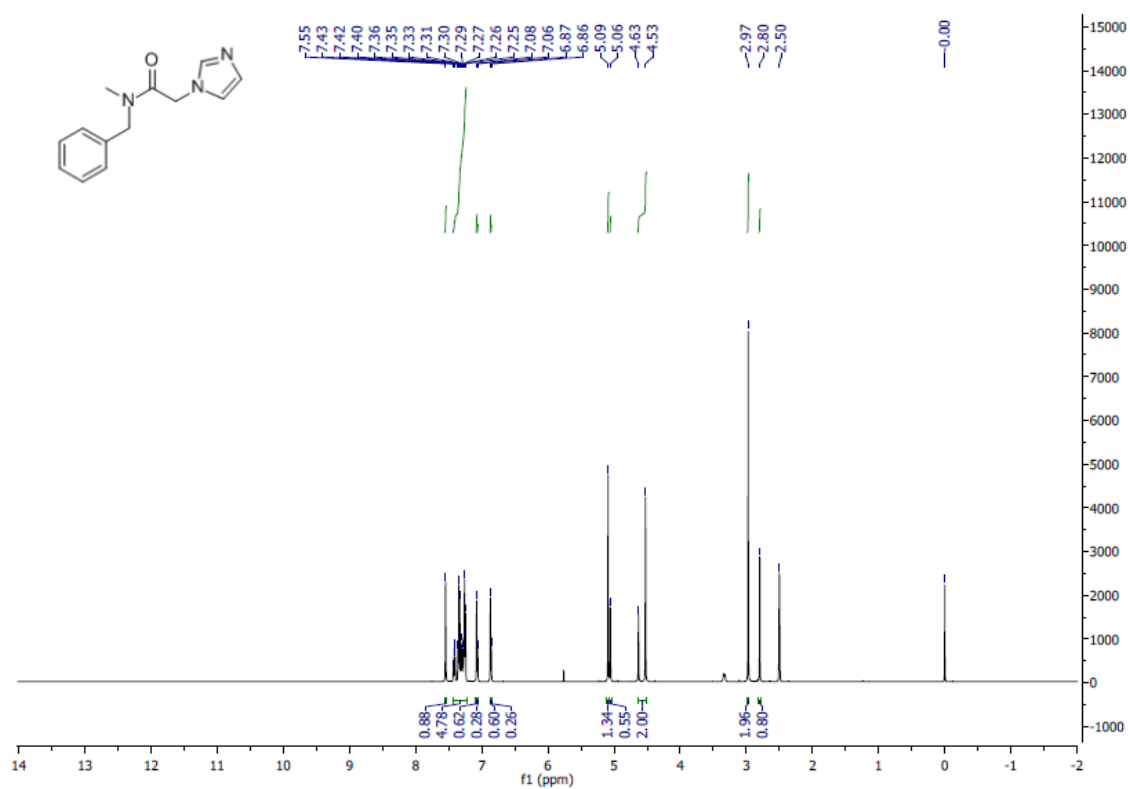


Figure S9.  $^1\text{H}$  NMR (500 MHz,  $\text{DMSO-}d_6$ ) of compound 7g.

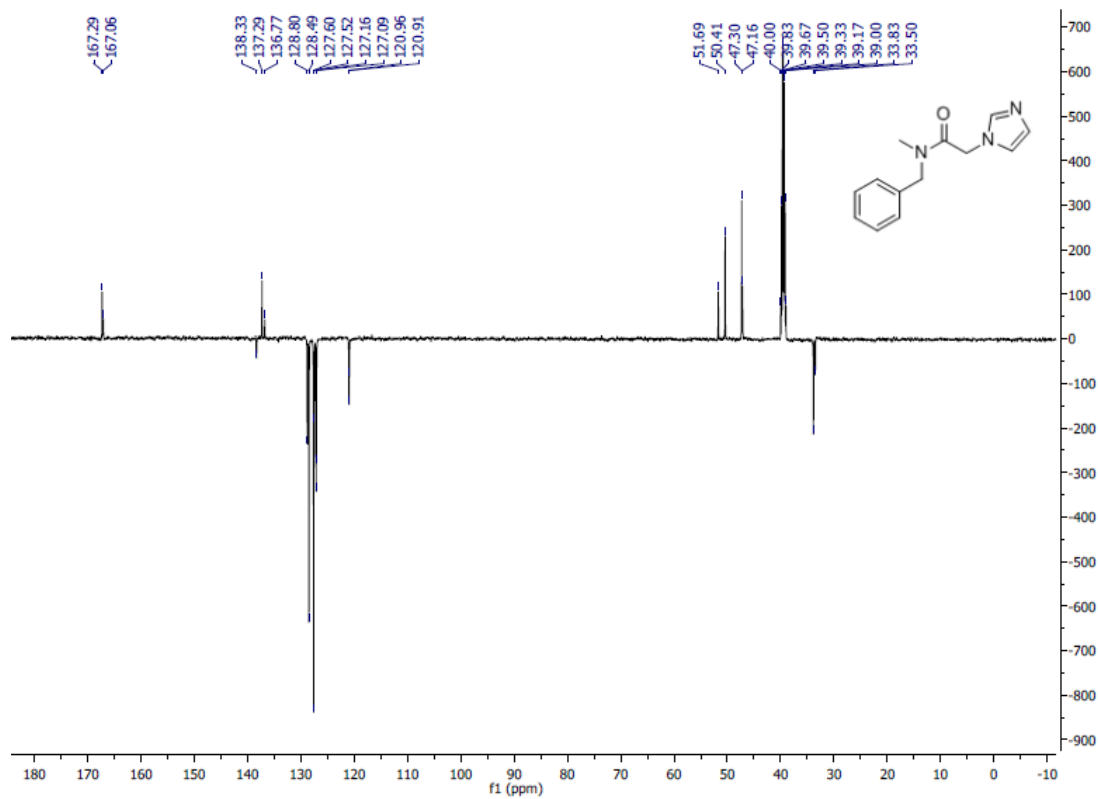


Figure S10.  $^{13}\text{C}$  NMR (125 MHz,  $\text{DMSO-}d_6$ ) of compound 7g.

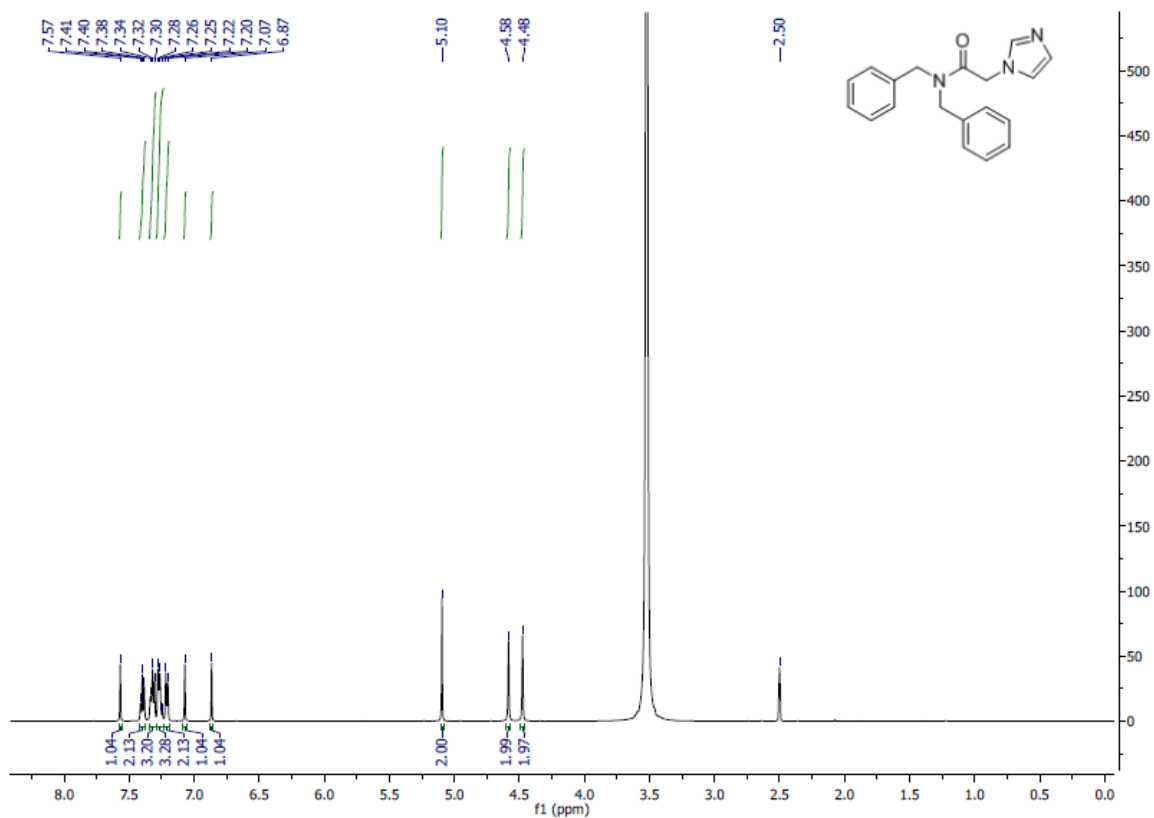


Figure S11.  $^1\text{H}$  NMR (500 MHz,  $\text{DMSO-}d_6$ ) of compound 7h.

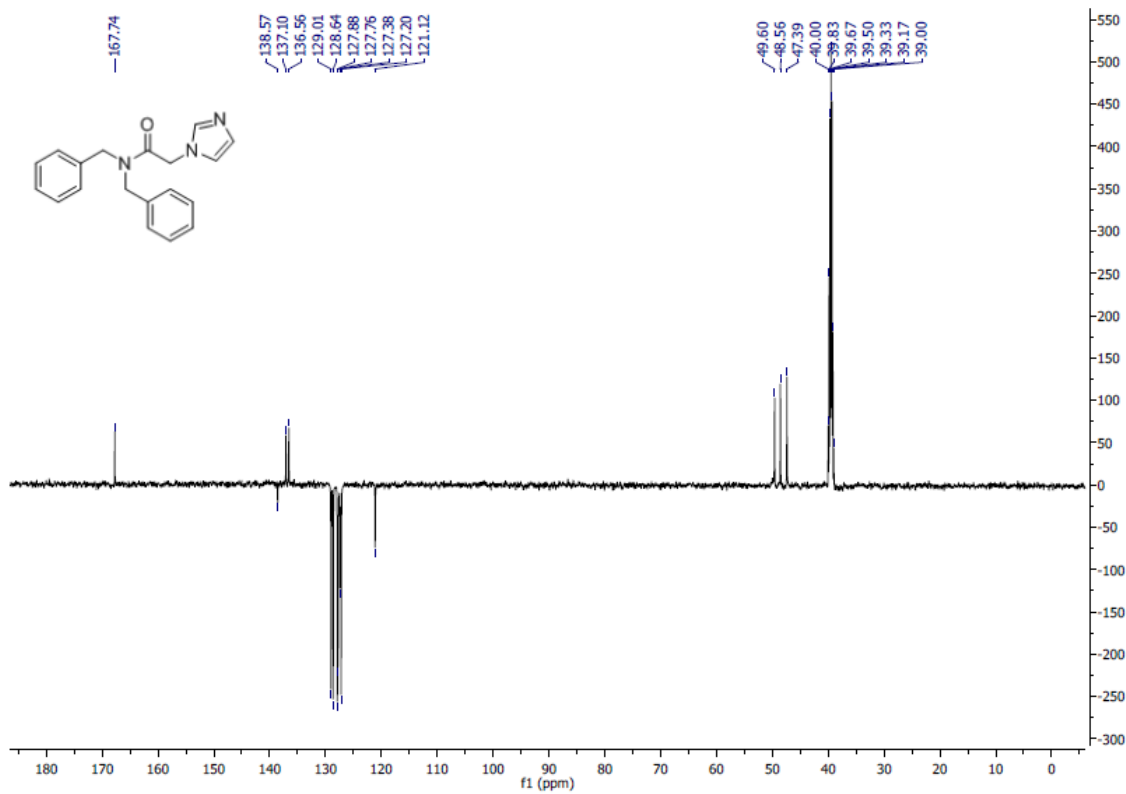
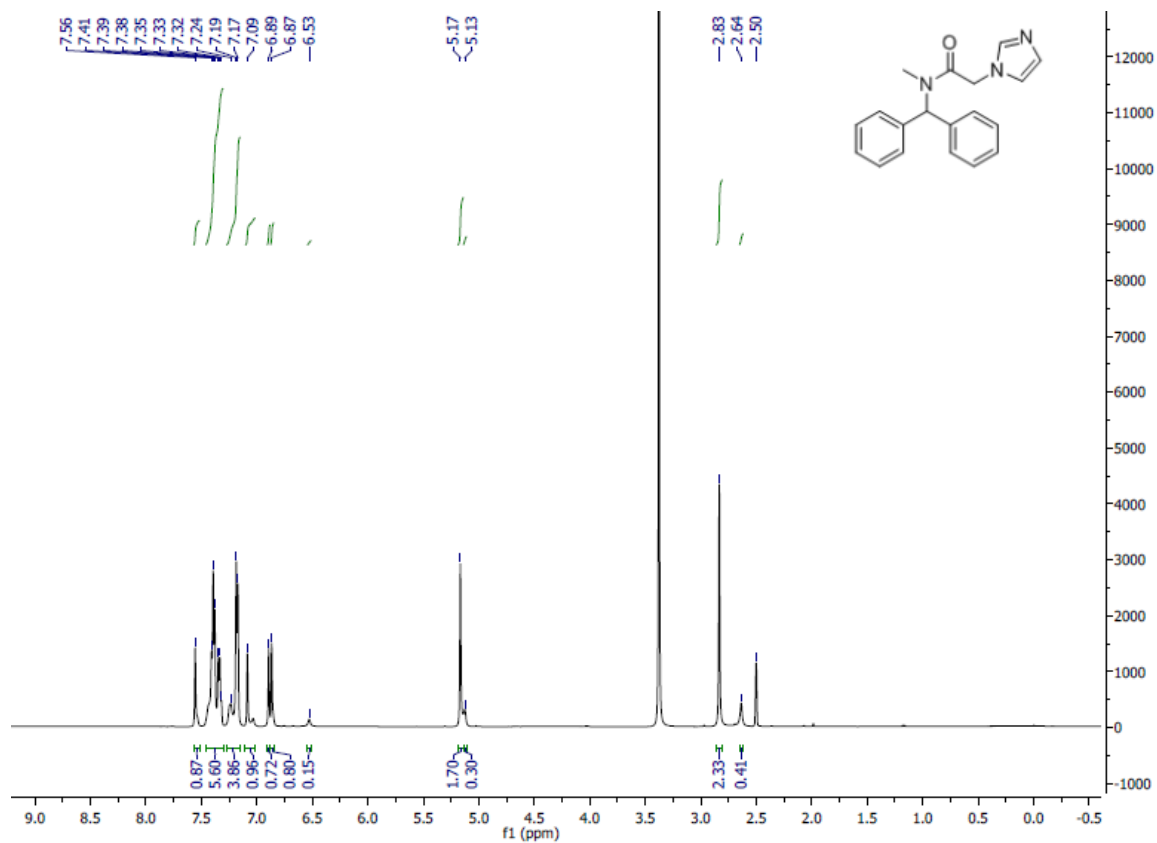
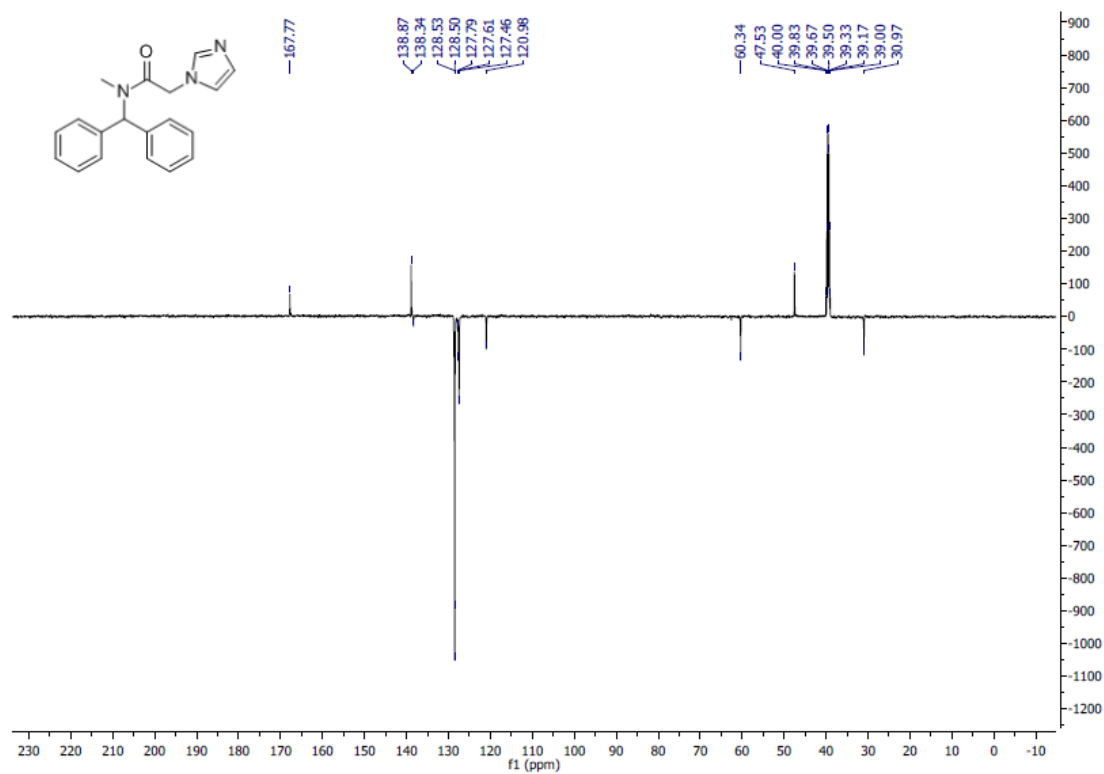


Figure S12.  $^{13}\text{C}$  NMR (125 MHz,  $\text{DMSO-}d_6$ ) of compound 7h.



**Figure S13.** <sup>1</sup>H NMR (500 MHz, DMSO-*d*<sub>6</sub>) of compound **7i**.



**Figure S14.** <sup>13</sup>C NMR (125 MHz, DMSO-*d*<sub>6</sub>) of compound **7i**.

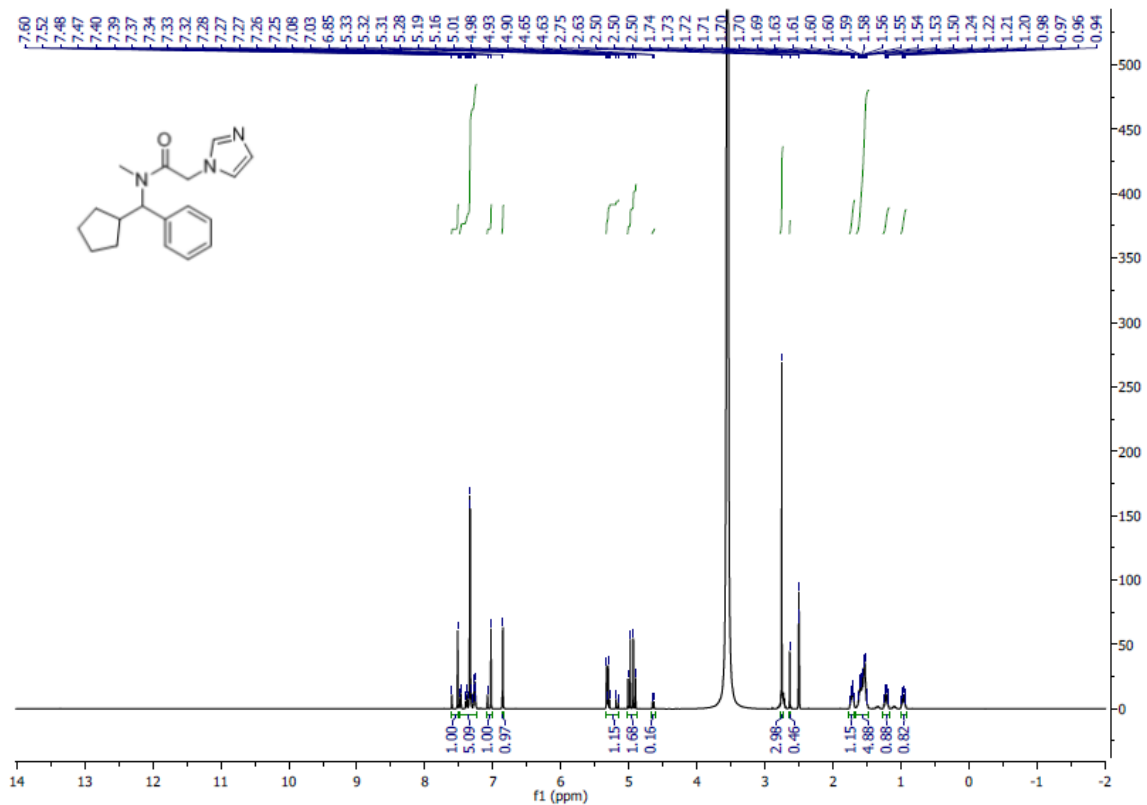


Figure S15. <sup>1</sup>H NMR (500 MHz, DMSO-*d*<sub>6</sub>) of compound 7j.

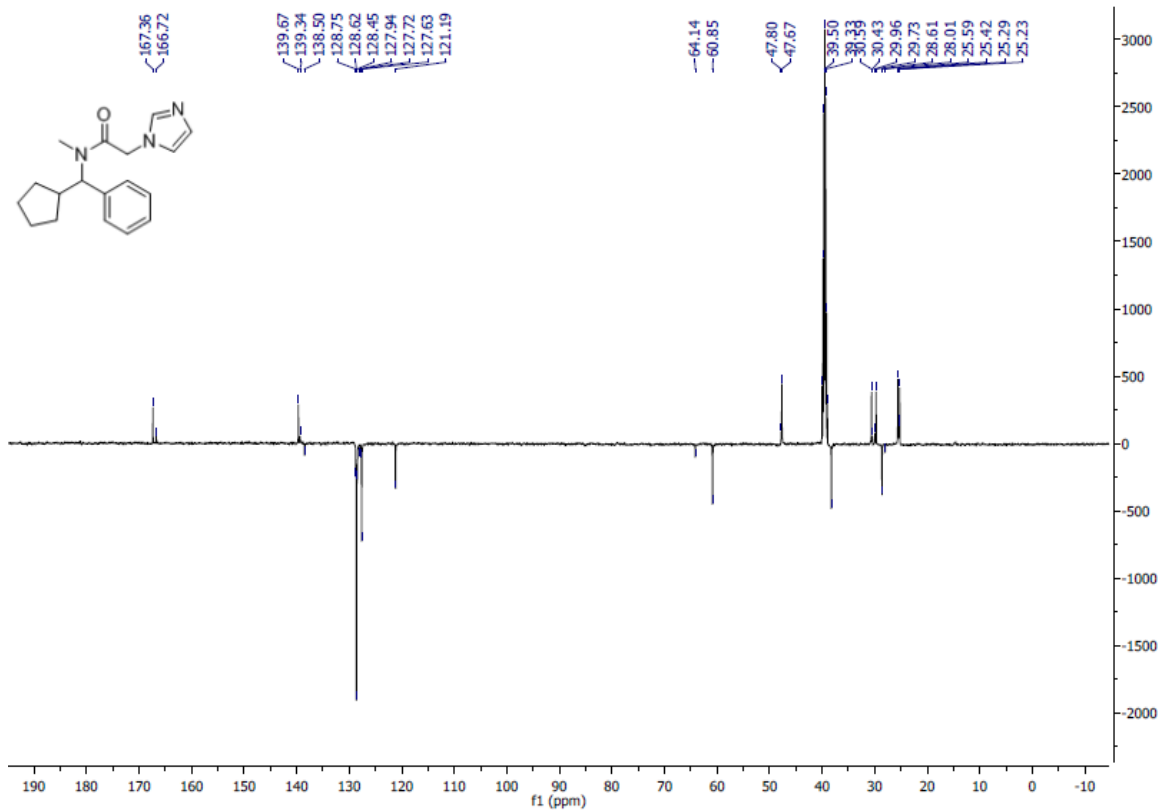


Figure S16. <sup>13</sup>C NMR (125 MHz, DMSO-*d*<sub>6</sub>) of compound 7j.

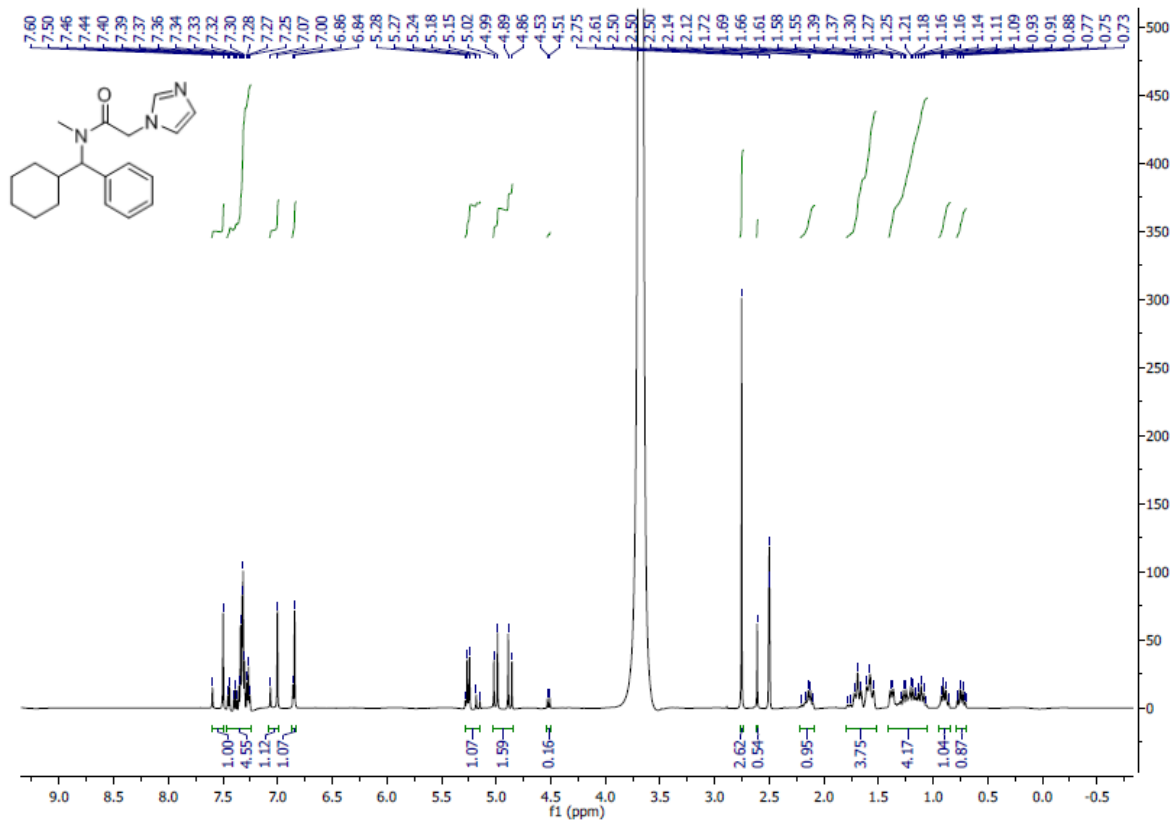


Figure S17. <sup>1</sup>H NMR (500 MHz, DMSO-*d*<sub>6</sub>) of compound 7k.

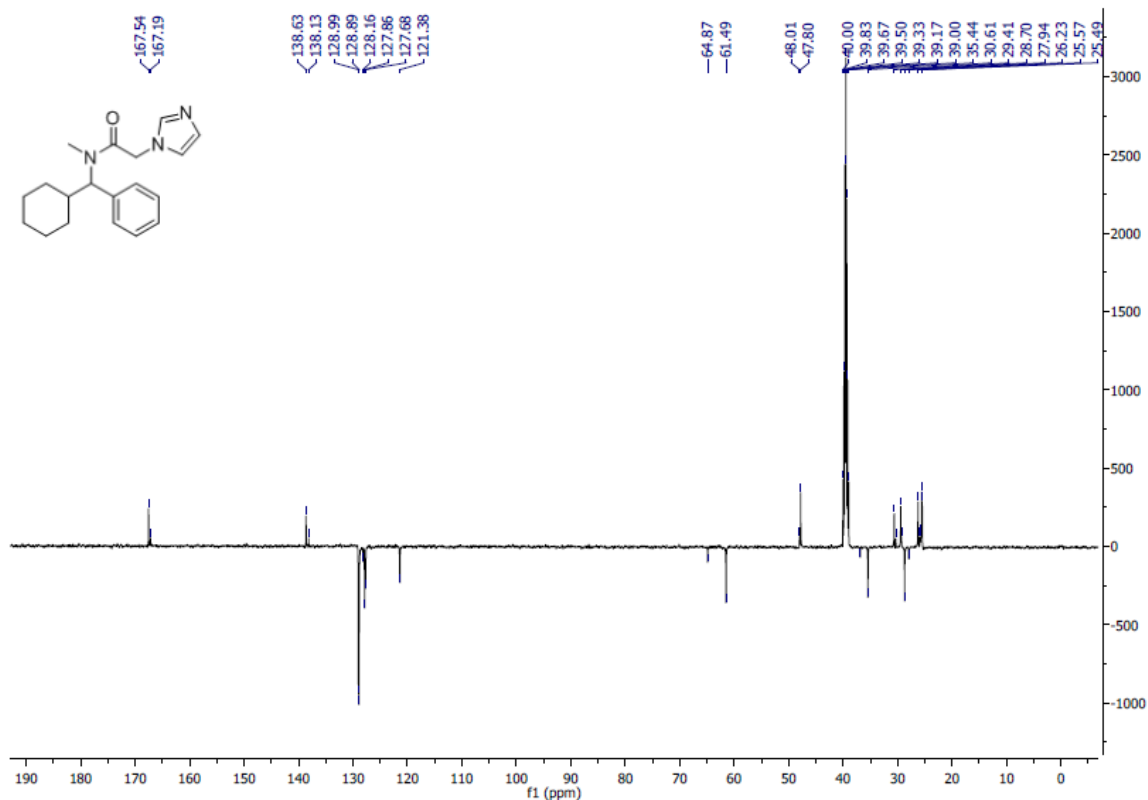
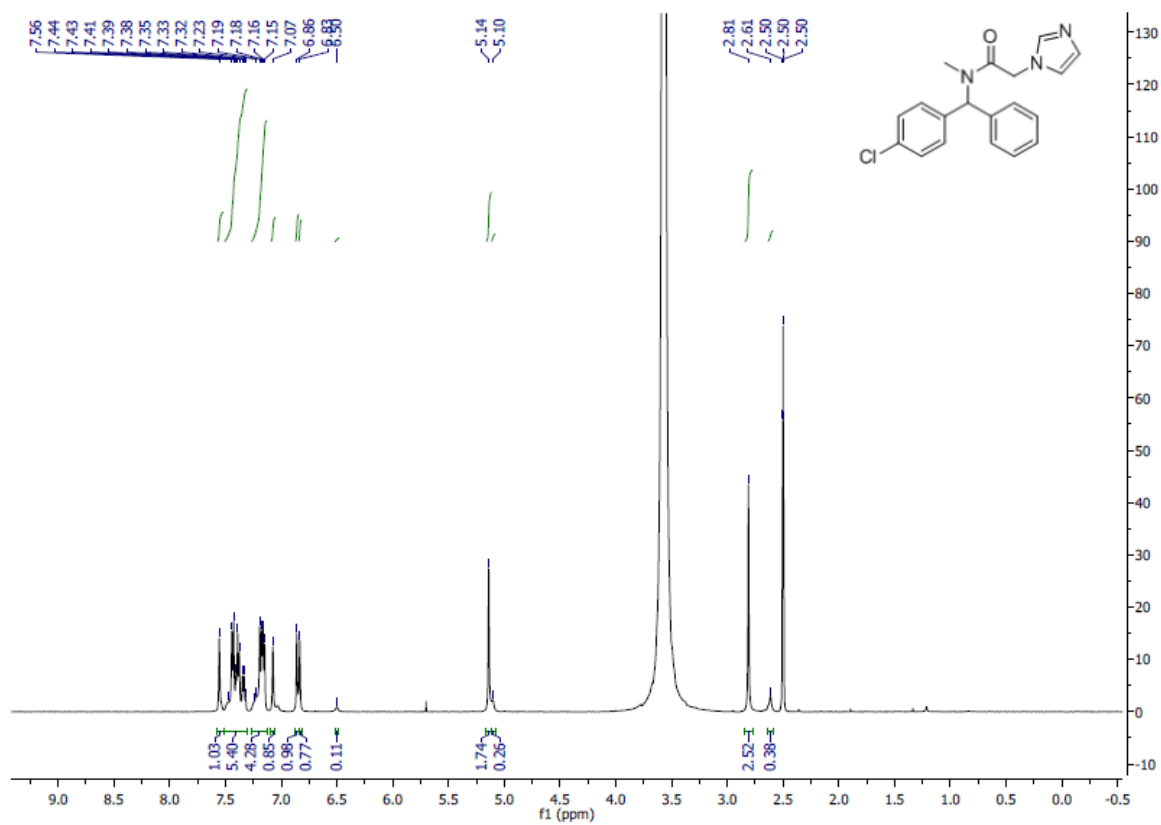
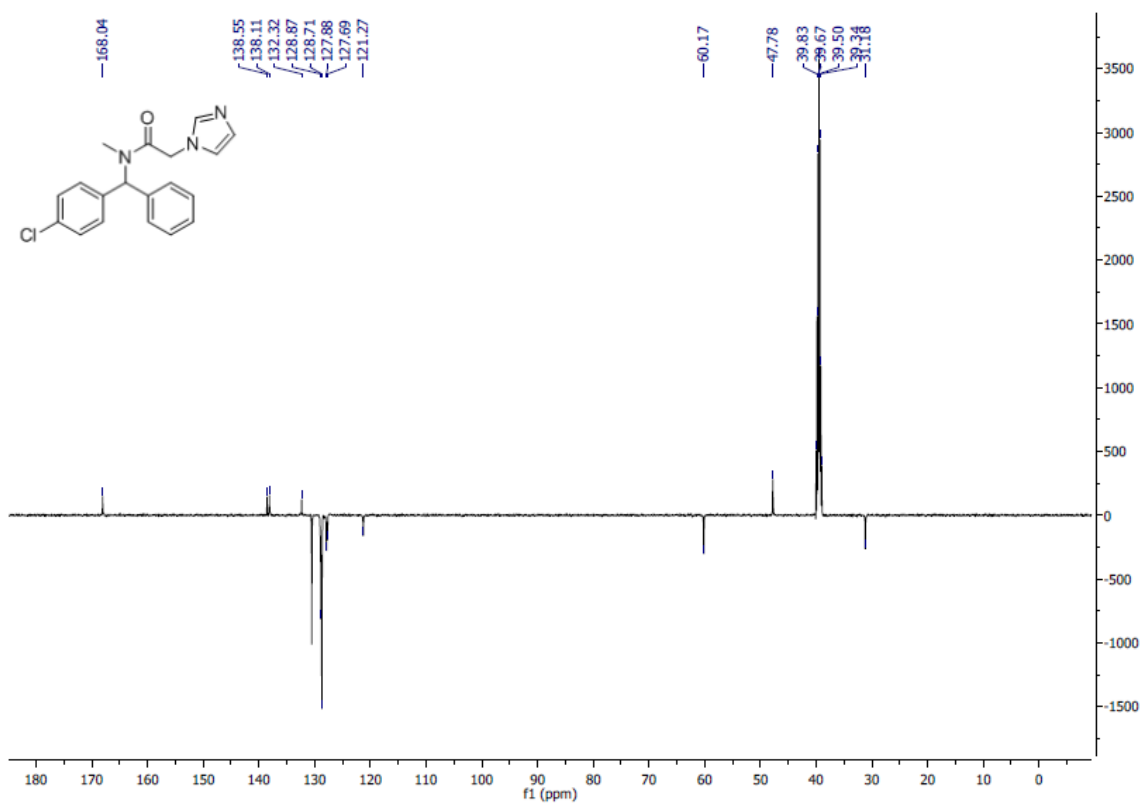


Figure S18. <sup>13</sup>C NMR (125 MHz, DMSO-*d*<sub>6</sub>) of compound 7k.





**Figure S19.**  $^1\text{H}$  NMR (500 MHz,  $\text{DMSO-}d_6$ ) of compound **7I**.



**Figure S20.**  $^{13}\text{C}$  NMR (125 MHz,  $\text{DMSO-}d_6$ ) of compound **7I**.

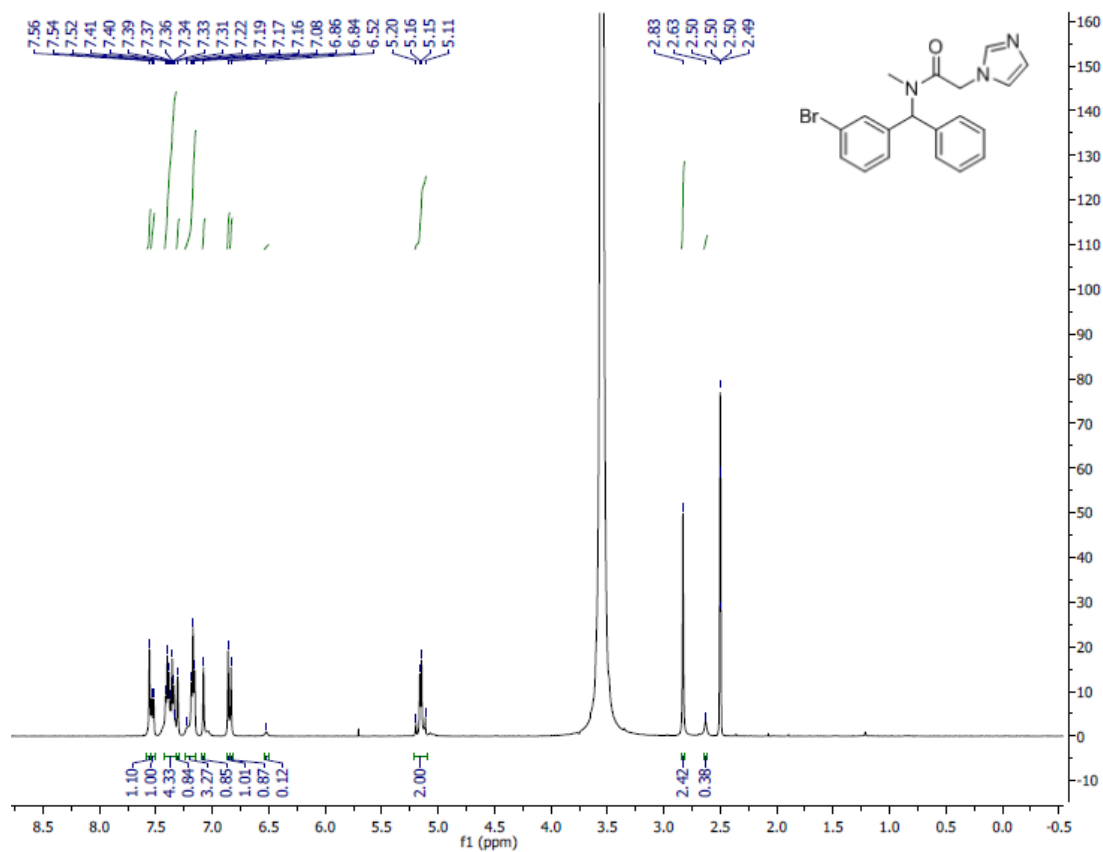


**Figure S21.** <sup>1</sup>H NMR (500 MHz, DMSO-*d*<sub>6</sub>) of compound 7m.

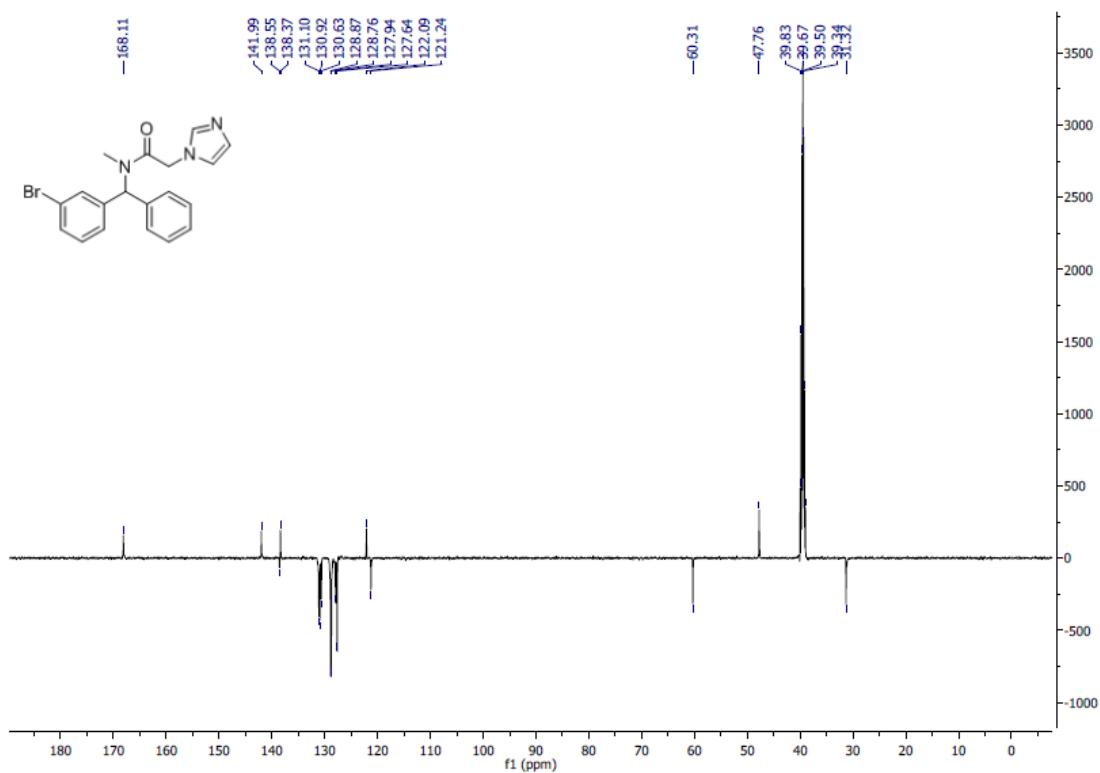


**Figure S22.** <sup>13</sup>C NMR (125 MHz, DMSO-*d*<sub>6</sub>) of compound 7m.

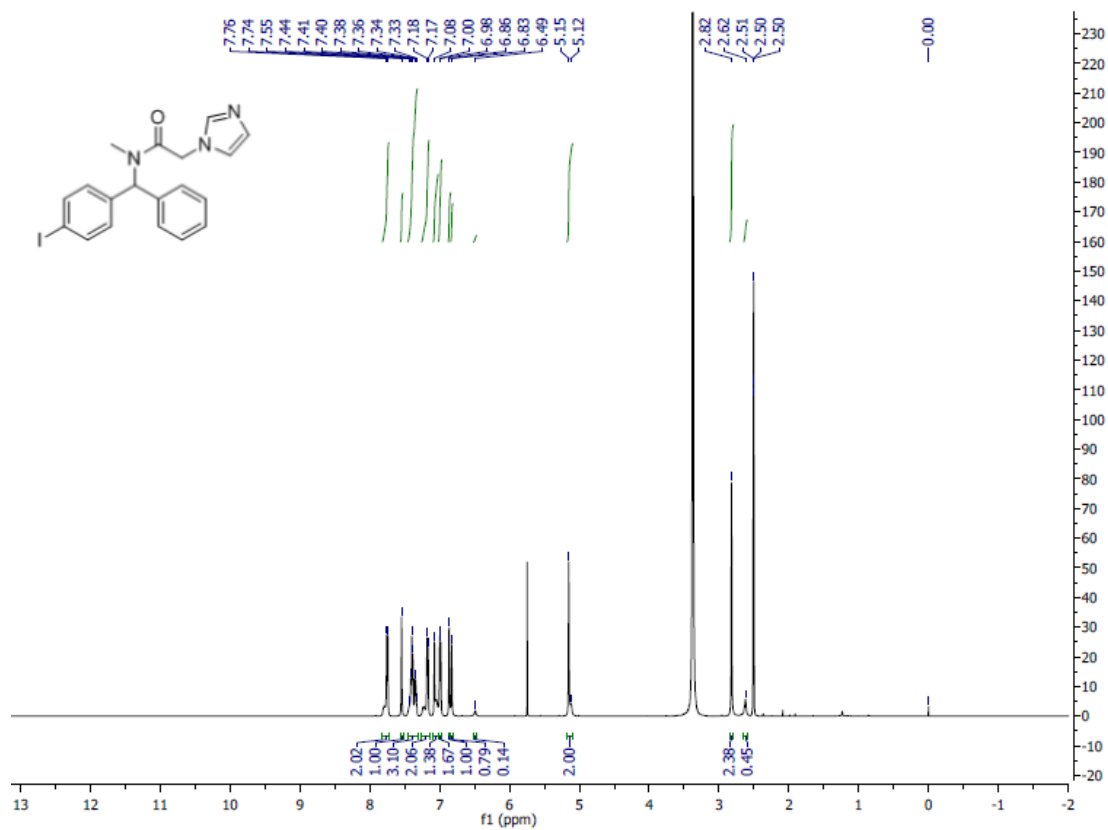


Figure S23.  $^1\text{H}$  NMR (500 MHz,  $\text{DMSO-}d_6$ ) of compound 7n.

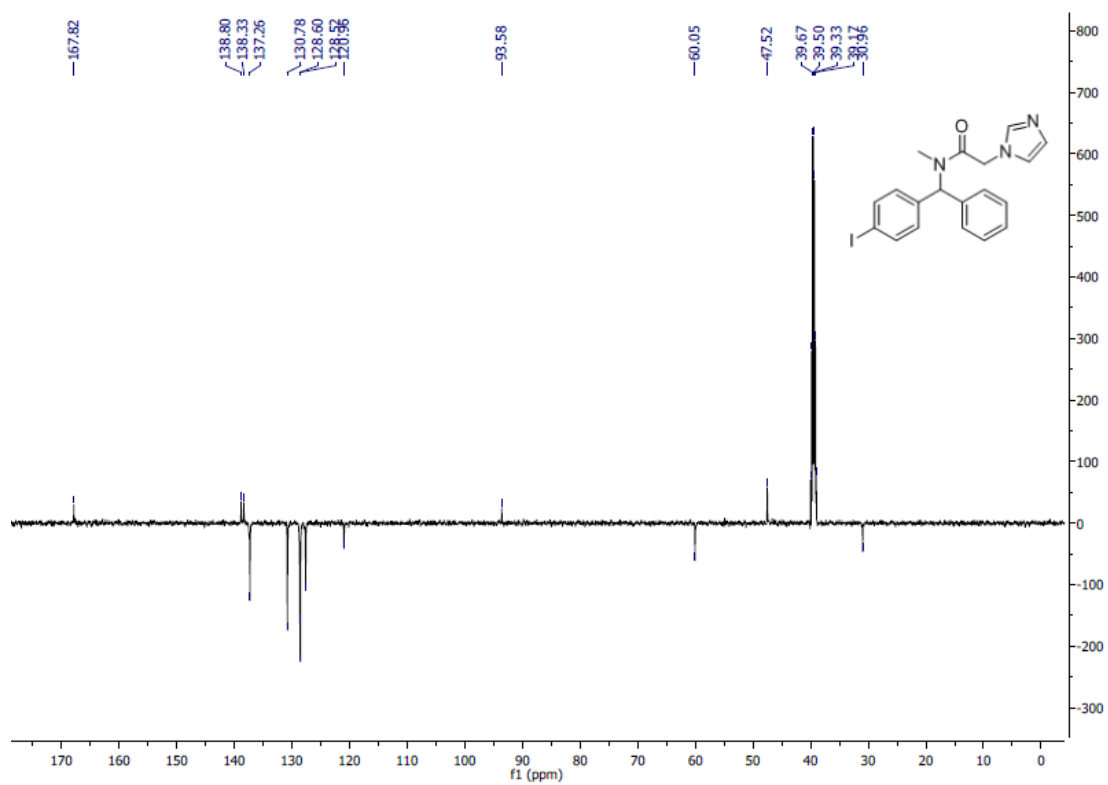
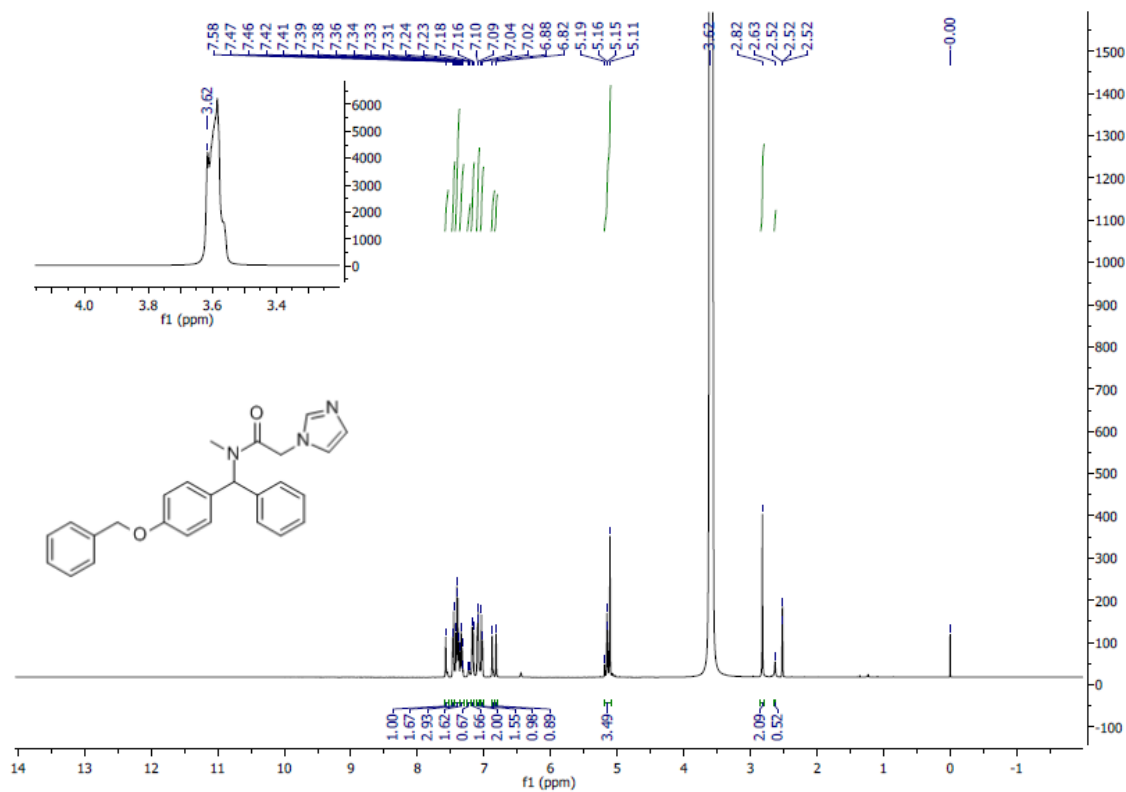
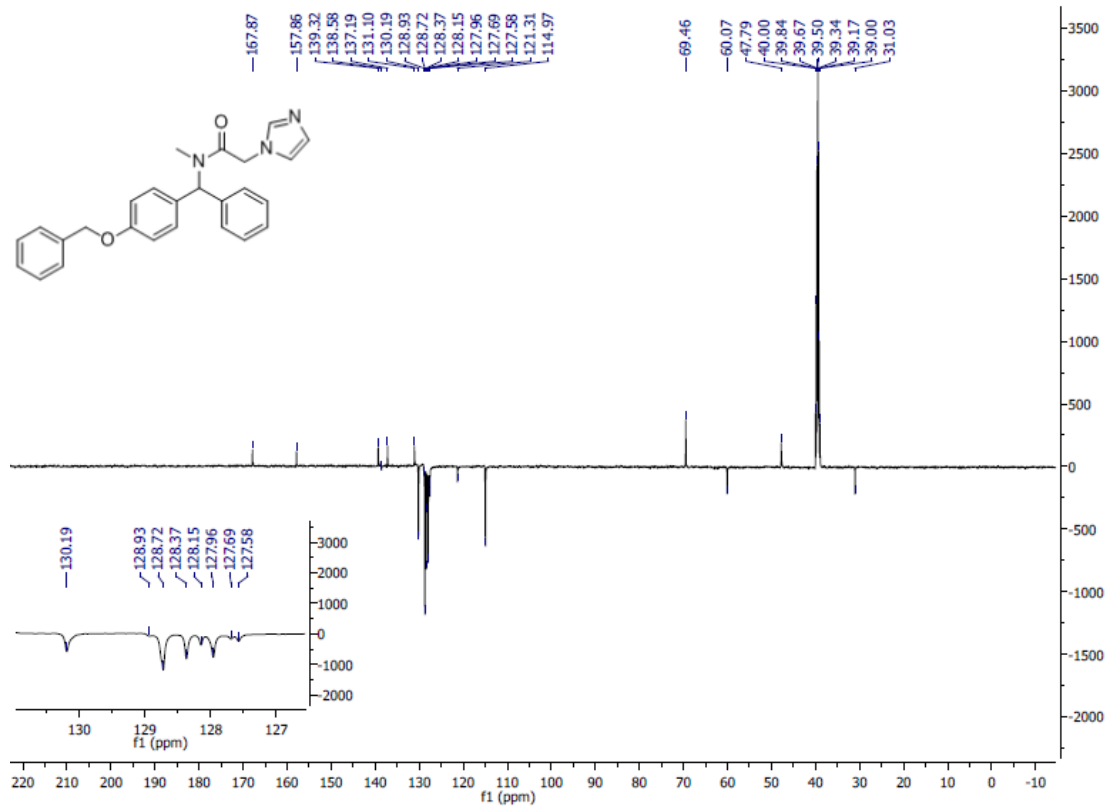


Figure S24.  $^{13}\text{C}$  NMR (125 MHz,  $\text{DMSO-}d_6$ ) of compound 7n.



**Figure S25.** <sup>1</sup>H NMR (500 MHz, DMSO-*d*<sub>6</sub>) of compound **7o**.



**Figure S26.** <sup>13</sup>C NMR (125 MHz, DMSO-*d*<sub>6</sub>) of compound **7o**.

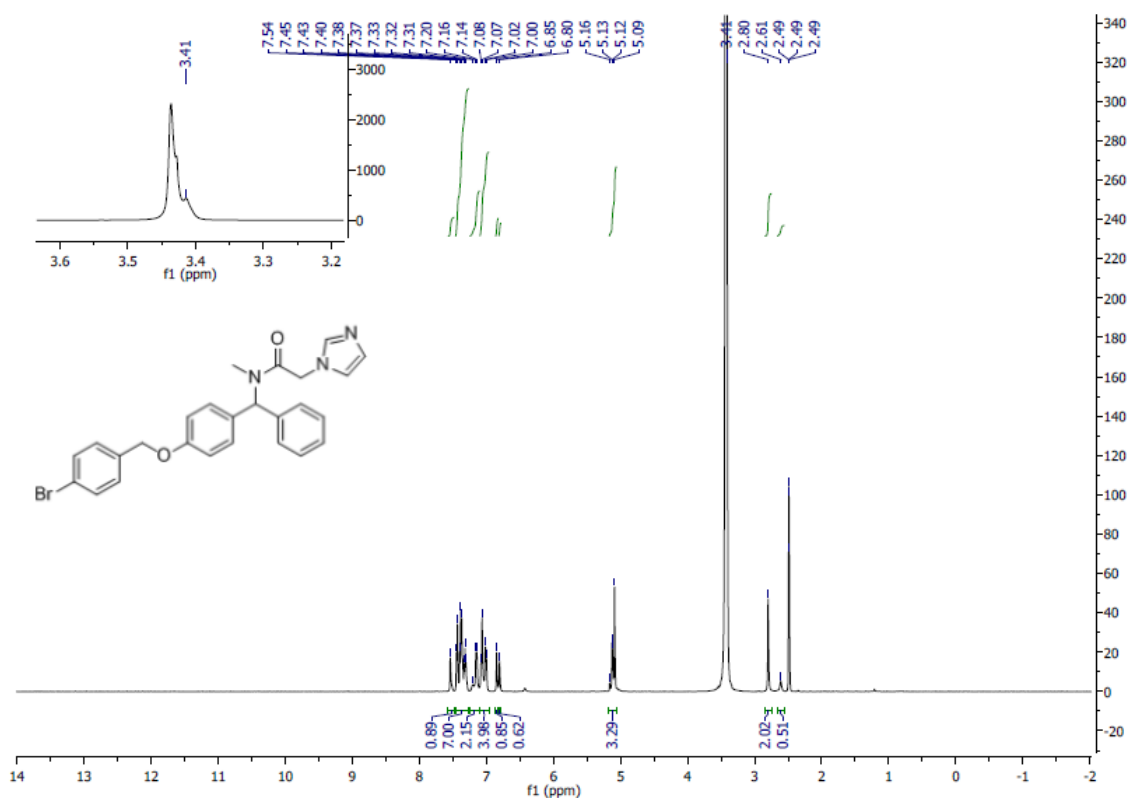


Figure S27.  $^1\text{H NMR}$  (500 MHz,  $\text{DMSO-}d_6$ ) of compound 7p.

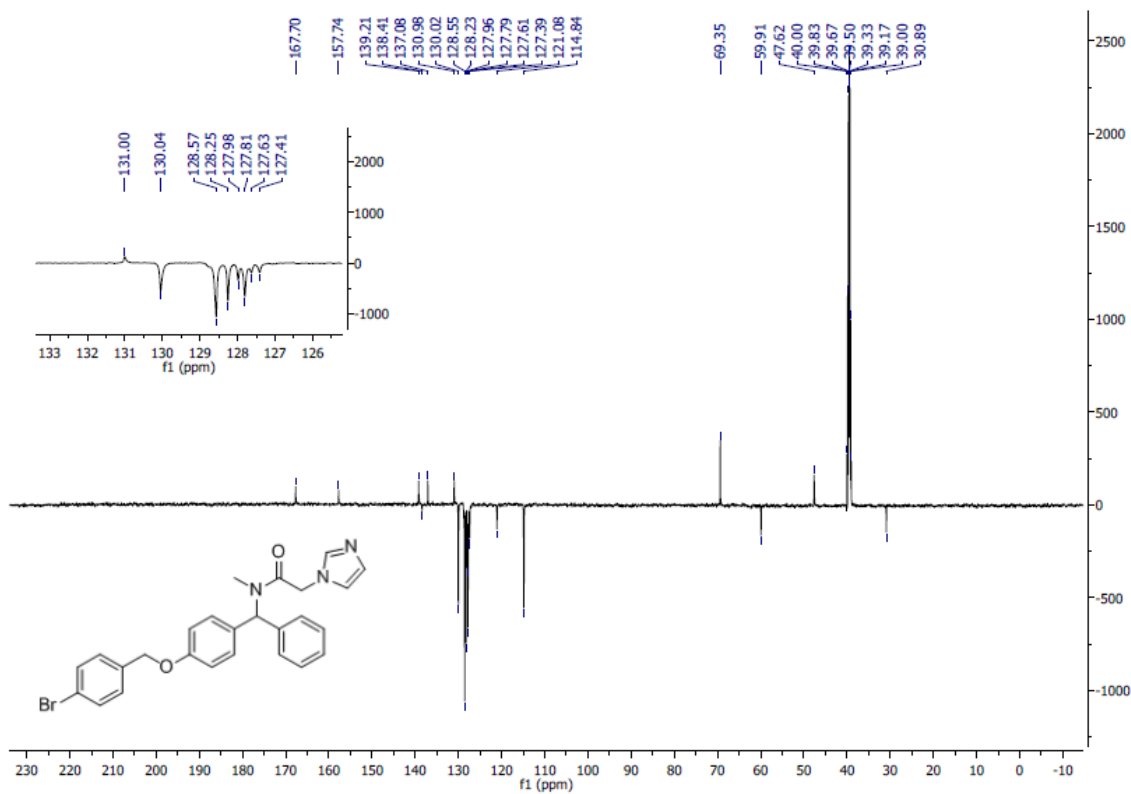
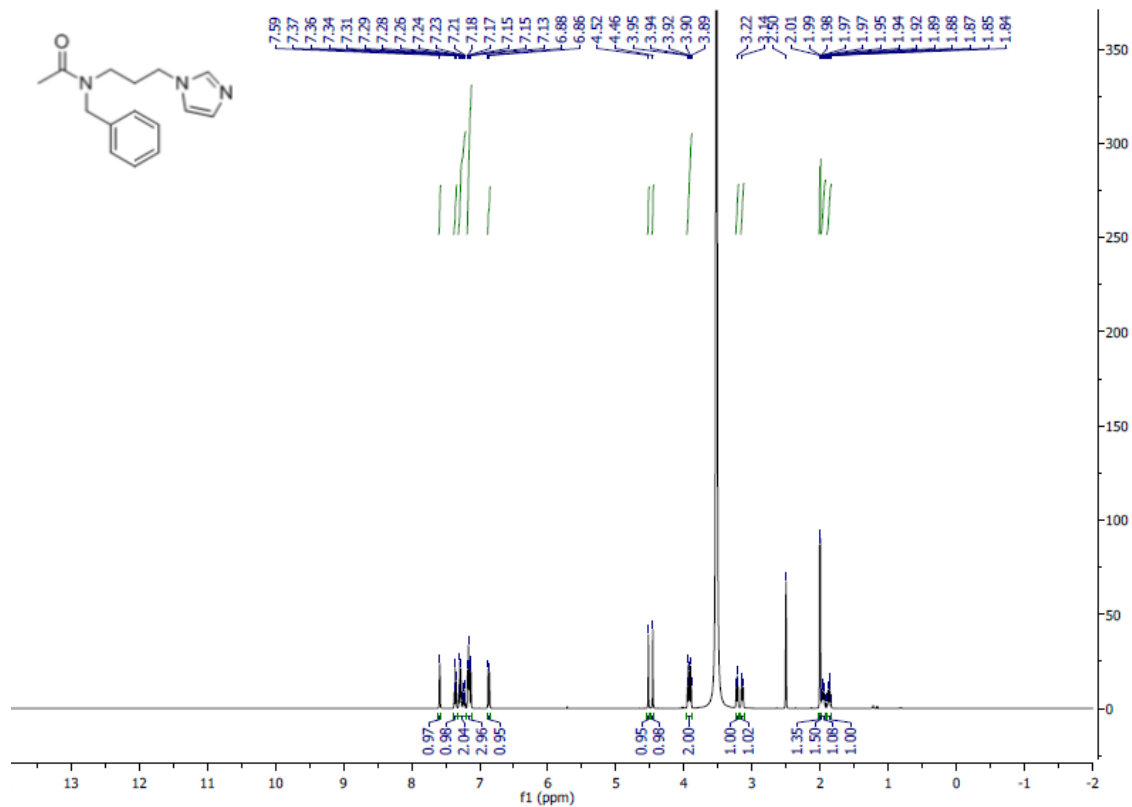
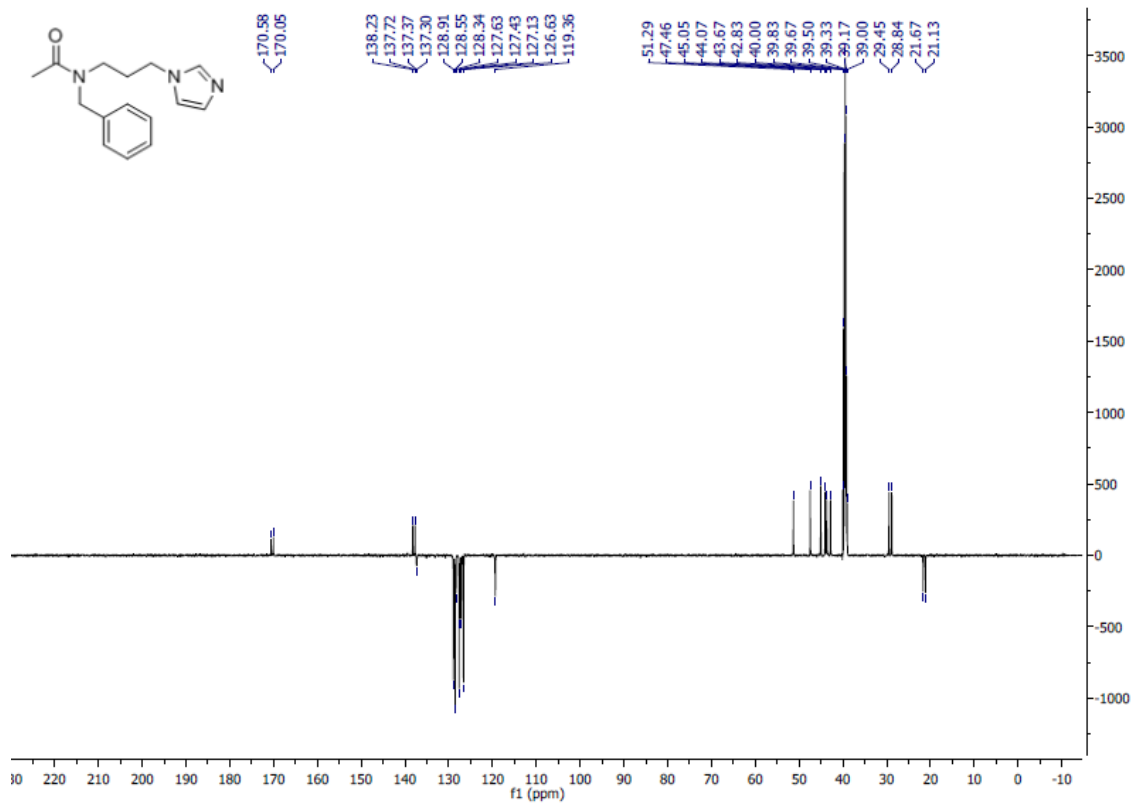


Figure S28.  $^{13}\text{C NMR}$  (125 MHz,  $\text{DMSO-}d_6$ ) of compound 7p.



**Figure S29.** <sup>1</sup>H NMR (500 MHz, DMSO-*d*<sub>6</sub>) of compound 11a.



**Figure S30.** <sup>13</sup>C NMR (125 MHz, DMSO-*d*<sub>6</sub>) of compound 11a.

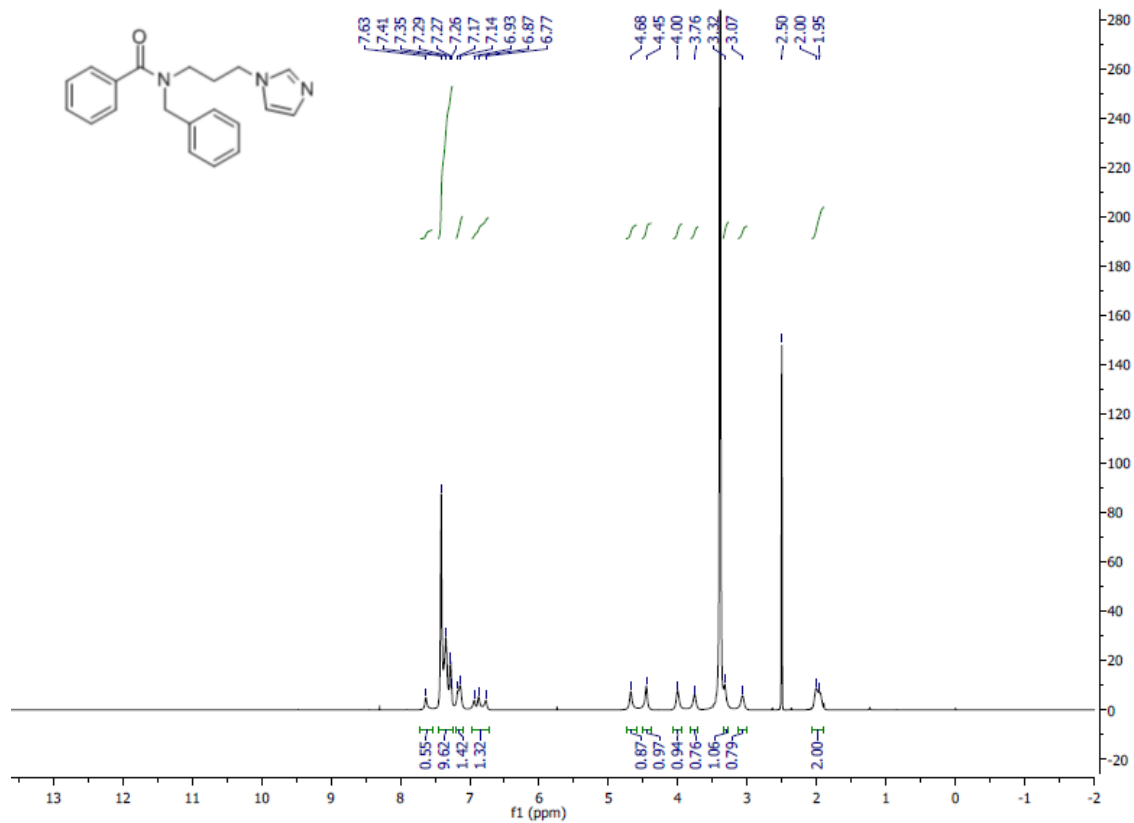


Figure S31. <sup>1</sup>H NMR (500 MHz, DMSO-*d*<sub>6</sub>) of compound 11b.

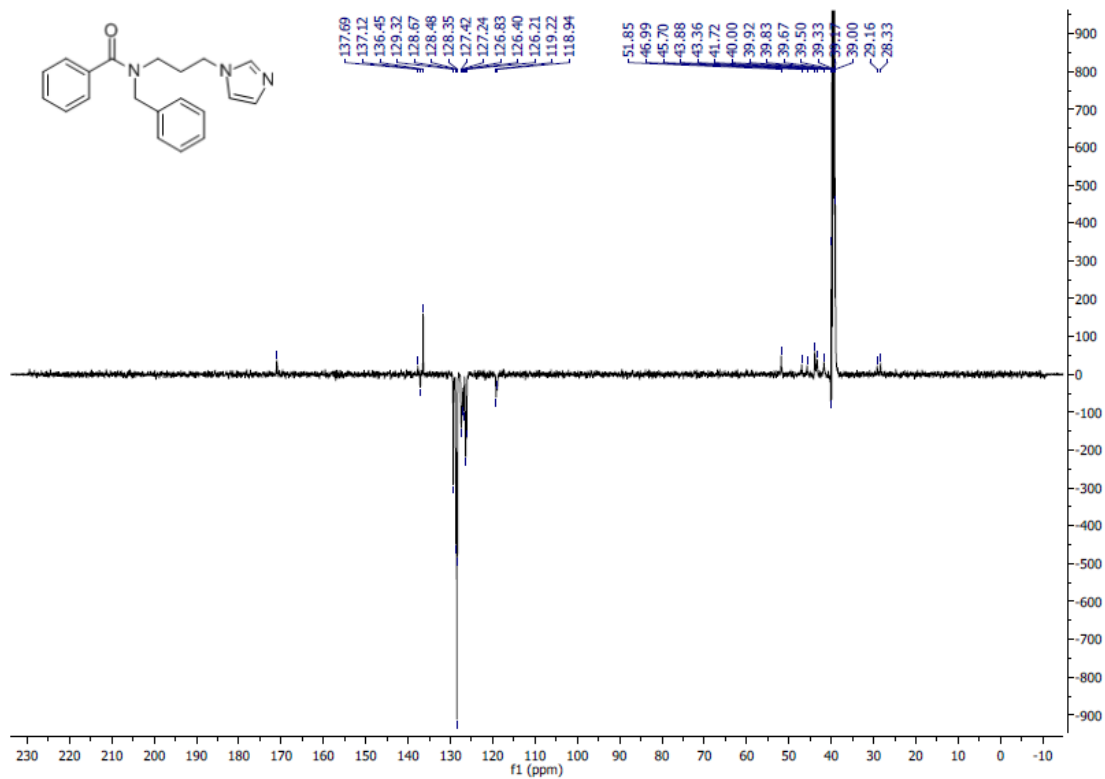


Figure S32. <sup>13</sup>C NMR (125 MHz, DMSO-*d*<sub>6</sub>) of compound 11b.

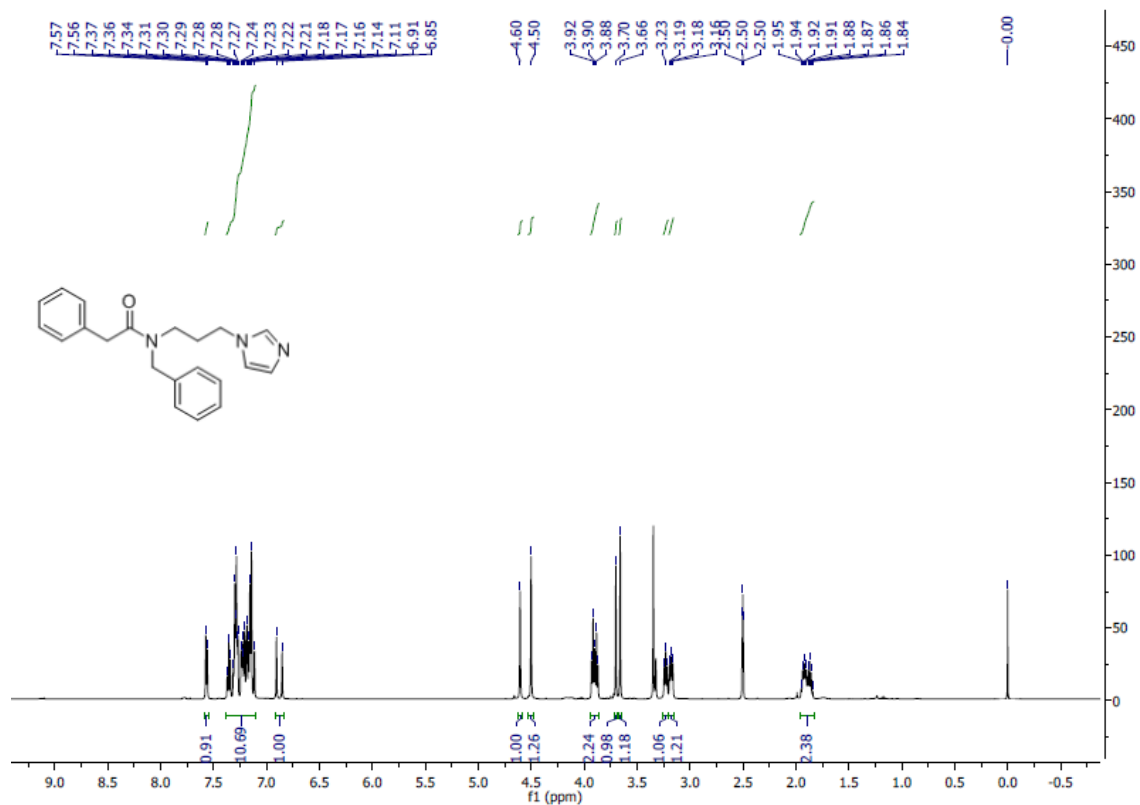


Figure S33. <sup>1</sup>H NMR (500 MHz, DMSO-*d*<sub>6</sub>) of compound 11c.

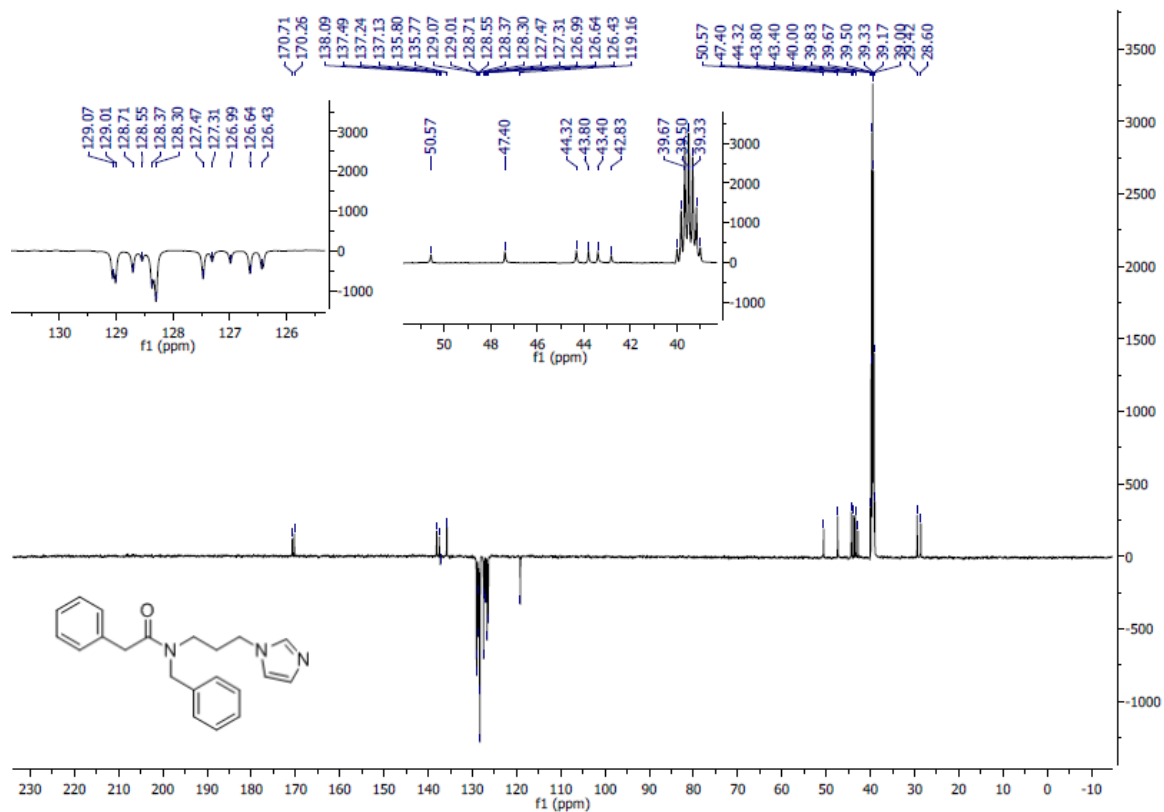
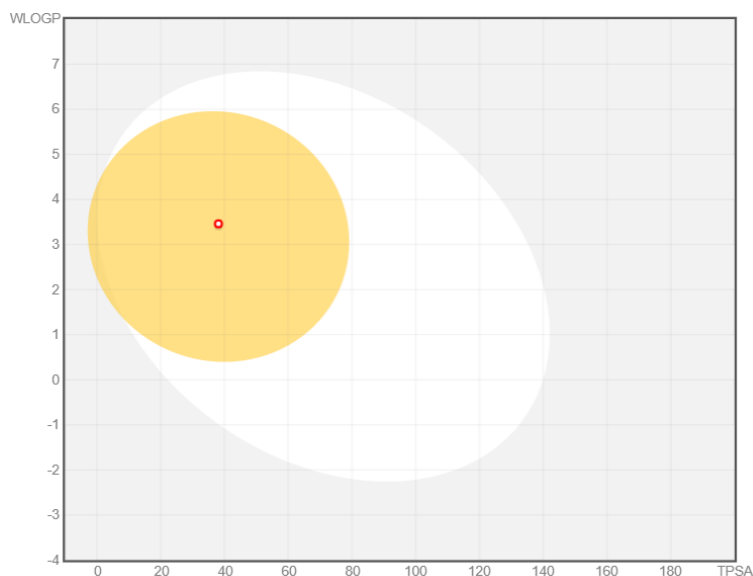


Figure S34. <sup>13</sup>C NMR (125 MHz, DMSO-*d*<sub>6</sub>) of compound 11c.





**Figure S35.** BOILED-Egg plot. Points located in the BOILED-Egg's yellow are the compounds predicted to permeate the BBB passively, differently the ones in the white are the molecules predicted to be only passively absorbed by the gastrointestinal tract. The red dot indicate that the compound is not transported by the P-glycoprotein.

**Table S2.** Results of SwissADME calculations.

Formula	$C_{19}H_{18}ClN_3O$
MW	339.82
#Heavy atoms	24
#Aromatic heavy atoms	17
Fraction Csp3	0.16
#Rotatable bonds	6
#H-bond acceptors	2
#H-bond donors	0
MR	94.99
TPSA	38.13
iLOGP	2.7
XLOGP3	3.46
WLOGP	3.46

---

MLOGP	2.55
Silicos-IT Log P	3.12
Consensus Log P	3.06
ESOL Log S	-4.25
ESOL Solubility (mg/ml)	1.89E-02
ESOL Solubility (mol/l)	5.56E-05
ESOL Class	Moderately soluble
Ali Log S	-3.94
Ali Solubility (mg/ml)	3.88E-02
Ali Solubility (mol/l)	1.14E-04
Ali Class	Soluble
Silicos-IT LogSw	-6.15
Silicos-IT Solubility (mg/ml)	2.39E-04
Silicos-IT Solubility (mol/l)	7.03E-07
Silicos-IT class	Poorly soluble
GI absorption	High
BBB permeant	Yes
Pgp substrate	No
CYP1A2 inhibitor	Yes
CYP2C19 inhibitor	Yes
CYP2C9 inhibitor	Yes
CYP2D6 inhibitor	Yes
CYP3A4 inhibitor	Yes
log Kp (cm/s)	-5.92
Lipinski #violations	0
Ghose #violations	0
Veber #violations	0
Egan #violations	0
Muegge #violations	0

---

Bioavailability Score	0.55
PAINS #alerts	0
Brenk #alerts	0
Leadlikeness #violations	0
Synthetic Accessibility	2.74

**Table S3.** Results of pkCSM calculations.

Property	Model Name	Predicted Value
Absorption	Water solubility	-3.102 log mol/L
Absorption	Caco2 permeability	1.82 log Papp in 10 <sup>-6</sup> cm/s
Absorption	Intestinal absorption (human)	94.698 % Absorbed
Absorption	Skin Permeability	-2.739 log Kp
Absorption	P-glycoprotein substrate	Yes
Absorption	P-glycoprotein I inhibitor	Yes
Absorption	P-glycoprotein II inhibitor	Yes
Distribution	VDss (human)	0.715
Distribution	Fraction unbound (human)	0.019
Distribution	BBB permeability	0.265 log BB
Distribution	CNS permeability	-1.482 log PS
Metabolism	CYP2D6 substrate	No
Metabolism	CYP3A4 substrate	Yes
Metabolism	CYP1A2 inhibitor	Yes
Metabolism	CYP2C19 inhibitor	Yes
Metabolism	CYP2C9 inhibitor	No
Metabolism	CYP2D6 inhibitor	Yes
Metabolism	CYP3A4 inhibitor	Yes
Excretion	Total Clearance	0.662 log ml/min/kg
Excretion	Renal OCT2 substrate	Yes
Toxicity	AMES toxicity	No

Toxicity	Max. tolerated dose (human)	0.854 log mg/kg/day
Toxicity	hERG I inhibitor	No
Toxicity	hERG II inhibitor	Yes
Toxicity	Oral Rat Acute Toxicity (LD50)	2.236 mol/kg
Toxicity	Oral Rat Chronic Toxicity (LOAEL)	1.246 log mg/kg_bw/day
Toxicity	Hepatotoxicity	No
Toxicity	Skin Sensitisation	No
Toxicity	T.Pyriformis toxicity	0.285 log ug/L
Toxicity	Minnow toxicity	1.058 log mM

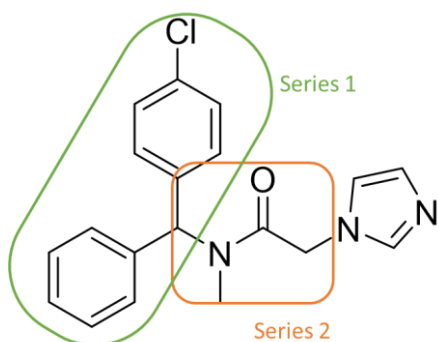


**Figure S36.** Series 1 and 2 of the scaffold-hopping analysis in **71**.

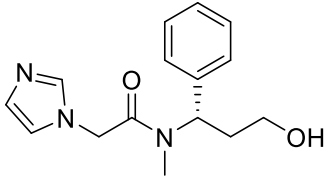
**Table S4.** Series 1 derived from isosteric replacement.

Entry	Structure	Predicted pIC <sub>50</sub>
1		6.6
2		6.4

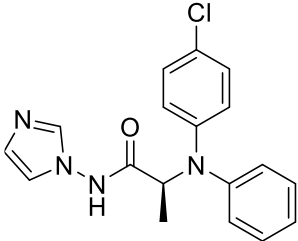
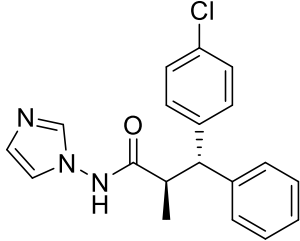
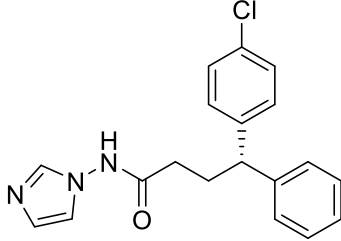
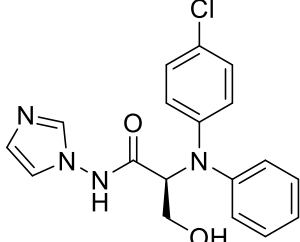
---

3		6.3
4		6.3
5		6.3
6		6.3
7		6.2
8		6.2
9		6.1

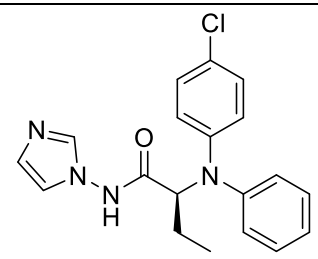
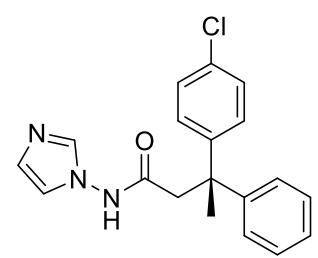
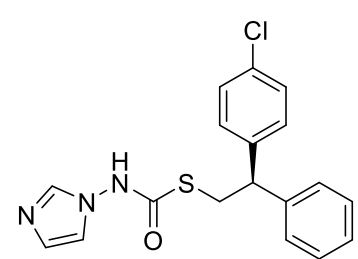
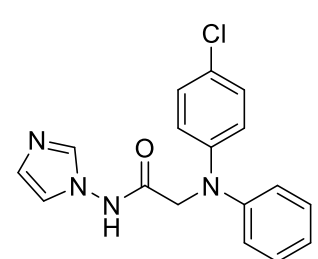
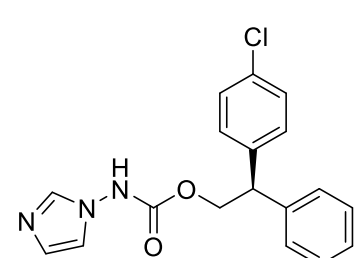
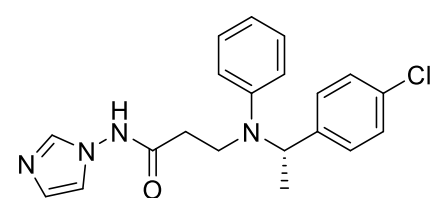
---

10		6.1
----	---	-----

**Table S5.** Series 2 derived from isosteric replacement.

Entry	Structure	Predicted $pIC_{50}$
1		6.2
2		6
3		6
4		6

---

5		6
6		6
7		5.9
8		5.9
9		5.9
10		5.9

---

# Growing the molecular architecture of imidazole-like ligands in HO-1 complexes

Giuseppe Floresta <sup>a,1,\*</sup>, Antonino N. Fallica <sup>b,1</sup>, Loredana Salerno <sup>b</sup>, Valeria Sorrenti <sup>b</sup>, Valeria Pittalà <sup>b,\*</sup>, Antonio Rescifina <sup>b</sup>

<sup>a</sup> Department of Analytical, Environmental and Forensic Sciences, King's College London, London, UK

<sup>b</sup> Department of Drug and Health Sciences, University of Catania, Catania – Italy

Authors contribution

<sup>1</sup>These authors contributed equally

\*Corresponding authors:

Giuseppe Floresta: giuseppe.floresta@kcl.ac.uk

Valeria Pittalà: vpittala@unict.it

## Table of contents

Fig. S1. Spark's libraries used for the growing experiments	S43
Fig. S2. Forge's parameters used for the conformation hunt	S44
Fig. S3. Forge's parameters used for the alignment	S44
Fig. S4. <sup>1</sup> H NMR (500 MHz, CDCl <sub>3</sub> ) of compound <b>8</b>	S45
Fig. S5. <sup>13</sup> C NMR (125 MHz, CDCl <sub>3</sub> ) of compound <b>8</b>	S45
Fig. S6. <sup>1</sup> H NMR (500 MHz, DMSO- <i>d</i> <sub>6</sub> ) of compound <b>9</b>	S46
Fig. S7. <sup>13</sup> C NMR (125 MHz, DMSO- <i>d</i> <sub>6</sub> ) of compound <b>9</b>	S46
Fig. S8. <sup>1</sup> H NMR (500 MHz, DMSO- <i>d</i> <sub>6</sub> ) of compound <b>10</b>	S47
Fig. S9. <sup>13</sup> C NMR (125 MHz, DMSO- <i>d</i> <sub>6</sub> ) of compound <b>10</b>	S47
Fig. S10. <sup>1</sup> H NMR (500 MHz, CDCl <sub>3</sub> ) of compound <b>11</b>	S48
Fig. S11. <sup>13</sup> C NMR (125 MHz, CDCl <sub>3</sub> ) of compound <b>11</b>	S48
Fig. S12. <sup>1</sup> H NMR (500 MHz, CDCl <sub>3</sub> ) of compound <b>12</b>	S49



Fig. S13. <sup>13</sup> C NMR (125 MHz, CDCl <sub>3</sub> ) of compound <b>12</b>	S49
Fig. S14. <sup>1</sup> H NMR (500 MHz, DMSO- <i>d</i> <sub>6</sub> ) of compound <b>13</b>	S50
Fig. S15. <sup>13</sup> C NMR (125 MHz, DMSO- <i>d</i> <sub>6</sub> ) of compound <b>13</b>	S50
Table S1. Ligand growing molecules resulting from step 1	S51
Table S2. Ligand growing molecules resulting from step 2 (from molecule <b>3</b> )	S62
Table S3. Ligand growing molecules resulting from step 2 (from molecule <b>4</b> )	S73
Table S4. Ligand growing molecules resulting from step 2 (from molecule <b>5</b> )	S87
Table S5. Data used for IC <sub>50</sub> calculations	S98
Fig. S16. 2D interactions of <b>8</b> inside HO-1	S100
Fig. S17. 2D interactions of <b>9</b> inside HO-1	S100
Fig. S18. 2D interactions of <b>10</b> inside HO-1	S101
Fig. S19. 2D interactions of <b>11</b> inside HO-1	S101
Fig. S20. 2D interactions of <b>12</b> inside HO-1	S102
Fig. S21. 2D interactions of <b>13</b> inside HO-1	S102
Fig. S22. Poses of molecule <b>8–13</b> inside HO-1	S103
Fig. S23. Poses of molecule <b>8</b> and <b>9</b> inside HO-1	S103
Fig. S24. Poses of molecule <b>11</b> and <b>13</b> inside HO-1	S104
Fig. S25. Poses of molecule <b>10</b> and <b>12</b> inside HO-1	S104
Fig. S26. BOILED-Egg plot	S105
Table S6. ADMET result for molecules <b>8–13</b> from pkCSM	S105
Table S7. ADMET result for molecules <b>8–13</b> from swissadme	S106

## Spark Search

Calculation Method: Ligand Growing

Select one or more databases to search. Filter by name

Name	Fragments	Description
<input checked="" type="checkbox"/> Crystallographic		
<input checked="" type="checkbox"/> COD		
<input checked="" type="checkbox"/> COD	440047	Crystallography Open Database fragments, crystallographic conformations
<input checked="" type="checkbox"/> Fragments		
<input checked="" type="checkbox"/> ChEMBL		
<input checked="" type="checkbox"/> ChEMBL_common	231851	ChEMBL_26 common fragments (seen >12 times). Released under CC BY-SA 3.0 ( <a href="http://creativecommons.org/licenses/by-sa/3.0/">http://creativecommons.org/licenses/by-sa/3.0/</a> ).
<input checked="" type="checkbox"/> Commercial		
<input checked="" type="checkbox"/> VeryCommon	67888	Commercial very common fragments (seen more than 725 times)
<input checked="" type="checkbox"/> Common	112949	Commercial common fragments (seen 215-724 times)
<input checked="" type="checkbox"/> LessCommon	211480	Commercial less common fragments (seen 65-214 times)
<input checked="" type="checkbox"/> Reagents		
<input checked="" type="checkbox"/> eMolecules		
<input checked="" type="checkbox"/> eMolecules_acid	46489	Acids, delete the -COOH (eMolecules Tier 1,2,3 2021-03-01)
<input checked="" type="checkbox"/> eMolecules_aci...	26209	Acids, keep the CO (eMolecules Tier 1,2,3 2021-03-01)
<input checked="" type="checkbox"/> eMolecules_alc...	21329	Aliphatic alcohols, delete the O (eMolecules Tier 1,2,3 2021-03-01)
<input checked="" type="checkbox"/> eMolecules_alc...	22344	Alcohols, keep the O (eMolecules Tier 1,2,3 2021-03-01)
<input checked="" type="checkbox"/> eMolecules_alip...	9883	Aliphatic halide (eMolecules Tier 1,2,3 2021-03-01)
<input checked="" type="checkbox"/> eMolecules_alky...	3501	Alkynes, delete the -C#C (eMolecules Tier 1,2,3 2021-03-01)
<input checked="" type="checkbox"/> eMolecules_aro...	9931	Aromatic alcohols, keep the O (eMolecules Tier 1,2,3 2021-03-01)
<input checked="" type="checkbox"/> eMolecules_aro...	20716	Aromatic amines, keep the N (eMolecules Tier 1,2,3 2021-03-01)
<input checked="" type="checkbox"/> eMolecules_aro...	45893	Aromatic halide (eMolecules Tier 1,2,3 2021-03-01)
<input checked="" type="checkbox"/> eMolecules_bor...	4705	Aromatic boronic acids, delete -B(OH) <sub>2</sub> (eMolecules Tier 1,2,3 2021-03-01)
<input checked="" type="checkbox"/> eMolecules_cya...	17340	Cyano groups, delete -CN (eMolecules Tier 1,2,3 2021-03-01)
<input checked="" type="checkbox"/> eMolecules_isoc...	593	Isocyanates, keep -NCO (eMolecules Tier 1,2,3 2021-03-01)
<input checked="" type="checkbox"/> eMolecules_olefin	3797	Olefins, delete the -C=C (eMolecules Tier 1,2,3 2021-03-01)
<input checked="" type="checkbox"/> eMolecules_pri...	21917	Primary aliphatic amines, delete N (eMolecules Tier 1,2,3 2021-03-01)
<input checked="" type="checkbox"/> eMolecules_pri...	12830	Primary aliphatic amines, keep N (eMolecules Tier 1,2,3 2021-03-01)
<input checked="" type="checkbox"/> eMolecules_pri...	7766	Primary aliphatic halide (eMolecules Tier 1,2,3 2021-03-01)
<input checked="" type="checkbox"/> eMolecules_pri...	26281	Primary aromatic amines, delete N (eMolecules Tier 1,2,3 2021-03-01)
<input checked="" type="checkbox"/> eMolecules_red...	24466	Aldehydes/ketones, delete the O and reduce C (eMolecules Tier 1,2,3 2021-03-01)
<input checked="" type="checkbox"/> eMolecules_sec...	17416	Secondary aliphatic amines, keep N (eMolecules Tier 1,2,3 2021-03-01)
<input checked="" type="checkbox"/> eMolecules_sulf...	5252	Sulfonic acids, delete the -SO <sub>2</sub> X (eMolecules Tier 1,2,3 2021-03-01)
<input checked="" type="checkbox"/> eMolecules_sulf...	3160	Sulfonic acids, keep the -SO <sub>2</sub> (eMolecules Tier 1,2,3 2021-03-01)
<input checked="" type="checkbox"/> eMolecules_thiol	826	Aliphatic thiols, delete S (eMolecules Tier 1,2,3 2021-03-01)
<input checked="" type="checkbox"/> eMolecules_thiolS	2143	Thiols, keep S (eMolecules Tier 1,2,3 2021-03-01)
<input checked="" type="checkbox"/> Theoretical		
<input checked="" type="checkbox"/> VEHICLE		
<input checked="" type="checkbox"/> VEHICLE	170467	Ring systems from the VEHICLE database ( <a href="ftp://ftp.ebi.ac.uk/pub/databases/chembi/VEHICLE/">ftp://ftp.ebi.ac.uk/pub/databases/chembi/VEHICLE/</a> ).

**Figure S1.** Spark's libraries used for the growing experiments.

Conformation Hunt   Alignment   Build Model

Calculation Method: [Custom]   Save As...   Delete

Delete existing conformations

Perform Conformation Hunt

Maximum number of conformations   500

No. of high-T dynamics runs for flexible rings   20

Gradient cutoff for conformer minimization   0,100 kcal/mol/A

Filter duplicate conformers at RMS   0,50 A

Energy window   2,50 kcal/mol

Acyclic secondary amide handling   Use input amide geometry

Turn off Coulombic and attractive vdW forces

Use external tool for conformation generation

**Figure S2.** Forge's parameters used for the conformation hunt.

Conformation Hunt   Alignment   Build Model

Calculation Method: Normal   Save As...   Delete

Delete existing alignments

Perform Alignment

Invert achiral imported confs

Take shortcuts in alignments

Maximum-common-substructure conformers and alignment

Matching rules   Normal (element + hybridisation)

Allow conformations to move

Perform Scoring

Score method for multiple references   Weighted Average

Fraction of score from shape similarity   0.50

Reference into db fieldpoints weight   0.50

Hardness of protein excluded volume   Soft

Add/remove field constraints   Mark field points

**Figure S3.** Forge's parameters used for the alignment.

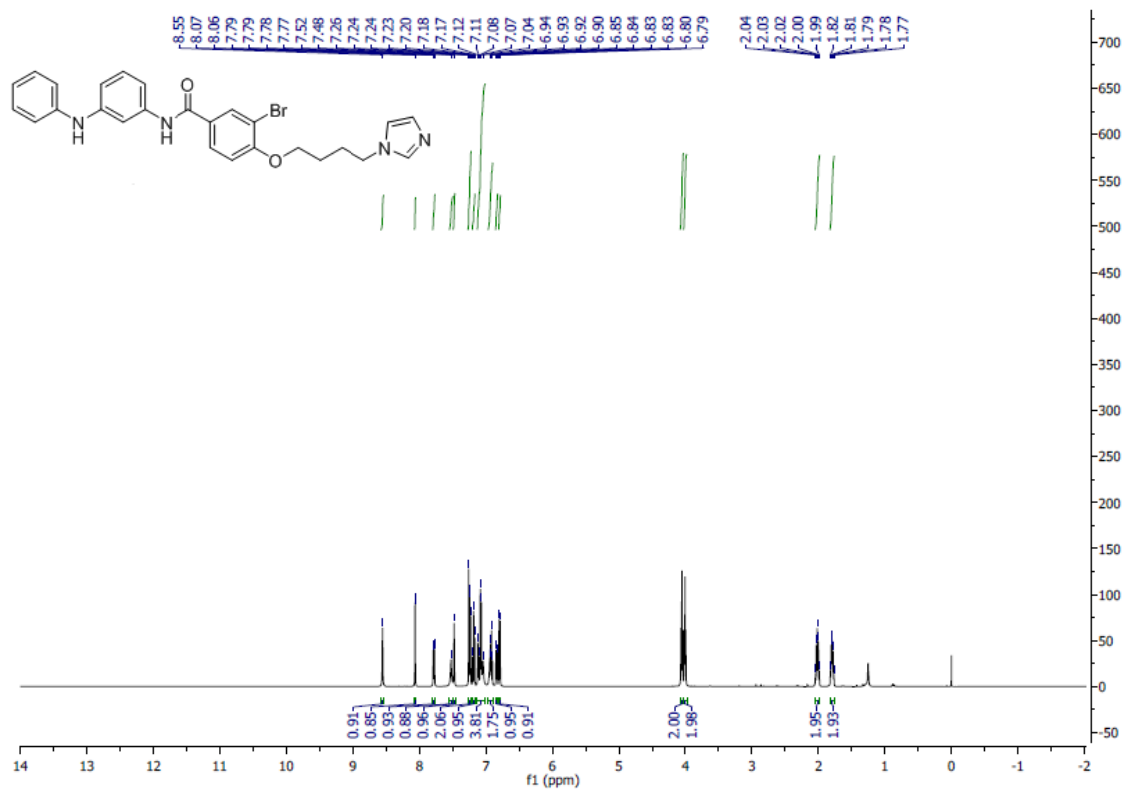


Figure S4. <sup>1</sup>H NMR (500 MHz, CDCl<sub>3</sub>) of compound 8.

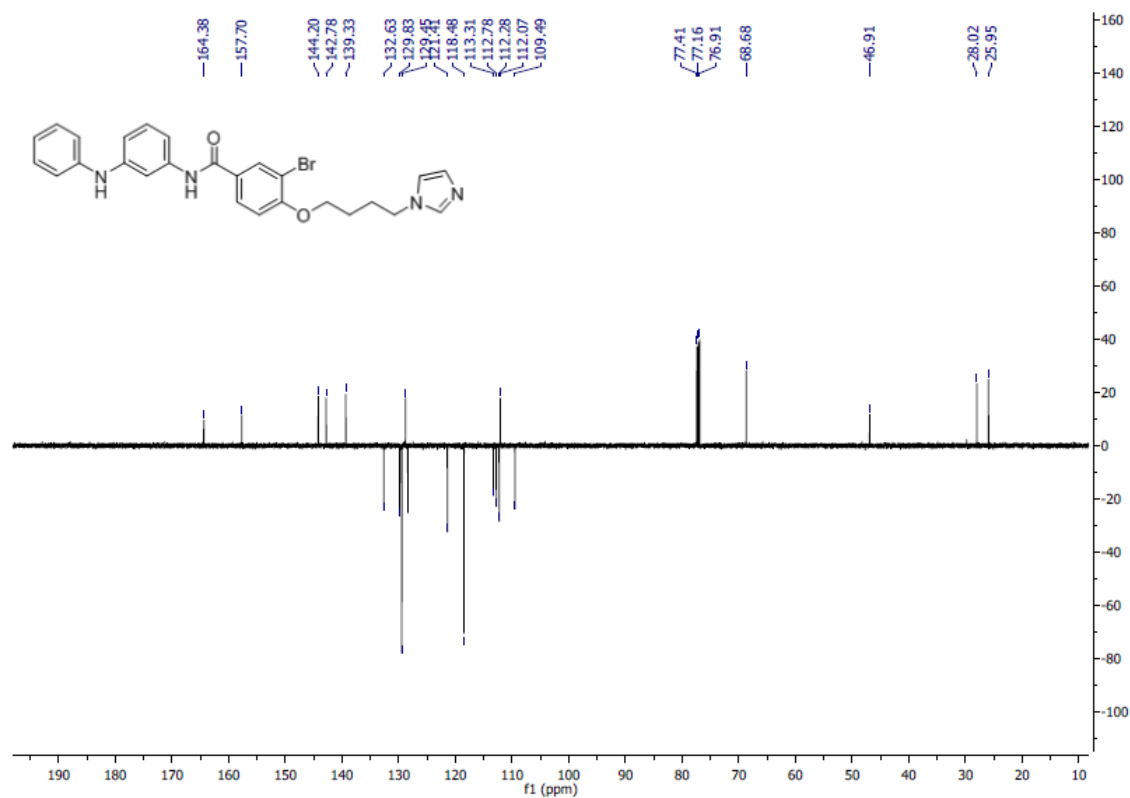
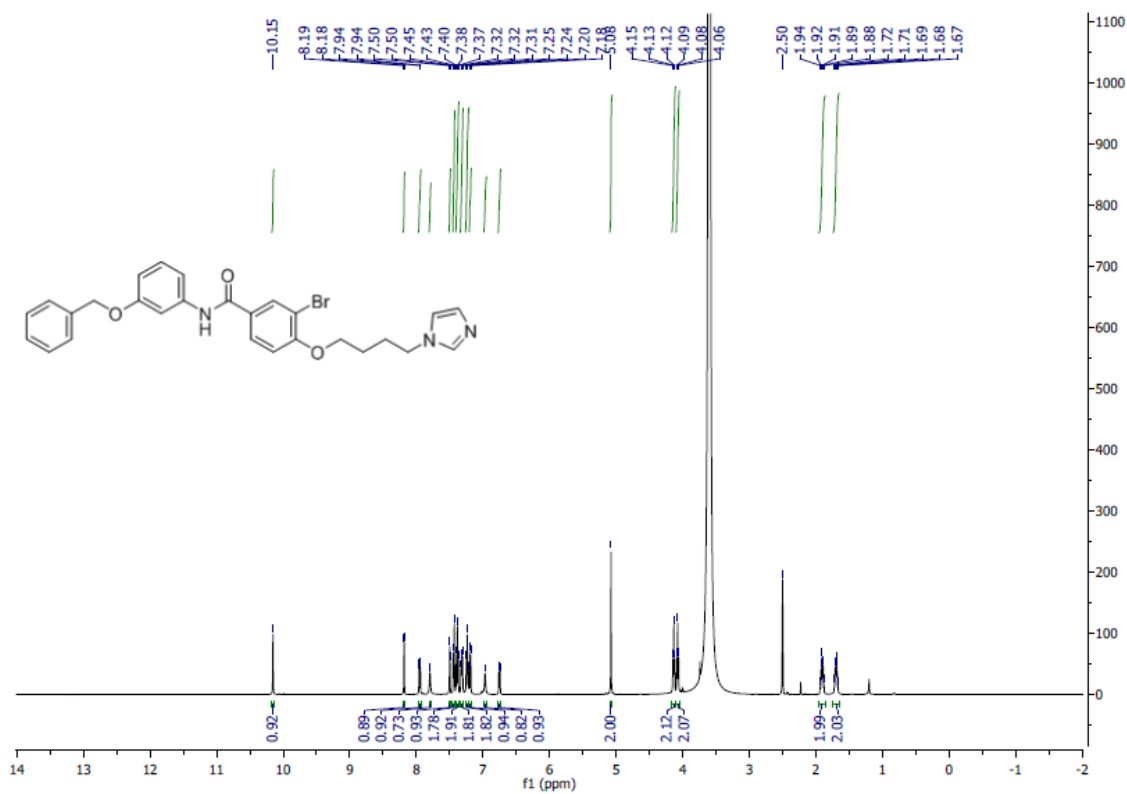
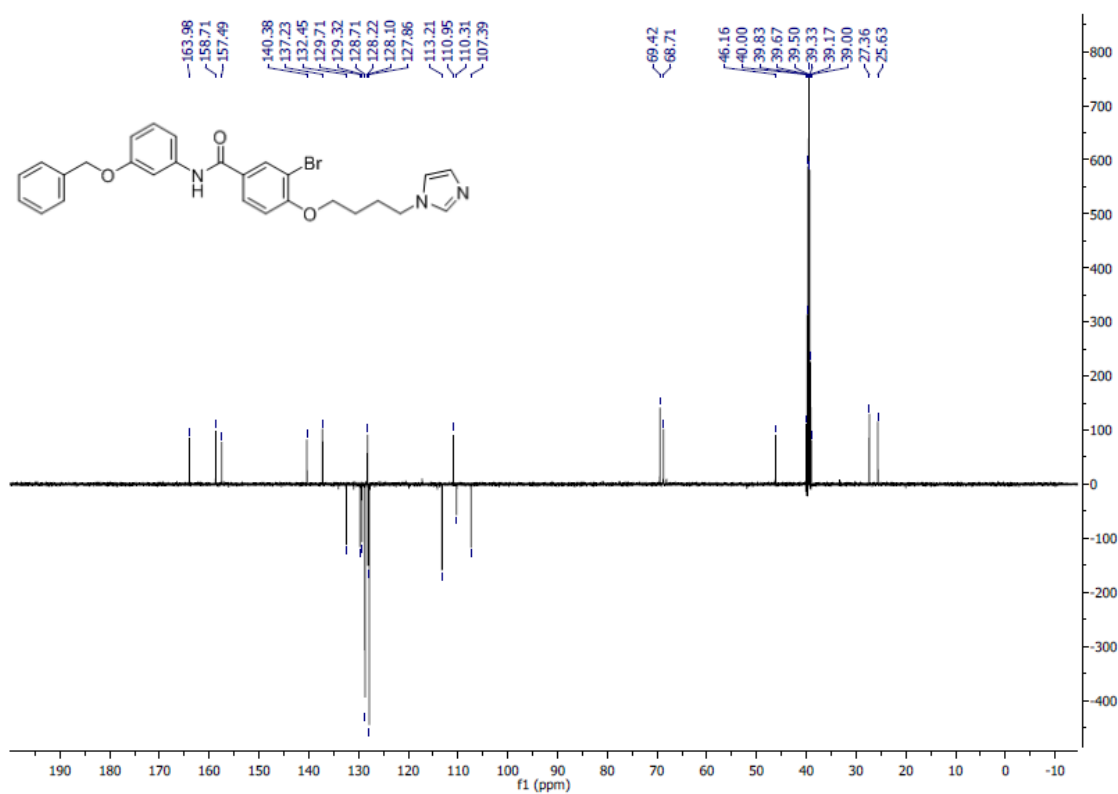


Figure S5. <sup>13</sup>C NMR (125 MHz, CDCl<sub>3</sub>) of compound 8.



**Figure S6.** <sup>1</sup>H NMR (500 MHz, DMSO-*d*<sub>6</sub>) of compound **9**.



**Figure S7.** <sup>13</sup>C NMR (125 MHz, DMSO-*d*<sub>6</sub>) of compound **9**.

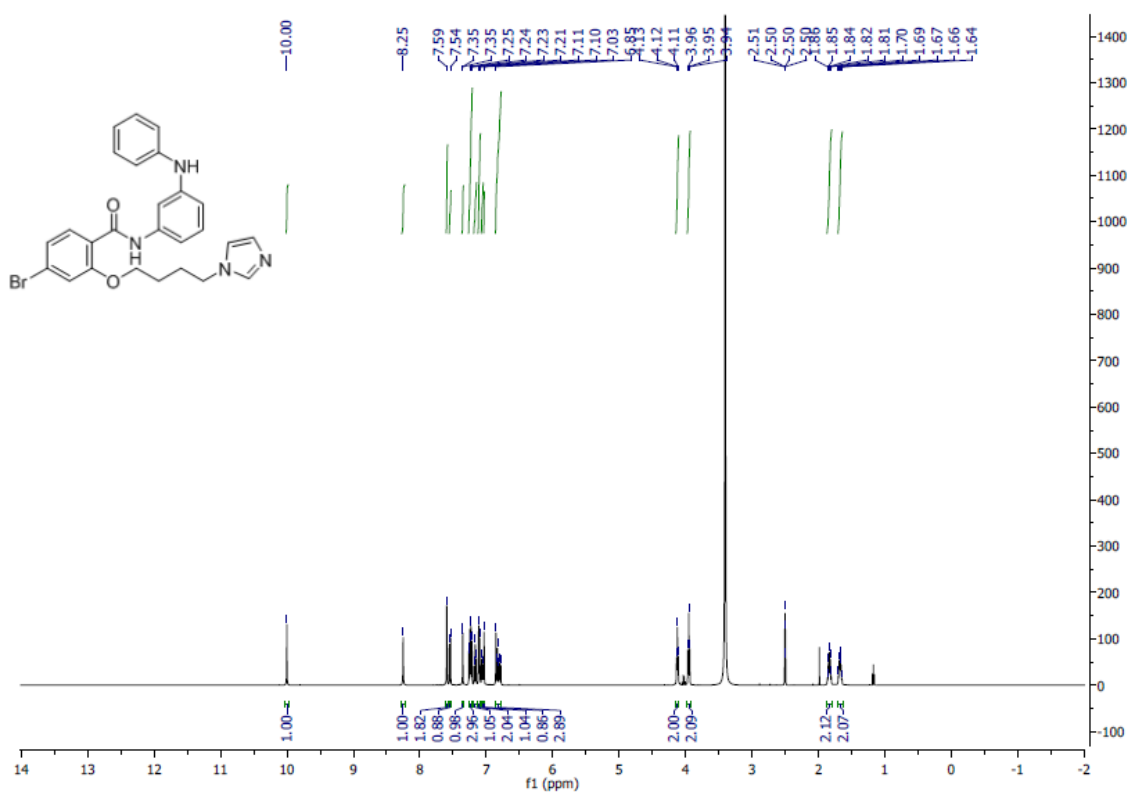


**Figure S8.**  $^1\text{H}$  NMR (500 MHz,  $\text{DMSO}-d_6$ ) of compound **10**.

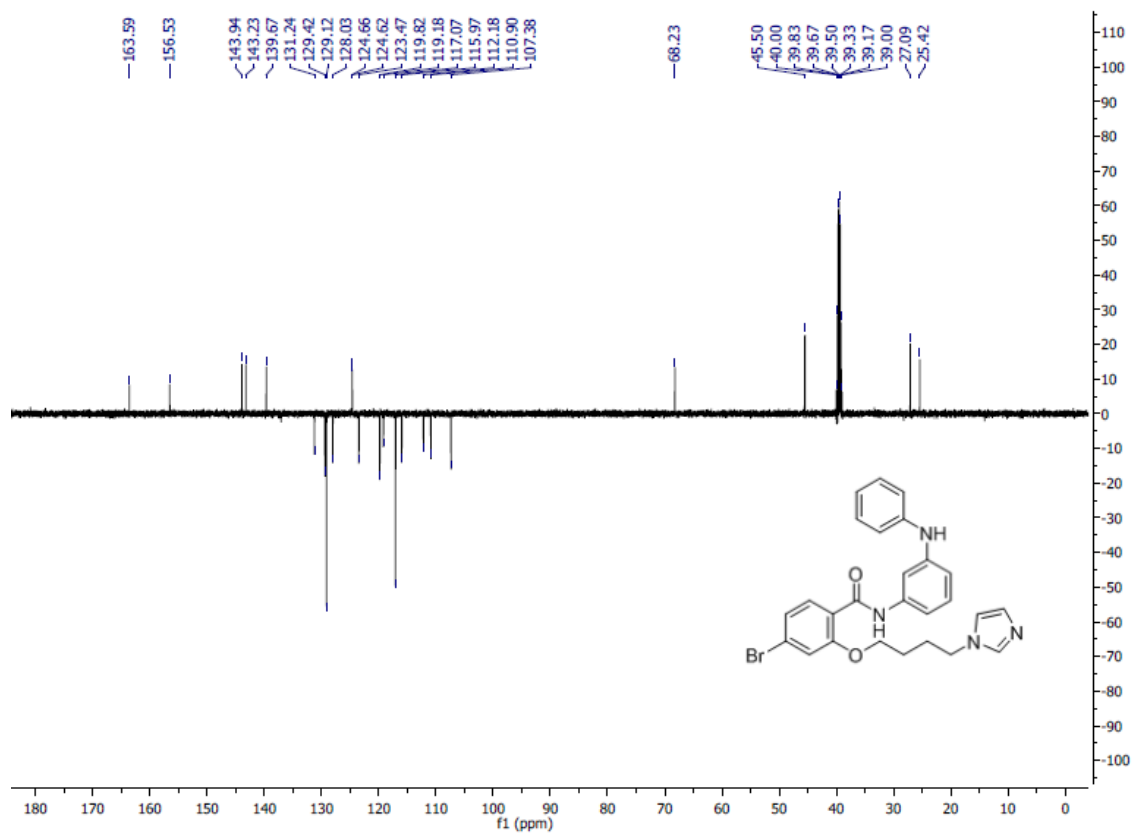


**Figure S9.**  $^{13}\text{C}$  NMR (125 MHz,  $\text{DMSO}-d_6$ ) of compound **10**.

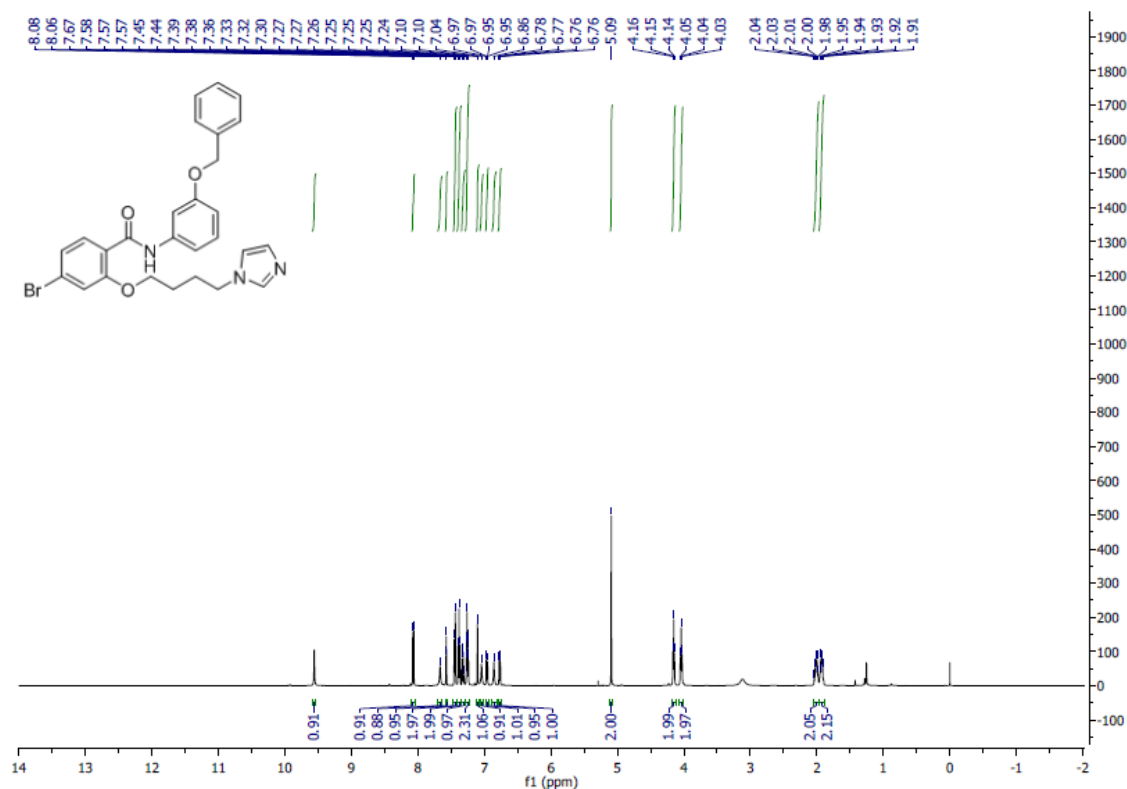


Figure S10. <sup>1</sup>H NMR (500 MHz, CDCl<sub>3</sub>) of compound 11.

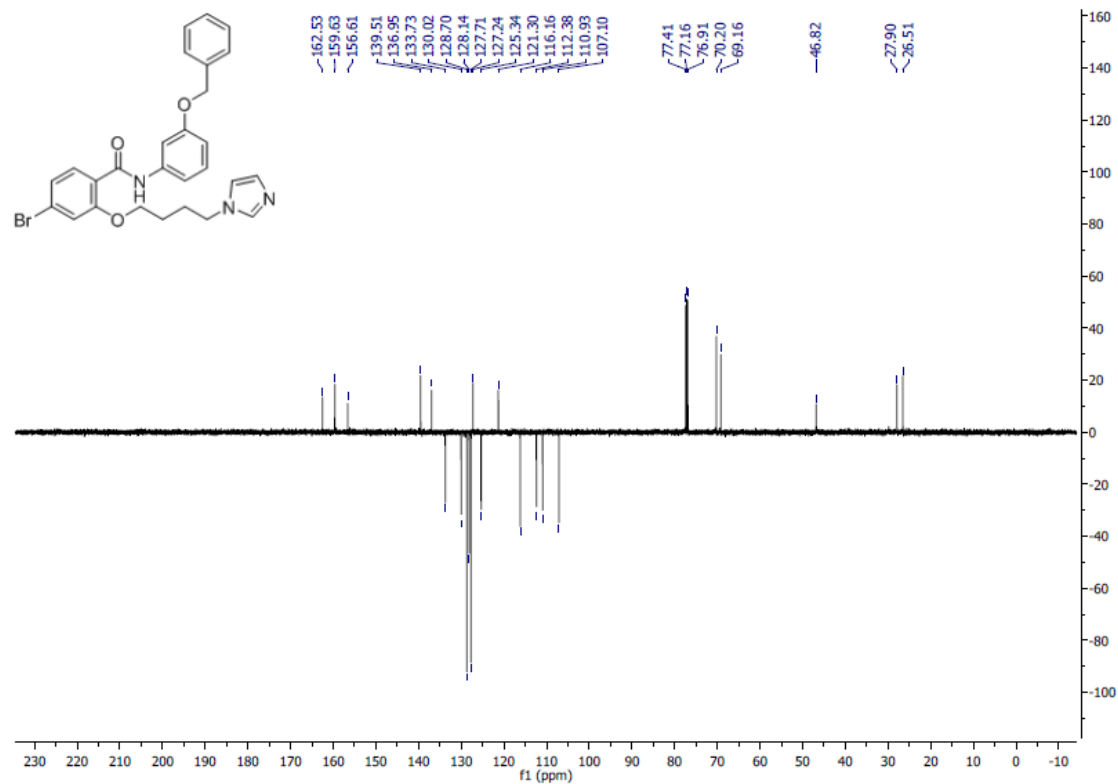


Figure S11. <sup>13</sup>C NMR (125 MHz, CDCl<sub>3</sub>) of compound 11.

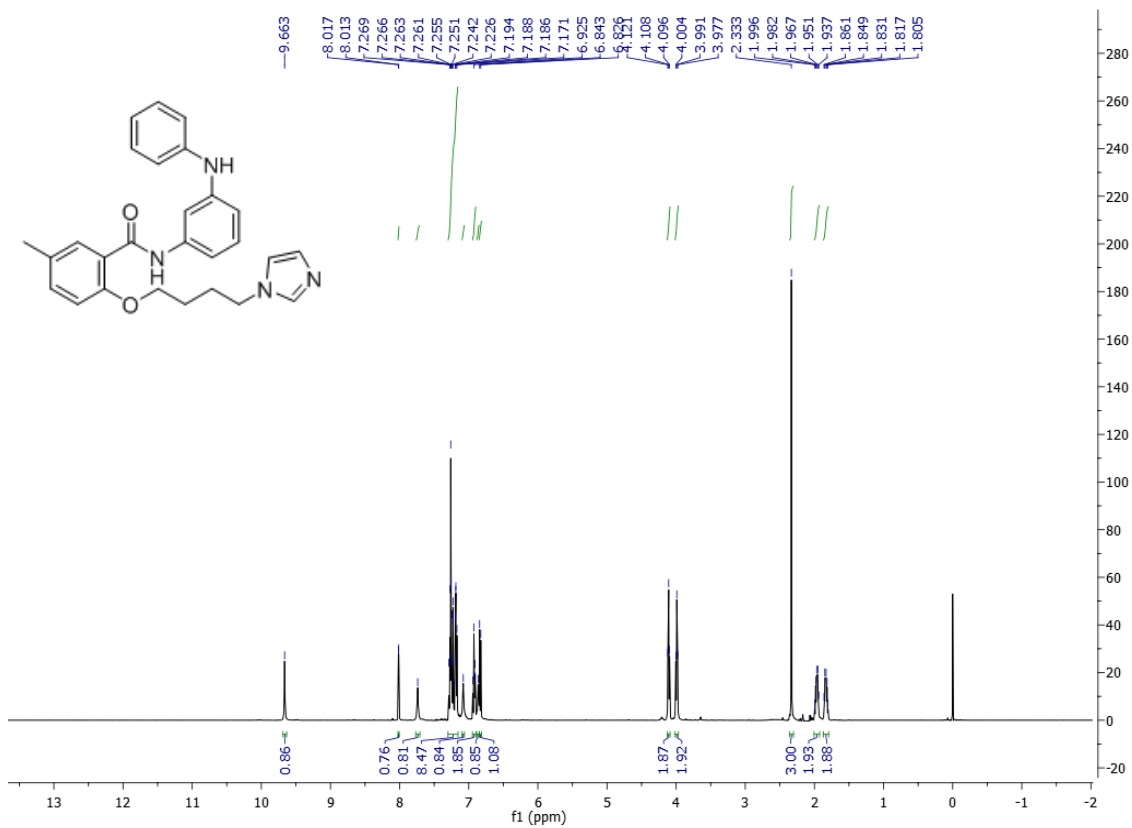


Figure S12. <sup>1</sup>H NMR (500 MHz, CDCl<sub>3</sub>) of compound 12.

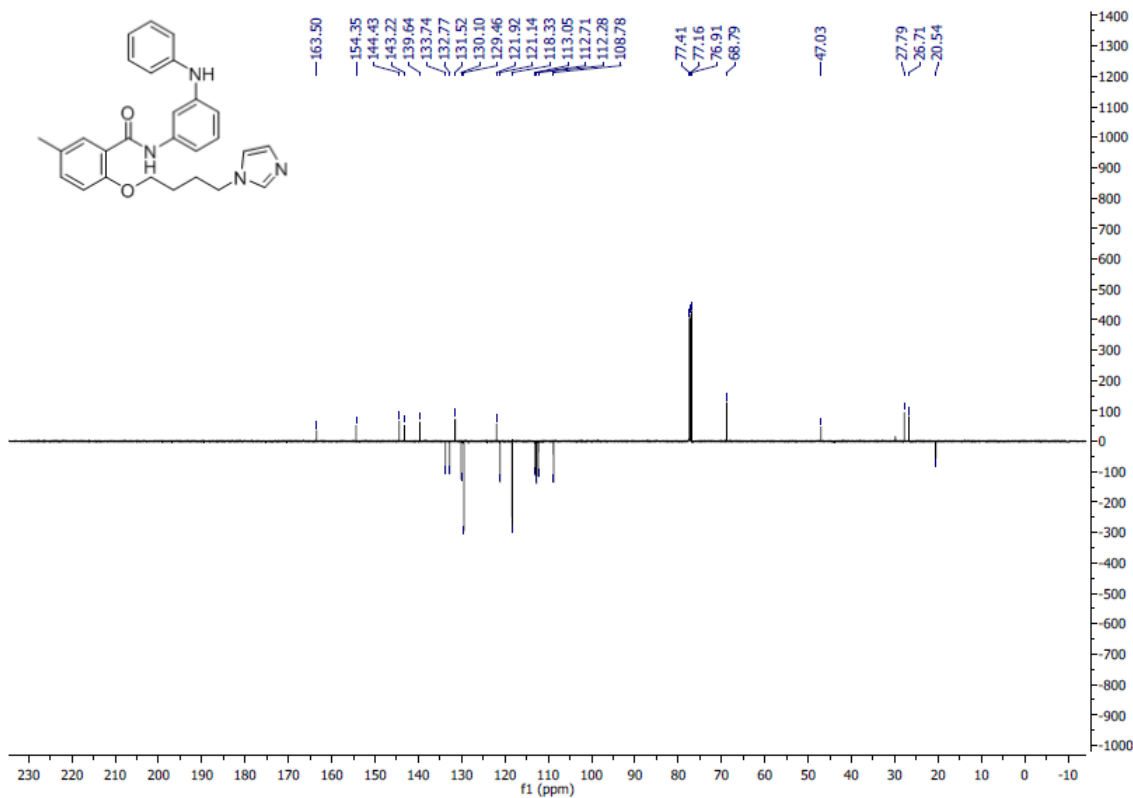


Figure S13. <sup>13</sup>C NMR (125 MHz, CDCl<sub>3</sub>) of compound 12.



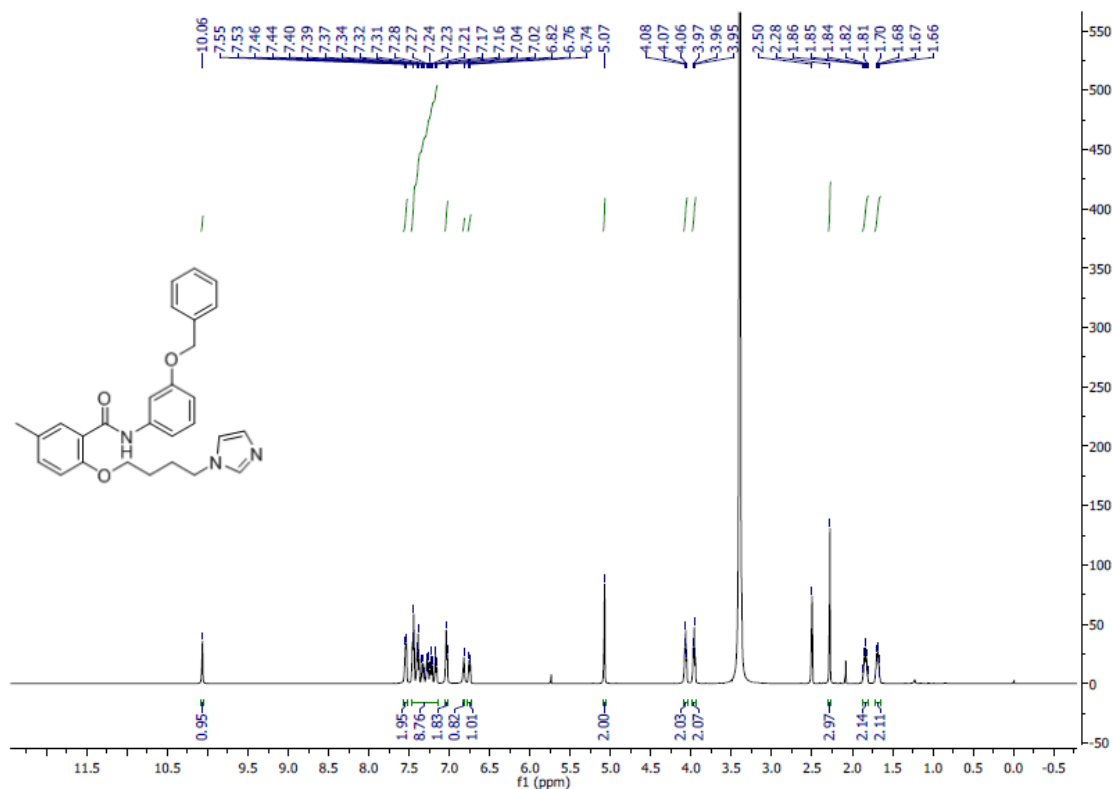


Figure S14.  $^1\text{H}$  NMR (500 MHz,  $\text{DMSO}-d_6$ ) of compound 13.

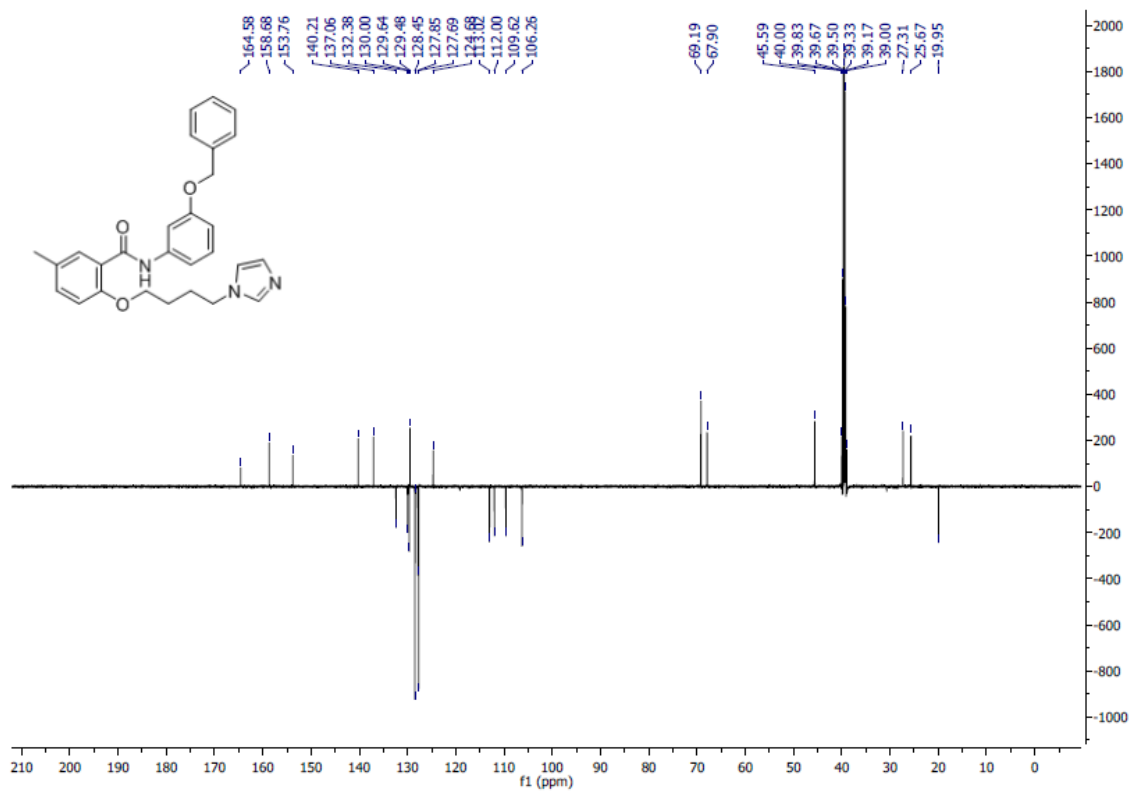


Figure S15.  $^{13}\text{C}$  NMR (125 MHz,  $\text{DMSO}-d_6$ ) of compound 13.

**Table S1.** Ligand growing molecules resulting from step 1.

Index	Structure	3D-QSAR IC <sub>50</sub> μM	Docking K <sub>i</sub> μM	Average
1	BrC1ccc(c(OCCCCn2encc2)c1)C(=O)N	17.01	29.94	23.47
2	BrC1cc(c(OCCCCn2encc2)C(=O)N	20.31	30.84	25.58
3	O=C(N)c1cc(c(OCCCCn2encc2)C	20.31	32.91	26.61
4	O=C(N1CCC[C@H](C1)CCCCn2encc2)c3cccn3	34.55	20.54	27.55
5	O=C(c1scc(C)c1NCCCCn2encc2)N	34.55	26.32	30.44
6	BrC#CC(=O)N(CCCCCn1encc1)C	24.24	37.48	30.86
7	Clc1enc(c(NCCCCn2encc2)c1)-c3encc3	34.55	29.94	32.24
8	BrC1c(NCCCCn2encc2)c3cccc3cn1	20.31	44.32	32.31
9	Clc1ccc(c(NCCCCn2encc2)c1)C(=O)NC	28.94	35.72	32.33
10	N(CCCCCn1encc1)c2eccne2-c3cccc3	41.25	24.38	32.81
11	O=C(OC)C1=CN(C(=C[C@H]1CCCCn2encc2)C)C	28.94	37.09	33.02
12	s1ccc(-c2encc2NCCCCn3encc3)c1	34.55	32.87	33.71
13	O=C1CC[C@H](N1Cc2cc(C)cc2)CCCCn3encc3	41.25	27.05	34.15
14	O=C(NC)c1cccc(N)c1OCCCCn2encc2	14.25	56.87	35.56
15	BrC1cccc(-n2c(NCCCCn3encc3)cn2)c1	24.24	47.23	35.74
16	BrC1cc(F)c(c(NCCCCn2encc2)c1)C#C	41.25	30.80	36.03
17	Fe1cccc(-c2c(NCCCCn3encc3)ccn2)c1	28.94	43.80	36.37
18	O=C(N1CCC[C@H]1CCCCn2encc2)[C@H]3CCCO3	49.24	23.51	36.37
19	Cc1enc(n1CCCCn2encc2)C3CC3	49.24	23.85	36.54
20	Clc1ccc(s1)-c2c(NCCCCn3encc3)ccn2	49.24	24.80	37.02
21	O=C(OCC)[C@H]1[C@@H](CCCCn2encc2)c3ccnc3O1	10.00	64.59	37.30
22	Fe1cccc1NC(=O)[C@H]2C[C@H]2CCCCn3encc3	34.55	40.36	37.46
23	Clc1ccc(Cl)cc1[C@H](CCCCn2encc2)C#N	24.24	52.74	38.49
24	O=C(OC)c1cn2CCCCc2c1CCCCn3encc3	17.01	60.69	38.85
25	BrC1cc(Cl)cc(OCCCCn2encc2)c1F	49.24	31.01	40.12
26	Fe1ccc(cc1NCCCCn2encc2)C	14.25	66.03	40.14
27	O=C(OC)c1cc(c(cc1NCCCCn2encc2)C)C	28.94	54.91	41.93
28	O=C(OCC)c1c(n(C)cn1)CCCCn2encc2	24.24	60.84	42.54
29	O=C(N1CSC[C@H]1CCCCn2encc2)c3cccs3	49.24	36.00	42.62
30	C[C@H](CCCCn1encc1)Cn2enc3cccc32	58.78	27.26	43.02
31	BrC1cc(F)cc([C@H](O)CCCCn2encc2)c1	58.78	27.30	43.04
32	O=C1CC[C@H](N1Cc2cc(o2)C)CCCCn3encc3	24.24	62.28	43.26
33	BrC1ccc(S)c(NCCCCn2encc2)c1	20.31	66.98	43.65
34	O=C(N(CCCCCn1encc1)C)Cc2cccs2	24.24	64.93	44.59
35	Fe1ccc(CN2C(=O)CC[C@H]2CCCCn3encc3)cc1	11.94	78.28	45.11
36	Clc1c(NCCCCn2encc2)c(no1)-c3cccc(Cl)c3	49.24	41.31	45.28
37	Fe1cccc(-n2c(NCCCCn3encc3)c(C)cn2)c1	41.25	50.07	45.66
38	CCc1c(NCCCCn2encc2)c(nen1)CC	34.55	56.80	45.67
39	BrC1cnn(c1CCCCn2encc2)CC(C)C	20.31	72.04	46.17
40	n1(CC2CCC2)c(NCCCCn3encc3)ccn1	8.38	84.30	46.34
41	Clc1c(cc(NCCCCn2encc2)c(C(OC)=O)c1)C	58.78	34.71	46.75
42	FCc1c(NCCCCn2encc2)ccn1	17.01	77.47	47.24

43	<chem>O=C1C(N)=C(NCCCCn2cncc2)c3cccc3O1</chem>	70.17	25.25	47.71
44	<chem>Fe1cnc(c(NCCCCn2cncc2)c1)C(=O)N</chem>	49.24	46.44	47.84
45	<chem>CO/N=C/c1cccc1NCCCCn2cncc2</chem>	41.25	54.77	48.01
46	<chem>Clc1ccc(s1)C(=O)N2CCC[C@@H]2CCCCn3cncc3</chem>	49.24	48.92	49.08
47	<chem>O=C(N1CCC[C@@H](C1)CCCCn2cncc2)c3cccc3</chem>	83.77	15.22	49.49
48	<chem>O=C(OC)[C@H]1C[C@@H](CCCCn2cncc2)c3ccsc3S1</chem>	58.78	41.31	50.05
49	<chem>S(CCCCN1cncc1)Cc2csc(n2)-c3csc3</chem>	70.17	33.21	51.69
50	<chem>Clc1ccc(F)c(S(=O)(=O)CCCCn2cncc2)c1</chem>	34.55	68.92	51.74
51	<chem>Cc1cc(-c2c(NCCCCn3cncc3)ccn2)cs1</chem>	49.24	54.41	51.83
52	<chem>Brclnnc1NCCCCn2cncc2)-c3nccn3</chem>	20.31	83.75	52.03
53	<chem>OCc1c(C)cccc1NCCCCn2cncc2</chem>	24.24	80.13	52.19
54	<chem>Clc1c(nn(c1NCCCCn2cncc2)-c3cccc3)C</chem>	20.31	87.31	53.81
55	<chem>Cc1cncc(-n2cccc2)c1NCCCCn3cncc3</chem>	34.55	73.26	53.91
56	<chem>Cc1enn(c1NCCCCn2cncc2)-c3cccc3</chem>	34.55	73.65	54.10
57	<chem>Brclncc(c1NCCCCn2cncc2)C(OC)=O</chem>	58.78	49.43	54.10
58	<chem>O=C(OC)C1=CC[C@@H](C[C@@H]1CCCCn2cncc2)C</chem>	100.00	10.36	55.18
59	<chem>Brclccc(c(NCCCCn2cncc2)c1)C(F)F</chem>	41.25	69.28	55.27
60	<chem>Brclc(NCCCCn2cncc2)c(Cl)cn1</chem>	58.78	51.79	55.29
61	<chem>O=S(=O)(CCCCn1cncc1)c2csc2C(OC)=O</chem>	49.24	64.84	57.04
62	<chem>O=C(NC)c1cccc(c1NCCCCn2cncc2)C</chem>	41.25	73.45	57.35
63	<chem>O=C1CC[C@@H](N1Cc2cccc2)CCCCn3cncc3</chem>	41.25	74.61	57.93
64	<chem>Brclncc(OCCCCn2cncc2)c1</chem>	41.25	75.49	58.37
65	<chem>[O-][N+](=O)c1c(OCCCCn2cncc2)c3cccc3nn1</chem>	70.17	48.16	59.16
66	<chem>O=C(OCC)c1en(cc1NCCCCn2cncc2)C</chem>	34.55	84.85	59.70
67	<chem>Cc1cncc(OCC)c(NCCCCn2cncc2)c1</chem>	83.77	36.38	60.07
68	<chem>Fe1cnc(-c2cccc2NCCCCn3cncc3)cc1</chem>	49.24	72.60	60.92
69	<chem>Clc1ccc(C(=O)N2CCO[C@@H]2CCCCn3cncc3)cc1</chem>	49.24	72.60	60.92
70	<chem>Clc1c(CCCCCn2cncc2)c(no1)-c3cccc(F)c3</chem>	70.17	52.06	61.12
71	<chem>O=C(OC)c1csc1NCCCCn2cncc2</chem>	41.25	82.35	61.80
72	<chem>C[C@@H](n1cncc1-c2cccc2)CCCCn3cncc3</chem>	41.25	83.53	62.39
73	<chem>n1(CCCCNc2cccc2-n3cncc3)cncc1</chem>	100.00	25.42	62.71
74	<chem>O=C(OCC)c1cccc1CCCCn2cncc2</chem>	70.17	55.63	62.90
75	<chem>Fe1ccc(c(NCCCCn2cncc2)c1)C(OC)=O</chem>	58.78	67.59	63.19
76	<chem>S=C(N)c1cccc1NCCCCn2cncc2</chem>	49.24	77.57	63.41
77	<chem>O=C(N1CCC[C@@H](C1)CCCCn2cncc2)c3cc(on3)C</chem>	70.17	56.65	63.41
78	<chem>Clc1cccc(-c2c(CCCCCn3cncc3)c(no2)C)c1</chem>	17.01	110.30	63.66
79	<chem>Brclcccc1NC(=O)[C@@H]2C[C@@H]2CCCCn3cncc3</chem>	24.24	103.37	63.81
80	<chem>Fe1ccc(F)c(c1NCCCCn2cncc2)C(OC)=O</chem>	119.38	8.35	63.86
81	<chem>Clc1ccc(-c2c(NCCCCn3cncc3)ccn2)cc1</chem>	20.31	109.31	64.81
82	<chem>Fe1c(F)cc(NCCCCn2cncc2)c(C(=O)NC)c1</chem>	41.25	89.72	65.48
83	<chem>O=C(N(CCCCN1cncc1)C)c2ccc3cccc3n2</chem>	83.77	47.23	65.50
84	<chem>CCc1ccc(cc1NCCCCn2cncc2)CC</chem>	49.24	82.35	65.79
85	<chem>Clc1c(F)cc(NCCCCn2cncc2)c(c1)C(OC)=O</chem>	49.24	84.74	66.99
86	<chem>Clc1c(F)cc(c(NCCCCn2cncc2)c1)C(OC)=O</chem>	58.78	75.49	67.13
87	<chem>Fe1cc(N)c([N+])([O-])=O)c(CCCCCn2cncc2)c1</chem>	83.77	50.66	67.21

88	<chem>O=Cc1cccc1OCCCCn2ence2</chem>	41.25	93.53	67.39
89	<chem>BrC1ccc(F)c([C@@H](O)CCCCn2ence2)c1</chem>	28.94	106.36	67.65
90	<chem>Fe1cccc(-n2c(NCCCCn3ence3)cc(n2)C)c1</chem>	119.38	16.15	67.77
91	<chem>Oc1cccc(NCCCCn2ence2)c1C(OC)=O</chem>	41.25	95.25	68.25
92	<chem>OC=1CCC[C@H](CCCCn2ence2)C1C(OCC)=O</chem>	83.77	53.09	68.43
93	<chem>BrC1cc(NCCCCn2ence2)c(OCC)c(c1)C</chem>	24.24	113.06	68.65
94	<chem>Clc1cc(Cl)cc(CCCCCn2ence2)c1[N+](O-)=O</chem>	100.00	37.48	68.74
95	<chem>Clc1ccc(C(C)C)cc1NCCCCn2ence2</chem>	41.25	97.12	69.18
96	<chem>BrC1ccc(c(NCCCCn2ence2)c1)CC</chem>	100.00	38.82	69.41
97	<chem>Cc1c(NCCCCn2ence2)c([nH]n1)-c3cccc3</chem>	83.77	56.06	69.92
98	<chem>O=C(N1CCC[C@@H]1CCCCn2ence2)c3enn(c3)C</chem>	28.94	111.17	70.05
99	<chem>BrC1enn(c1CCCCn2ence2)-c3cccc3</chem>	17.01	123.18	70.10
100	<chem>FC(F)c1cccc1NCCCCn2ence2</chem>	83.77	56.58	70.17
101	<chem>Cc1c(NCCCCn2ence2)cc(c(n1)C)C</chem>	17.01	123.66	70.34
102	<chem>O=C(OCC)c1enn(c1CCCCn2ence2)C</chem>	49.24	91.49	70.36
103	<chem>O=C(OC)c1cccc(c1CCCCn2ence2)C</chem>	58.78	82.89	70.83
104	<chem>Clc1ccc(-n2c(NCCCCn3ence3)ccn2)cc1</chem>	17.01	124.95	70.98
105	<chem>Clc1ccc(c(NCCCCn2ence2)c1)C(F)F</chem>	41.25	101.90	71.57
106	<chem>s1c2c(nc1N3CCCC[C@@H]3CCCCn4ence4)ccn2</chem>	70.17	73.07	71.62
107	<chem>O=C(OC)c1cc2c(n1CCCCn3ence3)cc(o2)C</chem>	70.17	73.17	71.67
108	<chem>BrC1c(NCCCCn2ence2)c(C)ccn1</chem>	58.78	85.29	72.03
109	<chem>O=C(OC)c1cccn1CCCCn2ence2</chem>	28.94	115.58	72.26
110	<chem>Cc1c(CCCCCn2ence2)c(no1)-c3cccc(c3)C</chem>	41.25	103.50	72.37
111	<chem>Cc1cn(-c2cccc2NCCCCn3ence3)cn1</chem>	119.38	25.55	72.46
112	<chem>Fe1ccc(NCCCCn2ence2)c(NC3CC3)c1</chem>	34.55	110.88	72.71
113	<chem>O=Cc1ccc2cccc2c1OCCCCn3ence3</chem>	119.38	26.12	72.75
114	<chem>BrC1ccc(NC(=O)C)c(OCCCCn2ence2)c1</chem>	70.17	75.49	72.83
115	<chem>BrC1enn(c1CCCCn2ence2)CCF</chem>	100.00	46.56	73.28
116	<chem>C[C@H]1Cc2c([C@H](C1)CCCCn3ence3)c(no2)-c4cccc4</chem>	28.94	119.09	74.02
117	<chem>O=C(NC1CCCC1)[C@@]2(CCC[NH+]2CCCCn3ence3)C</chem>	8.38	139.72	74.05
118	<chem>Oc1cccc(CCCCCn2ence2)c1C(OC)=O</chem>	28.94	120.33	74.64
119	<chem>N(CCCCCn1ence1)c2ccnc2-n3cnc3</chem>	17.01	132.30	74.66
120	<chem>BrC1cc(OCCCCn2ence2)c(F)cc1C</chem>	58.78	91.01	74.90
121	<chem>O=C(N(CCCCCn1ence1)C)c2cc(no2)C</chem>	49.24	100.59	74.91
122	<chem>BrC1cn2c(c(OCCCCn3ence3)c1)ccn2</chem>	119.38	31.62	75.50
123	<chem>n12c3cccc3nc1-c4cccc4N[C@@H]2CCCCn5ence5</chem>	34.55	116.49	75.52
124	<chem>BrC1ccc(c(NCCCCn2ence2)c1)C=O</chem>	20.31	131.62	75.96
125	<chem>Clc1ccc([N+](O-)=O)c(C(=O)CCCCn2ence2)c1</chem>	100.00	51.93	75.96
126	<chem>O=C(OC)c1csc(c1OCCCCn2ence2)C</chem>	83.77	68.57	76.17
127	<chem>Clc1ccnc(c1OCCCCn2ence2)C(OC)=O</chem>	34.55	118.63	76.59
128	<chem>BrC1ccc(c(CCCCCn2ence2)c1)C(O-)=O</chem>	20.31	133.17	76.74
129	<chem>O=C(N1CCC[C@@H](C1)CCCCn2ence2)c3ccc(o3)C</chem>	58.78	95.00	76.89
130	<chem>N#Cc1cn(n1)-c2cccc2NCCCCn3ence3</chem>	100.00	53.99	77.00
131	<chem>Fe1ccc(c(OCCCCn2ence2)c1)C=O</chem>	70.17	83.86	77.02
132	<chem>Cc1cc(nc(-n2c(NCCCCn3ence3)ccn2)n1)C</chem>	34.55	120.96	77.76

133	<chem>Fc1ccc(cc1[C@@H](O)CCCCn2ncc2)C</chem>	58.78	96.87	77.82
134	<chem>CC#CC[C@@H](CCCCn1ncc1)c2ccccc2</chem>	100.00	55.77	77.89
135	<chem>O=C(OC)c1ccc(cc1NCCCCn2ncc2)C</chem>	49.24	107.62	78.43
136	<chem>O=C(Nc1ccccc1NCCCCn2ncc2)C=C</chem>	83.77	73.17	78.47
137	<chem>Cc1ccc(OCC2(CC2)CCCCn3ncc3)cc1</chem>	41.25	115.74	78.49
138	<chem>Clc1c(Cl)cccc1NC(=O)/C=C\CCCCn2ncc2</chem>	58.78	98.77	78.78
139	<chem>Fc1cc(F)ccc1N2CC[C@@H]([NH+](CC2)CCCCn3ncc3)C</chem>	142.51	15.58	79.04
140	<chem>FC(F)c1ccc(cc1NCCCCn2ncc2)C</chem>	58.78	101.77	80.27
141	<chem>Cc1cccc2c1nc3c(n2)cccc3NCCCCn4ncc4</chem>	83.77	77.07	80.42
142	<chem>Brc1ccc(F)c([C@H](CCCCn2ncc2)CC=C)c1</chem>	119.38	42.13	80.75
143	<chem>Cc1cnn(C2CCCC2)c1NCCCCn3ncc3</chem>	24.24	137.56	80.90
144	<chem>Brc1cc(c(F)c(OCCCCn2ncc2)c1)C(F)F</chem>	41.25	121.12	81.18
145	<chem>Clc1cc(O)c(F)c(NCCCCn2ncc2)c1</chem>	70.17	92.44	81.31
146	<chem>Brc1cnn(c1NCCCCn2ncc2)-c3ccccc3</chem>	70.17	93.41	81.79
147	<chem>N(CCCCCn1ncc1)c2ccccc2-c3ncc3</chem>	70.17	94.14	82.15
148	<chem>O=C(OCC)c1c(NCCCCn2ncc2)cnn1C</chem>	119.38	45.25	82.31
149	<chem>O=C(OCC)c1c([C@H](CCCCn2ncc2)C)con1</chem>	100.00	64.93	82.46
150	<chem>O=C(OCC)c1c(snn1)CCCCn2ncc2</chem>	100.00	65.78	82.89
151	<chem>O=C(Sc1ccc(cc1)C)[C@@H](CCCCn2ncc2)C</chem>	119.38	47.23	83.30
152	<chem>Brc1ccc(s1)C(=O)N(CCCCCn2ncc2)C</chem>	28.94	137.74	83.34
153	<chem>Brc1c(cc(c(NCCCCn2ncc2)c1)C(OC)=O)C</chem>	83.77	83.64	83.71
154	<chem>Sc1cc(F)cc(OCCCCn2ncc2)c1F</chem>	83.77	83.75	83.76
155	<chem>Ic1c(NCCCCn2ncc2)c(C)cen1</chem>	83.77	84.19	83.98
156	<chem>Brc1ccc(c(NCCCCn2ncc2)c1F)C=O</chem>	70.17	98.13	84.15
157	<chem>s1cccc1[C@H](CCCCn2ncc2)C3cccs3</chem>	70.17	98.39	84.28
158	<chem>Fc1ccc(c(c1NCCCCn2ncc2)C(OC)=O)C</chem>	70.17	99.55	84.86
159	<chem>Cc1cnn([C@@H]2CCC[C@@H]2CCCCn3ncc3)c1</chem>	119.38	50.73	85.05
160	<chem>Brc1ccc(Cl)c(N)c1OCCCCn2ncc2</chem>	119.38	51.12	85.25
161	<chem>Cc1cnc(c(NCCCCn2ncc2)c1)C#C</chem>	58.78	111.75	85.26
162	<chem>Ic1ccc(F)c(NCCCCn2ncc2)c1</chem>	142.51	30.64	86.58
163	<chem>C[C@H](CCCCn1ncc1)CSc2ccc(cc2)C</chem>	100.00	73.55	86.77
164	<chem>Brc1cc(O)c(F)c(NCCCCn2ncc2)c1</chem>	119.38	55.12	87.25
165	<chem>Fc1ccc(F)cc1NC(=O)[C@@H]2C[C@@H]2CCCCn3ncc3</chem>	49.24	125.44	87.34
166	<chem>Clc1ccc(F)cc1[C@@H](O)CCCCn2ncc2</chem>	58.78	116.19	87.48
167	<chem>Brc1c(N)ccc(c1OCCCCn2ncc2)C(OC)=O</chem>	119.38	56.28	87.83
168	<chem>O=C(N1CCC[C@@H](C1)CCCCn2ncc2)c3cc(no3)C</chem>	142.51	33.21	87.86
169	<chem>Clc1cc(N)c(F)c(OCCCCn2ncc2)c1</chem>	70.17	106.36	88.27
170	<chem>[O-][N+](=O)c1ccc(cc1CCCCn2ncc2)C</chem>	58.78	117.86	88.32
171	<chem>O=C1CS[C@@H](N1Cc2ccco2)CCCCn3ncc3</chem>	41.25	135.96	88.60
172	<chem>O=C(OC)c1cc2COc2cc1NCCCCn3ncc3</chem>	49.24	128.41	88.82
173	<chem>Clc1cccc(c1NCCCCn2ncc2)C(OC)=O</chem>	49.24	128.91	89.07
174	<chem>Brc1c(F)cc(cc1OCCCCn2ncc2)C</chem>	83.77	95.12	89.44
175	<chem>[O-][N+](=O)c1c(n(C)n1)CCCCn2ncc2</chem>	34.55	144.52	89.54
176	<chem>Brc1nn(-c2c(CCCCCn3ncc3)ccn2)cn1</chem>	70.17	109.16	89.67

177	Clc1ccnc(c1NCCCCn2ence2)C(F)(F)F	83.77	96.62	90.19
178	O=C1c2ccccc2[C@H]3[C@@H](CCCCn4ence4)c5ccccc5N13	49.24	131.28	90.26
179	Brc1cc(NCCCCn2ence2)c(OC)c(c1)C	142.51	39.38	90.94
180	Cc1enc(o1)-c2ccccc2NCCCCn3ence3	24.24	157.66	90.95
181	Sc1nnc(n1CCCCn2ence2)CCC	34.55	147.94	91.25
182	Fe1enc(c(NCCCCn2ence2)c1)C(OC)=O	83.77	100.06	91.92
183	Fe1ccc(-c2c(NCCCCn3ence3)n(C)en2)cc1	119.38	64.76	92.07
184	Clc1enc(c(OCCCCn2ence2)c1)C#N	58.78	126.92	92.85
185	Brc1cc(F)c(F)c(N(CCCCCn2ence2)C)c1	142.51	45.96	94.23
186	Cc1c(CCCCCn2ence2)c(on1)-c3ccc(cc3)C	28.94	161.39	95.17
187	Fe1cccc(c1NCCCCn2ence2)C(=O)NC	100.00	90.78	95.39
188	Clc1c(Cl)ccc(c1NCCCCn2ence2)C(OC)=O	100.00	91.01	95.51
189	Brc1c(F)cc(c(NCCCCn2ence2)c1)C(OC)=O	100.00	91.37	95.68
190	Clc1enc(c(NCCCCn2ence2)c1)CO	119.38	72.70	96.04
191	Brc1ccc2c([C@H](CCCCn3ence3)CCO2)c1	100.00	92.08	96.04
192	Clc1ccc(OCCCCn2ence2)cc1C	83.77	108.74	96.25
193	Brc1ccc(Cl)c([C@H](CCCCn2ence2)CO)c1	119.38	73.84	96.61
194	O=Cc1cccc(c1NCCCCn2ence2)CC	142.51	50.79	96.65
195	S(CCCCCn1ence1)Cc2nnc(o2)C3CC3	49.24	145.27	97.26
196	Clc1cccc(c1NCCCCn2ence2)C(=O)NC	83.77	113.50	98.63
197	S(CCCCCn1ence1)Cc2nc(no2)-c3csc3	100.00	97.50	98.75
198	O=C(N)c1cc2ccccc2cc1OCCCCn3ence3	41.25	157.66	99.45
199	O=C(Nc1cccc1C#N)[C@@H]2C[C@@H]2CCCCn3ence3	170.13	29.44	99.78
200	o1cccc1-e2c(NCCCCn3ence3)ccn2	119.38	81.29	100.33
201	O=C(N1CCC[C@H](C1)CCCCn2ence2)c3cn(C)cn3	49.24	151.44	100.34
202	Brc1ccc(-n2c(NCCCCn3ence3)ccn2)cc1	49.24	151.64	100.44
203	Clc1cc(NCCCCn2ence2)c(c(C)c1)C(OC)=O	100.00	101.24	100.62
204	FC(F)(F)c1ccc(cc1NCCCCn2ence2)C	83.77	117.55	100.66
205	Brc1cc(cc(NCCCCn2ence2)c1)C(OC)=O)C	119.38	82.24	100.81
206	Brc1esc([C@@H](O)CCCCn2ence2)c1	142.51	59.21	100.86
207	Fe1ccc(cc1[C@H](CCCCn2ence2)CC#N)C	58.78	143.21	101.00
208	O=C(N)c1cccc(N)c1NCCCCn2ence2	17.01	185.70	101.36
209	Oc1cccc(c1NCCCCn2ence2)C(OC)=O	170.13	33.00	101.56
210	Fe1cccc(-n2c(NCCCCn3ence3)ccn2)c1	24.24	179.30	101.77
211	O=C(OC)c1ccc(cc1CCCCn2ence2)C	119.38	84.63	102.00
212	O=C(N(CCCCCn1ence1)C(C)C)C2CC2	58.78	146.03	102.41
213	S=C1N(OCCCCn2ence2)CCS1	28.94	176.99	102.96
214	Brc1ccc(c(NCCCCn2ence2)c1)F)C(OC)=O	100.00	106.36	103.18
215	Clc1cccc(-n2c(NCCCCn3ence3)ccn2)c1	41.25	165.21	103.23
216	Fe1cc(c(c(NCCCCn2ence2)c1)C)C=O	142.51	64.34	103.42
217	Fe1cccc(-n2cccn2)c1NCCCCn3ence3	83.77	123.50	103.63
218	F[C@@H](CCCCn1ence1)c2ccccc2[N+](=[O-])=O	49.24	159.93	104.59
219	S=C1NN=C(O1)c2ccccc2NCCCCn3ence3	41.25	168.02	104.64
220	N1(CCC[C@H](C1)CCCCn2ence2)c3c4ccccc4n3	119.38	90.78	105.08

221	<chem>Clc1c(F)cc(cc1CCCCn2cncc2)C</chem>	100.00	110.16	105.08
222	<chem>O=C(OC)c1c(NCCCCn2cncc2)cc(C)cn1</chem>	41.25	169.78	105.51
223	<chem>CC(Cc1c(CCCCCn2cncc2)cccn1)C</chem>	142.51	69.55	106.03
224	<chem>FC(F)Oc1c(NCCCCn2cncc2)c(on1)C</chem>	20.31	193.08	106.69
225	<chem>Clc1cc(NCCCCn2cncc2)c(c(n1)C)C(OC)=O</chem>	70.17	143.40	106.78
226	<chem>O(C1CCC1)c2c(NCCCCn3cncc3)cccn2</chem>	70.17	144.71	107.44
227	<chem>O=C(OC)c1c(NCCCCn2cncc2)c3cncc3s1</chem>	58.78	157.05	107.91
228	<chem>Clc1ccc(F)c([C@H](CCCCn2cncc2)C(F)F)c1</chem>	24.24	193.83	109.04
229	<chem>O=C(OC(C)(C)C)N1CC=C[C@H]1CCCCn2cncc2</chem>	49.24	169.56	109.40
230	<chem>F[C@H]1C[NH+](C@H)(C1)C(=O)NC)CCCCn2cncc2</chem>	119.38	99.55	109.46
231	<chem>Cc1enc(c(NCCCCn2cncc2)c1)C</chem>	119.38	99.81	109.59
232	<chem>Brclc(F)cc(NCCCCn2cncc2)c(c1)C(OC)=O</chem>	83.77	135.61	109.69
233	<chem>Brclcc(c(c(NCCCCn2cncc2)c1)C)C#N</chem>	41.25	178.37	109.81
234	<chem>Clc1c(Cl)cc(NCCCCn2cncc2)c(c1)C(OC)=O</chem>	83.77	136.49	110.13
235	<chem>O=C(OCC)[C@H]1[C@@H]2CCC[C@@H]2C[NH+]1CCCCn3cncc3</chem>	142.51	79.10	110.80
236	<chem>Brclcc(c(o1)CCCCn2cncc2)C(OC)=O</chem>	70.17	151.64	110.90
237	<chem>Clc1c(F)cc(F)cc1OCCCCn2cncc2</chem>	58.78	163.50	111.14
238	<chem>o1c2cccc2nc1N3CCCC[C@@H]3CCCCn4cncc4</chem>	100.00	122.86	111.43
239	<chem>Brclcc(Cl)c([N+](O-)=O)c(CCCCCn2cncc2)c1</chem>	142.51	81.18	111.85
240	<chem>O=C(OCC)c1ccoc1CCCCn2cncc2</chem>	170.13	53.85	111.99
241	<chem>O=C(NC)c1cccc1N(CCCCCn2cncc2)C</chem>	142.51	82.14	112.32
242	<chem>O=C(OC)c1c(sc1NCCCCn2cncc2)C)C</chem>	70.17	154.82	112.50
243	<chem>Brclccc(c(NCCCCn2cncc2)c1C)C(OC)=O</chem>	142.51	83.32	112.91
244	<chem>Brclsc([C@H]([NH2+]C2CC2)CCCCn3cncc3)c1</chem>	100.00	125.93	112.97
245	<chem>Clc1ccc2c(c(NCCCCn3cncc3)c4c(n2)CCCC4)c1</chem>	28.94	197.65	113.29
246	<chem>Fe1cccc1-c2c(NCCCCn3cncc3)cn[nH]2</chem>	142.51	84.52	113.51
247	<chem>O=C1c2cccc2[C@@H]3N1CC[NH+]3CCCCn4cncc4</chem>	70.17	158.07	114.12
248	<chem>O=C(N1CCC[C@@H]1CCCCn2cncc2)c3cccs3</chem>	11.94	216.74	114.34
249	<chem>O=C(OC)c1c(sec1NCCCCn2cncc2)C</chem>	142.51	86.97	114.74
250	<chem>Cc1ccc(-n2cccc2)c(NCCCCn3cncc3)c1</chem>	20.31	209.27	114.79
251	<chem>Brclcc(O)c(F)c([C@@H](O)CCCCn2cncc2)c1</chem>	83.77	146.03	114.90
252	<chem>O=C(N1CCC[C@@H](C1)CCCCn2cncc2)c3ccco3</chem>	170.13	60.69	115.41
253	<chem>Ic1cc(F)cc(OCCCCn2cncc2)c1</chem>	203.09	28.16	115.63
254	<chem>Brclccnc(c1NCCCCn2cncc2)C</chem>	49.24	182.12	115.68
255	<chem>O=C(OCC)C1=C(NC[NH2+][C@@H]1CCCCn2cncc2)C</chem>	119.38	112.47	115.93
256	<chem>O=C1CCC[C@@H](N1Cc2cccc2)CCCCn3cncc3</chem>	70.17	162.02	116.10
257	<chem>Clc1ccc(c(CCCCCn2cncc2)c1)C#C</chem>	170.13	62.12	116.12
258	<chem>o1c(nc(n1)C2CC2)[C@@H]3CCC[C@@H]3CCCCn4cncc4</chem>	83.77	149.68	116.72
259	<chem>O=C(OCC)c1ccncc1CCCCn2cncc2</chem>	83.77	150.07	116.92
260	<chem>O=Cc1ccc2CCCCc2c1OCCCCn3cncc3</chem>	142.51	91.61	117.06
261	<chem>Fe1cc(F)cc(O[C@@H]2CCC[C@@H]2CCCCn3cncc3)c1</chem>	119.38	115.14	117.26
262	<chem>N#Cc1ccc(OC)c(NCCCCn2cncc2)c1</chem>	83.77	152.82	118.30
263	<chem>O=C(OC)c1ccoc1CCCCn2cncc2</chem>	142.51	94.14	118.32
264	<chem>Fe1cc(F)cc(c1NCCCCn2cncc2)C(OC)=O</chem>	100.00	136.85	118.42

265	<chem>Fc1ccc(NCCCCn2cnc2)c(C(=O)NC)c1</chem>	58.78	178.14	118.46
266	<chem>S(CCCCN1cnc1)Cc2nc(o2)-c3ccc3</chem>	100.00	137.03	118.51
267	<chem>O=C(NCC)C1=CNC=C[C@@H]1CCCCn2cnc2</chem>	100.00	137.56	118.78
268	<chem>O=C(N1CCC[C@@H]1CCCCn2cnc2)c3ccsc3</chem>	170.13	68.92	119.53
269	<chem>Br1ccc(c(NCCCCn2cnc2)c1)C([O-])=O</chem>	34.55	204.70	119.63
270	<chem>Br1cnn(c1CCCCn2cnc2)CC(F)(F)F</chem>	142.51	97.63	120.07
271	<chem>Br1cc(NCCCCn2cnc2)c(s1)C</chem>	70.17	171.78	120.97
272	<chem>Cl1ccc(F)c(CCCCN2cnc2)c1</chem>	142.51	99.68	121.09
273	<chem>n1(CCCC[C@H]2c3ccccc3C#Cc4ccccc4C2)cnc1</chem>	170.13	72.70	121.41
274	<chem>Sc1nnc(n1CCCCn2cnc2)-c3ccc3</chem>	17.01	226.53	121.77
275	<chem>O=C(OC)c1c(CCCCN2cnc2)c3ccccc3[nH]1</chem>	142.51	101.77	122.14
276	<chem>O=C(OCC)c1c[nH]c(c1CCCCn2cnc2)C</chem>	100.00	144.33	122.17
277	<chem>Br1cnc(F)c(OCCCN2cnc2)c1</chem>	203.09	43.12	123.11
278	<chem>Fc1ccc(c(CCCCN2cnc2)c1)-c3en(nc3)C</chem>	70.17	176.07	123.12
279	<chem>N#Cc1c(cc(c1NCCCCn2cnc2)C)C</chem>	170.13	77.57	123.85
280	<chem>s1ccc(-c2noc(n2)CCCCCn3cnc3)c1</chem>	203.09	46.20	124.64
281	<chem>O=C(N1CCCC[C@H]1CCCCn2cnc2)c3ccc(o3)C</chem>	14.25	235.53	124.89
282	<chem>Ic1ccc(OC)c(NCCCCn2cnc2)c1</chem>	142.51	107.76	125.13
283	<chem>[O-][N+](=O)c1cc2ccccc2cc1CCCCn3cnc3</chem>	170.13	80.34	125.23
284	<chem>O=C(NCC)c1ccccc1NCCCCn2cnc2</chem>	49.24	201.27	125.26
285	<chem>Br1ccnc(c1OCCCN2cnc2)C(OC)=O</chem>	242.45	10.66	126.55
286	<chem>Cl1c(NCCCCn2cnc2)c(n[nH]1)C(OCC)=O</chem>	170.13	83.75	126.94
287	<chem>Cl1c(F)ccc(c1NCCCCn2cnc2)C(OC)=O</chem>	100.00	154.22	127.11
288	<chem>Fc1c(ccc([N+](O-)=O)c1NCCCCn2cnc2)C</chem>	119.38	135.61	127.49
289	<chem>Cl1ccc(-n2cccn2)c(NCCCCn3cnc3)c1</chem>	142.51	115.43	128.97
290	<chem>Fc1ccc(C2CC2)cc1NCCCCn3cnc3</chem>	83.77	174.25	129.01
291	<chem>Cl1ccc(-n2c(NCCCCn3cnc3)cc(n2)C)cc1</chem>	28.94	230.69	129.81
292	<chem>O=C(OCC)N1CC=C[C@H](CCCCn2cnc2)C1</chem>	119.38	140.45	129.91
293	<chem>Cn1c2c(N(C[C@H]3CCCN23)CCCCn4cnc4)c(n1)C</chem>	170.13	89.84	129.98
294	<chem>O=C1CS[C@@H](N1CC(C)C)CCCCn2cnc2</chem>	41.25	218.72	129.98
295	<chem>Cl1c(Cl)cc(NCCCCn2cnc2)c(c1)C=O</chem>	203.09	57.54	130.32
296	<chem>O=S(=O)(CCCN1cnc1)c2c(sc(c2C(OC)=O)C)C</chem>	142.51	119.25	130.88
297	<chem>O=C(OCC)c1cc[nH]c1CCCCn2cnc2</chem>	242.45	19.94	131.19
298	<chem>Br1ccc([N+](O-)=O)c(CCCCN2cnc2)c1</chem>	170.13	92.56	131.34
299	<chem>Cl1cnc(F)c(CCCCN2cnc2)c1</chem>	119.38	145.84	132.61
300	<chem>Br1ccc(c(CCCCN2cnc2)c1)C=O</chem>	119.38	147.17	133.28
301	<chem>n1(c(CCCCN2cnc2)ccn1)-c3cnc3</chem>	83.77	183.78	133.77
302	<chem>Cl1ccc(-n2cnc(c2)C)c(NCCCCn3cnc3)c1</chem>	83.77	185.94	134.85
303	<chem>Br1cc(F)c(F)c(NCCCCn2cnc2)c1F</chem>	142.51	127.58	135.04
304	<chem>Br1ccc(F)c([C@H](CCCCn2cnc2)C#N)c1</chem>	41.25	229.79	135.52
305	<chem>O=C(OC(C)C)N1CCC[C@@]1(CCCCN2cnc2)C</chem>	34.55	237.07	135.81
306	<chem>Cc1cnc(n1CCCCn2cnc2)C3CCC3</chem>	70.17	202.06	136.11
307	<chem>S(CCCCN1cnc1)Cc2nc(no2)-c3cccs3</chem>	142.51	129.75	136.13
308	<chem>O=C(N1CCC[C@H](C1)CCCCn2cnc2)c3cccs3</chem>	83.77	188.86	136.31
309	<chem>Br1ccc(F)c([C@H](CCCCn2cnc2)C=C)c1</chem>	83.77	189.60	136.68
310	<chem>Fc1ccc(CC)cc1OCCCN2cnc2</chem>	142.51	134.21	138.36



311	FC(F)c1c(NCCCCn2cnc2)c(C)ccn1	203.09	74.90	139.00
312	Fe1c(cc(c(NCCCCn2cnc2)c1)C(OC)=O)C	242.45	37.00	139.72
313	Ic1c(cc(cc1NCCCCn2cnc2)C)C	242.45	37.53	139.99
314	Clc1ccc(-n2c(NCCCCn3cnc3)cc(n2)C)nn1	170.13	109.88	140.00
315	Clc1cccc(c1CCCCn2cnc2)C(OC)=O	142.51	137.56	140.04
316	Fe1ccc(c(NCCCCn2cnc2)c1)C=O	58.78	221.87	140.32
317	Cc1c[nH]c(n1)-c2cccc2NCCCCn3cnc3	142.51	138.82	140.66
318	Cc1c2c([nH]n1)cccc2NCCCCn3cnc3	119.38	162.02	140.70
319	Clc1c(NCCCCn2cnc2)c(-n3cnc3)ncn1	119.38	162.02	140.70
320	s1cccc1-c2c(NCCCCn3cnc3)cccn2	58.78	222.74	140.76
321	Brc1ccc(F)c([C@H](CCCCn2cnc2)C(F)F)c1	242.45	39.89	141.17
322	Brc1cnc(c(NCCCCn2cnc2)c1)CO	242.45	41.37	141.91
323	O=C(OCC)c1c(sec1NCCCCn2cnc2)C	170.13	114.24	142.18
324	Cc1noc(n1)C2([NH2+]CCCCn3cnc3)CCCC2	100.00	184.74	142.37
325	O=C1COC[C@@H](N1Cc2cccc2)CCCCn3cnc3	142.51	142.66	142.58
326	O=C(OCC)c1c(NCCCCn2cnc2)c(no1)C	58.78	227.12	142.95
327	F[C@H]1CN([C@@H](CCCCn2cnc2)C1)c3nnc(o3)C	83.77	202.85	143.31
328	O=C(OC)[C@@H]([NH2+]CCCCn1cnc1)CC	242.45	44.72	143.58
329	Cc1cc(SC)c(NCCCCn2cnc2)c(SC)n1	203.09	85.29	144.19
330	O=C(OCC)c1cnc1NCCCCn2cnc2	142.51	146.79	144.65
331	Cc1cnc(OC2CC2)c1NCCCCn3cnc3	83.77	206.04	144.90
332	Clc1ccc(c(CCCCCn2cnc2)c1)C(OC)=O	119.38	170.66	145.02
333	CC(c1cn(nn1)CCCCCn2cnc2)=C	242.45	49.30	145.87
334	Brc1cc(F)cc(c1NCCCCn2cnc2)C(OC)=O	49.24	243.94	146.59
335	Brc1ccc(c(NCCCCn2cnc2)c1)CO	170.13	124.31	147.22
336	O([C@H]1CCC[C@@H]1CCCCn2cnc2)CC3CCC3	100.00	195.10	147.55
337	Brc1cnc([C@@H](O)CCCCn2cnc2)c1	203.09	92.08	147.59
338	Cc1cc([nH]n1)-c2cccc2NCCCCn3cnc3	170.13	125.12	147.62
339	o1cnc1-c2cccc2NCCCCn3cnc3	203.09	92.20	147.65
340	O=C(OC)c1c(NCCCCn2cnc2)c3c(s1)CCCC3	170.13	126.10	148.11
341	Fe1ccc([N+]([O-])=O)c(CCCCCn2cnc2)c1	203.09	93.53	148.31
342	Clc1cnc(c1NCCCCn2cnc2)C	100.00	197.90	148.95
343	Brc1cnc(c(NCCCCn2cnc2)c1)C(=O)C	100.00	198.16	149.08
344	O=C(OCC)c1c(CCCCCn2cnc2)c(on1)C	58.78	241.73	150.25
345	Fe1ccc(F)c([C@@H](O)CCCCn2cnc2)c1	170.13	130.77	150.45
346	O=C(OCC)c1ccsc1CCCCn2cnc2	242.45	59.13	150.79
347	O=C(OCC)N1CCC[C@@H](C1)CCCCn2cnc2	170.13	131.62	150.87
348	CSCc1cccc1NCCCCn2cnc2	242.45	59.90	151.17
349	O=C(OC)c1c(NCCCCn2cnc2)c3cccc3[nH]1	170.13	133.51	151.82
350	Clc1ccc(c(SCCCn2cnc2)c1)C(OC)=O	83.77	220.43	152.10
351	Fe1ccc(NCCCCn2cnc2)c(C(OC)=O)c1	203.09	101.51	152.30
352	Fe1cc(cc(CCCCCn2cnc2)c1C#N)C	170.13	134.73	152.43
353	O=C(Nc1ncs1)[C@H]2[C@H](C2(C)C)CCCCn3cnc3	170.13	138.64	154.38
354	Clc1ccc2c(nc(SCCCn3cnc3)o2)c1	242.45	66.46	154.45
355	Oc1cccc(CCCCCn2cnc2)c1[N+]([O-])=O	170.13	139.00	154.56
356	Fe1c(c(F)c(cc1NCCCCn2cnc2)C)C([O-])=O	34.55	274.90	154.73

357	Clc1ccc([N+](O-)=O)c(S(=O)(=O)CCCCn2cnc2)c1	170.13	139.36	154.74
358	Fe1cccc(c1NCCCCn2cnc2)C(OC)=O	58.78	251.66	155.22
359	Br1cc(c(F)c(OCCCCn2cnc2)c1)C#N	142.51	168.68	155.60
360	CC([C@@H]([NH2+])CCCCn1cnc1)c2nc(no2)C)C	203.09	108.32	155.70
361	C[C@@H](Cn1cnc2CCCCc21)CCCCn3cnc3	142.51	169.78	156.14
362	Br1ccc(c(OCCCCn2cnc2)c1F)C#N	242.45	71.39	156.92
363	O=C1C2([NH2+][C@@H](N1CCOC)CCCCn3cnc3)CC2	203.09	111.17	157.13
364	S=C(N)c1ccc(cc1NCCCCn2cnc2)C	58.78	255.62	157.20
365	Br1cc(F)nc(OCCCCn2cnc2)c1	289.43	29.90	159.66
366	N#Cc1ccc2nc3ccccc3n2c1NCCCCn4cnc4	41.25	280.31	160.78
367	Br1cc(F)c([N+](O-)=O)c(OCCCCn2cnc2)c1	203.09	119.09	161.09
368	O=C(OC)c1ccc(nc1CCCCn2cnc2)C	100.00	222.74	161.37
369	Cc1ccn(n1)-c2ccccc2CCCCn3cnc3	242.45	85.07	163.76
370	Fe1ccc(C(=O)N2CCC[C@@H]2CCCCn3cnc3)cc1	242.45	86.74	164.59
371	Br1ccnc(Cl)c1NCCCCn2cnc2	203.09	126.26	164.68
372	FC(F)Oc1c(OCCCCn2cnc2)cccn1	242.45	88.33	165.39
373	Br1ccc([N+](O-)=O)c(OCCCCn2cnc2)c1C	119.38	211.73	165.56
374	Fe1cc(c(NCCCCn2cnc2)cn1)C(OC)=O	170.13	161.18	165.65
375	Br1cc(F)c(F)c(OCCCCn2cnc2)c1	142.51	189.35	165.93
376	Clc1ccc(-n2c(OCCCCn3cnc3)ccn2)cc1	170.13	162.66	166.39
377	Br1cccc(OC(F)F)c1CCCCn2cnc2	289.43	44.20	166.81
378	Cc1cnc(O[C@H]2CCC[C@@H]2CCCCn3cnc3)nc1	119.38	214.78	167.08
379	Fe1c(F)cc(cc1OCCCCn2cnc2)C	142.51	191.83	167.17
380	Ic1ccc(F)c(OCCCCn2cnc2)c1	142.51	193.58	168.05
381	Fe1ccc2c([C@H](CCCCn3cnc3)CC(=N2)C(OC)=O)c1	242.45	95.25	168.85
382	Br1cccc(c1CCCCn2cnc2)C(OC)=O	119.38	218.72	169.05
383	Clc1ccc(c(NCCCCn2cnc2)c1)C(=S)N	242.45	95.74	169.09
384	Br1ccc(-n2cccn2)c(NCCCCn3cnc3)c1	242.45	95.87	169.16
385	Cc1ccc(OC)c(NCCCCn2cnc2)c1	203.09	135.26	169.17
386	Br1ccc(F)c(NCCCCn2cnc2)c1O	49.24	298.35	173.79
387	CCc1c(OCCCCn2cnc2)c(no1)CC	83.77	264.05	173.91
388	Br1nc(OCCCCn2cnc2)c(s1)C(OCC)=O	142.51	208.46	175.48
389	O=C(OCC)C1=CCCC[C@@H]1CCCCn2cnc2	203.09	148.13	175.61
390	Fe1cccc(OCCCCn2cnc2)c1C#N	170.13	184.50	177.31
391	[O-][N+](=O)c1ccccc1NCCCCn2cnc2	58.78	297.19	177.98
392	n1(OCCCCn2ccccc2-n3cccn3)cnc1	203.09	154.42	178.76
393	Br1ccc(F)c(c1NCCCCn2cnc2)C#N	289.43	69.74	179.58
394	Fe1c(ccc(F)c1[C@@H](O)CCCCn2cnc2)C	289.43	70.83	180.13
395	Clc1c(F)cc(cc1[C@@H](O)CCCCn2cnc2)C	242.45	118.47	180.46
396	o1c(nnc1CCCCn2cnc2)-c3ccc[nH]3	58.78	304.22	181.50
397	Fe1ccc(c(OCCCCn2cnc2)c1)C#N	242.45	120.96	181.70
398	Br1cnc(F)c([C@H](CCCCn2cnc2)C)c1	345.51	19.00	182.26
399	FC(F)c1ccccc1NCCCCn2cnc2)C	289.43	75.49	182.46
400	O=C(OC)c1c(NCCCCn2cnc2)cccn1	142.51	222.74	182.62
401	Cc1ccc(SC)c(NCCCCn2cnc2)c1	142.51	224.77	183.64
402	[O-][N+](=O)c1ccc(OC)cc1CCCCn2cnc2	203.09	166.50	184.80

403	s1cccc1-c2nnc(o2)C[NH2+]CCCCn3cncc3	289.43	82.35	185.89
404	O=C(OCC)c1csc1CCCCn2cncc2	289.43	83.10	186.26
405	O=C(N([C@H]1CCC[C@H]1CCCCn2cncc2)C)C3CCC3	119.38	253.30	186.34
406	Clc1cnc(F)c(OCCCCn2cncc2)c1	289.43	86.52	187.97
407	Fe1c(F)ccc(c1NCCCCn2cncc2)C(OC)=O	242.45	134.03	188.24
408	Br1cccc(c1NCCCCn2cncc2)C(OC)=O	10.00	366.79	188.39
409	Cc1nc(-c2ccccc2NCCCCn3cncc3)cs1	242.45	135.79	189.12
410	Br1c(Cl)c(F)c(F)c(OCCCCn2cncc2)c1	289.43	89.95	189.69
411	O=C(N1CCC[C@H](C1)CCCCn2cncc2)c3c(C)ccs3	203.09	177.45	190.27
412	Br1cc(F)c(c(NCCCCn2cncc2)c1)C(OC)=O	242.45	138.82	190.63
413	O=C(Nc1cccc(c1C)C)/C=C\CCCCn2cncc2	242.45	141.73	192.09
414	Br1cc(F)c(OCC)c(CCCCCn2cncc2)c1	289.43	95.37	192.40
415	O=C(NO)c1cccc(c1OCCCCn2cncc2)C	142.51	242.67	192.59
416	o1cncc1-c2ccccc2NCCCCn3cncc3	289.43	95.99	192.71
417	Br1cc(NCCCCn2cncc2)c(c(C)c1)C(OC)=O	289.43	96.37	192.90
418	Clc1cc(c(CCCCCn2cncc2)cc1)C#N	142.51	245.53	194.02
419	Cc1enn(-c2ccccc2OCCCCn3cncc3)c1	345.51	47.29	196.40
420	O=C(OC)c1c(ccc1NCCCCn2cncc2)C#N	289.43	103.64	196.53
421	O=C(OC)c1csc1CCCCn2cncc2	242.45	153.02	197.73
422	N#Cc1cccn1CCCCn2cncc2	242.45	153.82	198.13
423	Clc1ccc(F)cc1OCCCCn2cncc2	289.43	110.88	200.15
424	O=C(OC)c1cccc(c1NCCCCn2cncc2)C	289.43	112.04	200.73
425	O=S(=O)(CCCC)CCCCn1cncc1	289.43	114.69	202.06
426	Br1cnc(OC)c(OCCCCn2cncc2)c1	289.43	116.64	203.03
427	Clc1cc(cc(CCCCCn2cncc2)c1F)C	170.13	237.68	203.90
428	Fe1cccc(NCCCCn2cncc2)c1C(OC)=O	49.24	358.78	204.01
429	O=C(OC)[C@H]1CCCC[NH+]1CCCCn2cncc2	289.43	119.25	204.34
430	Fe1ccc(C(C)C)cc1NCCCCn2cncc2	170.13	239.23	204.68
431	N1(CCC[C@H](C1)CCCCn2cncc2)c3cnccn3	170.13	239.54	204.83
432	Fe1cc(F)cc(NCCCCn2cncc2)c1OCC	203.09	206.84	204.97
433	Br1cnc(c(CCCCCn2cncc2)c1)C#N	203.09	211.73	207.41
434	O=C(NC)c1c(CCCCCn2cncc2)c3ccccc3[nH]1	289.43	125.93	207.68
435	BrC=1C=CC(=O)N(CCCCCn2cncc2)C1	289.43	126.26	207.84
436	Clc1ccc(-n2cncc2)c(NCCCCn3cncc3)c1	345.51	71.11	208.31
437	Cc1noc(n1)[C@H]2[C@H](CCCCn3cncc3)CCO2	412.46	9.20	210.83
438	Clc1cc(F)cc(NCCCCn2cncc2)c1C(OC)=O	203.09	219.01	211.05
439	Br1cc(F)cc(c1CCCCn2cncc2)C(OC)=O	345.51	78.49	212.00
440	Clc1cc(Cl)cc(NCCCCn2cncc2)c1OCC	203.09	221.01	212.05
441	Clc1cncc(c1CCCCn2cncc2)C(OC)=O	242.45	182.12	212.28
442	Clc1c(F)c(NCCCCn2cncc2)cc(c1)C	203.09	224.48	213.78
443	Br1cc(NCCCCn2cncc2)c(F)c(c1)C	289.43	139.00	214.21
444	[NH+]1(CCCCn2cncc2)CCCC[C@H]1Cc3cccn3	289.43	139.72	214.57
445	Clc1cnc(c(NCCCCn2cncc2)c1)C(OC)=O	49.24	385.35	217.29
446	O=C(OC)N1c2ccccc2C[C@H]1CCCCn3cncc3	345.51	90.19	217.85
447	Br1c2c(OCCCCn3cncc3)cccc2[nH]n1	58.78	378.90	218.84

448	<chem>S=C(N)c1c(F)cccc1NCCCCn2cncc2</chem>	345.51	94.26	219.89
449	<chem>Br1cc(F)c(OCC)c(NCCCCn2cncc2)c1</chem>	242.45	197.90	220.17
450	<chem>Clc1ccc(OC(F)F)c(NCCCCn2cncc2)c1</chem>	119.38	321.27	220.33
451	<chem>S(CCCn1cncc1)Cc2noc(n2)-c3cccs3</chem>	170.13	271.36	220.74
452	<chem>CC1(C(OB(O1)/C=C\2CCCC[NH+](C2)CCCCn3cncc3)(C)C)C</chem>	70.17	372.55	221.36
453	<chem>O=C(OC)c1ccc(cc1CCCCn2cncc2)C#N</chem>	412.46	30.33	221.40
454	<chem>Br1ccc(c(NCCCCn2cncc2)c1)CC#N</chem>	412.46	31.01	221.73
455	<chem>O=C(OC)c1cnccc1NCCCCn2cncc2</chem>	119.38	324.21	221.79
456	<chem>Br1ccc(F)c(S(=O)(=O)CCCCn2cncc2)c1</chem>	203.09	240.79	221.94
457	<chem>FC(F)c1c(NCCCCn2cncc2)ccs1</chem>	100.00	345.52	222.76
458	<chem>O=C(OCC)c1ccncc1S(C)CCCCn2cncc2</chem>	242.45	203.38	222.91
459	<chem>Br1cnc(c(C)CCCCn2cncc2)c1C(OC)=O</chem>	345.51	100.85	223.18
460	<chem>Fe1cccc(NCCCCn2cncc2)c1-c3nc[nH]n3</chem>	289.43	157.05	223.24
461	<chem>Br1cc(F)c(OC)c(NCCCCn2cncc2)c1</chem>	119.38	341.94	230.66
462	<chem>O=C(N1CCC[C@H]1)CCCCn2cncc2)c3cnccn3</chem>	289.43	174.02	231.72
463	<chem>FC(F)(F)c1ccc(F)cc1OCCCCn2cncc2</chem>	170.13	297.19	233.66
464	<chem>Clc1c2c(cccc2NCCCCn3cncc3)ccn1</chem>	345.51	123.18	234.35
465	<chem>Fe1cccc(-n2cncc2)c1NCCCCn3cncc3</chem>	345.51	125.60	235.56
466	<chem>O=Cc1ccc(cc1NCCCCn2cncc2)C</chem>	289.43	182.12	235.77
467	<chem>Clc1ccc(c(C)CCCCn2cncc2)c1)C#N</chem>	289.43	204.17	246.80
468	<chem>O=C(OC)c1ccc(c(N)c1OCCCCn2cncc2)C</chem>	49.24	458.62	253.93
469	<chem>O=S(=O)(N)c1ccc(c1NCCCCn2cncc2)C</chem>	412.46	100.85	256.66
470	<chem>[O-][N+](=O)c1ccc(c1NCCCCn2cncc2)CC</chem>	345.51	179.30	262.41
471	<chem>Br1cc(F)c(OC)c(C)CCCCn2cncc2)c1</chem>	345.51	185.70	265.61
472	<chem>Br1ccc(SC)c(NCCCCn2cncc2)c1</chem>	412.46	128.58	270.52
473	<chem>CC1(COC(=N1)c2ccccc2NCCCCn3cncc3)C</chem>	345.51	206.84	276.18
474	<chem>N(C1CCC1)c2ccccc2NCCCCn3cncc3</chem>	203.09	351.86	277.47
475	<chem>Br1cccc(OCC)c1NCCCCn2cncc2</chem>	412.46	144.52	278.49
476	<chem>Oc1ccc(c(NCCCCn2cncc2)c1)C(OC)=O</chem>	492.39	92.08	292.24
477	<chem>o1ccc(n1)-c2ccccc2CCCCn3cncc3</chem>	492.39	106.92	299.65
478	<chem>n1(CC2CCC2)c(C)CCCCn3cncc3)ccn1</chem>	100.00	506.86	303.43
479	<chem>BrC1=CNC(=O)C(C)CCCCn2cncc2)=C1</chem>	587.80	37.43	312.62
480	<chem>O=C(NCCC)C1([NH2+])CCCCn2cncc2)CC1</chem>	492.39	139.72	316.06
481	<chem>Clc1cc(cc(OCCCCn2cncc2)c1)FC</chem>	119.38	528.37	323.87
482	<chem>O=C(OC)c1c(C)cccc1NCCCCn2cncc2</chem>	587.80	75.29	331.55
483	<chem>Clc1cccc1NC(=O)[C@H]2C[C@H]2CCCCn3cncc3</chem>	587.80	80.03	333.92
484	<chem>O=C(OC)c1cc2c(cc1NCCCCn3cncc3)cc[nH]2</chem>	492.39	182.12	337.25
485	<chem>Fe1cccc(NC2CC2)c1NCCCCn3cncc3</chem>	587.80	126.75	357.28
486	<chem>Cc1ccc(O[C@H]2CCC[NH+](C2)CCCCn3cncc3)cc1</chem>	492.39	226.23	359.31
487	<chem>Clc1ccc(F)c(c1NCCCCn2cncc2)C(OC)=O</chem>	289.43	475.60	382.51
488	<chem>n1(CCCCCc2c[nH]nc2-c3cnccn3)cncc1</chem>	587.80	188.62	388.21
489	<chem>O=C(OC)c1c(NCCCCn2cncc2)c(C)ccn1</chem>	70.17	710.50	390.33
490	<chem>Fe1ccc(C[NH3+])cc1NCCCCn2cncc2</chem>	701.70	113.06	407.38
491	<chem>Br1cc(F)c(F)c(C)CCCCn2cncc2)c1</chem>	492.39	322.95	407.67
492	<chem>Br1ccc(F)c([C@H](C)CCCCn2cncc2)CO)c1</chem>	83.77	769.08	426.43

493	Cc1noc(n1)CC2([NH2+]CCCCn3cncc3)CC2	701.70	165.00	433.35
494	O=C(OCC)[C@@H]1CC[NH2+][C@@H]1CCCCn2cncc2	587.80	282.87	435.34
495	O=C(OC)c1csc(c1NCCCCn2cncc2)C	142.51	732.04	437.28
496	Cc1nnc(o1)C23CC(C[NH+]3CCCCn4cncc4)C2	701.70	195.86	448.78
497	Br1cccc(OCC#C)c1CCCCn2cncc2	837.68	170.66	504.17
498	O=C(OC)c1c(NCCCCn2cncc2)c3c([nH]1)CCCC3	1000.00	56.94	528.47
499	Cn1cc(-c2ccccc2NCCCCn3cncc3)cn1	837.68	296.03	566.85
500	O=C(NCC1CC1)[C@@H]2CSC[NH+]2CCCCn3cncc3	1701.25	145.27	923.26

**Table S2.** Ligand growing molecules resulting from step 2 (from molecule 3).

Index	Structure	3D-QSAR IC <sub>50</sub> μM	Dockin g K <sub>i</sub> μM	Averag e
1	Br1ccc(c(OCCCCn2cncc2)c1)C(=O)Nc3cccc(Nc4ccccc4)c3	0.63	0.75	0.69
2	Br1ccc(c(OCCCCn2cncc2)c1)C(Oc3ccc(c(NCC)c3)C)=O	0.50	0.94	0.72
3	Br1ccc(c(OCCCCn2cncc2)c1)C(=O)NC(=O)c3c(nc(o3)CCC)C	1.26	0.54	0.90
4	Br1ccc(c(OCCCCn2cncc2)c1)C(=O)Nc3ccc4c(SCC4)c3	1.26	0.62	0.94
5	Br1ccc(c(OCCCCn2cncc2)c1)C(=O)Nc3ccccc3C(=O)NCC	1.00	1.12	1.06
6	Br1cnc(NC(=O)c2ccc(Br)cc2OCCCCn3cncc3)c(O)c1	1.26	0.99	1.13
7	Br1ccc(c(OCCCCn2cncc2)c1)C(=O)Nc3ccc(F)c(NC(=O)C)c3	1.58	0.81	1.20
8	Br1ccc(c(OCCCCn2cncc2)c1)C(=O)Nc3cccc4c3COC4	1.58	1.38	1.48
9	Br1ccc(c(OCCCCn2cncc2)c1)C(=O)Nc3c(F)ccc(O)c3	2.00	1.07	1.53
10	Br1ccc(c(OCCCCn2cncc2)c1)C(=O)Nc3cc(Cl)cc(F)c3OC	2.00	1.49	1.74
11	Br1ccc(c(OCCCCn2cncc2)c1)C(Oc3c4cc(F)ccc4cn3)=O	3.16	0.38	1.77
12	Br1cc(c(cc1NC(=O)c2ccc(Br)cc2OCCCCn3cncc3)C)C	3.16	0.62	1.89
13	Br1ccc(c(OCCCCn2cncc2)c1)C(=O)Nc3c4cc(F)ccc4cn3	2.51	1.30	1.91
14	Br1ccc(c(OCCCCn2cncc2)c1)C(=O)Nc3cccc(OCc4ccccc4)c3	2.51	1.52	2.02
15	Br1ccc(OC(=O)c2ccc(Br)cc2OCCCCn3cncc3)cc1C[NH+](C)C	2.00	2.04	2.02
16	Br1ccc(c(OCCCCn2cncc2)c1)C(Oc3c4cc(ccc4cn3)C)=O	3.98	0.26	2.12
17	Br1ccc(c(OCCCCn2cncc2)c1)C(=O)Nc3ccc(cc3)C#C	3.98	0.53	2.26
18	Br1ccc(c(OCCCCn2cncc2)c1)C(=O)Nc3cccc4ccn43	3.98	0.68	2.33
19	Br1cc(NC(=O)c2ccc(Br)cc2OCCCCn3cncc3)c(OC)cc1C	3.16	1.53	2.35
20	Br1ccc(c(OCCCCn2cncc2)c1)C(Oc3cccc4c3nc(o4)CC)=O	3.98	0.73	2.36
21	Br1cc(Cl)cnc1[C@H](NC(=O)c2ccc(Br)cc2OCCCCn3cncc3)C	3.98	0.82	2.40
22	Br1ccc(C(=O)CSc2cc(ccc2N)C)c(OCCCCn3cncc3)c1	3.98	0.87	2.42
23	Br1ccc(c(OCCCCn2cncc2)c1)C(=O)Nc3c(Cl)ccc(N)c3	3.98	0.93	2.46
24	Br1ccc(c(OCCCCn2cncc2)c1)C(Oc3c(F)cc(c(Cl)c3)C)=O	3.98	0.98	2.48
25	Br1ccc(c(OCCCCn2cncc2)c1)C(Oc3ccc(c(CC)c3)C)=O	3.98	1.02	2.50
26	Br1ccc(c(OCCCCn2cncc2)c1)C(=O)Nc3cccc4c3cc[nH]4	3.98	1.05	2.52
27	Br1ccc(c(OCCCCn2cncc2)c1)C(=O)Nc3cccc4C=CCc43	3.98	1.05	2.52
28	Br1ccc(c(OCCCCn2cncc2)c1)C(=O)Nc3c4cc(Cl)ccc4c(Cl)cn3	5.01	0.25	2.63
29	Br1cc(NC(=O)c2ccc(Br)cc2OCCCCn3cncc3)ccc1CC	5.01	0.57	2.79
30	Br1ccc(c(OCCCCn2cncc2)c1)C(=O)Nc3c(OC)nc(cc3)C	3.98	1.61	2.79
31	Ic1cccc(NC(=O)c2ccc(Br)cc2OCCCCn3cncc3)n1	3.98	1.61	2.80

32	<chem>BrC1c(scc1C)NC(=O)c2ccc(Br)cc2OCCCN3nccc3</chem>	3.98	2.23	3.11
33	<chem>Br1ccc(C(=O)N[C@@H]2CCCC[C@@H]2NS(=O)(=O)C)c(OCCCN3nccc3)c1</chem>	5.01	1.28	3.15
34	<chem>Br1ccc(c(OCCCN2nccc2)c1)C(=O)Nc3ccc4c3cc([nH]4)C</chem>	3.98	2.35	3.17
35	<chem>Br1ccc(c(OCCCN2nccc2)c1)C(=O)Nc3ccc4c(OCC4)c3</chem>	6.31	0.12	3.21
36	<chem>Br1ccc(c(OCCCN2nccc2)c1)C(=O)Nc3csc3Br</chem>	3.16	3.52	3.34
37	<chem>Br1ccc(c(OCCCN2nccc2)c1)C(=O)Nc3ccc4c(N(CC4)C(=O)N)c3</chem>	6.31	0.42	3.36
38	<chem>Br1ccc(c(OCCCN2nccc2)c1)C(=O)Nc3ccccc3CCC</chem>	6.31	0.66	3.49
39	<chem>Br1c(NC(=O)c2ccc(Br)cc2OCCCN3nccc3)ccc4c1cc[nH]4</chem>	6.31	0.73	3.52
40	<chem>Br1ccc(c(OCCCN2nccc2)c1)C(Oc3c(ccn3)C#C)=O</chem>	6.31	0.79	3.55
41	<chem>Br1ccc(c(OCCCN2nccc2)c1)C(=O)Nc3cccc(N)c3</chem>	6.31	0.81	3.56
42	<chem>Ic1cc(F)enc1OC(=O)c2ccc(Br)cc2OCCCN3nccc3</chem>	6.31	1.00	3.66
43	<chem>Br1ccc(c(OCCCN2nccc2)c1)C(Oc3ccccc(C4CC4)c3)=O</chem>	6.31	1.05	3.68
44	<chem>Br1ccc(c(OCCCN2nccc2)c1)C(=O)Nc3ccccc3CSC</chem>	3.98	3.39	3.69
45	<chem>Br1ccc(c(OCCCN2nccc2)c1)C(=O)Nc3ccc(F)c(Cl)c3OC</chem>	6.31	1.22	3.77
46	<chem>Br1ccc(c(OCCCN2nccc2)c1)C(=O)Nc3ccc(O)c(O)c3</chem>	6.31	1.26	3.78
47	<chem>Br1ccc(c(OCCCN2nccc2)c1)C(Oc3ccc(Br)s3)=O</chem>	3.98	3.66	3.82
48	<chem>Br1ccc(c(OCCCN2nccc2)c1)C(=O)Nc3ccc(Cl)c4ccnc34</chem>	6.31	1.57	3.94
49	<chem>Br1cc(F)enc1[C@H](NC(=O)c2ccc(Br)cc2OCCCN3nccc3)C</chem>	7.94	0.38	4.16
50	<chem>Br1ccc(c(OCCCN2nccc2)c1)C(=O)Nc3c4cc(ccc4cn3)C</chem>	7.94	0.50	4.22
51	<chem>Br1ccc(c(OCCCN2nccc2)c1)C(=O)Nc3ccc(cc3C#C)C</chem>	7.94	0.56	4.25
52	<chem>Br1ccc(c(OCCCN2nccc2)c1)C(=O)Nc3c4c([nH]n3)ccc(n4)C(OC)=O</chem>	7.94	0.83	4.39
53	<chem>Br1ccc(c(OCCCN2nccc2)c1)C(Oc3cc4c(F)cccc4n3)=O</chem>	7.94	0.94	4.44
54	<chem>Br1ccc(c(OCCCN2nccc2)c1)C(=O)NC[C@H]3C[C@@H]3C(F)F</chem>	6.31	2.76	4.53
55	<chem>Br1ccc(c(OCCCN2nccc2)c1)C(=O)Nc3c(Br)c(F)ccn3</chem>	7.94	1.19	4.57
56	<chem>Br1ccc(c(OCCCN2nccc2)c1)C(Oc3cc(ccn3)C(F)F)=O</chem>	7.94	1.24	4.59
57	<chem>Br1ccc(c(OCCCN2nccc2)c1)C(=O)Nc3ccc(c(S)c3)C</chem>	7.94	1.31	4.63
58	<chem>Br1ccc(c(OCCCN2nccc2)c1)C(=O)Nc3c(Cl)ccc(NC(=O)C)c3</chem>	7.94	1.64	4.79
59	<chem>Br1ccc(c(OCCCN2nccc2)c1)C(Oc3ncc(Cl)n3)=O</chem>	7.94	1.70	4.82
60	<chem>Br1ccc(c(OCCCN2nccc2)c1)C(=O)Nc3cc[nH]c3C(OCC)=O</chem>	7.94	1.78	4.86
61	<chem>Ic1c(OC(=O)c2ccc(Br)cc2OCCCN3nccc3)ncn1</chem>	7.94	2.14	5.04
62	<chem>Br1ccc(c(OCCCN2nccc2)c1)C(Oc3ncc(c(n3)C)C)=O</chem>	7.94	2.27	5.11
63	<chem>Br1ccc(c(OCCCN2nccc2)c1)C(=O)Nc3ccccc(O)c3F</chem>	7.94	2.37	5.16
64	<chem>Br1ccc(c(OCCCN2nccc2)c1)C(Oc3ncc4ccccc4n3)=O</chem>	10.00	0.40	5.20
65	<chem>Br1ccc(c(OCCCN2nccc2)c1)C(=O)/C=C/c3cc(Cl)cc(F)c3C</chem>	10.00	0.47	5.24
66	<chem>Br1ccc(c(OCCCN2nccc2)c1)C(=O)NCc3cc([nH+]c(N)c3)C</chem>	10.00	0.52	5.26
67	<chem>Br1ccc(c(OCCCN2nccc2)c1)C(=O)Nc3ccc4cc(F)enc34</chem>	10.00	0.57	5.29
68	<chem>Br1ccc(c(OCCCN2nccc2)c1)C(=O)Nc3c[nH]c(c3C(OCC)=O)C</chem>	7.94	2.64	5.29
69	<chem>Br1ccc(c(OCCCN2nccc2)c1)C(=O)Nc3ccc(c(F)c3)C</chem>	10.00	0.58	5.29
70	<chem>Br1ccc(c(OCCCN2nccc2)c1)C(=O)Nc3ccc(c(Cl)c3Br)C</chem>	10.00	0.68	5.34
71	<chem>Br1ccc(c(OCCCN2nccc2)c1)C(=O)Nc3ccc4cc(sc34)C(OC)=O</chem>	10.00	0.75	5.38
72	<chem>Br1ccc(c(OCCCN2nccc2)c1)C(=O)Nc3cc(F)ccc3OCC</chem>	7.94	2.88	5.41
73	<chem>Br1ccc(c(OCCCN2nccc2)c1)C(=O)Nc3c(Cl)cc(c(F)c3)C</chem>	10.00	1.09	5.55
74	<chem>Br1ccc(c(OCCCN2nccc2)c1)C(=O)Nc3ccc4c3OCC[C@H]4O</chem>	10.00	1.15	5.57
75	<chem>Br1ccc(c(OCCCN2nccc2)c1)C(=O)NCc3c(Cl)c(F)cc(c3)C</chem>	10.00	1.22	5.61

76	<chem>BrC1ccc(c(OCCCCn2cncc2)c1)C(=O)Nc3cc(cc(c3)C)C</chem>	10.00	1.23	5.62
77	<chem>BrC1ccc(c(OCCCCn2cncc2)c1)C(=O)Nc3cccc(F)c3COC</chem>	10.00	1.33	5.66
78	<chem>BrC1ccc(c(OCCCCn2cncc2)c1)C(=O)Nc3cccc4c3nc(o4)C(OC)=O</chem>	10.00	1.37	5.69
79	<chem>BrC1ccc(c(OCCCCn2cncc2)c1)C(Oc3ccc(s3)C)=O</chem>	7.94	3.44	5.69
80	<chem>BrC1ccc(c(OCCCCn2cncc2)c1)C(=O)Nc3ccc(F)cc3NC4CC4</chem>	10.00	1.48	5.74
81	<chem>BrC1ccc(NC(=O)c2ccc(Br)cc2OCCCCn3cncc3)c(c1)C#C</chem>	10.00	1.51	5.75
82	<chem>Ic1cccn1OC(=O)c2ccc(Br)cc2OCCCCn3cncc3</chem>	10.00	1.54	5.77
83	<chem>BrC1ccc(c(OCCCCn2cncc2)c1)C(=O)NCc3cnn(n3)CC</chem>	5.01	6.59	5.80
84	<chem>BrC1ccc(c(OCCCCn2cncc2)c1)C(=O)Nc3csc4cncnc43</chem>	10.00	1.61	5.81
85	<chem>BrC1ccc(NC(=O)c2ccc(Br)cc2OCCCCn3cncc3)c(C4CC4)c1</chem>	10.00	1.81	5.90
86	<chem>BrC1ccc(c(OCCCCn2cncc2)c1)C(=O)Nc3cccc3SC(C)C</chem>	10.00	1.98	5.99
87	<chem>BrC1ccc(C(=O)N[C@@H]2CCC[C@@H]2SC)c(OCCCCn3cncc3)c1</chem>	7.94	4.20	6.07
88	<chem>BrC1ccc(c(OCCCCn2cncc2)c1)C(=O)Nc3ccc(N)cc3OC</chem>	10.00	2.28	6.14
89	<chem>BrC1ccc(c(OCCCCn2cncc2)c1)C(=O)Nc3ccc(N)cc3</chem>	10.00	2.53	6.26
90	<chem>BrC1ccc(c(OCCCCn2cncc2)c1)C(Oc3cccc(Cl)c3)=O</chem>	10.00	2.82	6.41
91	<chem>BrC1ccc(c(OCCCCn2cncc2)c1)C(=O)Nc3ccc(c4cc([nH]c34)C(=O)N)C</chem>	12.59	0.31	6.45
92	<chem>BrC1ccc(c(OCCCCn2cncc2)c1)C(=O)N[C@H]3c4cc(OC)c(F)cc4CC3</chem>	12.59	0.35	6.47
93	<chem>BrC1ccc(c(OCCCCn2cncc2)c1)C(=O)Nc3c4cc(Br)sc4ccn3</chem>	10.00	2.96	6.48
94	<chem>BrC1ccc(c(OCCCCn2cncc2)c1)C(=O)Nc3cccc(NC(=O)C=C)c3</chem>	12.59	0.42	6.51
95	<chem>BrC1ccc(c(OCCCCn2cncc2)c1)C(=O)Nc3cccc4c(Cl)cccc43</chem>	12.59	0.45	6.52
96	<chem>BrC1ccc(C(=O)N[C@@H](c2nnc(o2)C)C)c(OCCCCn3cncc3)c1</chem>	12.59	0.54	6.57
97	<chem>BrC1ccc(c(OCCCCn2cncc2)c1)C(=O)Nc3cccc4c3ncc(OC)n4</chem>	12.59	0.59	6.59
98	<chem>BrC1ccc(c(OCCCCn2cncc2)c1)C(Oc3c4ccc(Cl)cc4[nH]n3)=O</chem>	12.59	0.62	6.60
99	<chem>BrC1ccc(c(OCCCCn2cncc2)c1)C(=O)Nc3cccc3OC(F)(F)F</chem>	12.59	0.66	6.63
100	<chem>BrC1ccc(c(OCCCCn2cncc2)c1)C(=O)Nc3cc(Cl)cc4c3OCC(=O)N4</chem>	12.59	0.77	6.68
101	<chem>BrC1ccc(c(OCCCCn2cncc2)c1)C(Oc3cccc(NC(=O)C=C)c3)=O</chem>	12.59	0.82	6.70
102	<chem>BrC1ccc(c(OCCCCn2cncc2)c1)C(=O)N[C@H]3c4cc(Br)cn4CC3</chem>	12.59	0.95	6.77
103	<chem>BrC1ccc(c(OCCCCn2cncc2)c1)C(Oc3c4cc(sc4ccn3)C)=O</chem>	12.59	1.04	6.81
104	<chem>BrC1cc(Cl)cn1OC(=O)c2ccc(Br)cc2OCCCCn3cncc3</chem>	12.59	1.11	6.85
105	<chem>BrC1ccc(c(OCCCCn2cncc2)c1)C(=O)Nc3cccc4c3nccn4</chem>	12.59	1.16	6.87
106	<chem>BrC1ccc(c(OCCCCn2cncc2)c1)C(=O)Nc3ccc(Cl)cc3C</chem>	12.59	1.21	6.90
107	<chem>BrC1ccc(c(OCCCCn2cncc2)c1)C(=O)Nc3c(Cl)cccc3O</chem>	12.59	1.39	6.99
108	<chem>BrC1ccc(c(OCCCCn2cncc2)c1)C(=O)Nc3ccc4c(c3)c(c[nH]4)C(OC)=O</chem>	12.59	1.48	7.03
109	<chem>BrC1ccc(c(OCCCCn2cncc2)c1)C(=O)Nc3ccc(nc3OCC)C</chem>	12.59	1.67	7.13
110	<chem>BrC1ccc(c(OCCCCn2cncc2)c1)C(=O)NCC/C=C=CC</chem>	12.59	1.83	7.21
111	<chem>BrC1ccnc(OC(=O)c2ccc(Br)cc2OCCCCn3cncc3)c1C=C</chem>	12.59	1.97	7.28
112	<chem>BrC1ccc(c(OCCCCn2cncc2)c1)C(=O)Nc3c(Br)c(Cl)ccn3</chem>	12.59	2.00	7.29
113	<chem>BrC1ccc(c(OCCCCn2cncc2)c1)C(Oc3cc(ccn3)C(=O)C)=O</chem>	12.59	2.21	7.40
114	<chem>BrC1ccc(c(OCCCCn2cncc2)c1)C(=O)NCc3cn(mn3)C4CC4</chem>	12.59	2.34	7.47
115	<chem>BrC1ccc(c(OCCCCn2cncc2)c1)C(=O)Nc3cccc(CS(=O)(=O)C)c3</chem>	12.59	2.35	7.47
116	<chem>BrC1ccc(c(OCCCCn2cncc2)c1)C(=O)Nc3cccc(C(C)C)c3F</chem>	12.59	2.54	7.56
117	<chem>BrC1ccc(c(OCCCCn2cncc2)c1)C(=O)NCc3cc(sc3)C(F)(F)F</chem>	12.59	2.84	7.71
118	<chem>BrC1ccc(c(OCCCCn2cncc2)c1)C(=O)Nc3cc(c(c3)C)C)C</chem>	15.85	0.41	8.13
119	<chem>BrC1ccc(c(OCCCCn2cncc2)c1)C(=O)Nc3cccc4c3cns4</chem>	12.59	3.75	8.17

120	<chem>BrC1ccc(c(OCCCCn2cncc2)c1)C(=O)Nc3ccccc4cnccn34</chem>	15.85	0.61	8.23
121	<chem>BrC1ccc(c(OCCCCn2cncc2)c1)C(Oc3c4cc(Cl)ccc4[nH]n3)=O</chem>	15.85	0.63	8.24
122	<chem>BrC1ccc(c(OCCCCn2cncc2)c1)C(=O)Nc3ccccc4cc(Br)cncc34</chem>	15.85	0.65	8.25
123	<chem>BrC1ccc(c(OCCCCn2cncc2)c1)C(=O)NCc3ccc(o3)-c4ccoc4</chem>	15.85	0.66	8.26
124	<chem>BrC1ccc(c(OCCCCn2cncc2)c1)C(=O)Nc3ccccc4cc(oc34)C</chem>	15.85	0.70	8.27
125	<chem>BrC1ccc(c(OCCCCn2cncc2)c1)C(=O)Nc3ccc(Br)c(c3F)C</chem>	15.85	0.71	8.28
126	<chem>BrC1ccc(c(OCCCCn2cncc2)c1)C(Oc3c4cc(nn4ccn3)C5CC5)=O</chem>	15.85	0.81	8.33
127	<chem>BrC1ccc(c(OCCCCn2cncc2)c1)C(Oc3c(N)c(Cl)ccn3)=O</chem>	15.85	0.96	8.40
128	<chem>BrC1ccc(c(OCCCCn2cncc2)c1)C(Oc3ncc(s3)C)=O</chem>	15.85	0.97	8.41
129	<chem>BrC1ccc(c(OCCCCn2cncc2)c1)C(=O)Nc3ccccc3</chem>	15.85	1.13	8.49
130	<chem>BrC1ccc(c(OCCCCn2cncc2)c1)C(=O)Nc3ccccc(NN)c3</chem>	15.85	1.21	8.53
131	<chem>BrC1ccc(c(OCCCCn2cncc2)c1)C(=O)Nc3ccccc4ccsc43</chem>	15.85	1.26	8.55
132	<chem>BrC1ccc(c(OCCCCn2cncc2)c1)C(=O)CNc3ccccc(c3)C(OC)=O</chem>	15.85	1.28	8.57
133	<chem>BrC1cc2c(OCO2)c(NC(=O)c3ccc(Br)cc3OCCCCn4cncc4)c1</chem>	15.85	1.29	8.57
134	<chem>BrC1ccc(c(OCCCCn2cncc2)c1)C(=O)Nc3ccccc4c3nc([nH]4)C</chem>	15.85	1.38	8.61
135	<chem>BrC1ccc(c(OCCCCn2cncc2)c1)C(=O)N/C=C(/CC)C=C</chem>	12.59	4.67	8.63
136	<chem>BrC1ccc(c(OCCCCn2cncc2)c1)C(=O)Nc3ccc(Br)cc3OC</chem>	15.85	1.50	8.67
137	<chem>BrC1c(Cl)ccc1NC(=O)c2ccc(Br)cc2OCCCCn3cncc3</chem>	15.85	1.53	8.69
138	<chem>BrC1ccc(c(OCCCCn2cncc2)c1)C(=O)Nc3ccccc3SC(F)F</chem>	15.85	1.54	8.69
139	<chem>BrC1ccc(c(OCCCCn2cncc2)c1)C(=O)Nc3ccc(S)cc3C</chem>	15.85	1.59	8.72
140	<chem>BrC1ccc(c(OCCCCn2cncc2)c1)C(=O)Nc3ccc(S)cc3F</chem>	15.85	1.64	8.74
141	<chem>BrC1ccc(c(OCCCCn2cncc2)c1)C(=O)Nc3cc(OC)cc4c3nc(Cl)s4</chem>	15.85	1.64	8.75
142	<chem>BrC1ccc(c(OCCCCn2cncc2)c1)C(=O)Nc3ccc(cc3SC)C</chem>	15.85	1.66	8.76
143	<chem>BrC1ccc(c(OCCCCn2cncc2)c1)C(=O)NCe3cn(nc3)CC#CC</chem>	15.85	1.84	8.84
144	<chem>BrC1ccc(c(OCCCCn2cncc2)c1)C(=O)NC[C@H]3C[C@@H]3c4ccn(n4)C</chem>	15.85	1.94	8.89
145	<chem>BrC1ccc(c(OCCCCn2cncc2)c1)C(=O)Nc3ccccc(Cl)c3SC</chem>	15.85	1.95	8.90
146	<chem>BrC1ccc(c(OCCCCn2cncc2)c1)C(=O)Nc3csnc3OC</chem>	12.59	7.70	10.14
147	<chem>BrC1ccc(c(OCCCCn2cncc2)c1)C(=O)c3nnc(o3)Cc4ccccc(F)c4</chem>	19.95	0.35	10.15
148	<chem>BrC1ccc(c(OCCCCn2cncc2)c1)C(=O)Nc3ccc(cc3C)C#C</chem>	19.95	0.38	10.16
149	<chem>BrC1ccc(c(OCCCCn2cncc2)c1)C(=O)Nc3c(CC)cccn3</chem>	19.95	0.46	10.21
150	<chem>BrC1ccc(c(OCCCCn2cncc2)c1)C(=O)Nc3ccc(OC(F)F)cc3Cl</chem>	19.95	0.50	10.22
151	<chem>BrC1ccc(c(OCCCCn2cncc2)c1)C(=O)Nc3ccc(C(C)C)c(c3)C</chem>	19.95	0.55	10.25
152	<chem>BrC1ccc(c(OCCCCn2cncc2)c1)C(Oc3cc(cc(n3)C)C(F)(F)F)=O</chem>	19.95	0.55	10.25
153	<chem>BrC1ccc(c(OCCCCn2cncc2)c1)C(=O)Nc3cc(F)cc4c3cc[nH]4</chem>	19.95	0.57	10.26
154	<chem>BrC1ccc(c(OCCCCn2cncc2)c1)C(=O)Nc3ccccc4cc(O)cncc34</chem>	19.95	0.61	10.28
155	<chem>BrC1ccc(c(OCCCCn2cncc2)c1)C(Oc3ccc4CCc4c3)=O</chem>	19.95	0.61	10.28
156	<chem>BrC1ccc(c(OCCCCn2cncc2)c1)C(=O)Nc3ccc(c(Cl)c3C)C</chem>	19.95	0.64	10.30
157	<chem>BrC1cc(Br)ccc1NC(=O)c2ccc(Br)cc2OCCCCn3cncc3</chem>	19.95	0.69	10.32
158	<chem>BrC1ccc(c(OCCCCn2cncc2)c1)C(=O)Cc3ccc(n3-c4cnccc4)C</chem>	19.95	0.72	10.34
159	<chem>BrC1ccc(c(OCCCCn2cncc2)c1)C(=O)Nc3ccc4CCc4c3</chem>	19.95	0.75	10.35
160	<chem>BrC1ccc(c(OCCCCn2cncc2)c1)C(=O)Nc3ccc(F)c(O)c3</chem>	19.95	0.87	10.41
161	<chem>BrC1ccc(c(OCCCCn2cncc2)c1)C(Oc3c4c(ccs4)ccn3)=O</chem>	19.95	1.02	10.49
162	<chem>BrC1ccc(c(OCCCCn2cncc2)c1)C(=O)N[C@H]3c4cc([N+])([O-])=O)ccc4CC3</chem>	19.95	1.10	10.53
163	<chem>BrC1ccc(NC(=O)c2ccc(Br)cc2OCCCCn3cncc3)c(Cl)c1Cl</chem>	19.95	1.17	10.56



164	<chem>BrC1ccc(c(OCCCCn2cncc2)c1)C(=O)Nc3c(Cl)cc(cc3F)C</chem>	19.95	1.32	10.64
165	<chem>BrC1ccc(c(OCCCCn2cncc2)c1)C(Oc3ccccc3C=C)=O</chem>	19.95	1.51	10.73
166	<chem>BrC1ccc(c(OCCCCn2cncc2)c1)C(=O)Nc3ccccc(F)c3OC</chem>	19.95	1.52	10.74
167	<chem>BrC1ccc(c(OCCCCn2cncc2)c1)C(=O)Nc3ccccc(NS(=O)(=O)C)c3</chem>	19.95	1.54	10.74
168	<chem>BrC1ccc(c(OCCCCn2cncc2)c1)C(=O)Nc3ccccc(Cl)c3OC4CC4</chem>	19.95	1.63	10.79
169	<chem>BrC1ccc(c(OCCCCn2cncc2)c1)C(=O)Nc3cc(O)c(Cl)cn3</chem>	19.95	1.69	10.82
170	<chem>BrC1ccc(c(OCCCCn2cncc2)c1)C(=O)Nc3ccccc3CC(C)C</chem>	19.95	1.79	10.87
171	<chem>BrC1ccc(c(OCCCCn2cncc2)c1)C(Oc3c(Cl)c(F)ccn3)=O</chem>	19.95	2.12	11.04
172	<chem>BrC1ccc(c(OCCCCn2cncc2)c1)C(=O)NCc3ccc(o3)[C@@H]4[C@H](C4)C</chem>	19.95	2.23	11.09
173	<chem>BrC1ccc(c(OCCCCn2cncc2)c1)C(Oc3enc(cc3)C)=O</chem>	19.95	2.25	11.10
174	<chem>BrC1ccc(c(OCCCCn2cncc2)c1)C(Oc3ccccc4c3nc(o4)C)=O</chem>	19.95	2.69	11.32
175	<chem>BrC1ccc(c(OCCCCn2cncc2)c1)C(=O)Nc3c(OC(C)C)ncn3</chem>	19.95	3.01	11.48
176	<chem>BrC1ccc(c(OCCCCn2cncc2)c1)C(=O)NCc3ccccc3Cl</chem>	19.95	3.21	11.58
177	<chem>BrC1ccc(c(OCCCCn2cncc2)c1)C(=O)NCc3csc(Br)c3</chem>	19.95	3.39	11.67
178	<chem>BrC1ccc(c(OCCCCn2cncc2)c1)C(=O)Nc3c(scc3)OC</chem>	19.95	4.74	12.35
179	<chem>BrC1ccc(c(OCCCCn2cncc2)c1)C(=O)NC[C@@H]3CC[C@@H]3C(OC)=O</chem>	19.95	5.16	12.56
180	<chem>BrC1ccc(c(OCCCCn2cncc2)c1)C(=O)Cc3ccc(n3-c4ccc(Cl)cn4)C</chem>	25.12	0.28	12.70
181	<chem>BrC1ccc(c(OCCCCn2cncc2)c1)C(Oc3ccccc4ccc(cc34)C=C)=O</chem>	25.12	0.30	12.71
182	<chem>BrC1ccc(c(OCCCCn2cncc2)c1)C(Oc3ccccc4c3nc([nH]4)C(F)F)=O</chem>	25.12	0.31	12.71
183	<chem>BrC1ccc(c(OCCCCn2cncc2)c1)C(=O)Nc3ccc4cc[nH]c4n3</chem>	25.12	0.32	12.72
184	<chem>BrC1ccc(-n2ccccc2CC(=O)c3ccc(Br)cc3OCCCCn4cncc4)cc1</chem>	25.12	0.34	12.73
185	<chem>BrC1ccc(c(OCCCCn2cncc2)c1)C(Oc3ccccc4ccc(F)cc34)=O</chem>	25.12	0.34	12.73
186	<chem>BrC1ccc(C(=O)Cc2cccn2-c3ccc(F)cc3)c(OCCCCn4cncc4)c1</chem>	25.12	0.37	12.74
187	<chem>BrC1ccc(c(OCCCCn2cncc2)c1)C(=O)Nc3ccccc4c3OC(F)(F)C(F)(F)O4</chem>	25.12	0.38	12.75
188	<chem>BrC1c(O)nc(NC(=O)c2ccc(Br)cc2OCCCCn3cncc3)cc1</chem>	25.12	0.41	12.76
189	<chem>BrC1ccc(c(OCCCCn2cncc2)c1)C(=O)Nc3cc(F)ccc3CC</chem>	25.12	0.42	12.77
190	<chem>BrC1ccc(c(OCCCCn2cncc2)c1)C(=O)Nc3ccccc(c3)C#C</chem>	25.12	0.61	12.86
191	<chem>BrC1ccc(c(OCCCCn2cncc2)c1)C(=O)Nc3ccc(cn3)C#C</chem>	25.12	0.66	12.89
192	<chem>BrC1c(O)nc(NC(=O)c2ccc(Br)cc2OCCCCn3cncc3)cc1C</chem>	25.12	0.67	12.89
193	<chem>BrC1ccc(c(OCCCCn2cncc2)c1)C(=O)Nc3ccc(Cl)c(O)c3</chem>	25.12	0.67	12.90
194	<chem>BrC1ccc(c(OCCCCn2cncc2)c1)C(=O)NCc3c(Cl)ccc(c3)C</chem>	25.12	0.80	12.96
195	<chem>BrC1ccc(c(OCCCCn2cncc2)c1)C(Oc3c4c(N)cccc4[nH]n3)=O</chem>	25.12	0.82	12.97
196	<chem>BrC1ccc(NC(=O)c2ccc(Br)cc2OCCCCn3cncc3)cc1C=C</chem>	25.12	0.86	12.99
197	<chem>BrC1ccc(c(OCCCCn2cncc2)c1)C(=O)/C=C/c3ccc(o3)COC(=O)C</chem>	25.12	0.86	12.99
198	<chem>BrC1ccc(c(OCCCCn2cncc2)c1)C(=O)NCc3noc(n3)[C@@H]4CCCCO4</chem>	25.12	0.92	13.02
199	<chem>BrC1ccc(c(OCCCCn2cncc2)c1)C(=O)Nc3ccccc4c(O)ccnc43</chem>	25.12	0.95	13.03
200	<chem>BrC1ccc(c(OCCCCn2cncc2)c1)C(=O)Nc3ccc(Cl)c(c3)C=C</chem>	25.12	0.97	13.04
201	<chem>BrC1ccc(c(OCCCCn2cncc2)c1)C(Oc3cc(Cl)cc(n3)C)=O</chem>	25.12	1.09	13.11
202	<chem>BrC1ccc(c(OCCCCn2cncc2)c1)C(=O)Nc3ccc(cc3OC(F)F)C</chem>	25.12	1.12	13.12
203	<chem>BrC1ccc(c(OCCCCn2cncc2)c1)C(=O)N[C@H](CC)c3cn(mn3)C</chem>	25.12	1.16	13.14
204	<chem>BrC1ccc(c(OCCCCn2cncc2)c1)C(=O)Nc3ccccc4c3CN(CC)C4=O</chem>	25.12	1.22	13.17
205	<chem>BrC1ccc(c(OCCCCn2cncc2)c1)C(=O)Nc3ccccc(F)c3OC(F)F</chem>	25.12	1.23	13.17
206	<chem>BrC1ccc(c(OCCCCn2cncc2)c1)C(=O)Nc3ccccc(n3)C#C</chem>	25.12	1.28	13.20

207	Br1ccc(Cl)ccc1NC(=O)c2ccc(Br)cc2OCCCCn3cnc3	25.12	1.41	13.26
208	Br1ccc(c(OCCCCn2cnc2)c1)C(=O)NCc3cc(-c4ccsc4)cs3	25.12	1.48	13.30
209	Br1ccc(c(OCCCCn2cnc2)c1)C(=O)NCC(CC)CC	19.95	6.68	13.32
210	Br1ccc(c(OCCCCn2cnc2)c1)C(=O)Nc3ccnc3OC4CCC4	25.12	1.55	13.34
211	Br1ccc(c(OCCCCn2cnc2)c1)C(=O)Nc3ccc(Cl)c(S)c3	25.12	1.89	13.50
212	Br1ccc(c(OCCCCn2cnc2)c1)C(Oc3c4cc([N+](O-])=O)ccc4[nH]n3)=O	25.12	2.46	13.79
213	Br1ccc(c(OCCCCn2cnc2)c1)C(=O)Nc3cccc(Cl)n3	25.12	2.99	14.05
214	Br1ccc(c(OCCCCn2cnc2)c1)C(=O)NCc3ccc(S(=O)(=O)C)s3	25.12	3.85	14.49
215	Br1ccc(c(OCCCCn2cnc2)c1)C(=O)NCc3ccc(o3)CSC	25.12	4.24	14.68
216	Br1ccc(c(OCCCCn2cnc2)c1)C(=O)/C=C/SC	19.95	11.66	15.81
217	Br1ccc(c(OCCCCn2cnc2)c1)C(=O)Nc3cccc4c3oc5CCCCc45	31.62	0.19	15.90
218	Br1ccc(c(OCCCCn2cnc2)c1)C(=O)Nc3cc(O)cc4ccccc34	31.62	0.19	15.91
219	Br1csc2ccc(NC(=O)c3ccc(Br)cc3OCCCCn4cnc4)cc12	31.62	0.36	15.99
220	Br1ccc(c(OCCCCn2cnc2)c1)C(=O)Nc3cc(ccc3C4CC4)C	31.62	0.41	16.02
221	Br1ccc(c(OCCCCn2cnc2)c1)C(=O)Nc3cccc4cc(Cl)cnc34	31.62	0.45	16.03
222	Br1ccc(c(OCCCCn2cnc2)c1)C(=O)Nc3c[nH]c4ccc(Cl)cc43	31.62	0.46	16.04
223	Br1ccc(c(OCCCCn2cnc2)c1)C(=O)NCc3cc(O)n4c(n3)ccn4	31.62	0.52	16.07
224	Br1ccc(c(OCCCCn2cnc2)c1)C(=O)Nc3c(Cl)cc(c(O)c3)C	31.62	0.58	16.10
225	Br1ccc(c(OCCCCn2cnc2)c1)C(=O)Nc3cccn4c3nc(n4)C5CCC5	31.62	0.59	16.11
226	Br1ccc(c(OCCCCn2cnc2)c1)C(=O)Nc3cc(cc4c3cc[nH]4)C	31.62	0.60	16.11
227	Br1ccc(c(OCCCCn2cnc2)c1)C(=O)Nc3ccc(c4c3cn[nH]4)C	31.62	0.64	16.13
228	Br1ccc(c(OCCCCn2cnc2)c1)C(=O)Nc3ccc(cc3C(F)F)C	31.62	0.64	16.13
229	Br1ccc(c(OCCCCn2cnc2)c1)C(SCc3cccc(F)c3)=O	31.62	0.78	16.20
230	Br1ccc(c(OCCCCn2cnc2)c1)C(=O)Nc3ccc4c(n3)cc[nH]4	31.62	0.82	16.22
231	Br1ccc(c(OCCCCn2cnc2)c1)C(=O)NC[C@H](Cc3cccs3)C	31.62	1.01	16.32
232	Br1ccc(c(OCCCCn2cnc2)c1)C(=O)Nc3cccc3OCC#C	31.62	1.19	16.41
233	Br1ccc(c(OCCCCn2cnc2)c1)C(=O)NCC(=O)NC3CCC(CC3)C	31.62	1.19	16.41
234	Br1ccc(Cl)c(NC(=O)c2ccc(Br)cc2OCCCCn3cnc3)cc1C	31.62	1.22	16.42
235	Br1ccc(C(=O)NC[C@@H]2CCSCCC2)c(OCCCCn3cnc3)c1	31.62	1.34	16.48
236	Ic1cccc(O)c1NC(=O)c2ccc(Br)cc2OCCCCn3cnc3	31.62	1.49	16.56
237	Br1ccc(c(OCCCCn2cnc2)c1)C(=O)Nc3c(Cl)nc(cc3)C	31.62	1.64	16.63
238	Br1ccc(c(OCCCCn2cnc2)c1)C(=O)Nc3ccc(Cl)cc3SCC	31.62	1.64	16.63
239	Br1ccc(c(OCCCCn2cnc2)c1)C(=O)Nc3c(OCC#C)cccn3	31.62	1.68	16.65
240	Br1ccc(c(OCCCCn2cnc2)c1)C(=O)Nc3cccc(c3)CF	31.62	1.97	16.79
241	Br1ccc(c(OCCCCn2cnc2)c1)C(=O)NCCC[C@H]3CCCO3	31.62	2.33	16.97
242	Br1ccc(c(OCCCCn2cnc2)c1)C(=O)Nc3ccc(Cl)cc3	31.62	2.35	16.98
243	Br1ccc(c(OCCCCn2cnc2)c1)C(=O)NCCCSC(C)C	19.95	14.07	17.01
244	Br1ccc(c(OCCCCn2cnc2)c1)C(=O)Nc3cccc3SC	31.62	2.58	17.10
245	Br1ccc(c(OCCCCn2cnc2)c1)C(=O)Nc3ccc(Br)s3	31.62	2.60	17.11
246	Br1ccc(c(OCCCCn2cnc2)c1)C(=O)Nc3cccc(c3O)C	31.62	4.79	18.21
247	Br1ccc(c(OCCCCn2cnc2)c1)C(=O)Nc3ccsc3OCC	31.62	4.87	18.25
248	Br1ccc(c(OCCCCn2cnc2)c1)C(OCC3(O)CCC3)=O	31.62	5.02	18.32
249	Br1ccc(c(OCCCCn2cnc2)c1)C(=O)Nc3ccc(c(Cl)c3)C#C	39.81	0.44	20.12
250	Br1ccc(c(OCCCCn2cnc2)c1)C(=O)Nc3ccc(CC)c(F)c3	39.81	0.45	20.13

251	<chem>BrC1ccc(c(OCCCCn2encc2)c1)C(=O)NC[C@H]3C[C@@H]3c4cccc(F)c4</chem>	39.81	0.48	20.15
252	<chem>BrC1ccc(c(OCCCCn2encc2)c1)C(=O)Nc3cccc4cc(ene34)C</chem>	39.81	0.59	20.20
253	<chem>BrC1ccc(C(=O)Cc2ccn2-c3ccc(Cl)cc3)c(OCCCCn4encc4)c1</chem>	39.81	0.60	20.20
254	<chem>BrC1ccc(c(OCCCCn2encc2)c1)C(=O)CCc3cc(Cl)c(cc3)C</chem>	39.81	0.64	20.23
255	<chem>BrC1ccc(c(OCCCCn2encc2)c1)C(=O)Nc3cccc(OC(=O)CC)c3</chem>	39.81	0.72	20.26
256	<chem>BrC1ccc(C(=O)N[C@H]2Cc3c(OC)cccc3CC2)c(OCCCCn4encc4)c1</chem>	39.81	0.74	20.28
257	<chem>BrC1ccc(c(OCCCCn2encc2)c1)C(=O)Nc3cccc4c3cco4</chem>	39.81	0.77	20.29
258	<chem>BrC1ccc(c(OCCCCn2encc2)c1)C(=O)Nc3c[nH]c4c(Cl)ccnc34</chem>	39.81	0.78	20.30
259	<chem>BrC1ccc(c(OCCCCn2encc2)c1)C(=O)Nc3cccc4c3nc[nH]4</chem>	39.81	0.83	20.32
260	<chem>BrC1ccc(c(OCCCCn2encc2)c1)C(=O)Nc3c(Cl)cc(Cl)c(O)c3</chem>	39.81	0.93	20.37
261	<chem>BrC1ccc(c(OCCCCn2encc2)c1)C(=O)Nc3cccc4c3nc(Cl)[nH]4</chem>	39.81	0.96	20.39
262	<chem>BrC1ccc(c(OCCCCn2encc2)c1)C(=O)Nc3ccc(Br)cc3OC4CC4</chem>	39.81	1.00	20.40
263	<chem>Ic1cc(ene1OC(=O)c2ccc(Br)cc2OCCCCn3encc3)C</chem>	39.81	1.00	20.41
264	<chem>BrC1c(NC(=O)c2ccc(Br)cc2OCCCCn3encc3)cccc1C</chem>	39.81	1.09	20.45
265	<chem>BrC1ccc(c(OCCCCn2encc2)c1)C(=O)Nc3cccc3OC(F)F</chem>	39.81	1.28	20.55
266	<chem>BrC1ccc(c(OCCCCn2encc2)c1)C(Oc3c(F)ccn3)=O</chem>	39.81	1.31	20.56
267	<chem>BrC1ccc(c(OCCCCn2encc2)c1)C(=O)Nc3c(F)cc(cc3)C</chem>	39.81	1.39	20.60
268	<chem>BrC1ccc(c(OCCCCn2encc2)c1)C(=O)Nc3cccc4ccnc43</chem>	39.81	1.59	20.70
269	<chem>BrC1ccc(c(OCCCCn2encc2)c1)C(=O)Nc3cc(Cl)c(N)cc3</chem>	39.81	1.66	20.74
270	<chem>BrC1ccc(c(OCCCCn2encc2)c1)C(Oc3cc(F)cc(n3)C)=O</chem>	39.81	1.70	20.76
271	<chem>BrC1ccc(c(OCCCCn2encc2)c1)C(=O)Nc3cccc(F)c3SC</chem>	39.81	1.83	20.82
272	<chem>BrC1ccc(c(OCCCCn2encc2)c1)C(=O)Nc3ccc(cc3S)C</chem>	39.81	1.84	20.83
273	<chem>BrC1ccc(c(OCCCCn2encc2)c1)C(=O)NCc3csc(n3)-c4cccs4</chem>	39.81	2.16	20.98
274	<chem>BrC1c(O)cc(F)cc1NC(=O)c2ccc(Br)cc2OCCCCn3encc3</chem>	39.81	2.30	21.06
275	<chem>BrC1ccc(c(OCCCCn2encc2)c1)C(=O)Nc3ccc(F)cc3SC</chem>	39.81	2.70	21.26
276	<chem>BrC1ccc(c(OCCCCn2encc2)c1)C(OCC3(O)CCCC3)=O</chem>	39.81	2.84	21.33
277	<chem>BrC1c(NC(=O)c2ccc(Br)cc2OCCCCn3encc3)ccs1</chem>	39.81	3.38	21.59
278	<chem>BrC1ccc(c(OCCCCn2encc2)c1)C(=O)Nc3cccc(O)c3OC</chem>	39.81	3.47	21.64
279	<chem>BrC1ccc(c(OCCCCn2encc2)c1)C(=O)NC[C@@H]3[C@@H](F)CC3</chem>	39.81	7.31	23.56
280	<chem>BrC1ccc2c([C@H](NC(=O)c3ccc(Br)cc3OCCCCn4encc4)CC2)c1</chem>	50.12	0.25	25.18
281	<chem>BrC1ccc(c(OCCCCn2encc2)c1)C(OC(=O)Nc3cccc3C#C)=O</chem>	50.12	0.30	25.21
282	<chem>BrC1ccc(C(=O)N[C@H]2c3cc(F)c(F)cc3CC2)c(OCCCCn4encc4)c1</chem>	50.12	0.30	25.21
283	<chem>BrC1ccc(c(OCCCCn2encc2)c1)C(=O)Nc3ccc4ccoc4c3</chem>	50.12	0.35	25.23
284	<chem>BrC1ccc(c(OCCCCn2encc2)c1)C(=O)CC(=O)N3c4cccc4CC3</chem>	50.12	0.47	25.29
285	<chem>BrC1ccc(c(OCCCCn2encc2)c1)C(=O)Nc3cccc(c3)-c4ncc(Br)cn4</chem>	50.12	0.50	25.31
286	<chem>BrC1ccc(c(OCCCCn2encc2)c1)C(=O)Nc3cccc4c3CC[NH+](C4)CC</chem>	50.12	0.70	25.41
287	<chem>BrC1ccc(c(OCCCCn2encc2)c1)C(=O)Nc3cc(F)cc4c3cn[nH]4</chem>	50.12	0.76	25.44
288	<chem>BrC1ccc(C(=O)Cc2cnn3ccc(OC(=O)C)cc23)c(OCCCCn4encc4)c1</chem>	50.12	0.79	25.45
289	<chem>BrC1ccc(c(OCCCCn2encc2)c1)C(=O)Nc3cccc(F)c3CC</chem>	50.12	0.81	25.46
290	<chem>BrC1ccc(Cl)c([C@H](NC(=O)c2ccc(Br)cc2OCCCCn3encc3)C)c1</chem>	50.12	0.83	25.48
291	<chem>BrC1ccc(C(=O)NC[C@H]2C[C@@H]2C3CCCC3)c(OCCCCn4encc4)c1</chem>	50.12	0.83	25.48
292	<chem>BrC1ccc(c(OCCCCn2encc2)c1)C(=O)Nc3ccc(F)cc3C4CC4</chem>	50.12	0.86	25.49
293	<chem>BrC1ccc(c(OCCCCn2encc2)c1)C(=O)N[C@H]3c4cc(Cl)sc4CCC3</chem>	50.12	0.91	25.51
294	<chem>BrC1ccc(c(OCCCCn2encc2)c1)C(=O)Nc3ccc(Br)c(c3)C</chem>	50.12	1.04	25.58

295	<chem>Br1ccc(c(OCCCCn2encc2)c1)C(=O)Nc3ccc(c(N)c3)C</chem>	50.12	1.12	25.62
296	<chem>Br1ccc(c(OCCCCn2encc2)c1)C(=O)Nc3ccc(Cl)c(O)c3Cl</chem>	50.12	1.15	25.63
297	<chem>Br1ccc(c(OCCCCn2encc2)c1)C(=O)Nc3cccc4COCCc43</chem>	50.12	1.18	25.65
298	<chem>Br1ccc(c(OCCCCn2encc2)c1)C(=O)Nc3c(OCC)ncn3</chem>	50.12	1.20	25.66
299	<chem>Br1ccc(c(OCCCCn2encc2)c1)C(=O)CSc3ccc4c(OCCCO4)c3</chem>	50.12	1.40	25.76
300	<chem>Br1ccoc1CNC(=O)c2ccc(Br)cc2OCCCCn3encc3</chem>	50.12	1.45	25.78
301	<chem>Br1ccc(c(OCCCCn2encc2)c1)C(=O)Nc3ccc(F)cc3OC</chem>	50.12	1.46	25.79
302	<chem>Br1ccc(c(OCCCCn2encc2)c1)C(=O)Nc3c(Cl)cc(cc3)C</chem>	50.12	1.53	25.83
303	<chem>Br1ccc(C(=O)N[C@H]2c3c(nc(Br)s3)CCC2)c(OCCCCn4encc4)c1</chem>	50.12	1.54	25.83
304	<chem>Ic1cccc(NC(=O)c2ccc(Br)cc2OCCCCn3encc3)c1</chem>	50.12	1.65	25.88
305	<chem>Br1ccc(c(OCCCCn2encc2)c1)C(=O)Nc3cccc(Cl)c3O</chem>	50.12	1.67	25.90
306	<chem>Br1ccc(c(OCCCCn2encc2)c1)C(=O)Nc3cccc3CS(=O)(=O)C</chem>	50.12	1.80	25.96
307	<chem>Br1ccc(c(OCCCCn2encc2)c1)C(=O)Nc3cccc(NC(=O)C[NH3+])c3</chem>	50.12	2.19	26.16
308	<chem>Br1ccc(c(OCCCCn2encc2)c1)C(=O)Nc3c(ncn3)CO</chem>	50.12	2.48	26.30
309	<chem>Br1ccc(c(OCCCCn2encc2)c1)C(=O)NCCn3cc(Cl)en3</chem>	50.12	7.55	28.83
310	<chem>Br1ccc(c(OCCCCn2encc2)c1)C(=O)CC=3C(=O)CCC3c4ccc(F)cc4</chem>	63.10	0.14	31.62
311	<chem>Br1ccc(C(=O)Cc2cccn2-c3ccc(c(Cl)c3)C)c(OCCCCn4encc4)c1</chem>	63.10	0.24	31.67
312	<chem>Br1ccc(c(OCCCCn2encc2)c1)C(=O)Nc3cc(O)c(c(c3)C)C</chem>	63.10	0.45	31.77
313	<chem>Br1ccc(c(OCCCCn2encc2)c1)C(=O)Nc3ccc(F)c(O)c3F</chem>	63.10	0.47	31.78
314	<chem>Br1ccc(c(OCCCCn2encc2)c1)C(=O)Nc3c(F)cc(en3)C</chem>	63.10	0.47	31.78
315	<chem>Br1ccc(c(OCCCCn2encc2)c1)C(=O)N[C@H]3c4cc(ccc4CC3)C</chem>	63.10	0.65	31.87
316	<chem>Br1ccc(c(OCCCCn2encc2)c1)C(=O)Nc3ccc(N)c4c3non4</chem>	63.10	0.88	31.99
317	<chem>Br1ccc(c(OCCCCn2encc2)c1)C(=O)Nc3ccc(F)c4c3C[C@H](O4)C</chem>	63.10	0.90	32.00
318	<chem>Br1ccc(c(OCCCCn2encc2)c1)C(=O)Nc3c(Cl)ccc(c3)C</chem>	63.10	0.92	32.01
319	<chem>Br1ccc(c(OCCCCn2encc2)c1)C(=O)Nc3c[nH]c4ccc(OC)nc34</chem>	63.10	0.93	32.01
320	<chem>Br1ccc(c(OCCCCn2encc2)c1)C(=O)NC[C@H]3C[C@@H]3C4CC</chem>	63.10	0.95	32.02
321	<chem>Br1ccc(c(OCCCCn2encc2)c1)C(=O)Nc3ccc(Br)cc3OC(C)C</chem>	63.10	0.97	32.03
322	<chem>Br1ccc(c(OCCCCn2encc2)c1)C(=O)Nc3ccc(N)c4ccnc43</chem>	63.10	1.09	32.09
323	<chem>Br1ccc(c(OCCCCn2encc2)c1)C(=O)Nc3cccc4c3nco4</chem>	63.10	1.12	32.11
324	<chem>Br1ccc(c(OCCCCn2encc2)c1)C(Oc3cccc(-c4enco4)c3)=O</chem>	63.10	1.28	32.19
325	<chem>Br1ccc(c(OCCCCn2encc2)c1)C(=O)Nc3ccc(cc3)C</chem>	63.10	1.31	32.20
326	<chem>Br1ccc(C(=O)N[C@H]2c3c(nc([nH]3)C)CCC2)c(OCCCCn4encc4)c</chem>	63.10	1.39	32.24
327	<chem>Br1ccc(c(OCCCCn2encc2)c1)C(=O)Nc3ccc(cc3Br)C</chem>	63.10	1.61	32.35
328	<chem>Br1ccc(c(OCCCCn2encc2)c1)C(=O)N[C@H]3CC=CCC3</chem>	63.10	2.39	32.74
329	<chem>Br1ccc(c(OCCCCn2encc2)c1)C(=O)Nc3cccc4c3nes4</chem>	63.10	2.65	32.88
330	<chem>Br1ccc(c(OCCCCn2encc2)c1)C(=O)Nc3cccc(c3F)CO</chem>	63.10	2.71	32.90
331	<chem>Br1ccc(c(OCCCCn2encc2)c1)C(=O)Nc3cccn4cccc34</chem>	63.10	2.88	32.99
332	<chem>Br1ccc(c(OCCCCn2encc2)c1)C(=O)NC[C@H]3CC[C@@H]3C(F)</chem>	63.10	4.88	33.99
333	<chem>Br1ccc(c(OCCCCn2encc2)c1)C(OCC3cc(es3)COC)=O</chem>	63.10	6.82	34.96
334	<chem>Br1ccc(c(OCCCCn2encc2)c1)C(=O)NCC3=Cc4cccc4OC3</chem>	79.43	0.32	39.87
335	<chem>Br1ccc(C(=O)N[C@H]2c3cc(C(C)C)ccc3CC2)c(OCCCCn4encc4)c</chem>	79.43	0.39	39.91
336	<chem>Br1c(NC(=O)c2ccc(Br)cc2OCCCCn3encc3)ccc4c1CCC4</chem>	79.43	0.41	39.92

337	<chem>BrC1c(O)cc2CC[C@@H](NC(=O)c3ccc(Br)cc3OCCCCn4cncc4)c2c1</chem>	79.43	0.50	39.97
338	<chem>Br1ccc(c(OCCCCn2cncc2)c1)C(=O)NC[C@H]3C[C@@H]3c4cn(nc4)C</chem>	79.43	0.50	39.97
339	<chem>Br1ccc(c(OCCCCn2cncc2)c1)C(=O)Nc3ccc4ccccc(OC)c4n3</chem>	79.43	0.52	39.98
340	<chem>Br1ccc(c(OCCCCn2cncc2)c1)C(=O)Nc3ccc(CC)cc3</chem>	79.43	0.59	40.01
341	<chem>Br1ccc(c(OCCCCn2cncc2)c1)C(=O)Nc3ccc4CCc4n3</chem>	79.43	0.60	40.01
342	<chem>Br1ccc(c(OCCCCn2cncc2)c1)C(=O)Nc3ccc(F)cc3CC</chem>	79.43	0.65	40.04
343	<chem>Br1ccc(cc1NC(=O)c2ccc(Br)cc2OCCCCn3cncc3)C</chem>	79.43	0.66	40.05
344	<chem>Br1ccc(C(=O)COc2ccccc(S(=O)(=O)C)c2)c(OCCCCn3cncc3)c1</chem>	79.43	0.66	40.05
345	<chem>Br1ccc(c(OCCCCn2cncc2)c1)C(=O)Nc3ccc(c4cc([nH]c34)C([O-])=O)C</chem>	79.43	0.68	40.05
346	<chem>Br1ccc(c(OCCCCn2cncc2)c1)C(=O)Nc3cc(O)cc4c3cn[nH]4</chem>	79.43	0.68	40.06
347	<chem>Br1cc(NC(=O)c2ccc(Br)cc2OCCCCn3cncc3)c4c([nH]c(c4)C)c1</chem>	79.43	0.76	40.10
348	<chem>Br1ccc(c(OCCCCn2cncc2)c1)C(=O)Nc3ccc4c(cc([nH]4)C)c3F</chem>	79.43	0.77	40.10
349	<chem>Br1ccc(C(=O)Cc2enn(c2-c3ccc(cc3)C)C)c(OCCCCn4cncc4)c1</chem>	79.43	0.78	40.11
350	<chem>Br1ccc(c(OCCCCn2cncc2)c1)C(=O)Nc3ccc(F)c(NC(=O)N)c3</chem>	79.43	0.82	40.13
351	<chem>Br1ccc(c(OCCCCn2cncc2)c1)C(=O)Nc3cccc4c3C[NH+](C5CC5)C4</chem>	79.43	0.83	40.13
352	<chem>Br1ccc(C(=O)CSc2nnc(o2)-c3ccc[nH]3)c(OCCCCn4cncc4)c1</chem>	79.43	0.86	40.14
353	<chem>Br1ccc(c(OCCCCn2cncc2)c1)C(=O)Nc3c(Cl)ccc(O)c3</chem>	79.43	0.90	40.17
354	<chem>Br1ccc(c(OCCCCn2cncc2)c1)C(=O)N[C@H](C)C#Cc3ccc(Cl)cc3</chem>	79.43	0.94	40.18
355	<chem>Br1ccc(c(OCCCCn2cncc2)c1)C(=O)Nc3cccc3-c4ccc(s4)C</chem>	79.43	0.95	40.19
356	<chem>Br1ccc(c(OCCCCn2cncc2)c1)C(=O)Nc3ccc4ccsc4c3</chem>	79.43	1.00	40.22
357	<chem>Br1c(OC)cccc1NC(=O)c2ccc(Br)cc2OCCCCn3cncc3</chem>	79.43	1.45	40.44
358	<chem>Br1ccc(c(OCCCCn2cncc2)c1)C(=O)Nc3cc(cs3)C</chem>	79.43	1.58	40.51
359	<chem>Br1ccc(c(OCCCCn2cncc2)c1)C(=O)Nc3cccc(SC)c3</chem>	79.43	1.66	40.55
360	<chem>Br1ccc(c(OCCCCn2cncc2)c1)C(=O)Nc3ccc(N)c(OC)n3</chem>	79.43	1.87	40.65
361	<chem>Br1ccc(c(OCCCCn2cncc2)c1)C(Oc3cc(Br)c(F)cn3)=O</chem>	79.43	1.92	40.68
362	<chem>Br1ccc(c(OCCCCn2cncc2)c1)C(=O)Nc3cccc3OC4CC4</chem>	79.43	2.22	40.82
363	<chem>Br1ccc(c(OCCCCn2cncc2)c1)C(=O)NCc3csc(CC)c3</chem>	79.43	3.42	41.43
364	<chem>Br1ccc(c(OCCCCn2cncc2)c1)C(=O)C[C@H](F)c3ccc(s3)C</chem>	79.43	3.88	41.66
365	<chem>Br1ccc(c(OCCCCn2cncc2)c1)C(=O)NCC3[C@H]([C@@H]3C)C</chem>	79.43	4.49	41.96
366	<chem>Br1ccc(c(OCCCCn2cncc2)c1)C(=O)NCC[C@@H](OC)C</chem>	79.43	7.91	43.67
367	<chem>Br1ccc(c(OCCCCn2cncc2)c1)C(=O)NC[C@H](COCC)C</chem>	79.43	8.14	43.79
368	<chem>Br1ccc(C(=O)N[C@@H]2CCC[C@H](OC(F)(F)F)C2)c(OCCCCn3cncc3)c1</chem>	100.00	0.31	50.15
369	<chem>Br1ccc(c(OCCCCn2cncc2)c1)C(=O)Nc3enc4c(n3)cc[nH]4</chem>	100.00	0.34	50.17
370	<chem>Br1cc(c(N)cc1NC(=O)c2ccc(Br)cc2OCCCCn3cncc3)C</chem>	100.00	0.56	50.28
371	<chem>Br1ccc(c(OCCCCn2cncc2)c1)C(=O)N[C@H]3Cc4c(CC3)c[nH]n4</chem>	100.00	0.66	50.33
372	<chem>Br1ccc(c(OCCCCn2cncc2)c1)C(=O)Nc3ccc(c([n+][3][O-])C)C</chem>	100.00	0.69	50.34
373	<chem>Br1ccc(c(OCCCCn2cncc2)c1)C(=O)Nc3c(F)enc(NCC)n3</chem>	100.00	0.69	50.35
374	<chem>Br1ccc(C(=O)N[C@@H]2CCC3(OCCO3)C2)c(OCCCCn4cncc4)c1</chem>	100.00	0.74	50.37
375	<chem>Br1ccc(c(OCCCCn2cncc2)c1)C(=O)Nc3cccc(n3)C4CC4</chem>	100.00	0.80	50.40
376	<chem>Br1ccc(c(OCCCCn2cncc2)c1)C(=O)NCc3csc(C4CCCC4)c3</chem>	100.00	0.84	50.42
377	<chem>Br1ccc(C(=O)N[C@H]2c3c(CCC2)cccn3)c(OCCCCn4cncc4)c1</chem>	100.00	0.84	50.42
378	<chem>Br1ccc(c(OCCCCn2cncc2)c1)C(=O)Nc3cccc(c3F)C</chem>	100.00	0.85	50.42
379	<chem>Br1ccc(c(OCCCCn2cncc2)c1)C(=O)Nc3cccc4c(c([nH]c34)C)C</chem>	100.00	0.89	50.45

380	<chem>Br1ccc(c(OCCCCn2ence2)c1)C(=O)Nc3cccc4C[C@H](Oc34)C</chem>	100.00	0.98	50.49
381	<chem>Br1ccc(c(OCCCCn2ence2)c1)C(=O)Nc3cccc3NC=C</chem>	100.00	1.01	50.50
382	<chem>Br1ccc(C(=O)N[C@@H](c2cc3CCCN3n2)C)c(OCCCCn4ence4)c1</chem>	100.00	1.07	50.53
383	<chem>Br1ccc(c(OCCCCn2ence2)c1)C(=O)Nc3ccc(F)c(n3)C</chem>	100.00	1.24	50.62
384	<chem>Br1ccc(c(OCCCCn2ence2)c1)C(=O)Nc3cc(cc(n3)C)C</chem>	100.00	1.27	50.64
385	<chem>Br1cc(Cl)c(NC(=O)c2ccc(Br)cc2OCCCCn3ence3)nc1C</chem>	100.00	1.34	50.67
386	<chem>Br1ccc(c(OCCCCn2ence2)c1)C(=O)Nc3cc(cc4c3OCC(=O)N4)C</chem>	100.00	1.44	50.72
387	<chem>Br1ccc(c(OCCCCn2ence2)c1)C(=O)Nc3cccc(n3)C(OC)=O</chem>	100.00	1.66	50.83
388	<chem>Br1ccc(c(OCCCCn2ence2)c1)C(=O)Nc3cccc(Cl)c3N</chem>	100.00	1.82	50.91
389	<chem>Br1ccc(c(OCCCCn2ence2)c1)C(=O)Nc3cccc(Cl)c3S</chem>	100.00	2.56	51.28
390	<chem>Br1ccc(c(OCCCCn2ence2)c1)C(=O)Nc3ccc(Cl)cc3COC</chem>	100.00	3.21	51.61
391	<chem>Br1ccc(c(OCCCCn2ence2)c1)C(=O)Nc3csc(c3C(OCC)=O)C</chem>	100.00	3.64	51.82
392	<chem>Br1ccc(C(=O)Nc2c[nH+]ccc2NN)c(OCCCCn3ence3)c1</chem>	100.00	4.55	52.27
393	<chem>Br1ccc(c(OCCCCn2ence2)c1)C(=O)NCc3ccc(o3)C</chem>	100.00	4.67	52.34
394	<chem>Br1ccc(c(OCCCCn2ence2)c1)C(=O)NS(=O)(=O)[C@H](COC)C</chem>	100.00	7.20	53.60
395	<chem>Br1ccc(C(=O)Cc2c(scn2)-c3ccc(Cl)cc3)c(OCCCCn4ence4)c1</chem>	125.89	0.27	63.08
396	<chem>Br1c(c(NC(=O)c2ccc(Br)cc2OCCCCn3ence3)cc(c1C)C)C</chem>	125.89	0.40	63.14
397	<chem>Br1ccc(C(=O)N[C@@H](c2nc(no2)C3CC3)C)c(OCCCCn4ence4)c1</chem>	125.89	0.40	63.15
398	<chem>Br1ccc(C(=O)Cc2cccn2-c3cccc(c3)C)c(OCCCCn4ence4)c1</chem>	125.89	0.49	63.19
399	<chem>Br1cn(-c2cccc(NC(=O)c3ccc(Br)cc3OCCCCn4ence4)c2)cn1</chem>	125.89	0.53	63.21
400	<chem>Br1ccc(c(OCCCCn2ence2)c1)C(=O)Nc3ccc(F)cc3C#C</chem>	125.89	0.58	63.24
401	<chem>Br1ccc(c(OCCCCn2ence2)c1)C(SCc3csc(n3)-c4csc4)=O</chem>	125.89	0.62	63.26
402	<chem>Ic1ccc(NC(=O)c2ccc(Br)cc2OCCCCn3ence3)cc1</chem>	125.89	1.04	63.46
403	<chem>Br1cc(Cl)c(NC(=O)c2ccc(Br)cc2OCCCCn3ence3)cc1</chem>	125.89	1.13	63.51
404	<chem>Br1ccc(c(OCCCCn2ence2)c1)C(=O)NC[C@H]3CCCN(S(=O)(=O)C)C3</chem>	125.89	1.16	63.52
405	<chem>Br1ccc(c(OCCCCn2ence2)c1)C(=O)Nc3cccc4c3nc(s4)C</chem>	125.89	1.22	63.56
406	<chem>Br1ccc(c(OCCCCn2ence2)c1)C(=O)Nc3cccc(F)c3Cl</chem>	125.89	1.25	63.57
407	<chem>Br1ccc(c(OCCCCn2ence2)c1)C(=O)Nc3cc(ccc3OC(F)F)C</chem>	125.89	1.31	63.60
408	<chem>Br1ccc(c(OCCCCn2ence2)c1)C(=O)Nc3cccc4c3cc(OC)cn4</chem>	125.89	1.37	63.63
409	<chem>Br1ccc(c(OCCCCn2ence2)c1)C(=O)Nc3cccc(Cl)c3F</chem>	125.89	1.57	63.73
410	<chem>Br1ccc(c(OCCCCn2ence2)c1)C(=O)Nc3ccc(Cl)cn3</chem>	125.89	1.70	63.79
411	<chem>Br1ccc(c(OCCCCn2ence2)c1)C(=O)Nc3ccc(Cl)cc3Cl</chem>	125.89	1.76	63.83
412	<chem>Br1ccc(C(=O)N[C@@H]2CCC[C@H](OC(F)F)C2)c(OCCCCn3ence3)c1</chem>	125.89	1.81	63.85
413	<chem>Br1ccc(c(OCCCCn2ence2)c1)C(Oc3ccc(cc3)C)=O</chem>	125.89	1.90	63.90
414	<chem>Br1ccc(c(OCCCCn2ence2)c1)C(=O)NCc3coc(n3)CC</chem>	125.89	2.02	63.96
415	<chem>Br1cc(Cl)c(OC)c(NC(=O)c2ccc(Br)cc2OCCCCn3ence3)c1</chem>	125.89	2.37	64.13
416	<chem>Br1ccc(c(OCCCCn2ence2)c1)C(=O)NC[C@H]3CCC[C@H]3OC</chem>	125.89	2.81	64.35
417	<chem>Br1ccc(c(OCCCCn2ence2)c1)C(=O)Nc3c(Br)ccs3</chem>	125.89	4.93	65.41
418	<chem>Br1ccc(c(OCCCCn2ence2)c1)C(=O)NCc3csc(n3)CSC</chem>	125.89	5.53	65.71
419	<chem>Br1ccc(c(OCCCCn2ence2)c1)C(=O)NCC3SCCS3</chem>	125.89	16.32	71.11
420	<chem>Br1ccc(c(OCCCCn2ence2)c1)C(=O)/C=C/c3cc(F)cc(c3Cl)C</chem>	158.49	0.32	79.40
421	<chem>Br1ccc(c(OCCCCn2ence2)c1)C(Oc3ccc(c4c3CCC4)C)=O</chem>	158.49	0.37	79.43
422	<chem>Br1ccc(c(OCCCCn2ence2)c1)C(=O)Nc3cccc4ccc(OC)cc43</chem>	158.49	0.41	79.45
423	<chem>Br1ccc(c(OCCCCn2ence2)c1)C(=O)Nc3cccn4ccc(nc34)C(F)(F)F</chem>	158.49	0.57	79.53

424	<chem>Br1ccc(c(OCCCCn2ence2)c1)C(=O)Nc3cccc4c3nc([nH]4)NC(=O)C</chem>	158.49	0.60	79.54
425	<chem>Br1ccc(C(=O)CNe2c(F)ccc(Cl)c2)c(OCCCCn3ence3)c1</chem>	158.49	0.66	79.57
426	<chem>Br1ccc(c(OCCCCn2ence2)c1)C(=O)Nc3c(Cl)cc(c(c3)C)C</chem>	158.49	0.78	79.64
427	<chem>Br1ccc(NC(=O)c2ccc(Br)cc2OCCCCn3ence3)cc1</chem>	158.49	0.83	79.66
428	<chem>Br1ccc(c(OCCCCn2ence2)c1)C(=O)Nc3ccc(Br)o3</chem>	158.49	1.02	79.75
429	<chem>Br1ccc(C(=O)[C@@H]2[C@H](O2)c3cccc(F)c3)c(OCCCCn4ence4)c1</chem>	158.49	1.23	79.86
430	<chem>Br1cccc(NC(=O)c2ccc(Br)cc2OCCCCn3ence3)c1F</chem>	158.49	1.24	79.86
431	<chem>Br1ccc(c(OCCCCn2ence2)c1)C(=O)Nc3cccc4c3C[C@H](O4)CC</chem>	158.49	1.42	79.95
432	<chem>Br1ccc(c(OCCCCn2ence2)c1)C(=O)Nc3ccc(Cl)cc3F</chem>	158.49	1.50	79.99
433	<chem>Br1ccc(c(OCCCCn2ence2)c1)C(=O)Nc3csc(c3C)C</chem>	158.49	1.92	80.20
434	<chem>Br1ccc(c(OCCCCn2ence2)c1)C(=O)CCc3csc(n3)C(C)C</chem>	158.49	2.64	80.57
435	<chem>Br1ccc(c(OCCCCn2ence2)c1)C(=O)NCc3nc(ns3)CC</chem>	158.49	2.74	80.62
436	<chem>Br1cc2c(NC(=O)c3ccc(Br)cc3OCCCCn4ence4)ccnc2cc1C</chem>	199.53	0.42	99.97
437	<chem>Br1ccc(c(OCCCCn2ence2)c1)C(=O)Nc3ccc(cc3C4CC4)C</chem>	199.53	0.66	100.09
438	<chem>Br1ccc(C(=O)CNe2c(F)nc(NC)n2)c(OCCCCn3ence3)c1</chem>	199.53	0.81	100.17
439	<chem>Br1ccc(NC(=O)c2ccc(Br)cc2OCCCCn3ence3)c4c1O[C@@H](C4)CC</chem>	199.53	0.92	100.22
440	<chem>Br1ccc(c(OCCCCn2ence2)c1)C(=O)Nc3cccc3Cl</chem>	199.53	1.03	100.28
441	<chem>Br1ccc(c(OCCCCn2ence2)c1)C(=O)Nc3cccc(Cl)c3</chem>	199.53	1.24	100.38
442	<chem>Br1c(ccc(NC(=O)c2ccc(Br)cc2OCCCCn3ence3)n1)C</chem>	199.53	1.28	100.41
443	<chem>Br1ccc(c(OCCCCn2ence2)c1)C(=O)Nc3ccc(S)cc3</chem>	199.53	1.54	100.53
444	<chem>Br1ccc(c(OCCCCn2ence2)c1)C(=O)Nc3c(Cl)c(F)cc(c3)C</chem>	199.53	1.73	100.63
445	<chem>Br1ccc(c(OCCCCn2ence2)c1)C(=O)Nc3ccc(SC)en3</chem>	199.53	1.85	100.69
446	<chem>Br1ccc(c(OCCCCn2ence2)c1)C(=O)Nc3c(Cl)sc3</chem>	199.53	3.92	101.72
447	<chem>Br1ccc(c(OCCCCn2ence2)c1)C(=O)Nc3c(F)ccc(NC(=O)C)c3</chem>	251.19	0.31	125.75
448	<chem>Br1c(F)cc2CC[C@@H](NC(=O)c3ccc(Br)cc3OCCCCn4ence4)c2c1</chem>	251.19	0.46	125.82
449	<chem>Br1c(NC(=O)c2ccc(Br)cc2OCCCCn3ence3)ccc(c1C)C</chem>	251.19	0.56	125.87
450	<chem>Br1ccc(c(OCCCCn2ence2)c1)C(=O)Nc3ccc(c(c3Cl)C)C</chem>	251.19	0.63	125.91
451	<chem>Br1ccc(c(OCCCCn2ence2)c1)C(=O)Nc3cccc3CC=C(C)C</chem>	251.19	0.75	125.97
452	<chem>Br1ccc(c(OCCCCn2ence2)c1)C(=O)Nc3ccc(Cl)c(Cl)c3Cl</chem>	251.19	0.86	126.03
453	<chem>Br1ccc(C(=O)N[C@@H]2CCC([C@@H](C2)C)(C)C)c(OCCCCn3ence3)c1</chem>	251.19	0.96	126.07
454	<chem>Ic1ccc(CCNC(=O)c2ccc(Br)cc2OCCCCn3ence3)cc1</chem>	251.19	0.97	126.08
455	<chem>Br1ccc(c(OCCCCn2ence2)c1)C(=O)Nc3c(Cl)cc(cc3)CO</chem>	251.19	1.44	126.32
456	<chem>Ic1nc(NC(=O)c2ccc(Br)cc2OCCCCn3ence3)cc1C</chem>	251.19	1.50	126.34
457	<chem>Ic1c(OC)cccc1NC(=O)c2ccc(Br)cc2OCCCCn3ence3</chem>	251.19	1.96	126.57
458	<chem>Br1ccc(c(OCCCCn2ence2)c1)C(=O)NC[C@H]3CCC[C@H](OC)C3</chem>	251.19	2.01	126.60
459	<chem>Br1cccc(NC(=O)c2ccc(Br)cc2OCCCCn3ence3)c1COC</chem>	251.19	2.18	126.69
460	<chem>Br1ccc(c(OCCCCn2ence2)c1)C(=O)Nc3ccc(Cl)c(Br)n3</chem>	251.19	2.28	126.74
461	<chem>Br1ccc(c(OCCCCn2ence2)c1)C(=O)Nc3cccc4c3nc(Br)s4</chem>	251.19	2.30	126.75
462	<chem>Br1ccc(c(OCCCCn2ence2)c1)C(=O)Nc3cccc3NS(=O)(=O)C</chem>	251.19	2.83	127.01
463	<chem>Br1ccc(c(OCCCCn2ence2)c1)C(=O)Nc3cc(OC)c(Cl)en3</chem>	251.19	3.65	127.42
464	<chem>Br1cc(NC(=O)c2ccc(Br)cc2OCCCCn3ence3)cc(c1C)C</chem>	316.23	0.41	158.32
465	<chem>Br1ccc(c(OCCCCn2ence2)c1)C(=O)NCc3cc(F)ccc3F</chem>	316.23	0.48	158.35
466	<chem>Br1ccc(c(OCCCCn2ence2)c1)C(=O)Nc3cccc(NC(=O)CC)c3</chem>	316.23	0.58	158.40

467	<chem>BrC1ccc(c(OCCCCn2cncc2)c1)C(=O)Nc3cccc4c3OC(F)(F)O4</chem>	316.23	0.59	158.41
468	<chem>BrC1ccc(c(OCCCCn2cncc2)c1)C(=O)Nc3cc(F)cc4c3OCC4</chem>	316.23	0.73	158.48
469	<chem>BrC1ccc(c(OCCCCn2cncc2)c1)C(=O)Nc3cccc4c3O[C@@H](C(=O)N4)C</chem>	316.23	0.74	158.49
470	<chem>BrC1ccc(c(OCCCCn2cncc2)c1)C(=O)NCe3cnn(C4CCCC4)c3</chem>	316.23	0.93	158.58
471	<chem>BrC1ccc(C(=O)Cc2cccc(F)c2OC(C)C)c(OCCCCn3cncc3)c1</chem>	316.23	1.10	158.66
472	<chem>BrC1ccc(c(OCCCCn2cncc2)c1)C(=O)Nc3c(Cl)nc(CC)cc3</chem>	316.23	1.35	158.79
473	<chem>BrC1cccc1NC(=O)c2ccc(Br)cc2OCCCCn3cncc3</chem>	316.23	1.48	158.85
474	<chem>BrC1ccc(c(OCCCCn2cncc2)c1)C(=O)Nc3cccc(OC)c3N</chem>	316.23	1.71	158.97
475	<chem>BrC1ccc(c(OCCCCn2cncc2)c1)C(=O)Nc3cccc4cc[nH]c43</chem>	316.23	1.79	159.01
476	<chem>BrC1ccc(NC(=O)c2ccc(Br)cc2OCCCCn3cncc3)c(SC)c1</chem>	316.23	1.80	159.02
477	<chem>BrC1ccc(c(OCCCCn2cncc2)c1)C(=O)Nc3c(O)ccc(Br)n3</chem>	316.23	2.20	159.21
478	<chem>BrC1ccc(C(=O)CNC2c(Cl)enc(NC)n2)c(OCCCCn3cncc3)c1</chem>	316.23	4.23	160.23
479	<chem>BrC1ccc(c(OCCCCn2cncc2)c1)C(=O)NC[C@H](CC(F)F)C</chem>	316.23	4.59	160.41
480	<chem>BrC1ccc2c([C@H](NC(=O)c3ccc(Br)cc3OCCCCn4cncc4)CS2)c1</chem>	398.11	0.33	199.22
481	<chem>BrC1ccc(c(OCCCCn2cncc2)c1)C(=O)Nc3ccc(CC)c(Cl)n3</chem>	398.11	0.67	199.39
482	<chem>BrC1ccc(c(OCCCCn2cncc2)c1)C(=O)Nc3c(Cl)cc(cc3)C#C</chem>	398.11	0.86	199.48
483	<chem>BrC1ccc(C(=O)Cc2c[nH]c(c2CC)C)c(OCCCCn3cncc3)c1</chem>	398.11	1.09	199.60
484	<chem>BrC1ccc(c(OCCCCn2cncc2)c1)C(=O)N[C@@H]3CCC[C@H](C4CC4)C3</chem>	398.11	1.10	199.60
485	<chem>BrC1ccc(c(OCCCCn2cncc2)c1)C(=O)Nc3c4c(ccs4)ccn3</chem>	398.11	1.41	199.76
486	<chem>BrC1ccc(c(OCCCCn2cncc2)c1)C(=O)NCe3c(nc(o3)C)C</chem>	398.11	3.82	200.96
487	<chem>BrC1ccc(c(OCCCCn2cncc2)c1)C(=O)Cc3ccc(n3-c4cccc4)C</chem>	501.19	0.51	250.85
488	<chem>BrC1ccc(c(OCCCCn2cncc2)c1)C(=O)Nc3c(F)cc(Cl)cn3</chem>	501.19	0.74	250.96
489	<chem>BrC1ccc(c(OCCCCn2cncc2)c1)C(=O)Nc3ccn(c3)C(=O)C</chem>	501.19	1.01	251.10
490	<chem>BrC1ccc(c(OCCCCn2cncc2)c1)C(=O)Nc3ccc(N)c(OCC)n3</chem>	501.19	1.85	251.52
491	<chem>BrC1ccc(c(OCCCCn2cncc2)c1)C(=O)Nc3cccc(Cl)c3OCC</chem>	501.19	2.19	251.69
492	<chem>BrC1ccc(c(OCCCCn2cncc2)c1)C(=O)Nc3cccc4CCCCc34</chem>	630.96	0.57	315.76
493	<chem>BrC1ccc(c(OCCCCn2cncc2)c1)C(=O)Nc3csc4cccc43</chem>	630.96	0.61	315.78
494	<chem>BrC1ccc(c(OCCCCn2cncc2)c1)C(=O)Nc3cccc4c3CC(F)(F)C4</chem>	630.96	0.75	315.85
495	<chem>BrC1ccc(c(OCCCCn2cncc2)c1)C(=O)Nc3cc(Cl)c(c(Cl)c3)C</chem>	630.96	0.90	315.93
496	<chem>BrC1ccc(c(OCCCCn2cncc2)c1)C(=O)NCe3cn(nc3C)CC</chem>	794.33	2.69	398.51
497	<chem>BrC1ccc(c(OCCCCn2cncc2)c1)C(=O)N[C@@H](c3cnn(C(C)C)c3)C</chem>	1000.00	0.50	500.25
498	<chem>BrC1ccc(c(OCCCCn2cncc2)c1)C(=O)Nc3cccc4c3cc(s4)C(OC)=O</chem>	1000.00	2.09	501.04
499	<chem>BrC1ccc(F)cc1CNC(=O)c2ccc(Br)cc2OCCCCn3cncc3</chem>	1258.93	1.04	629.98
500	<chem>BrC1ccc(c(OCCCCn2cncc2)c1)C(=O)Nc3ccc(F)cc3OC(F)F</chem>	1584.89	0.88	792.89

**Table S3.** Ligand growing molecules resulting from step 2 (from molecule 4).

Index	Structure	3D-QSAR IC <sub>50</sub> μM	Docking K <sub>i</sub> μM	Average
1	<chem>BrC1cc(C(=O)N2CCC[C@H](C2)c3nccn3)ccc1OCCCCn4cncc4</chem>	1.58	0.79	1.19
2	<chem>BrC1cc(C(=O)Nc2cccc(Nc3cccc3)c2)ccc1OCCCCn4cncc4</chem>	2.00	0.53	1.26
3	<chem>BrC1cc(C(=O)C2CN(C2)C(=O)c3cccs3)ccc1OCCCCn4cncc4</chem>	1.58	1.63	1.61



4	<chem>Brc1cc(C(=O)Cc2noc(n2)C3CCC3)ccc1OCCCCn4cncc4</chem>	2.51	0.91	1.71
5	<chem>Brc1cc(C(=O)N2CCC[C@@H]2C(=O)NCC(C)C)ccc1OCCCCn3cncc3</chem>	1.00	2.45	1.73
6	<chem>Brc1cc(ccc1OCCCCn2cncc2)C(=O)Nc3nnc(s3)NS(=O)(=O)C</chem>	2.00	1.46	1.73
7	<chem>Brc1cc(C(=O)c2cccc(S(=O)(=O)C)c2N)ccc1OCCCCn3cncc3</chem>	3.16	0.30	1.73
8	<chem>Brc1cc(C(=O)N2CC[C@@H](NC(=O)[C@H]3CCCO3)C2)ccc1OCCCCn4cncc4</chem>	3.16	1.10	2.13
9	<chem>Brc1cc(C(=O)c2cccc(NC3CCC3)c2)ccc1OCCCCn4cncc4</chem>	3.98	0.34	2.16
10	<chem>Brc1cc(C(=O)C(=O)[C@@H]2C[C@@H]2c3cccc(Cl)c3)ccc1OCCCCn4cncc4</chem>	3.98	0.36	2.17
11	<chem>Brc1cc(C(=O)NCCc2cccc(Br)c2)ccc1OCCCCn3cncc3</chem>	3.16	1.33	2.25
12	<chem>Brc1cc(C(=O)c2cccc(NC(=O)c3ccoc3)c2)ccc1OCCCCn4cncc4</chem>	3.98	0.64	2.31
13	<chem>Brc1cc(C(=O)[C@H]2CCCN(C2)c3c4nncn4ccn3)ccc1OCCCCn5cncc5</chem>	3.98	0.84	2.41
14	<chem>Brc1cc(C(=O)c2cccc(NC(=O)[C@@H]3CCCO3)c2)ccc1OCCCCn4cncc4</chem>	3.98	0.87	2.42
15	<chem>Brc1cc(C(=O)[C@H](CC[C@H]2CCCO2)C)ccc1OCCCCn3cncc3</chem>	2.51	2.75	2.63
16	<chem>Brc1cc(ccc1OCCCCn2cncc2)C(=O)Nc3ccc(nn3)C(F)(F)F</chem>	5.01	0.26	2.63
17	<chem>Brc1cc(C(=O)c2cccc(N3CCCS3(=O)=O)c2)ccc1OCCCCn4cncc4</chem>	5.01	0.26	2.64
18	<chem>Brc1cc(C(=O)c2cccc(NC(=O)C3([NH3+])CC3)c2)ccc1OCCCCn4cncc4</chem>	3.98	1.46	2.72
19	<chem>Brc1cc(C(=O)[C@H]2CCCN(C2)c3c(ncc(n3)C)C)ccc1OCCCCn4cncc4</chem>	5.01	0.43	2.72
20	<chem>Brc1cc(C(=O)c2ccc(Sc3ccc(Cl)cc3)o2)ccc1OCCCCn4cncc4</chem>	5.01	0.49	2.75
21	<chem>Brc1cc(C(=O)N2CC[C@@H]2c3cccc(F)c3)ccc1OCCCCn4cncc4</chem>	5.01	0.68	2.84
22	<chem>Brc1cc(ccc1OCCCCn2cncc2)C(=O)Nc3cccc(OCc4cccc4)c3</chem>	3.98	1.74	2.86
23	<chem>Brc1cc(C(=O)N[C@@H](Cc2cncn2)C)ccc1OCCCCn3cncc3</chem>	5.01	1.31	3.16
24	<chem>Brc1cc(C(=O)c2cccc(c2)-c3nccn3)ccc1OCCCCn4cncc4</chem>	6.31	0.17	3.24
25	<chem>Brc1cc(C(=O)c2cccc(C(=O)N3CCSCC3)c2)ccc1OCCCCn4cncc4</chem>	6.31	0.23	3.27
26	<chem>Brc1cc(C(=O)CCc2cccc(F)c2)ccc1OCCCCn3cncc3</chem>	5.01	1.61	3.31
27	<chem>Brc1cc(C(=O)[C@H]2CCCN(C2)c3ncc4COCCc4n3)ccc1OCCCCn5cncc5</chem>	6.31	0.48	3.40
28	<chem>Brc1cc(C(=O)CCS(=O)(=O)c2cccc2)ccc1OCCCCn3cncc3</chem>	5.01	1.82	3.41
29	<chem>Brc1cc(C(=O)N2CCC[C@H](C2)c3noc(n3)C4CC4)ccc1OCCCCn5cncc5</chem>	6.31	0.54	3.43
30	<chem>Brc1cc(C(=O)Cc2coc(n2)C3CC3)ccc1OCCCCn4cncc4</chem>	5.01	2.15	3.58
31	<chem>Brc1cc(ccc1OCCCCn2cncc2)C(=O)N(Cc3en(CC)cc3)C</chem>	2.00	5.23	3.61
32	<chem>Brc1cc(C(=O)CCNe2cccc2F)ccc1OCCCCn3cncc3</chem>	6.31	1.01	3.66
33	<chem>Brc1cc(C(=O)N2C[C@@H](CC2)Cc3nccs3)ccc1OCCCCn4cncc4</chem>	6.31	1.16	3.74
34	<chem>Brc1cc(C(=O)[C@@H]2CN(S(=O)(=O)CC)CC2)ccc1OCCCCn3cncc3</chem>	6.31	1.32	3.82
35	<chem>Brc1cc(C(=O)CCNS(=O)(=O)NC)ccc1OCCCCn2cncc2</chem>	3.98	3.78	3.88
36	<chem>Brc1cc(C(=O)c2cccc3cc[nH]c23)ccc1OCCCCn4cncc4</chem>	7.94	0.15	4.05
37	<chem>Brc1cc(C(=O)c2cccc(Oc3ccc(Cl)cc3)c2)ccc1OCCCCn4cncc4</chem>	7.94	0.26	4.10
38	<chem>Brc1cc(C(=O)c2cccc(n2)C[NH+]3CCCC3)ccc1OCCCCn4cncc4</chem>	7.94	0.38	4.16
39	<chem>Brc1cc(C(=O)NCCNc2nc(cs2)C)ccc1OCCCCn3cncc3</chem>	6.31	2.05	4.18
40	<chem>Brc1cc(C(=O)NCCc2cccc2O)ccc1OCCCCn3cncc3</chem>	7.94	0.49	4.22
41	<chem>Brc1cc(C(=O)Cc2noc(n2)C3CCCC3)ccc1OCCCCn4cncc4</chem>	7.94	0.71	4.33
42	<chem>Brc1cc(C(=O)CNc2nnc(o2)C(F)F)ccc1OCCCCn3cncc3</chem>	7.94	0.75	4.35

43	<chem>BrC1cc(C(=O)c2cccc(NCC#C)c2)ccc1OCCCCn3nccc3</chem>	7.94	1.03	4.48
44	<chem>BrC1cc(C(=O)c2cccc(/C(=[NH+]/C(C)C)N)c2)ccc1OCCCCn3nccc3</chem>	7.94	1.11	4.52
45	<chem>BrC1cc(ccc1OCCCCn2nccc2)C(=O)C(=O)NCc3nc4cccc4o3</chem>	7.94	1.15	4.54
46	<chem>BrC1cc(C(=O)CCSc2nccc(n2)C)ccc1OCCCCn3nccc3</chem>	6.31	2.93	4.62
47	<chem>BrC1cc(C(=O)N2CC[C@H](Oc3ncc(Br)cn3)C2)ccc1OCCCCn4nccc4</chem>	7.94	1.30	4.62
48	<chem>BrC1cc(C(=O)N2CC=C(C2)c3cccc(OC)c3)ccc1OCCCCn4nccc4</chem>	7.94	1.33	4.64
49	<chem>BrC1cc(C(=O)C2noc(n2)[C@H]3CCCO3)ccc1OCCCCn4nccc4</chem>	7.94	1.36	4.65
50	<chem>BrC1cc(ccc1OCCCCn2nccc2)C(=O)Nc3ccc(C4CCCC4)cc3</chem>	7.94	1.37	4.65
51	<chem>BrC1cc(C(=O)c2cccc(OC(=O)N(C)C)c2)ccc1OCCCCn3nccc3</chem>	7.94	1.45	4.70
52	<chem>BrC1cc(C(=O)[C@H](CCC2CCCC2)C)ccc1OCCCCn3nccc3</chem>	7.94	1.64	4.79
53	<chem>BrC1cc(C(=O)C/C=N/NCC#C)ccc1OCCCCn2nccc2</chem>	6.31	3.75	5.03
54	<chem>BrC1cc(C(=O)c2c(Cl)ccc(N3CCCCS3(=O)=O)c2)ccc1OCCCCn4nccc4</chem>	10.00	0.09	5.05
55	<chem>BrC1cc(ccc1OCCCCn2nccc2)C(SCCOC(C)C)=O</chem>	2.51	7.77	5.14
56	<chem>BrC1cc(C(=O)c2csc(n2)CCC(C)C)ccc1OCCCCn3nccc3</chem>	7.94	2.33	5.14
57	<chem>BrC1cc(C(=O)N2CC[C@@H](NC(=O)C(C)C)C2)ccc1OCCCCn3nccc3</chem>	10.00	0.55	5.28
58	<chem>BrC1cc(C(=O)[C@@]2(O)CCCN(C2)c3nccc3)ccc1OCCCCn4nccc4</chem>	10.00	0.64	5.32
59	<chem>BrC1cc(C(S(=O)(=O)c2enn(C3CCCC3)c2)=O)ccc1OCCCCn4nccc4</chem>	10.00	0.92	5.46
60	<chem>BrC1cc(C(=O)[C@@H]2CN(CC2)c3ccc(Cl)cc3F)ccc1OCCCCn4nccc4</chem>	10.00	1.09	5.54
61	<chem>BrC1cc(C(=O)[C@H](Cc2ccc(Cl)cc2)C)ccc1OCCCCn3nccc3</chem>	10.00	1.12	5.56
62	<chem>BrC1cc(ccc1OCCCCn2nccc2)C(SCCCC(C)(C)C#N)=O</chem>	5.01	6.16	5.59
63	<chem>BrC1cc(C(=O)c2cccc(NC(=O)c3ccsc3)c2)ccc1OCCCCn4nccc4</chem>	10.00	1.37	5.68
64	<chem>BrC1cc(C(=O)N2CC[C@@H](NS(=O)(=O)CC)C2)ccc1OCCCCn3nccc3</chem>	3.98	7.46	5.72
65	<chem>BrC1cc(C(=O)NC2CC[NH+](C3CCSCC3)CC2)ccc1OCCCCn4nccc4</chem>	10.00	1.44	5.72
66	<chem>BrC1cc(ccc1OCCCCn2nccc2)C(=O)NCC(=O)NC3CCCC3</chem>	10.00	1.57	5.78
67	<chem>BrC1cc(ccc1OCCCCn2nccc2)C(=O)Nc3ccc(-n4ccnc4)nn3</chem>	10.00	1.71	5.85
68	<chem>BrC1cc(C(=O)[C@@H](CC)C(=O)C(=O)NCC)ccc1OCCCCn2nccc2</chem>	7.94	3.78	5.86
69	<chem>BrC1cc(C(=O)c2cc(N3C(=O)CCS3(=O)=O)ccc2C)ccc1OCCCCn4nccc4</chem>	10.00	1.77	5.88
70	<chem>BrC1cc(ccc1OCCCCn2nccc2)C(=O)CC(Oc3cccc(CC)c3)=O</chem>	10.00	1.77	5.89
71	<chem>BrC1cc(ccc1OCCCCn2nccc2)C(=O)N(CC(=O)NCC(C)C)C</chem>	7.94	3.91	5.93
72	<chem>BrC1cc(C(=O)C(=O)N(Cc2nccc2)C)ccc1OCCCCn3nccc3</chem>	10.00	1.87	5.93
73	<chem>BrC1cc(C(=O)C(=O)NCc2ncc(Br)s2)ccc1OCCCCn3nccc3</chem>	6.31	5.64	5.98
74	<chem>BrC1cc(C(=O)N(CCC2(O)CCCC2)C)ccc1OCCCCn3nccc3</chem>	10.00	2.28	6.14
75	<chem>BrC1cc(C(=O)c2cccc(Oc3ccc(nn3)C)c2)ccc1OCCCCn4nccc4</chem>	12.59	0.15	6.37
76	<chem>BrC1cc(C(S(=O)(=O)CCC2CC2)=O)ccc1OCCCCn3nccc3</chem>	10.00	2.77	6.39
77	<chem>BrC1cc(C(=O)c2cccc(C[NH+]3CCCCC3)c2)ccc1OCCCCn4nccc4</chem>	12.59	0.56	6.58
78	<chem>BrC1cc(C(=O)c2cccc(OCC(F)(F)F)c2)ccc1OCCCCn3nccc3</chem>	12.59	0.66	6.62
79	<chem>BrC1cc(C(OCCc2ncc3cccc3c2)=O)ccc1OCCCCn4nccc4</chem>	12.59	0.68	6.63
80	<chem>BrC1cc(C(=O)NCCc2nnc3cccc32)ccc1OCCCCn4nccc4</chem>	12.59	0.72	6.65
81	<chem>BrC1cc(C(=O)N2CC(Cc3cccc(Br)c3)C2)ccc1OCCCCn4nccc4</chem>	12.59	0.76	6.67

82	<chem>BrC1cc(C(S(=O)(=O)CCC(OCC)=O)=O)ccc1OCCCCn2ncc2</chem>	10.00	3.37	6.69
83	<chem>BrC1cc(C(=O)[C@H]2CNC(NC(OC)=O)=N2)ccc1OCCCCn3ncc3</chem>	10.00	3.42	6.71
84	<chem>BrC1cc(C(=O)Cc2cn3cc(Cl)ccc3n2)ccc1OCCCCn4ncc4</chem>	12.59	0.83	6.71
85	<chem>BrC1cc(C(=O)N2CCC[C@@H]2C(=O)N3CCC(CC3)C)ccc1OCCCCn4ncc4</chem>	12.59	0.84	6.71
86	<chem>BrC1cc(C(=O)C(=O)c2ccc(C3CCCC3)cc2)ccc1OCCCCn4ncc4</chem>	12.59	0.84	6.72
87	<chem>BrC1cc(C(=O)COC(=O)Cc2cccc(F)c2)ccc1OCCCCn3ncc3</chem>	12.59	1.07	6.83
88	<chem>BrC1cc(C(=O)Nc2ccc(N3CCSCC3)cc2C)ccc1OCCCCn4ncc4</chem>	10.00	3.71	6.85
89	<chem>BrC1cc(ccc1OCCCCn2ncc2)C(=O)NCc3nnc(o3)C(C)C</chem>	12.59	1.12	6.85
90	<chem>BrC1cc(C(=O)C(=O)NCc2nc(C3CC3)cs2)ccc1OCCCCn4ncc4</chem>	12.59	1.20	6.90
91	<chem>BrC1cc(C(=O)CCS(=O)(=O)c2ccc(Cl)cc2)ccc1OCCCCn3ncc3</chem>	12.59	1.20	6.90
92	<chem>BrC1cc(C(=O)N2CCc3cc(N4CCOCC4)ccc32)ccc1OCCCCn5ncc5</chem>	12.59	1.22	6.90
93	<chem>BrC1cc(C(=O)N2CC[C@H](OC(=O)N(C)C)C2)ccc1OCCCCn3ncc3</chem>	12.59	1.52	7.06
94	<chem>BrC1cc(ccc1OCCCCn2ncc2)C(=O)C(=O)N(Cc3ccccc3)C</chem>	12.59	1.64	7.11
95	<chem>BrC1cc(C(=O)CCn2c3ccccc3nn2)ccc1OCCCCn4ncc4</chem>	12.59	1.66	7.13
96	<chem>BrC1cc(C(S(=O)(=O)CC[NH2+]C2CC2=O)ccc1OCCCCn3ncc3</chem>	6.31	8.28	7.29
97	<chem>BrC1cc(C(=O)NC[C@H](O)c2ccc(Cl)s2)ccc1OCCCCn3ncc3</chem>	12.59	2.52	7.56
98	<chem>BrC1cc(C(=O)N(CCc2ccc(O)cc2)C)ccc1OCCCCn3ncc3</chem>	12.59	2.83	7.71
99	<chem>BrC1cc(C(=O)CCSc2ccc(Cl)cc2)ccc1OCCCCn3ncc3</chem>	12.59	3.10	7.84
100	<chem>BrC1cc(C(=O)CCCOC(=O)C)ccc1OCCCCn2ncc2</chem>	12.59	3.13	7.86
101	<chem>BrC1cc(ccc1OCCCCn2ncc2)C(=O)c3cc(C(=O)NC4CC4)ccn3</chem>	15.85	0.36	8.10
102	<chem>BrC1cc(C(=O)c2cccc(OC(=O)c3cccs3)c2)ccc1OCCCCn4ncc4</chem>	15.85	0.40	8.12
103	<chem>BrC1cc(C(=O)N2CCC[C@H](NC(=O)C(C)C)C2)ccc1OCCCCn3ncc3</chem>	15.85	0.44	8.14
104	<chem>BrC1cc(C(=O)[C@@H]2[C@H](C2)C(=O)N3CCC[C@H](C3)C)ccc1OCCCCn4ncc4</chem>	15.85	0.59	8.22
105	<chem>BrC1cc(C(=O)N[C@H]2C[C@H]2c3ccc(Cl)cc3)ccc1OCCCCn4ncc4</chem>	15.85	0.94	8.39
106	<chem>BrC1cc(ccc1OCCCCn2ncc2)C(=O)Nc3ccc(N4CCSCC4)cc3</chem>	15.85	1.12	8.48
107	<chem>BrC1cc(C(=O)CCCCCS)ccc1OCCCCn2ncc2</chem>	5.01	12.02	8.52
108	<chem>BrC1cc(C(=O)[C@H]2CCCN(C2)c3ccc(OC)nn3)ccc1OCCCCn4ncc4</chem>	15.85	1.22	8.53
109	<chem>BrC1cc(C(S(=O)(=O)CCc2cccc(F)c2)=O)ccc1OCCCCn3ncc3</chem>	15.85	1.72	8.78
110	<chem>BrC1cc(C(=O)[C@H](CSc2ccc(F)cc2)C)ccc1OCCCCn3ncc3</chem>	15.85	2.04	8.94
111	<chem>BrC1cc(C(S(=O)(=O)C[C@H]2COCC(O2)(C)C)=O)ccc1OCCCCn3ncc3</chem>	15.85	2.08	8.96
112	<chem>BrC1cc(C(=O)C[NH+]2CC(n3cc(en3)C)C2)ccc1OCCCCn4ncc4</chem>	12.59	5.61	9.10
113	<chem>BrC1cc(C(=O)N2CCC[C@H](C2)C3OCCO3)ccc1OCCCCn4ncc4</chem>	15.85	2.37	9.11
114	<chem>BrC1cc(C(=O)N2C[C@H](Nc3ncc3)CC2)ccc1OCCCCn4ncc4</chem>	15.85	2.51	9.18
115	<chem>BrC1cc(ccc1OCCCCn2ncc2)C(Sc3nc(ns3)-c4cccc(c4)C)=O</chem>	15.85	2.60	9.22
116	<chem>BrC1cc(C(=O)CCCNC(=O)C(C)(C)C)ccc1OCCCCn2ncc2</chem>	15.85	2.88	9.36
117	<chem>BrC1cc(C(=O)[C@](O)(CCC=C(C)C)C)ccc1OCCCCn2ncc2</chem>	15.85	3.45	9.65
118	<chem>BrC1cc(C(S(=O)(=O)CC[NH+]2CCNCC2)=O)ccc1OCCCCn3ncc3</chem>	15.85	3.73	9.79
119	<chem>BrC1cc(C(=O)CCC[NH2+][C@H](CC)C)ccc1OCCCCn2ncc2</chem>	10.00	9.92	9.96
120	<chem>BrC1cc(C(=O)CC[NH2+]C2CCCC2)ccc1OCCCCn3ncc3</chem>	15.85	4.24	10.04

121	<chem>BrC1cc(C(=O)c2cccc(c2)-c3ccc(Cl)cc3Cl)ccc1OCCCCn4cncc4</chem>	19.95	0.32	10.14
122	<chem>BrC1cc(C(=O)N(CCC[NH+](C)C)C)ccc1OCCCCn2cncc2</chem>	12.59	7.77	10.18
123	<chem>BrC1cc(ccc1OCCCCn2cncc2)C(=O)Nc3ccc(NS(=O)(=O)C)nn3</chem>	19.95	0.42	10.19
124	<chem>BrC1cc(C(=O)Nc2ccc(S(=O)(=O)C)nn2)ccc1OCCCCn3cncc3</chem>	19.95	0.43	10.19
125	<chem>BrC1cc(C(SCCCCC)=O)ccc1OCCCCn2cncc2</chem>	7.94	12.48	10.21
126	<chem>BrC1cc(ccc1OCCCCn2cncc2)C(=O)C(=O)c3cc(n[nH]3)C4CCCC4</chem>	19.95	0.58	10.26
127	<chem>BrC1cc(C(=O)NCCc2nc3c([nH]2)CCCC3)ccc1OCCCCn4cncc4</chem>	19.95	0.58	10.27
128	<chem>BrC1cc(C(=O)N2CCc3cc(N4CCCC4)ccc32)ccc1OCCCCn5cncc5</chem>	19.95	0.59	10.27
129	<chem>BrC1cc(ccc1OCCCCn2cncc2)C(SCC(=O)NC3CCOCC3)=O</chem>	15.85	4.89	10.37
130	<chem>BrC1cc(C(=O)CCS(=O)(=O)c2cccc(Cl)c2)ccc1OCCCCn3cncc3</chem>	19.95	0.87	10.41
131	<chem>BrC1cc(C(=O)COCC[NH+]2CCCC2)ccc1OCCCCn3cncc3</chem>	12.59	8.31	10.45
132	<chem>BrC1cc(C(=O)Cc2noc(n2)C3CCCC3)ccc1OCCCCn4cncc4</chem>	19.95	0.97	10.46
133	<chem>BrC1cc(C(=O)CCC[NH2+]C2CCCC2)ccc1OCCCCn3cncc3</chem>	15.85	5.30	10.58
134	<chem>BrC1cccc(NCC(=O)C(=O)c2ccc(OCCCCn3cncc3)c(Br)c2)c1</chem>	19.95	1.45	10.70
135	<chem>BrC1cc(C(=O)[C@H](COc2cccc(c2)C)C)ccc1OCCCCn3cncc3</chem>	19.95	1.75	10.85
136	<chem>BrC1cc(C(=O)c2cccc(C[NH2+]C3CC3)c2)ccc1OCCCCn4cncc4</chem>	19.95	1.87	10.91
137	<chem>BrC1cc(C(=O)CC2CC[NH+](C3CCSCC3)CC2)ccc1OCCCCn4cncc4</chem>	19.95	1.97	10.96
138	<chem>BrC1cc(C(=O)N[C@@H](C(=O)NC2CC2)C)ccc1OCCCCn3cncc3</chem>	19.95	2.00	10.97
139	<chem>BrC1cc(C(=O)NC2CC[NH+](C3CCC3)CC2)ccc1OCCCCn4cncc4</chem>	19.95	2.24	11.10
140	<chem>BrC1cc(ccc1OCCCCn2cncc2)C(SCCCC(F)(F)F)=O</chem>	19.95	2.39	11.17
141	<chem>BrC1cc(C(=O)[C@H](CC(=O)c2cccs2)C)ccc1OCCCCn3cncc3</chem>	19.95	2.53	11.24
142	<chem>BrC1cc(C(=O)C[C@H](O)Cc2cccen2)ccc1OCCCCn3cncc3</chem>	19.95	2.70	11.32
143	<chem>BrC1cc(C(=O)[C@H]2C[C@@H]2C(=O)NCCOC)ccc1OCCCCn3cncc3</chem>	15.85	6.91	11.38
144	<chem>BrC1cc(C(=O)C(=O)CCc2nc(no2)C)ccc1OCCCCn3cncc3</chem>	19.95	3.01	11.48
145	<chem>BrC1cc(C(=O)N(CCc2nccs2)C)ccc1OCCCCn3cncc3</chem>	19.95	3.07	11.51
146	<chem>BrC1cc(C(S(=O)(=O)CCCC(C)(C)C)=O)ccc1OCCCCn2cncc2</chem>	19.95	3.14	11.55
147	<chem>BrC1cc(C(=O)[C@H]2C[C@@H]2C(=O)NCCC)ccc1OCCCCn3cncc3</chem>	19.95	3.17	11.56
148	<chem>BrC1cc(C(=O)CCCOc2cccc2)ccc1OCCCCn3cncc3</chem>	19.95	3.34	11.65
149	<chem>BrC1cc(C(=O)CCOc2ncc(Br)cn2)ccc1OCCCCn3cncc3</chem>	19.95	3.78	11.87
150	<chem>BrC1cc(C(=O)N(CCCCC)C)ccc1OCCCCn2cncc2</chem>	19.95	4.35	12.15
151	<chem>BrC1cc(ccc1OCCCCn2cncc2)C(SCC[NH2+]CC(C)C)=O</chem>	19.95	4.64	12.30
152	<chem>BrC1cc(C(=O)C(=O)C(NC(OC)=O)(C)C)ccc1OCCCCn2cncc2</chem>	19.95	4.74	12.34
153	<chem>BrC1cc(C(=O)[C@H](CCCCC)C)ccc1OCCCCn2cncc2</chem>	19.95	4.85	12.40
154	<chem>BrC1cc(C(S[C@@H](C[NH2+]C(C)C)C)=O)ccc1OCCCCn2cncc2</chem>	19.95	5.22	12.59
155	<chem>BrC1cc(C(=O)c2cc(NC(=O)C(C)(C)C)ccc2)ccc1OCCCCn3cncc3</chem>	25.12	0.07	12.59
156	<chem>BrC1cc(C(=O)[C@@H]2c3c(CC[NH2+]2)c4cc(CC)ccc4[nH]3)ccc1OCCCCn5cncc5</chem>	25.12	0.34	12.73
157	<chem>BrC1cc(C(=O)c2cccc(NC3C[NH2+]C3)c2)ccc1OCCCCn4cncc4</chem>	25.12	0.40	12.76
158	<chem>BrC1cc(C(S(=O)(=O)N2C[C@H]2c3ccccc3)=O)ccc1OCCCCn4cncc4</chem>	25.12	0.46	12.79
159	<chem>BrC1cc(C(=O)N2CC[C@@H](NC(=O)C3CCCC3)C2)ccc1OCCCCn4cncc4</chem>	25.12	0.48	12.80
160	<chem>BrC1cc(C(=O)N2CCO[C@@H](C2)c3cccc(F)c3)ccc1OCCCCn4cncc4</chem>	25.12	0.53	12.83

161	<chem>Brc1cc(C(=O)[C@@H]2CN(CC2)C(=O)c3cc[nH]n3)ccc1OCCCCn4cncc4</chem>	25.12	0.54	12.83
162	<chem>Brc1cc(C(=O)[C@H]2C[C@@H]2C(=O)Nc3ccc(Cl)cc3)ccc1OCCCCn4cncc4</chem>	25.12	0.56	12.84
163	<chem>Brc1cc(ccc1OCCCCn2cncc2)C(=O)NCc3nnc4ccc(Cl)cn43</chem>	25.12	0.64	12.88
164	<chem>Brc1cc(C(=O)c2csn3necnn3o2)ccc1OCCCCn4cncc4</chem>	25.12	0.67	12.90
165	<chem>Brc1cc(C(=O)N2CC(Nc3cc(ccc3)C#N)C2)ccc1OCCCCn4cncc4</chem>	25.12	0.70	12.91
166	<chem>Brc1cc(ccc1OCCCCn2cncc2)C(=O)CNC(=O)/C=C/c3cnccc3</chem>	25.12	0.72	12.92
167	<chem>Brc1cc(C(=O)N2CC[NH+](C@H)3CS(=O)(=O)CC3)CC2)ccc1OCCCCn4cncc4</chem>	25.12	0.75	12.93
168	<chem>Brc1cc(C(S(=O)(=O)C/C=C/C)=O)ccc1OCCCCn2cncc2</chem>	19.95	5.95	12.95
169	<chem>Brc1cc(ccc1OCCCCn2cncc2)C(=O)Nc3ccc(nn3)-c4ccc(F)cc4</chem>	25.12	0.95	13.03
170	<chem>Brc1cc(ccc1OCCCCn2cncc2)C(=O)CSCc3nc4cccc4s3</chem>	25.12	0.96	13.04
171	<chem>Brc1cc(C(=O)CC#CCn2cncc2)ccc1OCCCCn3cncc3</chem>	25.12	1.11	13.11
172	<chem>Brc1cc(ccc1OCCCCn2cncc2)C(=O)Cc3coc(n3)-c4ccc(F)c(F)c4</chem>	25.12	1.33	13.22
173	<chem>Brc1cc(C(=O)N[C@@H]2C[C@H]2c3cccc3F)ccc1OCCCCn4cncc4</chem>	25.12	1.39	13.25
174	<chem>Brc1cc(C(=O)C[NH+](Cc2ccc(Cl)cc2)C)ccc1OCCCCn3cncc3</chem>	25.12	1.66	13.39
175	<chem>Brc1cc(C(=O)C(=O)NCc2csc(n2)N)ccc1OCCCCn3cncc3</chem>	25.12	1.85	13.49
176	<chem>Brc1cc(C(S(=O)(=O)C[C@H]2C[C@H]3COC[C@H]3O2)=O)ccc1OCCCCn4cncc4</chem>	25.12	1.90	13.51
177	<chem>Brc1cc(C(=O)N2C[C@H](CC2)c3nc(cc(n3)C)C)ccc1OCCCCn4cncc4</chem>	25.12	1.94	13.53
178	<chem>Brc1cc(C(=O)[C@H](COc2ccccc2F)C)ccc1OCCCCn3cncc3</chem>	25.12	2.04	13.58
179	<chem>Brc1cc(C(=O)N2CC[C@@H](Oc3ncccn3)C2)ccc1OCCCCn4cncc4</chem>	25.12	2.25	13.68
180	<chem>Brc1cc(C(=O)N2CC[C@@H](NC(=O)c3cccs3)C2)ccc1OCCCCn4cncc4</chem>	25.12	2.35	13.73
181	<chem>Brc1cc(C(=O)C(=O)[C@H]2[C@H](C2)C(=O)N3CCCC3)ccc1OCCCCn4cncc4</chem>	25.12	2.70	13.91
182	<chem>Brc1cc(C(=O)[C@@]2(O)CCCN(C2)c3cc(nen3)C)ccc1OCCCCn4cncc4</chem>	25.12	3.09	14.10
183	<chem>Brc1cc(ccc1OCCCCn2cncc2)C(Sc3nc(SC)ns3)=O</chem>	19.95	9.64	14.80
184	<chem>Brc1cc(C(=O)[C@H](C(OCCCC)=O)C)ccc1OCCCCn2cncc2</chem>	25.12	5.18	15.15
185	<chem>Brc1cc(C(=O)[C@H]2CCC[C@H](C2)c3cccc(Cl)c3)ccc1OCCCCn4cncc4</chem>	31.62	0.18	15.90
186	<chem>Brc1cc(ccc1OCCCCn2cncc2)C(=O)C(=O)NCc3c4e(on3)CCCC4</chem>	31.62	0.42	16.02
187	<chem>Brc1cc(ccc1OCCCCn2cncc2)C(=O)Cc3ccc([nH+]c3)N4CCCCC4</chem>	31.62	0.48	16.05
188	<chem>Brc1cc(C(=O)c2ccccc2cenn3CC(C)C)ccc1OCCCCn4cncc4</chem>	31.62	0.53	16.07
189	<chem>Brc1cc(C(=O)Cc2coc(n2)-c3cccc(F)c3)ccc1OCCCCn4cncc4</chem>	31.62	0.57	16.10
190	<chem>Brc1cc(C(=O)N2CCC[C@H](C2)c3cccc(c3)C)ccc1OCCCCn4cncc4</chem>	31.62	0.57	16.10
191	<chem>Brc1cc(C(=O)N2C[C@@H]([C@H]3CCC[C@H]32)c4ccccc4)ccc1OCCCCn5cncc5</chem>	31.62	0.60	16.11
192	<chem>Brc1cc(C(=O)[C@H](Sc2nc3nc(cc(n3n2)C)C)C)ccc1OCCCCn4cncc4</chem>	31.62	0.66	16.14
193	<chem>Brc1cc(C(=O)N2CC(Oc3cc(Cl)ccc3)C2)ccc1OCCCCn4cncc4</chem>	31.62	0.67	16.14
194	<chem>Brc1cc(C(=O)[C@H]2C[C@@H]2C(=O)Nc3cccc(Br)c3)ccc1OCCCCn4cncc4</chem>	31.62	0.78	16.20
195	<chem>Brc1cc(C(=O)c2cenn2Cc3ccc(Cl)cc3)ccc1OCCCCn4cncc4</chem>	31.62	0.85	16.23
196	<chem>Brc1cc(C(=O)c2ccc(c2)C(=O)NC(C)C)ccc1OCCCCn3cncc3</chem>	31.62	0.85	16.23

197	<chem>Brc1cc(C(=O)N2CCC[C@@H]2c3noc(n3)CC)ccc1OCCCCn4cnc4</chem>	31.62	0.92	16.27
198	<chem>Brc1cc(C(=O)c2cccc(NC(=O)c3cccs3)c2)ccc1OCCCCn4cnc4</chem>	31.62	1.11	16.37
199	<chem>Brc1cc(C(=O)C[NH2+][C@H]2Cc3ccc(Cl)cc3C2)ccc1OCCCCn4cnc4</chem>	31.62	1.12	16.37
200	<chem>Brc1cc(C(=O)C(=O)[C@H]2C[C@@H]2C3CCCC3)ccc1OCCCCn4cnc4</chem>	31.62	1.13	16.38
201	<chem>Brc1cc(C(=O)CNC(=O)c2cn3ccsc3n2)ccc1OCCCCn4cnc4</chem>	31.62	1.23	16.43
202	<chem>Brc1cc(C(=O)[C@H]2C[C@@H]2C(=O)NCc3ccco3)ccc1OCCCCn4cnc4</chem>	31.62	1.26	16.44
203	<chem>Brc1cc(C(=O)C[C@@H]2CN(CC2)C(=O)C3CC3)ccc1OCCCCn4cnc4</chem>	31.62	1.26	16.44
204	<chem>Brc1cc(ccc1OCCCCn2cnc2)C(OCCn3c4ccccc4n3)=O</chem>	31.62	1.67	16.64
205	<chem>Brc1cc(C(S(=O)(=O)CCC2CCCC2)=O)ccc1OCCCCn3cnc3</chem>	31.62	1.74	16.68
206	<chem>Brc1cc(C(=O)CCS(=O)(=O)N2CC[NH+](CC2)C)ccc1OCCCCn3cnc3</chem>	31.62	1.86	16.74
207	<chem>Brc1cc(C(=O)c2cccc(COCC)c2)ccc1OCCCCn3cnc3</chem>	31.62	1.88	16.75
208	<chem>Brc1cc(ccc1OCCCCn2cnc2)C(SCc3cc(Cl)ccn3)=O</chem>	25.12	8.45	16.78
209	<chem>Brc1cc(C(SCCC[C@@H]2CCC[NH2+]2)=O)ccc1OCCCCn3cnc3</chem>	31.62	2.27	16.94
210	<chem>Brc1cc(C(=O)CC#CCN2C(=O)CCO2)ccc1OCCCCn3cnc3</chem>	31.62	2.39	17.00
211	<chem>Brc1cc(ccc1OCCCCn2cnc2)C(Oc3ccc(OC(C)C)cc3)=O</chem>	31.62	2.55	17.09
212	<chem>Brc1cc(C(=O)N2CC[C@H](OCC3CC3)C2)ccc1OCCCCn4cnc4</chem>	31.62	2.81	17.21
213	<chem>Brc1cc(C(=O)NC2CC[NH+](C3CCCC3)CC2)ccc1OCCCCn4cnc4</chem>	31.62	2.96	17.29
214	<chem>Brc1cc(C(=O)[C@H]2C[C@@H]2C(=O)NCCCC)ccc1OCCCCn3cnc3</chem>	31.62	3.00	17.31
215	<chem>Brc1cc(C(=O)CCOc2cccc(c2)C)ccc1OCCCCn3cnc3</chem>	31.62	3.03	17.33
216	<chem>Brc1cc(C(=O)[C@H](O)CSC2CCCC2)ccc1OCCCCn3cnc3</chem>	31.62	3.28	17.45
217	<chem>Brc1cc(C(=O)C(OCC(=O)Nc2ncsc2)=O)ccc1OCCCCn3cnc3</chem>	31.62	3.35	17.49
218	<chem>Brc1cc(C(=O)CSCc2cccc(Cl)c2)ccc1OCCCCn3cnc3</chem>	31.62	3.65	17.64
219	<chem>Brc1cc(C(=O)/C=C/COCC)ccc1OCCCCn2cnc2</chem>	25.12	10.23	17.67
220	<chem>Brc1cc(ccc1OCCCCn2cnc2)C(SCC[NH2+]C(C)C)=O</chem>	25.12	10.35	17.73
221	<chem>Brc1cc(C(=O)C(=O)NCc2nccc(n2)C)ccc1OCCCCn3cnc3</chem>	31.62	3.86	17.74
222	<chem>Brc1cc(C(=O)C[NH2+][C@H](COCC)C)ccc1OCCCCn2cnc2</chem>	15.85	19.78	17.82
223	<chem>Brc1cc(C(=O)C(=O)NCc2nccc(s2)CC)ccc1OCCCCn3cnc3</chem>	31.62	6.59	19.11
224	<chem>Brc1cc(C(=O)c2cccc(c2)C#Cc3cccs3)ccc1OCCCCn4cnc4</chem>	39.81	0.13	19.97
225	<chem>Brc1cc(C(=O)N2CCCc3ccc(C(C)C)cc3C2)ccc1OCCCCn4cnc4</chem>	39.81	0.15	19.98
226	<chem>Brc1cc(C(=O)c2c3ccc(S(=O)(=O)C)cc3[nH]c2)ccc1OCCCCn4cnc4</chem>	39.81	0.19	20.00
227	<chem>Brc1cc(ccc1OCCCCn2cnc2)C(=O)c3nccc(Nc4cccc(Br)c4)c3</chem>	39.81	0.20	20.01
228	<chem>Brc1cc(C(=O)N2CCC[C@H](C2)c3n[nH]c(n3)C4CC4)ccc1OCCCCn5cnc5</chem>	39.81	0.36	20.08
229	<chem>Brc1cc(C(=O)c2cccc(C/[NH+]=C(N)C)c2)ccc1OCCCCn3cnc3</chem>	39.81	0.41	20.11
230	<chem>Brc1cc(C(=O)N2CC[C@H](Oc3cccc(n3)C)C2)ccc1OCCCCn4cnc4</chem>	39.81	0.50	20.15
231	<chem>Brc1cc(C(=O)N2CC[C@H](Nc3ccccc3)C2)ccc1OCCCCn4cnc4</chem>	39.81	0.50	20.16
232	<chem>Brc1cc(C(=O)[C@H]2C[C@@H]2C(=O)Nc3cc(cc(c3)C)C)ccc1OCCCCn4cnc4</chem>	39.81	0.53	20.17
233	<chem>Brc1cc(C(=O)CC2CCN(CC2)c3cccc[nH+]3)ccc1OCCCCn4cnc4</chem>	39.81	0.63	20.22

234	Br1cccc(N2C[C@H](CC2)C(=O)c3ccc(OCCCCn4cncc4)c(Br)c3)c1	39.81	0.72	20.26
235	Br1cc(C(=O)c2cccc(OCCC)c2)ccc1OCCCCn3cncc3	39.81	0.85	20.33
236	Br1cc(ccc1OCCCCn2cncc2)C(=O)Nc3ccc(N4CCC(CC4)C)cc3	39.81	0.89	20.35
237	Br1cc(C(S(=O)(=O)CCc2cccc(Cl)c2)=O)ccc1OCCCCn3cncc3	39.81	0.93	20.37
238	Br1cc(ccc1OCCCCn2cncc2)C(=O)Nc3cc(F)c(N4CCOCC4)cc3	39.81	1.00	20.41
239	Br1cc(C(=O)C(=O)c2ccc([C@H]3C[NH2+]CCC3)cc2)ccc1OCCCn4cncc4	39.81	1.01	20.41
240	Br1cc(C(=O)N2CCC[C@@H](C[NH+]3CCN(CC3)C)C2)ccc1OCCCCn4cncc4	39.81	1.04	20.42
241	Br1cc(C(=O)NC2CCN(CC2)c3cccc(c3)C)ccc1OCCCCn4cncc4	39.81	1.09	20.45
242	Br1cc(C(=O)c2cccc(NCC(C)(C)C)c2)ccc1OCCCCn3cncc3	39.81	1.11	20.46
243	Br1cc(C(=O)[C@@H]2CN(CC2)C(=O)C(C)C)ccc1OCCCCn3cncc3	39.81	1.17	20.49
244	Br1cc(C(=O)c2cccc(C[NH+](C(C)C)C)c2)ccc1OCCCCn3cncc3	39.81	1.60	20.71
245	Br1cc(C(=O)CCNc2cccc(Cl)c2)ccc1OCCCCn3cncc3	39.81	1.79	20.80
246	Br1cc(ccc1OCCCCn2cncc2)C(=O)C(=O)NCc3nc(CC)c[nH]3	39.81	1.81	20.81
247	Br1cc(C(SCC[NH2+]C2CCCC2)=O)ccc1OCCCCn3cncc3	39.81	1.93	20.87
248	Br1cc(C(S(=O)(=O)NC[C@@H]2C[NH+](CCO2)C)=O)ccc1OCCCCn3cncc3	39.81	1.94	20.88
249	Br1cc(C(=O)C(=O)c2coc(n2)CC3CC3)ccc1OCCCCn4cncc4	39.81	2.28	21.05
250	Br1cc(ccc1OCCCCn2cncc2)C(SCCOc3cccc3)=O	39.81	2.47	21.14
251	Br1cc(C(=O)C(=O)N(Cc2ccc(Br)o2)C)ccc1OCCCCn3cncc3	39.81	2.54	21.18
252	Br1cc(C(=O)CCC[NH+]2CCCCC2)ccc1OCCCCn3cncc3	39.81	2.97	21.39
253	Br1cc(C(S(=O)(=O)CCC2CCC2)=O)ccc1OCCCCn3cncc3	39.81	3.07	21.44
254	Br1cc(C(=O)C(=O)CCn2cc(Br)en2)ccc1OCCCCn3cncc3	39.81	3.27	21.54
255	Br1cc(C(=O)/C=C/CC[NH2+]CCC)ccc1OCCCCn2cncc2	31.62	12.27	21.95
256	Br1cc(C(=O)C[NH+](Cc2cc(Cl)en2)C)ccc1OCCCCn3cncc3	39.81	4.08	21.95
257	Br1c(OCCCCn2cncc2)ccc(C(S(=O)(=O)[C@@H](C[NH2+]C3CC3)C)=O)c1	39.81	4.19	22.00
258	Br1cc(C(=O)CCCc2ncn2C)ccc1OCCCCn3cncc3	39.81	4.20	22.01
259	Br1cc(C(=O)CCOc2c(Cl)ccc(Br)c2)ccc1OCCCCn3cncc3	39.81	4.66	22.23
260	Br1cc(C(=O)C[NH+](Cc2ccc(Cl)s2)C)ccc1OCCCCn3cncc3	39.81	5.15	22.48
261	Br1cc(ccc1OCCCCn2cncc2)C(SCCC[NH2+]C(C)C)=O	39.81	6.66	23.24
262	Br1cc(C(=O)Cc2ncc(s2)C[NH+](C)C)ccc1OCCCCn3cncc3	31.62	15.28	23.45
263	Br1cc(ccc1OCCCCn2cncc2)C(SCCC[C@@H]([NH2+]C)C)=O	39.81	7.31	23.56
264	Br1cc(ccc1OCCCCn2cncc2)C(=O)N(CC(=O)NC(C)(C)C)C	39.81	7.35	23.58
265	Br1cc(C(=O)CC[C@@H]2CO2)ccc1OCCCCn3cncc3	39.81	7.50	23.65
266	Br1cc(C(=O)CCCC[NH2+]C2CC2)ccc1OCCCCn3cncc3	39.81	7.73	23.77
267	Br1cc(C(=O)CCNC(=O)NCC)ccc1OCCCCn2cncc2	39.81	8.83	24.32
268	Br1cc(C(=O)N(CCC(N)=[NH2+]C)ccc1OCCCCn2cncc2	39.81	8.90	24.36
269	Br1cc(ccc1OCCCCn2cncc2)C(SC[C@@H](C[NH2+]CC)C)=O	39.81	8.98	24.39
270	Br1cc(C(S(=O)(=O)CCOC(C)C)=O)ccc1OCCCCn2cncc2	39.81	9.12	24.46
271	Br1cc(C(=O)N2CCC[C@@H]2c3nnc4CCCCn43)ccc1OCCCCn5cncc5	50.12	0.15	25.13
272	Br1cc(C(=O)[C@H]2CCCN(C2)c3nccn3)ccc1OCCCCn4cncc4	50.12	0.28	25.20
273	Br1cc(C(=O)[C@H]2CCCN(C2)c3ncc(F)en3)ccc1OCCCCn4cncc4	50.12	0.29	25.20

274	<chem>Brc1cc(C(=O)[C@H]2C[C@@H]2C(=O)Nc3c(F)cc(F)cc3)ccc1OCCCCn4cncc4</chem>	50.12	0.41	25.26
275	<chem>Brc1cc(C(=O)N2CC(=CCC2)c3ccccc3)ccc1OCCCCn4cncc4</chem>	50.12	0.42	25.27
276	<chem>Brc1cc(C(=O)N2CCC[C@H](Oc3ncccc3)C2)ccc1OCCCCn4cncc4</chem>	50.12	0.43	25.27
277	<chem>Brc1cc(C(=O)N2CC(c3csc(n3)N)=CCC2)ccc1OCCCCn4cncc4</chem>	50.12	0.54	25.33
278	<chem>Brc1cc(ccc1OCCCCn2cncc2)C(=O)Nc3ccc(N4CC[NH2+][C@H](C4)C)nn3</chem>	50.12	0.58	25.35
279	<chem>Brc1cc(C(=O)N2CCC[C@@H](Nc3cc(F)ccc3)C2)ccc1OCCCCn4cncc4</chem>	50.12	0.61	25.36
280	<chem>Brc1cc(C(=O)[C@H]2CCN(C2)c3ccc(F)c(F)c3)ccc1OCCCCn4cncc4</chem>	50.12	0.68	25.40
281	<chem>Brc1cc(ccc1OCCCCn2cncc2)C(=O)Cc3noc(n3)-c4cc(Cl)ccc4</chem>	50.12	0.74	25.43
282	<chem>Brc1cc(C(=O)N2CCC[C@H](OCC3CC3)C2)ccc1OCCCCn4cncc4</chem>	50.12	0.85	25.48
283	<chem>Brc1cc(C(=O)Cc2cc(no2)CC(C)C)ccc1OCCCCn3cncc3</chem>	50.12	0.93	25.52
284	<chem>Brc1cc(C(=O)[C@H]2CCCN(C2)c3ccc(cc3F)C#N)ccc1OCCCCn4cncc4</chem>	50.12	0.95	25.53
285	<chem>Brc1cc(ccc1OCCCCn2cncc2)C(=O)Nc3ccc(N4CCCCC4)nn3</chem>	50.12	1.01	25.56
286	<chem>Brc1cc(C(S(=O)(=O)C[C@H]2CC3(CCCC3)CO2)=O)ccc1OCCCCn4cncc4</chem>	50.12	1.16	25.64
287	<chem>Brc1cc(C(=O)C[NH+]2CCC([NH+]3CCCC3)CC2)ccc1OCCCCn4cncc4</chem>	50.12	1.16	25.64
288	<chem>Brc1cc(C(=O)N2CC[C@H](n3cc(Cl)cn3)C2)ccc1OCCCCn4cncc4</chem>	50.12	1.22	25.67
289	<chem>Brc1cc(C(=O)C(=O)CCc2cccc(Br)c2)ccc1OCCCCn3cncc3</chem>	50.12	1.31	25.71
290	<chem>Brc1c(OCCCCn2cncc2)ccc(C(S(=O)(=O)N(CC3CCCC3)C)=O)c1</chem>	50.12	1.35	25.73
291	<chem>Brc1cc(C(=O)Cc2noc(n2)CCCC)ccc1OCCCCn3cncc3</chem>	50.12	1.45	25.78
292	<chem>Brc1cc(C(=O)c2cccc(c2N)C(OCC)=O)ccc1OCCCCn3cncc3</chem>	50.12	1.64	25.88
293	<chem>Brc1cc(C(=O)N(CCC[C@H]2CCCO2)C)ccc1OCCCCn3cncc3</chem>	50.12	1.76	25.94
294	<chem>Brc1cc(C(=O)N2CCC[C@@H](C3(OCCO3)C)C2)ccc1OCCCCn4cncc4</chem>	50.12	1.80	25.96
295	<chem>Ic1cccc(OCCC(=O)c2ccc(OCCCCn3cncc3)c(Br)c2)c1</chem>	50.12	1.84	25.98
296	<chem>Brc1cc(ccc1OCCCCn2cncc2)C(OCCc3cccc(Br)c3)=O</chem>	50.12	1.90	26.01
297	<chem>Brc1cc(C(=O)N2CCC[C@H](C2)COCC)ccc1OCCCCn3cncc3</chem>	50.12	2.42	26.27
298	<chem>Brc1cc(ccc1OCCCCn2cncc2)C(SC[C@H]([NH3+])C(OCC)=O)=O</chem>	50.12	2.51	26.31
299	<chem>Brc1cc(C(=O)CCOc2cc(cc2)C)C)ccc1OCCCCn3cncc3</chem>	50.12	2.73	26.42
300	<chem>Brc1cc(C(S(=O)(=O)CCC2CCCC2)=O)ccc1OCCCCn3cncc3</chem>	50.12	2.75	26.44
301	<chem>Brc1cc(C(=O)C(=O)NCc2nc(CC)cs2)ccc1OCCCCn3cncc3</chem>	50.12	2.88	26.50
302	<chem>Brc1cc(C(=O)C(=O)CCN2C(=O)C=CC(=O)N2)ccc1OCCCCn3cncc3</chem>	50.12	2.97	26.54
303	<chem>Brc1cc(C(=O)CNC2nnc(o2)CCC)ccc1OCCCCn3cncc3</chem>	50.12	3.22	26.67
304	<chem>Brc1cc(ccc1OCCCCn2cncc2)C(=O)N(c3ccc(C[NH2+])cn3)C</chem>	50.12	3.24	26.68
305	<chem>Brc1cc(C(=O)CCCNC(=O)C=C(C)C)ccc1OCCCCn2cncc2</chem>	50.12	3.36	26.74
306	<chem>Brc1cc(C(=O)[C@H](O)CCC#CC)ccc1OCCCCn2cncc2</chem>	50.12	3.68	26.90
307	<chem>Brc1cc(C(=O)N2CC[C@@H](C2)C(=O)N[C@H](CC)C)ccc1OCCCCn3cncc3</chem>	50.12	4.23	27.17
308	<chem>Brc1cc(ccc1OCCCCn2cncc2)C(SCC[NH2+])C3CCCC3)=O</chem>	50.12	4.43	27.28
309	<chem>Brc1cc(C(=O)N2CC[C@H](C[NH2+])C(C)(C)C2)ccc1OCCCCn3cncc3</chem>	50.12	4.81	27.46
310	<chem>Brc1cc(C(=O)[C@H](C[NH2+])CCCC)C)ccc1OCCCCn2cncc2</chem>	50.12	5.89	28.00



311	<chem>Brc1cc(ccc1OCCCCn2cncc2)C(SC[C@@H](C[NH2+]C)C)=O</chem>	39.81	16.63	28.22
312	<chem>Brc1cc(C(=O)CC[C@@H](C[NH2+]CC)C)ccc1OCCCCn2cncc2</chem>	50.12	6.48	28.30
313	<chem>Brc1cc(ccc1OCCCCn2cncc2)C(SC/C=C/CS)=O</chem>	50.12	7.23	28.68
314	<chem>Brc1cc(C(=O)CC2CC[NH+](CC2)CCO)ccc1OCCCCn3cncc3</chem>	50.12	11.13	30.62
315	<chem>Brc1cc(C(=O)[C@H](CC[NH2+]CC)C)ccc1OCCCCn2cncc2</chem>	50.12	11.64	30.88
316	<chem>Brc1cc(C(=O)c2cccc(NC3CCOCC3)c2)ccc1OCCCCn4cncc4</chem>	63.10	0.26	31.68
317	<chem>Brc1cc(C(=O)C(=O)c2cn(-c3cccc(Cl)c3)cn2)ccc1OCCCCn4cncc4</chem>	63.10	0.33	31.71
318	<chem>Brc1cc(C(=O)CNC(=O)[C@H]2Cc3cc(F)ccc3O2)ccc1OCCCCn4cncc4</chem>	63.10	0.41	31.75
319	<chem>Brc1cc(C(=O)[C@H]2CCCN(C2)c3cccc(n3)C#N)ccc1OCCCCn4cncc4</chem>	63.10	0.48	31.79
320	<chem>Brc1cc(C(=O)C(=O)[C@@H]2CC[C@H](C2)c3cccc3)ccc1OCCCCn4cncc4</chem>	63.10	0.49	31.79
321	<chem>Brc1cc(C(=O)C2CN(C2)C(=O)c3cccc(Cl)c3)ccc1OCCCCn4cncc4</chem>	63.10	0.56	31.83
322	<chem>Brc1cc(C(=O)[C@H](C(OC2C[C@@H]3CC[C@H]([NH+]3C)C2)=O)C)ccc1OCCCCn4cncc4</chem>	63.10	0.61	31.85
323	<chem>Brc1cc(C(=O)N2CC[C@H](C2)C(=O)Nc3cccc3)ccc1OCCCCn4cncc4</chem>	63.10	0.72	31.91
324	<chem>Brc1cc(C(=O)N2CCC[C@H](C2)c3c4c([nH]n3)ncn4)ccc1OCCCCn5cncc5</chem>	63.10	0.85	31.97
325	<chem>Brc1cc(C(=O)[C@H](c2noc(n2)-c3ccc(Cl)cc3)C)ccc1OCCCCn4cncc4</chem>	63.10	0.87	31.98
326	<chem>Brc1cc(ccc1OCCCCn2cncc2)C(=O)C(=O)Nc3cc4c(s3)CCCC4</chem>	63.10	0.87	31.98
327	<chem>Brc1cc(ccc1OCCCCn2cncc2)C(OCOC(=O)c3cccc3)=O</chem>	63.10	0.89	31.99
328	<chem>Brc1cc(C(=O)[C@H]2CCCN(C2)c3cccc([nH+]3)C)ccc1OCCCCn4cncc4</chem>	63.10	0.94	32.02
329	<chem>Brc1cc(C(=O)N2CCC[C@H]2C(=O)C3CCCC3)ccc1OCCCCn4cncc4</chem>	63.10	0.99	32.04
330	<chem>Brc1cc(C(=O)NCCc2ccc3c(c2)cc[nH]3)ccc1OCCCCn4cncc4</chem>	63.10	1.23	32.16
331	<chem>Brc1cc(C(=O)CCCc2cccc(Br)c2)ccc1OCCCCn3cncc3</chem>	63.10	1.25	32.17
332	<chem>Brc1cc(C(=O)[C@H]2C[C@H]([NH2+]C2)C(=O)N3CSCC3)ccc1OCCCCn4cncc4</chem>	63.10	1.27	32.18
333	<chem>Brc1cc(C(=O)N2CCC[C@H](NC(=O)[C@@H]3CCCO3)C2)ccc1OCCCCn4cncc4</chem>	63.10	1.28	32.19
334	<chem>Brc1cc(C(=O)COC(=O)Cc2ccc(F)cc2)ccc1OCCCCn3cncc3</chem>	63.10	1.31	32.20
335	<chem>Brc1cc(C(=O)N2CCC[C@H](C2)c3nc(c[nH]3)C)ccc1OCCCCn4cncc4</chem>	63.10	1.36	32.23
336	<chem>Brc1cc(C(=O)[C@H](c2n[nH]c(n2)C(C)C)C)ccc1OCCCCn3cncc3</chem>	63.10	1.39	32.24
337	<chem>Brc1cc(C(=O)[C@H]2CCCN(C2)c3c(ccn3)C#N)ccc1OCCCCn4cncc4</chem>	63.10	1.44	32.27
338	<chem>Brc1cc(C(=O)[C@H](O)COc2cccc2)ccc1OCCCCn3cncc3</chem>	63.10	1.50	32.30
339	<chem>Brc1cc(C(=O)[C@H](COc2ccc(F)cc2F)C)ccc1OCCCCn3cncc3</chem>	63.10	1.51	32.30
340	<chem>Brc1cc(C(=O)CCSc2nc(cc(n2)N)C)ccc1OCCCCn3cncc3</chem>	63.10	1.62	32.36
341	<chem>Brc1cc(ccc1OCCCCn2cncc2)C(OCCc3ccc(cc3)C)=O</chem>	63.10	1.63	32.36
342	<chem>Brc1cc(C(=O)C[NH+](Cc2cc(ccc2)C#N)C)ccc1OCCCCn3cncc3</chem>	63.10	1.64	32.37
343	<chem>Brc1cc(C(=O)CSCc2cc(ccc2)C#N)ccc1OCCCCn3cncc3</chem>	63.10	1.95	32.52
344	<chem>Brc1cc(C(=O)NC2CCN(CC2)c3ccc(c[nH+]3)C)ccc1OCCCCn4cncc4</chem>	63.10	1.96	32.53
345	<chem>Brc1cc(C(=O)CCCc2nnc3cccn32)ccc1OCCCCn4cncc4</chem>	63.10	2.16	32.63
346	<chem>Brc1cc(ccc1OCCCCn2cncc2)C(=O)Nc3ccc(SC)cn3</chem>	63.10	2.25	32.67
347	<chem>Brc1cc(ccc1OCCCCn2cncc2)C(=O)N(Cc3cc(no3)CC)C</chem>	63.10	2.36	32.73

348	<chem>BrC1cc(ccc1OCCCCn2ncc2)C(OCCn3cc(nn3)C[NH3+])=O</chem>	63.10	2.53	32.81
349	<chem>BrC1cc(C(=O)C(=O)CCn2cc(Cl)cn2)ccc1OCCCCn3ncc3</chem>	63.10	2.78	32.94
350	<chem>BrC1cc(C(=O)CNC(=O)[C@@H]2CSCC[NH2+])ccc1OCCCCn3ncc3</chem>	63.10	2.84	32.97
351	<chem>BrC1cc(C(=O)CCNc2ncc(N)en2)ccc1OCCCCn3ncc3</chem>	63.10	3.08	33.09
352	<chem>BrC1cc(C(=O)CC[NH+](CC2CCCC2)C)ccc1OCCCCn3ncc3</chem>	63.10	3.73	33.41
353	<chem>BrC1cc(ccc1OCCCCn2ncc2)C(SCC3c3ccc3)=O</chem>	63.10	4.56	33.83
354	<chem>BrC1cc(ccc1OCCCCn2ncc2)C(=O)Nc3nnc(s3)COC</chem>	63.10	4.82	33.96
355	<chem>BrC1cc(C(OC2CC([NH2+]CC)C2)=O)ccc1OCCCCn3ncc3</chem>	63.10	5.46	34.28
356	<chem>BrC1cc(C(S(=O)(=O)CC[NH2+]C(C)C)=O)ccc1OCCCCn2ncc2</chem>	63.10	5.78	34.44
357	<chem>BrC1cc(C(=O)Nc2ccc([nH+]c2C)N3CCOCC3)ccc1OCCCCn4ncc4</chem>	63.10	5.84	34.47
358	<chem>BrC1cnn(CCNC(=O)c2ccc(OCCCCn3ncc3)c(Br)c2)c1</chem>	63.10	5.86	34.48
359	<chem>BrC1cc(C(=O)CCSCCC[NH3+])ccc1OCCCCn2ncc2</chem>	50.12	23.90	37.01
360	<chem>BrC1cc(ccc1OCCCCn2ncc2)C(SC[C@@H]([NH2+]CCC)C)=O</chem>	63.10	13.26	38.18
361	<chem>BrC1cc(C(S(=O)(=O)CCOCC)=O)ccc1OCCCCn2ncc2</chem>	63.10	13.26	38.18
362	<chem>BrC1cc(C(=O)CCCC[NH+](C)C)ccc1OCCCCn2ncc2</chem>	63.10	16.05	39.57
363	<chem>BrC1cc(C(=O)N2CCC[C@@H](NC(=O)C(F)(F)F)C2)ccc1OCCCCn3ncc3</chem>	79.43	0.16	39.80
364	<chem>BrC1cc(C(=O)[C@H]2CCCN(C2)c3ccc(cen3)C#N)ccc1OCCCCn4ncc4</chem>	79.43	0.23	39.83
365	<chem>BrC1cc(C(=O)[C@H]2CCCN(C2)c3cnn(c3)C)ccc1OCCCCn4ncc4</chem>	79.43	0.34	39.89
366	<chem>BrC1cc(C(=O)N2c3ccc(cc3CC2)-c4csc(n4)C)ccc1OCCCCn5ncc5</chem>	79.43	0.35	39.89
367	<chem>BrC1cc(C(=O)[C@H]2CCCN(C2)c3ccc(Cl)nn3)ccc1OCCCCn4ncc4</chem>	79.43	0.40	39.92
368	<chem>BrC1cc(ccc1OCCCCn2ncc2)C(SCCC[NH2+]CC)=O</chem>	50.12	29.86	39.99
369	<chem>BrC1cc(C(=O)c2cc(Nc3cc(on3)C)ccn2)ccc1OCCCCn4ncc4</chem>	79.43	0.55	39.99
370	<chem>BrC1cc(C(=O)[C@H]2CCCN(C2)c3nccc(n3)C)ccc1OCCCCn4ncc4</chem>	79.43	0.56	40.00
371	<chem>BrC1cc(C(=O)c2cccc(C3=[NH+]C[C@@H](N3)C)c2)ccc1OCCCCn4ncc4</chem>	79.43	0.59	40.01
372	<chem>BrC1cc(C(=O)[C@H]2CCCN(C2)c3cccc3F)ccc1OCCCCn4ncc4</chem>	79.43	0.91	40.17
373	<chem>BrC1cc(C(=O)CN2CC[NH+](C[C@@H]3CS(=O)(=O)CC3)CC2)ccc1OCCCCn4ncc4</chem>	79.43	0.94	40.19
374	<chem>BrC1cc(ccc1OCCCCn2ncc2)C(SCC3c3cccc3N)=O</chem>	79.43	0.99	40.21
375	<chem>BrC1cc(C(=O)N2C[C@H](CC2)C(=O)Nc3cc(on3)C)ccc1OCCCCn4ncc4</chem>	79.43	1.10	40.27
376	<chem>BrC1cc(C(=O)N2CC[C@@H](Oc3cccc(F)c3)C2)ccc1OCCCCn4ncc4</chem>	79.43	1.30	40.37
377	<chem>BrC1cc(C(=O)N2CCO[C@@H](C2)c3ccc(Cl)s3)ccc1OCCCCn4ncc4</chem>	79.43	1.50	40.47
378	<chem>BrC1cc(C(=O)[C@H]2CCCN(C2)c3c(F)ccn3)ccc1OCCCCn4ncc4</chem>	79.43	1.51	40.47
379	<chem>BrC1cc(C(=O)[C@@H]2CN(CC2)C(=O)CC(C)C)ccc1OCCCCn3ncc3</chem>	79.43	1.71	40.57
380	<chem>BrC1cc(ccc1OCCCCn2ncc2)C(OCCc3cccc(c3)C)=O</chem>	79.43	1.80	40.62
381	<chem>BrC1cc(C(=O)CNC(=O)C[NH+]2CCCCC2)ccc1OCCCCn3ncc3</chem>	79.43	1.90	40.67
382	<chem>BrC1cc(ccc1OCCCCn2ncc2)C(SCC(OC3CCCC3)=O)=O</chem>	79.43	2.06	40.75
383	<chem>BrC1cc(C(=O)Cc2nc(no2)CC3CC3)ccc1OCCCCn4ncc4</chem>	79.43	2.69	41.06
384	<chem>BrC1cc(C(=O)NCCc2ncc(s2)C)ccc1OCCCCn3ncc3</chem>	79.43	3.03	41.23

385	<chem>Brc1cc(C(=O)[C@@H]2CN(CC2)C(=O)CCC)ccc1OCCCCn3cnc3</chem>	79.43	3.08	41.26
386	<chem>Brc1cc(C(=O)CCCNc2ccccc2)ccc1OCCCCn3cnc3</chem>	79.43	3.17	41.30
387	<chem>Brc1cc(C(=O)CCC[NH+](C2CCCC2)C)ccc1OCCCCn3cnc3</chem>	79.43	3.51	41.47
388	<chem>Brc1cc(C(=O)Cc2oc(n2)CC(C)C)ccc1OCCCCn3cnc3</chem>	79.43	3.66	41.55
389	<chem>Brc1cc(C(S[C@@H](C[NH2+])C2CC2)C(=O)ccc1OCCCCn3cnc3</chem>	79.43	3.86	41.65
390	<chem>Brc1cc(C(=O)CSc2[nH]nc(n2)CC)ccc1OCCCCn3cnc3</chem>	79.43	4.01	41.72
391	<chem>Brc1cc(C(=O)CCN2cc(Cl)c(n2)C)ccc1OCCCCn3cnc3</chem>	79.43	4.01	41.72
392	<chem>Brc1cc(C(=O)Cn2cc(nn2)CCCC)ccc1OCCCCn3cnc3</chem>	79.43	4.01	41.72
393	<chem>Brc1cc(C(=O)[C@H](CCC(OC)=O)C)ccc1OCCCCn2cnc2</chem>	79.43	4.10	41.77
394	<chem>Brc1cc(C(=O)CCC[NH2+]C2CCCC2)ccc1OCCCCn3cnc3</chem>	79.43	4.57	42.00
395	<chem>Brc1cc(ccc1OCCCCn2cnc2)C(=O)C(=O)NCc3c[nH]c(n3)C(C)C</chem>	79.43	4.82	42.12
396	<chem>Brc1cc(C(=O)C[NH+](Cc2cc(Br)cs2)C)ccc1OCCCCn3cnc3</chem>	79.43	5.15	42.29
397	<chem>Brc1cc(C(=O)CCCOC2COCC2)ccc1OCCCCn3cnc3</chem>	79.43	5.25	42.34
398	<chem>Brc1cc(C(=O)c2cccc(NC(=O)C(Br)=C)c2)ccc1OCCCCn3cnc3</chem>	79.43	5.67	42.55
399	<chem>Brc1cc(C(=O)N(CC[NH2+]C2CC2)C)ccc1OCCCCn3cnc3</chem>	79.43	5.67	42.55
400	<chem>Brc1cc(C(SCC[NH+]2CCC(F)CC2)=O)ccc1OCCCCn3cnc3</chem>	79.43	6.73	43.08
401	<chem>Brc1cc(C(=O)CCN2cc(Br)cn2)ccc1OCCCCn3cnc3</chem>	79.43	8.32	43.88
402	<chem>Brc1cc(ccc1OCCCCn2cnc2)C(SCC[NH2+][C@@H](CC)C)=O</chem>	79.43	9.54	44.49
403	<chem>Brc1cc(C(=O)CCCCC(C)C)ccc1OCCCCn2cnc2</chem>	79.43	9.94	44.68
404	<chem>Brc1cc(C(=O)CNCC[NH2+]CC)ccc1OCCCCn2cnc2</chem>	63.10	27.73	45.41
405	<chem>Brc1cc(C(S(=O)(=O)CC[NH2+]CC)=O)ccc1OCCCCn2cnc2</chem>	79.43	14.90	47.17
406	<chem>Brc1cc(C(=O)CCOCC[NH+](C)C)ccc1OCCCCn2cnc2</chem>	79.43	16.02	47.73
407	<chem>Brc1cc(C(=O)c2cccc3c2ccc(n3)C)ccc1OCCCCn4cnc4</chem>	100.00	0.10	50.05
408	<chem>Brc1cc(C(=O)c2cccc(S(=O)(=O)C3CCCC3)c2)ccc1OCCCCn4cnc4</chem>	100.00	0.14	50.07
409	<chem>Brc1cc(C(=O)[C@H]2CC[C@@H](C2)c3cccc(F)c3)ccc1OCCCCn4cnc4</chem>	100.00	0.15	50.08
410	<chem>Brc1cc(C(=O)[C@H]2CCCN(C2)c3cccc(F)c3)ccc1OCCCCn4cnc4</chem>	100.00	0.53	50.27
411	<chem>Brc1cc(C(=O)Cc2c(oc(n2)-c3cccc(F)c3)C)ccc1OCCCCn4cnc4</chem>	100.00	0.63	50.32
412	<chem>Brc1cc(C(=O)c2cccc(OC3CC[NH+](CC3)C)c2)ccc1OCCCCn4cnc4</chem>	100.00	0.69	50.35
413	<chem>Brc1cc(C(=O)c2cccc(C[NH+]3CCC(CC3)C)c2)ccc1OCCCCn4cnc4</chem>	100.00	0.74	50.37
414	<chem>Brc1cc(ccc1OCCCCn2cnc2)C(=O)Nc3ccc(N4CCCC4)nn3</chem>	100.00	0.78	50.39
415	<chem>Brc1cc(C(=O)[C@H]2CN(c3ccc(CC)cc3)C(O2)=O)ccc1OCCCCn4cnc4</chem>	100.00	0.83	50.41
416	<chem>Brc1cc(C(=O)[C@H]2CCN(S(=O)(=O)c3ccccc3)C2)ccc1OCCCCn4cnc4</chem>	100.00	0.87	50.43
417	<chem>Brc1cc(C(=O)C(=O)[C@@H]2CC[NH+](C3CCCC3)C2)ccc1OCCCCn4cnc4</chem>	100.00	0.89	50.44
418	<chem>Brc1cc(C(=O)N2CCO[C@H](C2)c3nc(O)cc(n3)C)ccc1OCCCCn4cnc4</chem>	100.00	0.98	50.49
419	<chem>Brc1cc(C(S(=O)(=O)Nc2ccc(SC)c2)=O)ccc1OCCCCn3cnc3</chem>	100.00	1.08	50.54
420	<chem>Brc1cc(C(=O)C[NH+]2CCN(CC2)c3cccc(Cl)c3)ccc1OCCCCn4cnc4</chem>	100.00	1.11	50.55
421	<chem>Brc1cc(C(=O)[C@@H]2C[NH+](CC2)Cc3ncn3C)ccc1OCCCCn4cnc4</chem>	100.00	1.15	50.57
422	<chem>Brc1cc(C(=O)CCNc2cc(Cl)ccc2Cl)ccc1OCCCCn3cnc3</chem>	100.00	1.22	50.61

423	<chem>Brc1cc(C(S(=O)(=O)NC(=O)CC2CCCC2)=O)ccc1OCCCCn3ncc3</chem>	100.00	1.25	50.62
424	<chem>Brc1cc(C(=O)CNC2nnc(o2)C(C)(C)C)ccc1OCCCCn3nccc3</chem>	100.00	1.29	50.64
425	<chem>Brc1cc(ccc1OCCCCn2nccc2)C(SCC3c4cccc4[nH]3)=O</chem>	100.00	1.36	50.68
426	<chem>Brc1cc(C(S(=O)(=O)CCc2ccccc2)=O)ccc1OCCCCn3nccc3</chem>	100.00	1.53	50.76
427	<chem>Brc1cc(C(=O)CCCc2ccc(Cl)cc2)ccc1OCCCCn3nccc3</chem>	100.00	1.53	50.77
428	<chem>Brc1cc(C(=O)N2CCO[C@@H](C2)c3cc(O)nc(n3)C)ccc1OCCCCn4nccc4</chem>	100.00	1.60	50.80
429	<chem>Brc1cc(C(S(=O)(=O)Nc2cc(Cl)c(Cl)cc2)=O)ccc1OCCCCn3nccc3</chem>	100.00	1.64	50.82
430	<chem>Brc1cc(C(=O)N2CC[C@@H](NC(=O)C=C)C2)ccc1OCCCCn3nccc3</chem>	100.00	1.79	50.89
431	<chem>Brc1cc(C(=O)[C@H]2CCCN(C2)c3nccn3)ccc1OCCCCn4nccc4</chem>	100.00	2.33	51.17
432	<chem>Brc1cc(C(=O)N2CC[C@H](NC(=O)N(C)C)C2)ccc1OCCCCn3nccc3</chem>	100.00	2.33	51.17
433	<chem>Brc1cc(C(=O)C/C=C/[C@@H]([NH3+])CS)ccc1OCCCCn2nccc2</chem>	79.43	23.18	51.31
434	<chem>Brc1cc(C(=O)[C@H]2CCC[C@H]2CCCC)ccc1OCCCCn3nccc3</chem>	100.00	2.66	51.33
435	<chem>Brc1cc(C(=O)NOCC[NH+]2CCCC2)ccc1OCCCCn3nccc3</chem>	100.00	3.19	51.60
436	<chem>Brc1cc(C(=O)N2CC[C@H](Oc3nccs3)C2)ccc1OCCCCn4nccc4</chem>	100.00	4.15	52.08
437	<chem>Brc1cc(C(=O)NCCc2csen2)ccc1OCCCCn3nccc3</chem>	100.00	4.21	52.10
438	<chem>Brc1cc(C(=O)C(=O)CCCC2CCCC2)ccc1OCCCCn3nccc3</chem>	100.00	4.82	52.41
439	<chem>Brc1cc(C(=O)C[NH+](Cc2ccc(Br)s2)C)ccc1OCCCCn3nccc3</chem>	100.00	4.83	52.42
440	<chem>Brc1cc(ccc1OCCCCn2nccc2)C(SCC[NH2+]CC3CC3)=O</chem>	100.00	6.77	53.39
441	<chem>Brc1cc(C(=O)CCCC[NH2+]C(C)C)ccc1OCCCCn2nccc2</chem>	100.00	9.48	54.74
442	<chem>Brc1cc(C(=O)[C@H](CCCC)CC)ccc1OCCCCn2nccc2</chem>	100.00	9.53	54.76
443	<chem>Brc1cc(C(S(=O)(=O)CCC[NH+](C)C)=O)ccc1OCCCCn2nccc2</chem>	100.00	10.29	55.15
444	<chem>Brc1cc(C(=O)C[C@H](C[NH2+]CC)C)ccc1OCCCCn2nccc2</chem>	100.00	14.72	57.36
445	<chem>Brc1cc(C(=O)CCCC[NH2+]CC)ccc1OCCCCn2nccc2</chem>	100.00	14.90	57.45
446	<chem>Brc1cc(C(=O)C[NH2+]CCCC)ccc1OCCCCn2nccc2</chem>	100.00	15.80	57.90
447	<chem>Brc1cc(C(=O)c2cccc(SC3CCCC3)c2)ccc1OCCCCn4nccc4</chem>	125.89	0.25	63.07
448	<chem>Brc1cc(C(=O)[C@H]2[C@H](C[NH+](C2)Cc3ccccc3)C)ccc1OCCCCn4nccc4</chem>	125.89	0.25	63.07
449	<chem>Brc1cc(C(=O)[C@H]2CCN(C2)c3ccccc3)ccc1OCCCCn4nccc4</chem>	125.89	0.49	63.19
450	<chem>Brc1cc(C(=O)[C@@H]2CC[NH+](C3CCCC3)C2)ccc1OCCCCn4nccc4</chem>	125.89	0.57	63.23
451	<chem>Brc1cc(C(=O)[C@H]2CC[NH+](C[C@H]2C)Cc3ccccc3)ccc1OCCCCn4nccc4</chem>	125.89	0.58	63.24
452	<chem>Brc1cc(C(=O)N2CC(Oc3ccccc3)C2)ccc1OCCCCn4nccc4</chem>	125.89	0.88	63.38
453	<chem>Brc1cc(C(S[C@@H]2C[C@@H]([NH2+]C2)C(=O)N(C)C)=O)ccc1OCCCCn3nccc3</chem>	125.89	1.11	63.50
454	<chem>Brc1cc(C(=O)CCNc2ccc3c(OCO3)c2)ccc1OCCCCn4nccc4</chem>	125.89	1.22	63.56
455	<chem>Brc1cc(ccc1OCCCCn2nccc2)C(=O)Nc3ccc(N4CCO[C@H](C4)C)cc3</chem>	125.89	1.27	63.58
456	<chem>Brc1cc(C(=O)CCC[NH+]2Cc3ccccc3C2)ccc1OCCCCn4nccc4</chem>	125.89	1.28	63.59
457	<chem>Brc1cc(C(=O)Cc2noc(n2)-c3cccs3)ccc1OCCCCn4nccc4</chem>	125.89	1.48	63.68
458	<chem>Brc1cc(C(=O)CCCc2ncc3ccccc32)ccc1OCCCCn4nccc4</chem>	125.89	1.95	63.92
459	<chem>Brc1cc(C(=O)CC#CC[NH+](C)C)ccc1OCCCCn2nccc2</chem>	125.89	2.10	64.00
460	<chem>Brc1cc(C(SCC[C@H]2CCCCO2)=O)ccc1OCCCCn3nccc3</chem>	125.89	2.27	64.08
461	<chem>Brc1cc(C(=O)C(=O)CCc2ccc(Cl)s2)ccc1OCCCCn3nccc3</chem>	125.89	2.37	64.13
462	<chem>Brc1cc(C(=O)CSCc2cc(no2)C)ccc1OCCCCn3nccc3</chem>	125.89	2.65	64.27

463	<chem>Brc1cc(C(=O)Cc2esc(n2)CCCC)ccc1OCCCCn3cncc3</chem>	125.89	3.19	64.54
464	<chem>Brc1cc(C(=O)CN2CC[NH+](C@H)(CC)C)CC2)ccc1OCCCCn3cncc3</chem>	125.89	3.83	64.86
465	<chem>Brc1cc(C(=O)C(=O)CCC(=O)NC2CC2)ccc1OCCCCn3cncc3</chem>	125.89	4.99	65.44
466	<chem>Brc1cc(C(=O)C[NH2+]Cc2csc(Br)c2)ccc1OCCCCn3cncc3</chem>	125.89	5.48	65.68
467	<chem>Brc1cc(C(=O)NCCCC(C)C)ccc1OCCCCn2cncc2</chem>	125.89	5.63	65.76
468	<chem>Brc1cc(C(=O)CCCC[n+]2cccc2)ccc1OCCCCn3cncc3</chem>	125.89	5.68	65.79
469	<chem>Brc1cc(C(=O)CNC(=O)C[NH2+]C2CC2)ccc1OCCCCn3cncc3</chem>	125.89	7.43	66.66
470	<chem>Brc1cc(C(=O)C/C(=[NH+]/CCC)N)ccc1OCCCCn2cncc2</chem>	125.89	14.11	70.00
471	<chem>Brc1cc(C(=O)[C@@H]2CN(CCC2)C(=O)N3CCCC3)ccc1OCCCCn4cncc4</chem>	158.49	0.36	79.42
472	<chem>Brc1cc(C(=O)c2cccc(n2)C(=O)N3CCCC3)ccc1OCCCCn4cncc4</chem>	158.49	0.58	79.53
473	<chem>Brc1cc(C(=O)N2c3ccc(CC)cc3CC2)ccc1OCCCCn4cncc4</chem>	158.49	0.83	79.66
474	<chem>Brc1cc(C(=O)CC#CC[NH+]2CCCC2)ccc1OCCCCn3cncc3</chem>	158.49	0.84	79.66
475	<chem>Brc1cc(C(=O)N2CC[NH2+][C@H](C2)c3ccc(OC)c3)ccc1OCCCCn4cncc4</chem>	158.49	0.86	79.67
476	<chem>Brc1cc(C(=O)C2CN(C2)C(=O)c3nc(C)cc3)ccc1OCCCCn4cncc4</chem>	158.49	0.86	79.67
477	<chem>Brc1cc(C(=O)C[NH+]2CCN(CC2)c3ccc(c3)C)ccc1OCCCCn4cncc4</chem>	158.49	0.97	79.73
478	<chem>Brc1cc(C(=O)[C@]2(O)CN(CC2)c3ccc[nH+]3)ccc1OCCCCn4cncc4</chem>	158.49	1.26	79.88
479	<chem>Brc1cc(C(=O)CNc2enc(C(C)(C)C)cn2)ccc1OCCCCn3cncc3</chem>	158.49	1.53	80.01
480	<chem>Brc1cc(C(=O)C2(CC2)C(=O)Nc3ccc(Cl)c3)ccc1OCCCCn4cncc4</chem>	158.49	1.74	80.11
481	<chem>Brc1cc(C(=O)CC2CC[NH+](C3CCOCC3)CC2)ccc1OCCCCn4cncc4</chem>	158.49	1.79	80.14
482	<chem>Brc1cc(C(=O)[C@H](NC(=O)C[NH2+]C2CC2)C)ccc1OCCCCn3cncc3</chem>	158.49	3.32	80.90
483	<chem>Brc1cc(C(=O)CC2CC[NH+](CC2)CCC)ccc1OCCCCn3cncc3</chem>	158.49	5.98	82.23
484	<chem>Brc1cc(C(=O)CC2CC[NH+](CC2)CC(F)(F)F)ccc1OCCCCn3cncc3</chem>	158.49	6.08	82.28
485	<chem>Brc1cc(C(=O)CCCC(=O)NCC)ccc1OCCCCn2cncc2</chem>	158.49	6.62	82.55
486	<chem>Brc1cc(ccc1OCCCCn2cncc2)C(SCC[NH2+]C3CC3)=O</chem>	158.49	9.32	83.90
487	<chem>Brc1cc(C(O)[C@@H](CCC[NH2+]C)C)=O)ccc1OCCCCn2cncc2</chem>	158.49	10.52	84.51
488	<chem>Brc1cc(C(=O)[C@H](Nc2ccc3CCc3c2)C)ccc1OCCCCn4cncc4</chem>	199.53	0.38	99.96
489	<chem>Brc1cc(C(=O)N2CCc3cc(ccc32)-c4cncc4)ccc1OCCCCn5cncc5</chem>	199.53	0.44	99.98
490	<chem>Brc1cc(C(=O)[C@H]2CCN(C2)C(=O)[C@H]3CC=CCC3)ccc1OCCCCn4cncc4</chem>	199.53	0.57	100.05
491	<chem>Brc1cc(C(=O)C2CN(C2)C(=O)C3CCCC3)ccc1OCCCCn4cncc4</chem>	199.53	0.96	100.25
492	<chem>Brc1cc(C(=O)CCOc2cccc(c2)C)ccc1OCCCCn3cncc3</chem>	199.53	1.99	100.76
493	<chem>Brc1cc(ccc1OCCCCn2cncc2)C(=O)Nc3ccc(OC(C)C)c(c3)C</chem>	199.53	2.76	101.14
494	<chem>Brc1cc(C(=O)[C@]2(O)CN(CC2)c3cc(nen3)C)ccc1OCCCCn4cncc4</chem>	199.53	2.91	101.22
495	<chem>Brc1cc(ccc1OCCCCn2cncc2)C(SCC[C@H]3CCCC[NH2+]3)=O</chem>	199.53	3.50	101.51
496	<chem>Brc1cc(C(=O)CC2CC[NH+](C3CC3)CC2)ccc1OCCCCn4cncc4</chem>	199.53	6.15	102.84
497	<chem>Brc1cc(ccc1OCCCCn2cncc2)C(SCC[NH2+]CC#C)=O</chem>	199.53	9.84	104.68
498	<chem>Brc1cc(C(=O)[C@H]2CCC[C@H](C2)c3ccc(Cl)cc3)ccc1OCCCCn4cncc4</chem>	251.19	0.54	125.86
499	<chem>Brc1ccc(N)c(NCCC(=O)c2ccc(OCCCCn3cncc3)c(Br)c2)c1</chem>	251.19	0.82	126.00
500	<chem>Brc1cc(C(=O)[C@H](CCc2ccccc2F)C)ccc1OCCCCn3cncc3</chem>	251.19	1.20	126.19

**Table S4.** Ligand growing molecules resulting from step 2 (from molecule 5).

Index	Structure	3D-QSAR IC <sub>50</sub> μM	Docking K <sub>i</sub> μM	Average
1	<chem>O=C(OC(=O)c1cc(ccc1OCCCCn2cncc2)C)c3cccc(OCC)c3</chem>	0.25	0.36	0.31
2	<chem>O=C(Nc1cccc2ccn(c12)C)c3cc(ccc3OCCCCn4cncc4)C</chem>	0.63	0.47	0.55
3	<chem>O=C(Nc1cccc2c1nc[nH]2)c3cc(ccc3OCCCCn4cncc4)C</chem>	0.63	0.59	0.61
4	<chem>Clc1ccc(NC(=O)C)cc1NC(=O)c2cc(ccc2OCCCCn3cncc3)C</chem>	1.00	0.23	0.61
5	<chem>Clc1ccc2c([C@H](NC(=O)c3cc(ccc3OCCCCn4cncc4)C)CC2)c1</chem>	1.58	0.11	0.85
6	<chem>O=C(Nc1cccc(Nc2cccc2)c1)c3cc(ccc3OCCCCn4cncc4)C</chem>	1.26	0.45	0.86
7	<chem>O=C(N[C@H](CC)c1nc(on1)C)c2cc(ccc2OCCCCn3cncc3)C</chem>	0.79	1.04	0.92
8	<chem>Brc1ccc(N)cc1C(OC(=O)c2cc(ccc2OCCCCn3cncc3)C)=O</chem>	1.58	0.33	0.96
9	<chem>Clc1ccc(Cl)c(c1)C(OC(=O)c2cc(ccc2OCCCCn3cncc3)C)=O</chem>	1.00	0.93	0.96
10	<chem>O=C(Nc1c2cc(nn2cn1)C3CCC3)c4cc(ccc4OCCCCn5cncc5)C</chem>	1.58	0.35	0.97
11	<chem>Brc1cc(N)ccc1NC(=O)c2cc(ccc2OCCCCn3cncc3)C</chem>	1.00	0.99	0.99
12	<chem>O=C(Oc1c2cccc2n(n1)C)c3cc(ccc3OCCCCn4cncc4)C</chem>	1.58	0.42	1.00
13	<chem>O=C(Nc1ccc(cc1)C)c2cc(ccc2OCCCCn3cncc3)C</chem>	1.26	0.77	1.01
14	<chem>O=C(Oc1cccc(CC)c1)C(=O)c2cc(ccc2OCCCCn3cncc3)C</chem>	1.26	0.77	1.02
15	<chem>Brc1ccc(Cl)c(c1)C(OC(=O)c2cc(ccc2OCCCCn3cncc3)C)=O</chem>	2.00	0.13	1.06
16	<chem>O=C(c1cc(ccc1OCCCCn2cncc2)C)C(Oc3cc(cc(c3)C)C)=O</chem>	1.58	0.58	1.08
17	<chem>O=C(Nc1cccn1-c2ccc(s2)C)c3cc(ccc3OCCCCn4cncc4)C</chem>	1.58	0.59	1.09
18	<chem>O=C(Nc1cc(OC)cc(N)c1)c2cc(ccc2OCCCCn3cncc3)C</chem>	1.00	1.18	1.09
19	<chem>Brc1ccc(NC(=O)c2cc(ccc2OCCCCn3cncc3)C)cc1</chem>	1.58	0.71	1.15
20	<chem>O=C(Nc1cccc(N)c1)c2cc(ccc2OCCCCn3cncc3)C</chem>	1.26	1.09	1.18
21	<chem>Brc1cnc2c(CNC(=O)c3cc(ccc3OCCCCn4cncc4)C)cn2c1</chem>	2.00	0.67	1.33
22	<chem>O=C(OC(=O)c1cc(ccc1OCCCCn2cncc2)C)N3C[C@H](C[C@H](C3)C)C</chem>	2.51	0.28	1.40
23	<chem>Fc1ccc(CNC(=O)c2cc(ccc2OCCCCn3cncc3)C)cc1C</chem>	2.51	0.73	1.62
24	<chem>O=C(Nc1cccc2cc[nH]c21)c3cc(ccc3OCCCCn4cncc4)C</chem>	2.51	0.75	1.63
25	<chem>O=C(Nc1cccc(OCc2cccc2)c1)c3cc(ccc3OCCCCn4cncc4)C</chem>	1.58	1.72	1.65
26	<chem>Fc1cc(N)cc(C(=O)NC(=O)c2cc(ccc2OCCCCn3cncc3)C)c1</chem>	3.16	0.24	1.70
27	<chem>O=C(NCc1ccc(o1)-c2ccc(o2)c3cc(ccc3OCCCCn4cncc4)C</chem>	3.16	0.27	1.72
28	<chem>O=C(c1cccc(CNC(=O)c2cc(ccc2OCCCCn3cncc3)C)c1)C</chem>	3.16	0.46	1.81
29	<chem>FC(F)(F)c1nc2c(o1)cccc2NC(=O)c3cc(ccc3OCCCCn4cncc4)C</chem>	3.16	0.78	1.97
30	<chem>Clc1ccc(NC(=O)c2cc(ccc2OCCCCn3cncc3)C)cc1</chem>	3.16	0.80	1.98
31	<chem>Brc1ccc(CNC(=O)c2cc(ccc2OCCCCn3cncc3)C)cc1C</chem>	3.16	0.81	1.99
32	<chem>Brc1cccc(NC(=O)c2cc(ccc2OCCCCn3cncc3)C)c1F</chem>	2.51	1.47	1.99
33	<chem>Fc1ccc2c(CCN(C2)C(=O)NC(=O)c3cc(ccc3OCCCCn4cncc4)C)c1</chem>	3.98	0.15	2.06
34	<chem>O=C(N1Cc2c(NC(=O)c3cc(ccc3OCCCCn4cncc4)C)n[nH]c2CC1)C</chem>	3.98	0.19	2.09
35	<chem>O=C(Nc1cccc1OC(=O)c2cc(ccc2OCCCCn3cncc3)C)C=C</chem>	2.00	2.19	2.09
36	<chem>Fc1cnc([C@H](NC(=O)c2cc(ccc2OCCCCn3cncc3)C)C)cc1</chem>	3.16	1.05	2.11
37	<chem>O=C(Nc1cccc1C)c2cc(ccc2OCCCCn3cncc3)C</chem>	2.51	1.75	2.13
38	<chem>O=C(Nc1c2ccsc2cn1)c3cc(ccc3OCCCCn4cncc4)C</chem>	3.16	1.24	2.20
39	<chem>Clc1ccc(OC)cc1NCC(=O)c2cc(ccc2OCCCCn3cncc3)C</chem>	3.98	0.58	2.28
40	<chem>Brc1ccc(N)c(c1)C(OC(=O)c2cc(ccc2OCCCCn3cncc3)C)=O</chem>	3.98	0.60	2.29

41	<chem>C1c1enc(nc1NCC(=O)c2cc(ccc2OCCCCn3cncc3)C)N</chem>	3.98	0.67	2.32
42	<chem>O=C(Nc1nc(co1)C)c2cc(ccc2OCCCCn3cncc3)C</chem>	2.51	2.66	2.59
43	<chem>O=C(NC(=O)c1cccc(OC)c1O)c2cc(ccc2OCCCCn3cncc3)C</chem>	5.01	0.22	2.62
44	<chem>O=C(NCc1cn(n1)CC)c2cc(ccc2OCCCCn3cncc3)C</chem>	3.16	2.09	2.62
45	<chem>O=C(NCCc1ccc(s1)C)c2cc(ccc2OCCCCn3cncc3)C</chem>	3.16	2.19	2.67
46	<chem>O=C(Nc1cccc1)c2cc(ccc2OCCCCn3cncc3)C</chem>	3.98	1.47	2.73
47	<chem>O=C(Nc1cccc1-c2cccs2)c3cc(ccc3OCCCCn4cncc4)C</chem>	5.01	0.56	2.78
48	<chem>O=C(Nc1ccc2c(c1)cc[nH]2)c3cc(ccc3OCCCCn4cncc4)C</chem>	5.01	0.58	2.80
49	<chem>O=C(N/C=C/c1ccc1)c2cc(ccc2OCCCCn3cncc3)C</chem>	5.01	0.65	2.83
50	<chem>OCc1ccnc1OC(=O)c2cc(ccc2OCCCCn3cncc3)C</chem>	3.98	1.71	2.84
51	<chem>O=C(NCc1ccc2c(c1)cc([nH]2)C)c3cc(ccc3OCCCCn4cncc4)C</chem>	5.01	0.71	2.86
52	<chem>Brc1ccc(NC(=O)c2cc(ccc2OCCCCn3cncc3)C)c4c1ccn4</chem>	5.01	0.77	2.89
53	<chem>FC(Sc1cccc1NC(=O)c2cc(ccc2OCCCCn3cncc3)C)F</chem>	5.01	0.77	2.89
54	<chem>O=C(c1cc(ccc1OCCCCn2cncc2)C)c3nc(no3)C4nc(on4)C</chem>	5.01	0.94	2.98
55	<chem>O=C(Nc1c2c(sc(c2)C)nen1)c3cc(ccc3OCCCCn4cncc4)C</chem>	5.01	0.98	3.00
56	<chem>Brc1cc(ccc1NC(=O)c2cc(ccc2OCCCCn3cncc3)C)C</chem>	5.01	1.02	3.02
57	<chem>O=C(c1cc(ccc1OCCCCn2cncc2)C)CNe3cccc(SC)c3</chem>	5.01	1.09	3.05
58	<chem>O=C(Nc1ccc(N)cc1)c2cc(ccc2OCCCCn3cncc3)C</chem>	5.01	1.15	3.08
59	<chem>O=C(N[C@@H](C1=CC=NN1)C)c2cc(ccc2OCCCCn3cncc3)C</chem>	5.01	1.19	3.10
60	<chem>O=C(c1cc(ccc1OCCCCn2cncc2)C)c3noc(n3)C4ccc(cc4)C</chem>	6.31	0.15	3.23
61	<chem>O=C(NC(=O)c1cc(cc(N)c1)C)c2cc(ccc2OCCCCn3cncc3)C</chem>	6.31	0.18	3.25
62	<chem>O=C(Oc1cccc2c(O)cccc12)c3cc(ccc3OCCCCn4cncc4)C</chem>	6.31	0.25	3.28
63	<chem>O=C(N1CCc2ccc(NC(=O)c3cc(ccc3OCCCCn4cncc4)C)cc21)N</chem>	6.31	0.27	3.29
64	<chem>O=C(Nc1c2cccc2n(c1)C)c3cc(ccc3OCCCCn4cncc4)C</chem>	6.31	0.28	3.29
65	<chem>Brc1nsc1CNC(=O)c2cc(ccc2OCCCCn3cncc3)C</chem>	5.01	1.61	3.31
66	<chem>O=C(N/C=C/C1CCCC1)C)c2cc(ccc2OCCCCn3cncc3)C</chem>	6.31	0.42	3.37
67	<chem>O=C(c1cc(ccc1OCCCCn2cncc2)C)c3nc(no3)C4cccc4</chem>	6.31	0.43	3.37
68	<chem>O=C(Oc1cccs1)c2cc(ccc2OCCCCn3cncc3)C</chem>	3.16	3.65	3.41
69	<chem>O=C(Nc1ccc2c(n1)ccs2)c3cc(ccc3OCCCCn4cncc4)C</chem>	6.31	0.51	3.41
70	<chem>Brc1enc(NC(=O)c2cc(ccc2OCCCCn3cncc3)C)c4c1ccs4</chem>	6.31	0.60	3.45
71	<chem>FC(F)Oc1cccc1NC(=O)c2cc(ccc2OCCCCn3cncc3)C</chem>	6.31	0.73	3.52
72	<chem>O=S(=O)(c1ccenc1NC(=O)c2cc(ccc2OCCCCn3cncc3)C)C</chem>	6.31	0.78	3.55
73	<chem>O=C(NCc1cc(-c2ccoc2)cs1)c3cc(ccc3OCCCCn4cncc4)C</chem>	6.31	0.85	3.58
74	<chem>O=C(NCc1c(nc(s1)CC)C)c2cc(ccc2OCCCCn3cncc3)C</chem>	5.01	2.28	3.65
75	<chem>O=C(NC[C@@H]1CC[C@@H](C1)C)c2cc(ccc2OCCCCn3cncc3)C</chem>	6.31	1.19	3.75
76	<chem>OC1(CCC1)COC(=O)c2cc(ccc2OCCCCn3cncc3)C</chem>	2.51	5.02	3.77
77	<chem>O=C(NC(=O)c1cc(ccc1OCCCCn2cncc2)C)[C@H]3CC(=NO3)c4ccc4</chem>	7.94	0.10	4.02
78	<chem>O=C(Nc1cccc2c1cc(nn2)C)c3cc(ccc3OCCCCn4cncc4)C</chem>	7.94	0.27	4.11
79	<chem>Fc1ccc2cnc(NC(=O)c3cc(ccc3OCCCCn4cncc4)C)c2c1</chem>	7.94	0.33	4.14
80	<chem>O=C(N[C@@H]1CC[C@H]([C@@H](C1)C)C)c2cc(ccc2OCCCCn3cncc3)C</chem>	7.94	0.35	4.15
81	<chem>Brc1cc(F)c(N)cc1C(OC(=O)c2cc(ccc2OCCCCn3cncc3)C)=O</chem>	7.94	0.36	4.15
82	<chem>O=C(c1cc(ccc1OCCCCn2cncc2)C)/C=C/c3ccc(o3)[C@@H]4C[C@@H]4C</chem>	7.94	0.40	4.17
83	<chem>O=C(NCc1sc(n1)-c2cccs2)c3cc(ccc3OCCCCn4cncc4)C</chem>	7.94	0.41	4.18
84	<chem>O=C(NCc1cc(cc(c1)C)C)c2cc(ccc2OCCCCn3cncc3)C</chem>	7.94	0.44	4.19

85	<chem>O=C(N[C@@H](c1enn(C(C)C)c1)C)c2cc(ccc2OCCCCn3ncc3)C</chem>	7.94	0.57	4.26
86	<chem>O=C(c1cc(ccc1OCCCCn2ncc2)C)CCc3nc(no3)C4CCCC4</chem>	7.94	0.59	4.26
87	<chem>O=C(Nc1cccc2c1cn[nH]2)c3cc(ccc3OCCCCn4ncc4)C</chem>	7.94	0.60	4.27
88	<chem>FC(F)(F)c1cc(cs1)CNC(=O)c2cc(ccc2OCCCCn3ncc3)C</chem>	7.94	0.88	4.41
89	<chem>O=C(Nc1cccc1C(OC)=O)c2cc(ccc2OCCCCn3ncc3)C</chem>	7.94	1.11	4.53
90	<chem>O=C(Nc1cc(c(s1)C)C)c2cc(ccc2OCCCCn3ncc3)C</chem>	7.94	1.15	4.55
91	<chem>O=C(Oc1cccc2CCCCc12)c3cc(ccc3OCCCCn4ncc4)C</chem>	7.94	1.23	4.58
92	<chem>O=C(Nc1c2c(nen1)nc(OC)n2)c3cc(ccc3OCCCCn4ncc4)C</chem>	7.94	1.28	4.61
93	<chem>Clc1ccc(CNC(=O)c2cc(ccc2OCCCCn3ncc3)C)cc1F</chem>	7.94	1.32	4.63
94	<chem>FC(F)Oc1cccnc1NC(=O)c2cc(ccc2OCCCCn3ncc3)C</chem>	7.94	1.52	4.73
95	<chem>O=C(Nc1cccc1SC)c2cc(ccc2OCCCCn3ncc3)C</chem>	7.94	1.53	4.73
96	<chem>O=C(N[C@@H]1CCc2ccc(cc21)C)c3cc(ccc3OCCCCn4ncc4)C</chem>	10.00	0.15	5.07
97	<chem>O=C(Oc1cccc1CCC)c2cc(ccc2OCCCCn3ncc3)C</chem>	7.94	2.22	5.08
98	<chem>O=C(Nc1ccc2CCc2c1)c3cc(ccc3OCCCCn4ncc4)C</chem>	10.00	0.19	5.10
99	<chem>O=C(NCC[NH+]1Cc2cccc2C1)c3cc(ccc3OCCCCn4ncc4)C</chem>	10.00	0.27	5.14
100	<chem>O=C(Nc1ccc2cc[nH]c2n1)c3cc(ccc3OCCCCn4ncc4)C</chem>	10.00	0.30	5.15
101	<chem>Brc1ccc(F)cc1CNC(=O)c2cc(ccc2OCCCCn3ncc3)C</chem>	10.00	0.39	5.20
102	<chem>O=S(=O)(Cc1cccc(NC(=O)c2cc(ccc2OCCCCn3ncc3)C)c1)C</chem>	10.00	0.46	5.23
103	<chem>O=C(OC(=O)c1cc(ccc1OCCCCn2ncc2)C)c3c(sc(c3)C)C</chem>	10.00	0.52	5.26
104	<chem>O=C(Nc1nccn1-c2cccc2)c3cc(ccc3OCCCCn4ncc4)C</chem>	10.00	0.53	5.26
105	<chem>Fc1cccc(CNC(=O)c2cc(ccc2OCCCCn3ncc3)C)c1</chem>	10.00	0.56	5.28
106	<chem>Brc1c(NC(=O)c2cc(ccc2OCCCCn3ncc3)C)ncc4c1cc[nH]4</chem>	10.00	0.57	5.28
107	<chem>Brc1ccc(cc1NC(=O)c2cc(ccc2OCCCCn3ncc3)C)C</chem>	10.00	0.57	5.29
108	<chem>O=C(Nc1c2nccc2ccn1)c3cc(ccc3OCCCCn4ncc4)C</chem>	10.00	0.59	5.30
109	<chem>O=C(Nc1snc1OC)c2cc(ccc2OCCCCn3ncc3)C</chem>	7.94	2.71	5.33
110	<chem>Oc1c(NC(=O)c2cc(ccc2OCCCCn3ncc3)C)cccc1C(C)C</chem>	10.00	0.67	5.34
111	<chem>Fc1c(F)ccc(NCC(=O)c2cc(ccc2OCCCCn3ncc3)C)c1</chem>	10.00	0.67	5.34
112	<chem>O=C(Nc1c2c(C)csc2nnc1)c3cc(ccc3OCCCCn4ncc4)C</chem>	10.00	0.68	5.34
113	<chem>O=C(CNc1ccc(N)c(OC)c1)c2cc(ccc2OCCCCn3ncc3)C</chem>	10.00	0.72	5.36
114	<chem>O=C(Nc1cccc2c1cc[nH]2)c3cc(ccc3OCCCCn4ncc4)C</chem>	10.00	0.85	5.42
115	<chem>O=C(Nc1c(CC)cccn1)c2cc(ccc2OCCCCn3ncc3)C</chem>	10.00	0.92	5.46
116	<chem>O=C(Nc1c(C)esc1C(OC)=O)c2cc(ccc2OCCCCn3ncc3)C</chem>	10.00	1.11	5.56
117	<chem>Clc1cccc1C(OC(=O)c2cc(ccc2OCCCCn3ncc3)C)=O</chem>	10.00	1.19	5.59
118	<chem>Fc1cccc(NC(=O)c2cc(ccc2OCCCCn3ncc3)C)c1O</chem>	10.00	1.30	5.65
119	<chem>O=C(c1cc(ccc1OCCCCn2ncc2)C)CSc3ccc4c(OCCCO4)c3</chem>	10.00	1.32	5.66
120	<chem>O=C(c1cc(ccc1OCCCCn2ncc2)C)c3nc(no3)[C@@H](OCC)C</chem>	10.00	2.05	6.03
121	<chem>O=C(NC(=O)c1cc(ccc1OCCCCn2ncc2)C)[C@H]3CC[C@@H](C3)c4cccc4</chem>	12.59	0.04	6.32
122	<chem>O=C(N1CCOC2(C1)CCCC2)NC(=O)c3cc(ccc3OCCCCn4ncc4)C</chem>	12.59	0.18	6.38
123	<chem>Oc1ccc(C(=O)NC(=O)c2cc(ccc2OCCCCn3ncc3)C)cc1OC</chem>	12.59	0.31	6.45
124	<chem>O=C(NCc1ccc(o1)-c2ccoc2)c3cc(ccc3OCCCCn4ncc4)C</chem>	12.59	0.34	6.47
125	<chem>O=C(NCc1cccc2c1nns2)c3cc(ccc3OCCCCn4ncc4)C</chem>	12.59	0.40	6.49
126	<chem>O=C(c1cc(ccc1OCCCCn2ncc2)C)CCc3ccc(c3)C(OC)=O</chem>	12.59	0.43	6.51
127	<chem>Brc1cscc1NC(=O)c2cc(ccc2OCCCCn3ncc3)C</chem>	10.00	3.05	6.52
128	<chem>O=C(OC(=O)c1cc(ccc1OCCCCn2ncc2)C)N3C[C@@H](O[C@@H](C3)C)C</chem>	12.59	0.46	6.53



129	<chem>O=C(Nc1cccc2c1cnn2C)c3cc(ccc3OCCCCn4cnc4)C</chem>	12.59	0.49	6.54
130	<chem>Clc1cc(Cl)cc2c(OC(=O)c3cc(ccc3OCCCCn4cnc4)C)ncnc12</chem>	12.59	0.53	6.56
131	<chem>Clc1c(ccc(CCC(=O)c2cc(ccc2OCCCCn3cnc3)C)c1)C</chem>	12.59	0.55	6.57
132	<chem>Clc1cccc(Cl)c1CNC(=O)c2cc(ccc2OCCCCn3cnc3)C</chem>	12.59	0.61	6.60
133	<chem>O=C(NCc1esnc1)c2cc(ccc2OCCCCn3cnc3)C</chem>	6.31	6.99	6.65
134	<chem>Oc1c(cccc1CC)C(=O)NC(=O)c2cc(ccc2OCCCCn3cnc3)C</chem>	12.59	0.73	6.66
135	<chem>Brc1cccc1NC(=O)c2cc(ccc2OCCCCn3cnc3)C</chem>	12.59	0.76	6.67
136	<chem>O=C(OC(=O)c1cc(ccc1OCCCCn2cnc2)C)c3c(C)ccc(c3)C</chem>	12.59	0.83	6.71
137	<chem>Clc1ccc(F)c(c1)C(OC(=O)c2cc(ccc2OCCCCn3cnc3)C)=O</chem>	12.59	0.91	6.75
138	<chem>O=C(N1C[C@H](O[C@H](C1)C)C)NC(=O)c2cc(ccc2OCCCCn3cnc3)C</chem>	12.59	0.99	6.79
139	<chem>O=C(NCC1CCC1)c2cc(ccc2OCCCCn3cnc3)C</chem>	7.94	5.68	6.81
140	<chem>O=C(c1cc(ccc1OCCCCn2cnc2)C)/C=C/Sc3cccc3</chem>	12.59	1.10	6.84
141	<chem>O=C(N1C[C@H](O[C@H](C1)C)CC)NC(=O)c2cc(ccc2OCCCCn3cnc3)C</chem>	12.59	1.34	6.97
142	<chem>O=C(N/C=C/C(C)C)C)c1cc(ccc1OCCCCn2cnc2)C</chem>	12.59	1.41	7.00
143	<chem>Brc1cccc(NC(=O)c2cc(ccc2OCCCCn3cnc3)C)c1C</chem>	12.59	1.67	7.13
144	<chem>Clc1ccc(c(CNC(=O)c2cc(ccc2OCCCCn3cnc3)C)c1)C</chem>	12.59	1.67	7.13
145	<chem>S=C(NC(=O)c1cc(ccc1OCCCCn2cnc2)C)c3cccc3</chem>	12.59	2.43	7.51
146	<chem>O=C(NCC[C@@H](OC)C)c1cc(ccc1OCCCCn2cnc2)C</chem>	10.00	5.18	7.59
147	<chem>Brc1c(C)ccnc1NC(=O)c2cc(ccc2OCCCCn3cnc3)C</chem>	12.59	2.86	7.73
148	<chem>O=C(NC(=O)c1cc(ccc1OCCCCn2cnc2)C)[C@H]3CCc4c(C3)c5ccc5[nH]4</chem>	15.85	0.03	7.94
149	<chem>O=C(N[C@H]1c2cccc(c2CC1)C)c3cc(ccc3OCCCCn4cnc4)C</chem>	15.85	0.10	7.97
150	<chem>Oc1cc(c2c(NCCC2)n1)C(=O)NC(=O)c3cc(ccc3OCCCCn4cnc4)C</chem>	15.85	0.14	8.00
151	<chem>O=C(NCCC1Cc2cccc2C1)c3cc(ccc3OCCCCn4cnc4)C</chem>	15.85	0.15	8.00
152	<chem>Brc1cc(c(cc1NC(=O)c2cc(ccc2OCCCCn3cnc3)C)C)C</chem>	15.85	0.20	8.02
153	<chem>O=C(c1cc(ccc1OCCCCn2cnc2)C)CNc3cccc(c3)C#C</chem>	15.85	0.26	8.05
154	<chem>FC(F)c1coc(NC(=O)c2cc(ccc2OCCCCn3cnc3)C)n1</chem>	15.85	0.29	8.07
155	<chem>O=C(N[C@H]1c2ccsc2CCC1)c3cc(ccc3OCCCCn4cnc4)C</chem>	15.85	0.33	8.09
156	<chem>O=C(N[C@@H](CCOC)C)c1cc(ccc1OCCCCn2cnc2)C</chem>	7.94	8.29	8.12
157	<chem>O=C(Nc1cccc2ccnc21)c3cc(ccc3OCCCCn4cnc4)C</chem>	15.85	0.39	8.12
158	<chem>Brc1ccc2c(c(OC(=O)c3cc(ccc3OCCCCn4cnc4)C)nn2C)c1</chem>	15.85	0.43	8.14
159	<chem>Fc1enc(NC)nc1NCC(=O)c2cc(ccc2OCCCCn3cnc3)C</chem>	15.85	0.50	8.18
160	<chem>O=C(Nc1cccn2c1nc(n2)CC)c3cc(ccc3OCCCCn4cnc4)C</chem>	15.85	0.50	8.18
161	<chem>Brc1ccc(NC(=O)c2cc(ccc2OCCCCn3cnc3)C)nc1C</chem>	15.85	0.52	8.18
162	<chem>O=C(CCc1ccc(o1)[C@@H]2[C@H](C2)C)c3cc(ccc3OCCCCn4cnc4)C</chem>	15.85	0.56	8.20
163	<chem>Brc1c(F)ccc(CNC(=O)c2cc(ccc2OCCCCn3cnc3)C)c1</chem>	15.85	0.56	8.21
164	<chem>O=C(Nc1cccc(NC(=O)N)c1)c2cc(ccc2OCCCCn3cnc3)C</chem>	15.85	0.58	8.21
165	<chem>O=C(Nc1cccc2c1cc([nH]2)C)c3cc(ccc3OCCCCn4cnc4)C</chem>	15.85	0.58	8.22
166	<chem>Brc1c(Cl)cccc1NC(=O)c2cc(ccc2OCCCCn3cnc3)C</chem>	15.85	0.60	8.22
167	<chem>Clc1cccc(Cl)c1NCC(=O)c2cc(ccc2OCCCCn3cnc3)C</chem>	15.85	0.60	8.23
168	<chem>O=C(c1cc(ccc1OCCCCn2cnc2)C)c3nc(no3)COCC</chem>	12.59	3.90	8.24
169	<chem>Brc1c(F)ccc(CSC(=O)c2cc(ccc2OCCCCn3cnc3)C)c1</chem>	15.85	0.64	8.25
170	<chem>Clc1ccc(Cl)cc1OCC(=O)c2cc(ccc2OCCCCn3cnc3)C</chem>	15.85	0.72	8.29
171	<chem>O=C(c1cc(ccc1OCCCCn2cnc2)C)CSc3cc(ccc3N)C</chem>	15.85	0.78	8.32

172	<chem>Fc1ccc(c(NC(=O)c2cc(ccc2OCCCCn3cncc3)C)c1)C(OC)=O</chem>	15.85	0.78	8.32
173	<chem>O=C(NCc1cccc(c1)C)c2cc(ccc2OCCCCn3cncc3)C</chem>	15.85	0.83	8.34
174	<chem>Brc1ccc(NC(=O)c2cc(ccc2OCCCCn3cncc3)C)c(c1)C(OC)=O</chem>	15.85	0.92	8.39
175	<chem>O=C(NC(=O)c1cc(ccc1OCCCCn2cncc2)C)c3ccn(n3)CCC</chem>	15.85	0.96	8.40
176	<chem>Brc1cccc(NC(=O)c2cc(ccc2OCCCCn3cncc3)C)c1COC</chem>	15.85	1.16	8.50
177	<chem>Clc1cccc(NC(=O)c2cc(ccc2OCCCCn3cncc3)C)n1</chem>	15.85	1.19	8.52
178	<chem>Oc1ccc(O)cc1NC(=O)c2cc(ccc2OCCCCn3cncc3)C</chem>	15.85	1.33	8.59
179	<chem>O=C(NCc1cccn1C)c2cc(ccc2OCCCCn3cncc3)C</chem>	15.85	1.47	8.66
180	<chem>O=C(Nc1cccc2c1OCCN2C)c3cc(ccc3OCCCCn4cncc4)C</chem>	15.85	1.85	8.85
181	<chem>O=C(N[C@@H](c1ccn(n1)C)C)c2cc(ccc2OCCCCn3cncc3)C</chem>	15.85	2.22	9.03
182	<chem>O=C(NC[C@H](c1ncc[nH]1)C)c2cc(ccc2OCCCCn3cncc3)C</chem>	15.85	2.57	9.21
183	<chem>O=C(NCC(CC)CC)c1cc(ccc1OCCCCn2cncc2)C</chem>	15.85	3.51	9.68
184	<chem>S=C(NC(=O)c1cc(ccc1OCCCCn2cncc2)C)c3ccccc3</chem>	15.85	3.69	9.77
185	<chem>O=C(NC(=O)c1cc(ccc1OCCCCn2cncc2)C)[C@H]3C[C@@H]3c4c ccc(c4)C</chem>	19.95	0.13	10.04
186	<chem>O=C(Nc1c2c([nH]c3ccccc32)ccn1)c4cc(ccc4OCCCCn5cncc5)C</chem>	19.95	0.16	10.06
187	<chem>Fc1ccc2c(c(NC(=O)c3cc(ccc3OCCCCn4cncc4)C)n[nH]2)c1</chem>	19.95	0.18	10.07
188	<chem>Fc1cc(F)cc(Cc2noc(n2)C(=O)c3cc(ccc3OCCCCn4cncc4)C)c1</chem>	19.95	0.18	10.07
189	<chem>Brc1ccc2c(c(NC(=O)c3cc(ccc3OCCCCn4cncc4)C)c[nH]2)c1</chem>	19.95	0.18	10.07
190	<chem>O=C(Nc1cccc1N2CCC[C@H](C2)C)c3cc(ccc3OCCCCn4cncc4)C</chem>	19.95	0.20	10.08
191	<chem>O=C1[C@@H](Oc2c(NC(=O)c3cc(ccc3OCCCCn4cncc4)C)cc(cc2N 1C)C)C</chem>	19.95	0.21	10.08
192	<chem>O=C(NC(=O)c1cccc(c1)-c2cccs2)c3cc(ccc3OCCCCn4cncc4)C</chem>	19.95	0.23	10.09
193	<chem>Clc1c(F)c(F)ccc1CNC(=O)c2cc(ccc2OCCCCn3cncc3)C</chem>	19.95	0.24	10.09
194	<chem>O=C(NCCc1nc2cccc2[nH]1)c3cc(ccc3OCCCCn4cncc4)C</chem>	19.95	0.30	10.13
195	<chem>FC(F)(F)Oc1cccc1NC(=O)c2cc(ccc2OCCCCn3cncc3)C</chem>	19.95	0.35	10.15
196	<chem>O=C(NCc1ccn(n1)C2CCCC2)c3cc(ccc3OCCCCn4cncc4)C</chem>	19.95	0.38	10.17
197	<chem>Brc1ccc(cc1C(=O)NC(=O)c2cc(ccc2OCCCCn3cncc3)C)C</chem>	19.95	0.44	10.20
198	<chem>O[C@@H]1CCc2cccc(NC(=O)c3cc(ccc3OCCCCn4cncc4)C)c2C1</chem>	19.95	0.47	10.21
199	<chem>Fc1ccc(NC(=O)c2cc(ccc2OCCCCn3cncc3)C)c(C)c1</chem>	19.95	0.53	10.24
200	<chem>Clc1ccc(NC(=O)c2cc(ccc2OCCCCn3cncc3)C)c(F)c1</chem>	19.95	0.60	10.28
201	<chem>O=S(=O)(N)c1ccccc1NC(=O)c2cc(ccc2OCCCCn3cncc3)C</chem>	19.95	0.62	10.29
202	<chem>O=C(OCC)c1cccc1NC(=O)c2cc(ccc2OCCCCn3cncc3)C</chem>	19.95	0.69	10.32
203	<chem>Clc1cccc(CNC(=O)c2cc(ccc2OCCCCn3cncc3)C)c1</chem>	19.95	0.72	10.34
204	<chem>O=C(Oc1cc(C(=O)C)ccn1)c2cc(ccc2OCCCCn3cncc3)C</chem>	19.95	0.78	10.37
205	<chem>O=C(N[C@@H]1CCCCC12OCCO2)c3cc(ccc3OCCCCn4cncc4)C</chem>	19.95	0.79	10.37
206	<chem>O=C(NCc1nc2CCCn12)c3cc(ccc3OCCCCn4cncc4)C</chem>	19.95	0.79	10.37
207	<chem>Clc1c(F)cccc1NC(=O)c2cc(ccc2OCCCCn3cncc3)C</chem>	19.95	0.84	10.40
208	<chem>O=C(CCc1cccc(N(C)C)c1)c2cc(ccc2OCCCCn3cncc3)C</chem>	19.95	0.87	10.41
209	<chem>Clc1cccc(NC(=O)c2cc(ccc2OCCCCn3cncc3)C)c1C</chem>	19.95	0.92	10.44
210	<chem>Ic1c(F)cccc1NC(=O)c2cc(ccc2OCCCCn3cncc3)C</chem>	19.95	0.96	10.45
211	<chem>O=C(NCC)c1cccc1NC(=O)c2cc(ccc2OCCCCn3cncc3)C</chem>	19.95	0.98	10.47
212	<chem>OCc1cc(ccc1OC(=O)c2cc(ccc2OCCCCn3cncc3)C)C</chem>	19.95	1.11	10.53
213	<chem>O=C(COc1cccc(C(C)C)c1)c2cc(ccc2OCCCCn3cncc3)C</chem>	19.95	1.29	10.62
214	<chem>O=C(NCc1ccn(CCC)c1)c2cc(ccc2OCCCCn3cncc3)C</chem>	19.95	1.35	10.65
215	<chem>OCc1ccnc(NC(=O)c2cc(ccc2OCCCCn3cncc3)C)n1</chem>	19.95	1.37	10.66

216	<chem>Brc1ccc(NC(=O)c2cc(ccc2OCCCCn3nccc3)C)c(Cl)c1</chem>	19.95	1.40	10.68
217	<chem>Clc1cccc(OC(=O)c2cc(ccc2OCCCCn3nccc3)C)c1CO</chem>	19.95	1.76	10.86
218	<chem>Clc1cccc(NC(=O)c2cc(ccc2OCCCCn3nccc3)C)c1N</chem>	19.95	1.82	10.88
219	<chem>Fc1cccc(NC2CC2)c1NC(=O)c3cc(ccc3OCCCCn4nccc4)C</chem>	19.95	1.88	10.92
220	<chem>O=C(N/C=C/CC)c1cc(ccc1OCCCCn2nccc2)C</chem>	15.85	6.26	11.05
221	<chem>OC1(CCCC1)COC(=O)c2cc(ccc2OCCCCn3nccc3)C</chem>	19.95	2.18	11.06
222	<chem>Brc1ccnc(NC(=O)c2cc(ccc2OCCCCn3nccc3)C)c1Cl</chem>	19.95	3.43	11.69
223	<chem>O=C(NCc1cn(nc1OC)C)c2cc(ccc2OCCCCn3nccc3)C</chem>	19.95	3.51	11.73
224	<chem>O=C(Nc1ccn(c1C(OCC)=O)C)c2cc(ccc2OCCCCn3nccc3)C</chem>	19.95	4.22	12.09
225	<chem>O=C(OC[C@H](CC)C)c1cc(ccc1OCCCCn2nccc2)C</chem>	19.95	4.99	12.47
226	<chem>O=C(c1cc(ccc1OCCCCn2nccc2)C)C#C[C@](O)(COC)C</chem>	19.95	5.18	12.57
227	<chem>O=C(Nc1cccc(-c2ccnc(n2)C)c1)c3cc(ccc3OCCCCn4nccc4)C</chem>	25.12	0.17	12.64
228	<chem>Brc1c(NC(=O)c2cc(ccc2OCCCCn3nccc3)C)ccc4cccc14</chem>	25.12	0.17	12.64
229	<chem>Clc1cc(cc(C(=O)NC(=O)c2cc(ccc2OCCCCn3nccc3)C)c1)C</chem>	25.12	0.26	12.69
230	<chem>O=C(NCc1cc(ccc1C)C)c2cc(ccc2OCCCCn3nccc3)C</chem>	25.12	0.30	12.71
231	<chem>O=C(Nc1cc(cc(c1)C)C)c2cc(ccc2OCCCCn3nccc3)C</chem>	25.12	0.31	12.71
232	<chem>Fc1ccc(Cc2nc(no2)C(=O)c3cc(ccc3OCCCCn4nccc4)C)cc1</chem>	25.12	0.33	12.72
233	<chem>O=C(NCc1noc(n1)C2CCC2)c3cc(ccc3OCCCCn4nccc4)C</chem>	25.12	0.38	12.75
234	<chem>Brc1cccc1/C=C/NC(=O)c2cc(ccc2OCCCCn3nccc3)C</chem>	25.12	0.38	12.75
235	<chem>O=C(Nc1ccc2c[nH]nc2c1)c3cc(ccc3OCCCCn4nccc4)C</chem>	25.12	0.41	12.76
236	<chem>Fc1ccc(-n2c(CC(=O)c3cc(ccc3OCCCCn4nccc4)C)cn2)cc1</chem>	25.12	0.51	12.82
237	<chem>Clc1ccc(Cl)c(CNC(=O)c2cc(ccc2OCCCCn3nccc3)C)c1</chem>	25.12	0.56	12.84
238	<chem>Fc1c(C)cccc1NC(=O)c2cc(ccc2OCCCCn3nccc3)C</chem>	25.12	0.57	12.84
239	<chem>O=C(Nc1cccc2c1CCC2)c3cc(ccc3OCCCCn4nccc4)C</chem>	25.12	0.63	12.87
240	<chem>Clc1cccc(C[C@@H](C(=O)c2cc(ccc2OCCCCn3nccc3)C)C)c1</chem>	25.12	0.63	12.88
241	<chem>O=C(NCc1enc(O)cc1)c2cc(ccc2OCCCCn3nccc3)C</chem>	25.12	0.67	12.89
242	<chem>Fc1c(C)ccc(CNC(=O)c2cc(ccc2OCCCCn3nccc3)C)c1</chem>	25.12	0.67	12.90
243	<chem>O=C(Nc1cccc(N)c1[N+](=[O-])=O)c2cc(ccc2OCCCCn3nccc3)C</chem>	25.12	0.74	12.93
244	<chem>Clc1ccc(Cl)c(/C=C/C(=O)c2cc(ccc2OCCCCn3nccc3)C)c1</chem>	25.12	0.76	12.94
245	<chem>O=C(Nc1cccc(c1)C)c2cc(ccc2OCCCCn3nccc3)C</chem>	25.12	0.77	12.94
246	<chem>Fc1ccc(NC(=O)c2cc(ccc2OCCCCn3nccc3)C)c(NC4CC4)c1</chem>	25.12	0.78	12.95
247	<chem>Clc1c(F)ccc(CNC(=O)c2cc(ccc2OCCCCn3nccc3)C)c1</chem>	25.12	0.78	12.95
248	<chem>O=C(Nc1c(c(c(s1)C)C)C)c2cc(ccc2OCCCCn3nccc3)C</chem>	25.12	0.80	12.96
249	<chem>S=C(NC(=O)c1cc(ccc1OCCCCn2nccc2)C)Nc3nc(en3)C</chem>	25.12	0.81	12.97
250	<chem>O=C(NC(=O)c1cc(ccc1OCCCCn2nccc2)C)c3csc(CCC)c3</chem>	25.12	0.85	12.98
251	<chem>O=C(NC(=O)c1cc(ccc1OCCCCn2nccc2)C)[C@H]3C[C@@H]3c4cnccc4</chem>	25.12	1.01	13.07
252	<chem>O=C(Nc1cccc2c1nco2)c3cc(ccc3OCCCCn4nccc4)C</chem>	25.12	1.05	13.08
253	<chem>Fc1ccc(OC)c(NC(=O)c2cc(ccc2OCCCCn3nccc3)C)c1</chem>	25.12	1.07	13.10
254	<chem>Brc1cccc(NC(=O)c2cc(ccc2OCCCCn3nccc3)C)c1</chem>	25.12	1.20	13.16
255	<chem>Fc1cccc1NC(=O)c2cc(ccc2OCCCCn3nccc3)C</chem>	25.12	1.26	13.19
256	<chem>O=C(NCc1sc(c1C)C)c2cc(ccc2OCCCCn3nccc3)C</chem>	25.12	1.52	13.32
257	<chem>O=C(Nc1cccc1CSC)c2cc(ccc2OCCCCn3nccc3)C</chem>	25.12	1.55	13.34
258	<chem>O=C(Nc1c(OCC#C)ccc1)c2cc(ccc2OCCCCn3nccc3)C</chem>	25.12	1.86	13.49
259	<chem>O=C(Nc1cccc1CC)c2cc(ccc2OCCCCn3nccc3)C</chem>	25.12	2.01	13.56
260	<chem>O=C(NCC#C)CNC(=O)c1cc(ccc1OCCCCn2nccc2)C</chem>	25.12	2.26	13.69

261	<chem>O=C(Oc1c(OCC)ccn1)c2cc(ccc2OCCCCn3encc3)C</chem>	25.12	2.35	13.73
262	<chem>O=C(Nc1c(cccn1)C(OC)=O)c2cc(ccc2OCCCCn3encc3)C</chem>	25.12	2.37	13.74
263	<chem>O=C(NC=C(C)C)c1cc(ccc1OCCCCn2encc2)C</chem>	25.12	2.97	14.05
264	<chem>O=C(NCc1esc(n1)CSC)c2cc(ccc2OCCCCn3encc3)C</chem>	25.12	3.47	14.30
265	<chem>O=C(NCCCC=C)c1cc(ccc1OCCCCn2encc2)C</chem>	25.12	6.02	15.57
266	<chem>FC(F)(F)c1ccc2c(c1)c(NC(=O)c3cc(ccc3OCCCCn4encc4)C)n[nH]2</chem>	31.62	0.08	15.85
267	<chem>Brc1cnc2c(c(NC(=O)c3cc(ccc3OCCCCn4encc4)C)n[nH]2)c1</chem>	31.62	0.17	15.90
268	<chem>Clc1ccc2c([C@H](NC(=O)c3cc(ccc3OCCCCn4encc4)C)CCC2)c1</chem>	31.62	0.18	15.90
269	<chem>Clc1ccc(NC(=O)c2cc(ccc2OCCCCn3encc3)C)c4c1ccn4</chem>	31.62	0.23	15.93
270	<chem>O=C(c1cc(ccc1OCCCCn2encc2)C)c3cnc(Oc4cccc4)cn3</chem>	31.62	0.31	15.97
271	<chem>O=C(Nc1cccc2cc([nH]c12)C)c3cc(ccc3OCCCCn4encc4)C</chem>	31.62	0.32	15.97
272	<chem>FC(F)(F)c1ccccc1NC(=O)c2cc(ccc2OCCCCn3encc3)C</chem>	31.62	0.37	16.00
273	<chem>Br1c(cc(c(NC(=O)c2cc(ccc2OCCCCn3encc3)C)c1)C)C</chem>	31.62	0.41	16.02
274	<chem>O=C(Nc1cccc(OC(=O)CC)c1)c2cc(ccc2OCCCCn3encc3)C</chem>	31.62	0.43	16.03
275	<chem>Clc1c(SC)ccc(NC(=O)c2cc(ccc2OCCCCn3encc3)C)c1</chem>	31.62	0.58	16.10
276	<chem>O=C(CCc1ccc(o1)-c2cccs2)c3cc(ccc3OCCCCn4encc4)C</chem>	31.62	0.60	16.11
277	<chem>O=C(Nc1cccc2COCCc21)c3cc(ccc3OCCCCn4encc4)C</chem>	31.62	0.61	16.12
278	<chem>O=C(NC1CCCC1)CNC(=O)c2cc(ccc2OCCCCn3encc3)C</chem>	31.62	0.64	16.13
279	<chem>Br1ccc(c(CNC(=O)c2cc(ccc2OCCCCn3encc3)C)c1)C</chem>	31.62	0.68	16.15
280	<chem>Br1cc(F)ccc1NC(=O)c2cc(ccc2OCCCCn3encc3)C</chem>	31.62	0.68	16.15
281	<chem>O=C(NC=C1CCCC1)c2cc(ccc2OCCCCn3encc3)C</chem>	31.62	0.70	16.16
282	<chem>Oc1cccc(c1NC(=O)c2cc(ccc2OCCCCn3encc3)C)C</chem>	31.62	0.76	16.19
283	<chem>Clc1c(C)ccnc1NC(=O)c2cc(ccc2OCCCCn3encc3)C</chem>	31.62	0.88	16.25
284	<chem>O=C(Nc1ccc(SC)cc1)c2cc(ccc2OCCCCn3encc3)C</chem>	31.62	0.91	16.27
285	<chem>O=C(NCCNC(=O)c1cc(ccc1OCCCCn2encc2)C)C3CCC3</chem>	31.62	0.91	16.27
286	<chem>O=C(COc1cccc(CC)c1)c2cc(ccc2OCCCCn3encc3)C</chem>	31.62	0.94	16.28
287	<chem>Clc1c(ccc(NC(=O)c2cc(ccc2OCCCCn3encc3)C)c1)C</chem>	31.62	1.03	16.33
288	<chem>O=C(OCc1noc(n1)CCC)c2cc(ccc2OCCCCn3encc3)C</chem>	31.62	1.17	16.40
289	<chem>O=C(Nc1ccc2c(ncs2)c1N)c3cc(ccc3OCCCCn4encc4)C</chem>	31.62	1.21	16.41
290	<chem>Br1cc(Cl)ccc1NC(=O)c2cc(ccc2OCCCCn3encc3)C</chem>	31.62	1.21	16.42
291	<chem>Clc1cnc(NC(=O)c2cc(ccc2OCCCCn3encc3)C)n1</chem>	31.62	1.29	16.46
292	<chem>Clc1cccc(NC(=O)c2cc(ccc2OCCCCn3encc3)C)c1OCC</chem>	31.62	1.83	16.73
293	<chem>Clc1c(c(nm1C)C)CNC(=O)c2cc(ccc2OCCCCn3encc3)C</chem>	31.62	2.16	16.89
294	<chem>O=C(Nc1cccc1SC(C)C)c2cc(ccc2OCCCCn3encc3)C</chem>	31.62	2.50	17.06
295	<chem>O=C(CCC1C[C@@H](O[C@@H](C1)C)C)c2cc(ccc2OCCCCn3encc3)C</chem>	31.62	2.80	17.21
296	<chem>Fc1c(OC)cccc1CCC(=O)c2cc(ccc2OCCCCn3encc3)C</chem>	31.62	3.15	17.39
297	<chem>O=C(c1cc(ccc1OCCCCn2encc2)C)CCSCC(OC)=O</chem>	31.62	4.97	18.29
298	<chem>O=C(NC[C@H](CCO)C)c1cc(ccc1OCCCCn2encc2)C</chem>	31.62	5.00	18.31
299	<chem>O=C(NC(=O)c1cc(ccc1OCCCCn2encc2)C)[C@H]3CC(=NO3)c4cnccc4</chem>	39.81	0.10	19.96
300	<chem>O=C(c1cc(ccc1OCCCCn2encc2)C)c3nnc(o3)Cc4cccc4</chem>	39.81	0.25	20.03
301	<chem>Clc1ccc(F)c(C(=O)NC(=O)c2cc(ccc2OCCCCn3encc3)C)c1</chem>	39.81	0.28	20.04
302	<chem>Fc1cc(F)ccc1CCNC(=O)c2cc(ccc2OCCCCn3encc3)C</chem>	39.81	0.37	20.09
303	<chem>O=C(Oc1c2cccc2cen1)c3cc(ccc3OCCCCn4encc4)C</chem>	39.81	0.37	20.09
304	<chem>O=C(NCc1ccc2c(c(c([nH]2)C)c1)c3cc(ccc3OCCCCn4encc4)C</chem>	39.81	0.40	20.11

305	O=C(Nc1cccc1-c2cn[nH]c2)c3cc(ccc3OCCCCn4cncc4)C	39.81	0.41	20.11
306	O=C(Nc1cccc1-c2cc[nH]n2)c3cc(ccc3OCCCCn4cncc4)C	39.81	0.41	20.11
307	Clc1ccc(F)c(NCC(=O)c2cc(ccc2OCCCCn3cncc3)C)c1	39.81	0.42	20.11
308	O=C(N1c2cccc2C[C@H]1C)CC(=O)c3cc(ccc3OCCCCn4cncc4)C	39.81	0.42	20.12
309	O=S(=O)(N1C[C@H](CC1)CNC(=O)c2cc(ccc2OCCCCn3cncc3)C)C	39.81	0.47	20.14
310	OCCCCNC(=O)c1cc(ccc1OCCCCn2cncc2)C	31.62	8.67	20.14
311	Clc1c(O)ccc(CNC(=O)c2cc(ccc2OCCCCn3cncc3)C)c1	39.81	0.76	20.28
312	Clc1c(Cl)cccc1NC(=O)c2cc(ccc2OCCCCn3cncc3)C	39.81	0.80	20.31
313	O=C(Nc1cccn2cncc12)c3cc(ccc3OCCCCn4cncc4)C	39.81	0.82	20.31
314	O=C(Cc1cccc1-c2ccc02)c3cc(ccc3OCCCCn4cncc4)C	39.81	0.89	20.35
315	O=C(c1cc(ccc1OCCCCn2cncc2)C)/C=C/c3cccc(c3)C	39.81	0.92	20.37
316	O=C(OCc1cc[nH+]c(NC)c1)c2cc(ccc2OCCCCn3cncc3)C	39.81	0.99	20.40
317	O=S(=O)(c1ccsc1NC(=O)c2cc(ccc2OCCCCn3cncc3)C)C	39.81	1.08	20.45
318	O=C(NCc1ncc(c1)C)c2cc(ccc2OCCCCn3cncc3)C	39.81	1.11	20.46
319	O=S(=O)(c1ccc(s1)CNC(=O)c2cc(ccc2OCCCCn3cncc3)C)C	39.81	1.11	20.46
320	Brc1c(F)ccc(OCC(=O)c2cc(ccc2OCCCCn3cncc3)C)c1	39.81	1.17	20.49
321	O=C(Nc1cccc(OC)c1N)c2cc(ccc2OCCCCn3cncc3)C	39.81	1.23	20.52
322	Clc1ccc(CNC(=O)c2cc(ccc2OCCCCn3cncc3)C)cc1N	39.81	1.30	20.55
323	Clc1cccc(NC(=O)c2cc(ccc2OCCCCn3cncc3)C)c1COC	39.81	1.32	20.56
324	O=C(NC(=O)c1cccc(c1)C(OC)=O)c2cc(ccc2OCCCCn3cncc3)C	39.81	1.32	20.56
325	O=C(NCc1ccc(OC)cc1)c2cc(ccc2OCCCCn3cncc3)C	39.81	1.32	20.57
326	O=C(Nc1cccc1OC)c2cc(ccc2OCCCCn3cncc3)C	39.81	1.52	20.66
327	O=C(c1cc(ccc1OCCCCn2cncc2)C)c3noc(n3)[C@@H](OC)C	39.81	1.62	20.71
328	O=C(c1cc(ccc1OCCCCn2cncc2)C)C(Oc3cc(ccc3)C)=O	39.81	1.90	20.86
329	Brc1cc(CNC(=O)c2cc(ccc2OCCCCn3cncc3)C)cs1	39.81	2.73	21.27
330	O=C(NC(=N)c1cnccc1)c2cc(ccc2OCCCCn3cncc3)C	39.81	3.10	21.45
331	O=C(Nc1cccc2cccc12)c3cc(ccc3OCCCCn4cncc4)C	50.12	0.27	25.19
332	O=C(Cc1c[nH]c2cccc(c21)C)c3cc(ccc3OCCCCn4cncc4)C	50.12	0.30	25.21
333	Clc1ccc2c(c(NC(=O)c3cc(ccc3OCCCCn4cncc4)C)ccn2)c1	50.12	0.31	25.22
334	Fc1ccc(cc1CNC(=O)c2cc(ccc2OCCCCn3cncc3)C)C	50.12	0.33	25.22
335	O=C(Nc1cccc(n1)C2CC2)c3cc(ccc3OCCCCn4cncc4)C	50.12	0.34	25.23
336	O=C(NC(=O)c1cc(ccc1OCCCCn2cncc2)C)c3cccc(SCC)c3	50.12	0.37	25.24
337	Oc1c(ccc(NC(=O)c2cc(ccc2OCCCCn3cncc3)C)c1)C	50.12	0.41	25.27
338	Clc1enc(NC)nc1NCC(=O)c2cc(ccc2OCCCCn3cncc3)C	50.12	0.43	25.28
339	O=C(NC[C@H]1CC[NH+]1C2CCCC2)c3cc(ccc3OCCCCn4cncc4)C	50.12	0.46	25.29
340	O=C(NCCc1cn2cccc2n1)c3cc(ccc3OCCCCn4cncc4)C	50.12	0.52	25.32
341	Fc1cc(ccc1NC(=O)c2cc(ccc2OCCCCn3cncc3)C)C#C	50.12	0.52	25.32
342	O=S(=O)(N1c2cc(NC(=O)c3cc(ccc3OCCCCn4cncc4)C)ccc2CC1)C	50.12	0.55	25.33
343	FC(F)(F)C(F)(F)CNC(=O)c1cc(ccc1OCCCCn2cncc2)C	50.12	0.67	25.39
344	O=C(Nc1ccc(c(c1)C)C)c2cc(ccc2OCCCCn3cncc3)C	50.12	0.68	25.40
345	O=C(Sc1c(-c2nc(on2)C)cccn1)c3cc(ccc3OCCCCn4cncc4)C	50.12	0.71	25.41
346	Brc1ccc(NC(=O)c2cc(ccc2OCCCCn3cncc3)C)c(C)c1	50.12	0.77	25.44
347	Oc1ccc([C@H](NC(=O)c2cc(ccc2OCCCCn3cncc3)C)C)cc1	50.12	0.77	25.45
348	Fc1cc(cc(OC)c1)CNC(=O)c2cc(ccc2OCCCCn3cncc3)C	50.12	0.86	25.49

349	FC(F)(F)c1ncc(s1)CNC(=O)c2cc(ccc2OCCCCn3encc3)C	50.12	0.99	25.56
350	Br1c(C)cccc1NC(=O)c2cc(ccc2OCCCCn3encc3)C	50.12	1.08	25.60
351	O=C(c1cc(ccc1OCCCCn2encc2)C)[C@H](Oe3cccc(OC)e3)C	50.12	1.11	25.61
352	O=S(=O)(N)c1cccc(NC(=O)c2cc(ccc2OCCCCn3encc3)C)c1C	50.12	1.32	25.72
353	O=C(Cc1cccc1-c2ccsc2)c3cc(ccc3OCCCCn4encc4)C	50.12	1.49	25.81
354	O=C(NCc1nnc(C(C)C)c1)c2cc(ccc2OCCCCn3encc3)C	50.12	3.75	26.93
355	O=C(NCC(CC)=C)c1cc(ccc1OCCCCn2encc2)C	50.12	3.86	26.99
356	O=C(NCCCOC=C)c1cc(ccc1OCCCCn2encc2)C	50.12	5.76	27.94
357	Clc1c(Cl)ccc([C@H]2C[C@@H]2C(=O)NC(=O)c3cc(ccc3OCCCCn4encc4)C)c1	63.10	0.20	31.65
358	Fe1cccc(c1)/C=C/C(=O)c2cc(ccc2OCCCCn3encc3)C	63.10	0.32	31.71
359	O=C(Nc1cccc2c1OCCC2)c3cc(ccc3OCCCCn4encc4)C	63.10	0.39	31.74
360	O=C(Nc1ccc(N)c2c1non2)c3cc(ccc3OCCCCn4encc4)C	63.10	0.44	31.77
361	Clc1ccc(O)c(NC(=O)c2cc(ccc2OCCCCn3encc3)C)c1	63.10	0.56	31.83
362	Fe1cc(ccc1NC(=O)c2cc(ccc2OCCCCn3encc3)C)C	63.10	0.60	31.85
363	Br1c2c(ncn2)ccc1NC(=O)c3cc(ccc3OCCCCn4encc4)C	63.10	0.68	31.89
364	O=C(N1CCO[C@@H](C1)CC)NC(=O)c2cc(ccc2OCCCCn3encc3)C	63.10	0.79	31.94
365	FC(F)c1cccc(CNC(=O)c2cc(ccc2OCCCCn3encc3)C)c1	63.10	0.80	31.95
366	Br1cnn(Cc2noc(n2)C(=O)c3cc(ccc3OCCCCn4encc4)C)c1	63.10	0.86	31.98
367	Clc1ccc(O)cc1NC(=O)c2cc(ccc2OCCCCn3encc3)C	63.10	0.92	32.01
368	Fe1c(OC)cccc1NC(=O)c2cc(ccc2OCCCCn3encc3)C	63.10	0.95	32.02
369	Fe1cc(OC)ccc1NC(=O)c2cc(ccc2OCCCCn3encc3)C	63.10	0.98	32.04
370	Clc1cccc1NC(=O)c2cc(ccc2OCCCCn3encc3)C	63.10	0.99	32.04
371	O=C(c1cc(ccc1OCCCCn2encc2)C)CNc3cc[nH+]c(NC)c3	63.10	1.22	32.16
372	O=C(NCc1c(C)ccs1)c2cc(ccc2OCCCCn3encc3)C	63.10	1.25	32.18
373	Oc1c(NC(=O)c2cc(ccc2OCCCCn3encc3)C)cccc1C	63.10	1.29	32.19
374	Clc1cccc(NC(=O)c2cc(ccc2OCCCCn3encc3)C)c1O	63.10	1.46	32.28
375	O=C(NCCc1cn2c(SCC2)n1)c3cc(ccc3OCCCCn4encc4)C	63.10	1.50	32.30
376	O=C(Cc1c(ncn1)-c2ccsc2)c3cc(ccc3OCCCCn4encc4)C	63.10	1.58	32.34
377	O=C(OCC(O)(C)C)c1cc(ccc1OCCCCn2encc2)C	63.10	4.35	33.72
378	Fe1ccc2c(CCC[C@H]2NC(=O)c3cc(ccc3OCCCCn4encc4)C)c1	79.43	0.08	39.75
379	O=C(Nc1c2cccc2[nH]n1)c3cc(ccc3OCCCCn4encc4)C	79.43	0.18	39.81
380	O=C(Nc1c[nH]c2cccc21)c3cc(ccc3OCCCCn4encc4)C	79.43	0.20	39.82
381	O=C(NC(=O)c1cc(ccc1OCCCCn2encc2)C)c3cc(N)ccc3C	79.43	0.22	39.83
382	O=C(Nc1cccc1C#C)c2cc(ccc2OCCCCn3encc3)C	79.43	0.28	39.86
383	O=C(N[C@H]1c2c(CCC1)ccn2)c3cc(ccc3OCCCCn4encc4)C	79.43	0.32	39.88
384	O=C(NCc1ccc2enn(c2c1)C)c3cc(ccc3OCCCCn4encc4)C	79.43	0.33	39.88
385	Fe1ccc(F)c(CNC(=O)c2cc(ccc2OCCCCn3encc3)C)c1	79.43	0.41	39.92
386	O=C(Nc1cccc2c1oc(n2)C)c3cc(ccc3OCCCCn4encc4)C	79.43	0.46	39.95
387	O=C(NCc1ccc(o1)[C@H]2[C@@H](C2)C)c3cc(ccc3OCCCCn4encc4)C	79.43	0.48	39.96
388	Clc1cccc(Cc2noc(n2)C(=O)c3cc(ccc3OCCCCn4encc4)C)c1	79.43	0.53	39.98
389	O=C(Nc1ccnc2ccc(OC)nc21)c3cc(ccc3OCCCCn4encc4)C	79.43	0.53	39.98
390	O=C(c1cc(ccc1OCCCCn2encc2)C)CNc3cc(ccc3)C)C	79.43	0.57	40.00
391	O=C(NCc1cc(-c2ccsc2)cs1)c3cc(ccc3OCCCCn4encc4)C	79.43	0.63	40.03

392	<chem>O=C(NC(=O)c1cc(ccc1OCCCCn2ence2)C)[C@H]3CCC[NH+](C3)CCC</chem>	79.43	0.63	40.03
393	<chem>O=C(NC[C@@H]1[C@H](OCC1)C(C)=C)c2cc(ccc2OCCCCn3ence3)C</chem>	79.43	0.64	40.04
394	<chem>O=C(N[C@H]1c2c(CCC1)en(n2)C(C)C)c3cc(ccc3OCCCCn4ence4)C</chem>	79.43	0.68	40.05
395	<chem>O=C(NCc1nc(n[nH]1)-c2ccco2)c3cc(ccc3OCCCCn4ence4)C</chem>	79.43	0.68	40.06
396	<chem>Clc1ccc(s1)C=2C[C@H](ON2)C(=O)NC(=O)c3cc(ccc3OCCCCn4ence4)C</chem>	79.43	0.68	40.06
397	<chem>O=C(NCc1ccc2c([nH]c(n2)C)c1)c3cc(ccc3OCCCCn4ence4)C</chem>	79.43	0.69	40.06
398	<chem>O=C(Nc1cccc2ccsc21)c3cc(ccc3OCCCCn4ence4)C</chem>	79.43	0.72	40.08
399	<chem>Brc1cccc1NCC(=O)c2cc(ccc2OCCCCn3ence3)C</chem>	79.43	0.83	40.13
400	<chem>O=C(NCc1nc(C2OCCO2)cs1)c3cc(ccc3OCCCCn4ence4)C</chem>	79.43	0.90	40.17
401	<chem>O=C(NNc1nc(O)cc(n1)C)c2cc(ccc2OCCCCn3ence3)C</chem>	79.43	0.91	40.17
402	<chem>Clc1cccc(NC(=O)c2cc(ccc2OCCCCn3ence3)C)c1F</chem>	79.43	0.96	40.20
403	<chem>FC(F)Oc1c(ccc(NC(=O)c2cc(ccc2OCCCCn3ence3)C)c1)C</chem>	79.43	1.16	40.30
404	<chem>Fc1cc(F)cc(NC(=O)c2cc(ccc2OCCCCn3ence3)C)c1OC</chem>	79.43	1.23	40.33
405	<chem>O=C(CNc1cccc1)c2cc(ccc2OCCCCn3ence3)C</chem>	79.43	1.35	40.39
406	<chem>Clc1cccc(NC(=O)c2cc(ccc2OCCCCn3ence3)C)c1OC</chem>	79.43	1.41	40.42
407	<chem>Sc1cccc1NC(=O)c2cc(ccc2OCCCCn3ence3)C</chem>	79.43	1.45	40.44
408	<chem>O=C(NC(=O)C(=O)NCc1cccs1)c2cc(ccc2OCCCCn3ence3)C</chem>	79.43	1.57	40.50
409	<chem>O=C(c1cc(ccc1OCCCCn2ence2)C)/C=C/C3CC3</chem>	79.43	1.59	40.51
410	<chem>O=C(N[C@@H]1C[C@H]2CC[C@@H]1O2)c3cc(ccc3OCCCCn4ence4)C</chem>	79.43	1.76	40.60
411	<chem>Clc1csc(CNC(=O)c2cc(ccc2OCCCCn3ence3)C)c1</chem>	79.43	2.06	40.75
412	<chem>Fc1cccc(NC(=O)c2cc(ccc2OCCCCn3ence3)C)c1S(=O)(=O)N</chem>	100.00	0.19	50.09
413	<chem>O=C(Nc1c2cc(ccc2ccn1)C)c3cc(ccc3OCCCCn4ence4)C</chem>	100.00	0.21	50.11
414	<chem>Fc1ccc(F)c(/C=C/C(=O)c2cc(ccc2OCCCCn3ence3)C)c1</chem>	100.00	0.29	50.14
415	<chem>Oc1cccc2c1cccc2NC(=O)c3cc(ccc3OCCCCn4ence4)C</chem>	100.00	0.31	50.15
416	<chem>Clc1ccc(NC)cc1C(=O)NC(=O)c2cc(ccc2OCCCCn3ence3)C</chem>	100.00	0.39	50.20
417	<chem>O[C@H]1Cc2cccc(NC(=O)c3cc(ccc3OCCCCn4ence4)C)c2C1</chem>	100.00	0.41	50.20
418	<chem>Brc1ccc(o1)NC(=O)c2cc(ccc2OCCCCn3ence3)C</chem>	100.00	0.62	50.31
419	<chem>Clc1cccc(NNC(=O)c2cc(ccc2OCCCCn3ence3)C)c1</chem>	100.00	0.66	50.33
420	<chem>Fc1cccc(NNC(=O)c2cc(ccc2OCCCCn3ence3)C)c1</chem>	100.00	0.68	50.34
421	<chem>O=C(Nc1cc(O)cc(c1)C)c2cc(ccc2OCCCCn3ence3)C</chem>	100.00	0.72	50.36
422	<chem>O=C(Nc1cccc2c1OCC[C@H]2OC)c3cc(ccc3OCCCCn4ence4)C</chem>	100.00	0.74	50.37
423	<chem>O=C(NCc1cnc1OC)c2cc(ccc2OCCCCn3ence3)C</chem>	100.00	0.80	50.40
424	<chem>O=C(c1cc(ccc1OCCCCn2ence2)C)CNc3cc[nH+]c(OC)c3</chem>	100.00	0.98	50.49
425	<chem>O=C(NC(=O)c1cccc(c1)C(=O)NC)c2cc(ccc2OCCCCn3ence3)C</chem>	100.00	1.10	50.55
426	<chem>O=C(NCc1c(nn(n1)CC)C)c2cc(ccc2OCCCCn3ence3)C</chem>	100.00	1.56	50.78
427	<chem>O=C(NCc1esc(n1)CCC)c2cc(ccc2OCCCCn3ence3)C</chem>	100.00	1.69	50.85
428	<chem>Brc1cnc(NC(=O)c2cc(ccc2OCCCCn3ence3)C)c1O</chem>	100.00	1.86	50.93
429	<chem>Clc1c(NC(=O)c2cc(ccc2OCCCCn3ence3)C)ccen1</chem>	100.00	2.13	51.06
430	<chem>O=C(Nc1cccc(n1)COC)c2cc(ccc2OCCCCn3ence3)C</chem>	100.00	2.68	51.34
431	<chem>O=C(N[C@@H]1CCC[C@@H]1SC)c2cc(ccc2OCCCCn3ence3)C</chem>	100.00	2.81	51.40
432	<chem>O=C(Nc1cc[n+](c2ccc(N)cc12)C)c3cc(ccc3OCCCCn4ence4)C</chem>	125.89	0.27	63.08
433	<chem>Brc1ccc(NC(=O)c2cc(ccc2OCCCCn3ence3)C)c(F)c1C</chem>	125.89	0.37	63.13
434	<chem>Fc1ccc(CCNC(=O)c2cc(ccc2OCCCCn3ence3)C)cc1</chem>	125.89	0.38	63.14

435	<chem>O=C(c1cc(ccc1OCCCCn2encc2)C)CNC3cc(cc(N)c3)C</chem>	125.89	0.39	63.14
436	<chem>Br1cc(N)cc(C(=O)NC(=O)c2cc(ccc2OCCCCn3encc3)C)c1</chem>	125.89	0.43	63.16
437	<chem>O=C(N1CCO[C@H](C(C)C)C1)NC(=O)c2cc(ccc2OCCCCn3encc3)C</chem>	125.89	0.43	63.16
438	<chem>O[C@H]1Cc2ccccc2[C@H]1[NH2+]CC(=O)c3cc(ccc3OCCCCn4encc4)C</chem>	125.89	0.44	63.17
439	<chem>O=C(OC)c1cccc(NCC(=O)c2cc(ccc2OCCCCn3encc3)C)c1</chem>	125.89	0.49	63.19
440	<chem>O=C(NCc1cccc(C2CC2)c1)c3cc(ccc3OCCCCn4encc4)C</chem>	125.89	0.51	63.20
441	<chem>O=C1CO2c(N1)ccc(CNC(=O)c3cc(ccc3OCCCCn4encc4)C)c2</chem>	125.89	0.52	63.21
442	<chem>O=C(NCCCc1ccccc1)c2cc(ccc2OCCCCn3encc3)C</chem>	125.89	0.60	63.24
443	<chem>O=C(N)Cc1cccc1NC(=O)c2cc(ccc2OCCCCn3encc3)C</chem>	125.89	0.70	63.29
444	<chem>Clc1cccc(CSC(=O)c2cc(ccc2OCCCCn3encc3)C)c1</chem>	125.89	0.74	63.32
445	<chem>O=C(NCC#CCC#C)c1cc(ccc1OCCCCn2encc2)C</chem>	125.89	0.83	63.36
446	<chem>O=C(Nc1ccccc1NC2CCC2)c3cc(ccc3OCCCCn4encc4)C</chem>	125.89	0.84	63.36
447	<chem>Br1cccc(CCC(=O)c2cc(ccc2OCCCCn3encc3)C)c1</chem>	125.89	1.02	63.46
448	<chem>O[C@H]1CCC[C@@H](NC(=O)c2cc(ccc2OCCCCn3encc3)C)C1</chem>	125.89	1.08	63.49
449	<chem>O=C(COc1cccc([C@H]([NH3+])C)c1)c2cc(ccc2OCCCCn3encc3)C</chem>	125.89	1.15	63.52
450	<chem>O=C(NCC1CCCC1)c2cc(ccc2OCCCCn3encc3)C</chem>	125.89	1.30	63.59
451	<chem>OC1CC(CCNC(=O)c2cc(ccc2OCCCCn3encc3)C)C1</chem>	125.89	1.35	63.62
452	<chem>O=C(c1cc(ccc1OCCCCn2encc2)C)c3nc(no3)[C@@H](OC)CC</chem>	125.89	2.44	64.17
453	<chem>O=C(CCNc1c(ncn1)C)c2cc(ccc2OCCCCn3encc3)C</chem>	125.89	7.20	66.55
454	<chem>O=C(c1cc(ccc1OCCCCn2encc2)C)/C=C/[NH2+]CCOC</chem>	125.89	8.84	67.37
455	<chem>O=C(CNc1cccc(CC)c1)c2cc(ccc2OCCCCn3encc3)C</chem>	158.49	0.46	79.47
456	<chem>O=C(Nc1ccccc1OCCO2)c3cc(ccc3OCCCCn4encc4)C</chem>	158.49	0.50	79.50
457	<chem>FC(F)(F)c1cccc(SCC(=O)c2cc(ccc2OCCCCn3encc3)C)c1</chem>	158.49	0.51	79.50
458	<chem>O=C(Nc1ccccc1CCCCc12)c3cc(ccc3OCCCCn4encc4)C</chem>	158.49	0.58	79.53
459	<chem>Fc1ccc(O)cc1NC(=O)c2cc(ccc2OCCCCn3encc3)C</chem>	158.49	0.72	79.61
460	<chem>O=C(C[C@@H](c1cccc(OC)c1)C)c2cc(ccc2OCCCCn3encc3)C</chem>	158.49	0.95	79.72
461	<chem>Br1cccc(C(=O)NC(=O)c2cc(ccc2OCCCCn3encc3)C)c1</chem>	158.49	1.05	79.77
462	<chem>O=C(NNc1ccc(OC)cc1)c2cc(ccc2OCCCCn3encc3)C</chem>	158.49	1.30	79.89
463	<chem>O=C(c1cc(ccc1OCCCCn2encc2)C)CNC3cn(nc3)C</chem>	158.49	1.40	79.94
464	<chem>Br1ccc(o1)[C@H](NC(=O)c2cc(ccc2OCCCCn3encc3)C)C</chem>	158.49	1.43	79.96
465	<chem>Fc1ccc(OCC#C)c(NC(=O)c2cc(ccc2OCCCCn3encc3)C)c1</chem>	158.49	1.49	79.99
466	<chem>O=C(CCc1cccc1C)c2cc(ccc2OCCCCn3encc3)C</chem>	158.49	1.60	80.04
467	<chem>Oc1cc(NC(=O)c2cc(ccc2OCCCCn3encc3)C)ccc1OC</chem>	158.49	2.01	80.25
468	<chem>Clc1cc(Cl)enc1NCCC(=O)c2cc(ccc2OCCCCn3encc3)C</chem>	158.49	2.04	80.27
469	<chem>O=C(N[C@@H](c1cccc(s1)CC)C)c2cc(ccc2OCCCCn3encc3)C</chem>	158.49	3.26	80.88
470	<chem>Br1cc(cc(C(=O)NC(=O)c2cc(ccc2OCCCCn3encc3)C)c1)C</chem>	199.53	0.30	99.91
471	<chem>Br1ccc2c(CCN2C(=O)CC(=O)c3cc(ccc3OCCCCn4encc4)C)c1</chem>	199.53	0.41	99.97
472	<chem>FC(F)(F)c1cnc(CNC(=O)c2cc(ccc2OCCCCn3encc3)C)c1</chem>	199.53	0.45	99.99
473	<chem>Fc1ccc(cc1NCC(=O)c2cc(ccc2OCCCCn3encc3)C)C</chem>	199.53	0.48	100.00
474	<chem>Clc1cc(Cl)cc(CNC(=O)c2cc(ccc2OCCCCn3encc3)C)c1</chem>	199.53	0.60	100.06
475	<chem>O=C(c1cc(ccc1OCCCCn2encc2)C)Cc3cccn3-c4enccc4</chem>	199.53	0.66	100.09
476	<chem>Clc1ccc(NC(=O)c2cc(ccc2OCCCCn3encc3)C)c(OC(F)F)c1</chem>	199.53	0.86	100.20



477	<chem>O=C(c1cc(ccc1OCCCCn2ncc2)C)C#CCCC[n+ ]3cccc(c3)C</chem>	199.53	0.90	100.21
478	<chem>Brc1c(OC)cccc1NC(=O)c2cc(ccc2OCCCCn3ncc3)C</chem>	199.53	1.19	100.36
479	<chem>O=C(C[NH2+ ] [C@H]1c2c(sc2)CCC1)c3cc(ccc3OCCCCn4ncc4)C</chem>	199.53	1.41	100.47
480	<chem>O=C(NCC(C1CC1)C2CC2)c3cc(ccc3OCCCCn4ncc4)C</chem>	199.53	2.75	101.14
481	<chem>Clc1cc2ccnc2c(NC(=O)c3cc(ccc3OCCCCn4ncc4)C)c1</chem>	251.19	0.38	125.79
482	<chem>O=C(Nc1cccc(CC)c1)c2cc(ccc2OCCCCn3ncc3)C</chem>	251.19	0.55	125.87
483	<chem>Brc1ccc(Cl)cc1NCC(=O)c2cc(ccc2OCCCCn3ncc3)C</chem>	251.19	0.56	125.87
484	<chem>Brc1ccc(Cl)c(NCC(=O)c2cc(ccc2OCCCCn3ncc3)C)c1</chem>	251.19	0.66	125.92
485	<chem>O=C(NCOc1ccc(cc1)C)c2cc(ccc2OCCCCn3ncc3)C</chem>	251.19	0.82	126.00
486	<chem>O=C(NC=C1CCCC1)c2cc(ccc2OCCCCn3ncc3)C</chem>	251.19	0.91	126.05
487	<chem>O=C(c1cc(ccc1OCCCCn2ncc2)C)CCC3=CCOCC3</chem>	251.19	1.39	126.29
488	<chem>O=C1CCOe2ccc(CNC(=O)c3cc(ccc3OCCCCn4ncc4)C)cc2N1</chem>	316.23	0.22	158.22
489	<chem>O=C(Nc1ccnc2ccc(N(C)C)cc12)c3cc(ccc3OCCCCn4ncc4)C</chem>	316.23	0.24	158.24
490	<chem>Clc1ccc2c([C@H](NC(=O)c3cc(ccc3OCCCCn4ncc4)C)CCS2)c1</chem>	316.23	0.26	158.24
491	<chem>O=C(Nc1ccnc2ccc(OC)cc21)c3cc(ccc3OCCCCn4ncc4)C</chem>	316.23	0.30	158.27
492	<chem>O=C(Nc1ccc2cccc(OC)c2n1)c3cc(ccc3OCCCCn4ncc4)C</chem>	316.23	0.31	158.27
493	<chem>Oc1c(/C=C/C(=O)c2cc(ccc2OCCCCn3ncc3)C)cccc1OC</chem>	316.23	0.43	158.33
494	<chem>O=C(CCCc1nc2c(s1)CCCC2)c3cc(ccc3OCCCCn4ncc4)C</chem>	316.23	1.16	158.69
495	<chem>O=C(c1cc(ccc1OCCCCn2ncc2)C)c3nc(no3)[C@H]4C[NH+ ]5C CCC[C@H]5CO4</chem>	398.11	0.16	199.13
496	<chem>O[C@H]1c2cccc(NC(=O)c3cc(ccc3OCCCCn4ncc4)C)c2OCC1</chem>	398.11	0.50	199.30
497	<chem>O=C(NCc1cccc(OC)c1)c2cc(ccc2OCCCCn3ncc3)C</chem>	398.11	0.94	199.52
498	<chem>Fc1ccc(NNC(=O)c2cc(ccc2OCCCCn3ncc3)C)cc1</chem>	398.11	0.97	199.54
499	<chem>O=C(Nc1c[nH+ ]ccc1N)c2cc(ccc2OCCCCn3ncc3)C</chem>	398.11	1.35	199.73
500	<chem>O=C(NCc1cc(cc(OC)c1)C)c2cc(ccc2OCCCCn3ncc3)C</chem>	501.19	0.43	250.81

**Table S5.** Data used for IC<sub>50</sub> calculations.

Compound	Percentage of inhibition @					
	100 μM	50 μM	25 μM	10 μM	5 μM	1 μM
<b>8</b>	100%	89%	60%	49%	35%	25%
<b>9</b>	58%	32%	15%	2%	0%	--

<b>10</b>	100%	95%	85%	80% (@12.5 μM)	68%	39% (@0.5 μM)
<b>11</b>	82%	48%	33%	13%	0%	--
<b>12</b>	100%	96%	88%	80% (@12.5 μM)	68%	41% (@0.5 μM)
<b>13</b>	95%	80%	42%	20%	0%	--

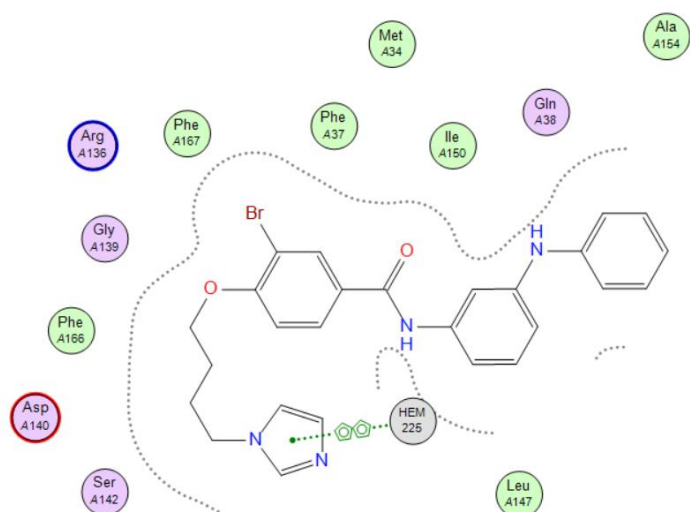


**Figure S16.** 2D interactions of **8** inside HO-1.

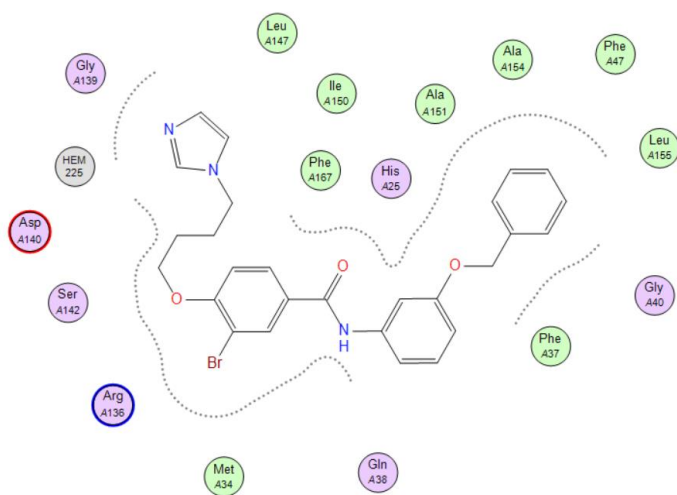


**Figure S17.** 2D interactions of **9** inside HO-1.

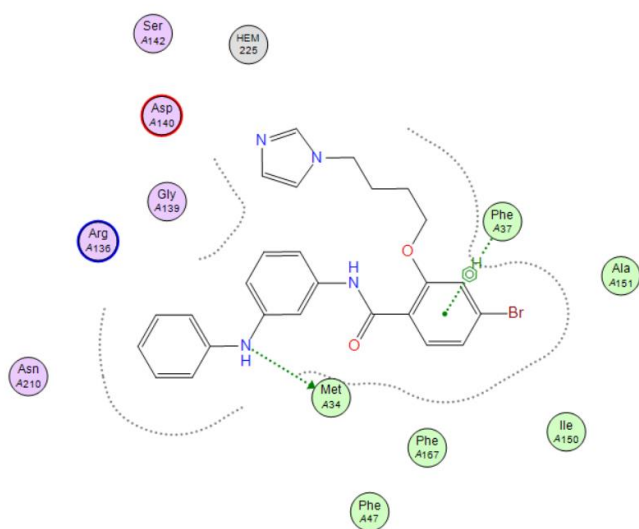


**Figure S18.** 2D interactions of **10** inside HO-1.

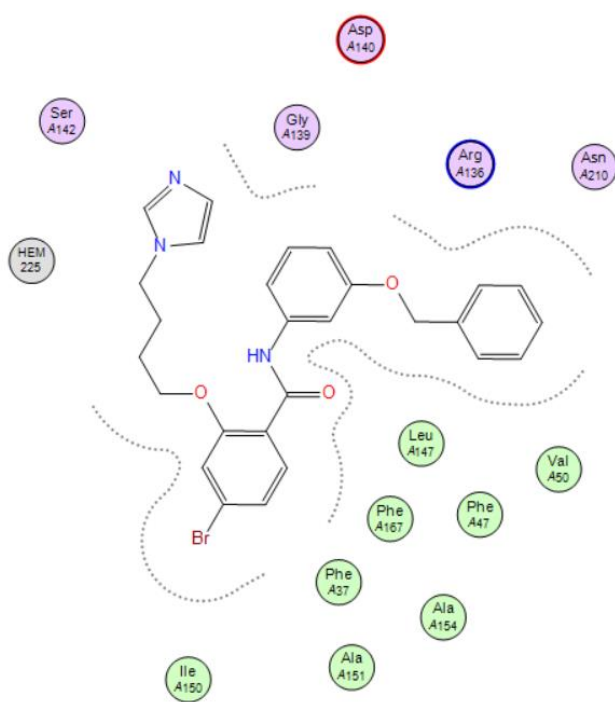


**Figure S19.** 2D interactions of **11** inside HO-1.

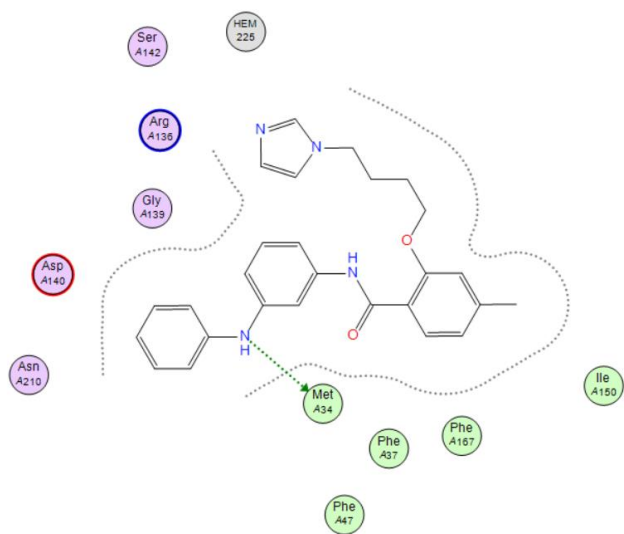


**Figure S20.** 2D interactions of **12** inside HO-1.

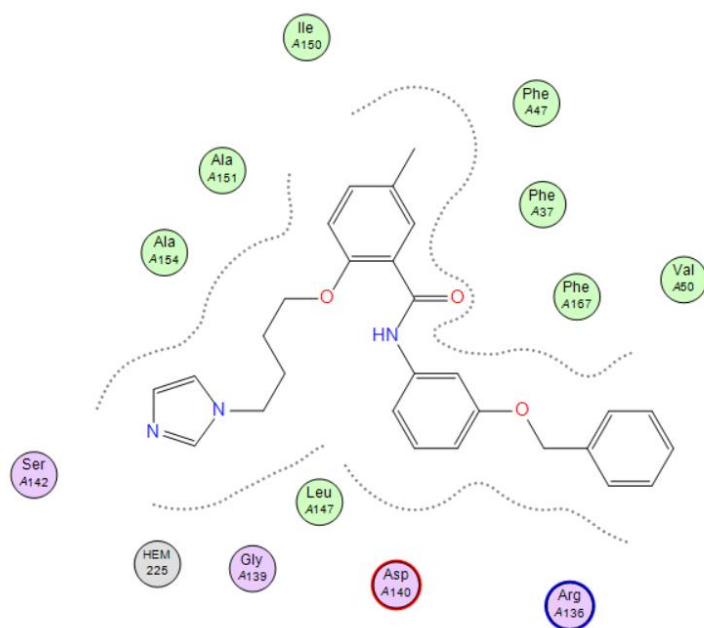


**Figure S21.** 2D interactions of **13** inside HO-1.

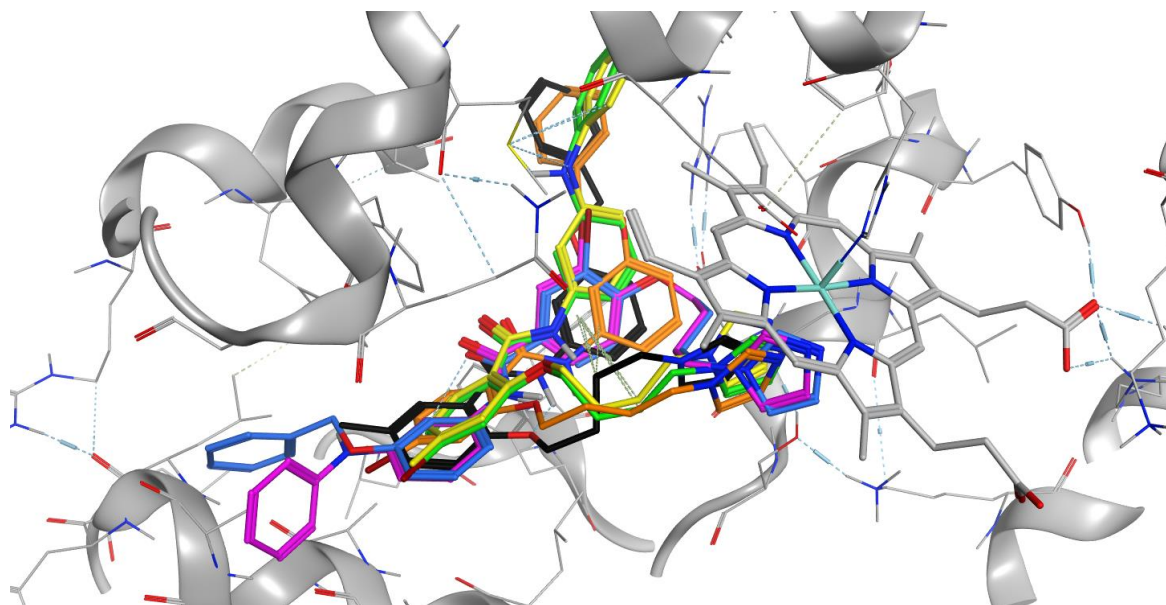


**Figure S22.** Poses of molecule **8–13** inside HO-1. **8** (purple), **9** (blue), **10** (green), **11** (orange), **12** (yellow), **13** (black).

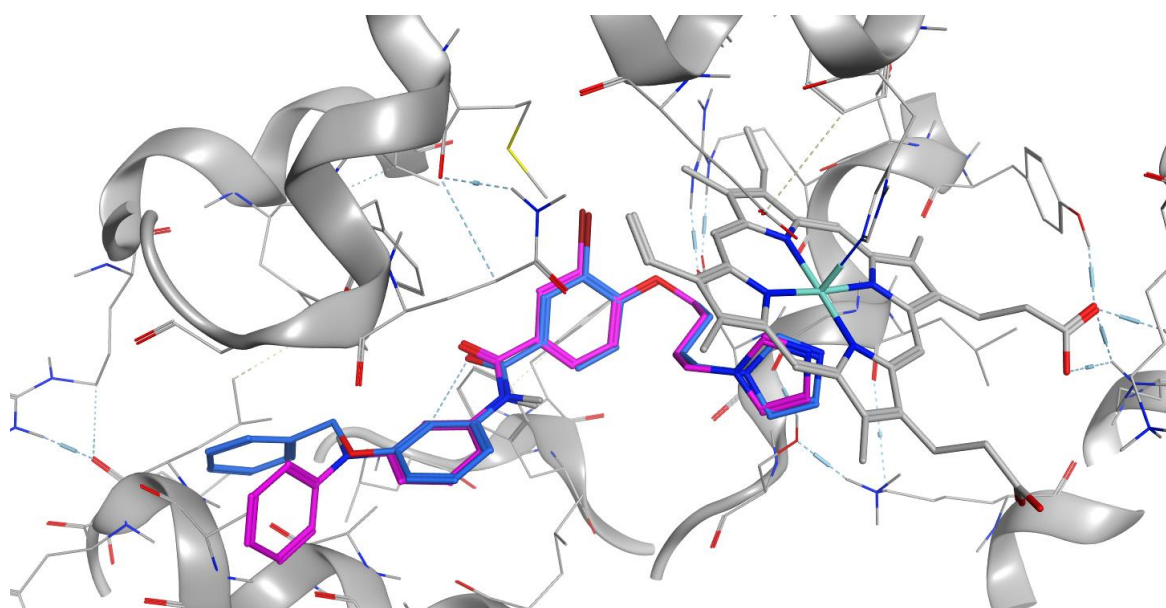


**Figure S23.** Poses of molecule **8** (purple) and **9** (blue) inside HO-1.

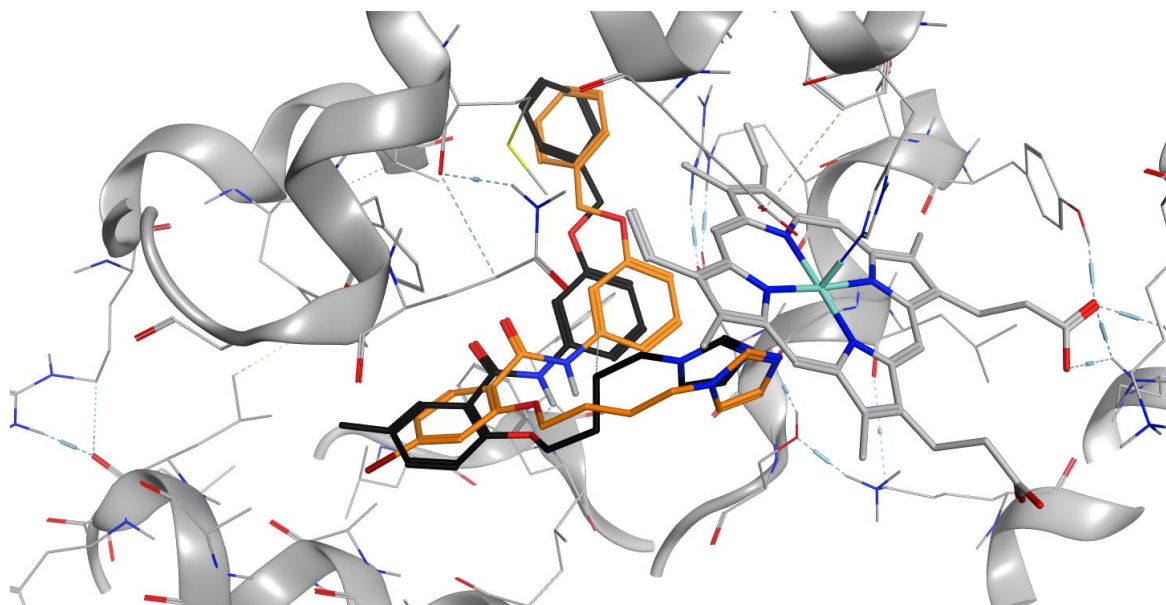


**Figure S24.** Poses of molecule **11** (orange) and **13** (black) inside HO-1.

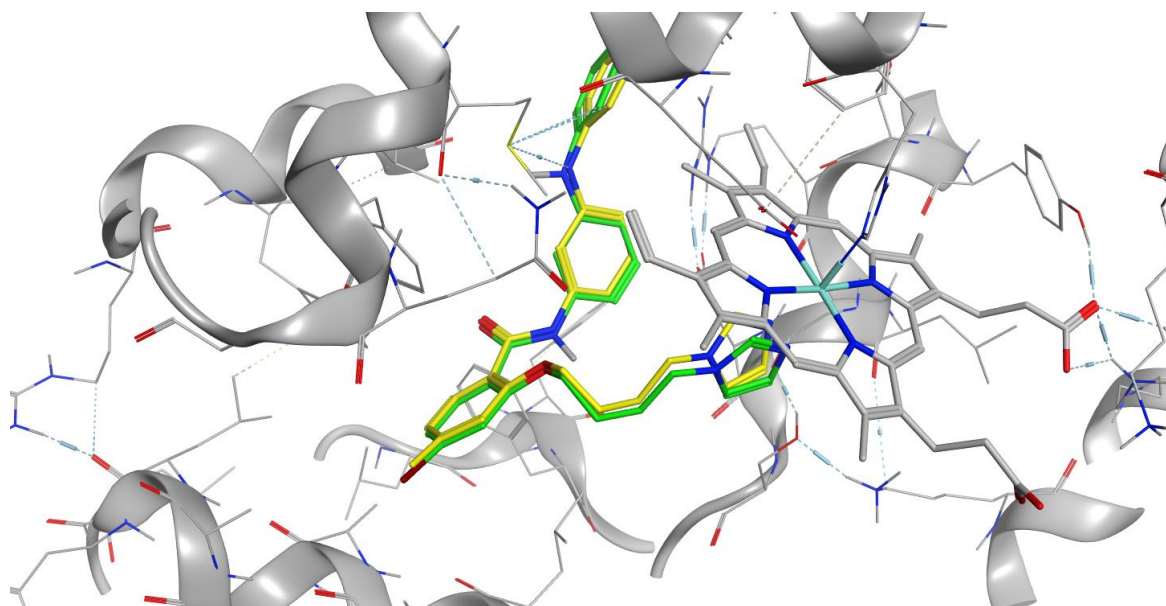


**Figure S25.** Poses of molecule **10** (green) and **12** (yellow) inside HO-1.

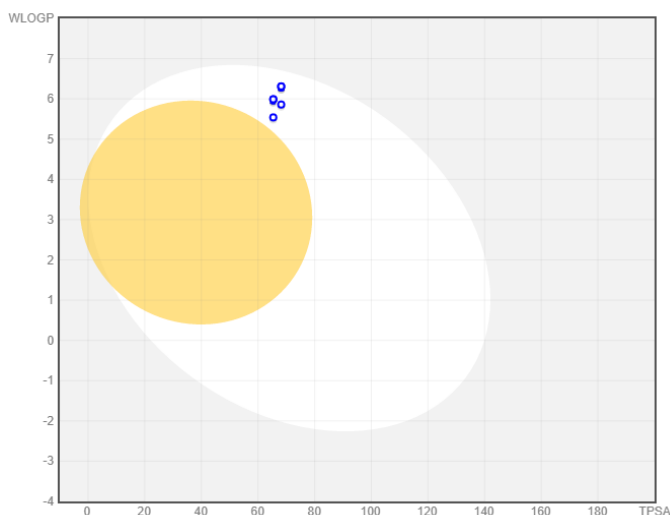


**Figure S26.** BOILED-Egg plot. Points located in the BOILED-Egg's yellow are the compounds predicted to permeate the BBB passively; differently, the ones in the white are the molecules predicted to be only passively absorbed by the gastrointestinal tract. The blue dot indicates that the compound is transported by the P-glycoprotein.

**Table S6.** ADMET result for molecules **8–13** from pkCSM.

	8	9	10	11	12	13	
Molecules							
Water solubility	-3.01	-3.332	-3.08	-3.32	-3.118	-3.243	Absorption
Caco2 permeability	0.481	0.333	0.563	1.139	0.469	0.451	Absorption
Intestinal	91.078	90.819	89.97	91.24	91.865	91.994	Absorption
Skin Permeability	-2.735	-2.735	-2.73	-2.73	-2.735	-2.735	Absorption
P-glycoprotein	Yes	Yes	Yes	Yes	Yes	Yes	Absorption
P-glycoprotein I	Yes	Yes	Yes	Yes	Yes	Yes	Absorption
P-glycoprotein II	Yes	Yes	Yes	Yes	Yes	Yes	Absorption
VDss (human)	0.648	0.321	0.515	0.282	0.362	0.442	Distribution
Fraction unbound	0.027	0	0	0	0	0	Distribution
BBB permeability	-0.612	-0.626	-0.52	-0.41	-0.357	-0.163	Distribution
CNS permeability	-2.039	-1.999	-2.09	-2.07	-2.191	-2.127	Distribution
CYP2D6 substrate	No	No	No	No	No	No	Metabolism
CYP3A4 substrate	Yes	Yes	Yes	Yes	Yes	Yes	Metabolism
CYP1A2 inhibitor	Yes	No	Yes	No	Yes	No	Metabolism
CYP2C19 inhibitor	Yes	Yes	Yes	Yes	Yes	Yes	Metabolism
CYP2C9 inhibitor	Yes	Yes	Yes	Yes	Yes	Yes	Metabolism
CYP2D6 inhibitor	Yes	Yes	Yes	Yes	Yes	Yes	Metabolism
CYP3A4 inhibitor	Yes	Yes	Yes	Yes	Yes	Yes	Metabolism
Total Clearance	1.099	0.932	1.043	1.017	1.048	1.022	Excretion
Renal OCT2	Yes	Yes	Yes	Yes	No	No	Excretion
AMES toxicity	Yes	Yes	Yes	No	Yes	Yes	Toxicity
Max. tolerated dose	0.389	0.446	0.372	0.480	0.203	0.308	Toxicity
hERG I inhibitor	Yes	Yes	Yes	No	No	No	Toxicity
hERG II inhibitor	Yes	Yes	Yes	Yes	Yes	Yes	Toxicity
Oral Rat Acute	2.518	2.816	2.547	2.828	2.532	2.501	Toxicity
Oral Rat Chronic	0.946	0.838	1.754	1.082	1.819	0.757	Toxicity
Hepatotoxicity	Yes	Yes	Yes	Yes	Yes	No	Toxicity
Skin Sensitisation	No	No	No	No	No	No	Toxicity
T. Pyriformis toxicity	0.285	0.285	0.285	0.285	0.285	0.285	Toxicity
Minnow toxicity	-1.329	-2.833	-3.14	-2.84	-2.348	-1.392	Toxicity



**Table S7.** ADMET result for molecules **8–13** from swissadme.

13	12	11	10	9	8	Molecules
65.4	68.2	65.4	68.2	65.4	68.2	TPSA
3.6	3.8	4.1	4.0	3.8	4.0	iLOGP
5.0	5.1	5.3	5.4	5.3	5.4	XLOGP3
5.5	5.9	6.0	6.3	6.0	6.3	WLOGP
3.2	3.2	3.5	3.6	3.5	3.6	MLOGP
5.2	4.5	5.4	4.7	5.4	4.7	Silicos-IT Log P
4.5	4.5	4.9	4.8	4.8	4.8	Consensus Log P
-5.5	-5.6	-6.1	-6.2	-6.1	-6.2	ESOL Log S
Moderately	Moderately	Poorly	Poorly	Poorly	Poorly	ESOL Class
-6.1	-6.2	-6.4	-6.6	-6.4	-6.6	All Log S
Poorly	Poorly	Poorly	Poorly	Poorly	Poorly	All Class
-9.7	-9.6	-10.1	-10.0	-10.1	-10.0	Silicos-IT LogSw
Poorly	Poorly	Insoluble	Insoluble	Insoluble	Insoluble	Silicos-IT class
High	High	High	High	High	High	GI absorption
No	No	No	No	No	No	BBB permeant
Yes	Yes	Yes	Yes	Yes	Yes	Pgp substrate
Yes	Yes	Yes	Yes	Yes	Yes	CYP1A2 inhibitor
Yes	Yes	Yes	Yes	Yes	Yes	CYP2C19 inhibitor
Yes	Yes	Yes	Yes	Yes	Yes	CYP2C9 inhibitor
Yes	Yes	Yes	Yes	Yes	Yes	CYP2D6 inhibitor
Yes	Yes	Yes	Yes	Yes	Yes	CYP3A4 inhibitor
-5.5	-5.4	-5.7	-5.6	-5.7	-5.6	log Kp (cm/s)
0	0	1	1	1	1	Lipinski #violations
1	2	3	3	3	3	Ghose #violations
1	1	1	1	1	1	Veber #violations
0	0	1	1	1	1	Egan #violations
0	1	1	1	1	1	Muegge #violations
1	1	1	1	1	1	Bioavailability Score
0	0	0	0	0	0	PAINS #alerts
0	0	0	0	0	0	Brenk #alerts
3	3	3	3	3	3	Leadlikeness

## From far west to east: joining the molecular architecture of imidazole-like ligands in HO-1 complexes

Giuseppe Floresta <sup>1,2,†</sup>, Antonino Nicolò Fallica <sup>1,†</sup>, Vincenzo Patamia <sup>1</sup>, Valeria Sorrenti <sup>1</sup>, Khaled Greish <sup>3</sup>, Antonio Rescifina <sup>1,\*</sup>, Valeria Pittalà <sup>1,\*</sup>

<sup>1</sup> Department of Drug and Health Sciences, University of Catania, V.le Andrea Doria 6, 95125 Catania, Italy;

<sup>2</sup> Department of Analytics, Environmental & Forensics, King's College London, London SE1 9NH, UK;

<sup>3</sup> Department of Molecular Medicine and Nanomedicine Unit, Princess Al-Jawhara Center for Molecular Medicine, College of Medicine and Medical Sciences, Arabian Gulf University, Manama 329, Bahrain.

### Author contributions

† These authors contributed equally

### \*Corresponding authors:

Antonio Rescifina: arescifina@unict.it

Valeria Pittalà: vpittala@unict.it

### Table of contents

Figures S1–16 NMR spectra of compounds.	S108–S115
Figure S17. Docked pose of <b>1</b> (light pink) and <b>4d</b> (blue) inside HO-1.	S116
Figure S18. Docked pose of <b>4a</b> (light pink), <b>4b</b> (green) and <b>4c</b> (blue) inside HO-1.	S116
Figure S19. Docked pose of <b>8a</b> (blue), <b>8b</b> (light pink) and <b>8c</b> (green) inside HO-1.	S117
Figure S20. Spark's libraries used for the growing experiments.	S118
Figure S21. Forge's parameters used for the conformation hunt.	S119
Figure S22. Forge's parameters used for the alignment.	S119
Table S1. $K_i$ $\mu$ M from docking, $IC_{50}$ $\mu$ M from QSAR and Average $\mu$ M calculated activity for the virtually evaluated compounds.	S120
Table S2. ECPF4 fingerprint similarity matrix values.	S130
Table S3. ECPF4 fingerprint similarity matrix values.	S130

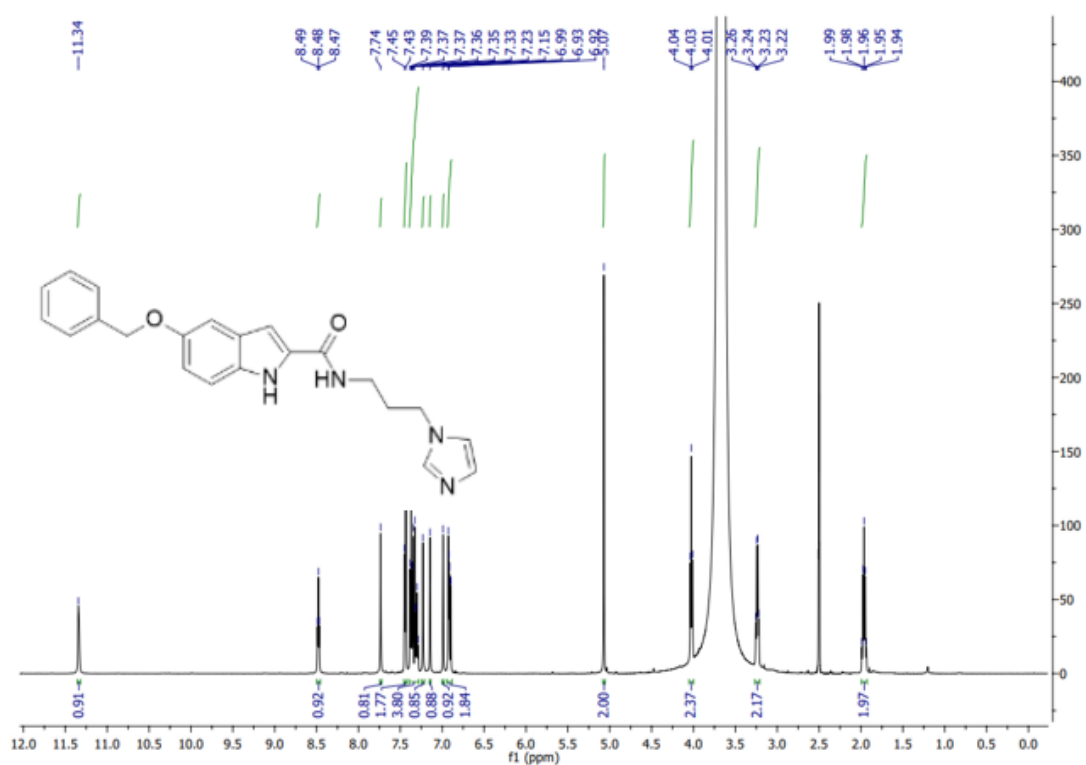


Figure S1.  $^1\text{H}$  NMR (500 MHz,  $\text{DMSO-}d_6$ ) of compound 1.

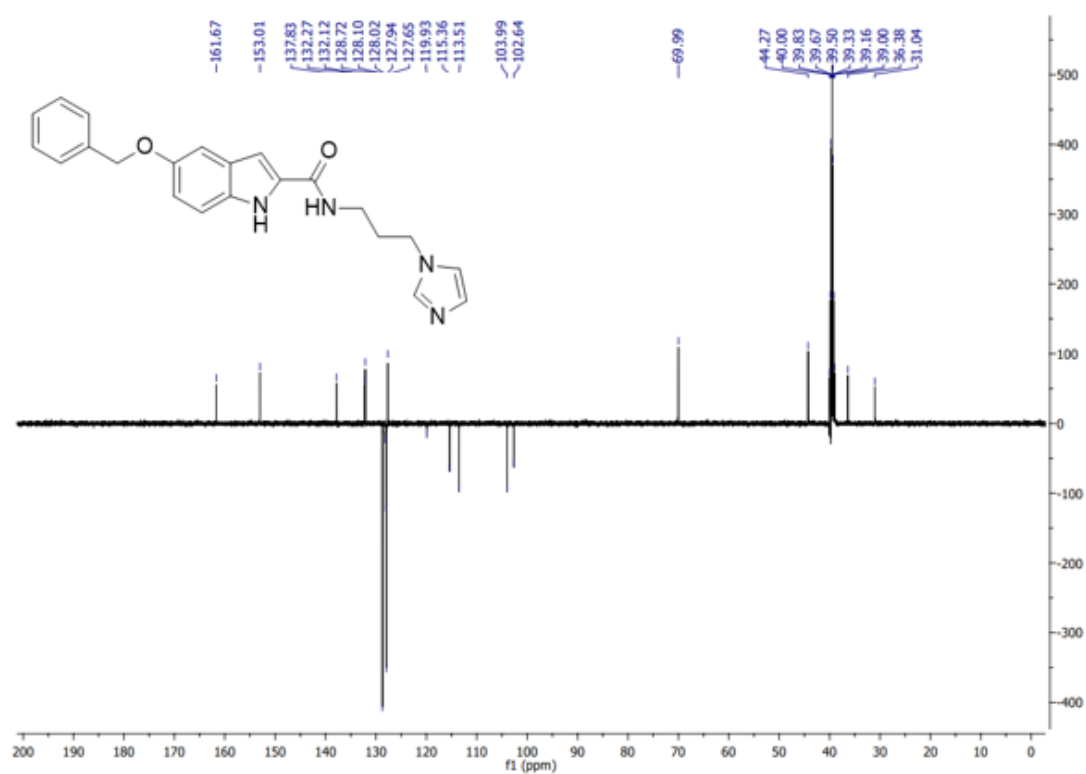


Figure S2.  $^{13}\text{C}$  NMR (500 MHz,  $\text{DMSO-}d_6$ ) of compound 1.

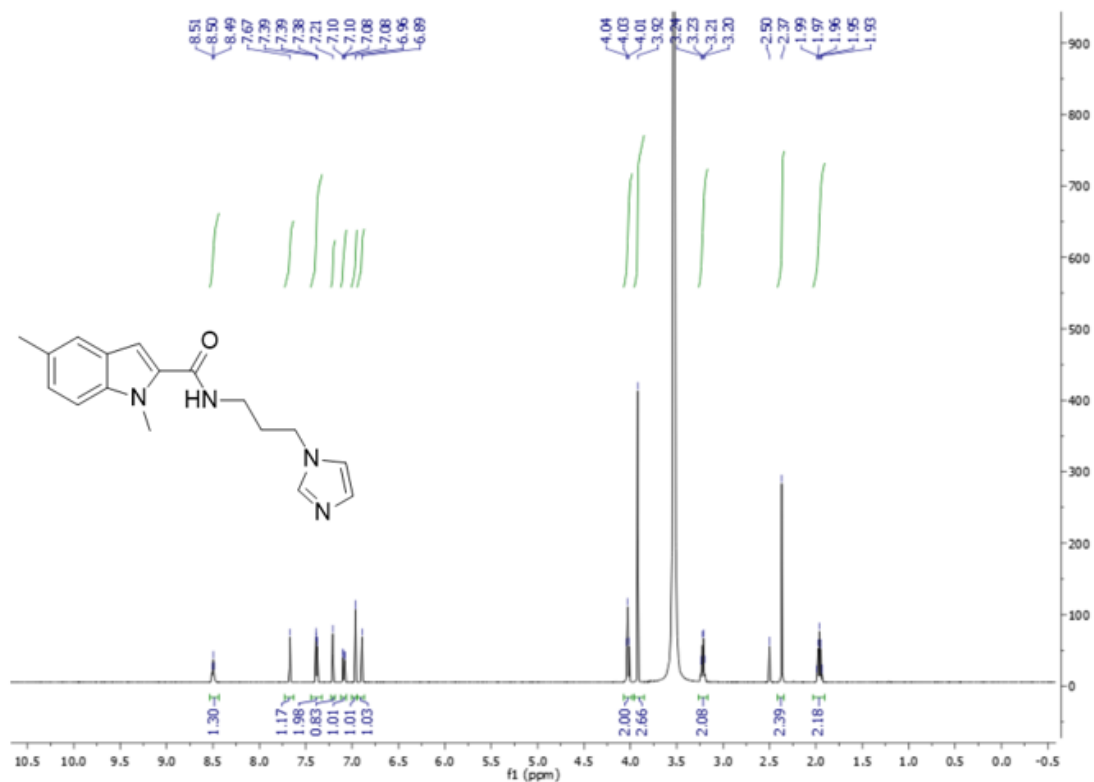


Figure S3. <sup>1</sup>H NMR (500 MHz, DMSO-*d*<sub>6</sub>) of compound 4a.

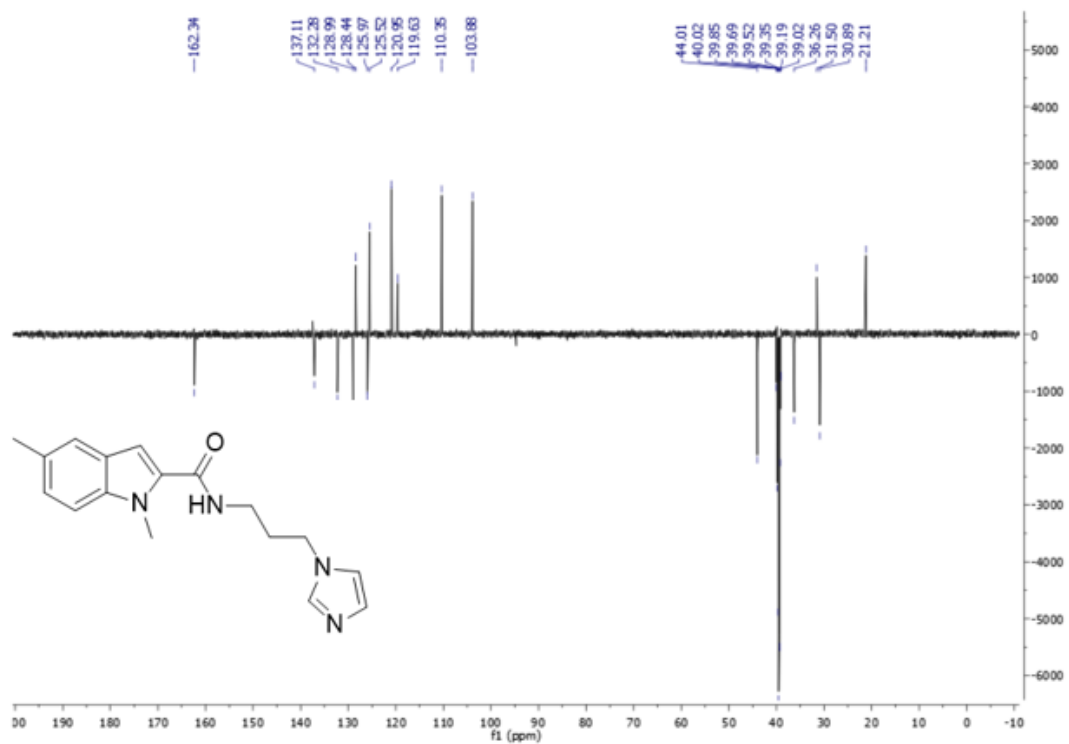


Figure S4. <sup>13</sup>C NMR (125 MHz, DMSO-*d*<sub>6</sub>) of compound 4a.

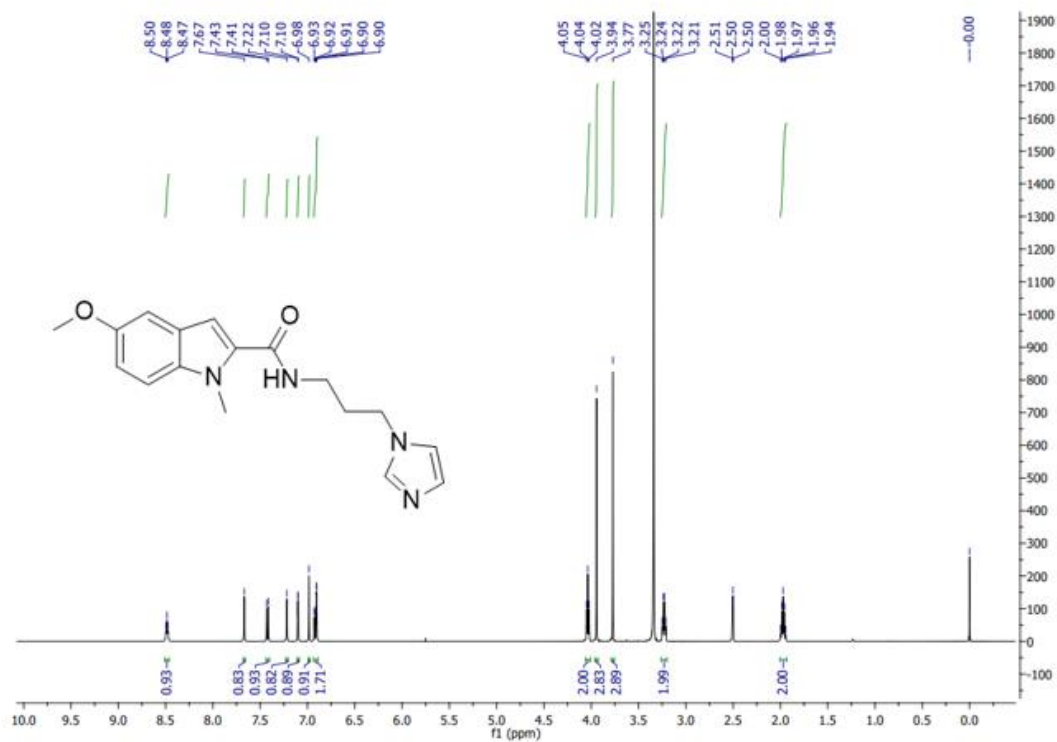


Figure S5.  $^1\text{H}$  NMR (500 MHz,  $\text{DMSO-}d_6$ ) of compound 4b.

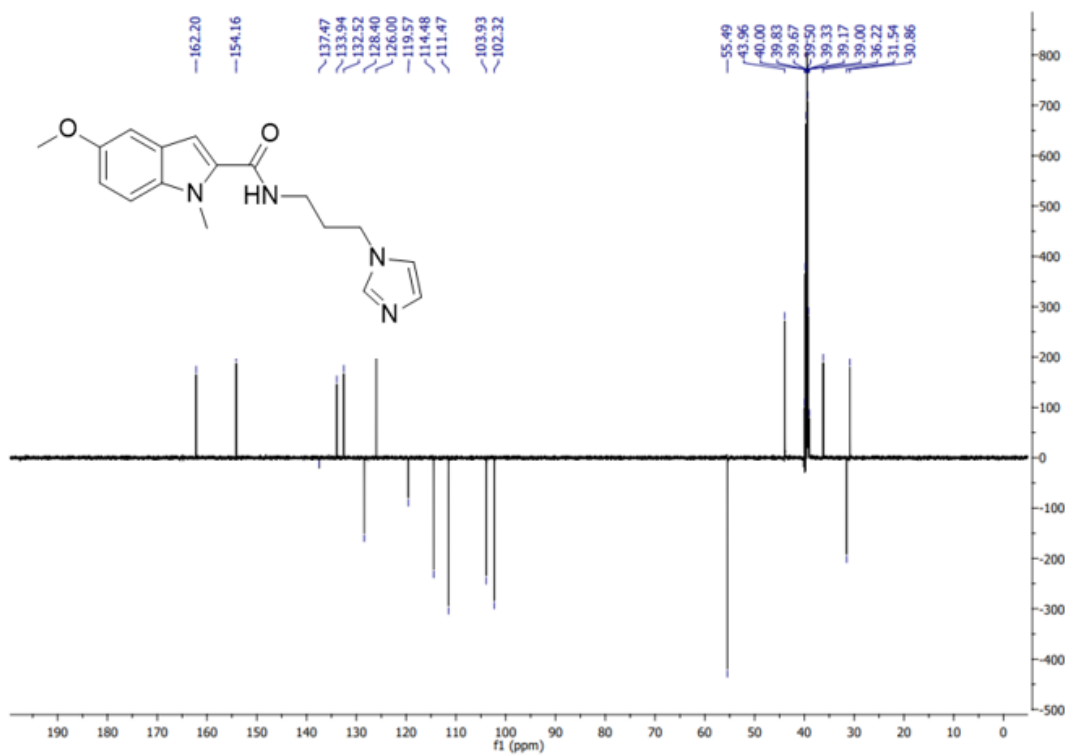


Figure S6.  $^{13}\text{C}$  NMR (125 MHz,  $\text{DMSO-}d_6$ ) of compound 4b.

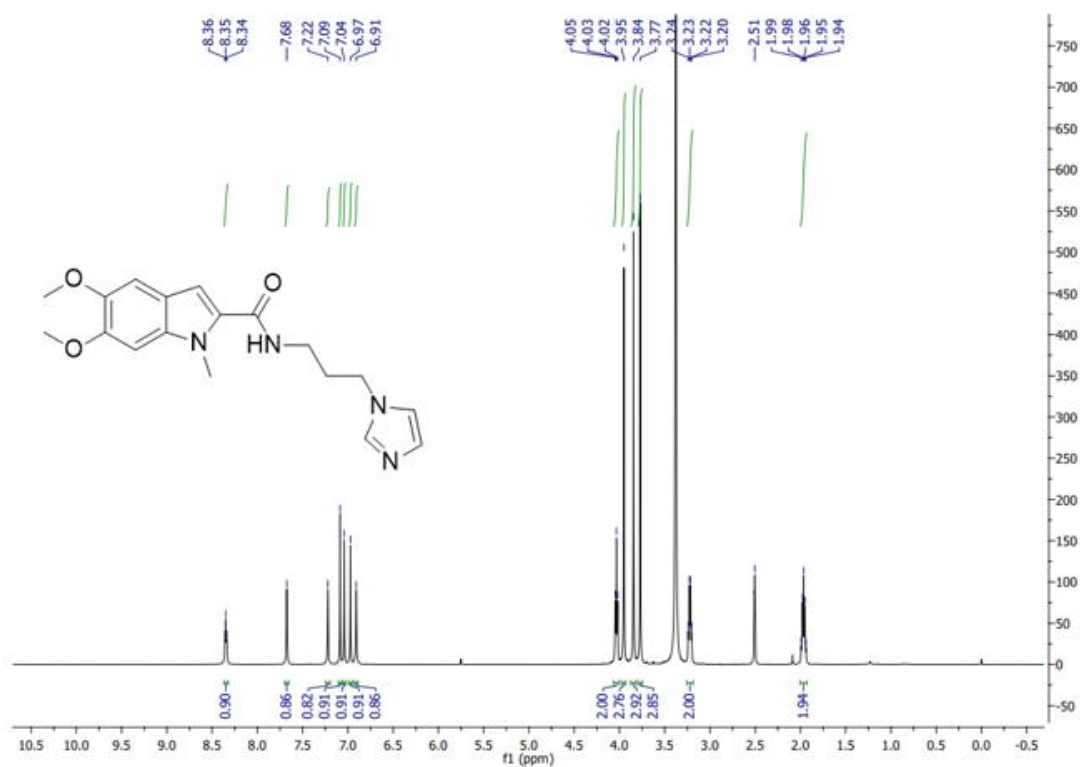


Figure S7.  $^1\text{H}$  NMR (500 MHz,  $\text{DMSO-}d_6$ ) of compound 4c.

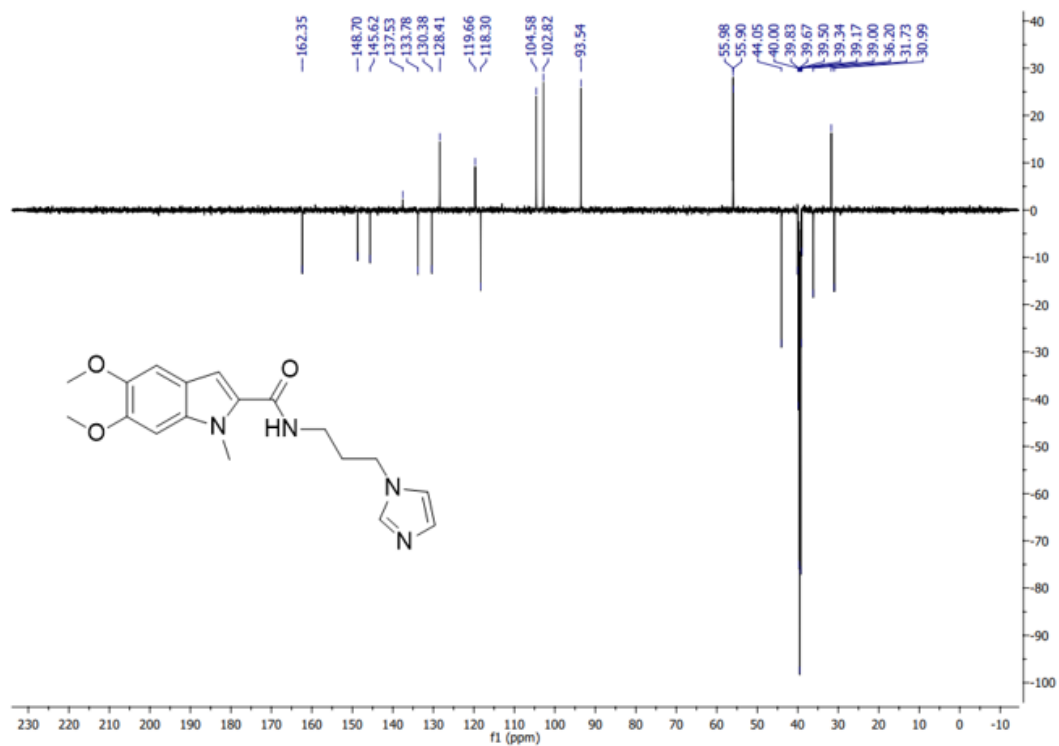


Figure S8.  $^{13}\text{C}$  NMR (125 MHz,  $\text{DMSO-}d_6$ ) of compound 4c.

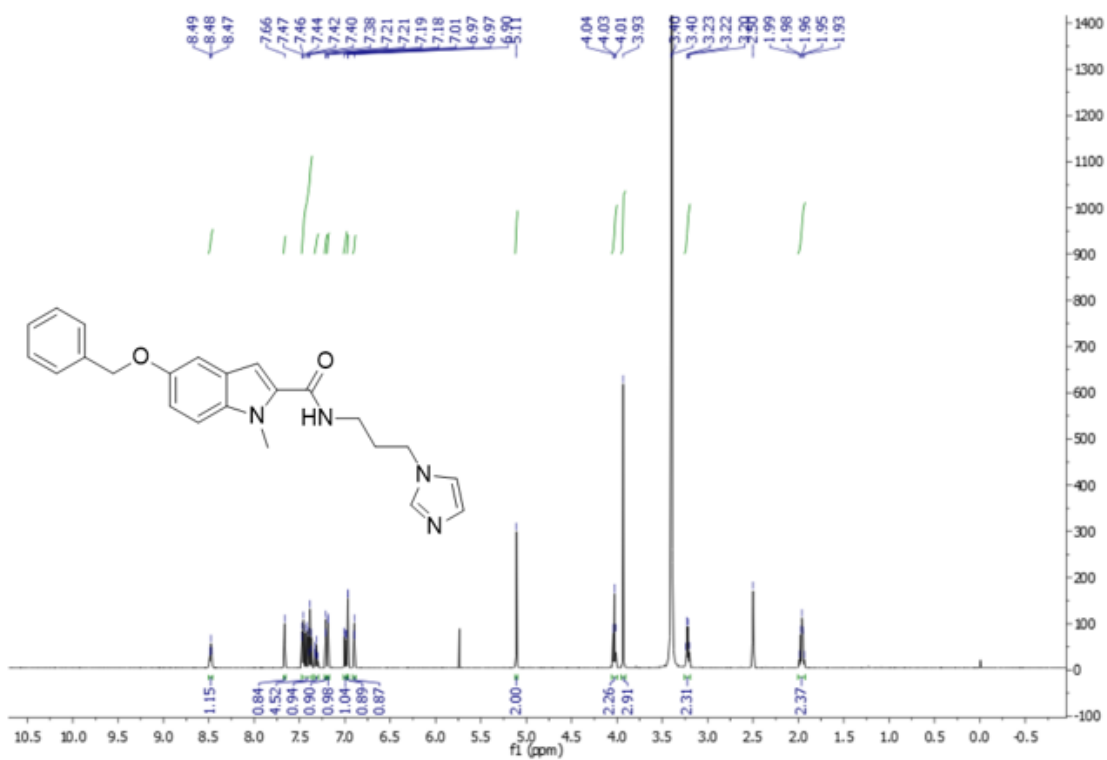


Figure S9.  $^1\text{H}$  NMR (500 MHz,  $\text{DMSO-}d_6$ ) of compound 4d.

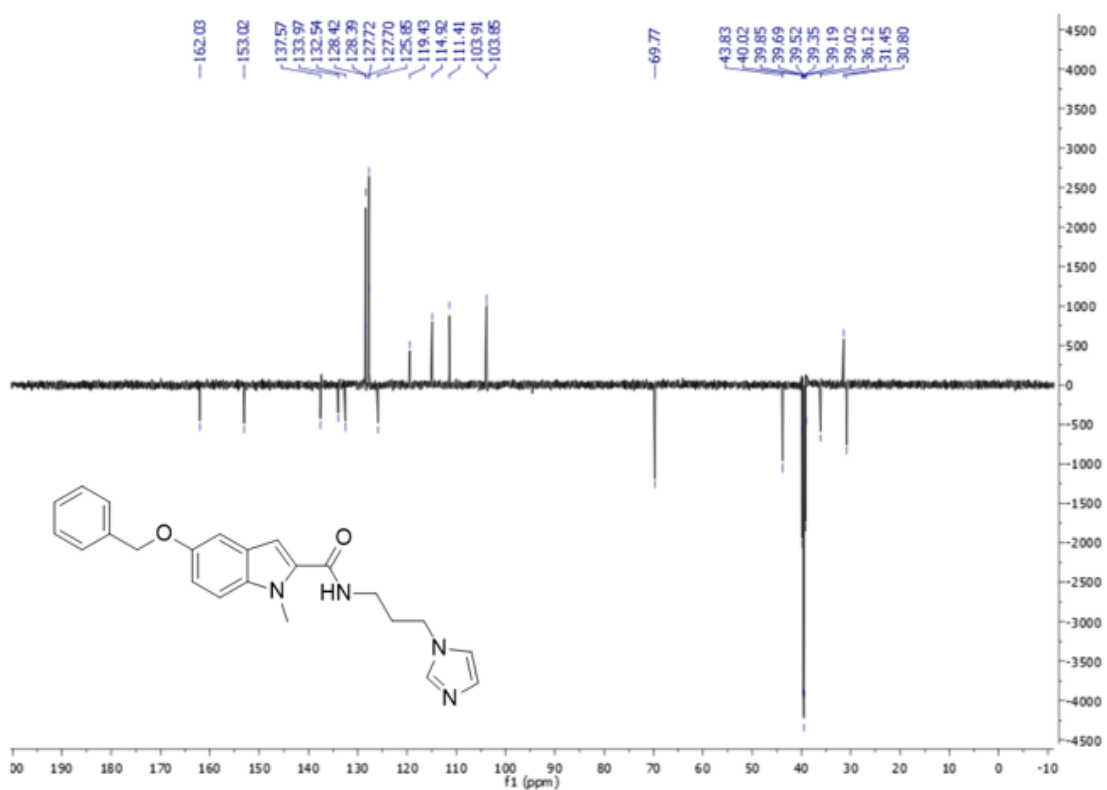


Figure S10.  $^{13}\text{C}$  NMR (125 MHz,  $\text{DMSO-}d_6$ ) of compound 4d.

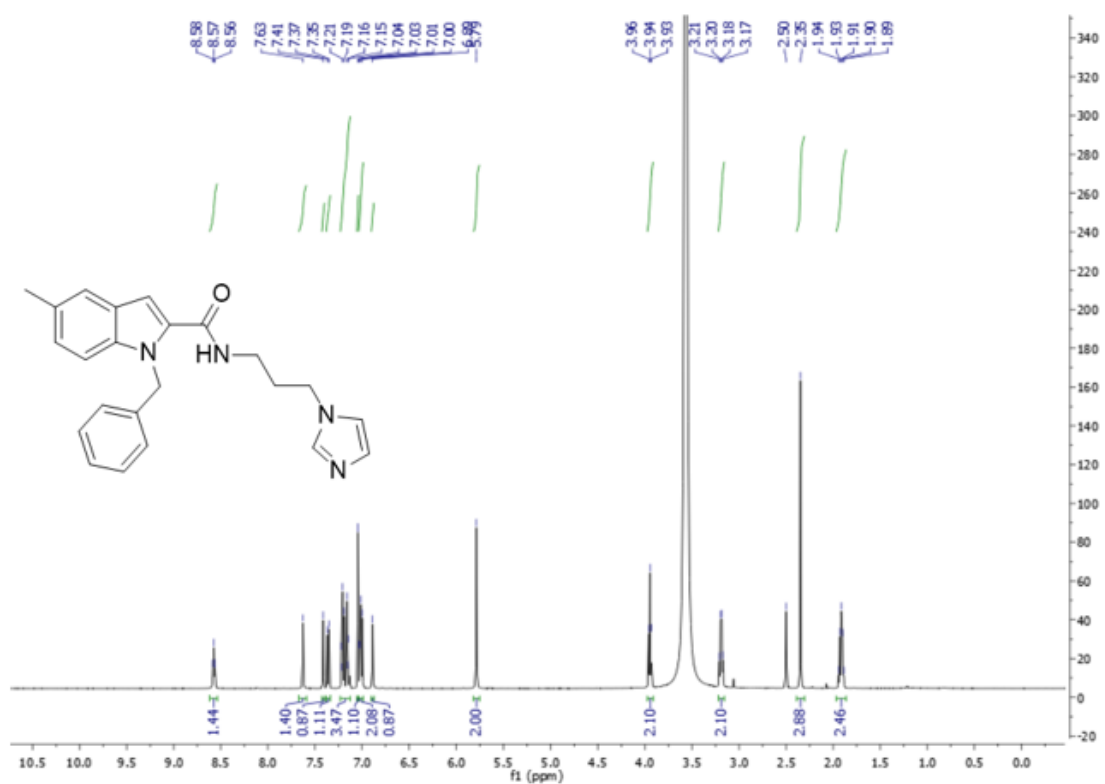


Figure S11. <sup>1</sup>H NMR (500 MHz, DMSO-*d*<sub>6</sub>) of compound 8a.

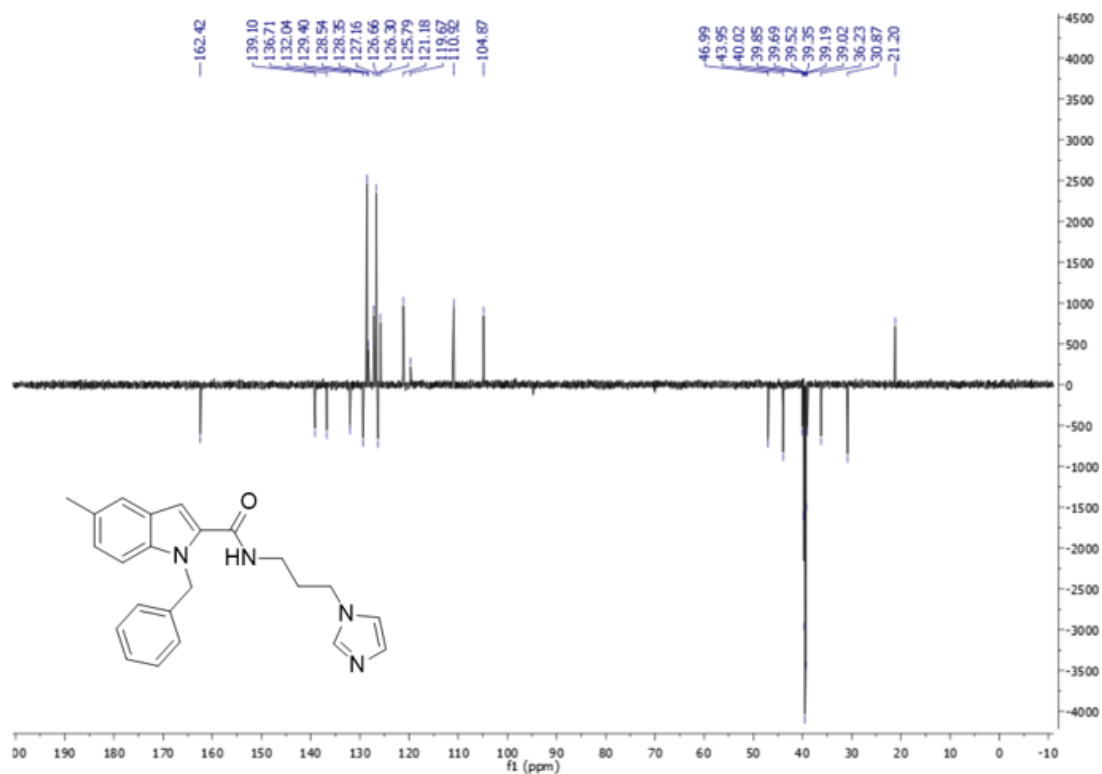
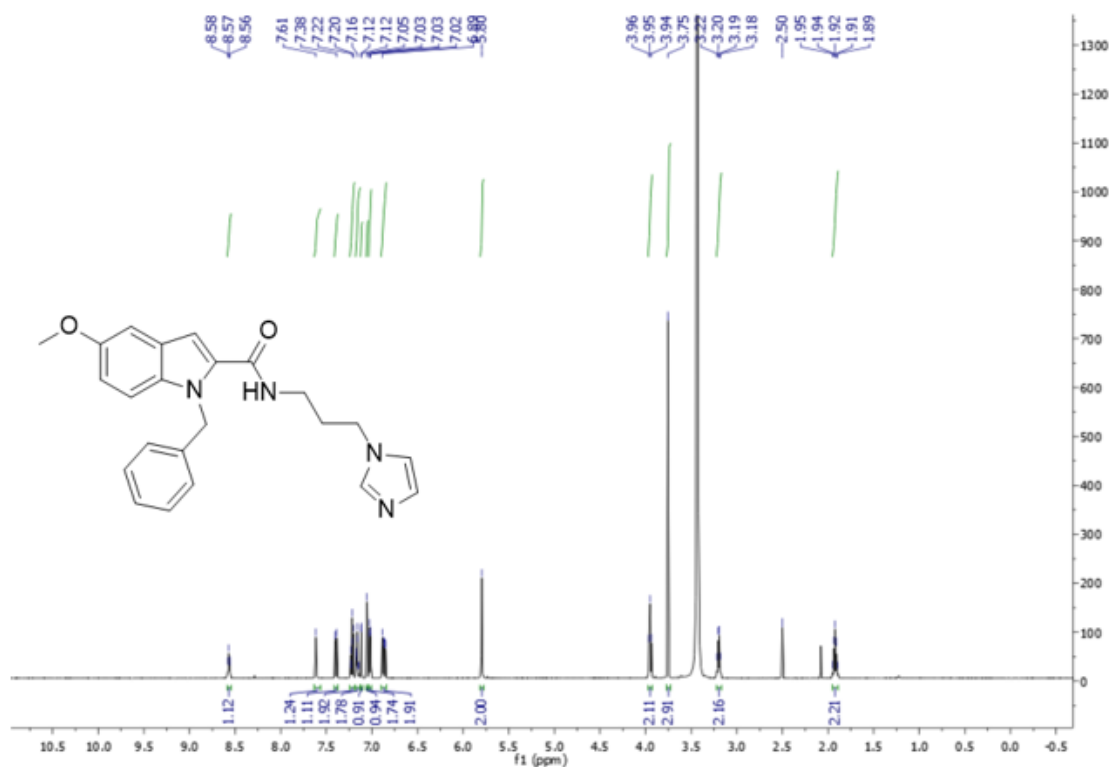
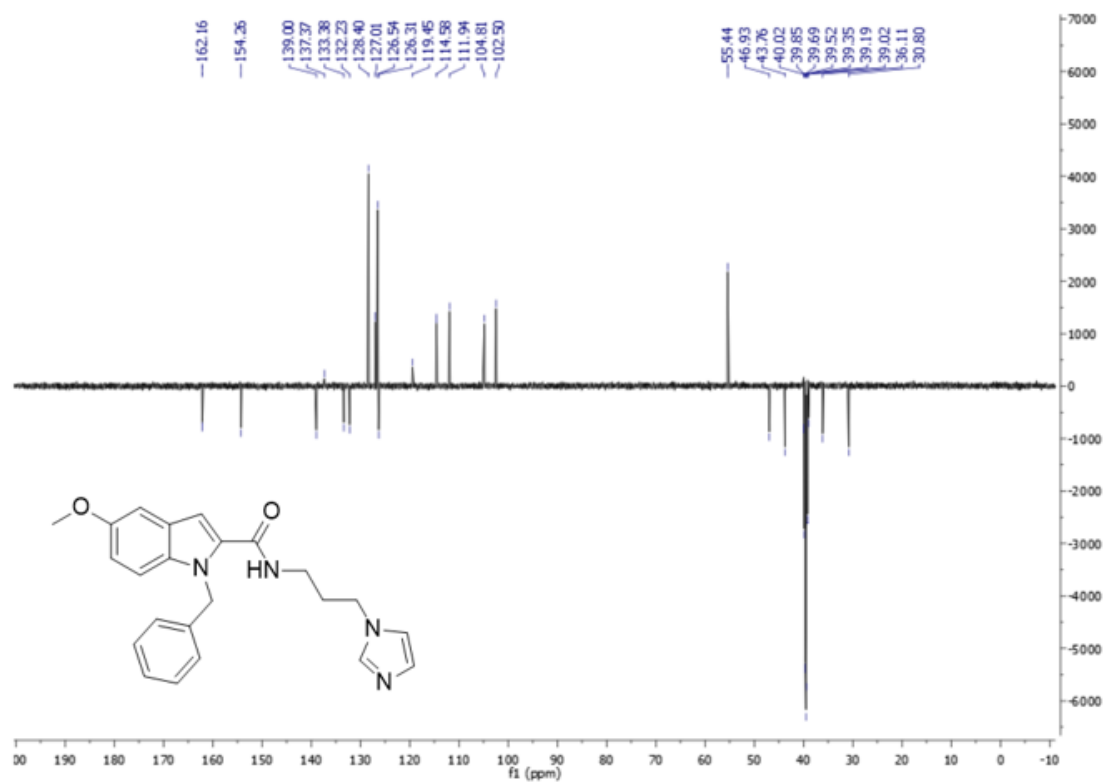


Figure S12. <sup>13</sup>C NMR (125 MHz, DMSO-*d*<sub>6</sub>) of compound 8a.





**Figure S13.**  $^1\text{H}$  NMR (500 MHz,  $\text{DMSO-}d_6$ ) of compound **8b**.



**Figure S14.**  $^{13}\text{C}$  NMR (125 MHz,  $\text{DMSO-}d_6$ ) of compound **8b**.

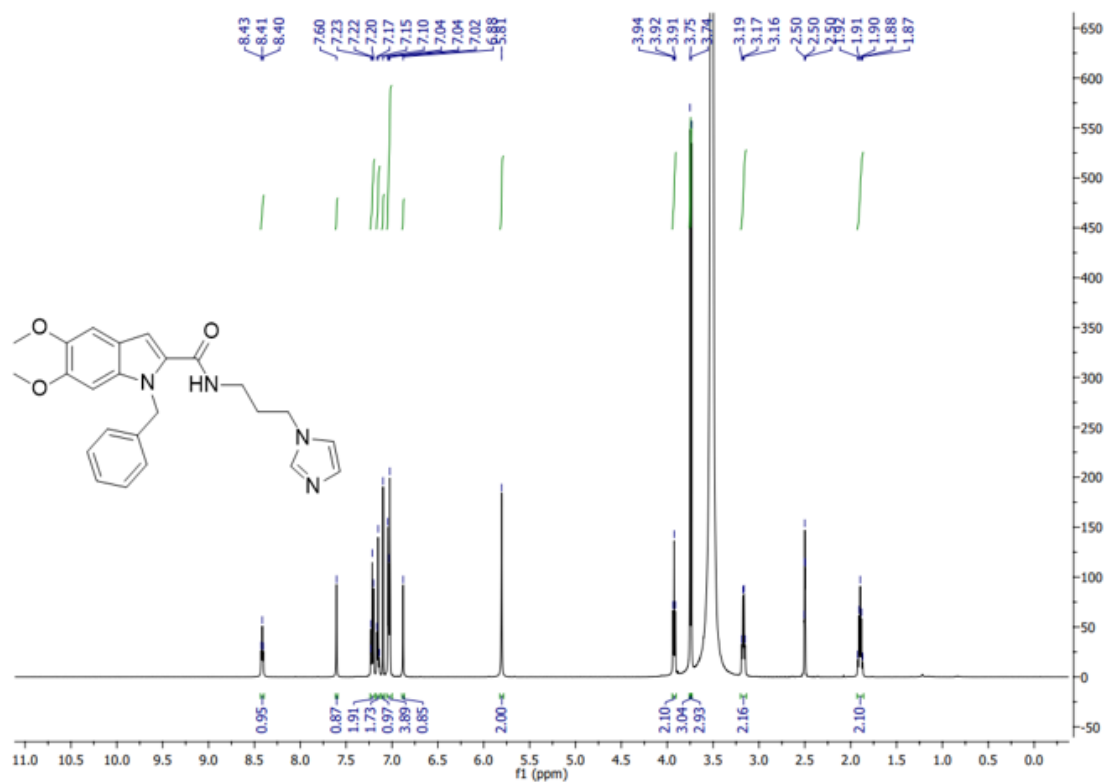


Figure S15.  $^1\text{H}$  NMR (500 MHz,  $\text{DMSO-}d_6$ ) of compound 8c.

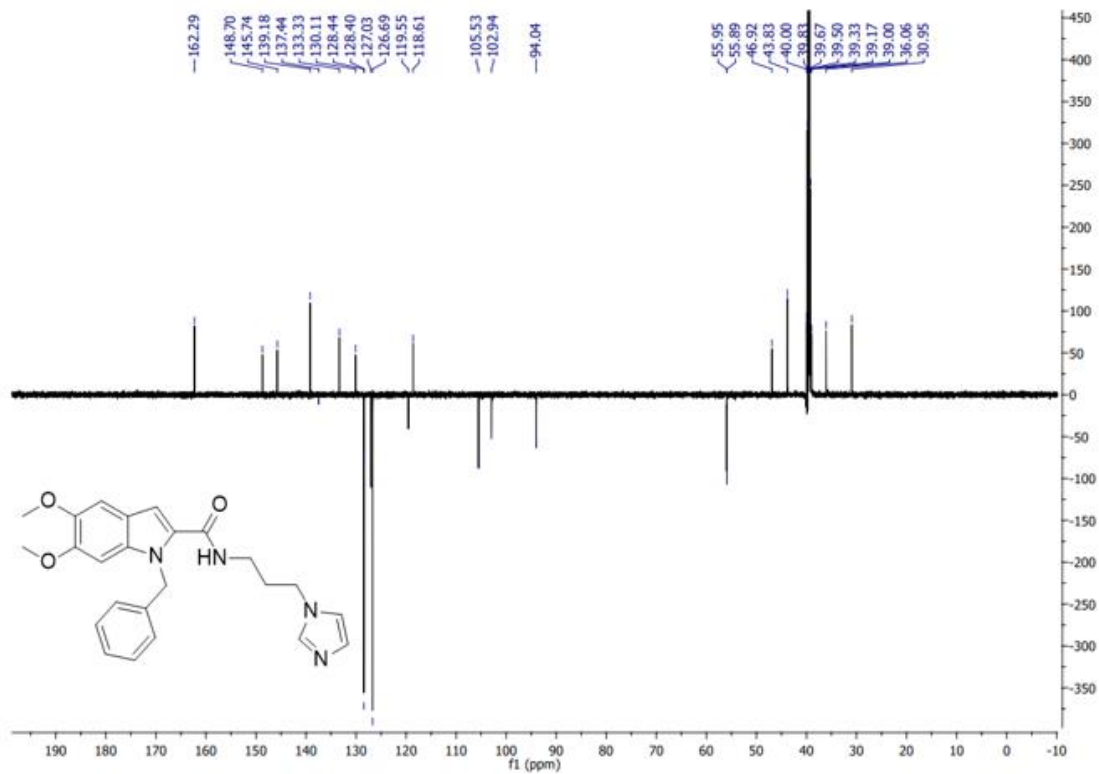
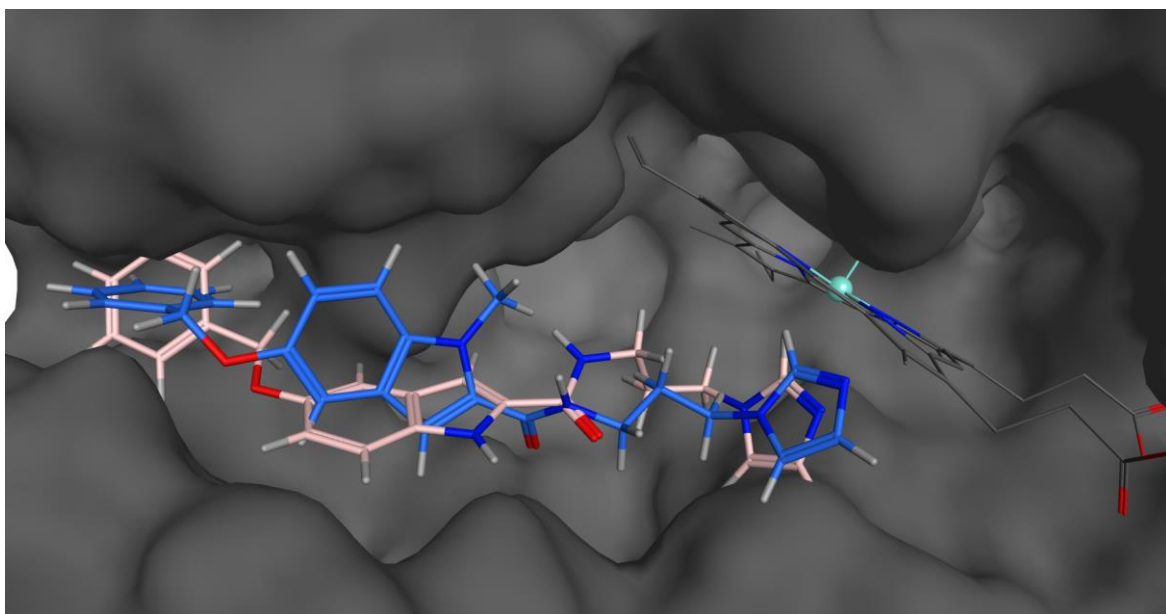
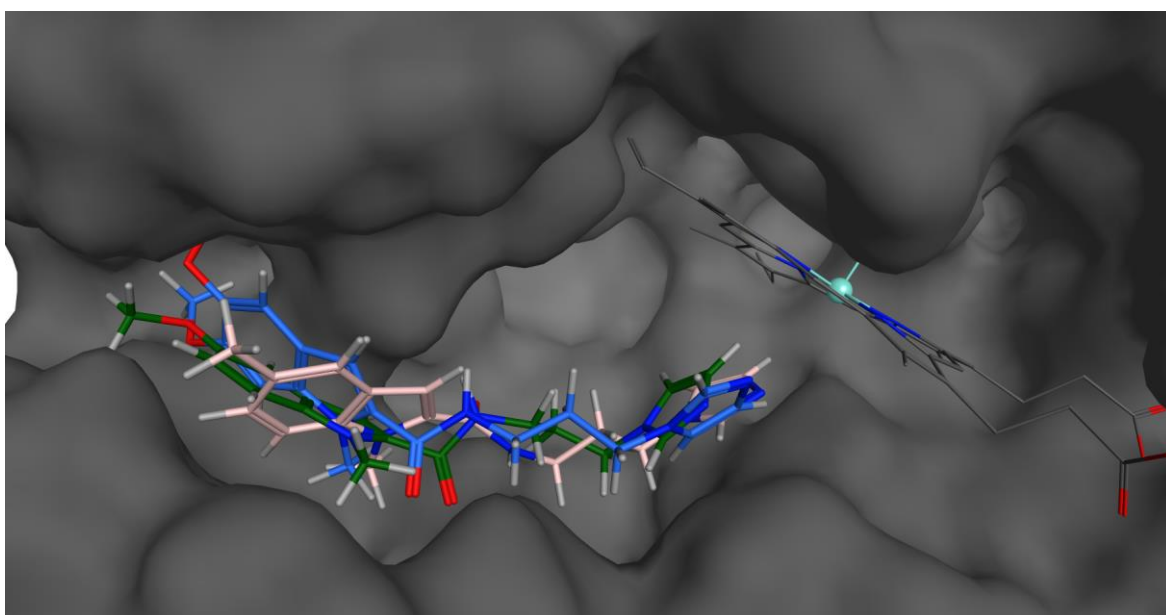


Figure S16.  $^{13}\text{C}$  NMR (125 MHz,  $\text{DMSO-}d_6$ ) of compound 8c.



**Figure S17.** Docked pose of **1** (light pink) and **4d** (blue) inside HO-1.



**Figure S18.** Docked pose of **4a** (light pink), **4b** (green) and **4c** (blue) inside HO-1.

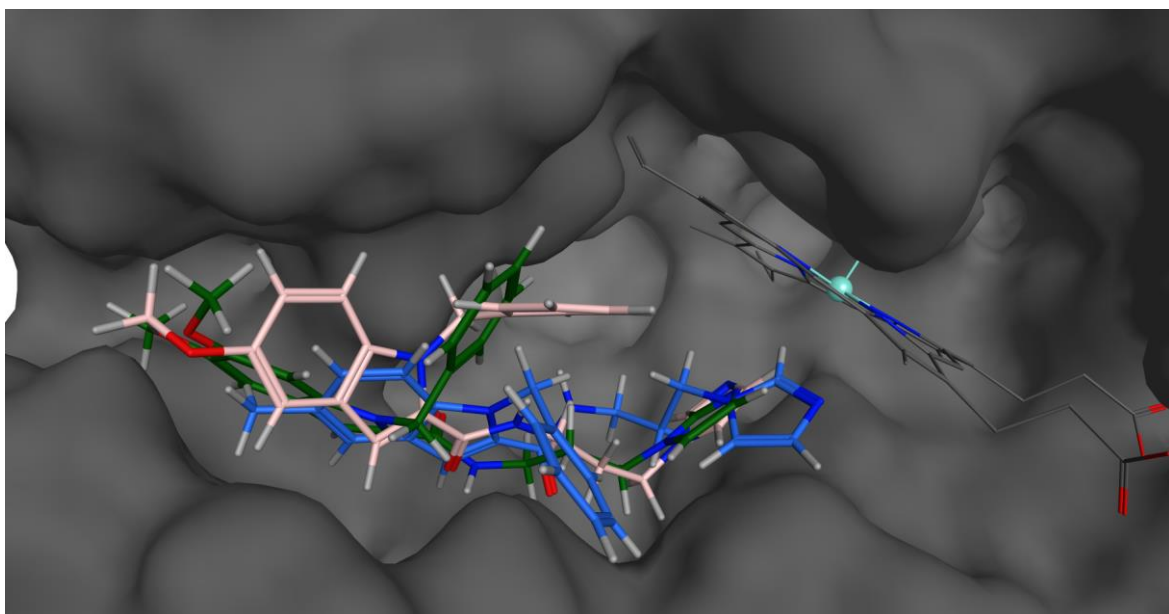


**Figure S19.** Docked pose of **8a** (blue), **8b** (light pink) and **8c** (green) inside HO-1.

## Spark Search

Calculation Method: Ligand Growing

Select one or more databases to search. Filter by name

Name	Fragments	Description
<input checked="" type="checkbox"/> Crystallographic		
<input checked="" type="checkbox"/> COD		
<input checked="" type="checkbox"/> COD	440047	Crystallography Open Database fragments, crystallographic conformations
<input checked="" type="checkbox"/> Fragments		
<input checked="" type="checkbox"/> ChEMBL		
<input checked="" type="checkbox"/> ChEMBL_common	231851	ChEMBL_26 common fragments (seen > 12 times). Released under CC BY-SA 3.0 ( <a href="http://creativecommons.org/licenses/by-sa/3.0/">http://creativecommons.org/licenses/by-sa/3.0/</a> ).
<input checked="" type="checkbox"/> Commercial		
<input checked="" type="checkbox"/> VeryCommon	67888	Commercial very common fragments (seen more than 725 times)
<input checked="" type="checkbox"/> Common	112949	Commercial common fragments (seen 215-724 times)
<input checked="" type="checkbox"/> LessCommon	211480	Commercial less common fragments (seen 65-214 times)
<input checked="" type="checkbox"/> Reagents		
<input checked="" type="checkbox"/> eMolecules		
<input checked="" type="checkbox"/> eMolecules_acid	46489	Acids, delete the -COOH (eMolecules Tier 1,2,3 2021-03-01)
<input checked="" type="checkbox"/> eMolecules_aci...	26209	Acids, keep the CO (eMolecules Tier 1,2,3 2021-03-01)
<input checked="" type="checkbox"/> eMolecules_alc...	21329	Aliphatic alcohols, delete the O (eMolecules Tier 1,2,3 2021-03-01)
<input checked="" type="checkbox"/> eMolecules_alc...	22344	Alcohols, keep the O (eMolecules Tier 1,2,3 2021-03-01)
<input checked="" type="checkbox"/> eMolecules_alip...	9883	Aliphatic halide (eMolecules Tier 1,2,3 2021-03-01)
<input checked="" type="checkbox"/> eMolecules_alky...	3501	Alkynes, delete the -C#C (eMolecules Tier 1,2,3 2021-03-01)
<input checked="" type="checkbox"/> eMolecules_aro...	9931	Aromatic alcohols, keep the O (eMolecules Tier 1,2,3 2021-03-01)
<input checked="" type="checkbox"/> eMolecules_aro...	20716	Aromatic amines, keep the N (eMolecules Tier 1,2,3 2021-03-01)
<input checked="" type="checkbox"/> eMolecules_aro...	45893	Aromatic halide (eMolecules Tier 1,2,3 2021-03-01)
<input checked="" type="checkbox"/> eMolecules_bor...	4705	Aromatic boronic acids, delete -B(OH) <sub>2</sub> (eMolecules Tier 1,2,3 2021-03-01)
<input checked="" type="checkbox"/> eMolecules_cya...	17340	Cyano groups, delete -CN (eMolecules Tier 1,2,3 2021-03-01)
<input checked="" type="checkbox"/> eMolecules_isoc...	593	Isocyanates, keep -NCO (eMolecules Tier 1,2,3 2021-03-01)
<input checked="" type="checkbox"/> eMolecules_olefin	3797	Olefins, delete the -C=C (eMolecules Tier 1,2,3 2021-03-01)
<input checked="" type="checkbox"/> eMolecules_pri...	21917	Primary aliphatic amines, delete N (eMolecules Tier 1,2,3 2021-03-01)
<input checked="" type="checkbox"/> eMolecules_pri...	12830	Primary aliphatic amines, keep N (eMolecules Tier 1,2,3 2021-03-01)
<input checked="" type="checkbox"/> eMolecules_pri...	7766	Primary aliphatic halide (eMolecules Tier 1,2,3 2021-03-01)
<input checked="" type="checkbox"/> eMolecules_pri...	26281	Primary aromatic amines, delete N (eMolecules Tier 1,2,3 2021-03-01)
<input checked="" type="checkbox"/> eMolecules_red...	24466	Aldehydes/ketones, delete the O and reduce C (eMolecules Tier 1,2,3 2021-03-01)
<input checked="" type="checkbox"/> eMolecules_sec...	17416	Secondary aliphatic amines, keep N (eMolecules Tier 1,2,3 2021-03-01)
<input checked="" type="checkbox"/> eMolecules_sulf...	5252	Sulfonic acids, delete the -SO <sub>2</sub> X (eMolecules Tier 1,2,3 2021-03-01)
<input checked="" type="checkbox"/> eMolecules_sulf...	3160	Sulfonic acids, keep the -SO <sub>2</sub> (eMolecules Tier 1,2,3 2021-03-01)
<input checked="" type="checkbox"/> eMolecules_thiol	826	Aliphatic thiols, delete S (eMolecules Tier 1,2,3 2021-03-01)
<input checked="" type="checkbox"/> eMolecules_thiolS	2143	Thiols, keep S (eMolecules Tier 1,2,3 2021-03-01)
<input checked="" type="checkbox"/> Theoretical		
<input checked="" type="checkbox"/> VEHICLE		
<input checked="" type="checkbox"/> VEHICLE	170467	Ring systems from the VEHICLE database ( <a href="ftp://ftp.ebi.ac.uk/pub/databases/chembl/VEHICLE/">ftp://ftp.ebi.ac.uk/pub/databases/chembl/VEHICLE/</a> ).

**Figure S20.** Spark's libraries used for the growing experiments.

Conformation Hunt   Alignment   Build Model

Calculation Method: [Custom]   Save As...   Delete

Delete existing conformations

Perform Conformation Hunt

Maximum number of conformations   500

No. of high-T dynamics runs for flexible rings   20

Gradient cutoff for conformer minimization   0,100 kcal/mol/Å

Filter duplicate conformers at RMS   0,50 Å

Energy window   2,50 kcal/mol

Acyclic secondary amide handling   Use input amide geometry

Turn off Coulombic and attractive vdW forces

Use external tool for conformation generation

**Figure S21.** Forge's parameters used for the conformation hunt.

Conformation Hunt   Alignment   Build Model

Calculation Method: [Normal]   Save As...   Delete

Delete existing alignments

Perform Alignment

Invert achiral imported confs

Take shortcuts in alignments

Maximum-common-substructure conformers and alignment

Matching rules   Normal (element + hybridisation)

Allow conformations to move

Perform Scoring

Score method for multiple references   Weighted Average

Fraction of score from shape similarity   0.50

Reference into db fieldpoints weight   0.50

Hardness of protein excluded volume   Soft

Add/remove field constraints   Mark field points

**Figure S22.** Forge's parameters used for the alignment.

**Table S1.**  $K_i$   $\mu\text{M}$  from docking,  $\text{IC}_{50}$   $\mu\text{M}$  from QSAR and average  $\mu\text{M}$  calculated activity for the virtually evaluated compounds (cut-off at 10  $\mu\text{M}$  average).

Structure	$K_i$ $\mu\text{M}$ from dockin g	$\text{IC}_{50}$ $\mu\text{M}$ from QSAR	Averag e $\mu\text{M}$
s1c(-c2noc(n2)-c3ceccc3)ccc1CNn4cnc4	0.44	1.58	1.01
O=C(Nc1nc(-c2ceccc2)cs1)C3CCN(n4cnc4)CC3	0.46	1.58	1.02
O=C(NCCn1cnc1)c2cc3cc(OCc4ceccc4)ccc3n2C (compound <b>4d</b> )	1.26	0.79	1.03
O=C(NCCn1cnc1)/C=C/Nc2ccc(-c3ceccc3)cc2	0.47	1.58	1.03
O=C(Nc1cc(n[nH]1)-c2ceccc2)c3ccc(-n4cnc4)cc3	0.13	2.00	1.06
O=C(N[C@@H]1COC2(C1)CC[NH+](CC2)Cn3cnc3)c4ceccc4	0.88	1.26	1.07
O=C(NCCn1cnc1)c2ccc(C3CCN(CC3)c4ceccc4)cc2	0.15	2.00	1.07
O=C(Nc1ceccc1)c2cc([nH]n2)-c3ccc(s3)-n4cnc4	0.17	2.00	1.08
O=C(NCCn1cnc1)[C@@H]2CCc3ccc(Oc4ceccc4)cc3C2	0.17	2.00	1.08
O=C(NCc1ceccc1)[C@@H]2CCC3(O2)CCN(n4cnc4)CC3	0.18	2.00	1.09
Clc1cc(-c2cc(no2)C(=O)NCCn3cnc3)ccc1-c4ceccc4	0.20	2.00	1.10
O=C(NCCn1cnc1)CSc2ccc(-c3ceccc3)cn2	1.41	0.79	1.10
O=C(NCCn1cnc1)c2ccc(s2)-c3ccc(o3)-c4ceccc4	0.21	2.00	1.10
O=C1C(OC2ceccc2)=COC(COC(=O)NCCn3cnc3)=C1	1.42	0.79	1.11
O=C(Nn1cnc1)C2CCN(CC2)c3nc(no3)-c4ceccc4	0.23	2.00	1.11
O=C(NCCn1cnc1)[C@@H]2CCN(CCC2)c3ceccc3	1.25	1.00	1.13
O=C(NC[C@@H]1Cc2cc(-c3ceccc3)ccc2O1)NCCn4cnc4	0.26	2.00	1.13
[nH+]1cc(ccc1N2CCC(Nn3cnc3)CC2)-c4ceccc4	0.35	2.00	1.17
O=C(Nn1cnc1)c2cnc(c2)-c3cnc(s3)-c4ceccc4	0.38	2.00	1.19
O=C(N1CCc2ccc(OC3ceccc3)cc2C1)NCCn4cnc4	0.38	2.00	1.19
O=C(NCCn1cnc1)c2cc3cc(OCc4ceccc4)ccc3[nH]2 (compound <b>1</b> )	0.39	2.00	1.19
O=S(=O)(c1ccc(s1)CNC(=O)NCCn2cnc2)c3ceccc3	0.80	1.58	1.19
O=C(Nc1nc2c(s1)CN(CC2)c3ceccc3)Cn4cnc4	0.42	2.00	1.21
O=C(N[C@@H]1CCN(C1)C(=O)NCCn2cnc2)Cc3ceccc3	1.17	1.26	1.21
O=C(NCCn1cnc1)[C@H](Sc2ccc(-c3ceccc3)cn2)C	0.87	1.58	1.23
O=C(NCCc1ccc(cc1C)-c2ceccc2)NCCn3cnc3	0.47	2.00	1.23
O=C(Nn1cnc1)c2ccc(-c3nc(no3)-c4ceccc4)cc2	0.07	2.51	1.29
O=C(NCCn1cnc1)c2cc3cc(OC)ccc3n2Cc4ceccc4 (compound <b>8b</b> )	0.07	2.51	1.29
S(CCCn1cnc1)c2ccc(-c3ceccc3)cc2	1.33	1.26	1.29
o1c(cc2c1ccc(N3CCN(n4cnc4)CC3)c2)-c5ceccc5	0.08	2.51	1.30
O=C(NCCn1cnc1)c2cc3cc(OC)c(OC)cc3n2Cc4ceccc4 (compound <b>8e</b> )	0.09	2.51	1.30
O=C(On1cnc1)c2ccc(-c3noc(n3)-c4ceccc4)cc2	0.11	2.51	1.31
s1c(Nn2cnc2)nnc1Nc3nc(-c4ceccc4)cs3	0.16	2.51	1.33
O=C(NCCc1ccc(-c2ceccc2)cc1)NCCn3cnc3	0.68	2.00	1.34
O=C(NCCn1cnc1)c2cc(no2)-c3ccc(-c4ceccc4)cc3	0.17	2.51	1.34
O=C(Nn1cnc1)c2ceccc(-n3cc(-c4ceccc4)cn3)c2	0.17	2.51	1.34
O=C(NCCn1cnc1)c2c(nc(s2)NNC(=O)c3ceccc3)C	0.76	2.00	1.38
O=C(NCCn1cnc1)c2cn(nn2)-c3ccc(-c4ceccc4)cc3	0.27	2.51	1.39
O=C(N1CCc2cc(Nc3ceccc3)ccc2CC1)NCCn4cnc4	0.27	2.51	1.39
O=C(NCCn1cnc1)/C=C/c2ccc3CN(Cc3c2)c4ceccc4	0.28	2.51	1.39
O=C(Nn1cnc1)c2cc(n[nH]2)-c3ccc(-c4ceccc4)cc3	0.29	2.51	1.40

N1(CCC(CC1)=Cn2cnc2)c3ccc(cc3)-c4cccc4	0.30	2.51	1.41
O=C(NCCcn1cnc1)[C@H]2CN(CCC2)C(=O)/C=C/c3cccc3	0.33	2.51	1.42
O=C(Nc1ccc(-n2cnc2)cn1)[C@H](Sc3cccc3)C	0.85	2.00	1.42
O=C(NCCcn1cnc1)NCc2ccc(o2)C(Oc3cccc3)=O	2.05	0.79	1.42
O=C(n1cnc1)Nc2nc(-c3ccc(-c4cccc4)cc3)c[nH]2	0.37	2.51	1.44
N1(CCC(Nn2cnc2)CC1)c3ccc(cc3)-c4cccc4	0.41	2.51	1.46
O=C(N[C@@H]1COc2cc(Oc3cccc3)ccc2C1)NCCcn4cnc4	0.43	2.51	1.47
O=C(NCCcn1cnc1)c2cc3cc(ccc3n2Cc4cccc4)C (compound <b>8a</b> )	0.47	2.51	1.49
o1c(nc(n1)-c2cc(on2)-n3cnc3)CNc4cccc4	0.52	2.51	1.51
O=C(NCCcn1cnc1)CSc2ncc(-c3cccc3)c(n2)N	2.26	0.79	1.53
s1c(ccc1-n2cnc2)-c3nnc(o3)CCc4cccc4	0.55	2.51	1.53
O=C(NC/C=C/n1cnc1)c2ccc(-c3cccc3)cc2	0.57	2.51	1.54
O=C(NC1CCN(n2cnc2)CC1)CSc3cccc3	1.10	2.00	1.55
N1(CCC(n2cnc2)CC1)c3cnc4ccc(cc4c3)-c5cccc5	0.01	3.16	1.59
n1(-n2cnc2)cc(-c3ccc4cnc(cc4c3)-c5cccc5)cn1	0.02	3.16	1.59
o1c(-c2cccc2)cc(n1)-c3ccc4c(CCN(n5cnc5)CC4)c3	0.02	3.16	1.59
[nH]1c(nc2cnc(-n3cnc3)cc21)-c4cccc(-c5cccc5)c4	0.04	3.16	1.60
O=C(Nn1cnc1)c2esc(n2)C3CCN(CC3)c4cccc4	0.70	2.51	1.60
O=C(Nc1enn(-n2cnc2)c1)c3cccc(-c4cccc4)c3	0.05	3.16	1.61
Clc1cc2c([nH]c(n2)-c3cccc3)cc1N4CCN(n5cnc5)CC4	0.06	3.16	1.61
O=C(NCCcn1cnc1)c2ccc(-c3noc(n3)-c4cccc4)cc2	0.10	3.16	1.63
o1c2cc(-c3cccc3)ccc2c(n1)C4CCN(n5cnc5)CC4	0.14	3.16	1.65
O=C(NCCcn1cnc1)CCc2cn(nn2)Cc3cccc3	2.30	1.00	1.65
O=C(N1CCN(CCC1)c2cc(n[nH]2)-c3cccc3)NCCcn4cnc4	0.14	3.16	1.65
O=C(NCCcn1cnc1)c2c(oc(n2)-c3cccc(-c4cccc4)c3)C	0.15	3.16	1.66
O=C(N1CCC(CC1)c2noc(n2)-c3cccc3)NCCcn4cnc4	0.15	3.16	1.66
N1(CC[C@]2(CCCN(C2)c3ncc(-n4cnc4)cn3)C1)c5cccc5	0.24	3.16	1.70
O=C(NC1CC(C1)c2cccc(e2)-c3cccc3)NCCcn4cnc4	0.27	3.16	1.72
O=C(NCCcn1cnc1)CSc2nnc([nH]2)Cc3cccc3	2.45	1.00	1.72
O=C(Nn1cnc1)c2cc([nH]n2)-c3ccc(s3)-c4cccc4	0.30	3.16	1.73
O=C(N/N=C/c1ccc(o1)-c2cccc2)Cn3cnc3	0.97	2.51	1.74
O=S(=O)(c1cc(-c2nnc(o2)NCCcn3cnc3)es1)c4cccc4	1.49	2.00	1.74
Cc1c(-c2cccc2)cc[n+](CCCC#Cn3cnc3)c1	0.36	3.16	1.76
O=C(NCCcn1cnc1)Cc2csc(n2)CCc3cccc3	2.54	1.00	1.77
o1c2ccc(-c3cccc3)cc2nc1NCCn4cnc4	0.39	3.16	1.77
O=C(N1CCN(CCC1)c2cccc2)c3cc(on3)NCCcn4cnc4	0.39	3.16	1.78
O=C(NCCcn1cnc1)c2cnc(s2)-c3ccc(-c4cccc4)cc3	0.40	3.16	1.78
O=C(NCCcn1cnc1)CCc2nc(no2)-c3cccc3	2.86	0.79	1.82
n1(CCCNe2cc(NCCc3cccc3)ncn2)cnc1	1.67	2.00	1.83
n1(Cc2cnc(nc2)-c3ccc(-c4cccc4)cc3)cnc1	0.52	3.16	1.84
s1c(nnc1-c2cccc2)/N=C/c3ccc(-n4cnc4)cc3	0.55	3.16	1.85
s1c2cc(Nn3cnc3)ccc2nc1SCc4cccc4	0.58	3.16	1.87
O([C@@H]1COc2nc(en2C1)-c3cccc3)CC#Cn4cnc4	0.58	3.16	1.87
O=C(N1CCC(CC1)COC(=O)NCCcn2cnc2)c3cccc3	0.62	3.16	1.89
O=C(NCc1cnc(Sc2cccc2)n1C)NCCcn3cnc3	1.33	2.51	1.92
O=C(NC1CCC(CC1)C(=O)NCCcn2cnc2)Cc3cccc3	0.74	3.16	1.95
O=C(NCCcn1cnc1)C/C(=N/NC(=O)Cc2cccc2)C	1.41	2.51	1.96



s1c2cc(On3cenc3)ccc2nc1SCc4cccc4	0.77	3.16	1.96
o1c(NCCCN2cenc2)nnc1C[C@@H]3CC[C@H](Nc4cccc4)C3	0.78	3.16	1.97
O=C(NCCCN1cenc1)NCc2cccc(c2)C(=O)c3cccc3	0.83	3.16	1.99
o1c2ccc(-c3cccc3)cc2nc1N4CCC(n5cnc5)CC4	0.03	3.98	2.00
Fc1cc(-c2nc3cc(-c4cccc4)ccc3[nH]2)ccc1-n5cenc5	0.05	3.98	2.02
O=C(Nc1cc(on1)-n2cenc2)c3cnc(c3)-c4cccc4	0.05	3.98	2.02
O=C(NCCCN1cenc1)C2CCC(CC2)CNC(=O)c3cccc3	0.87	3.16	2.02
[NH+]1(CCC[C@H](n2cenc2)CC1)Cc3cccc(-c4cccc4)c3	0.07	3.98	2.02
N1(CCCN(CC1)c2cccc2)c3ccc(Nn4cnc4)cc3	0.08	3.98	2.03
N1(n2cenc2)CCC(n3c4ccc(cc4nn3)-c5cccc5)CC1	0.14	3.98	2.06
Clc1c(-c2cccc2)ccc(CC3CCN(n4cnc4)CC3)c1	0.15	3.98	2.06
O=C(NCCCN1cenc1)c2cc3cc(NC(=O)c4cccc4)ccc3o2	0.15	3.98	2.07
O=C(N/N=C/c1ccc(s1)-c2cccc2)Cn3cnc3	1.62	2.51	2.07
N1(n2cenc2)CCN(CC1)c3ccc4c([nH]c(n4)-c5cccc5)n3	0.16	3.98	2.07
N1(CCC(CC1)c2cccc2)c3ccc(Nn4cnc4)nn3	0.16	3.98	2.07
O=C(Nn1cenc1)c2ccc(-n3cc(-c4cccc4)cn3)cc2	0.17	3.98	2.08
n1(-c2ccc(cc2)C#Cc3cn(nn3)-c4cccc4)ccnc1	0.18	3.98	2.08
O=C(NCCC(=O)NCCCN1cenc1)[C@@H]2C[C@@H]2c3cccc3	3.38	0.79	2.08
O=C(N[C@H](c1nc2ccc(-c3cccc3)cc2s1)C)NCCCN4cnc4	0.19	3.98	2.09
O1Cc2c(NCCCN3cnc3)nnn2C[C@@H]1c4ccc(-c5cccc5)cc4	0.22	3.98	2.10
O=C(Oc1cccc1)/C=C/COC(=O)NCCCN2cenc2	3.42	0.79	2.10
O=C(Oc1ccc(Nn2cenc2)cc1)/C=C/c3cccc3	0.26	3.98	2.12
n1(CCC#Cc2ccc(-c3cccc3)cc2)cnc1	0.28	3.98	2.13
S(Cc1cccc1)Cc2nc3cc(-n4cnc4)ccc3[nH]2	1.80	2.51	2.16
O=C(NCCCN1cenc1)c2c(n(nn2)-c3ccc(-c4cccc4)cc3)N	0.34	3.98	2.16
O=C(Nn1cenc1)c2cn(nn2)-c3ccc(-c4cccc4)cc3	0.35	3.98	2.17
O=C(N1CCC2(CC1)CO[C@H](C2)Cc3cccc3)NCCCN4cnc4	0.39	3.98	2.18
O=C1/C(CC[C@@H]1Cn2cnc2)=C/c3ccc(-c4cccc4)cc3	0.40	3.98	2.19
O=C(N1CCC2(CC[NH+](C2)Cc3cccc3)CC1)NCCCN4cnc4	0.49	3.98	2.24
O=C(NCCCN1cenc1)NC(=O)/C=C/c2ccc(-c3cccc3)cc2	0.50	3.98	2.24
O=C(N1CC[C@H](OCCc2cccc2)C1)NCCCN3cnc3	1.99	2.51	2.25
s1c(mnc1NCCCN2cenc2)-c3cccc(Oc4cccc4)c3	0.54	3.98	2.26
O=S(=O)(c1cc2c(s1)CCN(C2)C(=O)NCCCN3cnc3)c4cccc4	0.56	3.98	2.27
O=C(N1CCC[C@H](C1)CNC(=O)c2cccc2)NCCCN3cnc3	0.59	3.98	2.29
O=S(=O)(Nn1cenc1)c2ccc(s2)C#Cc3cccc3	0.60	3.98	2.29
O=C(NCCCN1cenc1)CCc2ccc(s2)-c3cccc3	2.59	2.00	2.29
O=C(Oc1cccc1)/C=C/c2ccc(Cn3cnc3)cc2	0.64	3.98	2.31
O=C(N1CCc2c(sc(n2)C(=O)NCCCN3cnc3)CC1)c4cccc4	0.83	3.98	2.40
o1c(nc(n1)-c2cc(on2)NCCCN3cnc3)CNc4cccc4	0.83	3.98	2.41
O=C(NCC[NH+]1CCC[C@@](C1)(c2cccc2)C)NCCCN3cnc3	0.87	3.98	2.43
[NH+]1(CCN(CC1)c2cccc2)CCC#Cn3cnc3	0.95	3.98	2.47
O=C(Nn1cenc1)C(=O)Nc2nnc(s2)Cc3cccc3	0.95	3.98	2.47
O=S(=O)(/N=C(/N/N=C(\C)C#Cn1cnc1)N)c2cccc2	0.97	3.98	2.48
S(c1cccc1)c2ccc(N3CCC(n4cnc4)CC3)nn2	1.03	3.98	2.51
n12ccc(-n3cnc3)nc1cc(n2)-c4ccc(-c5cccc5)cc4	0.06	5.01	2.53
O=C(Nc1nc(-n2cenc2)ns1)c3ccc(-c4cccc4)cc3	0.13	5.01	2.57
O=C(Nc1ccc(-c2cccc2)cc1)c3cc(-n4cnc4)n[nH]3	0.14	5.01	2.58

O=C(Nc1cc(-n2ccnc2)n[nH]1)c3ccc(-c4cccc4)cc3	0.14	5.01	2.58
O=C(Nc1nc2c(s1)C[C@H](CC2)c3cccc3)C(=O)n4ccnc4	0.14	5.01	2.58
O=C1C(=COc2cc(On3ccnc3)ccc12)/C=C/c4cccc4	0.16	5.01	2.59
O=C(NCCCN1cnc1)NCC#Cc2ccc(-c3cccc3)cc2	0.16	5.01	2.59
Fc1cc(-c2cc(no2)C(=O)NCCCN3cnc3)ccc1-c4cccc4	0.17	5.01	2.59
[NH+]1(C[C@H]2C([C@H](N2)C1)c3ccc(-c4cccc4)cc3)Cn5cnc5	0.19	5.01	2.60
O=C(Nc1cccc1)C#Cc2ccc(-n3ccnc3)cc2	0.20	5.01	2.61
O=C(NCCCN1cnc1)C(=O)Nc2cccc(Sc3cccc3)c2	1.24	3.98	2.61
O=C(c1ccc(/C=C/C(=O)NCCCN2cnc2)cc1)c3cccc3	0.21	5.01	2.61
N1(n2ccnc2)CCC(Nc3ccc(-c4cccc4)cc3)CC1	0.23	5.01	2.62
N(C1CCC(n2cnc2)CC1)c3ccc(-c4cccc4)cc3	0.24	5.01	2.62
O=C(c1ccc(C(=O)NC(=O)NCCCN2cnc2)cc1)c3cccc3	0.24	5.01	2.63
O=C(NCCCN1cnc1)c2nc3ccc(Nc4cccc4)cc3s2	0.25	5.01	2.63
O=C(Nn1cnc1)c2cnc([nH]2)-c3ccc(-c4cccc4)cc3	0.26	5.01	2.64
o1c(ccc1-c2ccc(-c3cccc3)cc2)/C=C/n4ccnc4	0.27	5.01	2.64
O=C(Oc1cccc(-n2ccc(c2)-c3cccc3)c1)NCCCN4cnc4	0.27	5.01	2.64
O=C(Nc1cccc1)c2cc(on2)-c3ccc(-n4ccnc4)cc3	0.29	5.01	2.65
O=C(NCCCN1cnc1)/C=C/Nc2cccc(-c3cccc3)c2	0.29	5.01	2.65
C/C(=N\c1cccc1)/C=N/Nc2ccc(-n3ccnc3)cc2	0.30	5.01	2.66
C/C(=N\nc1cnc1)/C=N/Nc2ccc(-c3cccc3)cc2	0.31	5.01	2.66
O=C(NCCCN1cnc1)NC/C=C/c2ccc(-c3cccc3)cc2	0.42	5.01	2.72
O=C(NCCCN1cnc1)c2c(nc(s2)N3C=NN(C3=O)c4cccc4)C	0.46	5.01	2.74
S(Cc1cccc1)c2ccc(CCN3cnc3)cc2	2.32	3.16	2.74
O=C(NCCCN1cnc1)CSc2nnc(o2)Cc3cccc3	4.50	1.00	2.75
[nH+]1cc(ccc1N2CCC(Cn3cnc3)CC2)-c4cccc4	0.50	5.01	2.75
O=C(Oc1cccc1)c2cccc(-n3c(NCCCN4cnc4)nnn3)c2	0.50	5.01	2.76
O=C(N/N=C/c1cccc1)C[NH+]2CCN(n3ccnc3)CC2	2.40	3.16	2.78
O=C(NCCc1ccc(s1)-c2cccc2)NCCCN3cnc3	1.61	3.98	2.80
O=C(On1cnc1)c2ccc(N/N=N/c3cccc3)cc2	0.64	5.01	2.83
O=C(Nn1cnc1)c2nnc(s2)[C@@H]3CCCN(C3)c4cccc4	0.70	5.01	2.86
s1c(CO/N=C/c2cccc2)cnc1NCCCN3cnc3	3.24	2.51	2.87
O=C(NCCCN1cnc1)NCc2ccc(Cc3cccc3)cc2	0.74	5.01	2.88
O=C(Oc1cccc1)/C=C/c2ccc(Sn3ccnc3)cc2	0.75	5.01	2.88
O=C(NCCCN1cnc1)c2cc3cc(ccc3n2)C	0.80	5.01	2.91
O=C(NCCCN1cnc1)NCc2cccc(Sc3cccc3)c2	0.80	5.01	2.91
O=C(NCCCN1cnc1)NCc2cccc(N(c3cccc3)C)c2	0.96	5.01	2.98
O=C(NCC(=O)NCCCN1cnc1)C2CCN(CC2)c3cccc3	1.00	5.01	3.01
O=C(Nn1cnc1)CNC(=O)c2ccc(s2)-c3cccc3	1.03	5.01	3.02
O=C(NCCCN1cnc1)c2ccc(s2)CNC(=O)c3cccc3	2.07	3.98	3.02
[NH+]1(C2CCN(CC2)c3cccc3)CCC(Nn4ccnc4)CC1	1.08	5.01	3.04
S(CCNc1cccc1)c2nnc(s2)NCCCN3cnc3	4.57	1.58	3.08
O=C(NCCc1cccc1)c2cnc(s2)NCCCN3cnc3	3.04	3.16	3.10
O=C(NCCCN1cnc1)c2ccc-3c(Cc4cc(-c5cccc5)ccc43)c2	0.05	6.31	3.18
O=C(Nc1cccc1)C[NH+]2CCC[C@H](C2)C(=O)NCCCN3cnc3	1.35	5.01	3.18
O=C(NCCCN1cnc1)NCc2nnc(s2)Sc3cccc3	1.36	5.01	3.19
[NH+]1(CCN(n2cnc2)CCC1)Cc3ccc(-c4cccc4)cc3	0.08	6.31	3.20
o1c2ccc(-n3ccnc3)cc2nc1-c4cnc(-c5cccc5)cc4	0.09	6.31	3.20

s1c2cc(-c3cccc3)enc2nc1N4CCC(n5cncc5)CC4	0.13	6.31	3.22
O=C(NC1CCC2(CC1)CCN(n3cncc3)CC2)c4cccc4	0.14	6.31	3.22
O=C(N[C@@H]1CCN(n2cncc2)C1)c3ccc(-c4cccc4)cc3	0.16	6.31	3.24
O(C1CCN(n2cncc2)CC1)c3ccc(-c4cccc4)cc3	0.17	6.31	3.24
O=C(On1cncc1)c2ccc(o2)-c3ccc(-c4cccc4)cc3	0.19	6.31	3.25
O=C(Nc1ccc2cc(sc2c1)-c3cccc3)Cn4cncc4	0.20	6.31	3.25
O=C(NCCcn1cncc1)n2cc(nn2)-c3ccc(-c4cccc4)cc3	0.20	6.31	3.26
O=C(NCCcn1cncc1)N/N=C\2[C@H](OC3(C2)CCN(CC3)c4cccc4)C	0.20	6.31	3.26
O=C(NCCcn1cncc1)c2nnc(o2)-c3cccc(-c4cccc4)c3	0.21	6.31	3.26
O=C(NCCcn1cncc1)Nc2cccc(c2)C#Cc3cccc3	0.21	6.31	3.26
O=C(NCCcn1cncc1)c2nc(no2)-c3ccc(-c4cccc4)cc3	0.22	6.31	3.27
O=C(Nc1ccc(-c2cccc2)cc1)[C@@H]3C[C@H](n4cncc4)C[NH2+]3	0.23	6.31	3.27
O=C(NCCcn1cncc1)[C@@H]2CC(=NO2)c3ccc(-c4cccc4)cc3	0.27	6.31	3.29
O=C(Nn1cncc1)c2cnn(n2)-c3ccc(-c4cccc4)cc3	0.28	6.31	3.30
O=C(Nn1cncc1)c2cnn(-c3ccc(-c4cccc4)cc3)c2	0.28	6.31	3.30
Cc1c(NCCcn2cncc2)c(on1)/C=C/c3ccc(s3)-c4cccc4	0.31	6.31	3.31
O=C(NCCcn1cncc1)C2CCN(CC2)c3ccc(c[nH+]3)-c4cccc4	0.33	6.31	3.32
O=C(NCCcn1cncc1)c2ncc(o2)-c3ccc(-c4cccc4)en3	0.33	6.31	3.32
O=C(NC[C@H](C1CCN(CC1)c2cccc2)C)NCCcn3cncc3	1.64	5.01	3.33
O=C(OC1CCCC(OC(=O)c2cccc2)CCC1)NCCcn3cncc3	0.37	6.31	3.34
O=C(NCCcn1cncc1)C/C=C/c2ccc(-c3cccc3)cc2	0.45	6.31	3.38
O=C(NC1CCN(n2cncc2)CC1)c3cc(on3)-c4cccc4	0.46	6.31	3.39
[NH+]1(C2CCN(CC2)c3cccc3)CCC(CC1)Cn4cncc4	0.46	6.31	3.39
O=C(NC1CCC(CC1)Cn2cncc2)/C=C/c3cccc3	0.48	6.31	3.40
O=C(NC1CCC(Oc2cccc2)CC1)/C=C/n3cncc3	0.56	6.31	3.44
n1(/C=C/CC/C=C/C=C/c2cccc2)cncc1	2.89	3.98	3.44
O=C(NCCcn1cncc1)c2csc(n2)-c3ccc(s3)-c4cccc4	0.59	6.31	3.45
O=C(NCC1CCN(n2cncc2)CC1)/C=C/c3cccc3	0.80	6.31	3.56
N/C(Nn1cncc1)=N\N=C\c2ccc(-c3cccc3)cc2	0.83	6.31	3.57
S(CC#CCc1cccc1)c2nnc(o2)-n3cncc3	0.87	6.31	3.59
S(CCOc1cccc1)c2nnc(o2)NCCcn3cncc3	4.70	2.51	3.61
o1c(nc(NCCcn2cncc2)n1)[C@@H]3CCC[NH+](C3)Cc4cccc4	0.96	6.31	3.63
O=C(N1CCC(CC1)CNC(=O)c2cccc2)NCCcn3cncc3	1.00	6.31	3.66
O=C(NCCcn1cncc1)c2cncc(C(=O)NCc3cccc3)c2	1.11	6.31	3.71
O=C(Nc1cccc1)Cn2cncc(n2)C(=O)NCCcn3cncc3	2.49	5.01	3.75
O=C(N1CC(C1)Cc2cnn(c2)-c3cccc3)NCCcn4cncc4	1.28	6.31	3.80
S(Sc1ccc(-c2cccc2)cc1)CCn3cncc3	1.35	6.31	3.83
O=C(NCCcn1cncc1)NCc2ccc(Oc3cccc3)cc2	1.39	6.31	3.85
O=C(OCC1CCN(CC1)c2cccc2)/C=C/n3cncc3	1.50	6.31	3.91
s1c(-c2nc3cc(-n4cncc4)ccc3[nH]2)ccc1-c5cccc5	0.06	7.94	4.00
C[n+]1c(en2ccc(-n3cncc3)cc21)-c4ccc(-c5cccc5)cc4	0.07	7.94	4.00
n1(-c2cncc(c2)C#Cc3cncc(-c4cccc4)cc3)cncc1	0.07	7.94	4.01
[NH+]1(CCCN(n2cncc2)CC1)Cc3cccc(-c4cccc4)c3	0.08	7.94	4.01
O=C(Oc1cccc1)c2ccc(o2)COC(=O)NCCcn3cncc3	3.02	5.01	4.02
N1(n2cncc2)CCC(CC1)c3nc4ccc(cc4[nH]3)-c5cccc5	0.10	7.94	4.02
N1(n2cncc2)CCN(CC1)c3ccc(Nc4cccc4)cc3	0.12	7.94	4.03
O=C(Nc1cc(on1)-n2cncc2)c3ccc(-c4cccc4)cc3	0.12	7.94	4.03

O=C(N1CCC(CC1)c2cc([nH]n2)-c3ccccc3)NCCCN4cncc4	0.13	7.94	4.04
O=C(NCCCN1cncc1)/C=C/c2ccc3cc(-c4ccccc4)ccc3c2	0.13	7.94	4.04
[NH+]1(Cc2ccccc(-n3ccnc3)c2)CCN(CCC1)c4ccccc4	0.15	7.94	4.05
O=C(c1ccccc1)c2cnc(N3CCC(n4cncc4)CC3)cc2	0.17	7.94	4.06
Clc1cc(-c2ccc(o2)/C=N/c3ccccc3)ccc1-n4cncc4	0.17	7.94	4.06
O=C(Oc1cncc1)c2cc(on2)-c3ccc(-c4ccccc4)cc3	0.18	7.94	4.06
O1C[C@H](n2ccnc2)CC31CCN(CC3)c4ccc(cc4)-c5ccccc5	0.19	7.94	4.06
Clc1c(noc1-c2ccc(-c3ccccc3)cc2)C(=O)NCCCN4cncc4	0.20	7.94	4.07
O=C(Nn1cncc1)c2ccc(N3CC[C@H](C3)c4ccccc4)cc2	0.21	7.94	4.07
O=C(NCCCN1cncc1)C2CCN(CC2)c3ccc(cc3)-c4ccccc4	0.21	7.94	4.07
O=C(NCCCN1cncc1)c2cc(N3CCC[C@H](C3)c4ccccc4)ncn2	0.23	7.94	4.09
N1(CCN(CCC1)c2ccc3nnc(n3n2)NCCCN4cncc4)c5ccccc5	0.25	7.94	4.10
O=C(NCCCN1cncc1)c2nc3cc(C(=O)c4ccccc4)ccc3o2	0.28	7.94	4.11
N(C1CCC(CC1)c2ccccc2)c3ccc(-n4cncc4)cc3	0.30	7.94	4.12
O=C(Nc1nc(C(=O)NCCCN2cncc2)cs1)Cc3ccccc3	1.95	6.31	4.13
O=C(c1ccccc1)/C=C/c2ccc(cc2)/C=N/n3cncc3	0.32	7.94	4.13
s1c(-c2csc(n2)-c3ccccc3)ccc1CCn4cncc4	0.37	7.94	4.15
O=C(Oc1ccc(Cn2cncc2)cc1)/C=C/c3ccccc3	0.37	7.94	4.16
[NH+]1(CCC(CC1)c2ccc(-c3ccccc3)cc2)Cn4cncc4	0.38	7.94	4.16
S=C(SCCc1nnc(o1)NCCCN2cncc2)c3ccccc3	2.06	6.31	4.18
[NH+]1(C2CCC(Nn3ccnc3)CC2)CCN(CC1)c4ccccc4	0.44	7.94	4.19
Cc1c[n+](CCCC#Cc2ccccc2)ccc1-n3cncc3	0.46	7.94	4.20
O=C(OCC#CCOc1ccccc1)NCCCN2cncc2	2.14	6.31	4.22
[NH+]1(CCC(C2CCN(CC2)c3ccccc3)CC1)Cn4cncc4	0.51	7.94	4.22
S(SC/C=C/n1cncc1)C/C=C/c2ccccc2	5.94	2.51	4.23
O=C(NCCCN1cncc1)c2ccccc2)C(=O)NCc3ccccc3	0.54	7.94	4.24
N1(CCC(Cn2cncc2)CC1)c3ncc(-c4ccccc4)cn3	0.55	7.94	4.24
O(C1CCN(CC1)c2ccccc2)c3ccc(-n4cncc4)cc3	0.56	7.94	4.25
[nH+]1cc(Nn2cncc2)ccc1N3CCN(CC3)c4ccccc4	0.57	7.94	4.26
[nH]1c2ccc(-n3cncc3)cc2nc1CCCc4ccccc4	0.60	7.94	4.27
O=C(NCCCN1cncc1)c2cc(no2)[C@@H]3CCCN(C3)c4ccccc4	0.62	7.94	4.28
O=S(=O)(N1CCC(CC1)C(=O)NCCCN2cncc2)Cc3ccccc3	0.65	7.94	4.30
o1c(nc(n1)CCn2cncc2)[C@@H]3CCN(C3)c4ccccc4	0.76	7.94	4.35
O=C(C1CCC(CC1)CNC(=O)NCCCN2cncc2)c3ccccc3	0.79	7.94	4.37
O=C(CCCc1nn2c(s1)nnc2NCCCN3cncc3)c4ccccc4	0.88	7.94	4.41
O=C(OCc1ccc(Oc2ccccc2)cc1)NCCCN3cncc3	0.89	7.94	4.42
O=C(Nc1ccccc1)C(=O)Nc2nnc(s2)Cn3cncc3	0.99	7.94	4.47
S(Cc1ncc(o1)-c2ccccc2)c3cncc(s3)-n4cncc4	1.02	7.94	4.48
O1[C@H](CCCCc2ccccc2)CC(NCCCN3cncc3)=N1	5.02	3.98	4.50
O=C(NCCCN1cncc1)NCc2ccc(s2)Cc3ccccc3	1.11	7.94	4.53
s1c(NCCCN2cncc2)nnc1CCSCc3ccccc3	4.10	5.01	4.56
O=C(N1CC(n2cc(nn2)Cc3ccccc3)C1)NCCCN4cncc4	1.42	7.94	4.68
O=C(NCCCN1cncc1)CCc2nc(no2)Cc3ccccc3	1.92	7.94	4.93
O=C(Oc1ccccc1)CSe2nnc(o2)NCCCN3cncc3	8.66	1.26	4.96
Cn1c(SCCCc2ccccc2)nnc1NCCCN3cncc3	2.04	7.94	4.99
N1(CCC(CC1)c2nc3ccc(-n4cncc4)en3n2)c5ccccc5	0.05	10.00	5.03
[nH]1c2ccc(-c3ccccc3)cc2nc1-c4ncc(-n5cncc5)cc4	0.07	10.00	5.03

Fc1enc(NCCCN2cnc2)nc1Ne3ccc(-c4cccc4)cc3	0.08	10.00	5.04
O=C1C=C(Nc2ccc(Nc3cccc3)cc12)C(=O)NCCCN4cnc4	0.09	10.00	5.05
N1(CCC(CC1)c2cc3cc(-n4cnc4)ccc3[nH]2)c5cccc5	0.10	10.00	5.05
O=C(NCCCN1cnc1)CSc2nnc(s2)Nc3cccc3	2.16	7.94	5.05
O=C(c1cc2cc(-n3cnc3)ccc2o1)/C=C/c4cccc4	0.12	10.00	5.06
O=C(NCCCN1cnc1)c2ccc(o2)-c3cccc(-c4cccc4)c3	0.14	10.00	5.07
N1(n2cnc2)CCC(n3c4cnc(cc4nn3)-c5cccc5)CC1	0.16	10.00	5.08
O=C(NCCCN1cnc1)C(=O)/C=C/c2cccc(-c3cccc3)c2	0.20	10.00	5.10
[NH+]1(CC2CCC(CC2)c3cccc3)CCC(n4cnc4)CC1	0.21	10.00	5.10
O1C[C@H](CC21CCN(CC2)c3cccc3)c4cnn(-n5cnc5)c4	0.23	10.00	5.12
O=C(Nc1ccc(-c2cccc2)cc1)[C@@H]3CCN(n4cnc4)C3	0.24	10.00	5.12
S(n1cnc1)C2COC(OC2)/C=C/C=C/c3cccc3	2.30	7.94	5.12
o1c(ncc1-c2ccc(-n3cnc3)cc2)/C=N/c4cccc4	0.26	10.00	5.13
N1(CCC(Cn2cnc2)CC1)c3ccc(nn3)-c4cccc4	0.26	10.00	5.13
O=C(NCCCN1cnc1)c2cnn(c2)-c3nc(-c4cccc4)cs3	0.27	10.00	5.13
O=C(N1CCN(CC1)c2ncc(-c3cccc3)cn2)NCCCN4cnc4	0.29	10.00	5.14
s1c(nnc1NCn2cnc2)-c3ccc(o3)-c4cccc4	0.33	10.00	5.17
C[C@@H]1C[NH+](CCN1c2ccc(-c3cccc3)cc2)Cn4cnc4	0.34	10.00	5.17
O=C(N1CC[C@H](CCC1)CCc2cccc2)NCCCN3cnc3	0.37	10.00	5.18
s1c2cc(Nc3cccc3)ccc2nc1SCn4cnc4	0.37	10.00	5.18
O=C(c1ccc(-n2cnc2)cc1)/C=C/C=C/c3cccc3	0.42	10.00	5.21
O=C(NC1CCN(n2cnc2)CC1)c3cc(n[nH]3)-c4cccc4	0.42	10.00	5.21
O=C(Nc1nc(ns1)-c2cccc2)c3ccc(-n4cnc4)cc3	0.47	10.00	5.24
[nH]1c2ccc(-n3cnc3)cc2nc1CCNc4cccc4	0.51	10.00	5.25
o1c(ccc1-c2cccc2)/C=C/C=N/Nn3cnc3	0.54	10.00	5.27
s1c(nnc1NCCCN2cnc2)/N=C/c3ccc(-c4cccc4)cc3	0.57	10.00	5.28
[n+]1(CCCC#Cn2cnc2)ccc(-c3cccc3)cc1	0.57	10.00	5.28
O=C(N1CC[C@@]2(C[C@H](Nc3cccc3)CCO2)C1)NCCCN4cnc4	0.70	10.00	5.35
O=S(=O)(C1CCN(CC1)C(=O)NCCCN2cnc2)Cc3cccc3	0.70	10.00	5.35
O=C(OC1CCC(N(c2cccc2)C)CC1)C#Cn3cnc3	0.70	10.00	5.35
O=C(Nc1nc(-c2cccc2)cs1)c3cnc(-n4cnc4)cn3	0.72	10.00	5.36
O=S(=O)(N1CC=C(CC1)c2cccc2)CC(=O)NCCCN3cnc3	0.73	10.00	5.36
O=C(NCCCN1cnc1)c2cnc(s2)-c3cnn(c3)-c4cccc4	0.73	10.00	5.36
O=C(NCCCN1cnc1)Ne2cccc(CCc3cccc3)c2	0.76	10.00	5.38
O=C(On1cnc1)CNC(=O)c2ccc(s2)-c3cccc3	0.88	10.00	5.44
O=C(NNC(=O)c1cccc1)CCC(=O)NCCCN2cnc2	4.58	6.31	5.45
S(Cn1cnc1)c2ccc(CCc3cccc3)cc2	3.01	7.94	5.48
S(Cc1noc(n1)-c2cccc2)c3nnc(NCCCN4cnc4)[nH]3	0.98	10.00	5.49
O=C(NCCCN1cnc1)CC[NH+]2CC=C(CC2)c3cccc3	1.08	10.00	5.54
N1(CCC(CC1)Cn2cc(NCCCN3cnc3)cn2)c4cccc4	1.09	10.00	5.55
O=C(NCCCN1cnc1)N/N=C\c2cccc(Oc3cccc3)c2	1.13	10.00	5.57
O=C(C(=O)NCCCN1cnc1)/C=C/c2ccc(s2)-c3cccc3	1.23	10.00	5.61
O=C(NCCCN1cnc1)C(=O)Nc2cccc(Oc3cccc3)c2	1.34	10.00	5.67
O=C(NCCCN1cnc1)c2nnc(s2)CSCc3cccc3	5.04	6.31	5.67
[NH+]1(CCC(n2cnc2)CC1)CCCCc3cccc3	1.50	10.00	5.75
O=C(NCCCN1cnc1)NCc2esc(n2)Nc3cccc3	1.87	10.00	5.94
N1(CCC(CC1)Cn2cc(NCCCN3cnc3)nn2)c4cccc4	1.96	10.00	5.98

O=C(NCCCN1cnc1)NCC[C@@H]2CN(CCC2)c3ccccc3	2.10	10.00	6.05
O=C(Oc1ccccc1)CCCO(=O)NCCCN2cnc2	10.62	1.58	6.10
n1(/C=C/C=C/CC/C=C/c2ccccc2)ccnc1	4.28	7.94	6.11
O=C(OCCCCc1ccccc1)NCCCN2cnc2	4.29	7.94	6.12
O=C(Nc1cnc(Oc2ccccc2)cc1)C(=O)NCCCN3cnc3	2.24	10.00	6.12
n1(-c2ccccc2)C#Cc3cnc(nc3)-c4ccccc4)ccnc1	0.02	12.59	6.31
O=C(NCc1nnc(s1)NCCCN2cnc2)Cc3ccccc3	2.62	10.00	6.31
O=C(NCCCN1cnc1)NCCCCc2ccccc2	7.63	5.01	6.32
Cn1c2ccc(cc2nc1-c3ccc(-n4ccnc4)cc3)-c5ccccc5	0.07	12.59	6.33
N1(n2cnc2)CCC(CC1)Cc3ccc(-c4ccccc4)cc3	0.11	12.59	6.35
Fc1cc(-c2ccccc2)ccc1OC3CCN(n4cnc4)CC3	0.11	12.59	6.35
s1c(nn2c1nnc2NCCCN3cnc3)-c4ccc(-c5ccccc5)cc4	0.13	12.59	6.36
Fc1c(-c2ccccc2)ccc(C[NH+])3CCN(n4cnc4)CC3)c1	0.14	12.59	6.37
Nc1nc(N2CCN(n3cnc3)CC2)nc4nc(nn14)-c5ccccc5	0.15	12.59	6.37
N1(CCC[C@H](C1)c2ccccc2)c3ccc4nnc(n4n3)NCCCN5cnc5	0.17	12.59	6.38
O=C(NCCCN1cnc1)c2cnn(-c3ccccc(-c4ccccc4)c3)c2	0.17	12.59	6.38
O=C(Nc1ccc(-n2cnc2)cc1)[C@@H]3C[C@H](C[NH2+])c4ccccc4	0.18	12.59	6.38
n1(C2CCC(CC3CCC(CC3)c4ccccc4)CC2)cnc1	0.21	12.59	6.40
Clc1cc(C=2C[C@H](ON2)C(=O)NCCCN3cnc3)ccc1-c4ccccc4	0.21	12.59	6.40
O(n1cnc1)C2CCN(CC2)c3ccc(nn3)-c4ccccc4	0.22	12.59	6.41
O=C(NCCCN1cnc1)c2ccccc2)C(=O)/C=C/c3ccccc3	0.24	12.59	6.42
O=C(NCCCN1cnc1)c2cc(on2)-c3ccc(-c4ccccc4)cc3	0.25	12.59	6.42
FC1(CN(C1)C(=O)NCCCN2cnc2)c3ccc(cc3)-c4ccccc4	0.25	12.59	6.42
O=C(Nc1ccccc1)c2ccc(N3CC[C@H](n4cnc4)C3)cc2	0.26	12.59	6.42
O=C([C@@H]1CCc2c(C1)cc(s2)C(=O)NCCCN3cnc3)c4ccccc4	0.27	12.59	6.43
[NH+]1(CC2CCC(n3cnc3)CC2)CCC(CC1)c4ccccc4	0.29	12.59	6.44
S(Cn1cnc1)c2nnc3c4cc(nn4cnc23)-c5ccccc5	0.29	12.59	6.44
O=C(NCCCN1cnc1)NCc2csc(n2)N(c3ccccc3)C	2.89	10.00	6.44
O=C(Nn1cnc1)c2nnc(n2)-c3ccc(-c4ccccc4)cc3	0.31	12.59	6.45
O=C(Nc1ccccc1)c2nnc(s2)[C@@H]3CCCN(n4cnc4)C3	0.32	12.59	6.46
O=C(OCn1cnc1)/C=C/c2ccc(-c3ccccc3)cc2	0.33	12.59	6.46
N1(n2cnc2)CCC3(CC(C3)CCc4ccccc4)CC1	0.36	12.59	6.47
[NH+]1(CC2CCN(n3cnc3)CC2)CCC(CC1)c4ccccc4	0.36	12.59	6.48
O=C(Nc1enn(-n2cnc2)c1)c3cc(on3)-c4ccccc4	0.37	12.59	6.48
o1c2ccc(-n3cnc3)cc2nc1CCC4ccccc4	0.47	12.59	6.53
O=C(NCCCN1cnc1)c2cc(no2)-c3enn(-c4ccccc4)c3	0.47	12.59	6.53
O(CCc1ccccc1)c2ccc3c(nc(o3)-n4cnc4)c2	0.47	12.59	6.53
O=C(NCCCN1cnc1)c2csc(n2)[C@@H]3C[C@H](CCO3)c4ccccc4	0.49	12.59	6.54
O=C(OCC1ccccc1)/C=C/c2ccc(-n3cnc3)cc2	0.50	12.59	6.54
[NH+]1(C2CCC(CC2)Cn3cnc3)CC=C(CC1)c4ccccc4	0.50	12.59	6.55
S(Cc1ccccc1)c2nc3ccc(On4cnc4)cc3[nH]2	0.51	12.59	6.55
O=C(NCCCN1cnc1)c2coc(n2)-c3coc(n3)-c4ccccc4	0.62	12.59	6.60
O=C(NCCCN1cnc1)NCc2nnc3C[C@H](CCn23)c4ccccc4	0.63	12.59	6.61
O=C(NCCCN1cnc1)/C=C/c2ccc3c(c2)ccn3-c4ccccc4	0.65	12.59	6.62
O=C(N[C@@H]1CC[NH+](C2CCN(n3cnc3)CC2)C1)c4ccccc4	0.66	12.59	6.62
O=C(Nc1cccc(CNc2ccccc2)c1)NCCCN3cnc3	0.74	12.59	6.66
o1cc(nc1-n2cnc2)C[NH2+][C@@H]3CCN(C3)c4ccccc4	0.76	12.59	6.67

O=C1N(n2ccnc2)C[C@H](O1)CNC(=O)/C=C/c3ccccc3	0.78	12.59	6.68
O=C(Nc1ccc(Nc2ccccc2)cc1)C(=O)NCCCn3cnc3	0.79	12.59	6.69
C/C(=C\Ce1ccccc1)/C=C/C=C(\C)/C=C/n2ccnc2	0.83	12.59	6.71
O=C(NCCCN1cnc1)N/N=C\c2ccc(Oc3ccccc3)cc2	0.86	12.59	6.73
O=C(NCCCN1cnc1)c2cnc(N3CCN(CC3)c4ccccc4)cc2	0.99	12.59	6.79
O(n1ccnc1)CC#CC#CCOc2ccccc2	3.62	10.00	6.81
s1c(C[NH+]2CC[C@H](C2)c3ccccc3)cnc1NCCCN4cnc4	1.20	12.59	6.89
O=C(OCCC1CCN(CC1)c2ccccc2)NCCCN3cnc3	1.22	12.59	6.90
O=C(Nc1cnc(C(=O)NCCCn2cnc2)c1)Cc3ccccc3	1.48	12.59	7.03
O=C(NC1CCC(Nc2ccccc2)CC1)C(=O)NCCCn3cnc3	1.53	12.59	7.06
O=C(NCCCN1cnc1)c2ccc(SCc3ccccc3)cc2	1.58	12.59	7.08
O=C(NCCCN1cnc1)c2nnc(s2)CNC(=O)c3ccccc3	1.70	12.59	7.14
S(CCOc1ccccc1)c2nnc(s2)NCCCN3cnc3	13.23	1.26	7.24
O=C(NCCCN1cnc1)c2ccc(s2)CCc3ccccc3	1.91	12.59	7.25
o1c(nnc1NCCCN2cnc2)C[NH2+]CCc3ccccc3	4.59	10.00	7.29
O=C(NCCCN1cnc1)c2ccc(N3CCN(CC3)c4ccccc4)cn2	2.13	12.59	7.36
s1c(NCCCc2ccccc2)nnc1NCCCN3cnc3	2.14	12.59	7.36
O=C(NCCCN1cnc1)C2CCC([NH2+]Cc3ccccc3)CC2	2.19	12.59	7.39
S(Cc1nnc(s1)SCn2cnc2)c3ccccc3	8.59	6.31	7.45
O=C(NCCCN1cnc1)CC/C=C/CCc2ccccc2	4.97	10.00	7.48
O=C(NCCCN1cnc1)CNC(=O)c2cc(n(n2)C)-c3ccccc3	2.49	12.59	7.54
O=C(NC[C@H]([NH3+])c1ccccc1)/C=C/C(=O)NCCCN2cnc2	2.55	12.59	7.57
S(CCC[NH+]1CCN(n2ccnc2)CC1)c3ccccc3	2.60	12.59	7.60
O=C(NCCCN1cnc1)CCCN2cc(-c3ccccc3)cn2	2.68	12.59	7.64
O=C(NCCCN1cnc1)CSc2nc(Sc3ccccc3)ns2	9.05	6.31	7.68
n1(CCCCc2ccccc2)cnc(NCCCN3cnc3)c1	2.92	12.59	7.75
O=C(NCCN1cc(-c2ccccc2)cn1)NCCCN3cnc3	2.95	12.59	7.77
O=C(Nc1ncc(s1)-n2cnc2)c3cccc(-c4ccccc4)c3	0.03	15.85	7.94
s1cc(-n2cnc2)nc1NN=C3CCC(CC3)c4ccccc4	0.06	15.85	7.96
o1c2ccc(-c3ccccc3)cc2nc1-c4cnc(-n5ccnc5)cc4	0.08	15.85	7.96
n1(nc2ccc(-n3cnc3)cc2n1)-c4ccc(-c5ccccc5)cc4	0.08	15.85	7.96
s1c(ccc1-n2cnc2)C#Cc3ccc(-c4ccccc4)cc3	0.08	15.85	7.97
O1c2ccc(On3cnc3)cc2CCC41CCN(CC4)c5ccccc5	0.09	15.85	7.97
Fe1cc(-c2nc3cc(-n4cnc4)ccc3[nH]2)ccc1-c5ccccc5	0.09	15.85	7.97
N1(CCC(CC1)c2nc3cc(-n4cnc4)ccc3[nH]2)c5ccccc5	0.10	15.85	7.97
O=C(c1ccc(N2CCC(n3cnc3)CC2)cc1)c4ccccc4	0.10	15.85	7.97
N1(n2cnc2)CCN(CC1)c3ccc4c([nH]c(n4)-c5ccccc5)c3	0.10	15.85	7.97
n1(-c2ccc(-c3nc4cc(-c5ccccc5)cnc4[nH]3)cc2)cnc1	0.11	15.85	7.98
O(CCCn1cc(NCCCN2cnc2)cn1)c3ccccc3	10.95	5.01	7.98
Fe1cc2c(onc2C3CCN(n4cnc4)CC3)cc1-c5ccccc5	0.13	15.85	7.99
O=C1c2e(CN1n3cnc3)ccc(n2)-c4ccc(-c5ccccc5)cc4	0.13	15.85	7.99
O=C(Nc1nnc(o1)-n2cnc2)c3ccc(-c4ccccc4)cc3	0.14	15.85	8.00
O=C(Nn1cnc1)c2cc(on2)-c3cccc(-c4ccccc4)c3	0.15	15.85	8.00
O=C(NCCCN1cnc1)c2cc(n(n2)C)-c3ccc(-c4ccccc4)cc3	0.16	15.85	8.01
o1c2cnc(cc2cc1C3CCN(n4cnc4)CC3)-c5ccccc5	0.17	15.85	8.01
O=C1c2cc(nn2C=NN1n3cnc3)-c4ccc(-c5ccccc5)cc4	0.17	15.85	8.01
C/C(=C\CC1CCC(CC1)c2ccccc2)/C=C/n3cnc3	0.20	15.85	8.03

s1c2c(nc1N3CCN(n4cnc4)CC3)CC[C@H](C2)c5ccccc5	0.22	15.85	8.03
[NH+]1(C2CCN(n3cnc3)CC2)CCC(Nc4ccccc4)CC1	0.23	15.85	8.04
O=C(NCCc1cnc1)c2ccc(s2)-c3ccc(-c4ccccc4)cc3	0.26	15.85	8.05
Clc1cc(CC2CCN(CC2)c3ccccc3)ccc1-n4cnc4	0.27	15.85	8.06
O=C(N[C@H]1CCN(n2cnc2)C1)c3ccc(-c4ccccc4)cn3	0.28	15.85	8.06
n1(CCCNc2nccc(Nc3ccc(-c4ccccc4)cc3)n2)cnc1	0.28	15.85	8.07
Cc1cc(ccc1N2CC[NH+](Cn3cnc3)CC2)-c4ccccc4	0.29	15.85	8.07
[NH+]1(CC2CCC(CC2)c3ccccc3)CCN(n4cnc4)CC1	0.30	15.85	8.07
O=C(NCCc1cnc1)c2cnn(-c3ccc(-c4ccccc4)cc3)c2	0.30	15.85	8.08
O=C(NCCc1cnc1)c2cnn(c2N)-c3ccc(-c4ccccc4)cc3	0.31	15.85	8.08
O=C(NCCc1cnc1)c2c(oc(n2)C3CCN(CC3)c4ccccc4)C	0.33	15.85	8.09
O=C(NCCc1cnc1)[C@@H]2COc3ccc(Oc4ccccc4)cc3C2	0.34	15.85	8.10
O=C(NCCc1cnc1)c2cnc(N3C[C@H]4[C@H](C4c5ccccc5)C3)nc2	0.35	15.85	8.10
O=C(NCCc1cnc1)[C@H]2COc3cc(Oc4ccccc4)ccc3C2	0.37	15.85	8.11
O=C(OCc1cn2c(n1)ccc(c2)-c3ccccc3)NCCc4cnc4	0.41	15.85	8.13
[NH+]1(CCN(CCC1)c2ccccc2)Cc3ccc(-n4cnc4)cc3	0.45	15.85	8.15
O=C(NCCc1cnc1)c2cn(nn2)-c3ccc(-c4ccccc4)cn3	0.46	15.85	8.16
O=C(/C=C/NCCc1cnc1)/C=C/c2ccc(-c3ccccc3)cc2	0.47	15.85	8.16
O=C(NCCc1cnc1)c2csc(n2)-c3ccc(o3)-c4ccccc4	0.47	15.85	8.16
O=C(OCn1cnc1)/C=C/c2ccc(o2)-c3ccccc3	0.49	15.85	8.17
O=C(NC1CC(C1)c2cc(nen2)-c3ccccc3)NCCc4cnc4	0.51	15.85	8.18
O=C(NCCc1cnc1)c2nnc(s2)C3CCN(CC3)c4ccccc4	0.53	15.85	8.19
s1cc(nc1CCc2ccccc2)-c3nc(-n4cnc4)cs3	0.55	15.85	8.20
O=C(NCCc1cnc1)/C=C/C=C/c2ccc(-c3ccccc3)cc2	0.57	15.85	8.21
S(CCNc1ccc(-n2cnc2)cc1)c3ccccc3	3.84	12.59	8.21
O=C(OCC1CCC(CC1)Cc2ccccc2)NCCc3cnc3	0.66	15.85	8.25
O=C(NCCc1cnc1)c2nnc(o2)-c3esc(c3)-c4ccccc4	0.68	15.85	8.27
O=C(NC[C@H]1[C@H]2CCN(C[C@H]2CO1)c3ccccc3)NCCc4cnc4	0.76	15.85	8.31
O=C(NCCc1cnc1)C(=O)NCc2ccc(-c3ccccc3)cc2	0.78	15.85	8.31
N1(CCC2(CC(C2)CCc3cnc3)CC1)c4ccccc4	0.78	15.85	8.31
O=C(NCCc1cnc1)/C=C/c2ccc(o2)/C=C/c3ccccc3	0.78	15.85	8.32
O=C(NCCc1cnc1)c2cc(N3CCN(CC3)c4ccccc4)nen2	0.79	15.85	8.32
[NH+]1(CCN(CC1)c2ccc(c[nH+]2)-c3ccccc3)Cn4cnc4	0.89	15.85	8.37
O=C(NCCc1cnc1)NCC[C@H]2CCO[C@H](C2)c3ccccc3	0.91	15.85	8.38
[n+]1(CCCC#Cc2ccccc2)cccc(NCCc3cnc3)c1	0.91	15.85	8.38
[n+]1(C[C@H]2[C@H](C2)Cc3ccccc3)ccc(NCCc4cnc4)cc1	0.91	15.85	8.38
O=C(NCCc1cnc1)CSc2nc(Cc3ccccc3)cs2	6.80	10.00	8.40
O=C(NCC1CCC(Oc2ccccc2)CC1)NCCc3cnc3	1.03	15.85	8.44
[NH+]1(C2CCC(n3cnc3)CC2)CCN(CC1)Cc4ccccc4	1.03	15.85	8.44
O=C(NCC1CCN(CC1)c2ccccc2)C(=O)NCCc3cnc3	1.18	15.85	8.51
O=C(NCC1CCN(CC1)c2ccccc2)/C=C/n3cnc3	1.31	15.85	8.58
O=C(NCCc1cnc1)NCc2ccc(N(c3ccccc3)C)cc2	1.42	15.85	8.63
O=C(NCCc1cnc1)NCOCCOc2ccccc2	10.99	6.31	8.65
Clc1c(Oc2ccccc2)ccc(CNC(=O)NCCc3cnc3)c1	1.49	15.85	8.67
[NH2+](C[C@H]1CCc2nnc(n2C1)NCCc3cnc3)Cc4ccccc4	1.72	15.85	8.78
O=C(NCCc1cnc1)Nc2cnc(SCc3ccccc3)c2	1.88	15.85	8.87





## List of papers (2018–2021)

1. Intagliata S, Salerno L, Ciaffaglione V, Leonardi C, Fallica AN, Carota G, Amata E, Marrazzo A, Pittalà V, Romeo G. Heme Oxygenase-2 (HO-2) as a Therapeutic Target: Activators and Inhibitors. *Eur J Med Chem.* **2019**, *183*, 111703. doi: 10.1016/j.ejmech.2019.111703.
2. Floresta G, Fallica AN, Romeo G, Sorrenti V, Salerno L, Rescifina A, Pittalà V. Identification of a potent heme oxygenase-2 (HO-2) inhibitor by targeting the secondary hydrophobic pocket of the HO-2 western region. *Bioorg Chem.* **2020**, *104*, 104310. doi: 10.1016/j.bioorg.2020.104310.
3. Salerno L, Vanella L, Sorrenti V, Consoli V, Ciaffaglione V, Fallica AN, Canale V, Zajdel P, Pignatello R, Intagliata S. Novel mutual prodrug of 5-fluorouracil and heme oxygenase-1 inhibitor (5-FU/HO-1 hybrid): design and preliminary in vitro evaluation. *J. Enzyme Inhib. Med. Chem.* **2021**, *36* (1), 1378-1386. doi: 10.1080/14756366.2021.1928111.
4. Fallica AN, Pittalà V, Modica MN, Salerno L, Romeo G, Marrazzo A, Helal MA, Intagliata S. Recent Advances in the Development of Sigma Receptors Ligands as Cytotoxic Agents: A Medicinal Chemistry Perspective. *J. Med. Chem.* **2021**, *64* (12), 7926-7962. doi:10.1021/acs.jmedchem.0c02265.
5. Fallica AN<sup>‡</sup>, Sorrenti V<sup>‡</sup>, D'Amico AG, Salerno L, Romeo G, Consoli V, Floresta G, Rescifina A, D'Agata V, Vanella L, Pittalà V. Discovery of novel acetamide-based heme oxygenase-1 inhibitors with potent in vitro antiproliferative activity. *J. Med. Chem.* **2021**, *64* (18), 13373-13393. doi: 10.1021/acs.jmedchem.1c00633.
6. Haider M, Elsherbeny A, Pittalà V, Fallica AN, Ali Alghamdi M, Greish K. The potential role of sildenafil in cancer management through EPR augmentation. *J. Pers. Med.* **2021**, *11* (6), 585. doi: 10.3390/jpm11060585.
7. Fallica AN, Barbaraci C, Amata E, Pasquinucci L, Turnaturi R, Dichiara M, Intagliata S, Gariboldi MB, Marras E, Orlandi VT, Ferroni C, Martini C, Rescifina A, Gentile D, Varchi G, Marrazzo A. Nitric Oxide Photo-donor Hybrids of Ciprofloxacin and Norfloxacin: Shift in Activity from Antimicrobial to Anticancer Agents. *J. Med. Chem.* **2021**, *64* (15), 11597-11613. doi: 10.1021/acs.jmedchem.1c00917.

8. Floresta G<sup>‡</sup>, Fallica AN<sup>‡</sup>, Salerno L, Sorrenti V, Pittalà V, Rescifina A. Growing the molecular architecture of imidazole-like ligands in HO-1 complexes. *Bioorg. Chem.* **2021**, *117*, 105428. doi: 10.1016/j.bioorg.2021.105428.
9. Floresta G<sup>†</sup>, Fallica AN<sup>†</sup>, Patamia V, Sorrenti V, Greish K, Rescifina A, Pittalà V. From far west to east: joining the molecular architecture of imidazole-like ligands in HO-1 complexes. *Pharmaceuticals.* **2021**, *14* (12), 1289. doi: /10.3390/ph14121289

## List of conference participations (2018–2021)

1. Fallica AN, Ciaffaglione V, Leonardi C, Dichiarà M, Barbaraci C, Catalfo A, Finocchiaro G, De Guidi G, Amata E, Marrazzo A. Synthesis of “NO-light activated” ciprofloxacin and norfloxacin derivatives as potential biofilm dispersant agents. Società Chimica Italiana, Congresso Congiunto delle Sezioni Sicilia e Calabria, 1–2 March, 2019.

### Poster presentation

2. Ciaffaglione V, Fallica AN, Leonardi C, Intagliata S, Dichiarà M, Barbaraci C, Carota G, Salerno L. Development of novel azole-based Heme Oxygenase-1 Inhibitors. Società Chimica Italiana, Congresso Congiunto delle Sezioni Sicilia e Calabria, 1–2 March, 2019.

### Contribution to poster presentation

3. Leonardi C, Pittalà V, Ciaffaglione V, Fallica AN, Intagliata S, Abdelghany S, Ben Khalaf N. Computer-aided approach to design protein Leishmania major Disulfide Isomerase (LmPDI) inhibitors. Società Chimica Italiana, Congresso Congiunto delle Sezioni Sicilia e Calabria, 1–2 March, 2019.

### Contribution to poster presentation

4. Pittalà V, Raffaele M, Salerno L, Fallica AN, Ciaffaglione V, Sorrenti V, Vanella L. A small-molecule inhibitor of heme oxygenase-1 enhances metformin antiproliferative activity. 11th Joint Meeting on Medicinal Chemistry, 27–30 June, 2019, Prague.

### Contribution to poster presentation

5. Fallica AN, Pittalà V, Rescifina A, Ciaffaglione V, Intagliata S, Floresta G. Rational design and synthesis of heme oxygenase 2 (HO-2) inhibitors by targeting the secondary hydrophobic pocket of the HO-2 western region. Italian Young Medicinal Chemistry Virtual Meeting (#IYMCVMEET), July 22-24, 2020.

### Poster presentation

6. Barbaraci C, Fallica AN, Marras E, Ignazzitto MT, Dichiarà M, Gariboldi M, Orlandi V, Varchi G, Marrazzo A. Shift in activity of ciprofloxacin and norfloxacin “NO-light activated” derivatives from antibiotics to anticancer agents: preliminary results. Italian Young Medicinal Chemistry Virtual Meeting (#IYMCVMEET), July 22-24, 2020.

### Contribution to poster presentation

7. Fallica AN, Ciaffaglione V, Intagliata S, Barbaraci C, Dichiarà M, Sorrenti V, Pittalà V. Targeting the heme oxygenase system with novel azole-based inhibitors possessing an amide

function. Workshop della Sezione Sicilia, Società Chimica Italiana, 3 December, 2020, Messina, Italy.

Poster presentation

8. Barbaraci C, Diciara M, Fallica AN, Ciaffaglione V, Intagliata S, Marrazzo A. Sigma-HDACi hybrid molecules as potential therapeutic treatment for uveal melanoma: design, synthesis and preliminary results. Workshop della Sezione Sicilia, Società Chimica Italiana, 3 December 2020, Messina, Italy.

Abstract

9. Fallica AN, Sorrenti V, D'Amico AG, Salerno L, Romeo G, Consoli V, Floresta G, Rescifina A, Vanella L, Pittalà V. Design, Synthesis and Molecular Modeling Studies of Novel Heme Oxygenase-1 Inhibitors with in Vitro Antiproliferative Effects on Glioblastoma. 13th Young Medicinal Chemist Symposium "Nuove prospettive in Chimica Farmaceutica (NPCF13), 26–29 April, 2021.

Poster presentation

10. Fallica AN, Floresta G, Sorrenti V, Pittalà V, Rescifina A. Identification of novel indole-2-carboxamides as heme oxygenase-1 (HO-1) inhibitors. MedChem2021 Paul Ehrlich Virtual Meeting, 26–28 July, 2021.

Poster presentation

11. Fallica AN, Barbaraci C, Ignazzitto MT, Tomarchio E, Gentile D, Amata E, Gariboldi MB, Orlandi VT, Rescifina A, Varchi G, Marrazzo A. Ciprofloxacin and Norfloxacin Nitric Oxide Photo-donor Hybrids: From Antibacterial to Anticancer Agents. XXVII Congresso Nazionale Della Società Chimica Italiana (SCI2021), 14–23 September, 2021.

Poster presentation

12. Floresta G, Fallica AN, Salerno L, Sorrenti V, Intagliata S, Rescifina A, Pittalà V. Structure-Guided Fragment-Based Approach to Identify New Heme Oxygenase-1 Inhibitors. XXVII Congresso Nazionale Della Società Chimica Italiana (SCI2021), 14–23 September, 2021.

Contribution to poster presentation